Structural and Sensitivity Analysis for the Primal and Dual Problems in the Physical and Material Spaces

Dissertation

DANIEL MATERNA

Structural and Sensitivity Analysis for the Primal and Dual Problems in the Physical and Material Spaces

von der Fakultät Architektur und Bauingenieurwesen
der Technischen Universität Dortmund
zur Verleihung des akademischen Grades
Doktor-Ingenieur (Dr.-Ing.)
genehmigte Dissertation

von
Dipl.-Ing. Daniel Materna

Dortmund, November 2009

Kontakt:
Dipl.-Ing. Daniel Materna
Numerische Methoden und Informationsverarbeitung
Fakultät Architektur und Bauingenieurwesen
Technische Universität Dortmund
August-Schmidt-Str. 8, D-44227 Dortmund
Email: *daniel.materna@tu-dortmund.de*
URL: *www.bauwesen.uni-dortmund.de/nmi*

Prüfungskommission:

Vorsitz:	Prof. Dr.-rer. nat. Bernhard Middendorf
1. Gutachter:	Prof. Dr.-Ing. Franz-Joseph Barthold
2. Gutachter:	Prof. Dr.-Ing. Friedel Hartmann

Tag der Einreichung:	13.07.2009
Tag der mündlichen Prüfung:	06.11.2009

Abstract

The present work is concerned with a complete and consistent representation of structural and sensitivity analysis for the primal and dual problems in structural mechanics. A complete description means that besides classical changes in the physical space (displacement space) also changes in the material space (geometry or design space) are allowed. This point of view yield a complexity of eight problems in structural mechanics. Based on a variational approach, these eight problems are completely derived in a continuous and finite element formulation for the model problem of nonlinear elasticity.

The above mentioned formulations are applied to mesh optimization (r-adaptivity) and shape optimization problems. First of all, in the framework of a complete primal problem, classical global r-adaptive mesh optimization strategies are considered and different error measures are introduced. Thereafter, a novel goal-oriented r-adaptive mesh optimization algorithm is proposed, in which the finite element mesh is optimized in such a way, that a chosen quantity of interest can be computed with high accuracy. Furthermore, shape optimization problems are investigated and the coherence to configurational mechanics is demonstrated.

Moreover, error estimators and improvement algorithms for first-order sensitivity relations are derived. Novel theorems for exact sensitivity relations for the state and a chosen quantity of interest are presented. These results are the basis for error estimators and for any improvement algorithms of design sensitivity relations. All of the required higher-order variations of the weak form of equilibrium are explicitly derived for shape design sensitivities. The efficiency and reliability of the error estimators and improvement algorithms are verified by means of numerical examples.

Kurzfassung

Die vorliegende Arbeit befasst sich mit der vollständigen und konsistenten Darstellung der Struktur- und Sensitivitätsanalyse für die primalen und dualen Probleme in der Strukturmechanik. Unter Vollständigkeit wird hier verstanden, dass neben den klassischen Veränderungen im physikalischen Raum (Verschiebungsraum) auch Veränderungen im materiellen Raum (Geometrie- oder Designraum) zulässig sind. Diese Betrachtungsweise führt zu einer Komplexität von acht Problemen in der Strukturmechanik. Basierend auf einem variationellen Zugang werden diese acht Probleme in der Arbeit vollständig kontinuierlich und diskret für das Modellproblem der nichtlinearen Elastizitätstheorie hergeleitet.

Die obigen Formulierungen werden anschließend auf Netzoptimierungsprobleme (r-Adaptivität) und Formoptimierungsprobleme angewendet. Zunächst werden im Rahmen eines vollständigen primalen Problems klassische globale r-adaptive Netzoptimierungsstrategien betrachtet und verschiedene Fehlermaße für r-Adaptivität eingeführt. Anschießend wird ein neuer zielorientierter r-adaptiver Netzoptimierungsalgorithmus entwickelt, mit dem ein gegebenes FE-Netz derart verbessert wird, dass eine gewählte Zielgröße möglichst genau berechnet werden kann. Ferner werden Formoptimierungsprobleme betrachtetet und die Beziehung zur Konfigurationsmechanik aufgezeigt.

Des Weiteren werden Fehlerschätzer und Verbesserungsalgorithmen für Sensitivitätsbeziehungen 1. Ordnung hergeleitet. Hierbei werden neue Theoreme für eine exakte Darstellung von Design-Sensitivitätsbeziehungen des Verschiebungsfeldes sowie für eine gewählte lokale Zielgröße formuliert. Diese bilden den Ausgangspunkt für Fehlerschätzer und Verbesserungsalgorithmen von Design-Sensitivitäten. Die hierfür benötigten höheren Variationen der schwachen Form des Gleichgewichts werden explizit für Formänderungen des materiellen Körpers bestimmt. Die Effizienz und Zuverlässigkeit der Fehlerschätzer und Verbesserungsalgorithmen wird anhand numerischer Beispiele verifiziert.

Preface

The research on the topic of the present thesis was performed during my time as a research assistant at the *Chair of Numerical Methods and Information Processing* at the *University of Dortmund* during the years 2004 to 2009.

First of all, I would like to thank Prof. Dr.-Ing. Franz-Joseph Barthold for his support and for providing me the freedom to choose my subjects of research. He has given me the opportunity to work in a relaxed environment, which is the basis for the success of scientific work. In addition, special thanks to all my colleagues at the university for creating a pleasant work atmosphere.

Furthermore, I would like to thank Prof. Dr.-Ing. Friedel Hartmann for kindly accepting to be the second reviewer of this thesis and for the interest in my work as well as his useful suggestions. Moreover, thanks to Prof. Dr.-rer. nat. Bernhard Middendorf for taking the chairmanship of the examination committee.

Finally, I would like to thank my family and my friends, especially Maria and my parents for their support.

Dortmund, November 2009 Daniel Materna

Contents

Chapter 1

Introduction

This chapter gives an introduction and motivation for the present work. The state of the art in this topic as well as open problems are stated. Furthermore, the goals as well as the structure of this work are presented.

1.1 State of the art and motivation

Physical problems are solved nowadays using numerical methods such as the *finite element method*. For the most problems a fixed initial or reference configuration is assumed and the considered problem is solved in order to find the corresponding state function, i.e. the deformed configuration under given prescribed loads. The solution of the problem with respect to the state is termed as *structural analysis*. The finite element formulation is based on variational or weak formulations of the considered *boundary value problem* (BVP) or *initial value problem* (IVP). The solution of a given nonlinear variational problem requires variations with respect to the state function or generally speaking variations in the *physical space*.

In some problems the requirement of a fixed initial or reference configuration is abandoned, i.e. the material configuration is allowed to change. A classical field is structural optimization such as shape or topology optimization, in which the initial configuration is changed in order to minimize a chosen objective functional under given constraints, see e.g. [13, 29, 58] and the references therein for an overview. The shape of the material configuration is described in an abstract sense by a design function. The variation of objective functionals and PDE-constraints due to variations in the design or material configuration is termed as *variational design sensitivity analysis*. The variations are required in order to solve the optimization problem using nonlinear programming algorithms. Proposed originally in [25], design sensitivity analysis has been largely developed in the last decades, see e.g. [27, 28, 104] for a widely overview with many references on this topic. The change in the state function and the objective functional due to design variations or variations in the material configuration are investigated. The solution of the sensitivity problems requires variations with respect to the design function or generally speaking variations in the *material space*.

Apart from structural optimization and sensitivity analysis other fields are concerned with variations in the material configuration. Configurational changes are studied in the field of *configurational mechanics* or *mechanics in the material space* and the so-called *configurational* or *material forces* or *material residuals* are used in the context of material inhomogeneities as well as any kinds of material defects, see e.g. the monographs [48, 60, 74] for an overview. Configurational mechanics as a branch of continuum mechanics is concerned with processes in which simultaneous deformation and configurational changes of a body take place. Configurational mechanics is also referred to as *Eshelbian mechanics*, which honors Eshelby's work associating the concept of material or configurational force on a material defect with the change of the overall energy of the system with respect to a *displacement* in the material space of such defects [39, 40].

Furthermore, the theory of configurational mechanics is used in computational mechanics. An interesting application is the optimization of finite element meshes (r-adaptivity) based on the minimization of the material residual or configurational forces on the mesh nodes, see e.g. [2, 20, 66, 77, 80, 101]. The resulting mesh is optimal with respect to the global energy of the primal problem. The mesh optimization problem has a long tradition. First steps for the optimization of finite element meshes based on a discrete formulation of energy minimization were outlined for instance in [23, 24, 41, 75]. The overall energy is minimized with respect to the state and the position of the nodes. The best mesh is defined as the one associated with the lowest potential energy. In fact, the authors obtained the same discrete indicators for mesh optimization like the above mentioned approach from configurational mechanics, but they have not called them material or configurational forces. In the context of sensitivity analysis these error indicators can be termed as the *sensitivity of the energy* with respect to changes of the nodal point positions. Hence, different communities use merely different designations for the same quantities.

Therefore, both shape sensitivity analysis and configurational mechanics deal with changes in the material configuration. Techniques known from shape sensitivity analysis can be used to obtain the relations from configurational mechanics if the overall energy of the problem is chosen as objective functional [6, 65, 66, 69]. For instance, in the particular case of fracture mechanics, if crack propagation is understood as a shape change, the expression of the energy release rate can be obtained through the shape derivative of the total potential energy [8, 100]. In the context of *topological-shape sensitivity analysis* this was investigated in [83].

Furthermore, changes in the material configuration are concerned in the context of the *inverse motion problem*, in which the deformed configuration and Cauchy traction are given and the undeformed configuration has to be calculated. Methods for formulating such inverse deformation problems in elasticity were initially proposed in [26, 93] and later on investigated for instance in [44, 45, 57, 61, 96].

In many theoretical and practical situations only certain *quantities of interest* have to be computed, such as pointwise stresses and displacements or average stresses at some given material point. Well-known *duality techniques* can be used in order to compute such quantities. The

original problem is referred to as the *primal problem* and the solution obtained from the structural analysis is termed as *primal solution*. A *dual* or *adjoint problem* has to be formulated for a given primal problem with respect to the chosen quantities of interest. The solution of the dual problem yields the corresponding *dual* or *adjoint solution*, which is the basis for duality techniques. In the context of structural mechanics such duality techniques are well-known as *Betti's principle* or *reciprocity relation* [49, 51]. The concept of duality is more general and not restricted to mechanical problems and interpretations. Dual problems and dual solutions are essential within *goal-oriented error analysis* and *mesh optimization techniques* in order to minimize the discretization error within numerical methods, see e.g. [4, 11, 37, 88]. Furthermore, in recent years the goal-oriented techniques have been used for combined model and discretization error analysis and adaptive algorithms, see e.g. [18, 84, 95] for an overview. Modeling error is a part of the error due to the natural imperfections in abstract models of actual physical phenomena. In the context of structural optimization and sensitivity analysis such duality techniques are known as *adjoint sensitivity method* [27, 28]. In fact, all those different terms are used synonymously for duality techniques. Hence, dual problems and dual solutions play an important role within different fields.

In summary, it can be stated that different fields are concerned with changes in the physical and material spaces but they are usually disconnected from each other. For a complete description of a variational problem with respect to possible changes in the physical and material spaces both variations have to be considered. Furthermore, additional to the primal problem also a dual problem corresponding to a chosen quantity should be considered. In the context of the above mentioned changes in the material configuration and sensitivity analysis it would be also of interest to study configurational changes for the dual problem itself. Therefore, the goal is to establish a complete description of the primal and dual problems with respect to structural analysis and sensitivity analysis in the physical and material spaces.

1.2 The goal and the structure of this work

In the present work a general framework for structural analysis and variational sensitivity analysis of the primal and dual problems is presented. A complete description of the primal and dual problems with respect to variations in the physical and material spaces is proposed.

A variational problem can be investigated with respect to changes in the physical space (variations in the state) and with respect to changes in the material space (variations in the design), which yield the physical and material problems. The solution of both problems is part of structural analysis. Furthermore, sensitivity analysis can be obtained for the physical and material problems. The same can be performed for the dual problem corresponding to a quantity of interest. Hence, a complete description has a complexity of eight problems, i.e.

$$\begin{array}{c}\text{structural \& sensitivity}\\ \text{analysis}\end{array} \times \begin{array}{c}\text{primal \& dual}\\ \text{problems}\end{array} \times \begin{array}{c}\text{physical \& material}\\ \text{spaces}\end{array} .$$

All these problems will be considered in the present work and with this complexity in mind, a problem formulation can be labeled as complete. Furthermore, in the context of sensitivity analysis it is also of interest to study the error of design sensitivity relations.

The work can be divided into three parts. The following summary outlines the main goals.

1. **The first main goal** is to establish a general and complete framework for the primal and dual problems in linear and nonlinear elasticity. The structural analysis and the variational sensitivity analysis of the primal and dual problems are investigated.

   - Structural and sensitivity analysis of the primal problem.
     A complete and consistent continuous and finite element formulation for variations in the physical and material spaces will be proposed, i.e. all variations are performed with respect to the state and the design.

   - Duality techniques in the physical and material spaces.
     The concept of duality as well as a general framework for dual problems in the physical and material spaces will be presented. In addition to the classical dual physical problem also a dual material as well as a dual formulation for the coupled physical and material problem will be derived.

   - Structural and sensitivity analysis of the dual problem.
     In the same manner as for the primal problem, a complete and consistent continuous and finite element formulation for variations in the physical and material spaces will be proposed.

2. **The second main goal** is to apply the derived relations to representative problems which are based on energy minimization principles.

   - Development of global and goal-oriented r-adaptive mesh optimization algorithms based on sensitivity relations in the physical and material spaces. Furthermore, error measures in the context of r-adaptivity will be studied.

   - The coherence of mechanics in the material space and structural optimization will be presented. As a particular application, the shape optimization problem in the context of configurational mechanics will be investigated.

3. **The third main goal** is to investigate the reliability and accuracy of design sensitivities. In particular, error analysis and improvement of variational sensitivity relations are considered.

   - Exact sensitivity relations for the state and a chosen quantity of interest based on exact integral remainder representations will be derived. A theorem for error analysis of sensitivity relations has to be developed.

   - Based on the exact representation an improvement algorithm for sensitivity relations is proposed, which yields an improved solution of the change in the state as well as a quantity of interest due to changes in the design.

The above summary reflects moreover the structure of the work. In particular, the work is divided into eleven chapters. Chapter 2 is concerned with some fundamental mathematical preliminaries and notations, which are used within this work. Subsequently, the underlying mechanical relations as well as important variations in the physical and material spaces are introduced in Chapter 3.

A complete framework for the primal problem is presented in Chapter 4. Firstly, an energy functional is introduced and all variations are performed with respect to the state and the design. Furthermore, the corresponding finite element formulations are derived. This yields a complete description of the primal problem with respect to possible changes in the physical and material spaces.

Chapter 5 is concerned with duality relations in the physical and material spaces. The general concept of duality is introduced and applied to the physical and material problems. This is based on an optimal control approach, which yields the framework for general variational problems.

With these duality relations at hand, a novel complete framework for the dual problem is proposed in Chapter 6. In the same manner as for the primal problem, an energy functional of the dual problem is introduced and all variations are performed with respect to the dual solution and the design. The resulting residuals and tangent forms are the basis for sensitivity relations of the dual solution itself. Subsequently, the corresponding complete finite element formulations are derived.

A direct application of the complete framework for the primal problem is r-adaptive mesh optimization, which is presented in Chapter 7. The nodal coordinates in the domain and the nodal coordinates in tangential direction on the boundaries are chosen as design variables and the primal energy is minimized with respect to the state and the nodal coordinates. The lowest potential energy of the primal problem yields the smallest discretization error on the current mesh. Furthermore, different error measures in the context of r-adaptivity are introduced and investigated. The potential of such r-adaptive algorithms is demonstrated by means of selected examples. The mesh can be optimized with respect to the overall energy of the primal problem.

Moreover, a novel goal-oriented r-adaptive mesh optimization algorithm is proposed in Chapter 8, which is based on the variational framework of the dual problem. The goal is to optimize the mesh in such a way, that a chosen quantity of interest can be computed with high accuracy. The error in a quantity of interest depends on the error in the corresponding dual solution. With this in mind, the mesh has to be optimized with respect to the dual solution. This is based on the simultaneous minimization of the primal and dual energy functionals.

Chapter 9 deals with the coherence of configurational mechanics and structural optimization. Both disciplines are concerned with changes in the material configuration but they use merely different designations for the same quantities. In particular, the shape optimization problem is considered and the relations to configurational mechanics are highlighted and demonstrated by means of numerical examples.

A novel error representation for sensitivity analysis is presented in Chapter 10. This is based on an exact integral remainder within the Taylor expansion. The remainder can be computed explicitly based on higher-order variations of the considered residual. With this at hand, an improvement algorithm for the sensitivity of the state is proposed. Furthermore, an exact sensitivity relation for quantities of interest is derived. This exact relation is the basis for an estimator of the change in the quantity of interest due to changes in the design.

Finally, Chapter 11 summarizes and discusses the present work and gives an outlook on future research topics.

A summary of important variations in the physical and material spaces, explicit formulations for selective model problems as well as some details on the numerical implementation are given in the appendices.

Some parts of this thesis are submitted or already published in peer-reviewed journals and conference proceedings as part of this doctoral thesis, see [65–73]. These references are also stated in the respective chapters.

Chapter 2

Preliminaries and notations

This chapter deals with some fundamental mathematical preliminaries and notations. The general concepts of variation, linearization and derivation are introduced, which are frequently used terms within this work.

2.1 Notation

In order to distinguish between vectors, tensors of different order and matrices the following notation is introduced.

Scalars and scalar functions are represented by nonbold symbols in italic shape, e.g. A, S, a, s or $\Gamma, \Sigma, \gamma, \sigma$.

Let $\{\boldsymbol{g}_1, \boldsymbol{g}_2, \dots, \boldsymbol{g}_n\}$ be the basis vectors of a given vector space. Then, we write vectors by using boldface letters in italic shape, e.g. $\boldsymbol{A} = A^i \boldsymbol{g}_i$ or $\boldsymbol{a} = a^i \boldsymbol{g}_i$ with the components A^i and a^i, respectively.

Second-order tensors $\mathbf{A} = A^{ij} \boldsymbol{g}_i \otimes \boldsymbol{g}_j$ or $\mathbf{a} = a^{ij} \boldsymbol{g}_i \otimes \boldsymbol{g}_j$ are written with bold-faced roman letters with the components A^{ij} and a^{ij}, respectively. Fourth-order tensors are indicated with a hollowed Roman font, i.e. for instance $\mathbb{A} = \mathsf{A}^{ijkl} \boldsymbol{g}_i \otimes \boldsymbol{g}_j \otimes \boldsymbol{g}_k \otimes \boldsymbol{g}_l$. Bold-face calligraphic letters are used for sixth-order tensors, i.e.

$$\boldsymbol{\mathcal{A}} = \mathcal{A}^{ijklmn} \boldsymbol{g}_i \otimes \boldsymbol{g}_j \otimes \boldsymbol{g}_k \otimes \boldsymbol{g}_l \otimes \boldsymbol{g}_m \otimes \boldsymbol{g}_n.$$

Furthermore, non-standard tensors of eighth-order are introduced and written using bold-faced Fraktur font letters, e.g.

$$\mathfrak{A} = \mathfrak{A}^{ijklmnop} \boldsymbol{g}_i \otimes \boldsymbol{g}_j \otimes \boldsymbol{g}_k \otimes \boldsymbol{g}_l \otimes \boldsymbol{g}_m \otimes \boldsymbol{g}_n \otimes \boldsymbol{g}_o \otimes \boldsymbol{g}_p$$

with the components $\mathfrak{A}^{ijklmnop}$.

Finally, matrices are symbolized by bold-faced sans-serif letters in italic shape, e.g. $\boldsymbol{\mathsf{A}} = [\mathsf{A}_{ij}]$ or a column matrix $\boldsymbol{\mathsf{a}} = [\mathsf{a}_i]$.

2.2 Directional derivative, variation and linearization

Within this work the concepts of variation and linearization are frequently used terms. The notation and some important relations are briefly introduced. For details about the fundamentals of variational calculus see the standard textbooks, e.g. [16, 42, 63].

2.2.1 Directional derivative and variation

Let $a(\boldsymbol{v};\boldsymbol{\eta})$ be a semilinear form, i.e. nonlinear with respect to the variable $\boldsymbol{v} \in \mathcal{V}$ and linear with respect to all arguments on the right of the semicolon, and let $J(\boldsymbol{v})$ be a possible nonlinear functional. Both are defined on a Hilbert space $\mathcal{V}$, i.e.

$$a : \mathcal{V} \times \mathcal{V} \to \mathbb{R},$$

$$J : \mathcal{V} \to \mathbb{R}.$$

We require that $a(\cdot;\cdot)$ is at least twice continuously differentiable. Then, the first and second directional derivatives with respect to $\boldsymbol{v}$ in directions $\{\boldsymbol{\mu}, \boldsymbol{\kappa}\} \in \mathcal{V}$ are introduced as

$$a'_v(\boldsymbol{v};\boldsymbol{\eta},\boldsymbol{\mu}) := \lim_{\varepsilon\to 0} \frac{1}{\varepsilon} \left[\, a(\boldsymbol{v}+\varepsilon\boldsymbol{\mu};\boldsymbol{\eta}) - a(\boldsymbol{v};\boldsymbol{\eta}) \,\right] = \left. \frac{d}{d\varepsilon}\, a(\boldsymbol{v}+\varepsilon\boldsymbol{\mu};\boldsymbol{\eta}) \right|_{\varepsilon=0},$$

$$\begin{aligned} a''_{vv}(\boldsymbol{v};\boldsymbol{\eta},\boldsymbol{\mu},\boldsymbol{\kappa}) &:= \lim_{\varepsilon\to 0} \frac{1}{\varepsilon} \left[\, a'_v(\boldsymbol{v}+\varepsilon\boldsymbol{\kappa};\boldsymbol{\eta},\boldsymbol{\mu}) - a'_v(\boldsymbol{v};\boldsymbol{\eta},\boldsymbol{\mu}) \,\right] \\ &= \left. \frac{d}{d\varepsilon}\, a'_v(\boldsymbol{v}+\varepsilon\boldsymbol{\kappa};\boldsymbol{\eta},\boldsymbol{\mu}) \right|_{\varepsilon=0}. \end{aligned}$$

Remark 2.1 *Note that for a fixed $\hat{\boldsymbol{v}}$ the operator $a'_v(\hat{\boldsymbol{v}};\boldsymbol{\eta},\boldsymbol{\mu})$ is a bilinear form, i.e. linear with respect to $\boldsymbol{\eta}$ and $\boldsymbol{\mu}$. Furthermore, the operator $a''_{vv}(\hat{\boldsymbol{v}};\boldsymbol{\eta},\boldsymbol{\mu},\boldsymbol{\kappa})$ is a trilinear form, i.e. linear with respect to $\{\boldsymbol{\eta},\boldsymbol{\mu},\boldsymbol{\kappa}\}$.*

Furthermore, if $J(\cdot)$ is a differentiable functional on $\mathcal{V}$, the following notation is used for the Gâteaux derivatives

$$J'_v(\boldsymbol{v};\boldsymbol{\eta}) := \lim_{\varepsilon\to 0} \frac{1}{\varepsilon} \left[\, J(\boldsymbol{v}+\varepsilon\boldsymbol{\eta}) - J(\boldsymbol{v}) \,\right] = \left. \frac{d}{d\varepsilon}\, J(\boldsymbol{v}+\varepsilon\boldsymbol{\eta}) \right|_{\varepsilon=0},$$

$$J''_{vv}(\boldsymbol{v};\boldsymbol{\eta},\boldsymbol{\mu}) := \lim_{\varepsilon\to 0} \frac{1}{\varepsilon} \left[\, J'_v(\boldsymbol{v}+\varepsilon\boldsymbol{\mu};\boldsymbol{\eta}) - J'_v(\boldsymbol{v};\boldsymbol{\eta}) \,\right] = \left. \frac{d}{d\varepsilon}\, J'_v(\boldsymbol{v}+\varepsilon\boldsymbol{\mu};\boldsymbol{\eta}) \right|_{\varepsilon=0}.$$

Remark 2.2 *Note that for a fixed $\hat{\boldsymbol{v}}$ the term $J'_v(\hat{\boldsymbol{v}};\boldsymbol{\eta})$ is a linear form, i.e. linear with respect to $\boldsymbol{\eta}$, and $J''_{vv}(\hat{\boldsymbol{v}};\boldsymbol{\eta},\boldsymbol{\mu})$ is a bilinear form, i.e. linear with respect to $\boldsymbol{\eta}$ and $\boldsymbol{\mu}$.*

Higher-order derivatives yield multilinear forms defined as above in a straightforward manner, e.g. $a'''_{vvv}(\hat{\boldsymbol{v}};\boldsymbol{\eta},\boldsymbol{\mu},\boldsymbol{\kappa},\boldsymbol{\xi})$ or $J'''_{vvv}(\boldsymbol{v};\boldsymbol{\eta},\boldsymbol{\mu},\boldsymbol{\kappa})$.

The directional derivative corresponds to the *variation* or sometimes called *variational derivative* of a functional $J(\cdot)$. In classical textbooks of mechanics and variational calculus this is often written using the δ symbol, i.e. the first variation of $J(\cdot)$ with respect to $\boldsymbol{v}$ is written as $\delta_v J(\boldsymbol{v};\delta\boldsymbol{v})$ or $\delta_v J(\boldsymbol{v})(\delta\boldsymbol{v})$, in which $\delta\boldsymbol{v}\in\mathcal{V}$. In fact, it holds true that

$$\delta_v J(\boldsymbol{v};\delta\boldsymbol{v}) = J'_v(\boldsymbol{v};\delta\boldsymbol{v})$$

and both notations are used within this work.

2.2.2 Partial-, total partial and total variation

The semilinear form $a(\cdot;\cdot)$ and the functional $J(\cdot)$ can also depend on a second nonlinear function $\boldsymbol{s}\in\mathcal{S}$, i.e. we consider the forms $a(\boldsymbol{v},\boldsymbol{s};\cdot)$ and $J(\boldsymbol{v},\boldsymbol{s})$, respectively, in which $\mathcal{S}$ is a Hilbert space.

The *partial derivative* or *partial variational derivative* with respect to $\boldsymbol{v}$ and $\boldsymbol{s}$ are written in form of

$$a'_v(\boldsymbol{v},\boldsymbol{s};\boldsymbol{\eta},\boldsymbol{\mu}) = \frac{d}{d\varepsilon}\, a(\boldsymbol{v}+\varepsilon\,\boldsymbol{\mu},\boldsymbol{s};\boldsymbol{\eta})\bigg|_{\varepsilon=0},$$

$$a'_s(\boldsymbol{v},\boldsymbol{s};\boldsymbol{\eta},\boldsymbol{\psi}) = \frac{d}{d\varepsilon}\, a(\boldsymbol{v},\boldsymbol{s}+\varepsilon\,\boldsymbol{\psi};\boldsymbol{\eta})\bigg|_{\varepsilon=0},$$

$$J'_v(\boldsymbol{v},\boldsymbol{s};\boldsymbol{\eta}) = \frac{d}{d\varepsilon}\, J(\boldsymbol{v}+\varepsilon\,\boldsymbol{\eta},\boldsymbol{s})\bigg|_{\varepsilon=0} \quad\text{and}\quad J'_s(\boldsymbol{v},\boldsymbol{s};\boldsymbol{\psi}) = \frac{d}{d\varepsilon}\, J(\boldsymbol{v},\boldsymbol{s}+\varepsilon\,\boldsymbol{\psi})\bigg|_{\varepsilon=0},$$

in which $\{\boldsymbol{\eta},\boldsymbol{\mu}\}\in\mathcal{V}$ and $\boldsymbol{\psi}\in\mathcal{S}$. In the same manner, the second and mixed variations are indicated as above by $(\cdot)''_{vv}$, $(\cdot)''_{ss}$ or $(\cdot)''_{vs}$.

The *total directional derivative* or *total variation* is written as

$$J' = J'_v(\boldsymbol{v},\boldsymbol{s};\boldsymbol{\eta}) + J'_s(\boldsymbol{v},\boldsymbol{s};\boldsymbol{\psi}) \quad\text{or}\quad \delta J = \delta_v J(\boldsymbol{v},\boldsymbol{s};\boldsymbol{\eta}) + \delta_s J(\boldsymbol{v},\boldsymbol{s};\boldsymbol{\psi}).$$

Furthermore, in many cases the function $\boldsymbol{v}$ depends directly on $\boldsymbol{s}$, i.e. $\boldsymbol{v}=\boldsymbol{v}(\boldsymbol{s})$. It is important to distinguish between the *total partial derivative* $D_s(\cdot)$ and the *explicit partial derivative* $\partial_s(\cdot)=\partial(\cdot)/\partial\boldsymbol{s}$ of a quantity $(\cdot)$ with respect to a variable $\boldsymbol{s}$ [35]. The total partial derivative of a function $\mathcal{F}(\boldsymbol{s}) := F(\boldsymbol{v}(\boldsymbol{s}),\boldsymbol{s})$ with respect to $\boldsymbol{s}$ and the explicit partial derivative are connected by the relation

$$D_s\mathcal{F}(\boldsymbol{s})\cdot d\boldsymbol{s} = \frac{\partial F}{\partial \boldsymbol{s}}\cdot d\boldsymbol{s} + \frac{\partial F}{\partial \boldsymbol{v}}\cdot\frac{\partial \boldsymbol{v}}{\partial \boldsymbol{s}}\, d\boldsymbol{s}.$$

By virtue of

$$d\boldsymbol{v} = \frac{\partial \boldsymbol{v}}{\partial \boldsymbol{s}}\, d\boldsymbol{s}$$

we have

$$D_s\mathcal{F}(\boldsymbol{s}) \cdot d\boldsymbol{s} = \frac{\partial F}{\partial \boldsymbol{s}} \cdot d\boldsymbol{s} + \frac{\partial F}{\partial \boldsymbol{v}} \cdot d\boldsymbol{v} = F'(\boldsymbol{v}, \boldsymbol{s}, d\boldsymbol{s}, d\boldsymbol{v}).$$

Hence, the total partial derivative $D_s\mathcal{F}$ with respect to $\boldsymbol{s}$ can be transformed to the total derivative F' and vice versa, i.e. $D_s\mathcal{F}(\boldsymbol{s}) \cdot d\boldsymbol{s} = F'(\boldsymbol{v}, \boldsymbol{s}, d\boldsymbol{s}, d\boldsymbol{v})$. This is of interest in order to eliminate $d\boldsymbol{v}$ and to obtain only a dependency on $d\boldsymbol{s}$.

2.2.3 Increment, variation and linearization

Within this work, it is important to highlight the distinction between an *increment* $\Delta_v J$ and the *variation* $\delta_v J$ of a functional J.

Definition 2.1 *Let $J(\boldsymbol{v})$ be a functional defined on some normed space. Then,*

$$\Delta_v J(\boldsymbol{v}; \Delta\boldsymbol{v}) := J(\boldsymbol{v} + \Delta\boldsymbol{v}) - J(\boldsymbol{v})$$

is the increment of J corresponding to the increment $\Delta\boldsymbol{v}$ in the variable $\boldsymbol{v}$.

In general $\Delta_v J(\boldsymbol{v}; \Delta\boldsymbol{v})$ is a nonlinear functional. A Taylor expansion yields

$$\begin{aligned}\Delta_v J(\boldsymbol{v}; \Delta\boldsymbol{v}) = J(\boldsymbol{v} + \Delta\boldsymbol{v}) - J(\boldsymbol{v}) &= J'_v(\boldsymbol{v}; \Delta\boldsymbol{v}) + r(\boldsymbol{v}, \Delta\boldsymbol{v}) \\ &= \delta_v J(\boldsymbol{v}; \Delta\boldsymbol{v}) + r(\boldsymbol{v}, \Delta\boldsymbol{v}),\end{aligned}$$

where the remainder $r(\boldsymbol{v}, \Delta\boldsymbol{v})$ is quadratic in $\Delta\boldsymbol{v}$ and given as

$$r(\boldsymbol{v}; \Delta\boldsymbol{v}) := \int_0^1 J''_{vv}(\boldsymbol{v} + \lambda\Delta\boldsymbol{v}; \Delta\boldsymbol{v}, \Delta\boldsymbol{v})\,(1 - \lambda)\, d\lambda.$$

The increment can be separated in a linear part and a nonlinear integral remainder. The linear part is the *directional derivative* $J'_v(\boldsymbol{v}, \Delta\boldsymbol{v})$ or *variational derivative* $\delta_v J(\boldsymbol{v}, \Delta\boldsymbol{v})$, i.e.

$$J'_v(\boldsymbol{v}; \Delta\boldsymbol{v}) = \left.\frac{d}{d\varepsilon}\, J(\boldsymbol{v} + \varepsilon\Delta\boldsymbol{v})\right|_{\varepsilon=0} = \delta_v J(\boldsymbol{v}, \Delta\boldsymbol{v}).$$

Definition 2.2 *Let $J(\boldsymbol{v})$ be a differentiable functional defined on some normed space. Then, the variation $\delta_v J$ is the principal linear part of the increment $\Delta_v J(\boldsymbol{v}; \Delta\boldsymbol{v})$, i.e.*

$$\delta_v J(\boldsymbol{v}; \Delta\boldsymbol{v}) := \Delta_v J(\boldsymbol{v}; \Delta\boldsymbol{v}) - r(\boldsymbol{v}; \Delta\boldsymbol{v}).$$

In the limit case we have

$$r(\boldsymbol{v}; \Delta\boldsymbol{v}) \to 0 \qquad \text{as} \qquad ||\Delta\boldsymbol{v}|| \to 0.$$

Hence, for small changes $\Delta\boldsymbol{v}$ we have $\delta_v J(\boldsymbol{v}; \Delta\boldsymbol{v}) \cong \Delta_v J(\boldsymbol{v}; \Delta\boldsymbol{v})$.

The functional J can also depend on a second nonlinear function $\boldsymbol{s}$. In this case the partial increments due to $\Delta\boldsymbol{v}$ and $\Delta\boldsymbol{s}$ are given in form of

$$\Delta_v J(\boldsymbol{v}, \boldsymbol{s}; \Delta\boldsymbol{v}) := J(\boldsymbol{v} + \Delta\boldsymbol{v}, \boldsymbol{s}) - J(\boldsymbol{v}, \boldsymbol{s}) = J'_v(\boldsymbol{v}, \boldsymbol{s}; \Delta\boldsymbol{v}) + r_v(\boldsymbol{v}, \boldsymbol{s}; \Delta\boldsymbol{v})$$

$$\Delta_s J(\boldsymbol{v}, \boldsymbol{s}; \Delta\boldsymbol{s}) := J(\boldsymbol{v}, \boldsymbol{s} + \Delta\boldsymbol{s}) - J(\boldsymbol{v}, \boldsymbol{s}) = J'_s(\boldsymbol{v}, \boldsymbol{s}; \Delta\boldsymbol{s}) + r_s(\boldsymbol{v}, \boldsymbol{s}; \Delta\boldsymbol{s})$$

where

$$r_v(\boldsymbol{v}, \boldsymbol{s}; \Delta\boldsymbol{v}) := \int_0^1 J''_{vv}(\boldsymbol{v} + \lambda\Delta\boldsymbol{v}, \boldsymbol{s}; \Delta\boldsymbol{v}, \Delta\boldsymbol{v})\,(1-\lambda)\,d\lambda,$$

$$r_s(\boldsymbol{v}, \boldsymbol{s}; \Delta\boldsymbol{s}) := \int_0^1 J''_{ss}(\boldsymbol{v}, \boldsymbol{s} + \lambda\Delta\boldsymbol{s}; \Delta\boldsymbol{s}, \Delta\boldsymbol{s})\,(1-\lambda)\,d\lambda.$$

Finally, in case of infinitesimal changes are considered it is called variation δJ and if finite changes are studied then it is called increment ΔJ. This distinction is important within error analysis of sensitivity relations, see Chapter 10.

Furthermore, the linearization of a given functional $J(\boldsymbol{v})$ in the direction $\Delta\boldsymbol{v}$ is written in form of

$$J(\boldsymbol{v} + \Delta\boldsymbol{v}) = J(\boldsymbol{v}) + D_v J(\boldsymbol{v}) \cdot \Delta\boldsymbol{v} + \mathcal{O}.$$

The term $\mathcal{O}$ denotes the remainder which is usually neglected. Therefore, only the abstract symbol $\mathcal{O}$ is used instead of an explicit expression of the remainder when linearization takes place.

2.2.4 Linear and nonlinear arguments in functionals and tangent forms

Different kind of functionals and tangent forms are investigated within this work. In order to distinguish between linear and nonlinear arguments the following notation with comma and semicolon is used. In general, arguments on the right hand side of a semicolon are the linear arguments. Let $\boldsymbol{v}$ and $\boldsymbol{s}$ be nonlinear arguments as well as $\boldsymbol{\eta}$ and $\boldsymbol{\mu}$ are linear functions. Then, the semilinear form $a(\boldsymbol{v}, \boldsymbol{s}; \boldsymbol{\eta})$ and its partial variation $a'_v(\boldsymbol{v}, \boldsymbol{s}; \boldsymbol{\eta}, \boldsymbol{\mu})$ are nonlinear in $\boldsymbol{v}$ and $\boldsymbol{s}$ but linear in $\boldsymbol{\eta}$ and $\boldsymbol{\mu}$, respectively.

The same holds true for functionals. Let $J(\boldsymbol{v}, \boldsymbol{s})$ be a nonlinear functional in $\boldsymbol{v}$ and $\boldsymbol{s}$. Then, the partial variations $J'_v(\boldsymbol{v}, \boldsymbol{s}; \boldsymbol{\eta})$ and $J''_{vv}(\boldsymbol{v}, \boldsymbol{s}; \boldsymbol{\eta}, \boldsymbol{\mu})$ are linear in $\boldsymbol{\eta}$ and $\boldsymbol{\mu}$, respectively.

Furthermore, sometimes a third nonlinear function $\boldsymbol{z}$ can appear and a second semicolon is used in order to indicate this. For instance, the functional $G^*(\boldsymbol{v}, \boldsymbol{s}; \boldsymbol{z}; \cdot)$ and its variation $G^{*\prime}_s(\boldsymbol{v}, \boldsymbol{s}; \boldsymbol{z}; \cdot, \cdot)$ are nonlinear is $\boldsymbol{v}$, $\boldsymbol{s}$ and $\boldsymbol{z}$ but linear in all arguments on the right of the second semicolon.

Chapter 3

Variations in the physical and material spaces

This chapter is concerned with some fundamental mechanical relations in the physical and material spaces. In the present work, changes in the deformed configuration as well as in the initial or reference configuration are investigated. Therefore, important variations in the physical and material spaces of kinematical quantities, energy functionals and stresses are stated. These different kinds of variations are required in the following chapters.

3.1 Kinematics

The present section represents a brief summary of fundamental relations of the underlying geometrically exact kinematic framework. Further details can be found in the standard textbooks, for instance [17, 55, 64, 87]. Moreover, a kinematic framework based on an *intrinsic formulation in local coordinates* has been presented in [5,7,9]. Some parts of the kinematical descriptions are based on this formulation.

3.1.1 The physical and material motion problems

We consider an open bounded material body with an undeformed reference configuration $\Omega_R \subset \mathbb{E}^3$ with a piecewise smooth, polyhedral and Lipschitz-continuous boundary $\Gamma = \partial\Omega_R$ such that $\Gamma = \Gamma_{\mathrm{D}} \cup \Gamma_{\mathrm{N}}$ and $\Gamma_{\mathrm{D}} \cap \Gamma_{\mathrm{N}} = \emptyset$, where Γ_{D} denotes the Dirichlet boundary and Γ_{N} the Neumann boundary, respectively. The corresponding deformed (current) configuration is denoted by $\Omega_t \subset \mathbb{E}^3$. The deformation of the material body from Ω_R into a deformed configuration Ω_t is given by the nonlinear mapping

$$\boldsymbol{\varphi} : \left\{ \begin{array}{lcl} \Omega_R \times I_t & \rightarrow & \Omega_t \subset \mathbb{E}^3 \\ (\boldsymbol{X}, t) & \mapsto & \boldsymbol{x} = \boldsymbol{\varphi}(\boldsymbol{X}, t) \end{array} \right. . \tag{3.1}$$

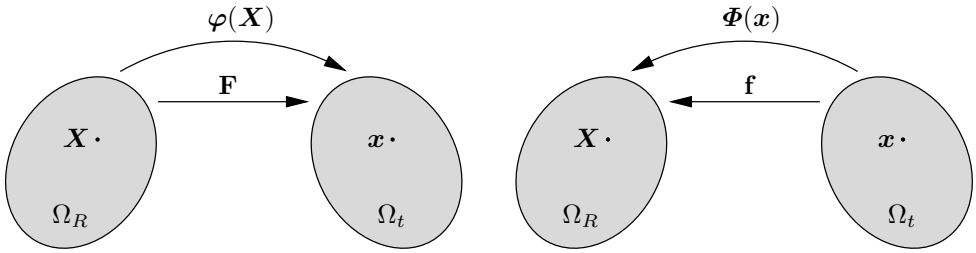

(a) Physical or direct motion problem (b) Material or inverse motion problem

Figure 3.1: Physical and material motion problems

Here, $\boldsymbol{\varphi}$ maps the material particle $\boldsymbol{X}$ from the reference configuration Ω_R to the spatial coordinates $\boldsymbol{x}$ in the deformed configuration Ω_t for any fixed time $t \in I_t$, see Fig. 3.1a. We use in this work for the gradient of a vector field $(\bullet)$ with respect to $\boldsymbol{x}$ and $\boldsymbol{X}$ the notation

$$\operatorname{grad}(\bullet) := \nabla_x(\bullet) \qquad \text{and} \qquad \operatorname{Grad}(\bullet) := \nabla_X(\bullet). \tag{3.2}$$

In the same manner, we use for the divergence operators the notation

$$\operatorname{div}(\bullet) := \nabla_x \cdot (\bullet) \qquad \text{and} \qquad \operatorname{Div}(\bullet) := \nabla_X \cdot (\bullet). \tag{3.3}$$

The deformation gradient, i.e. the tangent map of $\boldsymbol{\varphi}$ from the material tangent space $T_X\Omega_R$ to the spatial tangent space $T_x\Omega_t$ as well as its Jacobian J are given by

$$\mathbf{F} : T_X\Omega_R \to T_x\Omega_t \quad \text{with} \quad \mathbf{F} := \operatorname{Grad} \boldsymbol{\varphi} \quad \text{and} \quad J := \det \mathbf{F}. \tag{3.4}$$

The displacement at a time $t \in I_t$ is the vector field

$$\boldsymbol{u}(\boldsymbol{X}, t) = \boldsymbol{\varphi}(\boldsymbol{X}, t) - \boldsymbol{X}. \tag{3.5}$$

The corresponding displacement gradient is given as

$$\mathbf{H} = \operatorname{Grad} \boldsymbol{u}. \tag{3.6}$$

Furthermore, we assume that the deformation is bijective, sufficiently smooth and that $J > 0$, such that there exists the inverse deformation mapping

$$\boldsymbol{\Phi} : \left\{ \begin{array}{lll} \Omega_t \times I_t & \to & \Omega_R \subset \mathbb{E}^3 \\ (\boldsymbol{x}, t) & \mapsto & \boldsymbol{X} = \boldsymbol{\Phi}(\boldsymbol{x}, t) \end{array} \right. , \tag{3.7}$$

see Fig. 3.1b. The corresponding deformation gradient $\mathbf{f}$ and its Jacobian j are given by

$$\mathbf{f} : T_x\Omega_t \to T_X\Omega_R \quad \text{with} \quad \mathbf{f} := \operatorname{grad} \boldsymbol{\Phi} \quad \text{and} \quad j := \det \mathbf{f}. \tag{3.8}$$

The deformation gradients and Jacobians are related by

$$\mathbf{f} = \mathbf{F}^{-1} \qquad \text{and} \qquad j = J^{-1}. \tag{3.9}$$

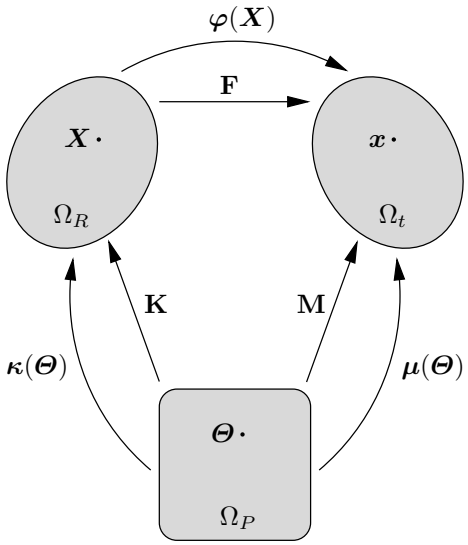

Figure 3.2: Enhanced kinematics

3.1.2 Enhanced kinematics

The above introduced kinematical settings in Ω_R and Ω_t can be enhanced by using the *intrinsic formulation* [82]. In the context of design sensitivity analysis this was proposed in [5,7,9]. Following the intrinsic concept, a given manifold can be described locally using an intrinsic coordinate system defined on an independent continuous parameter space Ω_P with local coordinates $\boldsymbol{\Theta}$. Without going into detail, this leads to two fundamental mappings, a design dependent *local reference placement mapping*

$$\boldsymbol{\kappa} : \left\{ \begin{array}{lcl} \Omega_P \times I_s & \rightarrow & \Omega_R \subset \mathbb{E}^3 \\ (\boldsymbol{\Theta}, s) & \mapsto & \boldsymbol{X} = \boldsymbol{\kappa}(\boldsymbol{\Theta}, s) \end{array} \right. \tag{3.10}$$

and a time dependent *local current placement mapping*

$$\boldsymbol{\mu} : \left\{ \begin{array}{lcl} \Omega_P \times I_t & \rightarrow & \Omega_t \subset \mathbb{E}^3 \\ (\boldsymbol{\Theta}, t) & \mapsto & \boldsymbol{x} = \boldsymbol{\mu}(\boldsymbol{\Theta}, t) \end{array} \right. \tag{3.11}$$

for any fixed time $t \in I_t$ and any design $s \in I_s$, see Fig. 3.2. Here, s is used as a general scalar (time-like) design variable, which parameterizes in an abstract sense the material body in the reference configuration Ω_R, i.e. $\Omega_R = \Omega_R(s)$. The corresponding tangent maps

$$\mathbf{K} : T_\Theta \Omega_P \rightarrow T_X \Omega_R \quad \text{and} \quad \mathbf{M} : T_\Theta \Omega_P \rightarrow T_x \Omega_t \tag{3.12}$$

as well as their Jacobians are given by

$$\mathbf{K} := \mathrm{GRAD}\,\boldsymbol{\kappa} \qquad J_K := \det \mathbf{K} \tag{3.13}$$

$$\mathbf{M} := \mathrm{GRAD}\,\boldsymbol{\mu} \qquad J_M := \det \mathbf{M}, \tag{3.14}$$

where $\mathrm{GRAD}(\bullet) := \nabla_\Theta(\bullet)$. With these mappings, the deformation map $\boldsymbol{\varphi}$ (3.1) and its tangent map can be written in the form

$$\boldsymbol{\varphi} = \boldsymbol{\mu} \circ \boldsymbol{\kappa}^{-1} \quad \text{and} \quad \mathbf{F} = \mathrm{Grad}\,\boldsymbol{\varphi} = \mathbf{M}\mathbf{K}^{-1} \tag{3.15}$$

and for the inverse mapping $\boldsymbol{\Phi}$ (3.7) follows

$$\boldsymbol{\Phi} = \boldsymbol{\kappa} \circ \boldsymbol{\mu}^{-1} \quad \text{and} \quad \mathbf{f} = \mathrm{grad}\,\boldsymbol{\Phi} = \mathbf{K}\mathbf{M}^{-1}, \tag{3.16}$$

respectively. The difference vector between the reference and current placements is the displacement $\boldsymbol{u} = \boldsymbol{x} - \boldsymbol{X}$, which can be written in terms of the local mappings $\boldsymbol{\kappa}$ and $\boldsymbol{\mu}$ as

$$\boldsymbol{u} = \boldsymbol{\mu}(\boldsymbol{\Theta}, t) - \boldsymbol{\kappa}(\boldsymbol{\Theta}, s). \tag{3.17}$$

Overall, $\mathbf{K}, \mathbf{M}$ and $\mathbf{F}$ are used to perform pull back and push forward transformations between Ω_R, Ω_t and Ω_P.

3.1.3 The generalized state and design functions

Within the above introduced kinematical framework different functions can be considered as the *state function*, i.e. the primary unknown of the problem. This can be the deformation $\boldsymbol{\varphi}$ or the displacement field $\boldsymbol{u}$. Furthermore, using the intrinsic formulation also the mapping $\boldsymbol{\mu}$ can be chosen as primary unknown.

Therefore, the *generalized state function* $\boldsymbol{v} \in \mathcal{V}$ is introduced in an abstract sense. The space $\mathcal{V}$ denotes a Hilbert space of states. The state function $\boldsymbol{v}$ can be the deformation $\boldsymbol{\varphi}$, the displacement field $\boldsymbol{u}$ or the local current placement mapping $\boldsymbol{\mu}$ depending on what is chosen as primary unknown.

The local reference placement mapping is parameterized by a time like design parameter s, i.e. $\boldsymbol{X} = \boldsymbol{\kappa}(\boldsymbol{\Theta}, s)$. With this in mind, in an abstract sense a *generalized design function* or *control function* $\boldsymbol{s} \in \mathcal{S}$ is introduced. The space $\mathcal{S}$ denotes a Hilbert space with all admissible design or control functions. Hence, the design function specifies the current reference configuration Ω_R, i.e. $\Omega_R = \Omega_R(\boldsymbol{s})$. The design function $\boldsymbol{s}$ can be the inverse deformation $\boldsymbol{\Phi}(\boldsymbol{x})$ for a given fixed Ω_t or it can be the local reference placement mapping $\boldsymbol{\kappa}$.

With these definitions, a quantity $(\cdot)$, which depends on the state variable $\boldsymbol{v}$ and the design variable $\boldsymbol{s}$ is denoted by $(\cdot)(\boldsymbol{v}, \boldsymbol{s})$. The partial variations of $(\cdot)(\boldsymbol{v}, \boldsymbol{s})$ with respect to $\boldsymbol{v}$ and $\boldsymbol{s}$ are denoted by $(\cdot)'_v$ and $(\cdot)'_s$, respectively. In the same manner, the second and mixed variations are indicated by $(\cdot)''_{vv}$, $(\cdot)''_{ss}$ or $(\cdot)''_{vs}$, see Section 2.2.

Remark 3.1 (Generalized state function vs. deformation and displacement) *The generalized state function $\boldsymbol{v}$ can be the deformation $\boldsymbol{\varphi}$ or the displacement field $\boldsymbol{u}$ depending on what is chosen as primary unknown. For the classical spatial motion problem with a fixed reference configuration Ω_R this distinction is not necessary, because the variations with respect to $\boldsymbol{\varphi}$ and $\boldsymbol{u}$ lead to the same results, i.e. we have $\delta\boldsymbol{\varphi} = \delta\boldsymbol{u}$ for a fixed $\boldsymbol{X}$. For instance, the deformation gradient $\mathbf{F}$ can be written as a function of $\boldsymbol{\varphi}$ or $\boldsymbol{u}$, i.e. $\bar{\mathbf{F}}(\boldsymbol{\varphi}) = \operatorname{Grad}\boldsymbol{\varphi}$ or $\tilde{\mathbf{F}}(\boldsymbol{u}) = \mathbf{I} + \mathbf{H}$. The variations of the deformation gradient $\mathbf{F}$ with respect to $\boldsymbol{\varphi}$ and $\boldsymbol{u}$ yield the same result, but the variations with respect to $\boldsymbol{X}$ are slightly different, see Section 3.2.1. Therefore, it is important to distinguish between $\boldsymbol{\varphi}$ and $\boldsymbol{u}$ for problems where variations of the reference configuration Ω_R are allowed. It is necessary to introduce a generalized state $\boldsymbol{v}$ in order to obtain a general description. Furthermore, the distinction is also important within sensitivity analysis, see Section 4.3.4.*

3.2 Variations of kinematical quantities

Variations of kinematical quantities with respect to changes in the physical and material spaces are considered. The reference configuration depends in an abstract sense on a design or control function $\boldsymbol{s}$. Therefore, the variations with respect to the reference configuration are indicated as $(\cdot)'_s$. The state function can be $\boldsymbol{\varphi}$ or $\boldsymbol{u}$ and $(\cdot)'_\varphi$ and $(\cdot)'_u$ is used, respectively.

Let $\mathcal{V}$ and $\mathcal{S}$ be Sobolev spaces for the state and the design, which are defined as

$$\mathcal{V} := \{\boldsymbol{\eta} \in [W^{1,p}(\Omega_R)]^3 : \boldsymbol{\eta} = \mathbf{0} \text{ on } \Gamma_{\mathrm{D}_u}\}, \tag{3.18}$$

$$\mathcal{S} := \{\boldsymbol{\psi} \in [W^{1,p}(\Omega_t)]^3 : \boldsymbol{\psi} = \mathbf{0} \text{ on } \Gamma_{\mathrm{D}_s}\} \tag{3.19}$$

with $p \geq 2$. Here, Γ_{D_u} denotes the Dirichlet boundary for the state and Γ_{D_s} is the corresponding design boundary. Additionally, some other geometrical or side constraints may be defined for the design function $\boldsymbol{s}$.

3.2.1 Variations of gradients

The variations of the gradients can be easily obtained using the tangent mappings $\mathbf{K}$ and $\mathbf{M}$ from Section 3.1.2. This is based on a multiplicative decomposition of the deformation gradients $\mathbf{F}$ and $\mathbf{f} = \mathbf{F}^{-1}$ using the local mappings $\mathbf{K}$ and $\mathbf{M}$, i.e. by using (3.15) and (3.16), respectively. For instance, $\mathbf{F} = \mathbf{M}\mathbf{K}^{-1}$ and the total variation is given as

$$\delta\mathbf{F} = \delta\mathbf{M}\mathbf{K}^{-1} + \mathbf{M}\delta[\mathbf{K}^{-1}]. \tag{3.20}$$

Using the relation[1] $\delta[\mathbf{K}^{-1}] = -\mathbf{K}^{-1}\delta\mathbf{K}\mathbf{K}^{-1}$ we obtain

$$\delta\mathbf{F} = \delta\mathbf{M}\mathbf{K}^{-1} - \mathbf{M}\mathbf{K}^{-1}\delta\mathbf{K}\mathbf{K}^{-1} = \operatorname{Grad}\delta\boldsymbol{\varphi} - \mathbf{F}\operatorname{Grad}\delta\boldsymbol{\Phi}, \tag{3.21}$$

[1] The variation of an inverse tensor $\mathbf{A}^{-1}$ can be computed using the identity $\mathbf{A}\mathbf{A}^{-1} = \mathbf{I}$. The variation $\delta(\mathbf{A}\mathbf{A}^{-1}) = \delta\mathbf{A}\mathbf{A}^{-1} + \mathbf{A}\delta[\mathbf{A}^{-1}] = \delta\mathbf{I} = \mathbf{0}$ yields $\delta[\mathbf{A}^{-1}] = -\mathbf{A}^{-1}\delta\mathbf{A}\mathbf{A}^{-1}$.

where the partial variations are identified as

$$\delta_{\varphi}\mathbf{F} = \operatorname{Grad}\delta\boldsymbol{\varphi} \qquad \delta_{\Phi}\mathbf{F} = -\mathbf{F}\operatorname{Grad}\delta\boldsymbol{\Phi}. \tag{3.22}$$

A complete list of variations and more details are given in Appendix A.

The deformation gradient $\mathbf{F}$ can be written as a function of $\boldsymbol{\varphi}$ or $\boldsymbol{u}$, i.e. $\bar{\mathbf{F}}(\boldsymbol{\varphi}) = \operatorname{Grad}\boldsymbol{\varphi}$ or $\tilde{\mathbf{F}}(\boldsymbol{u}) = \mathbf{I} + \mathbf{H}$, where $\mathbf{H} = \operatorname{Grad}\boldsymbol{u}$. The total variation of the deformation gradient reads

$$\begin{aligned}\bar{\mathbf{F}}'(\boldsymbol{\varphi}, \delta\boldsymbol{\varphi}, \delta\boldsymbol{\Phi}) &= \operatorname{Grad}\delta\boldsymbol{\varphi} - \mathbf{F}\operatorname{Grad}\delta\boldsymbol{\Phi} \\ &= \operatorname{Grad}\delta\boldsymbol{u} - \mathbf{H}\operatorname{Grad}\delta\boldsymbol{\Phi} \\ &= \tilde{\mathbf{F}}'(\boldsymbol{u}, \delta\boldsymbol{u}, \delta\boldsymbol{\Phi}) = \mathbf{H}'(\boldsymbol{u}, \delta\boldsymbol{u}, \delta\boldsymbol{\Phi})\end{aligned} \tag{3.23}$$

for all $\{\delta\boldsymbol{\varphi},\ \delta\boldsymbol{u}\} \in \mathcal{V}$ and $\delta\boldsymbol{\Phi} \in \mathcal{S}$, whereas the relation $\delta\boldsymbol{x} = \delta\boldsymbol{X} + \delta\boldsymbol{u}$ has been used. Hence, both formulations can be considered. The partial variations are given as $\bar{\mathbf{F}}'_{\varphi} = \operatorname{Grad}\delta\boldsymbol{\varphi}$ and $\bar{\mathbf{F}}'_{s} = -\mathbf{F}\operatorname{Grad}\delta\boldsymbol{\Phi}$ as well as $\tilde{\mathbf{F}}'_{u} = \operatorname{Grad}\delta\boldsymbol{u} = \mathbf{H}'_{u}$ and $\tilde{\mathbf{F}}'_{s} = -\mathbf{H}\operatorname{Grad}\delta\boldsymbol{\Phi} = \mathbf{H}'_{s}$, respectively. The partial variations with respect to $\boldsymbol{s}$ are different but the total variations yield the same results.

Finally, using the generalized state $\boldsymbol{v}$ we obtain

$$\mathbf{F}'(\boldsymbol{v}, \delta\boldsymbol{v}, \delta\boldsymbol{\Phi}) = \operatorname{Grad}\delta\boldsymbol{v} - \operatorname{Grad}\boldsymbol{v}\operatorname{Grad}\delta\boldsymbol{\Phi} \tag{3.24}$$

and hence the partial variations

$$\mathbf{F}'_{v} = \operatorname{Grad}\delta\boldsymbol{v}, \tag{3.25}$$

$$\mathbf{F}'_{s} = -\operatorname{Grad}\boldsymbol{v}\operatorname{Grad}\delta\boldsymbol{\Phi}. \tag{3.26}$$

3.2.2 Variations of strains

In the same manner, the variations of strain measures can be obtained by using the above described technique. The Green-Lagrange strain tensor

$$\mathbf{E} := \frac{1}{2}\left(\mathbf{F}^{T}\mathbf{F} - \mathbf{I}\right) \tag{3.27}$$

is considered within this work. The strain tensor can be expressed in terms of $\boldsymbol{\varphi}$ or $\boldsymbol{u}$. Let $\{\boldsymbol{\eta},\ \boldsymbol{\lambda}\} \in \mathcal{V}$ and $\{\psi,\ \boldsymbol{\chi}\} \in \mathcal{S}$ be admissible variations.

Then, the partial variations of $\mathbf{E}$ with respect to $\boldsymbol{v}$ and $\boldsymbol{s}$ are obtained as

$$\mathbf{E}'_v(\boldsymbol{v},\boldsymbol{\eta}) = \operatorname{sym}\{\mathbf{F}^T \operatorname{Grad}\boldsymbol{\eta}\}, \tag{3.28}$$

$$\mathbf{E}'_s(\boldsymbol{v},\boldsymbol{\psi}) = -\operatorname{sym}\{\mathbf{F}^T \operatorname{Grad}\boldsymbol{v}\ \operatorname{Grad}\boldsymbol{\psi}\}, \tag{3.29}$$

$$\mathbf{E}''_{vs}(\boldsymbol{v},\boldsymbol{\eta},\boldsymbol{\psi}) = -\operatorname{sym}\{\operatorname{Grad}\boldsymbol{\psi}^T\ \operatorname{Grad}\boldsymbol{v}^T \operatorname{Grad}\boldsymbol{\eta} + \mathbf{F}^T \operatorname{Grad}\boldsymbol{\eta}\ \operatorname{Grad}\boldsymbol{\psi}\}, \tag{3.30}$$

$$\mathbf{E}''_{vv}(\boldsymbol{\eta},\boldsymbol{\lambda}) = \operatorname{sym}\{\operatorname{Grad}\boldsymbol{\lambda}^T \operatorname{Grad}\boldsymbol{\eta}\}, \tag{3.31}$$

$$\begin{aligned}\mathbf{E}''_{ss}(\boldsymbol{v},\boldsymbol{\psi},\boldsymbol{\chi}) = \operatorname{sym}\{&\operatorname{Grad}\boldsymbol{\chi}^T \operatorname{Grad}\boldsymbol{v}^T \operatorname{Grad}\boldsymbol{v} \operatorname{Grad}\boldsymbol{\psi}\\ &+ \mathbf{F}^T \operatorname{Grad}\boldsymbol{v} \operatorname{Grad}\boldsymbol{\chi} \operatorname{Grad}\boldsymbol{\psi}\\ &+ \mathbf{F}^T \operatorname{Grad}\boldsymbol{v} \operatorname{Grad}\boldsymbol{\psi} \operatorname{Grad}\boldsymbol{\chi}\}.\end{aligned} \tag{3.32}$$

Note that due to symmetry, it holds true that $\mathbf{E}''_{vs}(\boldsymbol{v},\boldsymbol{\eta},\boldsymbol{\psi}) = \mathbf{E}''_{sv}(\boldsymbol{v},\boldsymbol{\psi},\boldsymbol{\eta})$.

If the deformation $\boldsymbol{\varphi}$ is chosen as unknown, i.e. $\boldsymbol{v} = \boldsymbol{\varphi}$, the strain tensor $\mathbf{E}$ is written in terms of $\boldsymbol{\varphi}$ as $\bar{\mathbf{E}}(\boldsymbol{\varphi}) = \frac{1}{2}(\operatorname{Grad}\boldsymbol{\varphi}^T \operatorname{Grad}\boldsymbol{\varphi} - \mathbf{I})$. The partial variations are given as

$$\bar{\mathbf{E}}'_\varphi(\boldsymbol{\varphi},\boldsymbol{\eta}) = \operatorname{sym}\{\mathbf{F}^T \operatorname{Grad}\boldsymbol{\eta}\}, \tag{3.33}$$

$$\bar{\mathbf{E}}'_s(\boldsymbol{\varphi},\boldsymbol{\psi}) = -\operatorname{sym}\{\mathbf{F}^T\mathbf{F}\ \operatorname{Grad}\boldsymbol{\psi}\}, \tag{3.34}$$

$$\bar{\mathbf{E}}''_{\varphi s}(\boldsymbol{\varphi},\boldsymbol{\eta},\boldsymbol{\psi}) = -\operatorname{sym}\{\operatorname{Grad}\boldsymbol{\psi}^T\,\mathbf{F}^T \operatorname{Grad}\boldsymbol{\eta} + \mathbf{F}^T \operatorname{Grad}\boldsymbol{\eta}\ \operatorname{Grad}\boldsymbol{\psi}\}, \tag{3.35}$$

$$\bar{\mathbf{E}}''_{\varphi\varphi}(\boldsymbol{\eta},\boldsymbol{\lambda}) = \operatorname{sym}\{\operatorname{Grad}\boldsymbol{\lambda}^T \operatorname{Grad}\boldsymbol{\eta}\}, \tag{3.36}$$

$$\begin{aligned}\bar{\mathbf{E}}''_{ss}(\boldsymbol{\varphi},\boldsymbol{\psi},\boldsymbol{\chi}) = \operatorname{sym}\{&\operatorname{Grad}\boldsymbol{\chi}^T\mathbf{F}^T\mathbf{F} \operatorname{Grad}\boldsymbol{\psi} + \mathbf{F}^T\mathbf{F} \operatorname{Grad}\boldsymbol{\chi} \operatorname{Grad}\boldsymbol{\psi}\\ &+ \mathbf{F}^T\mathbf{F} \operatorname{Grad}\boldsymbol{\psi} \operatorname{Grad}\boldsymbol{\chi}\}.\end{aligned} \tag{3.37}$$

On the other hand, if the displacement field $\boldsymbol{u}$ is chosen as unknown, i.e. $\boldsymbol{v} = \boldsymbol{u}$, the strain tensor $\mathbf{E}$ is written in terms of $\boldsymbol{u}$ in form of $\tilde{\mathbf{E}}(\boldsymbol{u}) = \frac{1}{2}((\mathbf{I} + \operatorname{Grad}\boldsymbol{u})^T(\mathbf{I} + \operatorname{Grad}\boldsymbol{u}) - \mathbf{I})$. Finally, the corresponding partial variations are obtained as

$$\tilde{\mathbf{E}}'_u(\boldsymbol{u},\boldsymbol{\eta}) = \operatorname{sym}\{\mathbf{F}^T \operatorname{Grad}\boldsymbol{\eta}\}, \tag{3.38}$$

$$\tilde{\mathbf{E}}'_s(\boldsymbol{u},\boldsymbol{\psi}) = -\operatorname{sym}\{\mathbf{F}^T\mathbf{H}\ \operatorname{Grad}\boldsymbol{\psi}\}, \tag{3.39}$$

$$\tilde{\mathbf{E}}''_{us}(\boldsymbol{u},\boldsymbol{\eta},\boldsymbol{\psi}) = -\operatorname{sym}\{\operatorname{Grad}\boldsymbol{\psi}^T\,\mathbf{H}^T \operatorname{Grad}\boldsymbol{\eta} + \mathbf{F}^T \operatorname{Grad}\boldsymbol{\eta}\ \operatorname{Grad}\boldsymbol{\psi}\}, \tag{3.40}$$

$$\tilde{\mathbf{E}}''_{uu}(\boldsymbol{\eta},\boldsymbol{\lambda}) = \operatorname{sym}\{\operatorname{Grad}\boldsymbol{\lambda}^T \operatorname{Grad}\boldsymbol{\eta}\}, \tag{3.41}$$

$$\begin{aligned}\tilde{\mathbf{E}}''_{ss}(\boldsymbol{u},\boldsymbol{\psi},\boldsymbol{\chi}) = \operatorname{sym}\{&\operatorname{Grad}\boldsymbol{\chi}^T\mathbf{H}^T\mathbf{H} \operatorname{Grad}\boldsymbol{\psi} + \mathbf{F}^T\mathbf{H} \operatorname{Grad}\boldsymbol{\chi} \operatorname{Grad}\boldsymbol{\psi}\\ &+ \mathbf{F}^T\mathbf{H} \operatorname{Grad}\boldsymbol{\psi} \operatorname{Grad}\boldsymbol{\chi}\},\end{aligned} \tag{3.42}$$

where $\mathbf{H} = \operatorname{Grad} \boldsymbol{u}$. The partial variations with respect to $\boldsymbol{u}$ and $\boldsymbol{\varphi}$ yield the same results, regardless of which is chosen as unknown, i.e.

$$\bar{\mathbf{E}}'_{\varphi} = \tilde{\mathbf{E}}'_{u} \qquad \text{and} \qquad \bar{\mathbf{E}}''_{\varphi\varphi} = \tilde{\mathbf{E}}''_{uu}. \tag{3.43}$$

But the partial variations with respect to $\boldsymbol{s}$ are different, i.e.

$$\bar{\mathbf{E}}'_{s} \neq \tilde{\mathbf{E}}'_{s} \qquad \text{and} \qquad \bar{\mathbf{E}}''_{ss} \neq \tilde{\mathbf{E}}''_{ss} \qquad \text{and} \qquad \bar{\mathbf{E}}''_{\varphi s} \neq \tilde{\mathbf{E}}''_{us}. \tag{3.44}$$

In the formulations with respect to $\boldsymbol{\varphi}$, the displacement gradient $\mathbf{H}$ is replaced by $\mathbf{F}$. But it can be easily proved that the total variations of both descriptions are the same, i.e.

$$\bar{\mathbf{E}}' = \bar{\mathbf{E}}'_{\varphi} + \bar{\mathbf{E}}'_{s} = \tilde{\mathbf{E}}'_{u} + \tilde{\mathbf{E}}'_{s} = \tilde{\mathbf{E}}'. \tag{3.45}$$

This is based on the same arguments as shown for the deformation gradient in (3.23). This demonstrates that the introduction of the generalized state $\boldsymbol{v}$ is useful, because the description in $\boldsymbol{\varphi}$ or $\boldsymbol{u}$ can be directly obtained from the formulation in $\boldsymbol{v}$.

In same manner, higher-order variations of $\mathbf{E}$ can be derived. A complete list is given in Appendix A.2.

3.3 Variations of energy terms

Variations of energy terms with respect to the state and the design are required within this work. A hyperelastic material is considered, i.e. it is assumed that a strain energy function W_R exists. Let C be the internal energy of a hyperelastic body. The energy can be written in terms of $\boldsymbol{\varphi}$ or the inverse deformation $\boldsymbol{\Phi}$, i.e.

$$C(\boldsymbol{\varphi}) = \int_{\Omega_R} W_R(\mathbf{F}) \, \mathrm{d}\Omega \quad \text{or} \quad \hat{C}(\boldsymbol{\Phi}) = \int_{\Omega_t} W_t(\mathbf{f}) \, \mathrm{d}\Omega, \tag{3.46}$$

where $W_R(\mathbf{F})$ and $W_t(\mathbf{f}) = j(\mathbf{f}) \, W_R$ are the strain energy functions in Ω_R and Ω_t, respectively. Both functionals express the same physical quantity, i.e. $C(\boldsymbol{\varphi}) = \hat{C}(\boldsymbol{\Phi})$. The partial variations are given as

$$C'_{\varphi} = \int_{\Omega_R} \mathbf{P} : \operatorname{Grad} \delta\boldsymbol{\varphi} \, \mathrm{d}\Omega = \int_{\Omega_t} \boldsymbol{\sigma} : \operatorname{grad} \delta\boldsymbol{\varphi} \, \mathrm{d}\Omega, \tag{3.47}$$

$$\hat{C}'_{s} = \int_{\Omega_t} \mathbf{p} : \operatorname{grad} \delta\boldsymbol{\Phi} \, \mathrm{d}\Omega = \int_{\Omega_R} \bar{\boldsymbol{\Sigma}} : \operatorname{Grad} \delta\boldsymbol{\Phi} \, \mathrm{d}\Omega, \tag{3.48}$$

where

$$\mathbf{P} := \frac{\partial W_R}{\partial \mathbf{F}} \qquad \text{and} \qquad \mathbf{p} := \frac{\partial W_t}{\partial \mathbf{f}}. \tag{3.49}$$

Here, $\mathbf{P}$ denotes the first Piola-Kirchhoff stress tensor and $\mathbf{p}$ is the counterpart of the inverse motion problem. Furthermore, $\boldsymbol{\sigma} = J^{-1}\mathbf{P}\mathbf{F}^T$ is the Cauchy stress tensor and

$$\bar{\boldsymbol{\Sigma}} := W_R\mathbf{I} - \mathbf{F}^T\frac{\partial W_R}{\partial \mathbf{F}} = W_R\mathbf{I} - \mathbf{F}^T\mathbf{P} \tag{3.50}$$

is the well-known energy momentum or Eshelby tensor [39, 40], which is the Piola transformation of the two-point tensor $\mathbf{p}$, i.e. $\bar{\boldsymbol{\Sigma}} = j^{-1}\mathbf{p}\mathbf{f}^T$. For a detailed discussion about the direct and inverse problems and their duality see e.g. [26, 35, 57, 61, 74, 93, 96].

The total variation of the internal energy can be written as

$$C' = \int_{\Omega_R} [\,\mathbf{P} : \operatorname{Grad}\delta\boldsymbol{\varphi} + \bar{\boldsymbol{\Sigma}} : \operatorname{Grad}\delta\boldsymbol{\Phi}\,]\,\mathrm{d}\Omega \tag{3.51}$$

$$= \int_{\Omega_R} [\,\mathbf{P} : \operatorname{Grad}\delta\boldsymbol{u} + \tilde{\boldsymbol{\Sigma}} : \operatorname{Grad}\delta\boldsymbol{\Phi}\,]\,\mathrm{d}\Omega, \tag{3.52}$$

whereas $\delta\boldsymbol{x} = \delta\boldsymbol{X} + \delta\boldsymbol{u}$ has been used. Here, we inserted the displacement $\boldsymbol{u}$ in (3.50) and obtained an energy momentum tensor in terms of the displacement field, i.e.

$$\tilde{\boldsymbol{\Sigma}} := W_R\mathbf{I} - \mathbf{H}^T\frac{\partial W_R}{\partial \mathbf{F}} = W_R\mathbf{I} - \mathbf{H}^T\mathbf{P}, \tag{3.53}$$

which is a modified version of the tensor $\bar{\boldsymbol{\Sigma}}$. These tensors are related by

$$\bar{\boldsymbol{\Sigma}} = \tilde{\boldsymbol{\Sigma}} - \mathbf{P}. \tag{3.54}$$

Both Eq. 3.51 and Eq. 3.52 express the same amount of energy change, i.e. the same total change of the internal energy due to variations $\delta\boldsymbol{X}$ and $\delta\boldsymbol{x}$ or $\delta\boldsymbol{u}$. The formulation in $\boldsymbol{u}$ is used in fracture mechanics and is called Newton-Eshelby tensor, see e.g. [90, 96].

Therefore, in terms of the generalized state $\boldsymbol{v}$ we can introduce the *generalized energy-momentum tensor* in form of

$$\boldsymbol{\Sigma}(\boldsymbol{v}) := W_R\mathbf{I} - \operatorname{Grad}\boldsymbol{v}^T\frac{\partial W_R}{\partial \mathbf{F}} = W_R\mathbf{I} - \operatorname{Grad}\boldsymbol{v}^T\mathbf{P}. \tag{3.55}$$

Let $\boldsymbol{\eta} \in \mathcal{V}$ and $\boldsymbol{\psi} \in \mathcal{S}$ be admissible variations. The variations of a functional $F = \int_{\Omega_R}(\cdot)\,\mathrm{d}\Omega$ with respect to $\boldsymbol{v} \in \mathcal{V}$ and $\boldsymbol{s} \in \mathcal{S}$ in terms of the reference configuration are given as

$$F'_v(\boldsymbol{v},\boldsymbol{\eta}) = \int_{\Omega_R}(\cdot)'_v(\boldsymbol{v},\boldsymbol{\eta})\,\mathrm{d}\Omega,$$

$$F'_s(\boldsymbol{v},\boldsymbol{\psi}) = \int_{\Omega_R}(\cdot)'_s(\boldsymbol{v},\boldsymbol{\psi}) + (\cdot)\operatorname{Div}\boldsymbol{\psi}\,d\Omega = \int_{\Omega_R}(\cdot)'_s(\boldsymbol{v},\boldsymbol{\psi}) + (\cdot)\mathbf{I} : \operatorname{Grad}\boldsymbol{\psi}\,\mathrm{d}\Omega.$$

For the internal energy (3.46) we have

$$C'_v(\boldsymbol{v},\boldsymbol{\eta}) = \int_{\Omega_R} \mathbf{P} : \operatorname{Grad}\boldsymbol{\eta}\,\mathrm{d}\Omega, \tag{3.56}$$

$$\begin{aligned} C'_s(\boldsymbol{v},\boldsymbol{\psi}) &= \int_{\Omega_R} \boldsymbol{\Sigma} : \operatorname{Grad}\boldsymbol{\psi}\,d\Omega \\ &= \int_{\Omega_R} -\operatorname{Grad}\boldsymbol{v}^T\mathbf{P} : \operatorname{Grad}\boldsymbol{\psi} + W_R\mathbf{I} : \operatorname{Grad}\boldsymbol{\psi}\,\mathrm{d}\Omega. \end{aligned} \tag{3.57}$$

Hence, the partial variations of the strain energy W_R with respect to $\boldsymbol{v}$ and $\boldsymbol{s}$ are identified as

$$\begin{aligned} (W_R)'_v(\boldsymbol{v},\boldsymbol{\eta}) &= \frac{\partial W_R}{\partial \mathbf{F}} : \mathbf{F}'_v(\boldsymbol{v},\boldsymbol{\eta}) = \mathbf{P} : \mathbf{F}'_v(\boldsymbol{v},\boldsymbol{\eta}) = \mathbf{P} : \operatorname{Grad}\boldsymbol{\eta} \\ &= \mathbf{F}\mathbf{S} : \operatorname{Grad}\boldsymbol{\eta} = \mathbf{S} : \mathbf{F}^T \operatorname{Grad}\boldsymbol{\eta} \\ &= \mathbf{S} : \mathbf{E}'_v(\boldsymbol{v},\boldsymbol{\eta}) \end{aligned} \tag{3.58}$$

$$\begin{aligned} (W_R)'_s(\boldsymbol{v},\boldsymbol{\psi}) &= \frac{\partial W_R}{\partial \mathbf{F}} : \mathbf{F}'_s(\boldsymbol{v},\boldsymbol{\psi}) = \mathbf{P} : \mathbf{F}'_s(\boldsymbol{v},\boldsymbol{\psi}) = -\mathbf{P} : \operatorname{Grad}\boldsymbol{v}\operatorname{Grad}\boldsymbol{\psi} \\ &= -\mathbf{F}\mathbf{S} : \operatorname{Grad}\boldsymbol{v}\operatorname{Grad}\boldsymbol{\psi} = -\mathbf{S} : \mathbf{F}^T \operatorname{Grad}\boldsymbol{v}\operatorname{Grad}\boldsymbol{\psi} \\ &= \mathbf{S} : \mathbf{E}'_s(\boldsymbol{v},\boldsymbol{\psi}) \end{aligned} \tag{3.59}$$

where

$$\mathbf{S} := \mathbf{F}^{-1}\mathbf{P} = J\,\mathbf{F}^{-1}\boldsymbol{\sigma}\mathbf{F}^{-T} \tag{3.60}$$

is the symmetric second Piola-Kirchhoff stress tensor.

Finally, the variations of the internal energy in (3.56) and (3.57) can be equivalently expressed in terms of $\mathbf{S}$ and the partial variations of $\mathbf{E}$, i.e.

$$C'_v(\boldsymbol{v},\boldsymbol{\eta}) = \int_{\Omega_R} \mathbf{S} : \mathbf{E}'_v(\boldsymbol{v},\boldsymbol{\eta})\,\mathrm{d}\Omega, \tag{3.61}$$

$$C'_s(\boldsymbol{v},\boldsymbol{\psi}) = \int_{\Omega_R} \mathbf{S} : \mathbf{E}'_s(\boldsymbol{v},\boldsymbol{\psi}) + W_R\mathbf{I} : \operatorname{Grad}\boldsymbol{\psi}\,\mathrm{d}\Omega. \tag{3.62}$$

3.4 Variations of stresses

In the above section the first and second Piola-Kirchhoff stress tensors $\mathbf{P}$ and $\mathbf{S}$ have been introduced. The variations of both stress tensors with respect to $\boldsymbol{v}$ and $\boldsymbol{s}$ are given by

$$\mathbf{P}'_v(\boldsymbol{v},\boldsymbol{\eta}) = \frac{\partial \mathbf{P}}{\partial \mathbf{F}} : \mathbf{F}'_v(\boldsymbol{v},\boldsymbol{\eta}) = \mathbb{A} : \mathbf{F}'_v(\boldsymbol{v},\boldsymbol{\eta}) = \mathbb{A} : \operatorname{Grad}\boldsymbol{\eta}, \tag{3.63}$$

$$\mathbf{P}'_s(\boldsymbol{v},\boldsymbol{\psi}) = \frac{\partial \mathbf{P}}{\partial \mathbf{F}} : \mathbf{F}'_s(\boldsymbol{v},\boldsymbol{\psi}) = \mathbb{A} : \mathbf{F}'_s(\boldsymbol{v},\boldsymbol{\psi}) = -\mathbb{A} : \operatorname{Grad}\boldsymbol{v}\operatorname{Grad}\boldsymbol{\psi}, \tag{3.64}$$

$$\mathbf{S}'_v(\boldsymbol{v},\boldsymbol{\eta}) = \frac{\partial \mathbf{S}}{\partial \mathbf{E}} : \mathbf{E}'_v(\boldsymbol{v},\boldsymbol{\eta}) = \mathbb{C} : \mathbf{E}'_v(\boldsymbol{v},\boldsymbol{\eta}) = \mathbb{C} : \mathbf{F}^T \operatorname{Grad} \boldsymbol{\eta}, \tag{3.65}$$

$$\mathbf{S}'_s(\boldsymbol{v},\boldsymbol{\psi}) = \frac{\partial \mathbf{S}}{\partial \mathbf{E}} : \mathbf{E}'_s(\boldsymbol{v},\boldsymbol{\psi}) = \mathbb{C} : \mathbf{E}'_s(\boldsymbol{v},\boldsymbol{\psi}) = -\mathbb{C} : \mathbf{F}^T \operatorname{Grad} \boldsymbol{v} \operatorname{Grad} \boldsymbol{\psi}, \tag{3.66}$$

where $\mathbb{A}$ and $\mathbb{C}$ are the so-called first and the second elasticity tensor, respectively, see e.g. [64]. Both fourth-order tensors are given as usual in form of

$$\mathbb{A} := \frac{\partial \mathbf{P}}{\partial \mathbf{F}} = \frac{\partial^2 W_R}{\partial \mathbf{F}\, \partial \mathbf{F}} \quad \text{and} \quad \mathbb{C} := \frac{\partial \mathbf{S}}{\partial \mathbf{E}} = \frac{\partial^2 W_R}{\partial \mathbf{E}\, \partial \mathbf{E}}. \tag{3.67}$$

Within this work also higher-order variations with respect to changes in the physical and material spaces are considered. Furthermore, all variational formulations in the following chapters are written in terms of the second Piola-Kirchhoff stress tensor $\mathbf{S}$ and the variations of the strain tensor $\mathbf{E}$ instead of $\mathbf{P}$ and $\mathbf{F}$. Therefore, only higher-order variations with respect to $\mathbf{S}$ are considered. The same can be performed in a straightforward manner for higher-order variations of $\mathbf{P}$.

To achieve this, the variations of $\mathbb{C}$ with respect to $\boldsymbol{v}$ and $\boldsymbol{s}$ are required. These terms are obtained in form of

$$\mathbb{C}'_v(\boldsymbol{v},\boldsymbol{\eta}) = \frac{\partial \mathbb{C}}{\partial \mathbf{E}} : \mathbf{E}'_v(\boldsymbol{v},\boldsymbol{\eta}) = \boldsymbol{\mathcal{D}} : \mathbf{E}'_v(\boldsymbol{v},\boldsymbol{\eta}), \tag{3.68}$$

$$\mathbb{C}'_s(\boldsymbol{v},\boldsymbol{\psi}) = \frac{\partial \mathbb{C}}{\partial \mathbf{E}} : \mathbf{E}'_s(\boldsymbol{v},\boldsymbol{\psi}) = \boldsymbol{\mathcal{D}} : \mathbf{E}'_s(\boldsymbol{v},\boldsymbol{\psi}), \tag{3.69}$$

where the sixth-order tensor $\boldsymbol{\mathcal{D}}$ is introduced as

$$\boldsymbol{\mathcal{D}} := \frac{\partial \mathbb{C}}{\partial \mathbf{E}}. \tag{3.70}$$

Furthermore, the variation of $\boldsymbol{\mathcal{D}}$ results in

$$\boldsymbol{\mathcal{D}}'_v(\boldsymbol{v},\boldsymbol{\eta}) = \frac{\partial \boldsymbol{\mathcal{D}}}{\partial \mathbf{E}} : \mathbf{E}'_v(\boldsymbol{v},\boldsymbol{\eta}) = \boldsymbol{\mathfrak{E}} : \mathbf{E}'_v(\boldsymbol{v},\boldsymbol{\eta}), \tag{3.71}$$

$$\boldsymbol{\mathcal{D}}'_s(\boldsymbol{v},\boldsymbol{\psi}) = \frac{\partial \boldsymbol{\mathcal{D}}}{\partial \mathbf{E}} : \mathbf{E}'_s(\boldsymbol{v},\boldsymbol{\psi}) = \boldsymbol{\mathfrak{E}} : \mathbf{E}'_s(\boldsymbol{v},\boldsymbol{\psi}), \tag{3.72}$$

where the eighth-order tensor $\boldsymbol{\mathfrak{E}}$ is defined by

$$\boldsymbol{\mathfrak{E}} := \frac{\partial \boldsymbol{\mathcal{D}}}{\partial \mathbf{E}}. \tag{3.73}$$

Finally, using the above variations of $\mathbb{C}$ the second and mixed variations of $\mathbf{S}$ are given by

$$\mathbf{S}''_{vv}(\boldsymbol{v},\boldsymbol{\eta},\boldsymbol{\lambda}) = \mathbb{C} : \mathbf{E}''_{vv}(\boldsymbol{\eta},\boldsymbol{\lambda}) + \mathbf{E}'_v(\boldsymbol{v},\boldsymbol{\eta}) : \boldsymbol{\mathcal{D}} : \mathbf{E}'_v(\boldsymbol{v},\boldsymbol{\lambda}), \tag{3.74}$$

$$\mathbf{S}''_{ss}(\boldsymbol{v},\boldsymbol{\psi},\boldsymbol{\chi}) = \mathbb{C} : \mathbf{E}''_{ss}(\boldsymbol{v},\boldsymbol{\psi},\boldsymbol{\chi}) + \mathbf{E}'_s(\boldsymbol{v},\boldsymbol{\psi}) : \boldsymbol{\mathcal{D}} : \mathbf{E}'_s(\boldsymbol{v},\boldsymbol{\chi}), \tag{3.75}$$

$$\mathbf{S}''_{vs}(\boldsymbol{v},\boldsymbol{\eta},\boldsymbol{\psi}) = \mathbb{C} : \mathbf{E}''_{vs}(\boldsymbol{v},\boldsymbol{\eta},\boldsymbol{\psi}) + \mathbf{E}'_v(\boldsymbol{v},\boldsymbol{\eta}) : \boldsymbol{\mathcal{D}} : \mathbf{E}'_s(\boldsymbol{v},\boldsymbol{\psi}), \tag{3.76}$$

$$\mathbf{S}''_{sv}(\boldsymbol{v},\boldsymbol{\psi},\boldsymbol{\eta}) = \mathbb{C} : \mathbf{E}''_{sv}(\boldsymbol{v},\boldsymbol{\psi},\boldsymbol{\eta}) + \mathbf{E}'_s(\boldsymbol{v},\boldsymbol{\psi}) : \boldsymbol{\mathcal{D}} : \mathbf{E}'_v(\boldsymbol{v},\boldsymbol{\eta}). \tag{3.77}$$

Note that due to symmetry $\mathbf{S}''_{sv}(\boldsymbol{v},\boldsymbol{\psi},\boldsymbol{\eta}) = \mathbf{S}''_{vs}(\boldsymbol{v},\boldsymbol{\eta},\boldsymbol{\psi})$. Furthermore, variations of $\mathbf{S}$ up to third-order are required. For instance, the variation $\mathbf{S}'''_{vvs}$ reads

$$\begin{aligned}\mathbf{S}'''_{vvs}(\boldsymbol{v},\boldsymbol{\eta},\boldsymbol{\lambda},\boldsymbol{\psi}) = \mathbb{C} : \mathbf{E}'''_{vvs}(\boldsymbol{\eta},\boldsymbol{\lambda},\boldsymbol{\psi}) + \mathbf{E}''_{vv}(\boldsymbol{\eta},\boldsymbol{\lambda}) : \boldsymbol{\mathcal{D}} : \mathbf{E}'_{s}(\boldsymbol{v},\boldsymbol{\psi}) \\ + \mathbf{E}''_{vs}(\boldsymbol{v},\boldsymbol{\eta},\boldsymbol{\psi}) : \boldsymbol{\mathcal{D}} : \mathbf{E}'_{v}(\boldsymbol{v},\boldsymbol{\lambda}) + \mathbf{E}'_{v}(\boldsymbol{v},\boldsymbol{\eta}) : \boldsymbol{\mathcal{D}} : \mathbf{E}''_{vs}(\boldsymbol{v},\boldsymbol{\lambda},\boldsymbol{\psi}) \\ + \mathbf{E}'_{v}(\boldsymbol{v},\boldsymbol{\eta}) : \boldsymbol{\mathfrak{E}} : \mathbf{E}'_{s}(\boldsymbol{v},\boldsymbol{\psi}) : \mathbf{E}'_{v}(\boldsymbol{v},\boldsymbol{\lambda}),\end{aligned} \tag{3.78}$$

where $\mathbf{E}'''_{vvs}$ is given in (A.34). Different other higher-order variations of $\mathbf{S}$ can be performed in the same way.

Explicit specifications of $\mathbf{P}$, $\mathbf{S}$, $\mathbb{C}$ and $\mathbb{A}$ as well as the non-standard tensors $\boldsymbol{\mathcal{D}}$ and $\boldsymbol{\mathfrak{E}}$ for a Neo-Hookean material are given in Appendix B.1.

Chapter 4

Structural and sensitivity analysis of the primal problem

The present chapter deals with variational balance laws and variational sensitivity analysis in the physical and material spaces for the primal problem. The balance laws are derived from an energy functional. Sensitivity relations for the primal physical and material problems are investigated, which are based on an invariant requirement of the considered variational problem. Furthermore, explicit formulations for the complete variational and discrete relations are derived.

4.1 Introduction

Variational methods are a common approach to derive balance laws in elasticity. The classical physical residual is given as the first variation of the energy functional of the primal problem with respect to the deformation, see e.g. [64]. The variation of the energy with respect to configurational changes leads to the material residual or weak form of the configurational or material force equilibrium, see for instance the monographs [48, 60, 74]. In the context of *Arbitrary Lagrangian-Eulerian* (ALE) formulations this was investigated for instance in [2, 61].

The variational approach is an elegant way to express a mathematical physical theory, which does not involve dissipative processes. But configurational variations are not restricted to elastic problems and variational approaches. Inelastic problems play an important role in many fields, e.g. elastic-plastic fracture mechanics, see e.g. [97] for an overview of different approaches and applications. In this work a pure variational setting for elasticity is considered. The extension to inelastic problems is addressed to future work.

In addition, the energy functional is an interesting objective functional in structural optimization, e.g. shape and topology optimization [14,32]. The minimization of the energy is directly related to the minimization of the compliance of the system or equivalently to the maximization of the stiffness. In this context, it is of interest to study the sensitivities of the governing variational equations.

Some parts of this chapter are published in [66, 69].

4.2 Energy minimization and variational balance laws

4.2.1 The energy functional

The model problem of nonlinear elasticity is considered and the attention is restricted to hyperelastic materials. Let $E(\boldsymbol{v}, \boldsymbol{s})$ be the total potential energy of a homogeneous elastic body. The energy depends on the *generalized state function* $\boldsymbol{v} \in \mathcal{V}$ and on a *generalized design* or *control function* $\boldsymbol{s} \in \mathcal{S}$, which specifies in an abstract sense the current reference configuration Ω_R, i.e. $\Omega_R = \Omega_R(\boldsymbol{s})$. The state function $\boldsymbol{v}$ can be the deformation $\boldsymbol{\varphi}$ or the displacement field $\boldsymbol{u}$ depending on what is chosen as primary unknown. The space $\mathcal{V}$ denotes the usual Sobolev space of states and $\mathcal{S}$ a Sobolev space with all admissible design functions. The total potential energy of the primal problem is given by

$$E(\boldsymbol{v}, \boldsymbol{s}) := C(\boldsymbol{v}, \boldsymbol{s}) - F(\boldsymbol{s}; \boldsymbol{v}), \tag{4.1}$$

where $C(\boldsymbol{v}, \boldsymbol{s})$ denotes the internal energy (3.46) and $F(\boldsymbol{s}; \cdot)$ is a functional associated with the external potential, i.e.

$$C(\boldsymbol{v}, \boldsymbol{s}) := \int_{\Omega_R} W_R \, \mathrm{d}\Omega \tag{4.2}$$

$$F(\boldsymbol{s}; \boldsymbol{v}) := \int_{\Omega_R} \boldsymbol{b}_R \cdot \boldsymbol{v} \, \mathrm{d}\Omega + \int_{\Gamma_\mathrm{N}} \bar{\boldsymbol{t}}_R \cdot \boldsymbol{v} \, \mathrm{d}\Gamma. \tag{4.3}$$

Here, $\boldsymbol{b}_R$ are physical body forces per unit volume in the reference configuration and $\bar{\boldsymbol{t}}_R$ are prescribed tractions imposed on the Neumann boundary Γ_N. Furthermore, we assume that $\boldsymbol{v} = \boldsymbol{0}$ on Γ_D.

The functional $F(\boldsymbol{s}; \boldsymbol{v})$ is linear in $\boldsymbol{v}$ but nonlinear in $\boldsymbol{s}$. This is indicated by the semicolon, i.e. all arguments right from the semicolon are linear. Furthermore, $C(\boldsymbol{v}, \boldsymbol{s})$ is nonlinear in $\boldsymbol{v}$ and $\boldsymbol{s}$.

4.2.2 The primal physical and material residuals

We consider the minimization of the primal energy with respect to $\boldsymbol{v}$ and $\boldsymbol{s}$. This ends in the following minimization problem.

Problem 4.1 *Find $\{\boldsymbol{v}, \boldsymbol{s}\} \in \mathcal{V} \times \mathcal{S}$ such that the primal energy functional (4.1) is minimized, i.e.*

$$E(\boldsymbol{v}, \boldsymbol{s}) = \min_{\{\boldsymbol{p}, \boldsymbol{r}\} \in \mathcal{V} \times \mathcal{S}} E(\boldsymbol{p}, \boldsymbol{r}). \tag{4.4}$$

The first-order optimality condition reads

$$E' = E'_v(\boldsymbol{v}, \boldsymbol{s})(\boldsymbol{\eta}) + E'_s(\boldsymbol{v}, \boldsymbol{s})(\boldsymbol{\psi}) = 0. \tag{4.5}$$

We assume that $\boldsymbol{\eta} \in \mathcal{V}$ and $\boldsymbol{\psi} \in \mathcal{S}$ are independent variations. Then, we have to solve the following variational problem. Find $\{\boldsymbol{v}, \boldsymbol{s}\} \in \mathcal{V} \times \mathcal{S}$ such that

$$\left\{ \begin{array}{c} E'_v(\boldsymbol{v}, \boldsymbol{s})(\boldsymbol{\eta}) \\ E'_s(\boldsymbol{v}, \boldsymbol{s})(\boldsymbol{\psi}) \end{array} \right\} = \left\{ \begin{array}{c} R(\boldsymbol{v}, \boldsymbol{s}; \boldsymbol{\eta}) \\ G(\boldsymbol{v}, \boldsymbol{s}; \boldsymbol{\psi}) \end{array} \right\} = \boldsymbol{0} \qquad \forall \{\boldsymbol{\eta}, \boldsymbol{\psi}\} \in \mathcal{V} \times \mathcal{S}. \tag{4.6}$$

The partial variation of E with respect to $\boldsymbol{v}$ leads to the *primal physical residual* $R : \mathcal{V} \to \mathbb{R}$, which is given by

$$R(\boldsymbol{v}, \boldsymbol{s}; \boldsymbol{\eta}) := E'_v(\boldsymbol{v}, \boldsymbol{s})(\boldsymbol{\eta}) = a(\boldsymbol{v}, \boldsymbol{s}; \boldsymbol{\eta}) - F(\boldsymbol{s}; \boldsymbol{\eta}). \tag{4.7}$$

In the same manner, variation with respect to changes in the design $\boldsymbol{s}$ yields the *primal material residual* $G : \mathcal{S} \to \mathbb{R}$, which is given as

$$G(\boldsymbol{v}, \boldsymbol{s}; \boldsymbol{\psi}) := E'_s(\boldsymbol{v}, \boldsymbol{s})(\boldsymbol{\psi}) = b(\boldsymbol{v}, \boldsymbol{s}; \boldsymbol{\psi}) - F'_s(\boldsymbol{s}; \boldsymbol{v}, \boldsymbol{\psi}). \tag{4.8}$$

The semilinear forms $a(\boldsymbol{v}, \boldsymbol{s}; \boldsymbol{\eta})$ and $b(\boldsymbol{v}, \boldsymbol{s}; \boldsymbol{\psi})$ contain the partial variations of the internal energy with respect to $\boldsymbol{v}$ and $\boldsymbol{s}$, i.e.

$$a(\boldsymbol{v}, \boldsymbol{s}; \boldsymbol{\eta}) := C'_v(\boldsymbol{v}, \boldsymbol{s}; \boldsymbol{\eta}), \tag{4.9}$$

$$b(\boldsymbol{v}, \boldsymbol{s}; \boldsymbol{\psi}) := C'_s(\boldsymbol{v}, \boldsymbol{s}; \boldsymbol{\psi}), \tag{4.10}$$

where $C'_v(\boldsymbol{v}, \boldsymbol{s}; \boldsymbol{\eta})$ and $C'_s(\boldsymbol{v}, \boldsymbol{s}; \boldsymbol{\psi})$ are given in (3.61) and (3.62), respectively.

Remark 4.1 *The material residual is also referred to as the weak form of the material or configurational force equilibrium as well as the weak form of the pseudo-momentum equation [48, 60, 74]. In the case of a homogeneous elastic body the material residual is the weak form of the inverse deformation problem. It should be noted, that the material residual can be the weak form of the direct deformation problem when the role of the spatial and material coordinates are interchanged. On the other hand, the inverse deformation problem and its weak form can be obtained by a re-parametrization of the direct deformation problem in terms of the inverse deformation $\boldsymbol{\Phi}$ [44, 45]. For a detailed discussion about the direct and inverse deformation problem and its duality see for instance [26, 57, 61, 93, 96].*

4.3 Variational sensitivity analysis

Variational design sensitivity analysis is a branch of structural optimization, e.g. shape or topology optimization, see e.g. [27, 28, 58, 104] and the reference therein for an overview. Variational sensitivity analysis based on a formulation in local coordinates has been presented in [7, 9]. In general, variations of the material configuration are considered and the changes of the state variables and the objective functional due to these variations are investigated. The variations are required in order to solve the optimization problem using nonlinear programming algorithms.

4.3.1 Sensitivity of the energy functional

The solution of structural optimization problems require the variations of the objective functional and the constraints due to variations in the design. In the context of structural optimization this is termed as *design sensitivity analysis*. The total variation of a given arbitrary objective functional $I(\boldsymbol{v}, \boldsymbol{s})$ is given by

$$\delta I = \delta_v I(\boldsymbol{v}, \boldsymbol{s})(\delta \boldsymbol{v}) + \delta_s I(\boldsymbol{v}, \boldsymbol{s})(\delta \boldsymbol{s}). \tag{4.11}$$

Within this chapter the primal energy $E(\boldsymbol{v}, \boldsymbol{s})$ is the objective functional which has to be minimized with respect to $\boldsymbol{v}$ and $\boldsymbol{s}$, i.e. the energy minimization problem (4.4) has to be solved. Therefore, for $I = E$ we have

$$\delta E = \delta_v E(\boldsymbol{v}, \boldsymbol{s})(\delta \boldsymbol{v}) + \delta_s E(\boldsymbol{v}, \boldsymbol{s})(\delta \boldsymbol{s}) = R(\boldsymbol{v}, \boldsymbol{s}; \delta \boldsymbol{v}) + G(\boldsymbol{v}, \boldsymbol{s}; \delta \boldsymbol{s}). \tag{4.12}$$

For a given solution $\boldsymbol{v} \in \mathcal{V}$ we have $R(\boldsymbol{v}, \boldsymbol{s}; \delta \boldsymbol{v}) = 0$. With this, the first part of the above sensitivity relation vanishes and it remains only the material residual, i.e.

$$\delta E = \delta_s E(\boldsymbol{v}, \boldsymbol{s})(\delta \boldsymbol{s}) = G(\boldsymbol{v}, \boldsymbol{s}; \delta \boldsymbol{s}). \tag{4.13}$$

Therefore, in the context of structural optimization, the material residual or configurational forces can be interpreted as the sensitivity of the energy with respect to variations in the design.

Remark 4.2 (Energy release rate) *The material residual or configurational forces are directly related to the well-known $\mathcal{J}$-integral, which is in linear fracture mechanics equal to the energy release rate $\mathcal{G}$ and is defined as the negative variation of E with respect to configurational changes, i.e.*

$$\mathcal{J} = \mathcal{G} = -\delta_s E(\boldsymbol{v}, \boldsymbol{s})(\delta \boldsymbol{s}) = -G(\boldsymbol{v}, \boldsymbol{s}; \delta \boldsymbol{s}). \tag{4.14}$$

4.3.2 Sensitivity of the physical residual

The following sensitivity analysis is based on an invariant requirement of the physical residual (4.7) with respect to variations $\delta \boldsymbol{v}$ and $\delta \boldsymbol{s}$. For a given solution $\{\boldsymbol{v}, \boldsymbol{s}\} \in \mathcal{V} \times \mathcal{S}$ of (4.6) we have $R(\boldsymbol{v}, \boldsymbol{s}; \boldsymbol{\eta}) = 0 \ \forall \, \boldsymbol{\eta} \in \mathcal{V}$. The total variation of the physical residual reads

$$R' = R'_v(\boldsymbol{v}, \boldsymbol{s}; \boldsymbol{\eta}, \delta \boldsymbol{v}) + R'_s(\boldsymbol{v}, \boldsymbol{s}; \boldsymbol{\eta}, \delta \boldsymbol{s}) = 0, \tag{4.15}$$

where the partial variations are given by

$$R'_v(\boldsymbol{v}, \boldsymbol{s}; \boldsymbol{\eta}, \delta \boldsymbol{v}) = a'_v(\boldsymbol{v}, \boldsymbol{s}; \boldsymbol{\eta}, \delta \boldsymbol{v}) \tag{4.16}$$

$$R'_s(\boldsymbol{v}, \boldsymbol{s}; \boldsymbol{\eta}, \delta \boldsymbol{s}) = a'_s(\boldsymbol{v}, \boldsymbol{s}; \boldsymbol{\eta}, \delta \boldsymbol{s}) - F'_s(\boldsymbol{s}; \boldsymbol{\eta}, \delta \boldsymbol{s}). \tag{4.17}$$

Note, that $R'_v = E''_{vv}$ and $R'_s = E''_{vs}$, respectively.

We introduce for the variations of the physical residual R with respect to $\boldsymbol{v}$ and $\boldsymbol{s}$ the operators

$$k(\boldsymbol{v}, \boldsymbol{s}; \boldsymbol{\eta}, \delta\boldsymbol{v}) := R'_v(\boldsymbol{v}, \boldsymbol{s}; \boldsymbol{\eta}, \delta\boldsymbol{v}), \tag{4.18}$$

$$p(\boldsymbol{v}, \boldsymbol{s}; \boldsymbol{\eta}, \delta\boldsymbol{s}) := R'_s(\boldsymbol{v}, \boldsymbol{s}; \boldsymbol{\eta}, \delta\boldsymbol{s}), \tag{4.19}$$

where $k(\boldsymbol{v}, \boldsymbol{s}; \cdot, \cdot)$ is the well-known *tangent physical stiffness operator* and we call $p(\boldsymbol{v}, \boldsymbol{s}; \cdot, \cdot)$ the *tangent pseudo load operator* for the physical problem. Both terms are bilinear forms $k : \mathcal{V} \times \mathcal{V} \to \mathbb{R}$ and $p : \mathcal{V} \times \mathcal{S} \to \mathbb{R}$.

With these notations the total variation yields the form

$$R' = k(\boldsymbol{v}, \boldsymbol{s}; \boldsymbol{\eta}, \delta\boldsymbol{v}) + p(\boldsymbol{v}, \boldsymbol{s}; \boldsymbol{\eta}, \delta\boldsymbol{s}) = 0\,. \tag{4.20}$$

After rearranging the above terms we can formulate the following sensitivity equation for the physical problem.

Problem 4.2 *Let $\delta\hat{\boldsymbol{s}} \in \mathcal{S}$ be a given fixed design variation. Find $\delta\boldsymbol{v} \in \mathcal{V}$ such that*

$$k(\boldsymbol{v}, \boldsymbol{s}; \boldsymbol{\eta}, \delta\boldsymbol{v}) = -Q_p(\boldsymbol{v}, \boldsymbol{s}; \boldsymbol{\eta}) \qquad \forall\, \boldsymbol{\eta} \in \mathcal{V}, \tag{4.21}$$

where

$$Q_p(\boldsymbol{v}, \boldsymbol{s}; \boldsymbol{\eta}) := p(\boldsymbol{v}, \boldsymbol{s}; \boldsymbol{\eta}, \delta\hat{\boldsymbol{s}}) = R'_s(\boldsymbol{v}, \boldsymbol{s}; \boldsymbol{\eta}, \delta\hat{\boldsymbol{s}}) \tag{4.22}$$

is the pseudo load *of the physical problem for the variation $\delta\hat{\boldsymbol{s}}$.*

This is a variational equation for the sensitivity of the state due to changes in the design. For a given variation in the design $\delta\hat{\boldsymbol{s}}$, we can calculate the variation in the state $\delta\boldsymbol{v}$.

Remark 4.3 (Pseudo load) *In general, the pseudo load operator $p(\boldsymbol{v}, \boldsymbol{s}; \boldsymbol{\eta}, \delta\boldsymbol{s})$ is a bilinear form $p : \mathcal{V} \times \mathcal{S} \to \mathbb{R}$. For a chosen fixed $\delta\hat{\boldsymbol{s}}$ it becomes a linear functional $Q_p : \mathcal{V} \to \mathbb{R}$ and is called* pseudo load *because it plays the role of a* load *in the sensitivity equation (4.21) and is denoted by $Q_p(\boldsymbol{v}, \boldsymbol{s}; \cdot)$, i.e. $Q_p(\boldsymbol{v}, \boldsymbol{s}; \cdot) = p(\boldsymbol{v}, \boldsymbol{s}; \cdot, \delta\hat{\boldsymbol{s}})$.*

4.3.3 Sensitivity of the material residual

In the same way we can perform the total variation of the material residual given in (4.8). For a given solution $\{\boldsymbol{v}, \boldsymbol{s}\} \in \mathcal{V} \times \mathcal{S}$ of (4.6) we have $G(\boldsymbol{v}, \boldsymbol{s}; \boldsymbol{\psi}) = 0\ \forall\, \boldsymbol{\psi} \in \mathcal{S}$. The total variation reads

$$G' = G'_v(\boldsymbol{v}, \boldsymbol{s}; \boldsymbol{\psi}, \delta\boldsymbol{v}) + G'_s(\boldsymbol{v}, \boldsymbol{s}; \boldsymbol{\psi}, \delta\boldsymbol{s}) = 0, \tag{4.23}$$

where the partial variations are given by

$$G'_v(\boldsymbol{v}, \boldsymbol{s}; \boldsymbol{\psi}, \delta\boldsymbol{v}) = b'_v(\boldsymbol{v}, \boldsymbol{s}; \boldsymbol{\psi}, \delta\boldsymbol{v}) - F'_s(\boldsymbol{s}; \delta\boldsymbol{v}, \boldsymbol{\psi}) \tag{4.24}$$

$$G'_s(\boldsymbol{v}, \boldsymbol{s}; \boldsymbol{\psi}, \delta\boldsymbol{s}) = b'_s(\boldsymbol{v}, \boldsymbol{s}; \boldsymbol{\psi}, \delta\boldsymbol{s}) - F''_{ss}(\boldsymbol{s}; \boldsymbol{v}, \boldsymbol{\psi}, \delta\boldsymbol{s})\,. \tag{4.25}$$

Note, that $G'_v = E''_{sv}$ and $G'_s = E''_{ss}$, respectively.

We introduce for the variations of the material residual G with respect to $\boldsymbol{v}$ and $\boldsymbol{s}$ the operators

$$d(\boldsymbol{v}, \boldsymbol{s}; \boldsymbol{\psi}, \delta\boldsymbol{s}) := G'_s(\boldsymbol{v}, \boldsymbol{s}; \boldsymbol{\psi}, \delta\boldsymbol{s}), \tag{4.26}$$

$$t(\boldsymbol{v}, \boldsymbol{s}; \boldsymbol{\psi}, \delta\boldsymbol{v}) := G'_v(\boldsymbol{v}, \boldsymbol{s}; \boldsymbol{\psi}, \delta\boldsymbol{v}), \tag{4.27}$$

where $d(\cdot;\cdot)$ is the so-called *tangent material stiffness* in order to highlight the duality to the tangent physical stiffness (4.18) and we call $t(\cdot;\cdot)$ the *tangent pseudo load operator* for the material problem, compare with Eq. 4.19. Both terms are bilinear forms $d : \mathcal{S} \times \mathcal{S} \to \mathbb{R}$ and $t : \mathcal{S} \times \mathcal{V} \to \mathbb{R}$.

As a result of the permutableness of variations, i.e.

$$G'_v = E''_{sv} = E''_{vs} = R'_s, \tag{4.28}$$

we obtain for the variation of G with respect to $\boldsymbol{v}$

$$\begin{aligned} G'_v(\boldsymbol{v}, \boldsymbol{s}; \cdot, \delta\boldsymbol{v}) &= R'_s(\boldsymbol{v}, \boldsymbol{s}; \delta\boldsymbol{v}, \cdot) = p(\boldsymbol{v}, \boldsymbol{s}; \delta\boldsymbol{v}, \cdot) \\ &= a'_s(\boldsymbol{v}, \boldsymbol{s}; \delta\boldsymbol{v}, \cdot) - F'_s(\boldsymbol{s}; \delta\boldsymbol{v}, \cdot)\,. \end{aligned} \tag{4.29}$$

Thus, due to symmetry, the partial variation G'_v leads to the tangent pseudo load operator of the physical problem (4.19), i.e.

$$t(\boldsymbol{v}, \boldsymbol{s}; \boldsymbol{\psi}, \delta\boldsymbol{v}) = p(\boldsymbol{v}, \boldsymbol{s}; \delta\boldsymbol{v}, \boldsymbol{\psi}). \tag{4.30}$$

Therefore, we have additional to specify only the material tangent operator $d(\boldsymbol{v}, \boldsymbol{s}; \cdot, \cdot) = G'_s$. With these notations, the total variation yields the form

$$G' = p(\boldsymbol{v}, \boldsymbol{s}; \delta\boldsymbol{v}, \boldsymbol{\psi}) + d(\boldsymbol{v}, \boldsymbol{s}; \boldsymbol{\psi}, \delta\boldsymbol{s}) = 0. \tag{4.31}$$

After rearranging the above terms we can formulate the following sensitivity equation for the material problem.

Problem 4.3 *Let $\delta\hat{\boldsymbol{v}} \in \mathcal{V}$ be a given fixed variation in the state. Find $\delta\boldsymbol{s} \in \mathcal{S}$ such that*

$$d(\boldsymbol{v}, \boldsymbol{s}; \boldsymbol{\psi}, \delta\boldsymbol{s}) = -Q_m(\boldsymbol{v}, \boldsymbol{s}; \boldsymbol{\psi}) \qquad \forall\, \boldsymbol{\psi} \in \mathcal{S}, \tag{4.32}$$

where

$$Q_m(\boldsymbol{v}, \boldsymbol{s}; \boldsymbol{\psi}) := p(\boldsymbol{v}, \boldsymbol{s}; \delta\hat{\boldsymbol{v}}, \boldsymbol{\psi}) = G'_v(\boldsymbol{v}, \boldsymbol{s}; \boldsymbol{\psi}, \delta\hat{\boldsymbol{v}}) \tag{4.33}$$

is the pseudo load *of the material problem for the variation $\delta\hat{\boldsymbol{v}}$.*

This is a variational equation for the sensitivity of the design due to changes in the state. For a given variation in the state $\delta\hat{\boldsymbol{v}}$, we can calculate the variation in the design $\delta\boldsymbol{s}$.

Remark 4.4 *It is interesting to note, that due to symmetry both the sensitivity of the state and the sensitivity of the design depend on the pseudo load operator $p(\cdot,\cdot)$. Therefore, this operator plays an important role for the solution of the minimization problems for $\boldsymbol{v}$ and $\boldsymbol{s}$.*

4.3.4 Sensitivity relations in terms of deformation and displacement

For the classical spatial motion or physical problem with a fixed reference configuration Ω_R the formulation in terms of the deformation $\boldsymbol{\varphi}$ or the displacement field $\boldsymbol{u}$ yield the same results. But if we consider problems with changes in the material configuration, i.e. if the reference configuration Ω_R is not fixed, we have to distinguish between $\boldsymbol{\varphi}$ and $\boldsymbol{u}$. We consider for instance the sensitivity equation (4.21). If the deformation $\boldsymbol{\varphi}$ is the unknown, the problem reads: Find $\delta\boldsymbol{\varphi} \in \mathcal{V}$ such that

$$k(\boldsymbol{\varphi}, \boldsymbol{s}; \boldsymbol{\eta}, \delta\boldsymbol{\varphi}) = -Q_p(\boldsymbol{\varphi}, \boldsymbol{s}; \boldsymbol{\eta}) \qquad \forall\, \boldsymbol{\eta} \in \mathcal{V}, \tag{4.34}$$

with $Q_p(\boldsymbol{\varphi}, \boldsymbol{s}; \boldsymbol{\eta}) = p(\boldsymbol{\varphi}, \boldsymbol{s}; \boldsymbol{\eta}, \delta\boldsymbol{s})$. This equation yields the change in the deformation $\delta\boldsymbol{\varphi}$ due to changes in the design $\delta\boldsymbol{X} = \delta\boldsymbol{s}$. The corresponding change in displacement field is obtained from the relation

$$\delta\boldsymbol{u} = \delta\boldsymbol{\varphi} - \delta\boldsymbol{X}. \tag{4.35}$$

On the other hand, if the displacement field $\boldsymbol{u}$ is the unknown, the problem reads: Find $\delta\boldsymbol{u} \in \mathcal{V}$ such that

$$k(\boldsymbol{u}, \boldsymbol{s}; \boldsymbol{\eta}, \delta\boldsymbol{u}) = -Q_p(\boldsymbol{u}, \boldsymbol{s}; \boldsymbol{\eta}) \qquad \forall\, \boldsymbol{\eta} \in \mathcal{V}, \tag{4.36}$$

with $Q_p(\boldsymbol{u}, \boldsymbol{s}; \boldsymbol{\eta}) = p(\boldsymbol{u}, \boldsymbol{s}; \boldsymbol{\eta}, \delta\boldsymbol{s})$. This equation yields the change in the displacement field $\delta\boldsymbol{u}$ due to changes $\delta\boldsymbol{X}$. The change in the deformation $\delta\boldsymbol{\varphi}$ and the change in the displacement $\delta\boldsymbol{u}$ are related by

$$\delta\boldsymbol{\varphi} = \delta\boldsymbol{u} + \delta\boldsymbol{X}. \tag{4.37}$$

Note that

$$k(\boldsymbol{\varphi}, \boldsymbol{s}; \cdot, \cdot) = k(\boldsymbol{u}, \boldsymbol{s}; \cdot, \cdot), \tag{4.38}$$

because $\mathbf{E}'_{\varphi} = \mathbf{E}'_{u}$ and $\mathbf{E}''_{\varphi\varphi} = \mathbf{E}''_{uu}$, i.e. all variations with respect to $\boldsymbol{\varphi}$ and $\boldsymbol{u}$ yield the same results. But

$$p(\boldsymbol{\varphi}, \boldsymbol{s}; \cdot, \delta\boldsymbol{s}) \neq p(\boldsymbol{u}, \boldsymbol{s}; \cdot, \delta\boldsymbol{s}) \tag{4.39}$$

and therefore

$$Q_p(\boldsymbol{\varphi}, \boldsymbol{s}; \cdot) \neq Q_p(\boldsymbol{u}, \boldsymbol{s}; \cdot). \tag{4.40}$$

Hence, if we have configurational changes $\delta\boldsymbol{X} \neq \mathbf{0}$, then we have $\delta\boldsymbol{\varphi} \neq \delta\boldsymbol{u}$. This is the reason why the distinction between $\delta\boldsymbol{\varphi}$ and $\delta\boldsymbol{u}$ is important, if configurational variations are concerned.

4.4 Finite element approximation

The finite element formulation is based on a conforming Galerkin method defined on meshes $\mathcal{T}_h = \{K\}$ with a mesh parameter h consisting of closed cells K. The boundary ∂K of each element K is assumed to be Lipschitz-continuous. On the mesh $\mathcal{T}_h$ we define finite dimensional element spaces $\mathcal{V}_h \subset \mathcal{V}$ and $\mathcal{S}_h \subset \mathcal{S}$ consisting of cellwise polynomial functions, see e.g. the standard textbooks [19, 56, 85].

4.4.1 The discrete energy minimization problem

The discrete state $\boldsymbol{v}_h \in \mathcal{V}_h \subset \mathcal{V}$ and discrete design $\boldsymbol{s}_h \in \mathcal{S}_h \subset \mathcal{S}$ are determined by the following discrete version of Problem 4.1.

Problem 4.4 *Find* $\{\boldsymbol{v}_h, \boldsymbol{s}_h\} \in \mathcal{V}_h \times \mathcal{S}_h$ *such that*

$$E(\boldsymbol{v}_h, \boldsymbol{s}_h) = \min_{\{\boldsymbol{p}_h, \boldsymbol{r}_h\} \in \mathcal{V}_h \times \mathcal{S}_h} E(\boldsymbol{p}_h, \boldsymbol{r}_h). \tag{4.41}$$

The corresponding optimality condition is given as follows. Find $\{\boldsymbol{v}_h, \boldsymbol{s}_h\} \in \mathcal{V}_h \times \mathcal{S}_h$ such that

$$\left\{ \begin{array}{l} R(\boldsymbol{v}_h, \boldsymbol{s}_h; \boldsymbol{\eta}_h) \\ \\ G(\boldsymbol{v}_h, \boldsymbol{s}_h; \psi_h) \end{array} \right\} = \boldsymbol{0} \qquad \forall \{\boldsymbol{\eta}_h, \psi_h\} \in \mathcal{V}_h \times \mathcal{S}_h. \tag{4.42}$$

4.4.2 Matrix representation of the residuals and tangent forms

For a matrix description of the derived residuals and tangent forms we introduce the discrete approximations for the state and the design, i.e. the nodal vector $\boldsymbol{v} \in \mathbb{R}^n$ and the vector of design variables $\boldsymbol{s} \in \mathbb{R}^m$. Here, n and m are the dimensions of the introduced approximation spaces, i.e. n denotes the number of the discrete state variables and m the number of the discrete design variables. We introduce in the same manner the discrete approximations for the corresponding variations and test functions, i.e. $\delta \boldsymbol{v} \in \mathbb{R}^n$ and $\boldsymbol{\eta} \in \mathbb{R}^n$ as well as $\delta \boldsymbol{s} \in \mathbb{R}^m$ and $\boldsymbol{\psi} \in \mathbb{R}^m$.

For given $\{\hat{\boldsymbol{v}}_h, \hat{\boldsymbol{s}}_h\}$, the discrete versions of the residuals and tangent forms are given as

$$R(\hat{\boldsymbol{v}}_h, \hat{\boldsymbol{s}}_h; \boldsymbol{\eta}_h) = \boldsymbol{\eta}^T \boldsymbol{R}, \tag{4.43}$$

$$G(\hat{\boldsymbol{v}}_h, \hat{\boldsymbol{s}}_h; \psi_h) = \boldsymbol{\psi}^T \boldsymbol{G}, \tag{4.44}$$

$$k(\hat{\boldsymbol{v}}_h, \hat{\boldsymbol{s}}_h; \boldsymbol{\eta}_h, \delta \boldsymbol{v}_h) = \boldsymbol{\eta}^T \boldsymbol{K} \delta \boldsymbol{v}, \tag{4.45}$$

$$p(\hat{\boldsymbol{v}}_h, \hat{\boldsymbol{s}}_h; \boldsymbol{\eta}_h, \delta \boldsymbol{s}_h) = \boldsymbol{\eta}^T \boldsymbol{P} \delta \boldsymbol{s}, \tag{4.46}$$

$$t(\hat{\boldsymbol{v}}_h, \hat{\boldsymbol{s}}_h; \boldsymbol{\psi}_h, \delta\boldsymbol{v}_h) = \boldsymbol{\psi}^T \boldsymbol{T} \delta\boldsymbol{v}, \tag{4.47}$$

$$d(\hat{\boldsymbol{v}}_h, \hat{\boldsymbol{s}}_h; \boldsymbol{\psi}_h, \delta\boldsymbol{s}_h) = \boldsymbol{\psi}^T \boldsymbol{D} \delta\boldsymbol{s}, \tag{4.48}$$

where the vectors and matrices associated to the functionals and bilinear forms are denoted by

$\boldsymbol{R} \in \mathbb{R}^n$	primal physical residual vector
$\boldsymbol{G} \in \mathbb{R}^m$	primal material residual vector
$\boldsymbol{K} \in \mathbb{R}^{n \times n}$	primal tangent physical stiffness matrix
$\boldsymbol{P} \in \mathbb{R}^{n \times m}$	primal tangent physical pseudo load matrix
$\boldsymbol{T} \in \mathbb{R}^{m \times n}$	primal tangent material pseudo load matrix
$\boldsymbol{D} \in \mathbb{R}^{m \times m}$	primal tangent material stiffness matrix.

Details on the formulation of the matrix representations are given in C.3 and C.4.

Note that due to (4.30) we have $\boldsymbol{T} = \boldsymbol{P}^T$. Figure 4.2 summarizes the complete discrete tangent forms in the physical and material spaces.

4.4.3 The discrete sensitivity equations

With the above definitions, the sensitivity of the primal energy (4.13) with respect to variations $\delta\boldsymbol{s}$ is given as

$$\delta_s E = \boldsymbol{G}^T \delta\boldsymbol{s}. \tag{4.49}$$

Furthermore, the discrete versions of the sensitivity equations for the physical (4.20) and material (4.31) residuals become

$$\delta\boldsymbol{R} = \boldsymbol{K}\delta\boldsymbol{v} + \boldsymbol{P}\delta\boldsymbol{s} = \boldsymbol{0} \qquad \text{or} \qquad \delta\boldsymbol{v} = -\boldsymbol{K}^{-1}\boldsymbol{P}\delta\boldsymbol{s}, \tag{4.50}$$

$$\delta\boldsymbol{G} = \boldsymbol{P}^T\delta\boldsymbol{v} + \boldsymbol{D}\delta\boldsymbol{s} = \boldsymbol{0} \qquad \text{or} \qquad \delta\boldsymbol{s} = -\boldsymbol{D}^{-1}\boldsymbol{P}^T\delta\boldsymbol{v}. \tag{4.51}$$

For chosen fixed variations $\delta\hat{\boldsymbol{s}}$ and $\delta\hat{\boldsymbol{v}}$ the discrete versions of the sensitivity equations for the physical (4.21) and material (4.32) problem are given by

$$\boldsymbol{K}\delta\boldsymbol{v} = -\boldsymbol{Q}_p \qquad \text{with} \qquad \boldsymbol{Q}_p := \boldsymbol{P}\delta\hat{\boldsymbol{s}}, \tag{4.52}$$

$$\boldsymbol{D}\delta\boldsymbol{s} = -\boldsymbol{Q}_m \qquad \text{with} \qquad \boldsymbol{Q}_m := \boldsymbol{P}^T\delta\hat{\boldsymbol{v}}. \tag{4.53}$$

Here, $\boldsymbol{Q}_p \in \mathbb{R}^n$ is the pseudo load vector of the physical residual problem associated to the functional $Q_p(\boldsymbol{v}_h, \boldsymbol{s}_h; \cdot)$ and $\boldsymbol{Q}_m \in \mathbb{R}^m$ is the pseudo load vector of the material residual problem associated to the functional $Q_m(\boldsymbol{v}_h, \boldsymbol{s}_h; \cdot)$.

Remark 4.5 (Sensitivity operator) *It is important to note, that we obtain with the relations from (4.50) directly a connection between the physical and the material spaces. Both spaces are connected by the transformation*

$$\delta \boldsymbol{v} = \boldsymbol{S}_p \, \delta \boldsymbol{s} \qquad \textit{with} \qquad \boldsymbol{S}_p := -\boldsymbol{K}^{-1} \boldsymbol{P}, \tag{4.54}$$

where $\boldsymbol{S}_p \in \mathbb{R}^{n \times m}$ denotes the sensitivity operator matrix *of the physical problem. With the knowledge of the pseudo load operator matrix $\boldsymbol{P}$, we can evaluate the sensitivity equation for arbitrary admissible variations $\delta \boldsymbol{s}$ in the material space. In the same manner, we obtain from (4.51) for the material problem the transformation*

$$\delta \boldsymbol{s} = \boldsymbol{S}_m \, \delta \boldsymbol{v} \qquad \textit{with} \qquad \boldsymbol{S}_m := -\boldsymbol{D}^{-1} \boldsymbol{P}^T, \tag{4.55}$$

where $\boldsymbol{S}_m \in \mathbb{R}^{m \times n}$ denotes the sensitivity operator matrix *of the material problem. With this, we can perform the sensitivity analysis for arbitrary admissible variations $\delta \boldsymbol{v}$ in the physical space.*

Remark 4.6 (Deformation vs. displacement) *The importance of the distinction between sensitivity relations in terms of the deformation $\boldsymbol{\varphi}$ and the displacement $\boldsymbol{u}$ has been shown in Section 4.3.4. We consider the discrete formulation in order to illustrate this important fact. The discrete nodal vectors of $\boldsymbol{\varphi}$ and $\boldsymbol{u}$ are introduced as $\boldsymbol{\varphi} \in \mathbb{R}^n$ and $\boldsymbol{u} \in \mathbb{R}^n$, respectively. The nodal coordinates X_i are chosen as the design variables, i.e. we set $\boldsymbol{s} = \boldsymbol{X} \in \mathbb{R}^n$. Let $\boldsymbol{P}(\boldsymbol{\varphi})$ be the pseudo load operator matrix corresponding to $p(\boldsymbol{\varphi}, \boldsymbol{s}; \cdot; \cdot)$ evaluated at the current deformation $\boldsymbol{\varphi}$. Furthermore, let $\boldsymbol{P}(\boldsymbol{u})$ be the same operator in terms of the actual displacement field $\boldsymbol{u}$, i.e. obtained from $p(\boldsymbol{u}, \boldsymbol{s}; \cdot; \cdot)$. Then, by means of $\operatorname{Grad} \boldsymbol{\varphi} = \mathbf{I} + \operatorname{Grad} \boldsymbol{u}$ we have*

$$\frac{d\boldsymbol{\varphi}}{d\boldsymbol{X}} = [\, \boldsymbol{I} + \frac{d\boldsymbol{u}}{d\boldsymbol{X}} \,] = \boldsymbol{S}_p(\boldsymbol{\varphi}) = -\boldsymbol{K}^{-1} \boldsymbol{P}(\boldsymbol{\varphi}) \qquad \textit{and} \qquad d\boldsymbol{\varphi} = \boldsymbol{S}_p(\boldsymbol{\varphi}) d\boldsymbol{X}, \tag{4.56}$$

$$\frac{d\boldsymbol{u}}{d\boldsymbol{X}} = \boldsymbol{S}_p(\boldsymbol{\varphi}) - \boldsymbol{I} = \boldsymbol{S}_p(\boldsymbol{u}) = -\boldsymbol{K}^{-1} \boldsymbol{P}(\boldsymbol{u}) \qquad \textit{and} \qquad d\boldsymbol{u} = \boldsymbol{S}_p(\boldsymbol{u}) d\boldsymbol{X}, \tag{4.57}$$

where $\boldsymbol{I} \in \mathbb{R}^{n \times n}$ denotes the identity matrix. Finally, the pseudo load operator matrices $\boldsymbol{P}(\boldsymbol{\varphi})$ and $\boldsymbol{P}(\boldsymbol{u})$ as well as the sensitivity operator matrices $\boldsymbol{S}_p(\boldsymbol{\varphi})$ and $\boldsymbol{S}_p(\boldsymbol{u})$ are related by

$$\boldsymbol{P}(\boldsymbol{\varphi}) = \boldsymbol{P}(\boldsymbol{u}) - \boldsymbol{K}\boldsymbol{I}, \tag{4.58}$$

$$\boldsymbol{S}_p(\boldsymbol{\varphi}) = \boldsymbol{I} + \boldsymbol{S}_p(\boldsymbol{u}). \tag{4.59}$$

Hence, $\boldsymbol{P}(\boldsymbol{\varphi}) \neq \boldsymbol{P}(\boldsymbol{u})$ and $\boldsymbol{S}_p(\boldsymbol{\varphi}) \neq \boldsymbol{S}_p(\boldsymbol{u})$. As in the continuous case (4.37), the change in the deformation $d\boldsymbol{\varphi}$ and the change in the displacement $d\boldsymbol{u}$ are related by

$$d\boldsymbol{\varphi} = d\boldsymbol{u} + d\boldsymbol{X}. \tag{4.60}$$

This has to be taken into account by evaluating the sensitivity relation (4.54).

Remark 4.7 (Sensitivity of the energy release rate) *As mentioned in Remark 4.2 the material residual G is directly related to the energy release rate $\mathcal{G}$, i.e. $\mathcal{G} = -G$. Therefore, the sensitivity of the material residual (4.31) can be used to calculate the sensitivity of $\mathcal{G}$, which can be derived as*

$$\delta\mathcal{G} = -\delta G = -G' = -[\, d(\boldsymbol{v}, \boldsymbol{s}; \boldsymbol{\psi}, \delta\boldsymbol{s}) + p(\boldsymbol{v}, \boldsymbol{s}; \delta\boldsymbol{v}, \boldsymbol{\psi})\,]\,. \tag{4.61}$$

In order to obtain a dependency only from the variation in the design $\delta\boldsymbol{s}$, we can substitute the sensitivity of the state (4.21) to eliminate $\delta\boldsymbol{v}$. With (4.50) and (4.51) we have

$$\delta\mathcal{G}_h = -G'(\boldsymbol{v}_h, \boldsymbol{s}_h; \boldsymbol{\psi}_h, \delta\boldsymbol{v}_h, \delta\boldsymbol{s}_h) = -\boldsymbol{\psi}^T \delta\boldsymbol{G} \tag{4.62}$$

where

$$\delta\boldsymbol{G} = \boldsymbol{D}\delta\boldsymbol{s} + \boldsymbol{P}^T\delta\boldsymbol{v} = [\, \boldsymbol{D} - \boldsymbol{P}^T\boldsymbol{K}^{-1}\boldsymbol{P}\,]\,\delta\boldsymbol{s}. \tag{4.63}$$

Hence, for a given variation in the design $\delta\boldsymbol{s}$ we can calculate the variation in the energy release rate or rather the variation in the material residual $\boldsymbol{G}$.

4.5 Solution of the energy minimization problem

The energy minimization problem can be solved using different algorithms. It can be solved simultaneously for $\{\boldsymbol{v}, \boldsymbol{s}\}$, i.e. by solving the coupled problem (4.6) or in a staggered way by using gradient-based methods or Newton type methods.

4.5.1 Solution of the coupled problem

A Newton method on the continuous level is applied in order to get the solution of (4.6). Let $\mathcal{Y} := \mathcal{V} \times \mathcal{S}$ be a product space and set $\boldsymbol{y} = \{\boldsymbol{v}, \boldsymbol{s}\} \in \mathcal{Y}$, $\Delta\boldsymbol{y} = \{\Delta\boldsymbol{v}, \Delta\boldsymbol{s}\} \in \mathcal{Y}$ as well as $\boldsymbol{\phi} = \{\boldsymbol{\eta}, \boldsymbol{\psi}\} \in \mathcal{Y}$. Furthermore, we set

$$B(\boldsymbol{y}; \boldsymbol{\phi}) := R(\boldsymbol{v}, \boldsymbol{s}; \boldsymbol{\eta}) + G(\boldsymbol{v}, \boldsymbol{s}; \boldsymbol{\psi}). \tag{4.64}$$

Then, the optimality condition (4.6) reads

$$B(\boldsymbol{y}; \boldsymbol{\phi}) = 0 \qquad \forall\, \boldsymbol{\phi} \in \mathcal{Y}. \tag{4.65}$$

A Taylor expansion yields

$$B(\boldsymbol{y} + \Delta\boldsymbol{y}; \boldsymbol{\phi}) = B(\boldsymbol{y}; \boldsymbol{\phi}) + B'(\boldsymbol{y}; \boldsymbol{\phi}, \Delta\boldsymbol{y}) + \mathcal{O} = 0\,. \tag{4.66}$$

The remainder $\mathcal{O}$ contains higher order terms which can be usually neglected. Each Newton step requires the solution of the linear system

$$h(\boldsymbol{y}; \boldsymbol{\phi}, \Delta\boldsymbol{y}) = -B(\boldsymbol{y}; \boldsymbol{\phi}) \qquad \forall\, \boldsymbol{\phi} \in \mathcal{Y}, \tag{4.67}$$

where $h(\boldsymbol{y};\boldsymbol{\phi},\Delta\boldsymbol{y}) := B'(\boldsymbol{y};\boldsymbol{\phi},\Delta\boldsymbol{y})$ denotes the Hessian. The Hessian contains the partial variations of R and G, i.e.

$$\begin{aligned} h(\boldsymbol{y};\boldsymbol{\phi},\Delta\boldsymbol{y}) = \quad & R'_v(\boldsymbol{v},\boldsymbol{s};\boldsymbol{\eta},\Delta\boldsymbol{v}) + R'_s(\boldsymbol{v},\boldsymbol{s};\boldsymbol{\eta},\Delta\boldsymbol{s}) \\ & + G'_v(\boldsymbol{v},\boldsymbol{s};\boldsymbol{\psi},\Delta\boldsymbol{v}) + G'_s(\boldsymbol{v},\boldsymbol{s};\boldsymbol{\psi},\Delta\boldsymbol{s}). \end{aligned} \tag{4.68}$$

The definitions of the sensitivities of the physical (4.20) and material residual (4.31) yield the explicit form of the variations of R and G, respectively, and the Hessian takes the form

$$\begin{aligned} h(\boldsymbol{y};\boldsymbol{\phi},\Delta\boldsymbol{y}) = \quad & k(\boldsymbol{v},\boldsymbol{s};\boldsymbol{\eta},\Delta\boldsymbol{v}) + p(\boldsymbol{v},\boldsymbol{s};\boldsymbol{\eta},\Delta\boldsymbol{s}) \\ & + p(\boldsymbol{v},\boldsymbol{s};\Delta\boldsymbol{v},\boldsymbol{\psi}) + d(\boldsymbol{v},\boldsymbol{s};\boldsymbol{\psi},\Delta\boldsymbol{s}). \end{aligned} \tag{4.69}$$

Finally, the solution of problem (4.6) requires the solution of the linear system

$$\left\{ \begin{array}{l} k(\boldsymbol{v},\boldsymbol{s};\boldsymbol{\eta},\Delta\boldsymbol{v}) + p(\boldsymbol{v},\boldsymbol{s};\boldsymbol{\eta},\Delta\boldsymbol{s}) = -R(\boldsymbol{v},\boldsymbol{s};\boldsymbol{\eta}) \\ p(\boldsymbol{v},\boldsymbol{s};\Delta\boldsymbol{v},\boldsymbol{\psi}) + d(\boldsymbol{v},\boldsymbol{s};\boldsymbol{\psi},\Delta\boldsymbol{s}) = -G(\boldsymbol{v},\boldsymbol{s};\boldsymbol{\psi}) \end{array} \right\} \tag{4.70}$$

in each Newton step.

After a standard finite element discretization by using the notations from Section 4.4.2, the system (4.70) takes the form

$$\left[\begin{array}{cc} \boldsymbol{K} & \boldsymbol{P} \\ \boldsymbol{P}^T & \boldsymbol{D} \end{array} \right] \left[\begin{array}{c} \Delta\boldsymbol{v} \\ \Delta\boldsymbol{s} \end{array} \right] = - \left[\begin{array}{c} \boldsymbol{R} \\ \boldsymbol{G} \end{array} \right] . \tag{4.71}$$

Remark 4.8 (Coupling of the physical and material problem) *The off-diagonal elements of the above saddle point problem are the pseudo load operators of the physical (4.19) and material residual (4.27). Hence, the physical and the material problems are coupled by the pseudo load operator $p(\cdot,\cdot)$.*

Remark 4.9 (Schur complement) *If we substitute the first equation of (4.71) into the second and vice versa, we can eliminate $\Delta\boldsymbol{v}$ or $\Delta\boldsymbol{s}$ by using the Schur complement in order to solve the problem one after the other and to minimize the size of the system. We obtain a formulation for the state variables*

$$[\,\boldsymbol{K} - \boldsymbol{P}\boldsymbol{D}^{-1}\boldsymbol{P}^T\,]\Delta\boldsymbol{v} = \boldsymbol{P}\boldsymbol{D}^{-1}\boldsymbol{G} - \boldsymbol{R} \tag{4.72}$$

or for the design variables

$$[\,\boldsymbol{D} - \boldsymbol{P}^T\boldsymbol{K}^{-1}\boldsymbol{P}\,]\Delta\boldsymbol{s} = \boldsymbol{P}^T\boldsymbol{K}^{-1}\boldsymbol{R} - \boldsymbol{G}\,. \tag{4.73}$$

This requires well-conditioned matrices $\boldsymbol{K}$ and $\boldsymbol{D}$ in order to compute the corresponding inverse matrices accurately and to obtain a stable solution algorithm.

Remark 4.10 (Problems within the numerical solution) *It seems, that the naturally best way to find a solution of the energy minimization problem (4.4) is a full Newton method, i.e. the simultaneous solution of the physical and material problem. The best convergence speed is expected and hence, the lowest computational cost. This optimization problem is non-convex in general and for real problems with a large number of design variables such an algorithm is very sensitive and not stable. Furthermore, the system (4.71) has a typical saddle point structure and we have to be careful by solving this system. Often a preconditioner is needed in order to obtain a well-conditioned system matrix. See for instance [15] and the references therein for preconditioners for this type of equations. Therefore, other solution algorithms should be considered.*

4.5.2 A staggered solution algorithm

The energy only in terms of $\boldsymbol{s}$. In order to solve the energy minimization problem in a staggered way, we introduce the functional

$$\mathcal{E}(\boldsymbol{s}) := E(\boldsymbol{v}(\boldsymbol{s}), \boldsymbol{s}). \tag{4.74}$$

A reformulation of Problem 4.1 only in terms of the design function $\boldsymbol{s}$ yields the following problem.

Problem 4.5 *Find $\boldsymbol{s} \in \mathcal{S}$ such that the energy $\mathcal{E}(\boldsymbol{s})$ is minimized, i.e.*

$$\mathcal{E}(\boldsymbol{s}) = \min_{\boldsymbol{r} \in \mathcal{S}} E(\boldsymbol{v}(\boldsymbol{r}), \boldsymbol{r}). \tag{4.75}$$

For a given solution $\boldsymbol{v}$ we have to solve $G(\boldsymbol{v}(\boldsymbol{s}), \boldsymbol{s}) = 0$ within a Newton or gradient-based algorithm. First, we have to solve the primal physical problem to provide a solution $\boldsymbol{v}$.

Solution of the primal physical problem. The primal physical problem is solved for a given fixed design $\boldsymbol{s}$. The variational equation of the primal problem is given in Eq. 4.7 as

$$R(\boldsymbol{v}, \boldsymbol{s}; \boldsymbol{\eta}) = 0 \qquad \forall\, \boldsymbol{\eta} \in \mathcal{V}.$$

The solution within a Newton scheme requires the linearization

$$R(\boldsymbol{v}, \boldsymbol{s}; \boldsymbol{\eta}) + D_v R(\boldsymbol{v}, \boldsymbol{s}; \boldsymbol{\eta}) \cdot \Delta\boldsymbol{v} + \mathcal{O} = 0. \tag{4.76}$$

The tangent operator $D_v R(\boldsymbol{v}, \boldsymbol{s}; \boldsymbol{\eta}) \cdot \Delta\boldsymbol{v} = R'_v(\boldsymbol{u}, \boldsymbol{s}; \boldsymbol{\eta}, \Delta\boldsymbol{v}) = k(\boldsymbol{v}, \boldsymbol{s}; \boldsymbol{\eta}, \Delta\boldsymbol{v})$ is the tangent physical stiffness operator (4.18). The remainder $\mathcal{O}$ contains higher order terms and is neglected. Hence, the solution of (4.7) requires the solution of the linear equation

$$k(\boldsymbol{v}, \boldsymbol{s}; \boldsymbol{\eta}, \Delta\boldsymbol{v}) = -R(\boldsymbol{v}, \boldsymbol{s}; \boldsymbol{\eta}) \qquad \forall\, \boldsymbol{\eta} \in \mathcal{V} \tag{4.77}$$

in every Newton step in order to compute the increment $\Delta\boldsymbol{v}$. The discrete version of (4.77) is given by

$$\boldsymbol{K}\Delta\boldsymbol{v} = -\boldsymbol{R}. \tag{4.78}$$

Solution of the primal material problem. The variational equation of the material problem is given in Eq. 4.8 and reads $G(\boldsymbol{v}, \boldsymbol{s}; \boldsymbol{\psi}) = 0$. In order to solve this nonlinear problem in a staggered way, we use the linearization

$$G(\boldsymbol{v}, \boldsymbol{s}; \boldsymbol{\psi}) + D_s G(\boldsymbol{v}(\boldsymbol{s}), \boldsymbol{s}; \boldsymbol{\psi}) \cdot \Delta\boldsymbol{s} + \mathcal{O} = 0. \tag{4.79}$$

The *material tangent operator* is introduced as

$$\begin{aligned} m(\boldsymbol{v}, \boldsymbol{s}; \boldsymbol{\psi}, \Delta\boldsymbol{s}) &:= D_s G(\boldsymbol{v}(\boldsymbol{s}), \boldsymbol{s}; \boldsymbol{\psi}) \cdot \Delta\boldsymbol{s} \\ &= \frac{d}{d\varepsilon} \left[G(\boldsymbol{v}, \boldsymbol{s} + \varepsilon\Delta\boldsymbol{s}; \boldsymbol{\psi}) + G(\boldsymbol{v}(\boldsymbol{s} + \varepsilon\Delta\boldsymbol{s}), \boldsymbol{s}; \boldsymbol{\psi}) \right] \Big|_{\varepsilon=0} . \end{aligned} \tag{4.80}$$

This is a bilinear form $m : \mathcal{S} \times \mathcal{S} \to \mathbb{R}$, which has to be evaluated for the current $\{\boldsymbol{v}, \boldsymbol{s}\}$. The remainder $\mathcal{O}$ is again neglected. Hence, we have to solve the linear equation

$$m(\boldsymbol{v}, \boldsymbol{s}; \boldsymbol{\psi}, \Delta\boldsymbol{s}) = -G(\boldsymbol{v}, \boldsymbol{s}; \boldsymbol{\psi}) \qquad \forall\, \boldsymbol{\psi} \in \mathcal{S} \tag{4.81}$$

in every Newton step in order to compute the increment $\Delta\boldsymbol{s}$.

The discrete formulation of (4.80) for given $\{\hat{\boldsymbol{v}}_h, \hat{\boldsymbol{s}}_h\}$ reads

$$\begin{aligned} m(\hat{\boldsymbol{v}}_h, \hat{\boldsymbol{s}}_h; \boldsymbol{\psi}_h, \Delta\boldsymbol{s}_h) &= \boldsymbol{\psi}^T \left[\frac{\partial \boldsymbol{G}}{\partial \boldsymbol{s}} + \frac{\partial \boldsymbol{G}}{\partial \boldsymbol{v}} \frac{\partial \boldsymbol{v}}{\partial \boldsymbol{s}} \right] \Delta\boldsymbol{s} \\ &= \boldsymbol{\psi}^T \left[\boldsymbol{D} - \boldsymbol{P}^T \boldsymbol{K}^{-1} \boldsymbol{P} \right] \Delta\boldsymbol{s}, \end{aligned} \tag{4.82}$$

where the relations $\partial\boldsymbol{G}/\partial\boldsymbol{v} = \boldsymbol{P}^T$ and $\partial\boldsymbol{v}/\partial\boldsymbol{s} = -\boldsymbol{K}^{-1}\boldsymbol{P}$ have been used. Finally, the staggered Newton algorithm for the material problem (4.81) becomes the discrete form

$$\boldsymbol{M}\Delta\boldsymbol{s} = -\boldsymbol{G} \qquad \text{with} \qquad \boldsymbol{M} := \boldsymbol{D} - \boldsymbol{P}^T \boldsymbol{K}^{-1} \boldsymbol{P}, \tag{4.83}$$

where $\boldsymbol{M} \in \mathbb{R}^{m \times m}$ denotes the discrete material tangent operator matrix corresponding to the bilinear form $m(\cdot, \cdot)$ from (4.80).

Alternatively, gradient based methods which are used in classical nonlinear programming can be considered in order to solve (4.75). For instance, a simple steepest descent method is given by the update rule

$$\boldsymbol{s}_{i+1} = \boldsymbol{s}_i + \Delta\boldsymbol{s}_i = \boldsymbol{s}_i - \varepsilon_i \, \boldsymbol{G}(\boldsymbol{v}_h(\boldsymbol{s}_{h,i}), \boldsymbol{s}_{h,i}), \tag{4.84}$$

where ε_i denotes the step size parameter which controls the decrease in the energy. The algorithm can be further improved by using quasi-Newton methods such as a BFGS method, see e.g. [81] for such solution algorithms.

Remark 4.11 (Applications) *The proposed full Newton and staggered solution algorithms can be applied to problems which are concerned with energy minimization. Applications to global and goal-oriented mesh optimization (r-adaptivity) are investigated in Chapter 7 and Chapter 8, respectively. Furthermore, the shape optimization problem is studied in Chapter 9.*

Remark 4.12 (Stability within the numerical solution) *As mentioned in Remark 4.10, the full Newton algorithm is very sensitive and not stable for a large number of design variables. The staggered solution method is more stable than the full Newton method but requires also a well-conditioned tangent matrix M. In many cases, the tangent matrix is ill-conditioned and becomes singular or close to singular during the iterations. Therefore, reasonable regularization methods have to be used in order to regularize the problem. This is discussed in detail in Section 7.5 for the mesh optimization problem.*

Remark 4.13 (Staggered Newton method vs. gradient based method) *The solution of the linear equation (4.83) is part of a staggered Newton method. If the problem is well-posed and the tangent matrix M is well-conditioned the algorithm converged very quickly to the solution. As mentioned above in many cases M is ill-conditioned and the computed new increment $\Delta\mathsf{s}$ results possibly not in a decrease of the energy. In contrast, a gradient based method yields in the most cases accurate search directions and is very stable. Therefore, by using quasi-Newton methods based on gradient information and an adequate and efficient line search algorithm the gradient method can be superior to the staggered Newton method because no regularization has to be taken into account.*

4.6 Explicit formulations for shape sensitivity

Explicit variational and discrete formulations of the derived residuals and tangent forms are stated in this section. In addition to the well-known classical physical residual $R(\boldsymbol{v}, \boldsymbol{s}; \cdot)$ and tangent stiffness $k(\boldsymbol{v}, \boldsymbol{s}; \cdot, \cdot)$, all variations of the primal energy are derived with respect to $\boldsymbol{v}$ and $\boldsymbol{s}$.

The formulations are obtained by using the variational framework in the physical and material spaces introduced in Chapter 3. All residuals and tangent forms are expressed in terms of the second Piola-Kirchhoff stress tensor $\mathbf{S}$ and the Green-Lagrange strain tensor $\mathbf{E}$ within this work. Alternatively, they can be written in terms of the first Piola-Kirchhoff stress $\mathbf{P}$ and $\mathbf{F}$.

Within this section the model problem of nonlinear elasticity is considered. The formulations for linearized elasticity are given for completeness in Section B.2.4.

4.6.1 Variational formulations of the primal residuals and tangent forms

The partial variations of the primal physical and material residuals have been introduced as

$$k(\boldsymbol{v}, \boldsymbol{s}; \boldsymbol{\eta}, \delta\boldsymbol{v}) = R'_v(\boldsymbol{v}, \boldsymbol{s}; \boldsymbol{\eta}, \delta\boldsymbol{v}) \qquad t(\boldsymbol{v}, \boldsymbol{s}; \boldsymbol{\psi}, \delta\boldsymbol{v}) = G'_v(\boldsymbol{v}, \boldsymbol{s}; \boldsymbol{\psi}, \delta\boldsymbol{v})$$

$$p(\boldsymbol{v}, \boldsymbol{s}; \boldsymbol{\eta}, \delta\boldsymbol{s}) = R_s(\boldsymbol{v}, \boldsymbol{s}; \boldsymbol{\eta}, \delta\boldsymbol{s}) \qquad d(\boldsymbol{v}, \boldsymbol{s}; \boldsymbol{\psi}, \delta\boldsymbol{s}) = G'_s(\boldsymbol{v}, \boldsymbol{s}; \boldsymbol{\psi}, \delta\boldsymbol{s}).$$

The residuals written in terms of $\mathbf{S}$ and $\mathbf{E}$ are given by

$$R(\boldsymbol{v},\boldsymbol{s};\boldsymbol{\eta}) = \int_{\Omega_R} \mathbf{S} : \mathbf{E}'_v(\boldsymbol{v},\boldsymbol{\eta})\,\mathrm{d}\Omega - F(\boldsymbol{s};\boldsymbol{\eta}) \tag{4.85}$$

$$G(\boldsymbol{v},\boldsymbol{s};\boldsymbol{\psi}) = \int_{\Omega_R} [\,\mathbf{S} : \mathbf{E}'_s(\boldsymbol{v},\boldsymbol{\psi}) + W_R\mathbf{I} : \mathrm{Grad}\,\boldsymbol{\psi}\,]\,\mathrm{d}\Omega - F'_s(\boldsymbol{s};\boldsymbol{v},\boldsymbol{\psi}) \tag{4.86}$$

and the explicit formulation of the tangent forms are obtained as

$$k(\boldsymbol{v},\boldsymbol{s};\boldsymbol{\eta},\delta\boldsymbol{v}) = \int_{\Omega_R} \{\,\mathbf{S} : \mathbf{E}''_{vv}(\boldsymbol{\eta},\delta\boldsymbol{v}) + \mathbf{E}'_v(\boldsymbol{v},\boldsymbol{\eta}) : \mathbb{C} : \mathbf{E}'_v(\boldsymbol{v},\delta\boldsymbol{v})\,\}\,\mathrm{d}\Omega, \tag{4.87}$$

$$\begin{aligned} p(\boldsymbol{v},\boldsymbol{s};\boldsymbol{\eta},\delta\boldsymbol{s}) = \int_{\Omega_R} \{\,&\mathbf{S} : \mathbf{E}''_{vs}(\boldsymbol{v},\boldsymbol{\eta},\delta\boldsymbol{s}) + \mathbf{E}'_v(\boldsymbol{v},\boldsymbol{\eta}) : \mathbb{C} : \mathbf{E}'_s(\boldsymbol{v},\delta\boldsymbol{s}) \\ &+ \mathbf{S} : \mathbf{E}'_v(\boldsymbol{v},\boldsymbol{\eta})\,\mathrm{Div}\,\delta\boldsymbol{s}\,\}\,\mathrm{d}\Omega \\ &- F'_s(\boldsymbol{s};\boldsymbol{\eta},\delta\boldsymbol{s}), \end{aligned} \tag{4.88}$$

$$\begin{aligned} t(\boldsymbol{v},\boldsymbol{s};\boldsymbol{\psi},\delta\boldsymbol{v}) = \int_{\Omega_R} \{\,&\mathbf{S} : \mathbf{E}''_{sv}(\boldsymbol{v},\boldsymbol{\psi},\delta\boldsymbol{v}) + \mathbf{E}'_s(\boldsymbol{v},\boldsymbol{\psi}) : \mathbb{C} : \mathbf{E}'_v(\boldsymbol{v},\delta\boldsymbol{v}) \\ &+ \mathbf{S} : \mathbf{E}'_v(\boldsymbol{v},\delta\boldsymbol{v})\,\mathrm{Div}\,\boldsymbol{\psi}\,\}\,\mathrm{d}\Omega \\ &- F'_s(\boldsymbol{s};\delta\boldsymbol{v},\boldsymbol{\psi}), \end{aligned} \tag{4.89}$$

$$\begin{aligned} d(\boldsymbol{v},\boldsymbol{s};\boldsymbol{\psi},\delta\boldsymbol{s}) = \int_{\Omega_R} \{\,&\mathbf{S} : \mathbf{E}''_{ss}(\boldsymbol{v},\boldsymbol{\psi},\delta\boldsymbol{s}) + \mathbf{E}'_s(\boldsymbol{v},\boldsymbol{\psi}) : \mathbb{C} : \mathbf{E}'_s(\boldsymbol{v},\delta\boldsymbol{s}) \\ &+ \mathbf{S} : [\,\mathbf{E}'_s(\boldsymbol{v},\boldsymbol{\psi})\,\mathrm{Div}\,\delta\boldsymbol{s} + \mathbf{E}'_s(\boldsymbol{v},\delta\boldsymbol{s})\,\mathrm{Div}\,\boldsymbol{\psi}\,] \\ &+ W_R\,[\,\mathrm{Div}\,\boldsymbol{\psi}\,\mathrm{Div}\,\delta\boldsymbol{s} - \mathbf{I} : \mathrm{Grad}\,\boldsymbol{\psi}\,\mathrm{Grad}\,\delta\boldsymbol{s}\,]\,\}\,\mathrm{d}\Omega \\ &- F''_{ss}(\boldsymbol{s};\boldsymbol{v},\boldsymbol{\psi},\delta\boldsymbol{s}). \end{aligned} \tag{4.90}$$

The explicit formulations of $F(\boldsymbol{s};\boldsymbol{\eta})$, $F'_s(\boldsymbol{s};\boldsymbol{v},\boldsymbol{\psi})$, $F'_s(\boldsymbol{s};\boldsymbol{\eta},\delta\boldsymbol{s})$ and $F''_{ss}(\boldsymbol{s};\boldsymbol{v},\boldsymbol{\psi},\delta\boldsymbol{s})$ depend on the form of the functional $F(\cdot)$. We consider for instance the potential $V_R(\boldsymbol{v})$ of physical body forces $\boldsymbol{b}_R$ per unit volume in the reference configuration, i.e. we choose the functional

$$F(\boldsymbol{s};\boldsymbol{v}) = -\int_{\Omega_R} V_R\,d\Omega = \int_{\Omega_R} \boldsymbol{b}_R\cdot\boldsymbol{v}\,\mathrm{d}\Omega. \tag{4.91}$$

Then, we have

$$F(\boldsymbol{s};\boldsymbol{\eta}) = \int_{\Omega_R} \boldsymbol{b}_R\cdot\boldsymbol{\eta}\,\mathrm{d}\Omega, \tag{4.92}$$

$$F'_s(\boldsymbol{s};\boldsymbol{\eta},\delta\boldsymbol{s}) = \int_{\Omega_R} \boldsymbol{b}_R\cdot\boldsymbol{\eta}\,\mathrm{Div}\,\delta\boldsymbol{s}\,\mathrm{d}\Omega, \tag{4.93}$$

$$F'_s(\boldsymbol{s};\boldsymbol{v},\boldsymbol{\psi}) = -\int_{\Omega_R} V_R\,\mathbf{I} : \operatorname{Grad}\boldsymbol{\psi}\,\mathrm{d}\Omega, \tag{4.94}$$

$$F''_{ss}(\boldsymbol{s};\boldsymbol{v},\boldsymbol{\psi},\delta\boldsymbol{s}) = -\int_{\Omega_R} V_R\,\left[\,\operatorname{Div}\boldsymbol{\psi}\operatorname{Div}\delta\boldsymbol{s} - \mathbf{I} : \operatorname{Grad}\boldsymbol{\psi}\operatorname{Grad}\delta\boldsymbol{s}\,\right]\,\mathrm{d}\Omega. \tag{4.95}$$

The derived residuals and tangent forms have the same structure with different variations of the Green-Lagrange strain tensor $\mathbf{E}$. But the terms obtained from variations with respect to $\boldsymbol{s}$ have additional terms as a result of the variation of the domain Ω_R.

4.6.2 Discrete formulations of the primal residuals and tangent matrices

The above residuals and tangent forms are discretized using the isoparametric concept, i.e. the state $\boldsymbol{v}_h$ and the geometry $\boldsymbol{X}_h$ are approximated by the same shape functions defined on a fixed parameter space. Details about the numerical implementation are given in Appendix C.

The nodal contributions of the discrete residual vectors are given by

$$\boldsymbol{R}_i^e = \int_{\Omega_R^e} \boldsymbol{B}_{vi}^T \underline{\boldsymbol{S}}\,\mathrm{d}\Omega - \boldsymbol{F}^e(\boldsymbol{s})_i, \tag{4.96}$$

$$\boldsymbol{G}_i^e = \int_{\Omega_R^e} \{\,\boldsymbol{B}_{si}^T \underline{\boldsymbol{S}} + W_R \boldsymbol{I}\boldsymbol{L}_i\}\,\mathrm{d}\Omega - \boldsymbol{F}_s^e(\boldsymbol{s};\boldsymbol{v})_i, \tag{4.97}$$

and the tangent matrices are obtained as

$$\boldsymbol{K}_{ij}^e = \int_{\Omega_R^e} \{\,\boldsymbol{B}_{vi}^T \boldsymbol{C}\boldsymbol{B}_{vj} + \boldsymbol{L}_i^T \boldsymbol{S}\boldsymbol{L}_j \boldsymbol{I}\,\}\,\mathrm{d}\Omega, \tag{4.98}$$

$$\begin{aligned}\boldsymbol{P}_{ij}^e = &\int_{\Omega_R^e} \{\,\boldsymbol{B}_{vi}^T \boldsymbol{C}\boldsymbol{B}_{sj} - \boldsymbol{L}_i^T \boldsymbol{S}\boldsymbol{L}_j \operatorname{Grad}\boldsymbol{v} - \boldsymbol{F}\boldsymbol{S}\boldsymbol{L}_j\boldsymbol{L}_i^T + \boldsymbol{F}\boldsymbol{S}\boldsymbol{L}_i\boldsymbol{L}_j^T\,\}\,\mathrm{d}\Omega \\ &- \boldsymbol{F}_s^e(\boldsymbol{s})_{ij},\end{aligned} \tag{4.99}$$

$$\begin{aligned}\boldsymbol{D}_{ij}^e = &\int_{\Omega_R^e} \{\,\boldsymbol{B}_{si}^T \boldsymbol{C}\boldsymbol{B}_{sj} + \boldsymbol{L}_i^T \boldsymbol{S}\boldsymbol{L}_j \operatorname{Grad}\boldsymbol{v}^T \operatorname{Grad}\boldsymbol{v} + \operatorname{Grad}\boldsymbol{v}^T \boldsymbol{F}\boldsymbol{S}\boldsymbol{L}_j\boldsymbol{L}_i^T \\ &\quad + \boldsymbol{L}_j\boldsymbol{L}_i^T \boldsymbol{S}^T\boldsymbol{F}^T \operatorname{Grad}\boldsymbol{v} - \operatorname{Grad}\boldsymbol{v}^T \boldsymbol{F}\boldsymbol{S}\boldsymbol{L}_i\boldsymbol{L}_j^T - \boldsymbol{L}_i\boldsymbol{L}_j^T \boldsymbol{S}^T\boldsymbol{F}^T \operatorname{Grad}\boldsymbol{v} \\ &\quad + W_R\,[\,\boldsymbol{L}_i\boldsymbol{L}_j^T - \boldsymbol{L}_j\boldsymbol{L}_i^T\,]\,\}\,\mathrm{d}\Omega \\ &- \boldsymbol{F}_{ss}^e(\boldsymbol{s};\boldsymbol{v})_{ij}.\end{aligned} \tag{4.100}$$

Here, $\boldsymbol{S}$ and $\boldsymbol{F}$ are the matrices corresponding to second Piola-Kirchhoff stress tensor $\mathbf{S}$ and the deformation gradient $\mathbf{F}$, respectively, as well as $\boldsymbol{C}$ is the matrix representation of the

fourth-order elasticity tensor $\mathbb{C}$. Due to the symmetry of $\mathbf{S}$ it is useful to use the *Voigt* notation in order to compute the residuals. For this we introduce the column matrix $\underline{\boldsymbol{S}}$. Furthermore, $\boldsymbol{I}$ denotes the identity matrix and $\boldsymbol{L}_i$ the gradient of the shape function ϕ_i. For instance, in the two-dimensional case these matrices are given by

$$\boldsymbol{S} = \begin{bmatrix} S_{11} & S_{12} \\ S_{21} & S_{22} \end{bmatrix}, \qquad \underline{\boldsymbol{S}} = \begin{bmatrix} S_{11} & S_{22} & S_{12} \end{bmatrix}^T, \tag{4.101}$$

$$\boldsymbol{I} = \begin{bmatrix} 1 & 0 \\ 0 & 1 \end{bmatrix}, \qquad \boldsymbol{L}_i = \begin{bmatrix} \phi_{i,1} \\ \phi_{i,2} \end{bmatrix}. \tag{4.102}$$

The matrices $\boldsymbol{B}_v$ and $\boldsymbol{B}_s$ are given in (C.8) and (C.12).

The quantities $\boldsymbol{F}^e(\boldsymbol{s})_i$ and $\boldsymbol{F}^e_s(\boldsymbol{s};\boldsymbol{v})_i$ are the element nodal vectors on a node i corresponding to the functionals $F(\boldsymbol{s};\cdot)$ and $F'_s(\boldsymbol{s};\boldsymbol{v},\cdot)$. In the same manner, $\boldsymbol{F}^e_s(\boldsymbol{s})_{ij}$ and $\boldsymbol{F}^e_{ss}(\boldsymbol{s};\boldsymbol{v})_{ij}$ are the element nodal matrices corresponding to the bilinear forms $F'_s(\boldsymbol{s};\cdot,\cdot)$ and $F''_{ss}(\boldsymbol{s};\boldsymbol{v},\cdot,\cdot)$, respectively. The residuals and tangent forms depend on the explicit form of the functional $F(\boldsymbol{s};\cdot)$. We choose the particular form (4.91), i.e.

$$F(\boldsymbol{s};\boldsymbol{v}) = -\int_{\Omega_R} V_R \, d\Omega = \int_{\Omega_R} \boldsymbol{b}_R \cdot \boldsymbol{v} \, \mathrm{d}\Omega.$$

With this, the discrete version of (4.92), (4.93), (4.94) and (4.95) are obtained as

$$\boldsymbol{F}^e(\boldsymbol{s})_i = \int_{\Omega^e_R} \phi_i \, \boldsymbol{b}_R \, \mathrm{d}\Omega, \tag{4.103}$$

$$\boldsymbol{F}^e_s(\boldsymbol{s};\boldsymbol{v})_i = -\int_{\Omega^e_R} V_R \, \boldsymbol{I}\boldsymbol{L}_i \, \mathrm{d}\Omega, \tag{4.104}$$

$$\boldsymbol{F}^e_s(\boldsymbol{s})_{ij} = \int_{\Omega^e_R} \phi_i \, \boldsymbol{b}_R \, \boldsymbol{L}_j^T \, \mathrm{d}\Omega, \tag{4.105}$$

$$\boldsymbol{F}^e_{ss}(\boldsymbol{s};\boldsymbol{v})_{ij} = -\int_{\Omega^e_R} V_R \, [\, \boldsymbol{L}_i \boldsymbol{L}_j^T - \boldsymbol{L}_j \boldsymbol{L}_i^T \,] \, \mathrm{d}\Omega. \tag{4.106}$$

Remark 4.14 (Control of the residuals and tangent forms) *The discrete formulations are directly obtained by discretization of the variational formulations from Section 4.6.1. The correctness of the derived residual vectors and tangent matrices have been checked by using a* global finite difference method*, see e.g. [81] for details about such methods.*

4.7 Complete energy variations of the primal problem

4.7.1 Variational formulation

The starting point of the above sensitivity relations is an energy functional, which depends on a state function and a design function. Different variations with respect to $\boldsymbol{v}$ and $\boldsymbol{s}$ can

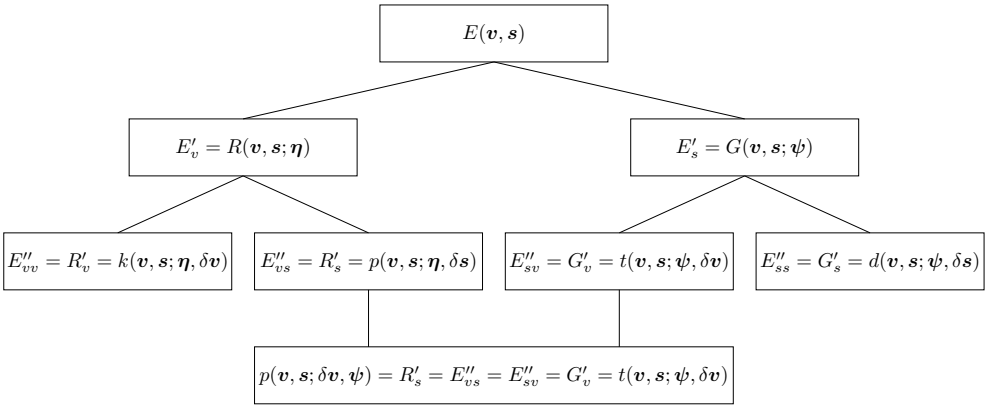

Figure 4.1: Summary of the complete energy variations and tangent forms for admissible variations $\{\boldsymbol{\eta}, \delta\boldsymbol{v}\} \in \mathcal{V}$ and $\{\boldsymbol{\psi}, \delta\boldsymbol{s}\} \in \mathcal{S}$

be performed. For the classical spatial motion or physical problem only the variations with respect to the state are required, i.e. $E'_v = R(\boldsymbol{v}, \boldsymbol{s}; \cdot)$ and $E''_{vv} = k(\boldsymbol{v}, \boldsymbol{s}; \cdot, \delta\boldsymbol{v})$. In the context of sensitivity analysis and structural optimization also the variation of the physical residual R with respect to $\boldsymbol{s}$ is investigated, i.e. $R'_s = E''_{vs} = p(\boldsymbol{v}, \boldsymbol{s}; \cdot, \delta\boldsymbol{s})$.

If we also consider the material problem, we have to compute the variations of the energy functional with respect to $\boldsymbol{s}$, i.e. $E'_s = G(\boldsymbol{v}, \boldsymbol{s}; \cdot)$ and $E''_{ss} = G'_s = d(\boldsymbol{v}, \boldsymbol{s}; \cdot, \delta\boldsymbol{s})$ as well as the mixed variation $E_{sv} = G'_v = t(\boldsymbol{v}, \boldsymbol{s}; \cdot, \delta\boldsymbol{v})$. This yields a complete framework for the physical and material problem. Due to symmetry and permutableness of variations, we have

$$p(\boldsymbol{v}, \boldsymbol{s}; \delta\boldsymbol{v}, \boldsymbol{\psi}) = R'_s = E''_{vs} = E''_{sv} = G'_v = t(\boldsymbol{v}, \boldsymbol{s}; \boldsymbol{\psi}, \delta\boldsymbol{v}). \tag{4.107}$$

Hence, it turns out that the physical and material problems are coupled by the pseudo load operator $p(\boldsymbol{v}, \boldsymbol{s}; \cdot, \cdot)$. Figure 4.1 summarizes the complete variations in the physical and material spaces.

4.7.2 Finite element formulation

The complete variations of the energy with respect to the state and the design yield the framework for the complete description of the physical or direct and material or inverse motion problem as well as corresponding sensitivity relations, see Fig. 4.1.

For classical problems with a fixed reference configuration Ω_R we can say that the finite element formulation is complete if we supply the physical residual vector $\boldsymbol{R}$ and the tangent physical stiffness matrix $\boldsymbol{K}$. From this we can solve the linear equation $\boldsymbol{K}\Delta\boldsymbol{v} = -\boldsymbol{R}$ in every Newton step in order to compute the increment in the state $\Delta\boldsymbol{v}$.

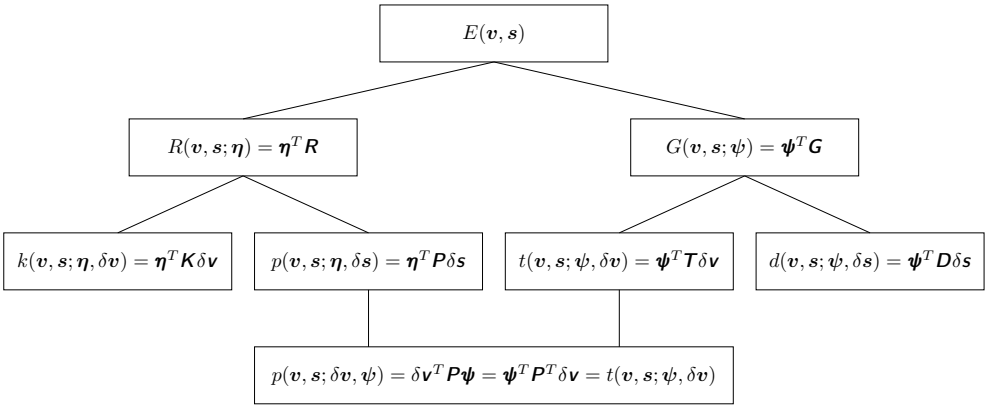

Figure 4.2: Summary of the complete discrete operators of the primal problem

But for problems with configurational variations, we can say that the formulation is complete if we supply additional the material residual $\boldsymbol{G}$, the pseudo load operator matrix $\boldsymbol{P}$ and the tangent material stiffness $\boldsymbol{D}$. With all these operators the formulation is complete in the sense that the energy depends on the state and the design and we allow changes in both variables, see Fig. 4.2.

Using the variational formulations for $k(\cdot, \cdot)$, $p(\cdot, \cdot)$ and $d(\cdot, \cdot)$ from (4.87), (4.88) and (4.90), the tangent matrices $\boldsymbol{P}$ and $\boldsymbol{D}$ can be computed and assembled in the same routine as the classical physical stiffness matrix $\boldsymbol{K}$ without considerable computational cost, because all of these matrices have the same structure. The matrix formulations are given in (4.98), (4.99) and (4.100), respectively.

The same holds true for the material residual $\boldsymbol{G}$, which can be computed in the same way as the classical physical residual vector $\boldsymbol{R}$. By means of all these operators the finite element formulation is complete. With this at hand, the physical and material problems can be solved and sensitivity analysis in the physical and material spaces can be performed.

4.8 Summary and concluding remarks

Variational balance laws and sensitivity relations for the primal physical and material problems have been proposed within this chapter. Due to symmetry both problems are coupled by the pseudo load operator $p(\boldsymbol{v}, \boldsymbol{s}; \cdot, \cdot)$. The obtained residuals and tangent forms can be used within different applications which are concerned with energy minimization. The proposed approach yields a complete framework for the solution of the classical physical or direct motion problem as well as for the material or inverse motion problem. Applications for the

Table 4.1: Summary of important variational and discrete sensitivity relations

Variational formulation	Discrete formulation
primal physical residual	
$\delta R = k(\boldsymbol{v}, \boldsymbol{s}; \cdot, \delta\boldsymbol{v}) + p(\boldsymbol{v}, \boldsymbol{s}; \cdot, \delta\boldsymbol{s})$	$\delta\boldsymbol{R} = \boldsymbol{K}\delta\boldsymbol{v} + \boldsymbol{P}\delta\boldsymbol{s}$
primal material residual	
$\delta G = p(\boldsymbol{v}, \boldsymbol{s}; \delta\boldsymbol{v}, \cdot) + d(\boldsymbol{v}, \boldsymbol{s}; \cdot, \delta\boldsymbol{s})$	$\delta\boldsymbol{G} = \boldsymbol{P}^T\delta\boldsymbol{v} + \boldsymbol{D}\delta\boldsymbol{s}$
primal pseudo load tangent form	
$p(\boldsymbol{v}, \boldsymbol{s}; \boldsymbol{\eta}, \delta\boldsymbol{s})$	$\boldsymbol{\eta}^T\boldsymbol{P}\delta\boldsymbol{s}$
primal pseudo load (physical)	
$Q_p(\boldsymbol{v}, \boldsymbol{s}; \boldsymbol{\eta}) = p(\boldsymbol{v}, \boldsymbol{s}; \boldsymbol{\eta}, \delta\hat{\boldsymbol{s}})$	$\boldsymbol{\eta}^T\boldsymbol{Q}_p = \boldsymbol{\eta}^T\boldsymbol{P}\delta\hat{\boldsymbol{s}}$
primal pseudo load (material)	
$Q_m(\boldsymbol{v}, \boldsymbol{s}; \psi) = p(\boldsymbol{u}, \boldsymbol{s}; \delta\hat{\boldsymbol{v}}, \psi)$	$\boldsymbol{\psi}^T\boldsymbol{Q}_m = \boldsymbol{\psi}^T\boldsymbol{P}^T\delta\hat{\boldsymbol{v}}$
sensitivity of $\boldsymbol{v}$	
$k(\boldsymbol{v}, \boldsymbol{s}; \cdot, \delta\boldsymbol{v}) = -Q_p(\boldsymbol{v}, \boldsymbol{s}; \cdot)$	$\boldsymbol{K}\delta\boldsymbol{v} = -\boldsymbol{Q}_p$
sensitivity of $\boldsymbol{s}$	
$d(\boldsymbol{v}, \boldsymbol{s}; \cdot, \delta\boldsymbol{s}) = -Q_m(\boldsymbol{v}, \boldsymbol{s}; \cdot)$	$\boldsymbol{D}\delta\boldsymbol{s} = -\boldsymbol{Q}_m$
sensitivity of E	
$\delta_s E = G(\boldsymbol{v}, \boldsymbol{s}; \delta\boldsymbol{s})$	$\delta_s E = \boldsymbol{G}^T\delta\boldsymbol{s}$

optimization of finite element meshes and shape optimization are studied in Chapter 7 and Chapter 9, respectively.

For the classical physical problem with a fixed reference configuration Ω_R the formulation in terms of the deformation $\boldsymbol{\varphi}$ or the displacement field $\boldsymbol{u}$ yield the same results. But if problems with changes in the material configuration are considered, i.e. if the reference configuration Ω_R is not fixed, we have to distinguish between $\boldsymbol{\varphi}$ and $\boldsymbol{u}$ within the sensitivity analysis.

Furthermore, a complete and consistent finite element formulation of the derived residuals and tangent forms has been given. All residuals and tangent matrices can be computed in the same routine as the usual physical residual vector and tangent stiffness matrix. The finite element formulation is complete if all residuals, i.e. $\boldsymbol{R}$ and $\boldsymbol{G}$, as well as all tangent matrices $\boldsymbol{K}$, $\boldsymbol{P}$ and $\boldsymbol{D}$ are supplied.

Finally, the most important variational and discrete sensitivity relations are summarized in Table 4.1.

Chapter 5

Duality techniques in the physical and material spaces

Duality relations in the physical and material spaces are investigated within this chapter. Additionally to the well-known dual physical problem, the corresponding dual material problem is introduced. Furthermore, a dual relation for the coupled physical and material problem is proposed. The derivation of the dual problems is based on a general optimal control approach, which yields the framework for general variational problems.

5.1 Introduction

The concept of duality plays an important role in many fields which deal with local quantities of interest, e.g. in structural mechanics, physics, optimization, control theory, computational methods and goal-oriented error estimation, see e.g. [4, 49, 62, 85].

In structural mechanics and mechanics in the physical space, duality relations are well-known as Betti's principle, also known as the reciprocity theorem. The quantities of interest are for instance displacements and pointwise stresses or average stresses. The corresponding *dual solutions* are *Green's functions* or *influence functions*, see e.g. [49, 51].

Green's functions play an important role in the solution of linear partial differential equations [34, 76]. Furthermore, they are a key component of boundary integral methods such as the *boundary element method* [50].

In structural optimization the dual problems are termed as *adjoint problems* and the corresponding solutions are referred to as *adjoint solutions*, see e.g. [27, 28].

In the context of configurational mechanics or mechanics in the material space, a reciprocity relation in the material space similar to the reciprocity relation for point loads in the physical space was proposed in [53, 54].

Within this work, a general variational approach for dual solutions in the physical and material spaces is investigated. In addition to the classical dual problem of the physical problem, also duality relations for the material problem as well as for the coupled physical and material problem are proposed. Some parts of this chapter are published in [73].

5.1.1 A linear model situation

The primal problem. For motivation a linear model problem is considered. Let for instance $\boldsymbol{u} \in \mathcal{V}$ be the solution of the so-called *primal problem* in the variational form

$$a(\boldsymbol{u}, \boldsymbol{\eta}) = F(\boldsymbol{\eta}) \quad \forall\, \boldsymbol{\eta} \in \mathcal{V}, \tag{5.1}$$

where $a(\cdot,\cdot) : \mathcal{V}\times\mathcal{V} \to \mathbb{R}$ denotes a bilinear form corresponding to the considered differential operator and $F(\cdot) : \mathcal{V} \to \mathbb{R}$ is a linear functional associated with the given external loads in a given space $\mathcal{V}$.

The quantity of interest. In duality techniques we are concerned with a certain *quantity of interest* or *general output* or *cost functional* $J(\boldsymbol{u})$, which can be every functional value which corresponds in some sense to the solution $\boldsymbol{u}$. The quantities of interest can be represented as linear or nonlinear functionals $J(\cdot) : \mathcal{V} \to \mathbb{R}$ of the solution. This could be point values, e.g. a component u_i or the derivatives $\partial_k u_i$ or the stress component $\sigma_{ij}(\boldsymbol{u})$ at some given point $\boldsymbol{X}$, i.e.

$$J(\boldsymbol{u}) = u_i(\boldsymbol{X}) \qquad \text{or} \qquad J(\boldsymbol{u}) = \partial_k u_i(\boldsymbol{X}) \qquad \text{or} \qquad J(\boldsymbol{u}) = \sigma_{ij}(\boldsymbol{X}). \tag{5.2}$$

Furthermore, it could be some integral value over a certain region Γ_r, e.g.

$$J(\boldsymbol{u}) = \int_{\Gamma_r} \partial_k u_i(\boldsymbol{X})\, \mathrm{d}\Gamma. \tag{5.3}$$

In general, every quantity of interest can be associated with a functional $J(\cdot)$.

The dual problem. For a chosen quantity of interest $J(\boldsymbol{u})$, the corresponding *dual* or *adjoint solution* or *generalized Green's function* $\boldsymbol{z} \in \mathcal{V}$ is determined by the *dual* or *adjoint problem*

$$a(\boldsymbol{\eta}, \boldsymbol{z}) = J(\boldsymbol{\eta}) \quad \forall\, \boldsymbol{\eta} \in \mathcal{V}. \tag{5.4}$$

The duality relation. A duality relation is in the linear case easily obtained. Obviously, by using (5.1) and (5.4) as well as the symmetry of $a(\cdot,\cdot)$, we have

$$J(\boldsymbol{u}) = a(\boldsymbol{u}, \boldsymbol{z}) = F(\boldsymbol{z}). \tag{5.5}$$

If the dual solution $\boldsymbol{z}$ is known, the quantity of interest $J(\boldsymbol{u})$ can be computed for arbitrary functionals $F(\cdot)$, i.e. $J(\boldsymbol{u}) = F(\boldsymbol{z})$.

For instance, let the displacement u_i at some material point $\boldsymbol{X}$ be the quantity of interest, i.e. $J(\boldsymbol{u}) = u_i(\boldsymbol{X})$. Furthermore, let

$$F(\boldsymbol{\eta}) = \int_{\Omega_R} \boldsymbol{b}_R \cdot \boldsymbol{\eta} \, \mathrm{d}\Omega$$

be the explicit form of the functional. Then, we have

$$J(\boldsymbol{u}) = u_i(\boldsymbol{X}) = \int_{\Omega_R} \boldsymbol{b}_R \cdot \boldsymbol{z} \, \mathrm{d}\Omega = F(\boldsymbol{z}).$$

Hence, $J(\boldsymbol{u})$ is given by the scalar product between the dual solution $\boldsymbol{z}$ and the given data $\boldsymbol{b}_R$. In structural mechanics this is well-known as Betti's principle and the dual solutions are the Green's functions or influence functions for $u_i(\boldsymbol{X})$. In the discrete case we have

$$u_i(\boldsymbol{X}) = \mathsf{z}^T \mathsf{F},$$

in which $\mathsf{z} \in \mathbb{R}^n$ is the discrete dual solution corresponding to u_i and $\mathsf{F} \in \mathbb{R}^n$ is the discrete load vector corresponding to the functional $F(\cdot)$.

Remark 5.1 (Computation of $J(\boldsymbol{u})$) *In general, there are two ways to compute $J(\boldsymbol{u})$. The first or classical way is to solve the primal problem (5.1). We obtain $J(\boldsymbol{u})$ directly from $\boldsymbol{u}$ or by a postprocessing step. The second way is indirect. We solve the dual problem (5.4) and obtain the dual solution $\boldsymbol{z}$. Afterwards, we evaluate Eq. 5.5 and get $J(\boldsymbol{u})$. The advantage of the second approach is that for a given dual solution $\boldsymbol{z}$ the quantity of interest $J(\boldsymbol{u})$ can be computed for arbitrary functionals $F(\cdot)$, i.e. for arbitrary given data.*

5.1.2 Regularized functionals for point values

From a mathematical point of view the energy of the dual problem $a(\boldsymbol{z}, \boldsymbol{z})$ is infinite for some dual solutions, because they are caused by point loads, which are represented by Dirac delta functions $\boldsymbol{\delta}(\boldsymbol{Y} - \boldsymbol{X})$, see e.g. [49, 51]. Hence, (5.4) may not be well-defined.

The quantity of interest can be written as

$$J(\boldsymbol{u}(\boldsymbol{X})) = \int_{\Omega} \boldsymbol{\delta}(\boldsymbol{Y} - \boldsymbol{X}) \cdot \boldsymbol{u}(\boldsymbol{Y}) \, \mathrm{d}\Omega_Y.$$

In order to avoid such infinite energy terms, we use for point values regularized functionals, e.g. for the point values from (5.2) we have

$$J_\varepsilon(\boldsymbol{u}) = \frac{1}{\Omega_\varepsilon} \int_{\Omega_\varepsilon} u_i(\boldsymbol{X}) \, \mathrm{d}\Omega \qquad \text{or} \qquad J_\varepsilon(\boldsymbol{u}) = \frac{1}{\Omega_\varepsilon} \int_{\Omega_\varepsilon} \partial_k u_i(\boldsymbol{X}) \, \mathrm{d}\Omega.$$

This corresponds with the mean value of the displacement or the derivative of the point value in a small domain

$$\Omega_\varepsilon := \{\, \boldsymbol{Y} \in \Omega \,:\, ||\boldsymbol{Y} - \boldsymbol{X}|| \leq \varepsilon \,\}$$

around the point $\boldsymbol{X}$, see e.g. [4]. The corresponding dual solutions behave like regularized Green's functions and Eq. 5.4 is well-defined. Alternatively, a mollifier function can be used, in which the Dirac function $\boldsymbol{\delta}(\boldsymbol{Y} - \boldsymbol{X})$ is approximated by mollifiers $\boldsymbol{\phi}_\varepsilon(\boldsymbol{Y} - \boldsymbol{X})$ [88]. The quantity of interest can be written as

$$J_\varepsilon(\boldsymbol{u}(\boldsymbol{X})) = \int_\Omega \boldsymbol{\phi}_\varepsilon(\boldsymbol{Y} - \boldsymbol{X}) \cdot \boldsymbol{u}(\boldsymbol{Y}) \, \mathrm{d}\Omega_Y,$$

where $\boldsymbol{\phi}_\varepsilon$ are infinitely smooth functions, see [85] for details.

With this in mind, we consider within this work always regularized functional for the quantity of interest such that the corresponding dual problems are well-defined. The corresponding dual solutions are regular and the dual energy $a(\boldsymbol{z}, \boldsymbol{z})$ has a finite value.

5.2 A general framework for duality techniques

The relation (5.5) holds in the exact form only for linear problems. Nevertheless, the duality approach can be extended to general nonlinear variational problems. Furthermore, the concept is more general and not restricted to mechanical problems and interpretations.

We consider an abstract optimal control approach, which yields a general framework for duality relations of variational problems. Such an approach is also used for instance within a posteriori error estimation techniques in finite element methods [4, 12].

Let $\boldsymbol{x} \in \mathcal{X}$ be the solution of a given (nonlinear) variational problem

$$A(\boldsymbol{x}; \boldsymbol{\eta}) = 0 \quad \forall\, \boldsymbol{\eta} \in \mathcal{X} \tag{5.6}$$

in a space $\mathcal{X}$. Furthermore, let $J(\boldsymbol{x}) : \mathcal{X} \to \mathbb{R}$ be the (possible nonlinear) quantity of interest with respect to the solution $\boldsymbol{x}$.

An optimal control approach ends in the following constraint optimization problem:

$$\min_{\boldsymbol{x} \in \mathcal{X}} J(\boldsymbol{x}) \qquad \text{subject to} \qquad A(\boldsymbol{x}; \boldsymbol{\eta}) = 0 \quad \forall\, \boldsymbol{\eta} \in \mathcal{X}. \tag{5.7}$$

The constraint is nothing but the variational problem (5.6). The corresponding Lagrangian functional reads

$$L(\boldsymbol{x}, \boldsymbol{g}) = J(\boldsymbol{x}) - A(\boldsymbol{x}; \boldsymbol{g}) \tag{5.8}$$

and the first-order optimality condition follows in the form

$$L'(\boldsymbol{x},\boldsymbol{g})(\boldsymbol{\nu},\boldsymbol{\eta}) = \left\{ \begin{array}{l} L'_x(\boldsymbol{x},\boldsymbol{g})(\boldsymbol{\nu}) \\ \\ L'_g(\boldsymbol{x},\boldsymbol{g})(\boldsymbol{\eta}) \end{array} \right\} = \left\{ \begin{array}{l} J'_x(\boldsymbol{x};\boldsymbol{\nu}) - A'_x(\boldsymbol{x};\boldsymbol{g},\boldsymbol{\nu}) \\ \\ -\, A(\boldsymbol{x};\boldsymbol{\eta}) \end{array} \right\} = 0 \tag{5.9}$$

for all $\{\boldsymbol{\nu},\boldsymbol{\eta}\} \in \mathcal{X} \times \mathcal{X}$. Here, $\boldsymbol{g} \in \mathcal{X}$ denotes the *dual* or *adjoint variable*. The first equation in (5.9) is the *dual* or *adjoint problem* and reads: Find $\boldsymbol{g} \in \mathcal{X}$ such that

$$A'_x(\boldsymbol{x};\boldsymbol{g},\boldsymbol{\nu}) = J'_x(\boldsymbol{x};\boldsymbol{\nu}) \qquad \forall\, \boldsymbol{\nu} \in \mathcal{X}, \tag{5.10}$$

with the tangent form $A'_x(\boldsymbol{x};\cdot,\cdot)$ and the linearized functional $J'_x(\boldsymbol{x};\cdot)$, i.e.

$$A'_x(\boldsymbol{x};\boldsymbol{g},\boldsymbol{\nu}) := \frac{d}{d\varepsilon}\, A(\boldsymbol{x}+\varepsilon\,\boldsymbol{\nu};\boldsymbol{g})\bigg|_{\varepsilon=0}, \qquad J'_x(\boldsymbol{x};\boldsymbol{\nu}) := \frac{d}{d\varepsilon}\, J(\boldsymbol{x}+\varepsilon\,\boldsymbol{\nu})\bigg|_{\varepsilon=0}. \tag{5.11}$$

The dual problem is a linear problem and is formulated at the current linearization point, i.e. at a given solution $\boldsymbol{x}$.

The second equation in (5.9) is just the variational equation of the primal problem (5.6). In the general nonlinear case, the solution of this equation within a Newton scheme requires the linearization $A(\boldsymbol{x};\boldsymbol{\eta}) + D_x A(\boldsymbol{x};\boldsymbol{\eta}) \cdot \Delta\boldsymbol{x} + \mathcal{O} = 0$. The tangent operator is given in (5.11) and denoted by $t(\boldsymbol{x};\boldsymbol{\eta},\Delta\boldsymbol{x}) := D_x A(\boldsymbol{x};\boldsymbol{\eta}) \cdot \Delta\boldsymbol{x} = A'_x(\boldsymbol{x};\boldsymbol{\eta},\Delta\boldsymbol{x})$. The term $\mathcal{O}$ denotes a remainder of higher-order and can usually be neglected. Hence, the solution of the nonlinear primal problem (5.6) requires the solution of the linear equation

$$t(\boldsymbol{x};\boldsymbol{\eta},\Delta\boldsymbol{x}) = -A(\boldsymbol{x};\boldsymbol{\eta}) \qquad \forall\, \boldsymbol{\eta} \in \mathcal{X} \tag{5.12}$$

in every Newton step in order to find the new increment $\Delta\boldsymbol{x}$.

By using (5.10) and (5.12) as well as the symmetry of the bilinear form $A'_x(\boldsymbol{x};\cdot,\cdot) = t(\boldsymbol{x};\cdot,\cdot)$, i.e. $A'_x(\boldsymbol{x};\boldsymbol{\eta},\Delta\boldsymbol{x}) = A'_x(\boldsymbol{x};\Delta\boldsymbol{x},\boldsymbol{\eta})$, we have

$$J'_x(\boldsymbol{x};\Delta\boldsymbol{x}) = t(\boldsymbol{x};\boldsymbol{g},\Delta\boldsymbol{x}) = -A(\boldsymbol{x};\boldsymbol{g}). \tag{5.13}$$

If the dual solution $\boldsymbol{g}$ is known, the change in the quantity of interest $J(\boldsymbol{x})$ can be computed for arbitrary functionals $A(\boldsymbol{x};\cdot)$, i.e. $J'_x(\boldsymbol{x};\Delta\boldsymbol{x}) = -A(\boldsymbol{x};\boldsymbol{g})$.

In order to make this relation more transparent we consider a discrete formulation. Let $J(\boldsymbol{x}_h) = x_i$ be the quantity of interest and let $\boldsymbol{g} \in \mathbb{R}^n$ be the discrete dual solution according to x_i as well as $\boldsymbol{J}_x \in \mathbb{R}^n$ be a discrete vector which corresponds to $J'_x(\boldsymbol{x}_h;\cdot)$. Furthermore, let $\boldsymbol{T} \in \mathbb{R}^{n\times n}$ be the tangent matrix and let $\boldsymbol{A} \in \mathbb{R}^n$ be a discrete vector corresponding to the bilinear form $t(\boldsymbol{x}_h;\cdot,\cdot)$ and the functional $A(\boldsymbol{x}_h;\cdot)$, respectively. With these, the discrete versions of (5.12) and (5.10), i.e. the discrete linearized primal problem and the discrete dual problem are given as

$$\boldsymbol{T}\Delta\boldsymbol{x} = -\boldsymbol{A} \qquad \text{and} \qquad \boldsymbol{T}^T\boldsymbol{g} = \boldsymbol{J}_x, \tag{5.14}$$

respectively. Due to the symmetry of the tangent form $A'_x(\boldsymbol{x};\cdot,\cdot)$, we have $\boldsymbol{T} = \boldsymbol{T}^T$. Then, the change in the quantity of interest $J'_x(\boldsymbol{x}_h;\Delta\boldsymbol{x}_h) = \Delta x_i$ at the current linearization point $\boldsymbol{x}$ is given from the discrete version of (5.13) in form of

$$\Delta x_i = \Delta\boldsymbol{x}^T\boldsymbol{J}_x = \Delta\boldsymbol{x}^T\boldsymbol{T}^T\boldsymbol{g} = \boldsymbol{g}^T\boldsymbol{T}\Delta\boldsymbol{x} = -\boldsymbol{g}^T\boldsymbol{A}. \tag{5.15}$$

5.3 The physical problem

The above described approach is now applied to the physical problem. The primal physical problem and the corresponding dual problem are introduced and a duality relation for physical quantities is derived.

5.3.1 The primal physical problem

The variational equation of the primal problem is given in Eq. 4.7 as

$$R(\boldsymbol{v}, \boldsymbol{s}; \boldsymbol{\eta}) = 0 \qquad \forall\, \boldsymbol{\eta} \in \mathcal{V}.$$

This equation is solved for a given fixed design $\boldsymbol{s}$. The solution within a Newton scheme requires the solution of the linearized equation (4.77) given by

$$k(\boldsymbol{v}, \boldsymbol{s}; \boldsymbol{\eta}, \Delta\boldsymbol{v}) = -R(\boldsymbol{v}, \boldsymbol{s}; \boldsymbol{\eta}) \qquad \forall\, \boldsymbol{\eta} \in \mathcal{V}. \tag{5.16}$$

5.3.2 The dual physical problem

Let $J(\cdot) : \mathcal{V} \to \mathbb{R}$ be a (possible nonlinear) quantity of interest for a given fixed $\boldsymbol{s}$. The optimal control approach from Section 5.2 is used with $\boldsymbol{x} = \boldsymbol{v}$ as the considered variable and $\mathcal{X} = \mathcal{V}$. This ends in the following constraint optimization problem:

$$\min_{\boldsymbol{v} \in \mathcal{V}} J(\boldsymbol{v}) \qquad \text{subject to} \qquad R(\boldsymbol{v}, \boldsymbol{s}; \boldsymbol{\eta}) = 0 \quad \forall\, \boldsymbol{\eta} \in \mathcal{V}. \tag{5.17}$$

Then, the Lagrangian functional reads

$$L(\boldsymbol{v}, \boldsymbol{z}) = J(\boldsymbol{v}) - R(\boldsymbol{v}, \boldsymbol{s}; \boldsymbol{z}) \tag{5.18}$$

and the optimality condition becomes

$$\left\{ \begin{array}{l} J'_v(\boldsymbol{v}; \delta\boldsymbol{v}) - R'_v(\boldsymbol{v}, \boldsymbol{s}; \boldsymbol{z}, \delta\boldsymbol{v}) \\ \\ \quad - R(\boldsymbol{v}, \boldsymbol{s}; \delta\boldsymbol{z}) \end{array} \right\} = \boldsymbol{0} \qquad \forall \{\delta\boldsymbol{v}, \delta\boldsymbol{z}\} \in \mathcal{V} \times \mathcal{V}. \tag{5.19}$$

The tangent form is the physical stiffness (4.87), i.e. $R'_v(\boldsymbol{v}, \boldsymbol{s}; \boldsymbol{z}, \cdot) = k(\boldsymbol{v}, \boldsymbol{s}; \boldsymbol{z}, \cdot)$. The first equation is the *dual physical problem*. Hence, the corresponding *dual physical solution* $\boldsymbol{z} \in \mathcal{V}$ is determined by

$$k(\boldsymbol{v}, \boldsymbol{s}; \boldsymbol{z}, \boldsymbol{\eta}) = J'_v(\boldsymbol{v}; \boldsymbol{\eta}) \qquad \forall\, \boldsymbol{\eta} \in \mathcal{V}. \tag{5.20}$$

The variation of J according to (5.11) is given from $J'_v(\boldsymbol{v}; \boldsymbol{\eta}) = \frac{d}{d\varepsilon} J(\boldsymbol{v} + \varepsilon\, \boldsymbol{\eta})\big|_{\varepsilon=0}$. The explicit form of $J'_v(\boldsymbol{v}; \cdot)$ depends on the chosen quantity of interest J.

With (5.16) and (5.20) and by using the symmetry of $k(\boldsymbol{v}, \boldsymbol{s}; \cdot, \cdot)$ we have

$$J'_v(\boldsymbol{v}; \Delta\boldsymbol{v}) = k(\boldsymbol{v}, \boldsymbol{s}; \boldsymbol{z}, \Delta\boldsymbol{v}) = -R(\boldsymbol{v}, \boldsymbol{s}; \boldsymbol{z}). \tag{5.21}$$

Finally, if the dual solution $\boldsymbol{z}$ is known, the change in the quantity of interest can be computed for arbitrary functionals $R(\cdot)$, i.e.

$$J'_v(\boldsymbol{v}; \Delta\boldsymbol{v}) = -R(\boldsymbol{v}, \boldsymbol{s}; \boldsymbol{z}). \tag{5.22}$$

We consider the discrete case. Let $J(\boldsymbol{v}_h) = v_i$ be the quantity of interest and let $\boldsymbol{z} \in \mathbb{R}^n$ be the vector with the discrete dual solution corresponding to v_i. Then, the discrete form of (5.22) for the change in the quantity of interest reads

$$\Delta v_i = -\boldsymbol{z}^T \boldsymbol{R}, \tag{5.23}$$

where $\boldsymbol{R} \in \mathbb{R}^n$ is the physical residual vector corresponding to $R(\boldsymbol{v}, \boldsymbol{s}; \cdot)$.

5.4 The material problem

In the same manner, a dual material problem can be introduced using the framework for duality techniques of variational equations. Furthermore, a duality relation for material quantities is proposed.

5.4.1 The primal material problem

The variational equation of the material problem is given in Eq. 4.8 and reads

$$G(\boldsymbol{v}, \boldsymbol{s}; \boldsymbol{\psi}) = 0 \qquad \forall\, \boldsymbol{\psi} \in \mathcal{S}.$$

In order to solve this nonlinear problem in a staggered way, we use the linearized equation (4.81) obtained in form of

$$m(\boldsymbol{v}, \boldsymbol{s}; \boldsymbol{\psi}, \Delta\boldsymbol{s}) = -G(\boldsymbol{v}, \boldsymbol{s}; \boldsymbol{\psi}) \qquad \forall\, \boldsymbol{\psi} \in \mathcal{S}. \tag{5.24}$$

The material tangent operator has been introduced as $m(\boldsymbol{v}, \boldsymbol{s}; \boldsymbol{\psi}, \Delta\boldsymbol{s}) := D_s G(\boldsymbol{v}, \boldsymbol{s}; \boldsymbol{\psi}) \cdot \Delta\boldsymbol{s}$, which has to be evaluated for the current $\{\boldsymbol{v}, \boldsymbol{s}\}$. This equation has to be solved in every Newton step in order to compute the increment $\Delta\boldsymbol{s}$.

5.4.2 The dual material problem

Let $J(\cdot) : \mathcal{S} \to \mathbb{R}$ be a quantity of interest for a given $\boldsymbol{v}(\boldsymbol{s})$. The optimal control approach from Sec. 5.2 with $\boldsymbol{x} = \boldsymbol{s}$ and $\mathcal{X} = \mathcal{S}$ ends in the following problem:

$$\min_{\boldsymbol{s}\in\mathcal{S}} J(\boldsymbol{s}) \qquad \text{subject to} \qquad G(\boldsymbol{v}, \boldsymbol{s}; \boldsymbol{\psi}) = 0 \quad \forall\, \boldsymbol{\psi} \in \mathcal{S}. \tag{5.25}$$

The corresponding Lagrangian functional reads

$$L(\boldsymbol{v}, \boldsymbol{s}, \boldsymbol{q}) = J(\boldsymbol{s}) - G(\boldsymbol{v}(\boldsymbol{s}), \boldsymbol{s}; \boldsymbol{q}) \tag{5.26}$$

and the first-order optimality condition follows in the form

$$\begin{aligned} L'(\boldsymbol{v}, \boldsymbol{s}, \boldsymbol{q})(\delta\boldsymbol{v}, \delta\boldsymbol{s}, \delta\boldsymbol{q}) &= L'_v(\boldsymbol{v}, \boldsymbol{s}, \boldsymbol{q})(\delta\boldsymbol{v}) + L'_s(\boldsymbol{v}, \boldsymbol{s}, \boldsymbol{q})(\delta\boldsymbol{s}) + L'_q(\boldsymbol{v}, \boldsymbol{s}, \boldsymbol{q})(\delta\boldsymbol{q}) \\ &= -G'_v(\boldsymbol{v}, \boldsymbol{s}; \boldsymbol{q}, \delta\boldsymbol{v}) + J'_s(\boldsymbol{s}; \delta\boldsymbol{s}) - G'_s(\boldsymbol{v}, \boldsymbol{s}; \boldsymbol{q}, \delta\boldsymbol{s}) \\ &\quad - G(\boldsymbol{v}, \boldsymbol{s}; \delta\boldsymbol{q}) = 0. \end{aligned} \tag{5.27}$$

By virtue of the relation between the total variation G' and the total partial variation $D_s G$ we can eliminate $\delta\boldsymbol{v}$ and obtain only a dependency on $\delta\boldsymbol{s}$, i.e.

$$\begin{aligned} G'(\boldsymbol{v}, \boldsymbol{s}; \boldsymbol{q})(\delta\boldsymbol{v}, \delta\boldsymbol{s}) &= G'_v(\boldsymbol{v}, \boldsymbol{s}; \boldsymbol{q}, \delta\boldsymbol{v}) + G'_s(\boldsymbol{v}, \boldsymbol{s}; \boldsymbol{q}, \delta\boldsymbol{s}) \\ &= m(\boldsymbol{v}, \boldsymbol{s}; \boldsymbol{q}, \delta\boldsymbol{s}) = D_s G(\boldsymbol{v}(\boldsymbol{s}), \boldsymbol{s}; \boldsymbol{q}) \cdot \delta\boldsymbol{s}. \end{aligned} \tag{5.28}$$

The optimality condition can be written as

$$L' = J'_s(\boldsymbol{s}; \delta\boldsymbol{s}) - m(\boldsymbol{v}, \boldsymbol{s}; \boldsymbol{q}, \delta\boldsymbol{s}) - G(\boldsymbol{v}, \boldsymbol{s}; \delta\boldsymbol{q}) = 0. \tag{5.29}$$

Under the assumption that $\delta\boldsymbol{s}$ and $\delta\boldsymbol{q}$ are independent variations we obtain the system

$$\left\{ \begin{array}{l} J'_s(\boldsymbol{s}; \delta\boldsymbol{s}) - m(\boldsymbol{v}, \boldsymbol{s}; \boldsymbol{q}, \delta\boldsymbol{s}) \\ \\ - G(\boldsymbol{v}, \boldsymbol{s}; \delta\boldsymbol{q}) \end{array} \right\} = \boldsymbol{0} \qquad \forall \{\delta\boldsymbol{s}, \delta\boldsymbol{q}\} \in \mathcal{S} \times \mathcal{S}. \tag{5.30}$$

The first equation is the *dual material problem*: Find the *dual material solution* $\boldsymbol{q} \in \mathcal{S}$ such that

$$m(\boldsymbol{v}, \boldsymbol{s}; \boldsymbol{q}, \boldsymbol{\psi}) = J'_s(\boldsymbol{s}; \boldsymbol{\psi}) \qquad \forall\, \boldsymbol{\psi} \in \mathcal{S}. \tag{5.31}$$

The second equation is just the primal material residual (4.8).

The variation of J according to (5.11) is given from $J'_s(\boldsymbol{s}; \boldsymbol{\psi}) = \frac{d}{d\varepsilon} J(\boldsymbol{s} + \varepsilon\, \boldsymbol{\psi})\big|_{\varepsilon=0}$. By using (5.24) and (5.31) as well as the symmetry of $m(\boldsymbol{v}, \boldsymbol{s}; \cdot, \cdot)$ we have

$$J'_s(\boldsymbol{s}; \Delta\boldsymbol{s}) = m(\boldsymbol{v}, \boldsymbol{s}; \boldsymbol{q}, \Delta\boldsymbol{s}) = -G(\boldsymbol{v}, \boldsymbol{s}; \boldsymbol{q}). \tag{5.32}$$

If the dual solution $\boldsymbol{q}$ is known $J'_s(\boldsymbol{s}; \Delta\boldsymbol{s})$ can be computed for any functionals $G(\cdot)$.

We consider the discrete case. Let $J(\boldsymbol{s}_h) = s_i$ be the quantity of interest and let $\boldsymbol{q} \in \mathbb{R}^m$ be the vector with the discrete dual solution corresponding to s_i. Then, the discrete form of (5.32) for the change in the quantity of interest reads

$$\Delta s_i = -\boldsymbol{q}^T \boldsymbol{G}, \tag{5.33}$$

where $\boldsymbol{G} \in \mathbb{R}^m$ is the material residual vector corresponding to $G(\boldsymbol{v}, \boldsymbol{s}; \cdot)$.

5.5 The coupled problem

As for the physical and material problems, a dual problem and a duality relation can be also established for the coupled physical and material problem. We use the notation from Section 4.5.1, i.e. we set $\boldsymbol{y} = \{\boldsymbol{v}, \boldsymbol{s}\} \in \mathcal{Y}$, $\Delta\boldsymbol{y} = \{\Delta\boldsymbol{v}, \Delta\boldsymbol{s}\} \in \mathcal{Y}$ as well as $\boldsymbol{\phi} = \{\boldsymbol{\eta}, \boldsymbol{\psi}\} \in \mathcal{Y}$, where $\mathcal{Y} := \mathcal{V} \times \mathcal{S}$.

5.5.1 The primal coupled problem

The variational equation of the coupled primal physical (4.7) and material problem (4.8) is given in (4.65) as

$$B(\boldsymbol{y}; \boldsymbol{\phi}) = R(\boldsymbol{v}, \boldsymbol{s}; \boldsymbol{\eta}) + G(\boldsymbol{v}, \boldsymbol{s}; \boldsymbol{\psi}) = 0 \qquad \forall\, \boldsymbol{\phi} \in \mathcal{Y}.$$

The solution of this problem ends in the linearized equation (4.67) given by

$$h(\boldsymbol{y}; \boldsymbol{\phi}, \Delta\boldsymbol{y}) = -B(\boldsymbol{y}; \boldsymbol{\phi}) \qquad \forall\, \boldsymbol{\phi} \in \mathcal{Y}, \tag{5.34}$$

where the Hessian $h(\boldsymbol{y}; \boldsymbol{\phi}, \Delta\boldsymbol{y})$ is given in (4.69). This equations has to be solved in each Newton step in order to compute the increment $\Delta\boldsymbol{y}$.

5.5.2 The dual coupled problem

Let $J(\cdot) : \mathcal{Y} \to \mathbb{R}$ be a quantity of interest. Then, we have to solve the following optimization problem:

$$\min_{\boldsymbol{y} \in \mathcal{Y}} J(\boldsymbol{y}) \qquad \text{subject to} \qquad B(\boldsymbol{y}; \boldsymbol{\phi}) = 0 \quad \forall\, \boldsymbol{\phi} \in \mathcal{Y}. \tag{5.35}$$

The corresponding Lagrangian functional is given by

$$L(\boldsymbol{y}; \boldsymbol{y}^*) = J(\boldsymbol{y}) - B(\boldsymbol{y}; \boldsymbol{y}^*) = J(\boldsymbol{v}, \boldsymbol{s}) - R(\boldsymbol{v}, \boldsymbol{s}; \boldsymbol{z}_c) - G(\boldsymbol{v}, \boldsymbol{s}; \boldsymbol{q}_c). \tag{5.36}$$

Here, $\boldsymbol{y}^* := \{\boldsymbol{z}_c, \boldsymbol{q}_c\} \in \mathcal{Y}$ is the dual or adjoint solution for the coupled problem, in which $\boldsymbol{z}_c \in \mathcal{V}$ is the dual solution for the physical problem and $\boldsymbol{q}_c \in \mathcal{S}$ the corresponding dual solution for the material problem. The index c indicates that the coupled problem is considered. We seek for stationary points of L which are candidates for optimal solutions of

$$L'(\boldsymbol{y}; \boldsymbol{y}^*)(\delta\boldsymbol{y}, \delta\boldsymbol{y}^*) = 0.$$

This leads to the following problem. Find $\boldsymbol{w} := \{\boldsymbol{v}, \boldsymbol{s}, \boldsymbol{z}_c, \boldsymbol{q}_c\} \in \mathcal{V} \times \mathcal{S} \times \mathcal{V} \times \mathcal{S}$ such that

$$\left\{ \begin{array}{l} L'_v(\boldsymbol{w})(\delta\boldsymbol{v}) \\ L'_s(\boldsymbol{w})(\delta\boldsymbol{s}) \\ L'_z(\boldsymbol{w})(\delta\boldsymbol{z}_c) \\ L'_q(\boldsymbol{w})(\delta\boldsymbol{q}_c) \end{array} \right\} = \left\{ \begin{array}{l} J'_v(\boldsymbol{v}, \boldsymbol{s}; \delta\boldsymbol{v}) - R'_v(\boldsymbol{v}, \boldsymbol{s}; \boldsymbol{z}_c, \delta\boldsymbol{v}) - G'_v(\boldsymbol{v}, \boldsymbol{s}; \boldsymbol{q}_c, \delta\boldsymbol{v}) \\ J'_s(\boldsymbol{v}, \boldsymbol{s}; \delta\boldsymbol{s}) - R'_s(\boldsymbol{v}, \boldsymbol{s}; \boldsymbol{z}_c, \delta\boldsymbol{s}) - G'_s(\boldsymbol{v}, \boldsymbol{s}; \boldsymbol{q}_c, \delta\boldsymbol{s}) \\ - R(\boldsymbol{v}, \boldsymbol{s}; \delta\boldsymbol{z}_c) \\ - G(\boldsymbol{v}, \boldsymbol{s}; \delta\boldsymbol{q}_c) \end{array} \right\} = \boldsymbol{0} \quad (5.37)$$

$\forall\, \{\delta\boldsymbol{v}, \delta\boldsymbol{s}, \delta\boldsymbol{z}_c, \delta\boldsymbol{q}_c\} \in \mathcal{V} \times \mathcal{S} \times \mathcal{V} \times \mathcal{S}$. The last two equations are just the primal physical and material problems given in (4.7) and (4.8).

The first two equations yield the *dual coupled problem*, which is given using the definition of the Hessian (4.69) as

$$\left\{ \begin{array}{l} k(\boldsymbol{v}, \boldsymbol{s}; \boldsymbol{z}_c, \delta\boldsymbol{v}) + p(\boldsymbol{v}, \boldsymbol{s}; \delta\boldsymbol{v}, \boldsymbol{q}_c) = J'_v(\boldsymbol{v}, \boldsymbol{s}; \delta\boldsymbol{v}) \\ p(\boldsymbol{v}, \boldsymbol{s}; \boldsymbol{z}_c, \delta\boldsymbol{s}) + d(\boldsymbol{v}, \boldsymbol{s}; \boldsymbol{q}_c, \delta\boldsymbol{s}) = J'_s(\boldsymbol{v}, \boldsymbol{s}; \delta\boldsymbol{s}) \end{array} \right\}, \quad (5.38)$$

compare with the linearized primal coupled problem (4.70). Let $J'(\boldsymbol{y}; \delta\boldsymbol{y})$ be the total variation of the functional J, i.e.

$$J'(\boldsymbol{y}; \delta\boldsymbol{y}) := J'_v(\boldsymbol{v}, \boldsymbol{s}; \delta\boldsymbol{v}) + J'_s(\boldsymbol{v}, \boldsymbol{s}; \delta\boldsymbol{s}). \quad (5.39)$$

Then, the dual coupled problem is given as follows. Find the dual solution $\boldsymbol{y}^* \in \mathcal{Y}$ such that

$$h(\boldsymbol{y}; \boldsymbol{y}^*, \boldsymbol{\phi}) = J'(\boldsymbol{y}; \boldsymbol{\phi}) \qquad \forall\, \boldsymbol{\phi} \in \mathcal{Y}. \quad (5.40)$$

Finally, a duality relation for the coupled problem is obtained by using (5.34) and (5.40) as well as the symmetry of $h(\boldsymbol{y}; \cdot, \cdot)$ in form of

$$J'(\boldsymbol{y}; \Delta\boldsymbol{y}) = h(\boldsymbol{y}; \boldsymbol{y}^*, \Delta\boldsymbol{y}) = -B(\boldsymbol{y}; \boldsymbol{y}^*). \quad (5.41)$$

This equation can be evaluated for arbitrary residuals $B(\boldsymbol{y}; \cdot)$ if the corresponding dual solutions $\boldsymbol{y}^* = \{\boldsymbol{z}_c, \boldsymbol{q}_c\}$ are known. The result is the total change in the quantity of interest with respect to $\boldsymbol{v}$ and $\boldsymbol{s}$. The index c indicates that the dual solutions are obtained using the coupled system. Note, that these dual solutions differ in general from the results which are obtained with (5.20) and (5.31), respectively. Because the consecutive solution of (5.20) and

(5.31) is part of a staggered solution scheme, i.e. a decoupled algorithm, and the increments $\{\Delta\boldsymbol{v}, \Delta\boldsymbol{s}\}$ differ from the results of (5.34).

We consider the discrete formulation in order to make the above relations more transparent. Let $J(\boldsymbol{y}_h) = y_i$ be the quantity of interest. Then, the discrete dual solution $\boldsymbol{y}^* = [\boldsymbol{z}_c^T \ \boldsymbol{q}_c^T]^T$ is the solution of the discrete version of (5.40) given as

$$\begin{bmatrix} \boldsymbol{K} & \boldsymbol{P} \\ \boldsymbol{P}^T & \boldsymbol{D} \end{bmatrix} \begin{bmatrix} \boldsymbol{z}_c \\ \boldsymbol{q}_c \end{bmatrix} = \begin{bmatrix} \boldsymbol{J}_v \\ \boldsymbol{J}_s \end{bmatrix}, \tag{5.42}$$

where $\boldsymbol{J}_v$ and $\boldsymbol{J}_s$ are the discrete vectors corresponding to the functionals $J'_v(\boldsymbol{y}; \cdot)$ and $J'_s(\boldsymbol{y}; \cdot)$, respectively.

The discrete version of the duality relation (5.41) reads

$$\Delta y_i = -\boldsymbol{y}^{*T} \boldsymbol{B} = -[\, \boldsymbol{z}_c^T \boldsymbol{R} + \boldsymbol{q}_c^T \boldsymbol{G} \,]. \tag{5.43}$$

Finally, if the dual solution $\boldsymbol{y}^*$ is known the total change in the quantity of interest can be computed for arbitrary residuals $\boldsymbol{B} = [\boldsymbol{R}^T \ \boldsymbol{G}^T]^T$.

Remark 5.2 (Energy as quantity of interest) *If we choose the overall primal potential energy E as quantity of interest, i.e. $J(\boldsymbol{v}, \boldsymbol{s}) = E(\boldsymbol{v}, \boldsymbol{s})$, the right hand side of (5.40) becomes*

$$J'(\boldsymbol{y}; \delta\boldsymbol{y}) = J'_v(\boldsymbol{v}, \boldsymbol{s}; \delta\boldsymbol{v}) + J'_s(\boldsymbol{v}, \boldsymbol{s}; \delta\boldsymbol{s}) = R(\boldsymbol{v}, \boldsymbol{s}; \delta\boldsymbol{v}) + G(\boldsymbol{v}, \boldsymbol{s}; \delta\boldsymbol{s}) = 0. \tag{5.44}$$

Hence, the dual solution $\boldsymbol{y}^*$ vanishes and the optimality condition (5.37) is reduced to the optimality condition of the primal physical problem (4.6).

5.6 An illustrative example

A plate with a slit loaded by a body load $\boldsymbol{b}_R$ is considered as indicated in Fig. 5.1a. The physical quantity of interest is the vertical component of the nodal displacement at a given point $\boldsymbol{P}$, i.e. $J(\boldsymbol{v}_h) = u_2(\boldsymbol{P})$. The material quantity of interest is the vertical component of the nodal coordinate at $\boldsymbol{P}$, i.e. $J(\boldsymbol{s}_h) = X_2(\boldsymbol{P})$.

The approximate dual solutions $\boldsymbol{z}_h$ and $\boldsymbol{q}_h$ are computed using the finite element method and the shown mesh by solving (5.20) and (5.31), respectively. The dual loads for the chosen quantities of interest are just unit loads in vertical direction.

The vertical component of the dual physical solution $\boldsymbol{z}_h$ and the dual material solution $\boldsymbol{q}_h$ are given in Fig. 5.1b and Fig. 5.1c, respectively. The dual solutions reflect the influence of the considered residual on the change in the physical and material quantity of interest, respectively. For instance, a large value of $\boldsymbol{z}$ in a certain domain Ω_i indicates that a physical residual in Ω_i causes a large change in u_2. In the same manner, a large value of $\boldsymbol{q}$ in Ω_i indicates that a material residual in Ω_i causes a large change in X_2. Hence, the dual solutions are the influence functions for the considered physical and material quantity, respectively.

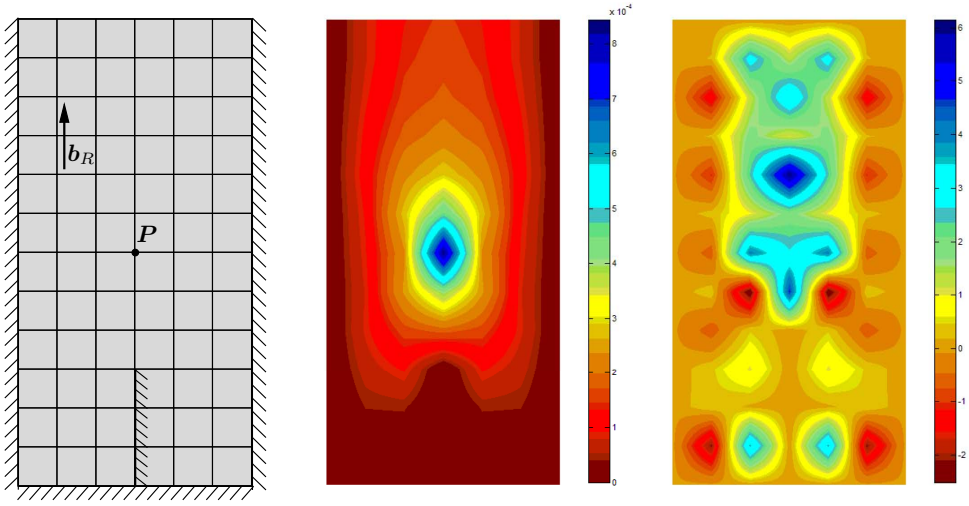

(a) primal problem

(b) dual physical solution z_2 for $J(\boldsymbol{v}_h) = u_2(\boldsymbol{P})$

(c) dual material solution q_2 for $J(\boldsymbol{s}_h) = X_2(\boldsymbol{P})$

Figure 5.1: Plate with a slit loaded by a body force $\boldsymbol{b}_R$: the dual physical solution $\boldsymbol{z}_h$ and the dual material solution $\boldsymbol{q}_h$ in vertical direction

5.7 Summary and concluding remarks

Duality techniques for the physical and material problems as well as for the coupled problem based on variational principles have been proposed. This was based on an optimal control approach, which yields the general framework for duality relations of variational equations. The form of the dual problem and the corresponding dual solution depend on the kind of the considered variational problem. The derived duality (sensitivity) relations are summarized in Box 5.1.

The dual problems in the physical and material spaces are always linear problems and formulated at the current linearization points $\{\boldsymbol{v}, \boldsymbol{s}\}$, i.e. at a given deformed state. If the dual solutions are known, a quantity of interest can be computed for arbitrary physical and material residuals, respectively.

The duality relations can be also interpreted as *sensitivity relations*, because they express the sensitivity of the considered quantity of interest with respect changes in the corresponding residual. For instance, for (5.22) we can write

$$\delta v_i = -\boldsymbol{z}^T \delta \boldsymbol{R}, \tag{5.45}$$

where $\delta \boldsymbol{R}$ denotes the variation in the physical residual. The variation in the quantity of interest δv_i is coupled with the variation $\delta \boldsymbol{R}$ by the dual solution or influence function $\boldsymbol{z}$. With this in mind, $\boldsymbol{z}$ could also be termed as *sensitivity function* .

	physical problem	
	variational	discrete
quantity of interest	$J(\boldsymbol{v}) = v_i$	$J(\boldsymbol{v}_h) = v_{h_i}$
primal physical problem	$R(\boldsymbol{v}, \boldsymbol{s}; \boldsymbol{\eta}) = 0$	$\boldsymbol{\eta}^T \boldsymbol{R}(\boldsymbol{v}, \boldsymbol{s}) = 0$
linearized primal problem	$k(\boldsymbol{v}, \boldsymbol{s}; \boldsymbol{\eta}, \Delta\boldsymbol{v}) = -R(\boldsymbol{v}, \boldsymbol{s}; \boldsymbol{\eta})$	$\boldsymbol{\eta}^T \boldsymbol{K} \Delta\boldsymbol{v} = -\boldsymbol{\eta}^T \boldsymbol{R}$
dual physical problem	$k(\boldsymbol{v}, \boldsymbol{s}; \boldsymbol{z}, \boldsymbol{\eta}) = J'_v(\boldsymbol{v}; \boldsymbol{\eta})$	$\boldsymbol{\eta}^T \boldsymbol{K} \boldsymbol{z} = \boldsymbol{\eta}^T \boldsymbol{J}_u$
duality (sensitivity) relation	$J'_v(\boldsymbol{v}; \Delta\boldsymbol{v}) = -R(\boldsymbol{v}, \boldsymbol{s}; \boldsymbol{z})$	$\Delta v_i = -\boldsymbol{z}^T \boldsymbol{R}$

	material problem	
	variational	discrete
quantity of interest	$J(\boldsymbol{s}) = s_i$	$J(\boldsymbol{s}_h) = s_{h_i}$
primal material problem	$G(\boldsymbol{v}(\boldsymbol{s}), \boldsymbol{s}; \boldsymbol{\psi}) = 0$	$\boldsymbol{\psi}^T \boldsymbol{G}(\boldsymbol{v}(\boldsymbol{s}), \boldsymbol{s}) = 0$
linearized primal problem	$m(\boldsymbol{v}, \boldsymbol{s}; \boldsymbol{\psi}, \Delta\boldsymbol{s}) = -G(\boldsymbol{v}, \boldsymbol{s}; \boldsymbol{\psi})$	$\boldsymbol{\psi}^T \boldsymbol{M} \Delta\boldsymbol{s} = -\boldsymbol{\psi}^T \boldsymbol{G}$
dual material problem	$m(\boldsymbol{v}, \boldsymbol{s}; \boldsymbol{q}, \boldsymbol{\psi}) = J'_s(\boldsymbol{s}; \boldsymbol{\psi})$	$\boldsymbol{\psi}^T \boldsymbol{M} \boldsymbol{q} = \boldsymbol{\psi}^T \boldsymbol{J}_s$
duality (sensitivity) relation	$J'_s(\boldsymbol{s}; \Delta\boldsymbol{s}) = -G(\boldsymbol{v}, \boldsymbol{s}; \boldsymbol{q})$	$\Delta s_i = -\boldsymbol{q}^T \boldsymbol{G}$

	coupled physical and material problem	
	variational	discrete
quantity of interest	$J(\boldsymbol{y}) = y_i$	$J(\boldsymbol{y}_h) = y_{h_i}$
primal coupled problem	$B(\boldsymbol{y}; \boldsymbol{\phi}) = 0$	$\boldsymbol{\phi}^T \boldsymbol{B} = \boldsymbol{\eta}^T \boldsymbol{R} + \boldsymbol{\psi}^T \boldsymbol{G} = 0$
linearized primal problem	$h(\boldsymbol{y}; \boldsymbol{\phi}, \Delta\boldsymbol{y}) = -B(\boldsymbol{y}; \boldsymbol{\phi})$	$\boldsymbol{\phi}^T \boldsymbol{H} \Delta\boldsymbol{y} = -\boldsymbol{\phi}^T \boldsymbol{B}$
dual coupled problem	$h(\boldsymbol{y}; \boldsymbol{y}^*, \boldsymbol{\phi}) = J'(\boldsymbol{y}; \boldsymbol{\phi})$	$\boldsymbol{\phi}^T \boldsymbol{H} \boldsymbol{y}^* = \boldsymbol{\phi}^T \boldsymbol{J}'$
duality (sensitivity) relation	$J'(\boldsymbol{y}; \Delta\boldsymbol{y}) = -B(\boldsymbol{y}; \boldsymbol{y}^*)$	$\Delta y_i = -\boldsymbol{y}^{*T} \boldsymbol{B}$ $= -[\, \boldsymbol{z}_c^T \boldsymbol{R} + \boldsymbol{q}_c^T \boldsymbol{G} \,]$

Box 5.1: Summary of variational and discrete duality relations

Chapter 6

Structural and sensitivity analysis of the dual problem

Variations in the physical and material spaces are considered for the dual problem. Based on an energy functional of the dual problem, balance laws and sensitivity relations for the dual solution itself as well as for a chosen quantity of interest are derived. The dual problem is embedded in the same framework as the primal problem and novel complete variational and discrete formulations for elasticity are proposed.

6.1 Introduction

As mentioned in Section 5.1, the dual physical problem plays an important role in structural mechanics as well as in computational methods for the computation of local quantities of interest, such as pointwise stresses and displacements or average stresses, see e.g. [51]. Furthermore, the concept of duality is essential within goal-oriented error analysis and mesh optimization techniques [4], see Section 8.1 and Section 8.2.1. But usually only variations with respect to the state are considered. As far as the author knows, configurational variations for the dual problem itself have not been studied so far.

The goal is now to embed the dual problem in the same framework as the primal problem. To achieve this, we introduce in addition to the usual primal energy functional $E(\boldsymbol{v}, \boldsymbol{s})$ an energy functional E^* and a strain energy function W_R^* for the dual problem. The variation of the dual energy with respect to configurational changes yields a novel *energy-momentum tensor for the dual problem*. In addition, a sensitivity relation for the dual solution itself is proposed, i.e. we are interested in the change of the dual solution due to configurational changes. The error in a chosen quantity of interest depends on the error in the corresponding dual solution. In this context, it is of interest to study the sensitivity of the dual solution and the quantity of interest. Some parts of this chapter are published in [71].

6.2 Energy minimization and variational balance laws

6.2.1 The dual problem

The dual physical problem has been introduced in Section 5.3.2 in (5.20). The dual problem corresponding to the chosen quantity of interest $J(\boldsymbol{v}, \boldsymbol{s})$ is formulated at the current linearization point, i.e. on a given deformed state $\boldsymbol{v}$. The dual solution $\boldsymbol{z} \in \mathcal{V}$ is determined by the linear equation

$$k(\boldsymbol{v}, \boldsymbol{s}; \boldsymbol{z}, \boldsymbol{\eta}) = J'_v(\boldsymbol{v}, \boldsymbol{s}; \boldsymbol{\eta}) \qquad \forall\, \boldsymbol{\eta} \in \mathcal{V}. \tag{6.1}$$

We introduce first an energy functional of the dual problem in order to use the same framework as for the primal problem.

6.2.2 The dual energy functional

Let $E^*(\boldsymbol{v})(\boldsymbol{z}, \boldsymbol{s})$ be the total potential energy of the dual problem. The energy depends on the state function $\boldsymbol{v} \in \mathcal{V}$ because the problem is formulated on a given deformed configuration. Furthermore, the energy depends on the same design function $\boldsymbol{s} \in \mathcal{S}$ as the state. We assume, that $J(\boldsymbol{v})$ is a regularized functional and well defined on $\mathcal{V}$. Then, the dual solution $\boldsymbol{z} \in \mathcal{V}$ is a minimizer of the corresponding energy functional of the dual problem

$$E^*(\boldsymbol{v})(\boldsymbol{z}, \boldsymbol{s}) := C^*(\boldsymbol{v})(\boldsymbol{z}, \boldsymbol{s}) - J'_v(\boldsymbol{v}, \boldsymbol{s}; \boldsymbol{z}), \tag{6.2}$$

where $C^*(\boldsymbol{v})(\boldsymbol{z}, \boldsymbol{s})$ denotes the *internal energy of the dual problem*. Furthermore, the functional $J'_v(\boldsymbol{v}, \boldsymbol{s}; \boldsymbol{z})$ contains the external potential energy, in which the explicit form of J'_v depends on the chosen quantity of interest.

By means of $k(\boldsymbol{v}, \boldsymbol{s}; \cdot, \cdot)$ given in (4.87), we introduce the *strain energy function of the dual problem*

$$W^*_R(\boldsymbol{v}, \boldsymbol{z}) := \frac{1}{2} \left[\mathbf{S}(\boldsymbol{v}) : \mathbf{E}''_{vv}(\boldsymbol{z}, \boldsymbol{z}) + \mathbf{E}'_v(\boldsymbol{v}, \boldsymbol{z}) : \mathbb{C} : \mathbf{E}'_v(\boldsymbol{v}, \boldsymbol{z}) \right] \tag{6.3}$$

such that the internal energy of the dual problem is given as

$$C^*(\boldsymbol{v})(\boldsymbol{z}, \boldsymbol{s}) := \frac{1}{2}\, k(\boldsymbol{v}, \boldsymbol{s}; \boldsymbol{z}, \boldsymbol{z}) = \int_{\Omega_R} W^*_R(\boldsymbol{v}, \boldsymbol{z})\, \mathrm{d}\Omega. \tag{6.4}$$

The energy functional of the dual problem $E^*(\boldsymbol{v})(\boldsymbol{z}, \boldsymbol{s})$ is constructed at a given deformed state and describes an energy quantity due to the linear dual solution $\boldsymbol{z}$ at this point.

Remark 6.1 (Construction of the dual energy functional) *The dual problem is formulated at a given deformed state $\boldsymbol{v}$ and the dual energy functional $E^*(\boldsymbol{v})(\boldsymbol{z}, \boldsymbol{s})$ is chosen in such a way that $E^{*\prime}_z(\boldsymbol{v})(\boldsymbol{z}, \boldsymbol{s})(\boldsymbol{\eta}) = k(\boldsymbol{v}, \boldsymbol{s}; \boldsymbol{z}, \boldsymbol{\eta}) - J'_v(\boldsymbol{v}, \boldsymbol{s}; \boldsymbol{\eta})$, i.e. the partial variation of E^* with respect to $\boldsymbol{z}$ yields just the variational dual problem (6.1).*

6.2.3 The dual physical and material residuals

The minimization of the dual energy with respect to $\boldsymbol{z}$ and $\boldsymbol{s}$ ends in the following minimization problem.

Problem 6.1 *Find $\{\boldsymbol{z}, \boldsymbol{s}\} \in \mathcal{V} \times \mathcal{S}$ such that the dual energy functional (6.2) is minimized, i.e.*

$$E^*(\boldsymbol{v})(\boldsymbol{z}, \boldsymbol{s}) = \min_{\{\boldsymbol{q},\boldsymbol{r}\}\in\mathcal{V}\times\mathcal{S}} E^*(\boldsymbol{v})(\boldsymbol{q}, \boldsymbol{r}). \tag{6.5}$$

The first-order optimality condition results in the following problem. Find $\{\boldsymbol{z}, \boldsymbol{s}\} \in \mathcal{V} \times \mathcal{S}$ such that

$$\left\{ \begin{array}{l} E_z^{*\prime}(\boldsymbol{v})(\boldsymbol{z}, \boldsymbol{s})(\boldsymbol{\eta}) \\ \\ E_s^{*\prime}(\boldsymbol{v})(\boldsymbol{z}, \boldsymbol{s})(\boldsymbol{\psi}) \end{array} \right\} = \left\{ \begin{array}{l} R^*(\boldsymbol{v}, \boldsymbol{s}; \boldsymbol{z}, \boldsymbol{\eta}) \\ \\ G^*(\boldsymbol{v}, \boldsymbol{s}; \boldsymbol{z}; \boldsymbol{\psi}) \end{array} \right\} = \boldsymbol{0} \qquad \forall \{\boldsymbol{\eta}, \boldsymbol{\psi}\} \in \mathcal{V} \times \mathcal{S}. \tag{6.6}$$

The partial variation of E^* with respect to $\boldsymbol{z}$ yields the *dual physical residual* $R^* : \mathcal{V} \to \mathbb{R}$ given as

$$R^*(\boldsymbol{v}, \boldsymbol{s}; \boldsymbol{z}, \boldsymbol{\eta}) := E_z^{*\prime}(\boldsymbol{v})(\boldsymbol{z}, \boldsymbol{s})(\boldsymbol{\eta}) = k(\boldsymbol{v}, \boldsymbol{s}; \boldsymbol{z}, \boldsymbol{\eta}) - J_v'(\boldsymbol{v}, \boldsymbol{s}; \boldsymbol{\eta}). \tag{6.7}$$

This is just the variational equation (6.1) for the dual problem. A variation with respect to changes in the design $\boldsymbol{s}$ leads to the *dual material residual* $G^* : \mathcal{S} \to \mathbb{R}$ in the form

$$G^*(\boldsymbol{v}, \boldsymbol{s}; \boldsymbol{z}; \boldsymbol{\psi}) := E_s^{*\prime}(\boldsymbol{v})(\boldsymbol{z}, \boldsymbol{s})(\boldsymbol{\psi}) = \frac{1}{2}\, k_s'(\boldsymbol{v}, \boldsymbol{s}; \boldsymbol{z}; \boldsymbol{\psi}) - J_{vs}''(\boldsymbol{v}, \boldsymbol{s}; \boldsymbol{z}, \boldsymbol{\psi}). \tag{6.8}$$

The dual material residual G^* represents the sensitivity of the energy functional $E^*(\boldsymbol{v})(\boldsymbol{z}, \boldsymbol{s})$ with respect to changes in the design $\boldsymbol{s}$. The change in the design causes a change in the gradients of the state $\boldsymbol{v}$ and therefore a change in the dual solution at this state. Finally, this ends in a change of the energy functional of the dual problem.

Remark 6.2 (Linear vs. nonlinear arguments) *The dual problem is a linear problem and the bilinear form $k(\boldsymbol{v}, \boldsymbol{s}; \boldsymbol{z}, \cdot)$ in the dual physical residual (6.7) is linear with respect to all arguments right from the semicolon. The variables left from the semicolon are the current evaluation points. In contrast, in the dual material residual (6.8), the dual solution $\boldsymbol{z}$ appears as a quadratic term, because the variation of the strain energy of the dual problem (6.3) with respect to $\boldsymbol{s}$ is still quadratic in $\boldsymbol{z}$. This important fact is indicated by the second semicolon in $k_s'(\boldsymbol{v}, \boldsymbol{s}; \boldsymbol{z}; \cdot)$, i.e.*

$$k_s'(\boldsymbol{v}, \boldsymbol{s}; \boldsymbol{z}; \cdot) := k_s'(\boldsymbol{v}, \boldsymbol{s}; \boldsymbol{z}, \boldsymbol{z}, \cdot), \tag{6.9}$$

Hence, in this semilinear form only the arguments right from the second semicolon are linear.

6.3 Variational sensitivity analysis

In the same manner as for the primal problem in Section 4.3, the sensitivities of the energy and the residuals are investigated. Furthermore, a sensitivity relation for the quantitiy of interest is considered.

6.3.1 Sensitivity of the energy functional

The sensitivity of the dual energy functional (6.2) is given as the total variation with respect to $\boldsymbol{z}$ and $\boldsymbol{s}$, i.e.

$$\begin{aligned} \delta E^* &= \delta_z E^*(\boldsymbol{v})(\boldsymbol{z},\boldsymbol{s})(\delta\boldsymbol{z}) + \delta_s E^*(\boldsymbol{v})(\boldsymbol{z},\boldsymbol{s})(\delta\boldsymbol{s}) \\ &= R^*(\boldsymbol{v},\boldsymbol{s};\boldsymbol{z},\delta\boldsymbol{z}) + G^*(\boldsymbol{v},\boldsymbol{s};\boldsymbol{z};\delta\boldsymbol{s}). \end{aligned} \tag{6.10}$$

For a given solution $\boldsymbol{z} \in \mathcal{V}$ of (6.1) we have $R^*(\boldsymbol{v},\boldsymbol{s};\boldsymbol{z},\delta\boldsymbol{z}) = 0$. Hence, the first contribution vanishes and the sensitivity relation becomes

$$\delta E^* = \delta_s E^*(\boldsymbol{v})(\boldsymbol{z},\boldsymbol{s})(\delta\boldsymbol{s}) = G^*(\boldsymbol{v},\boldsymbol{s};\boldsymbol{z};\delta\boldsymbol{s}). \tag{6.11}$$

Therefore, the dual material residual G^* can be interpreted as the sensitivity of the dual energy E^* with respect to configurational variations $\delta\boldsymbol{s}$.

6.3.2 Sensitivity of the physical residual

The change in the design yields a change in the state and in the quantity of interest as well as in the dual solution. In order to establish a sensitivity relation for the dual solution, we consider the dual physical residual $R^* = 0$ given in (6.7). The total variation reads

$$R^{*\prime} = R^{*\prime}_z(\boldsymbol{v},\boldsymbol{s};\delta\boldsymbol{z},\boldsymbol{\eta}) + R^{*\prime}_s(\boldsymbol{v},\boldsymbol{s};\boldsymbol{z},\boldsymbol{\eta},\delta\boldsymbol{s}) = 0. \tag{6.12}$$

The variation consists of two parts. Due to the fact that R^* is linear in $\boldsymbol{z}$ we have

$$k^*(\boldsymbol{v},\boldsymbol{s};\delta\boldsymbol{z},\boldsymbol{\eta}) := R^{*\prime}_z(\boldsymbol{v},\boldsymbol{s};\delta\boldsymbol{z},\boldsymbol{\eta}) = k(\boldsymbol{v},\boldsymbol{s};\delta\boldsymbol{z},\boldsymbol{\eta}). \tag{6.13}$$

Hence, the first part is the tangent stiffness operator $k(\cdot,\cdot)$ from (4.87). The second part is the *dual tangent pseudo load operator*

$$\begin{aligned} p^*(\boldsymbol{v},\boldsymbol{s};\boldsymbol{z},\boldsymbol{\eta},\delta\boldsymbol{s}) &:= R^{*\prime}_s(\boldsymbol{v},\boldsymbol{s};\boldsymbol{z},\boldsymbol{\eta},\delta\boldsymbol{s}) \\ &= k'_s(\boldsymbol{v},\boldsymbol{s};\boldsymbol{z},\boldsymbol{\eta},\delta\boldsymbol{s}) - J''_{vs}(\boldsymbol{v},\boldsymbol{s};\boldsymbol{\eta},\delta\boldsymbol{s}). \end{aligned} \tag{6.14}$$

This is a bilinear form $p^* : \mathcal{V} \times \mathcal{S} \to \mathbb{R}$. With these, (6.12) becomes

$$R^{*\prime} = k(\boldsymbol{v},\boldsymbol{s};\delta\boldsymbol{z},\boldsymbol{\eta}) + p^*(\boldsymbol{v},\boldsymbol{s};\boldsymbol{z},\boldsymbol{\eta},\delta\boldsymbol{s}) = 0. \tag{6.15}$$

A rearrangement of (6.15) leads to the following variational problem.

Problem 6.2 *Let $\delta\hat{\boldsymbol{s}} \in \mathcal{S}$ be a given fixed design variation. Find $\delta\boldsymbol{z} \in \mathcal{V}$ such that*

$$k(\boldsymbol{v}, \boldsymbol{s}; \delta\boldsymbol{z}, \boldsymbol{\eta}) = -Q_p^*(\boldsymbol{v}, \boldsymbol{s}; \boldsymbol{z}, \boldsymbol{\eta}) \quad \forall\, \boldsymbol{\eta} \in \mathcal{V}, \tag{6.16}$$

where

$$Q_p^*(\boldsymbol{v}, \boldsymbol{s}; \boldsymbol{z}, \cdot) := p^*(\boldsymbol{v}, \boldsymbol{s}; \boldsymbol{z}, \cdot, \delta\hat{\boldsymbol{s}}) \tag{6.17}$$

is the dual pseudo load *for a given fixed variation $\delta\hat{\boldsymbol{s}}$ at the current state $\{\boldsymbol{v}, \boldsymbol{s}, \boldsymbol{z}\}$.*

This is a variational equation for the sensitivity of the dual solution due to changes in the design. For a given variation in the design $\delta\hat{\boldsymbol{s}}$, we can calculate the variation in the dual solution $\delta\boldsymbol{z}$.

6.3.3 Sensitivity of the material residual

The sensitivity of the dual material residual (6.8) is given from the total variation of $G^* = 0$, i.e. we have

$$G^{*\prime} = G_z^{*\prime}(\boldsymbol{v}, \boldsymbol{s}; \boldsymbol{z}; \boldsymbol{\psi}, \delta\boldsymbol{z}) + G_s^{*\prime}(\boldsymbol{v}, \boldsymbol{s}; \boldsymbol{z}; \boldsymbol{\psi}, \delta\boldsymbol{s}) = 0. \tag{6.18}$$

The partial variations are introduced as

$$\begin{aligned} t^*(\boldsymbol{v}, \boldsymbol{s}; \boldsymbol{z}, \boldsymbol{\psi}, \delta\boldsymbol{z}) &:= G_z^{*\prime}(\boldsymbol{v}, \boldsymbol{s}; \boldsymbol{z}; \boldsymbol{\psi}, \delta\boldsymbol{z}) \\ &= \frac{1}{2}\, k_s'(\boldsymbol{v}, \boldsymbol{s}; \boldsymbol{z}, \delta\boldsymbol{z}; \boldsymbol{\psi}) - J_{vs}''(\boldsymbol{v}, \boldsymbol{s}; \delta\boldsymbol{z}, \boldsymbol{\psi}), \end{aligned} \tag{6.19}$$

$$\begin{aligned} d^*(\boldsymbol{v}, \boldsymbol{s}; \boldsymbol{z}; \boldsymbol{\psi}, \delta\boldsymbol{s}) &:= G_s^{*\prime}(\boldsymbol{v}, \boldsymbol{s}; \boldsymbol{z}; \boldsymbol{\psi}, \delta\boldsymbol{s}) \\ &= \frac{1}{2}\, k_{ss}''(\boldsymbol{v}, \boldsymbol{s}; \boldsymbol{z}; \boldsymbol{\psi}, \delta\boldsymbol{s}) - J_{vss}'''(\boldsymbol{v}, \boldsymbol{s}; \boldsymbol{z}, \boldsymbol{\psi}, \delta\boldsymbol{s}), \end{aligned} \tag{6.20}$$

where $d^*(\boldsymbol{v}, \boldsymbol{s}; \boldsymbol{z}; \boldsymbol{\psi}, \delta\boldsymbol{s})$ denotes the *dual tangent material stiffness operator*. For given fixed $\{\boldsymbol{v}, \boldsymbol{s}, \boldsymbol{z}\}$ these are bilinear forms $t^* : \mathcal{S}\times\mathcal{V} \to \mathbb{R}$ and $d^* : \mathcal{S}\times\mathcal{S} \to \mathbb{R}$. Due to permutableness of variations, i.e.

$$G_z^{*\prime} = (E^*)_{sz}'' = (E^*)_{zs}'' = R_s^{*\prime}, \tag{6.21}$$

we obtain for the variation of G^* with respect to $\boldsymbol{z}$

$$t^*(\boldsymbol{v}, \boldsymbol{s}; \boldsymbol{z}, \boldsymbol{\psi}, \delta\boldsymbol{z}) = p^*(\boldsymbol{v}, \boldsymbol{s}; \boldsymbol{z}, \delta\boldsymbol{z}, \boldsymbol{\psi}). \tag{6.22}$$

Hence, (6.18) can be written as

$$G^{*\prime} = p^*(\boldsymbol{v}, \boldsymbol{s}; \boldsymbol{z}, \delta\boldsymbol{z}, \boldsymbol{\psi}) + d^*(\boldsymbol{v}, \boldsymbol{s}; \boldsymbol{z}; \boldsymbol{\psi}, \delta\boldsymbol{s}) = 0. \tag{6.23}$$

After rearranging the above terms we can formulate the following problem.

Problem 6.3 *Let $\delta\hat{\boldsymbol{z}} \in \mathcal{V}$ be a given fixed variation. Find $\delta\boldsymbol{s} \in \mathcal{S}$ such that*

$$d^*(\boldsymbol{v}, \boldsymbol{s}; \boldsymbol{z}; \boldsymbol{\psi}, \delta\boldsymbol{s}) = -Q_m^*(\boldsymbol{v}, \boldsymbol{s}; \boldsymbol{z}, \boldsymbol{\psi}) \qquad \forall\, \boldsymbol{\psi} \in \mathcal{S}, \tag{6.24}$$

where

$$Q_m^*(\boldsymbol{v}, \boldsymbol{s}; \boldsymbol{z}, \cdot) := p^*(\boldsymbol{v}, \boldsymbol{s}; \boldsymbol{z}, \delta\hat{\boldsymbol{z}}, \cdot) \tag{6.25}$$

is the dual pseudo load *of the material problem for the variation $\delta\hat{\boldsymbol{z}}$.*

6.3.4 Sensitivity of the quantity of interest

The variation in the state $\delta\boldsymbol{v} \in \mathcal{V}$ due to a variation in the design $\delta\boldsymbol{s} \in \mathcal{S}$ is given by the variational equation (4.21) as

$$k(\boldsymbol{v}, \boldsymbol{s}; \boldsymbol{\eta}, \delta\boldsymbol{v}) = -Q_p(\boldsymbol{v}, \boldsymbol{s}; \boldsymbol{\eta}) \qquad \forall\, \boldsymbol{\eta} \in \mathcal{V}.$$

Furthermore, the dual solution $\boldsymbol{z}$ at the current linearization point is determined by (6.1), which is given by

$$k(\boldsymbol{v}, \boldsymbol{s}; \boldsymbol{z}, \boldsymbol{\eta}) = J_v'(\boldsymbol{v}, \boldsymbol{s}; \boldsymbol{\eta}) \qquad \forall\, \boldsymbol{\eta} \in \mathcal{V}.$$

Due to the symmetry of $k(\cdot, \cdot)$ we obtain a sensitivity relation for the quantity of interest in the form

$$J_v'(\boldsymbol{v}, \boldsymbol{s}; \delta\boldsymbol{u}) = k(\boldsymbol{v}, \boldsymbol{s}; \boldsymbol{z}, \delta\boldsymbol{v}) = -Q_p(\boldsymbol{v}, \boldsymbol{s}; \boldsymbol{z}). \tag{6.26}$$

Hence, the variation in a quantity of interest is given by the scalar product between the dual solution $\boldsymbol{z}$ and the pseudo load corresponding to the design variation $\delta\boldsymbol{s}$, i.e.

$$J_v'(\boldsymbol{v}, \boldsymbol{s}; \delta\boldsymbol{v}) = -Q_p(\boldsymbol{v}, \boldsymbol{s}; \boldsymbol{z}). \tag{6.27}$$

If the dual solution $\boldsymbol{z}$ is known, this equation can be evaluated for arbitrary pseudo loads $Q_p(\boldsymbol{v}, \boldsymbol{s}; \cdot) = p(\boldsymbol{v}, \boldsymbol{s}; \cdot, \delta\hat{\boldsymbol{s}}) = R_s'(\boldsymbol{v}, \boldsymbol{s}; \cdot, \delta\hat{\boldsymbol{s}})$, i.e. for arbitrary admissible design variations $\delta\boldsymbol{s}$. The pseudo load operator of the primal problem $p(\boldsymbol{v}, \boldsymbol{s}; \cdot, \delta\hat{\boldsymbol{s}})$ is given in (4.88).

6.4 Finite element approximation

6.4.1 The discrete energy minimization problem

The finite element formulation is based on a conforming Galerkin method as for the primal problem in Section 4.4.2. The discrete dual solution $\boldsymbol{z}_h \in \mathcal{V}_h \subset \mathcal{V}$ and discrete design $\boldsymbol{s}_h \in \mathcal{S}_h \subset \mathcal{S}$ are determined by the following discrete version of Problem 6.1.

Problem 6.4 *Find* $\{\boldsymbol{z}_h, \boldsymbol{s}_h\} \in \mathcal{V}_h \times \mathcal{S}_h$ *such that*

$$E^*(\boldsymbol{v}_h)(\boldsymbol{z}_h, \boldsymbol{s}_h) = \min_{\{\boldsymbol{q}_h, \boldsymbol{r}_h\} \in \mathcal{V}_h \times \mathcal{S}_h} E^*(\boldsymbol{v}_h)(\boldsymbol{q}_h, \boldsymbol{r}_h). \tag{6.28}$$

The optimality condition is given as follows. Find $\{\boldsymbol{z}_h, \boldsymbol{s}_h\} \in \mathcal{V}_h \times \mathcal{S}_h$ such that

$$\left\{ \begin{array}{l} R^*(\boldsymbol{v}_h, \boldsymbol{s}_h; \boldsymbol{z}_h, \boldsymbol{\eta}_h) \\ G^*(\boldsymbol{v}_h, \boldsymbol{s}_h; \boldsymbol{z}_h; \psi_h) \end{array} \right\} = \boldsymbol{0} \qquad \forall \{\boldsymbol{\eta}_h, \psi_h\} \in \mathcal{V}_h \times \mathcal{S}_h. \tag{6.29}$$

6.4.2 Matrix representation of the residuals and tangent forms

For a matrix description of the approximate dual solution $\boldsymbol{z}_h \in \mathcal{V}_h \subset \mathcal{V}$ we introduce the discrete approximations for the dual solution, i.e. the nodal vector $\boldsymbol{z} \in \mathbb{R}^n$ and the variation $\delta \boldsymbol{z} \in \mathbb{R}^n$.

For given $\{\hat{\boldsymbol{v}}_h, \hat{\boldsymbol{s}}_h, \hat{\boldsymbol{z}}_h\}$, the discrete versions of the residuals and tangent forms are given as

$$R^*(\hat{\boldsymbol{v}}_h, \hat{\boldsymbol{s}}_h; \hat{\boldsymbol{z}}_h, \boldsymbol{\eta}_h) = \boldsymbol{\eta}^T \boldsymbol{R}^*, \tag{6.30}$$

$$G^*(\hat{\boldsymbol{v}}_h, \hat{\boldsymbol{s}}_h; \hat{\boldsymbol{z}}_h; \psi_h) = \boldsymbol{\psi}^T \boldsymbol{G}^*, \tag{6.31}$$

$$k(\hat{\boldsymbol{v}}_h, \hat{\boldsymbol{s}}_h; \delta \boldsymbol{z}_h, \boldsymbol{\eta}_h) = \delta \boldsymbol{z}^T \boldsymbol{K} \boldsymbol{\eta} = \boldsymbol{\eta}^T \boldsymbol{K} \delta \boldsymbol{z}, \tag{6.32}$$

$$p^*(\hat{\boldsymbol{v}}_h, \hat{\boldsymbol{s}}_h; \hat{\boldsymbol{z}}_h, \boldsymbol{\eta}_h, \delta \boldsymbol{s}_h) = \boldsymbol{\eta}^T \boldsymbol{P}^* \delta \boldsymbol{s}, \tag{6.33}$$

$$t^*(\hat{\boldsymbol{v}}_h, \hat{\boldsymbol{s}}_h; \hat{\boldsymbol{z}}_h, \psi_h, \delta \boldsymbol{z}_h) = \boldsymbol{\psi}^T \boldsymbol{T}^* \delta \boldsymbol{z}, \tag{6.34}$$

$$d^*(\hat{\boldsymbol{v}}_h, \hat{\boldsymbol{s}}_h; \hat{\boldsymbol{z}}_h; \psi_h, \delta \boldsymbol{s}_h) = \boldsymbol{\psi}^T \boldsymbol{D}^* \delta \boldsymbol{s}, \tag{6.35}$$

where the vectors and matrices associated to the functionals and bilinear forms are denoted by

$\boldsymbol{R}^* \in \mathbb{R}^n$	dual physical residual vector
$\boldsymbol{G}^* \in \mathbb{R}^m$	dual material residual vector
$\boldsymbol{P}^* \in \mathbb{R}^{n \times m}$	dual tangent physical pseudo load matrix
$\boldsymbol{T}^* \in \mathbb{R}^{m \times n}$	dual tangent material pseudo load matrix
$\boldsymbol{D}^* \in \mathbb{R}^{m \times m}$	dual tangent material stiffness matrix.

Note that due to symmetry we have $\boldsymbol{T}^* = (\boldsymbol{P}^*)^T$. Details on the formulation of the matrix representations are given in C.3 and C.4.

6.4.3 The discrete sensitivity equations

The discrete sensitivity relation of the dual energy (6.11) with respect to variations $\delta \boldsymbol{s}$ reads

$$\delta_s E^* = \boldsymbol{G}^{*^T} \delta \boldsymbol{s}. \tag{6.36}$$

Furthermore, the total variations of the dual physical (6.15) and material (6.23) residuals become

$$\delta \boldsymbol{R}^* = \boldsymbol{K} \delta \boldsymbol{z} + \boldsymbol{P}^* \delta \boldsymbol{s} = \boldsymbol{0} \qquad \text{or} \qquad \delta \boldsymbol{z} = -\boldsymbol{K}^{-1} \boldsymbol{P}^* \delta \boldsymbol{s}, \tag{6.37}$$

$$\delta \boldsymbol{G}^* = \boldsymbol{P}^{*T} \delta \boldsymbol{z} + \boldsymbol{D}^* \delta \boldsymbol{s} = \boldsymbol{0} \qquad \text{or} \qquad \delta \boldsymbol{s} = -\boldsymbol{D}^{*-1} \boldsymbol{P}^{*T} \delta \boldsymbol{z}. \tag{6.38}$$

The discrete versions of the sensitivity equations for the dual physical (6.16) and material (6.24) problem are given by

$$\boldsymbol{K} \delta \boldsymbol{z} = -\boldsymbol{Q}_p^* \qquad \text{with} \qquad \boldsymbol{Q}_p^* := \boldsymbol{P}^* \delta \hat{\boldsymbol{s}}, \tag{6.39}$$

$$\boldsymbol{D}^* \delta \boldsymbol{s} = -\boldsymbol{Q}_m^* \qquad \text{with} \qquad \boldsymbol{Q}_m^* := \boldsymbol{P}^{*T} \delta \hat{\boldsymbol{z}}. \tag{6.40}$$

Here, $\boldsymbol{Q}_p^* \in \mathbb{R}^n$ is the dual pseudo load vector of the dual physical problem associated to the functional $Q_p^*(\boldsymbol{v}_h, \boldsymbol{s}_h; \boldsymbol{z}_h, \cdot)$ and $\boldsymbol{Q}_m^* \in \mathbb{R}^m$ is the pseudo load vector of the material residual problem associated to the functional $Q_m^*(\boldsymbol{v}_h, \boldsymbol{s}_h; \boldsymbol{z}_h, \cdot)$.

Remark 6.3 (Sensitivity operator) *In Remark 4.5 we have proposed a sensitivity relation for the state as $\delta \boldsymbol{v} = \boldsymbol{S}_p \, \delta \boldsymbol{s}$. In the same manner, we obtain with (6.37) directly a connection between the physical and the material spaces for the dual problem. Both spaces are connected by the transformation*

$$\delta \boldsymbol{z} = \boldsymbol{S}_p^* \, \delta \boldsymbol{s} \qquad \textit{with} \qquad \boldsymbol{S}_p^* := -\boldsymbol{K}^{-1} \boldsymbol{P}^*, \tag{6.41}$$

where $\boldsymbol{S}_p^* \in \mathbb{R}^{n \times m}$ denotes the dual sensitivity operator matrix *of the dual physical problem. With the knowledge of the pseudo load operator matrix $\boldsymbol{P}^*$, we can evaluate the sensitivity equation for arbitrary admissible variations $\delta \boldsymbol{s}$ in the material space. In the same manner, we obtain from (6.38) for the material problem the transformation*

$$\delta \boldsymbol{s} = \boldsymbol{S}_m^* \, \delta \boldsymbol{z} \qquad \textit{with} \qquad \boldsymbol{S}_m^* := -\boldsymbol{D}^{*-1} \boldsymbol{P}^{*T}, \tag{6.42}$$

where $\boldsymbol{S}_m^* \in \mathbb{R}^{m \times n}$ denotes the dual sensitivity operator matrix *of the material problem. With this, we can perform the sensitivity analysis for arbitrary admissible variations $\delta \boldsymbol{z}$ in the physical space.*

Finally, the sensitivity relation of the quantity of interest (6.27) becomes

$$J_v'(\boldsymbol{v}_h, \boldsymbol{s}_h; \delta \boldsymbol{v}_h) = -\boldsymbol{z}^T \boldsymbol{Q}_p, \tag{6.43}$$

where $\boldsymbol{Q}_p = \boldsymbol{P} \delta \boldsymbol{s}$ denotes the pseudo load vector defined in (4.52). Let for instance v_i be the quantity of interest, i.e. $J(\boldsymbol{v}_h, \boldsymbol{s}_h) = v_i$. Then, we have $J_v'(\boldsymbol{v}_h, \boldsymbol{s}_h; \delta \boldsymbol{v}_h) = \delta v_i$ and hence

$$\delta v_i = -\boldsymbol{z}^T \boldsymbol{Q}_p. \tag{6.44}$$

The dual solution has to be computed once and the sensitivity relation can be evaluated for arbitrary pseudo loads, i.e. for any admissible design variation $\delta \boldsymbol{s}$.

6.4.4 Computation of the dual solution

The discrete dual solution $\boldsymbol{z}_h \in \mathcal{V}_h$ corresponding to (6.1) is determined by the variational equation

$$k(\boldsymbol{v}_h, \boldsymbol{s}_h; \boldsymbol{\eta}_h, \boldsymbol{z}_h) = J'_v(\boldsymbol{v}_h, \boldsymbol{s}_h; \boldsymbol{\eta}_h) \quad \forall\, \boldsymbol{\eta}_h \in \mathcal{V}_h. \tag{6.45}$$

To solve this problem, we have to apply equivalent nodal forces j_k defined by the right-hand side $J'_v(\boldsymbol{v}_h, \boldsymbol{s}_h; \cdot)$. For a certain interpolation function $\phi_k \in \mathcal{V}_h$ we have

$$j_k = J'_v(\boldsymbol{v}_h, \boldsymbol{s}_h; \phi_k). \tag{6.46}$$

We consider for instance the stress component $S_{ij}(\boldsymbol{X})$ of the stress tensor $\mathbf{S}$ at some material point $\boldsymbol{X}$ as quantity of interest, i.e. $J(\boldsymbol{v}, \boldsymbol{s}) = S_{ij}(\boldsymbol{X})$ and $J'_v(\boldsymbol{v}, \boldsymbol{s}; \boldsymbol{\eta}) = (S_{ij})'_v(\boldsymbol{v}, \boldsymbol{\eta})(\boldsymbol{X})$, see also Example 6.1 in Section 6.5.2. The component $(S_{ij})'_v =: \Delta S_{ij}$ is given from the stress field $\mathbf{S}'_v(\boldsymbol{v}, \boldsymbol{\eta}) = \mathbb{C} : \mathbf{E}'_v(\boldsymbol{v}, \boldsymbol{\eta}) =: \Delta\mathbf{S}(\boldsymbol{v}, \boldsymbol{\eta})$. We use as interpolation functions ϕ_i the standard finite element shape functions. Hence, the equivalent nodal forces are given from

$$j_k = J'_v(\boldsymbol{v}_h, \boldsymbol{s}_h; \phi_k) = \Delta S_{ij}(\boldsymbol{v}_h, \phi_k)(\boldsymbol{X}). \tag{6.47}$$

The force j_k is the stress ΔS_{ij} at the point $\boldsymbol{X}$, which is caused by applying the shape function ϕ_k at the nodal coordinate k. The assembling of all element contributions yields the discrete nodal vector $\boldsymbol{J}_v$ corresponding to the functional $J'_v(\boldsymbol{v}_h, \boldsymbol{s}_h; \cdot)$.

The dual problem is formulated at a given linearization point, i.e. on a given deformed state $\boldsymbol{v}_h$. The tangent form $k(\boldsymbol{v}_h, \boldsymbol{s}_h; \cdot, \cdot)$ is just the tangent physical stiffness (4.87). Hence, in the discrete case we have to solve

$$\boldsymbol{K}\boldsymbol{z} = \boldsymbol{J}_v, \tag{6.48}$$

where $\boldsymbol{K}$ is the same tangent stiffness matrix as used in the last iteration within the solution process of the primal problem. Therefore, this matrix and its inverse are already known and have not to be additionally computed.

6.5 Explicit formulations for shape sensitivity

6.5.1 The energy-momentum tensor of the dual problem

The dual material residual (6.8) contains the variation of the internal energy (6.4) with respect to configurational changes, which is obtained as

$$\begin{aligned} C_s^{*\prime}(\boldsymbol{v})(\boldsymbol{z}, \boldsymbol{s})(\boldsymbol{\psi}) &= \frac{1}{2}\, k'_s(\boldsymbol{v}, \boldsymbol{s}; \boldsymbol{z}; \boldsymbol{\psi}) = \frac{1}{2}\, k'_s(\boldsymbol{v}, \boldsymbol{s}; \boldsymbol{z}, \boldsymbol{z}, \boldsymbol{\psi}) \\ &= \int_{\Omega_R} \{\, \frac{1}{2}\, [\, \mathbf{S} : \mathbf{E}'''_{vvs}(\boldsymbol{z}, \boldsymbol{z}, \boldsymbol{\psi}) + \mathbf{E}''_{vv}(\boldsymbol{z}, \boldsymbol{z}) : \mathbb{C} : \mathbf{E}'_s(\boldsymbol{v}, \boldsymbol{\psi}) \\ &\qquad + \mathbf{E}'_v(\boldsymbol{v}, \boldsymbol{z}) : \boldsymbol{\mathcal{D}} : \mathbf{E}'_s(\boldsymbol{v}, \boldsymbol{\psi}) : \mathbf{E}'_v(\boldsymbol{v}, \boldsymbol{z})\,] \\ &\qquad + \mathbf{E}''_{vs}(\boldsymbol{v}, \boldsymbol{z}, \boldsymbol{\psi}) : \mathbb{C} : \mathbf{E}'_v(\boldsymbol{v}, \boldsymbol{z}) + W^*_R(\boldsymbol{v}, \boldsymbol{z})\mathbf{I} : \operatorname{Grad} \boldsymbol{\psi}\, \}\, \mathrm{d}\Omega \end{aligned} \tag{6.49}$$

Stress increments:

$$\Delta_z \mathbf{S}^{(z)} := \mathbb{C} : \mathbf{E}''_{vv}(\boldsymbol{z},\boldsymbol{z}) = \mathbb{C} : \operatorname{Grad}\boldsymbol{z}^T \operatorname{Grad}\boldsymbol{z}, \tag{6.52}$$

$$\Delta_z \mathbf{S}^{(1)} := \mathbb{C} : \mathbf{E}'_{v}(\boldsymbol{v},\boldsymbol{z}) = \mathbb{C} : \mathbf{F}^T \operatorname{Grad}\boldsymbol{z}, \tag{6.53}$$

$$\Delta_z \mathbf{S}^{(2)} := \boldsymbol{\mathcal{D}} : \mathbf{E}'_{v}(\boldsymbol{v},\boldsymbol{z}) : \mathbf{E}'_{v}(\boldsymbol{v},\boldsymbol{z}) = \boldsymbol{\mathcal{D}} : \mathbf{F}^T \operatorname{Grad}\boldsymbol{z} : \mathbf{F}^T \operatorname{Grad}\boldsymbol{z}. \tag{6.54}$$

Elasticity tensor increments:

$$\Delta_z \mathbb{C}^{(z)} := \boldsymbol{\mathcal{D}} : \mathbf{E}''_{vv}(\boldsymbol{z},\boldsymbol{z}) = \boldsymbol{\mathcal{D}} : \operatorname{Grad}\boldsymbol{z}^T \operatorname{Grad}\boldsymbol{z}, \tag{6.55}$$

$$\Delta_z \mathbb{C}^{(1)} := \boldsymbol{\mathcal{D}} : \mathbf{E}'_{v}(\boldsymbol{v},\boldsymbol{z}) = \boldsymbol{\mathcal{D}} : \mathbf{F}^T \operatorname{Grad}\boldsymbol{z}, \tag{6.56}$$

$$\Delta_z \mathbb{C}^{(2)} := \boldsymbol{\mathfrak{E}} : \mathbf{E}'_{v}(\boldsymbol{v},\boldsymbol{z}) : \mathbf{E}'_{v}(\boldsymbol{v},\boldsymbol{z}) = \boldsymbol{\mathfrak{E}} : \mathbf{F}^T \operatorname{Grad}\boldsymbol{z} : \mathbf{F}^T \operatorname{Grad}\boldsymbol{z}, \tag{6.57}$$

where

$$\mathbb{C} := \frac{\partial \mathbf{S}}{\partial \mathbf{E}}, \qquad \boldsymbol{\mathcal{D}} := \frac{\partial \mathbb{C}}{\partial \mathbf{E}}, \qquad \boldsymbol{\mathfrak{E}} := \frac{\partial \boldsymbol{\mathcal{D}}}{\partial \mathbf{E}}. \tag{6.58}$$

Box 6.1: Stress and elasticity tensor increments for the dual physical problem

where

$$\begin{aligned}\mathbf{E}'''_{vvs}(\boldsymbol{\eta},\boldsymbol{\nu},\boldsymbol{\psi}) = -\operatorname{sym}\{ &\operatorname{Grad}\boldsymbol{\psi}^T \operatorname{Grad}\boldsymbol{\nu}^T \operatorname{Grad}\boldsymbol{\eta} \\ &+ \operatorname{Grad}\boldsymbol{\nu}^T \operatorname{Grad}\boldsymbol{\eta}\ \operatorname{Grad}\boldsymbol{\psi}\}.\end{aligned} \tag{6.50}$$

A more compact notation is given by

$$\begin{aligned}C_s^{*\prime}(\boldsymbol{v})(\boldsymbol{z},\boldsymbol{s})(\boldsymbol{\psi}) = \int_{\Omega_R} \{ \frac{1}{2} [\, &\mathbf{S} : \mathbf{E}'''_{vvs}(\boldsymbol{z},\boldsymbol{z},\boldsymbol{\psi}) + \Delta_z \mathbf{S}^{(z)} : \mathbf{E}'_s(\boldsymbol{v},\boldsymbol{\psi}) \\ &+ 2\,\Delta_z \mathbf{S}^{(1)} : \mathbf{E}''_{vs}(\boldsymbol{v},\boldsymbol{z},\boldsymbol{\psi}) + \Delta_z \mathbf{S}^{(2)} : \mathbf{E}'_s(\boldsymbol{v},\boldsymbol{\psi})\,] \\ &+ W_R^*(\boldsymbol{v},\boldsymbol{z})\mathbf{I} : \operatorname{Grad}\boldsymbol{\psi}\,\}\,\mathrm{d}\Omega\end{aligned} \tag{6.51}$$

The stresses (increments) $\Delta_z \mathbf{S}^{(z)}$, $\Delta_z \mathbf{S}^{(1)}$ and $\Delta_z \mathbf{S}^{(2)}$ are given in Box 6.1. For later use, the increments of the elasticity tensor have been introduced in the same manner in Box 6.1. The derivative of the fourth-order elasticity tensor $\mathbb{C}$ yields a sixth-order tensor $\boldsymbol{\mathcal{D}}$ and the second derivative leads to a eight-order tensor $\boldsymbol{\mathfrak{E}}$. The explicit specifications of these tensors for a classical compressible Neo-Hookean material are given in Appendix B.1.

The variation of the internal energy can be written in terms of an energy-momentum tensor. A straightforward calculation and rearrangement of (6.51) yields

$$C_s^{*\prime}(\boldsymbol{v})(\boldsymbol{z},\boldsymbol{s})(\boldsymbol{\psi}) = \int_{\Omega_R} \boldsymbol{\Sigma}^*(\boldsymbol{v},\boldsymbol{z}) : \operatorname{Grad}\boldsymbol{\psi}\,\mathrm{d}\Omega. \tag{6.59}$$

Here, a novel *energy-momentum tensor of the dual problem* $\boldsymbol{\Sigma}^*$ in form of

$$\boldsymbol{\Sigma}^*(\boldsymbol{v},\boldsymbol{z}) := W_R^*(\boldsymbol{v},\boldsymbol{z})\mathbf{I} - \operatorname{Grad}\boldsymbol{z}^T \frac{\partial W_R^*(\boldsymbol{v},\boldsymbol{z})}{\partial \operatorname{Grad}\boldsymbol{z}} - \operatorname{Grad}\boldsymbol{v}^T \frac{\partial W_R^*(\boldsymbol{v},\boldsymbol{z})}{\partial \operatorname{Grad}\boldsymbol{v}} \tag{6.60}$$

has been introduced, where

$$\frac{\partial W_R^*(\boldsymbol{v},\boldsymbol{z})}{\partial \operatorname{Grad}\boldsymbol{z}} = \operatorname{Grad}\boldsymbol{z}\,\mathbf{S} + \mathbf{F}\Delta_z\mathbf{S}^{(1)} \tag{6.61}$$

$$\frac{\partial W_R^*(\boldsymbol{v},\boldsymbol{z})}{\partial \operatorname{Grad}\boldsymbol{v}} = \operatorname{Grad}\boldsymbol{z}\,\Delta_z\mathbf{S}^{(1)} + \frac{1}{2}\,\mathbf{F}\,[\,\Delta_z\mathbf{S}^{(2)} + \Delta_z\mathbf{S}^{(z)}\,] \tag{6.62}$$

are just the derivatives of the strain energy W_R^* with respect to the gradient of the primal and dual solutions, compare with the energy-momentum tensor of the primal problem (3.55).

Remark 6.4 *The above derived terms in $\boldsymbol{\Sigma}^*$ are identified as the partial derivatives of W_R^* with respect to $\boldsymbol{v}$ and $\boldsymbol{z}$, respectively. The variation in $\boldsymbol{s}$ at a given deformed state causes a change in $\boldsymbol{v}$ and hence a change in $\boldsymbol{z}$ and the dual energy E^*. Therefore, two contributions appear in $\boldsymbol{\Sigma}^*$ due to these changes.*

Remark 6.5 *For the initial problem, i.e. at the undeformed state with $\boldsymbol{v} = \boldsymbol{u} = \mathbf{0}$, we obtain from (6.60) the energy-momentum or Eshelby tensor in terms of linear elasticity $\boldsymbol{\Sigma}(\boldsymbol{z})$, i.e.*

$$\boldsymbol{\Sigma}^*(\boldsymbol{u},\boldsymbol{z})\Big|_{\boldsymbol{u}=\mathbf{0}} = W_R(\boldsymbol{z})\,\mathbf{I} - \operatorname{Grad}\boldsymbol{z}^T\boldsymbol{\sigma}(\boldsymbol{z}) =: \boldsymbol{\Sigma}(\boldsymbol{z}), \tag{6.63}$$

with $W_R(\boldsymbol{z}) := \frac{1}{2}\,\boldsymbol{\varepsilon}(\boldsymbol{z}) : \mathbb{C} : \boldsymbol{\varepsilon}(\boldsymbol{z})$ and the linear Cauchy stress tensor $\boldsymbol{\sigma}(\boldsymbol{z}) := \mathbb{C} : \boldsymbol{\varepsilon}(\boldsymbol{z})$, where $\boldsymbol{\varepsilon}(\boldsymbol{z}) := \operatorname{sym}\{\operatorname{Grad}\boldsymbol{z}\}$.

Finally, the explicit form of the dual material residual (6.8) reads

$$G^*(\boldsymbol{v},\boldsymbol{s};\boldsymbol{z};\boldsymbol{\psi}) = \int_{\Omega_R} \boldsymbol{\Sigma}^*(\boldsymbol{v},\boldsymbol{z}) : \operatorname{Grad}\boldsymbol{\psi}\,\mathrm{d}\Omega - J''_{vs}(\boldsymbol{v},\boldsymbol{s};\boldsymbol{z},\boldsymbol{\psi}). \tag{6.64}$$

The explicit form of $J''_{vs}(\boldsymbol{v},\boldsymbol{s};\boldsymbol{z},\boldsymbol{\psi})$ depends on the chosen quantity of interest. An example is given in Section 6.5.2.

6.5.2 Variational formulation of the residuals and tangent forms

The explicit forms of the dual residuals and tangent forms are stated in this section in the same manner as for the primal problem in Section 4.6.1.

The partial variations of the dual physical and material residuals R^* and G^* have been introduced as

$$\begin{aligned} k^*(\boldsymbol{v},\boldsymbol{s};\delta\boldsymbol{z},\boldsymbol{\eta}) &= R^{*\prime}_z(\boldsymbol{v},\boldsymbol{s};\delta\boldsymbol{z},\boldsymbol{\eta}) & t^*(\boldsymbol{v},\boldsymbol{s};\boldsymbol{z},\boldsymbol{\psi},\delta\boldsymbol{z}) &= G^{*\prime}_z(\boldsymbol{v},\boldsymbol{s};\boldsymbol{z};\boldsymbol{\psi},\delta\boldsymbol{z}) \\ p^*(\boldsymbol{v},\boldsymbol{s};\boldsymbol{z},\boldsymbol{\eta},\delta\boldsymbol{s}) &= R^{*\prime}_s(\boldsymbol{v},\boldsymbol{s};\boldsymbol{z},\boldsymbol{\eta},\delta\boldsymbol{s}) & d^*(\boldsymbol{v},\boldsymbol{s};\boldsymbol{z};\boldsymbol{\psi},\delta\boldsymbol{s}) &= G^{*\prime}_s(\boldsymbol{v},\boldsymbol{s};\boldsymbol{z};\boldsymbol{\psi},\delta\boldsymbol{s}). \end{aligned}$$

The dual residuals written in terms of $\mathbf{S}$ and $\mathbf{E}$ are given by

$$\begin{aligned} R^*(\boldsymbol{v},\boldsymbol{s};\boldsymbol{z},\boldsymbol{\eta}) = \int_{\Omega_R} \{\, \mathbf{S} : \mathbf{E}''_{vv}(\boldsymbol{z},\boldsymbol{\eta}) + \Delta_z\mathbf{S}^{(1)} : \mathbf{E}'_v(\boldsymbol{v},\boldsymbol{\eta}) \,\}\,\mathrm{d}\Omega \\ - J'_v(\boldsymbol{v},\boldsymbol{s};\boldsymbol{\eta}), \end{aligned} \tag{6.65}$$

$$\begin{aligned} G^*(\boldsymbol{v},\boldsymbol{s};\boldsymbol{z};\boldsymbol{\psi}) = \int_{\Omega_R} \{\, \frac{1}{2}\, [\, \mathbf{S} : \mathbf{E}'''_{vvs}(\boldsymbol{z},\boldsymbol{z},\boldsymbol{\psi}) + \Delta_z\mathbf{S}^{(z)} : \mathbf{E}'_s(\boldsymbol{v},\boldsymbol{\psi}) \\ + 2\,\Delta_z\mathbf{S}^{(1)} : \mathbf{E}''_{vs}(\boldsymbol{v},\boldsymbol{z},\boldsymbol{\psi}) + \Delta_z\mathbf{S}^{(2)} : \mathbf{E}'_s(\boldsymbol{v},\boldsymbol{\psi})\,] \\ + W^*_R(\boldsymbol{v},\boldsymbol{z})\mathbf{I} : \mathrm{Grad}\,\boldsymbol{\psi}\,\}\,\mathrm{d}\Omega \\ - J''_{vs}(\boldsymbol{v},\boldsymbol{s};\boldsymbol{z},\boldsymbol{\psi}). \end{aligned} \tag{6.66}$$

The stress increments $\Delta_z\mathbf{S}^{(z)}$, $\Delta_z\mathbf{S}^{(1)}$ and $\Delta_z\mathbf{S}^{(2)}$ are given in (6.52), (6.53) and (6.54), respectively. Furthermore, the explicit formulation of the tangent forms are obtained as

$$\begin{aligned} k^*(\boldsymbol{v},\boldsymbol{s};\delta\boldsymbol{z},\boldsymbol{\eta}) &= k(\boldsymbol{v},\boldsymbol{s};\delta\boldsymbol{z},\boldsymbol{\eta}) \\ &= \int_{\Omega_R} \{\, \mathbf{S} : \mathbf{E}''_{vv}(\delta\boldsymbol{z},\boldsymbol{\eta}) + \mathbf{E}'_v(\boldsymbol{v},\delta\boldsymbol{z}) : \mathbb{C} : \mathbf{E}'_v(\boldsymbol{v},\boldsymbol{\eta}) \,\}\,\mathrm{d}\Omega, \end{aligned} \tag{6.67}$$

$$\begin{aligned} p^*(\boldsymbol{v},\boldsymbol{s};\boldsymbol{z},\boldsymbol{\eta},\delta\boldsymbol{s}) = \int_{\Omega_R} \{\, \mathbf{S} : \mathbf{E}'''_{vvs}(\boldsymbol{z},\boldsymbol{\eta},\delta\boldsymbol{s}) + \mathbf{E}''_{vv}(\boldsymbol{z},\boldsymbol{\eta}) : \mathbb{C} : \mathbf{E}'_s(\boldsymbol{v},\delta\boldsymbol{s}) \\ + \mathbf{E}''_{vs}(\boldsymbol{v},\boldsymbol{z},\delta\boldsymbol{s}) : \mathbb{C} : \mathbf{E}'_v(\boldsymbol{v},\boldsymbol{\eta}) \\ + \mathbf{E}'_v(\boldsymbol{v},\boldsymbol{z}) : \mathbb{C} : \mathbf{E}''_{vs}(\boldsymbol{v},\boldsymbol{\eta},\delta\boldsymbol{s}) \\ + \mathbf{E}'_v(\boldsymbol{v},\boldsymbol{\eta}) : \boldsymbol{\mathcal{D}} : \mathbf{E}'_v(\boldsymbol{v},\boldsymbol{z}) : \mathbf{E}'_s(\boldsymbol{v},\delta\boldsymbol{s}) \\ + [\, \mathbf{S} : \mathbf{E}''_{vv}(\boldsymbol{z},\boldsymbol{\eta}) + \mathbf{E}'_v(\boldsymbol{v},\boldsymbol{z}) : \mathbb{C} : \mathbf{E}'_v(\boldsymbol{v},\boldsymbol{\eta})\,]\,\mathrm{Div}\,\delta\boldsymbol{s} \,\}\,\mathrm{d}\Omega \\ - J''_{vs}(\boldsymbol{v},\boldsymbol{s};\boldsymbol{\eta},\delta\boldsymbol{s}), \end{aligned} \tag{6.68}$$

$$
\begin{aligned}
t^*(\boldsymbol{v},\boldsymbol{s};\boldsymbol{z},\boldsymbol{\psi},\delta\boldsymbol{z}) = \int_{\Omega_R} \{\, & \mathbf{S} : \mathbf{E}'''_{vvs}(\boldsymbol{z},\delta\boldsymbol{z},\boldsymbol{\psi}) + \mathbf{E}''_{vv}(\boldsymbol{z},\delta\boldsymbol{z}) : \mathbb{C} : \mathbf{E}'_s(\boldsymbol{v},\boldsymbol{\psi}) \\
& + \mathbf{E}''_{vs}(\boldsymbol{v},\boldsymbol{z},\boldsymbol{\psi}) : \mathbb{C} : \mathbf{E}'_v(\boldsymbol{v},\delta\boldsymbol{z}) \\
& + \mathbf{E}'_v(\boldsymbol{v},\boldsymbol{z}) : \mathbb{C} : \mathbf{E}''_{vs}(\boldsymbol{v},\delta\boldsymbol{z},\boldsymbol{\psi}) \\
& + \mathbf{E}'_v(\boldsymbol{v},\delta\boldsymbol{z}) : \boldsymbol{\mathcal{D}} : \mathbf{E}'_v(\boldsymbol{v},\boldsymbol{z}) : \mathbf{E}'_s(\boldsymbol{v},\boldsymbol{\psi}) \\
& + [\, \mathbf{S} : \mathbf{E}''_{vv}(\boldsymbol{z},\delta\boldsymbol{z}) + \mathbf{E}'_v(\boldsymbol{v},\boldsymbol{z}) : \mathbb{C} : \mathbf{E}'_v(\boldsymbol{v},\delta\boldsymbol{z}) \,] \operatorname{Div}\boldsymbol{\psi} \,\} \,\mathrm{d}\Omega \\
& - J''_{vs}(\boldsymbol{v},\boldsymbol{s};\delta\boldsymbol{z},\boldsymbol{\psi}),
\end{aligned}
\tag{6.69}
$$

$$
\begin{aligned}
d^*(\boldsymbol{v},\boldsymbol{s};\boldsymbol{z};\boldsymbol{\psi},\delta\boldsymbol{s}) = \int_{\Omega_R} \{\, & \frac{1}{2} [\, \mathbf{S} : \mathbf{E}''''_{vvss}(\boldsymbol{z},\boldsymbol{z},\boldsymbol{\psi},\delta\boldsymbol{s}) \\
& + \mathbf{E}'''_{vvs}(\boldsymbol{z},\boldsymbol{z},\boldsymbol{\psi}) : \mathbb{C} : \mathbf{E}'_s(\boldsymbol{v},\delta\boldsymbol{s}) \\
& + \mathbf{E}'''_{vvs}(\boldsymbol{z},\boldsymbol{z},\delta\boldsymbol{s}) : \mathbb{C} : \mathbf{E}'_s(\boldsymbol{v},\boldsymbol{\psi}) \\
& + \mathbf{E}''_{vv}(\boldsymbol{z},\boldsymbol{z}) : \mathbb{C} : \mathbf{E}''_{ss}(\boldsymbol{v},\boldsymbol{\psi},\delta\boldsymbol{s}) \\
& + \mathbf{E}''_{ss}(\boldsymbol{v},\boldsymbol{\psi},\delta\boldsymbol{s}) : \boldsymbol{\mathcal{D}} : \mathbf{E}'_v(\boldsymbol{v},\boldsymbol{z}) : \mathbf{E}'_v(\boldsymbol{v},\boldsymbol{z}) \\
& + \mathbf{E}'_s(\boldsymbol{v},\boldsymbol{\psi}) : \boldsymbol{\mathcal{D}} : \mathbf{E}''_{vv}(\boldsymbol{z},\boldsymbol{z}) : \mathbf{E}'_s(\boldsymbol{v},\delta\boldsymbol{s}) \\
& + \mathbf{E}'_s(\boldsymbol{v},\boldsymbol{\psi}) : \boldsymbol{\mathfrak{E}} : \mathbf{E}'_v(\boldsymbol{v},\boldsymbol{z}) : \mathbf{E}'_v(\boldsymbol{v},\boldsymbol{z}) : \mathbf{E}'_s(\boldsymbol{v},\delta\boldsymbol{s}) \,] \\
& + \mathbf{E}'''_{vss}(\boldsymbol{v},\boldsymbol{z},\boldsymbol{\psi},\delta\boldsymbol{s}) : \mathbb{C} : \mathbf{E}'_v(\boldsymbol{v},\boldsymbol{z}) \\
& + \mathbf{E}''_{vs}(\boldsymbol{v},\boldsymbol{z},\boldsymbol{\psi}) : \mathbb{C} : \mathbf{E}''_{vs}(\boldsymbol{v},\boldsymbol{z},\delta\boldsymbol{s}) \\
& + \mathbf{E}''_{vs}(\boldsymbol{v},\boldsymbol{z},\delta\boldsymbol{s}) : \boldsymbol{\mathcal{D}} : \mathbf{E}'_v(\boldsymbol{v},\boldsymbol{z}) : \mathbf{E}'_s(\boldsymbol{v},\boldsymbol{\psi}) \\
& + \mathbf{E}''_{vs}(\boldsymbol{v},\boldsymbol{z},\boldsymbol{\psi}) : \boldsymbol{\mathcal{D}} : \mathbf{E}'_v(\boldsymbol{v},\boldsymbol{z}) : \mathbf{E}'_s(\boldsymbol{v},\delta\boldsymbol{s}) \\
& + (W_R^*)'_s(\delta\boldsymbol{s}) \operatorname{Div}\boldsymbol{\psi} + (W_R^*)'_s(\boldsymbol{\psi}) \operatorname{Div}\delta\boldsymbol{s} \\
& + W_R^* \, [\operatorname{Div}\boldsymbol{\psi} \operatorname{Div}\delta\boldsymbol{s} - \mathbf{I} : \operatorname{Grad}\boldsymbol{\psi} \operatorname{Grad}\delta\boldsymbol{s} \,] \,\} \,\mathrm{d}\Omega \\
& - J'''_{vss}(\boldsymbol{v},\boldsymbol{s};\boldsymbol{z},\boldsymbol{\psi},\delta\boldsymbol{s}).
\end{aligned}
\tag{6.70}
$$

The bilinear form $d^*(\boldsymbol{v},\boldsymbol{s};\boldsymbol{z};\boldsymbol{\psi},\delta\boldsymbol{s})$ contains the variations of the strain energy function of the dual problem W_R^*. These terms are given by

$$
\begin{aligned}
(W_R^*)'_s(\boldsymbol{\psi}) = \frac{1}{2} [\, & \mathbf{S} : \mathbf{E}'''_{vvs}(\boldsymbol{z},\boldsymbol{z},\boldsymbol{\psi}) + \mathbf{E}''_{vv}(\boldsymbol{z},\boldsymbol{z}) : \mathbb{C} : \mathbf{E}'_s(\boldsymbol{v},\boldsymbol{\psi}) \\
& + \mathbf{E}'_s(\boldsymbol{v},\boldsymbol{\psi}) : \boldsymbol{\mathcal{D}} : \mathbf{E}'_v(\boldsymbol{v},\boldsymbol{z}) : \mathbf{E}'_v(\boldsymbol{v},\boldsymbol{z}) \,] \\
& + \mathbf{E}''_{vs}(\boldsymbol{v},\boldsymbol{z},\boldsymbol{\psi}) : \mathbb{C} : \mathbf{E}'_v(\boldsymbol{v},\boldsymbol{z}),
\end{aligned}
\tag{6.71}
$$

$$
\begin{aligned}
(W_R^*)'_s(\delta \boldsymbol{s}) = \frac{1}{2} \, [\, & \mathbf{S} : \mathbf{E}'''_{vvs}(\boldsymbol{z}, \boldsymbol{z}, \delta \boldsymbol{s}) + \mathbf{E}''_{vv}(\boldsymbol{z}, \boldsymbol{z}) : \mathbb{C} : \mathbf{E}'_s(\boldsymbol{v}, \delta \boldsymbol{s}) \\
& + \mathbf{E}'_s(\boldsymbol{v}, \delta \boldsymbol{s}) : \boldsymbol{\mathcal{D}} : \mathbf{E}'_v(\boldsymbol{v}, \boldsymbol{z}) : \mathbf{E}'_v(\boldsymbol{v}, \boldsymbol{z}) \,] \\
& + \mathbf{E}''_{vs}(\boldsymbol{v}, \boldsymbol{z}, \delta \boldsymbol{s}) : \mathbb{C} : \mathbf{E}'_v(\boldsymbol{v}, \boldsymbol{z}).
\end{aligned} \tag{6.72}
$$

Furthermore, the variation $\mathbf{E}''''_{vvss}(\boldsymbol{z}, \boldsymbol{z}, \boldsymbol{\psi}, \delta \boldsymbol{s})$ reads

$$
\begin{aligned}
\mathbf{E}''''_{vvss}(\boldsymbol{z}, \boldsymbol{z}, \boldsymbol{\psi}, \delta \boldsymbol{s}) = \operatorname{sym}\{ \; & \operatorname{Grad} \delta \boldsymbol{s}^T \operatorname{Grad} \boldsymbol{\psi}^T \operatorname{Grad} \boldsymbol{z}^T \operatorname{Grad} \boldsymbol{z} \\
& + \operatorname{Grad} \boldsymbol{\psi}^T \operatorname{Grad} \delta \boldsymbol{s}^T \operatorname{Grad} \boldsymbol{z}^T \operatorname{Grad} \boldsymbol{z} \\
& + \operatorname{Grad} \boldsymbol{\psi}^T \operatorname{Grad} \boldsymbol{z}^T \operatorname{Grad} \boldsymbol{z} \operatorname{Grad} \delta \boldsymbol{s} \\
& + \operatorname{Grad} \delta \boldsymbol{s}^T \operatorname{Grad} \boldsymbol{z}^T \operatorname{Grad} \boldsymbol{z} \operatorname{Grad} \boldsymbol{\psi} \\
& + \operatorname{Grad} \boldsymbol{z}^T \operatorname{Grad} \boldsymbol{z} \operatorname{Grad} \delta \boldsymbol{s} \operatorname{Grad} \boldsymbol{\psi} \\
& + \operatorname{Grad} \boldsymbol{z}^T \operatorname{Grad} \boldsymbol{z} \operatorname{Grad} \boldsymbol{\psi} \operatorname{Grad} \delta \boldsymbol{s} \, \}.
\end{aligned} \tag{6.73}
$$

The explicit forms of the contributions $J''_{vs}(\boldsymbol{v}, \boldsymbol{s}; \boldsymbol{\eta}, \delta \boldsymbol{s})$ and $J'''_{vss}(\boldsymbol{v}, \boldsymbol{s}; \boldsymbol{z}, \boldsymbol{\psi}, \delta \boldsymbol{s})$ depend on the chosen quantity of interest.

Example 6.1 As an example of a nonlinear functional J, we consider for instance the stress component $S_{ij}(\boldsymbol{X})$ of the stress tensor $\mathbf{S}$ at some material point $\boldsymbol{X}$ as quantity of interest, i.e. $J(\boldsymbol{v}, \boldsymbol{s}) = S_{ij}(\boldsymbol{X})$. The linearized functional follows in the form

$$
J'_v(\boldsymbol{v}, \boldsymbol{s}; \boldsymbol{\eta}) = (S_{ij})'_v(\boldsymbol{v}, \boldsymbol{\eta})(\boldsymbol{X}). \tag{6.74}
$$

The variation of $J'_v(\boldsymbol{v}, \boldsymbol{s}; \boldsymbol{z})$ with respect to $\boldsymbol{s}$ reads

$$
J''_{vs}(\boldsymbol{v}, \boldsymbol{s}; \boldsymbol{\eta}, \boldsymbol{\psi}) = (S_{ij})''_{vs}(\boldsymbol{v}, \boldsymbol{\eta}, \boldsymbol{\psi})(\boldsymbol{X}) \tag{6.75}
$$

and the second variation with respect to $\boldsymbol{s}$ is given as

$$
J'''_{vss}(\boldsymbol{v}, \boldsymbol{s}; \boldsymbol{\eta}, \boldsymbol{\psi}, \delta \boldsymbol{s}) = (S_{ij})'''_{vss}(\boldsymbol{v}, \boldsymbol{\eta}, \boldsymbol{\psi}, \delta \boldsymbol{s})(\boldsymbol{X}). \tag{6.76}
$$

The components $(S_{ij})'_v$, $(S_{ij})''_{vs}$ and $(S_{ij})'''_{vss}$ are given from the stress fields

$$
\mathbf{S}'_v(\boldsymbol{v}, \boldsymbol{\eta}) = \mathbb{C} : \mathbf{E}'_v(\boldsymbol{v}, \boldsymbol{\eta}), \tag{6.77}
$$

$$
\mathbf{S}''_{vs}(\boldsymbol{v}, \boldsymbol{\eta}, \boldsymbol{\psi}) = \mathbb{C} : \mathbf{E}''_{vs}(\boldsymbol{v}, \boldsymbol{\eta}, \boldsymbol{\psi}) + \mathbf{E}'_v(\boldsymbol{v}, \boldsymbol{\eta}) : \boldsymbol{\mathcal{D}} : \mathbf{E}'_s(\boldsymbol{v}, \boldsymbol{\psi}), \tag{6.78}
$$

$$
\begin{aligned}
\mathbf{S}'''_{vss}(\boldsymbol{v}, \boldsymbol{\eta}, \boldsymbol{\psi}, \delta \boldsymbol{s}) = & \, \mathbb{C} : \mathbf{E}'''_{vss}(\boldsymbol{v}, \boldsymbol{\eta}, \boldsymbol{\psi}, \delta \boldsymbol{s}) + \mathbf{E}''_{vs}(\boldsymbol{v}, \boldsymbol{\eta}, \boldsymbol{\psi}) : \boldsymbol{\mathcal{D}} : \mathbf{E}'_s(\boldsymbol{v}, \delta \boldsymbol{s}) \\
& + \mathbf{E}''_{vs}(\boldsymbol{v}, \boldsymbol{\eta}, \delta \boldsymbol{s}) : \boldsymbol{\mathcal{D}} : \mathbf{E}'_s(\boldsymbol{v}, \boldsymbol{\psi}) \\
& + \mathbf{E}'_v(\boldsymbol{v}, \boldsymbol{\eta}) : \boldsymbol{\mathcal{D}} : \mathbf{E}''_{ss}(\boldsymbol{v}, \boldsymbol{\psi}, \delta \boldsymbol{s}) \\
& + \mathbf{E}'_v(\boldsymbol{v}, \boldsymbol{\eta}) : \boldsymbol{\mathfrak{E}} : \mathbf{E}'_s(\boldsymbol{v}, \delta \boldsymbol{s}) : \mathbf{E}'_s(\boldsymbol{v}, \boldsymbol{\psi}).
\end{aligned} \tag{6.79}
$$

6.5.3 Discrete formulations of the dual residuals and tangent matrices

In the same manner as for the primal problem, the above dual residuals and tangent forms are discretized using the isoparametric concept as described in Appendix C.

The nodal contributions of the discrete residual vectors are given by

$$\boldsymbol{R}_i^{*e} = \int_{\Omega_R^e} \{\, \boldsymbol{B}_{zi}^T \underline{\boldsymbol{S}} + \boldsymbol{B}_{vi}^T \Delta_z \underline{\boldsymbol{S}}^{(1)} \,\} \,\mathrm{d}\Omega - \boldsymbol{J}_v^e(\boldsymbol{v}, \boldsymbol{s})_i, \tag{6.80}$$

$$\begin{aligned} \boldsymbol{G}_i^{*e} = \int_{\Omega_R^e} \{\, \frac{1}{2} \,[\, \boldsymbol{B}_{vvsi}^T \underline{\boldsymbol{S}} + \boldsymbol{B}_{si}^T \Delta_z \underline{\boldsymbol{S}}^{(z)} + 2\, \boldsymbol{B}_{vsi}^T \Delta_z \underline{\boldsymbol{S}}^{(1)} + \boldsymbol{B}_{si}^T \Delta_z \underline{\boldsymbol{S}}^{(2)} \,] \\ + W_R^* \, \boldsymbol{I} \boldsymbol{L}_i \,\} \,\mathrm{d}\Omega - \boldsymbol{J}_{vs}^e(\boldsymbol{v}, \boldsymbol{s}; \boldsymbol{z})_i, \end{aligned} \tag{6.81}$$

where $\underline{\boldsymbol{S}}$ is given in (4.101) and $\Delta_z \underline{\boldsymbol{S}}^{(z)}$, $\Delta_z \underline{\boldsymbol{S}}^{(1)}$ and $\Delta_z \underline{\boldsymbol{S}}^{(2)}$ are the column matrix representations of the symmetric stress increments $\Delta_z \mathbf{S}^{(z)}$, $\Delta_z \mathbf{S}^{(1)}$ and $\Delta_z \mathbf{S}^{(2)}$, respectively. For instance, the first increment has in the two-dimensional case the form

$$\Delta_z \underline{\boldsymbol{S}}^{(z)} = \left[\begin{array}{ccc} \Delta_z S_{11}^{(z)} & \Delta_z S_{22}^{(z)} & \Delta_z S_{12}^{(z)} \end{array} \right]^T. \tag{6.82}$$

The stress increments are defined in Box 6.1.

Furthermore, the corresponding dual tangent matrices are obtained as

$$\begin{aligned} \boldsymbol{K}_{ij}^{*e} &= \boldsymbol{K}_{ij}^e \\ &= \int_{\Omega_R^e} \{\, \boldsymbol{B}_{vi}^T \boldsymbol{C} \boldsymbol{B}_{vj} + \boldsymbol{L}_i^T \boldsymbol{S} \boldsymbol{L}_j \boldsymbol{I} \,\} \,\mathrm{d}\Omega, \end{aligned} \tag{6.83}$$

$$\begin{aligned} \boldsymbol{P}_{ij}^{*e} = \int_{\Omega_R^e} \{\, & \boldsymbol{B}_{zi}^T \boldsymbol{C} \boldsymbol{B}_{sj} - \boldsymbol{L}_i^T \boldsymbol{S} \boldsymbol{L}_j \,\mathrm{Grad}\, \boldsymbol{z} - \mathrm{Grad}\, \boldsymbol{z} \boldsymbol{S} \boldsymbol{L}_j \boldsymbol{L}_i^T \\ & - \boldsymbol{L}_i^T \Delta_z \boldsymbol{S}^{(1)} \boldsymbol{L}_j \,\mathrm{Grad}\, \boldsymbol{v} - \boldsymbol{F} \Delta_z \boldsymbol{S}^{(1)} \boldsymbol{L}_j \boldsymbol{L}_i^T \\ & + \boldsymbol{B}_{vi}^T \boldsymbol{C} \boldsymbol{B}_{vsj} + \boldsymbol{B}_{vi}^T \Delta_z \boldsymbol{C}^{(1)} \boldsymbol{B}_{sj} \\ & + \mathrm{Grad}\, \boldsymbol{z} \boldsymbol{S} \boldsymbol{L}_i \boldsymbol{L}_j^T + \boldsymbol{F} \Delta_z \boldsymbol{S}^{(1)} \boldsymbol{L}_i \boldsymbol{L}_j^T \,\} \,\mathrm{d}\Omega \\ & - \boldsymbol{J}_{vs}^e(\boldsymbol{v}, \boldsymbol{s})_{ij}, \end{aligned} \tag{6.84}$$

$$
\begin{aligned}
\boldsymbol{D}_{ij}^{*e} = \int_{\Omega_R^e} \{ & \operatorname{Grad} \boldsymbol{z}^T \operatorname{Grad} \boldsymbol{z} \boldsymbol{S}^T \boldsymbol{L}_j \boldsymbol{L}_i^T + \boldsymbol{L}_j \boldsymbol{L}_i^T \boldsymbol{S} \operatorname{Grad} \boldsymbol{z}^T \operatorname{Grad} \boldsymbol{z} \\
& + \boldsymbol{L}_i^T \boldsymbol{S} \boldsymbol{L}_j \operatorname{Grad} \boldsymbol{z}^T \operatorname{Grad} \boldsymbol{z} \\
& + 1/2 \, [\, \boldsymbol{B}_{vvsi}^T \boldsymbol{C} \boldsymbol{B}_{sj} + \boldsymbol{B}_{si}^T \boldsymbol{C} \boldsymbol{B}_{vvsj} \,] \\
& + 1/2 \, [\, \boldsymbol{L}_i^T \Delta_z \boldsymbol{S}^{(z)} \boldsymbol{L}_j \operatorname{Grad} \boldsymbol{v}^T \operatorname{Grad} \boldsymbol{v} + \boldsymbol{L}_j \boldsymbol{L}_i^T \Delta_z \boldsymbol{S}^{(z)} \boldsymbol{F}^T \operatorname{Grad} \boldsymbol{v} \\
& + \operatorname{Grad} \boldsymbol{v}^T \boldsymbol{F} \Delta_z \boldsymbol{S}^{(z)} \boldsymbol{L}_j \boldsymbol{L}_i^T \,] \\
& + 1/2 \, [\boldsymbol{L}_i^T \Delta_z \boldsymbol{S}^{(2)} \boldsymbol{L}_j \operatorname{Grad} \boldsymbol{v}^T \operatorname{Grad} \boldsymbol{v} + \boldsymbol{L}_j \boldsymbol{L}_i^T \Delta_z \boldsymbol{S}^{(2)} \boldsymbol{F}^T \operatorname{Grad} \boldsymbol{v} \\
& + \operatorname{Grad} \boldsymbol{v}^T \boldsymbol{F} \Delta_z \boldsymbol{S}^{(2)} \boldsymbol{L}_j \boldsymbol{L}_i^T] \\
& + 1/2 \, [\, \boldsymbol{B}_{si}^T \Delta_z \boldsymbol{C}^{(z)} \boldsymbol{B}_{sj} + \boldsymbol{B}_{si}^T \Delta_z \boldsymbol{C}^{(2)} \boldsymbol{B}_{sj} \,] \\
& + \operatorname{Grad} \boldsymbol{v}^T \operatorname{Grad} \boldsymbol{z} \Delta_z \boldsymbol{S}^{(1)} \boldsymbol{L}_j \boldsymbol{L}_i^T + \boldsymbol{L}_j \boldsymbol{L}_i^T \Delta_z \boldsymbol{S}^{(1)} \operatorname{Grad} \boldsymbol{z}^T \operatorname{Grad} \boldsymbol{v} \\
& + \boldsymbol{L}_i^T \Delta_z \boldsymbol{S}^{(1)} \boldsymbol{L}_j \operatorname{Grad} \boldsymbol{z}^T \operatorname{Grad} \boldsymbol{v} + \boldsymbol{L}_i^T \Delta_z \boldsymbol{S}^{(1)} \boldsymbol{L}_j \operatorname{Grad} \boldsymbol{v}^T \operatorname{Grad} \boldsymbol{z} \\
& + \boldsymbol{L}_j \boldsymbol{L}_i^T \Delta_z \boldsymbol{S}^{(1)} \boldsymbol{F}^T \operatorname{Grad} \boldsymbol{z} + \operatorname{Grad} \boldsymbol{z}^T \boldsymbol{F} \Delta_z \boldsymbol{S}^{(1)} \boldsymbol{L}_j \boldsymbol{L}_i^T \\
& + \boldsymbol{B}_{vsi}^T \boldsymbol{C} \boldsymbol{B}_{vsj} + \boldsymbol{B}_{si}^T \Delta_z \boldsymbol{C}^{(1)} \boldsymbol{B}_{vsj} + \boldsymbol{B}_{vsi}^T \Delta_z \boldsymbol{C}^{(1)} \boldsymbol{B}_{sj} \\
& + \boldsymbol{Y}_z \boldsymbol{L}_i \boldsymbol{L}_j^T + \boldsymbol{L}_i \boldsymbol{L}_j^T \boldsymbol{Y}_z^T + W_R^* \, [\, \boldsymbol{L}_i \boldsymbol{L}_j^T - \boldsymbol{L}_j \boldsymbol{L}_i^T \,] \, \} \, \mathrm{d}\Omega \\
- \boldsymbol{J}_{vss}^e & (\boldsymbol{v}, \boldsymbol{s}; \boldsymbol{z})_{ij} .
\end{aligned}
\tag{6.85}
$$

The quantities $\boldsymbol{J}_v^e(\boldsymbol{v}, \boldsymbol{s})_i$ and $\boldsymbol{J}_{vs}^e(\boldsymbol{v}, \boldsymbol{s}; \boldsymbol{z})_i$ are the element nodal vectors on a node i corresponding to the functionals $J_v'(\boldsymbol{v}, \boldsymbol{s}; \cdot)$ and $J_{vs}''(\boldsymbol{v}, \boldsymbol{s}; \boldsymbol{z}, \cdot)$. In the same manner, $\boldsymbol{J}_{vs}^e(\boldsymbol{v}, \boldsymbol{s})_{ij}$ and $\boldsymbol{J}_{vss}^e(\boldsymbol{v}, \boldsymbol{s}; \boldsymbol{z})_{ij}$ are the element nodal matrices corresponding to the bilinear forms $J_{vs}''(\boldsymbol{v}, \boldsymbol{s}; \cdot, \cdot)$ and $J_{vss}'''(\boldsymbol{v}, \boldsymbol{s}; \boldsymbol{z}, \cdot, \cdot)$.

The matrices $\boldsymbol{B}_{vvsi}$, $\boldsymbol{B}_{vsi}$ and $\boldsymbol{B}_{zi}$ are given in Appendix C in (C.20), (C.18) and (C.15), respectively. Furthermore,

$$
\begin{aligned}
\boldsymbol{Y}_z := & - \operatorname{Grad} \boldsymbol{z}^T [\operatorname{Grad} \boldsymbol{z} \boldsymbol{S} + \boldsymbol{F} \Delta_z \boldsymbol{S}^{(1)}] \\
& - \operatorname{Grad} \boldsymbol{v}^T [\operatorname{Grad} \boldsymbol{z} \Delta_z \boldsymbol{S}^{(1)} + \frac{1}{2} \boldsymbol{F} (\Delta_z \boldsymbol{S}^{(z)} + \Delta_z \boldsymbol{S}^{(2)})]
\end{aligned}
\tag{6.86}
$$

as well as $\Delta_z \boldsymbol{S}^{(z)}$, $\Delta_z \boldsymbol{S}^{(1)}$ and $\Delta_z \boldsymbol{S}^{(2)}$ are the matrix representation of the stress increments (6.52), (6.53) and (6.54). The matrices $\Delta_z \boldsymbol{C}^{(z)}$, $\Delta_z \boldsymbol{C}^{(1)}$ and $\Delta_z \boldsymbol{C}^{(2)}$ are the matrix representations of the fourth-order tensors (6.55), (6.56) and (6.57), respectively.

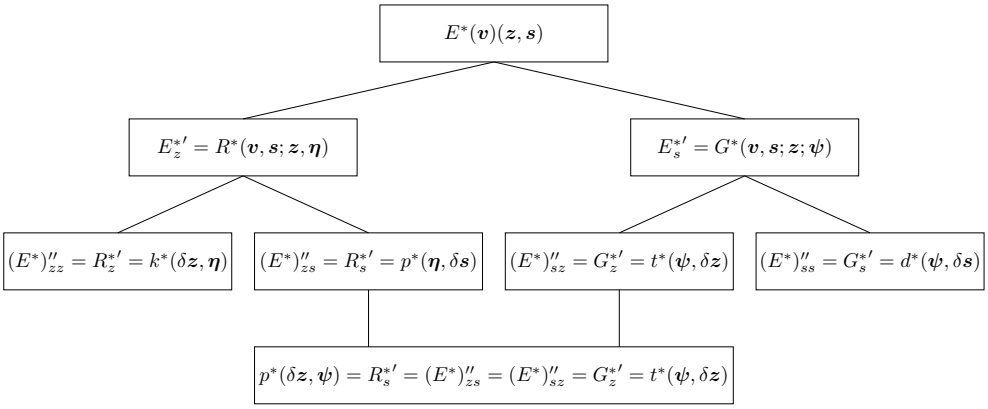

Figure 6.1: Summary of the complete energy variations of the dual problem for variations $\{\boldsymbol{\eta},\delta\boldsymbol{z}\} \in \mathcal{V}$ and $\{\boldsymbol{\psi},\delta\boldsymbol{s}\} \in \mathcal{S}$. The tangent forms have to be evaluated for given $\{\boldsymbol{v},\boldsymbol{s},\boldsymbol{z}\}$.

6.6 Complete energy variations of the dual problem

The energy functional of the dual problem $E^*(\boldsymbol{v})(\boldsymbol{z},\boldsymbol{s})$ is formulated on a given deformed state and depends on the dual solution $\boldsymbol{z}$ and a design function $\boldsymbol{s}$. The problem is completely described if both variables are considered. This is illustrated in Fig. 6.1.

In the same manner as mentioned for the primal problem in Section 4.7, the dual physical and material problems are coupled by the dual pseudo load operator $p^*(\boldsymbol{v},\boldsymbol{s};\boldsymbol{z},\cdot,\cdot)$, i.e.

$$p^*(\boldsymbol{v},\boldsymbol{s};\boldsymbol{z},\delta\boldsymbol{z},\boldsymbol{\psi}) = R^{*\prime}_s = (E^*)''_{zs} = (E^*)''_{sz} = G^{*\prime}_z = t^*(\boldsymbol{v},\boldsymbol{s};\boldsymbol{z},\boldsymbol{\psi},\delta\boldsymbol{z}).$$

In the context of the finite element method we can say that the element formulation is complete if the dual residuals $\boldsymbol{R}^*$ and $\boldsymbol{G}^*$ as well as dual tangent matrices $\boldsymbol{P}^*$ and $\boldsymbol{D}^*$ are supplied. These residuals and tangent matrices can efficiently be computed and assembled in the same routine as the quantities for the primal problem without considerable computational cost. By means of all residuals and tangent forms not only the analysis of the dual problem can be performed but also the sensitivity with respect to configurational changes.

6.7 Total change in the dual energy and the dual solution

The above derived sensitivity relations are obtained for a given fixed state $\boldsymbol{v}$, i.e. the deformed body can be associated with the reference configuration of the dual problem.

The change in the dual energy δE^* and the change in the dual solution $\delta \boldsymbol{z}$ from (6.11) and (6.16) are just the parts of the change for a given fixed state. The total change in the dual energy and the dual solution consist of additional parts due to the change in the state $\boldsymbol{v}$ itself.

Therefore, we assume in the following that $\boldsymbol{v}$ is not fixed. The total variations of the dual energy functional and the dual physical residual are considered.

6.7.1 The dual energy functional

The total variation of the dual energy (6.2) with respect to $\boldsymbol{z}$, $\boldsymbol{s}$ and $\boldsymbol{v}$ reads

$$\begin{aligned} \delta E^* &= \delta_z E^*(\boldsymbol{v})(\boldsymbol{z},\boldsymbol{s})(\delta \boldsymbol{z}) + \delta_s E^*(\boldsymbol{v})(\boldsymbol{z},\boldsymbol{s})(\delta \boldsymbol{s}) + \delta_v E^*(\boldsymbol{v})(\boldsymbol{z},\boldsymbol{s})(\delta \boldsymbol{v}) \\ &= R^*(\boldsymbol{v},\boldsymbol{s};\boldsymbol{z},\delta \boldsymbol{z}) + G^*(\boldsymbol{v},\boldsymbol{s};\boldsymbol{z};\delta \boldsymbol{s}) + L^*(\boldsymbol{v},\boldsymbol{s};\boldsymbol{z};\delta \boldsymbol{v}), \end{aligned} \tag{6.87}$$

where

$$L^*(\boldsymbol{v},\boldsymbol{s};\boldsymbol{z};\delta \boldsymbol{v}) := \delta_v E^*(\boldsymbol{v})(\boldsymbol{z},\boldsymbol{s})(\delta \boldsymbol{v}). \tag{6.88}$$

For a given solution $\boldsymbol{z} \in \mathcal{V}$ of (6.1) we have $R^*(\boldsymbol{v},\boldsymbol{s};\boldsymbol{z},\delta \boldsymbol{z}) = 0$ and the first contribution vanishes. Hence, we obtain

$$\delta E^* = G^*(\boldsymbol{v},\boldsymbol{s};\boldsymbol{z};\delta \boldsymbol{s}) + L^*(\boldsymbol{v},\boldsymbol{s};\boldsymbol{z};\delta \boldsymbol{v}). \tag{6.89}$$

The functional L^* becomes in the discrete case

$$L^*(\hat{\boldsymbol{v}}_h,\hat{\boldsymbol{s}}_h;\hat{\boldsymbol{z}}_h;\delta \boldsymbol{v}) = \delta \boldsymbol{v}^T \boldsymbol{L}^* = \boldsymbol{L}^{*T} \delta \boldsymbol{v}. \tag{6.90}$$

The total variation of the dual energy can be written as

$$\delta E^* = \boldsymbol{G}^{*T} \delta \boldsymbol{s} + \boldsymbol{L}^{*T} \delta \boldsymbol{v} = \boldsymbol{G}^{*T} \delta \boldsymbol{s} - \boldsymbol{L}^{*T} \boldsymbol{K}^{-1} \boldsymbol{P}\, \delta \boldsymbol{s} = [\,\boldsymbol{G}^{*T} - \boldsymbol{L}^{*T} \boldsymbol{K}^{-1} \boldsymbol{P}\,] \delta \boldsymbol{s}, \tag{6.91}$$

where the sensitivity relation for the state (4.54) has been used in order to eliminate $\delta \boldsymbol{v}$, i.e. $\delta \boldsymbol{v} = -\boldsymbol{K}^{-1} \boldsymbol{P} \delta \boldsymbol{s}$. This sensitivity relation depends only on changes in $\boldsymbol{s}$.

6.7.2 The dual physical residual

The total variation of the dual physical residual (6.7) becomes

$$\begin{aligned} R^{*\prime} &= R^{*\prime}_z(\boldsymbol{v},\boldsymbol{s};\delta \boldsymbol{z},\boldsymbol{\eta}) + R^{*\prime}_s(\boldsymbol{v},\boldsymbol{s};\boldsymbol{z},\boldsymbol{\eta},\delta \boldsymbol{s}) + R^{*\prime}_v(\boldsymbol{v},\boldsymbol{s};\boldsymbol{z},\boldsymbol{\eta},\delta \boldsymbol{v}) \\ &= k(\boldsymbol{v},\boldsymbol{s};\delta \boldsymbol{z},\boldsymbol{\eta}) + p^*(\boldsymbol{v},\boldsymbol{s};\boldsymbol{z},\boldsymbol{\eta},\delta \boldsymbol{s}) + b^*(\boldsymbol{v},\boldsymbol{s};\boldsymbol{z},\boldsymbol{\eta},\delta \boldsymbol{v}) = 0, \end{aligned} \tag{6.92}$$

where

$$b^*(\boldsymbol{v},\boldsymbol{s};\boldsymbol{z},\boldsymbol{\eta},\delta \boldsymbol{v}) := R^{*\prime}_v(\boldsymbol{v},\boldsymbol{s};\boldsymbol{z},\boldsymbol{\eta},\delta \boldsymbol{v}). \tag{6.93}$$

Hence, the total change in the dual solution is given by

$$k(\boldsymbol{v}, \boldsymbol{s}; \delta\boldsymbol{z}, \boldsymbol{\eta}) = -Q^*_{\text{full}}(\boldsymbol{v}, \boldsymbol{s}; \boldsymbol{z}, \boldsymbol{\eta}) \quad \forall\, \boldsymbol{\eta} \in \mathcal{V}, \tag{6.94}$$

with the *complete* or *full dual pseudo load*

$$Q^*_{\text{full}}(\boldsymbol{v}, \boldsymbol{s}; \boldsymbol{z}, \boldsymbol{\eta}) := p^*(\boldsymbol{v}, \boldsymbol{s}; \boldsymbol{z}, \boldsymbol{\eta}, \delta\boldsymbol{s}) + b^*(\boldsymbol{v}, \boldsymbol{s}; \boldsymbol{z}, \boldsymbol{\eta}, \delta\boldsymbol{v}). \tag{6.95}$$

We consider the discrete case. The bilinear form $b^*(\boldsymbol{v}, \boldsymbol{s}; \boldsymbol{z}, \boldsymbol{\eta}, \delta\boldsymbol{v})$ becomes the matrix representation

$$b^*(\hat{\boldsymbol{v}}_h, \hat{\boldsymbol{s}}_h; \hat{\boldsymbol{z}}_h, \boldsymbol{\eta}_h, \delta\boldsymbol{v}_h) = \boldsymbol{\eta}^T \boldsymbol{B}^* \delta\boldsymbol{v}, \tag{6.96}$$

with the tangent matrix $\boldsymbol{B}^* \in \mathbb{R}^{n\times n}$. This is just the partial derivative of discrete dual residual vector $\boldsymbol{R}^*$ with respect to $\boldsymbol{v}$, i.e. $\boldsymbol{B}^* = \partial \boldsymbol{R}^* / \partial \boldsymbol{v}$. For given solutions $\{\boldsymbol{v}_h, \boldsymbol{s}_h, \boldsymbol{z}_h\}$ the discrete residual reads $\boldsymbol{R}^*(\boldsymbol{v}, \boldsymbol{s}; \boldsymbol{z}) = \boldsymbol{0}$ and we have

$$\begin{aligned} \delta\boldsymbol{R}^* &= \frac{\partial \boldsymbol{R}^*}{\partial \boldsymbol{z}}\delta\boldsymbol{z} + \frac{\partial \boldsymbol{R}^*}{\partial \boldsymbol{s}}\delta\boldsymbol{s} + \frac{\partial \boldsymbol{R}^*}{\partial \boldsymbol{v}}\delta\boldsymbol{v} = \boldsymbol{K}\delta\boldsymbol{z} + \boldsymbol{P}^*\delta\boldsymbol{s} + \boldsymbol{B}^*\delta\boldsymbol{v} \\ &= \boldsymbol{K}\delta\boldsymbol{z} + \boldsymbol{P}^*\delta\boldsymbol{s} - \boldsymbol{B}^*\boldsymbol{K}^{-1}\boldsymbol{P}\delta\boldsymbol{s} = \boldsymbol{0}, \end{aligned} \tag{6.97}$$

where $\delta\boldsymbol{v} = -\boldsymbol{K}^{-1}\boldsymbol{P}\delta\boldsymbol{s}$ has been used. Hence, the total change in the dual solution due to configurational variations $\delta\boldsymbol{s}$ is given by the discrete version of (6.94) in form of

$$\boldsymbol{K}\delta\boldsymbol{z} = -\boldsymbol{Q}^*_{\text{full}} \qquad \text{with} \qquad \boldsymbol{Q}^*_{\text{full}} = [\,\boldsymbol{P}^* - \boldsymbol{B}^*\boldsymbol{K}^{-1}\boldsymbol{P}\,]\,\delta\boldsymbol{s}. \tag{6.98}$$

This is a linear equation, in which $\boldsymbol{K}$ is the same primal tangent physical stiffness matrix as used within the last solution iteration of the primal problem.

For linear problems the dual residual $\boldsymbol{R}^*$ depends not on $\boldsymbol{v}$ and hence the second term in the full pseudo load $\boldsymbol{Q}^*_{\text{full}}$ vanishes, i.e. $\boldsymbol{B}^*\boldsymbol{K}^{-1}\boldsymbol{P} = \boldsymbol{0}$, because of $\boldsymbol{B}^* = \partial \boldsymbol{R}^* / \partial \boldsymbol{v} = \boldsymbol{0}$.

Remark 6.6 (Sensitivity operator) *A connection between the physical and material spaces for the total change in the dual solution is directly obtained from (6.98), i.e. we have*

$$\delta\boldsymbol{z} = \boldsymbol{S}^*_{\text{full}}\,\delta\boldsymbol{s} \qquad \textit{with} \qquad \boldsymbol{S}^*_{\text{full}} := -\boldsymbol{K}^{-1}[\,\boldsymbol{P}^* - \boldsymbol{B}^*\boldsymbol{K}^{-1}\boldsymbol{P}\,], \tag{6.99}$$

where $\boldsymbol{S}^*_{\text{full}} \in \mathbb{R}^{n\times m}$ *denotes the* full dual sensitivity operator matrix *of the dual problem.*

6.7.3 Explicit formulations for shape sensitivity

In the same manner as in Section 6.5.2 and Section 6.5.3 the explicit variational and discrete formulations of the functional $L^*(\boldsymbol{v}, \boldsymbol{s}; \boldsymbol{z}; \delta\boldsymbol{v})$ and the tangent form $b^*(\boldsymbol{v}, \boldsymbol{s}; \boldsymbol{z}, \boldsymbol{\eta}, \delta\boldsymbol{v})$ are stated.

The partial variation of the dual energy E^* with respect to $\boldsymbol{v}$ reads

$$\begin{aligned} L^*(\boldsymbol{v},\boldsymbol{s};\boldsymbol{z};\delta\boldsymbol{v}) = \int_{\Omega_R} \frac{1}{2}\{\, \Delta_z \mathbf{S}^{(z)} : \mathbf{E}'_v(\boldsymbol{v},\delta\boldsymbol{v}) \\ + 2\,\Delta_z \mathbf{S}^{(1)} : \mathbf{E}''_{vv}(\boldsymbol{z},\delta\boldsymbol{v}) + \Delta_z \mathbf{S}^{(2)} : \mathbf{E}'_v(\boldsymbol{v},\delta\boldsymbol{v})\,\}\,\mathrm{d}\Omega \\ - J''_{vv}(\boldsymbol{v},\boldsymbol{s};\boldsymbol{z},\delta\boldsymbol{v}). \end{aligned} \tag{6.100}$$

The corresponding nodal vector contribution is obtained as

$$\begin{aligned} \boldsymbol{L}_i^{*e} = \int_{\Omega_R^e} \frac{1}{2}\{\boldsymbol{B}_{vi}^T \Delta_z \underline{\boldsymbol{S}}^{(z)} + 2\,\boldsymbol{B}_{zi}^T \Delta_z \underline{\boldsymbol{S}}^{(1)} + \boldsymbol{B}_{vi}^T \Delta_z \underline{\boldsymbol{S}}^{(2)}\}\,\mathrm{d}\Omega \\ - \boldsymbol{J}^e_{vv}(\boldsymbol{v},\boldsymbol{s};\boldsymbol{z})_i. \end{aligned} \tag{6.101}$$

Furthermore, the partial variation of the dual physical residual R^* with respect to $\boldsymbol{v}$ is given by

$$\begin{aligned} b^*(\boldsymbol{v},\boldsymbol{s};\boldsymbol{z},\boldsymbol{\eta},\delta\boldsymbol{v}) = \int_{\Omega_R} \{\, \mathbf{E}''_{vv}(\boldsymbol{z},\boldsymbol{\eta}) : \mathbb{C} : \mathbf{E}'_v(\boldsymbol{v},\delta\boldsymbol{v}) \\ + \mathbf{E}'_v(\boldsymbol{v},\boldsymbol{\eta}) : \mathbb{C} : \mathbf{E}''_{vv}(\boldsymbol{z},\delta\boldsymbol{v}) \\ + \mathbf{E}''_{vv}(\boldsymbol{\eta},\delta\boldsymbol{v}) : \mathbb{C} : \mathbf{E}'_v(\boldsymbol{v},\boldsymbol{z}) \\ + \mathbf{E}'_v(\boldsymbol{v},\boldsymbol{\eta}) : \boldsymbol{\mathcal{D}} : \mathbf{E}'_v(\boldsymbol{v},\boldsymbol{z}) : \mathbf{E}'_v(\boldsymbol{v},\delta\boldsymbol{v})\,\}\,\mathrm{d}\Omega \\ - J''_{vv}(\boldsymbol{v},\boldsymbol{s};\boldsymbol{\eta},\delta\boldsymbol{v}). \end{aligned} \tag{6.102}$$

The discrete tangent matrix representation is achieved in form of

$$\begin{aligned} \boldsymbol{B}_{ij}^{*e} = \int_{\Omega_R^e} \{\, \boldsymbol{B}_{zi}^T \boldsymbol{C} \boldsymbol{B}_{vj} + \boldsymbol{B}_{vi}^T \boldsymbol{C} \boldsymbol{B}_{zj} + \boldsymbol{L}_i^T \Delta_z \boldsymbol{S}^{(1)} \boldsymbol{L}_j \boldsymbol{I} + \boldsymbol{B}_{vi}^T \Delta_z \boldsymbol{C}^{(1)} \boldsymbol{B}_{vj}\,\}\,\mathrm{d}\Omega \\ - \boldsymbol{J}^e_{vv}(\boldsymbol{v},\boldsymbol{s})_{ij}. \end{aligned} \tag{6.103}$$

The stress increments $\Delta_z \mathbf{S}^{(i)}$ and the elasticity tensor increment $\Delta_z \mathbb{C}^{(1)}$ are given in Box 6.1. Details on the numerical implementation are stated in Appendix C.

6.8 An illustrative example

System and model problem. A L-shaped plate as indicated in Figure 6.2a is investigated. The plate is loaded by tractions $\bar{\boldsymbol{t}} = [0, -5]^T$. A compressible Neo-Hookean material with the strain energy function given in (B.20) is considered. The Lamé parameters are chosen as $\lambda = 5.769 \times 10^2$ and $\mu = 3.846 \times 10^2$, which correspond to $E = 10^3$ and $\nu = 0.3$. The discrete design variables $\boldsymbol{s}$ are the nodal coordinates of the mesh.

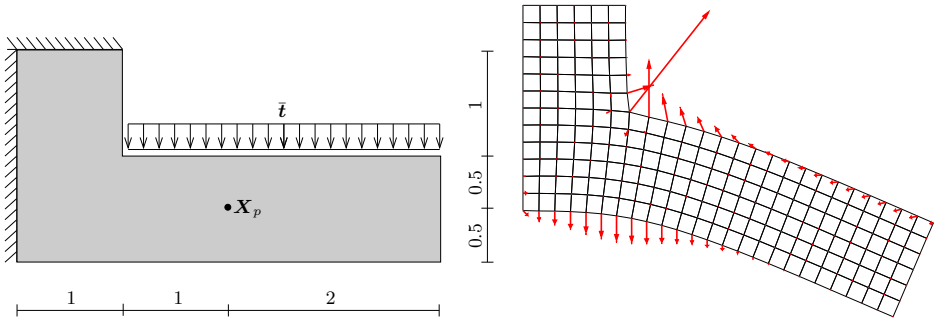

(a) primal problem (b) primal solution $\boldsymbol{u}_h$ and material residual $\boldsymbol{G}$

Figure 6.2: L-shaped plate: system of the primal problem and the primal material residual on the mesh nodes for the given deformed state

The quantity of interest and the dual problem. The stress component $S_{22}(\boldsymbol{X}_p)$ of the second Piola-Kirchhoff stress $\mathbf{S}$ at the point $\boldsymbol{X}_p$ is considered as quantity of interest, i.e. $J(\boldsymbol{u}, \boldsymbol{s}) = S_{22}(\boldsymbol{X}_p)$. The explicit expressions of the variations are given in Example 6.1 in Section 6.5.2.

Both the dual problem for the initial problem with $\boldsymbol{u}_h = \mathbf{0}$ and the dual problem formulated at the given deformed state $\boldsymbol{u}_h$ due to the primal load case $\bar{\boldsymbol{t}}$ are taken into consideration. The solution of the dual problem (6.45) for the chosen quantity of interest $J(\boldsymbol{u}, \boldsymbol{s}) = S_{22}(\boldsymbol{X}_p)$ requires the computation of the dual load J'_u given in (6.47). The corresponding discrete equivalent nodal forces $\boldsymbol{J}_u$ for the initial case ($\boldsymbol{u}_h = \mathbf{0}$) and the deformed state are shown in Fig. 6.3a and Fig. 6.3b, respectively. These loads cause the approximate dual solutions $\boldsymbol{z}_h$ shown in Fig. 6.3c and Fig. 6.3d. These are very rough approximations of the exact dual solutions, which have a discontinuity in the point $\boldsymbol{X}_p$. A good approximation of the dual solution on a highly local refined mesh for $\boldsymbol{u}_h = \mathbf{0}$ is given in Fig. 6.4. The figure shows a 3D plot of the vertical component z_y.

The change in the quantity of interest. If the dual solutions are known the change in the quantity of interest $J(\boldsymbol{u}, \boldsymbol{s})$ can be computed for arbitrary residuals $\boldsymbol{R}$, i.e. we have to evaluate (5.22) for any changes in the physical loads. Furthermore, if we have configurational changes $\delta\boldsymbol{s}$ we can compute the change in $J(\boldsymbol{u}, \boldsymbol{s})$ due to $\delta\boldsymbol{s}$, i.e. we have to evaluate Eq. 6.27. The discrete versions of (5.22) and (6.27) are given as

$$\delta S_{22}(\boldsymbol{X}_p) = -\boldsymbol{z}^T \boldsymbol{R} \qquad \text{and} \qquad \delta S_{22}(\boldsymbol{X}_p) = -\boldsymbol{z}^T \boldsymbol{Q}_p, \tag{6.104}$$

where $\boldsymbol{Q}_p = \boldsymbol{P}\delta\hat{\boldsymbol{s}}$ is the pseudo load vector corresponding to configurational variations $\delta\hat{\boldsymbol{s}}$. The new value of the quantity of interest is given by the update

$$J^{new} = J(\boldsymbol{u}_h, \boldsymbol{s}_h) + J'_u(\boldsymbol{u}_h, \boldsymbol{s}_h; \delta\boldsymbol{u}_h). \tag{6.105}$$

Hence, the stress component for the changed design is given by $S_{22}^{new} = S_{22} + \delta S_{22}$.

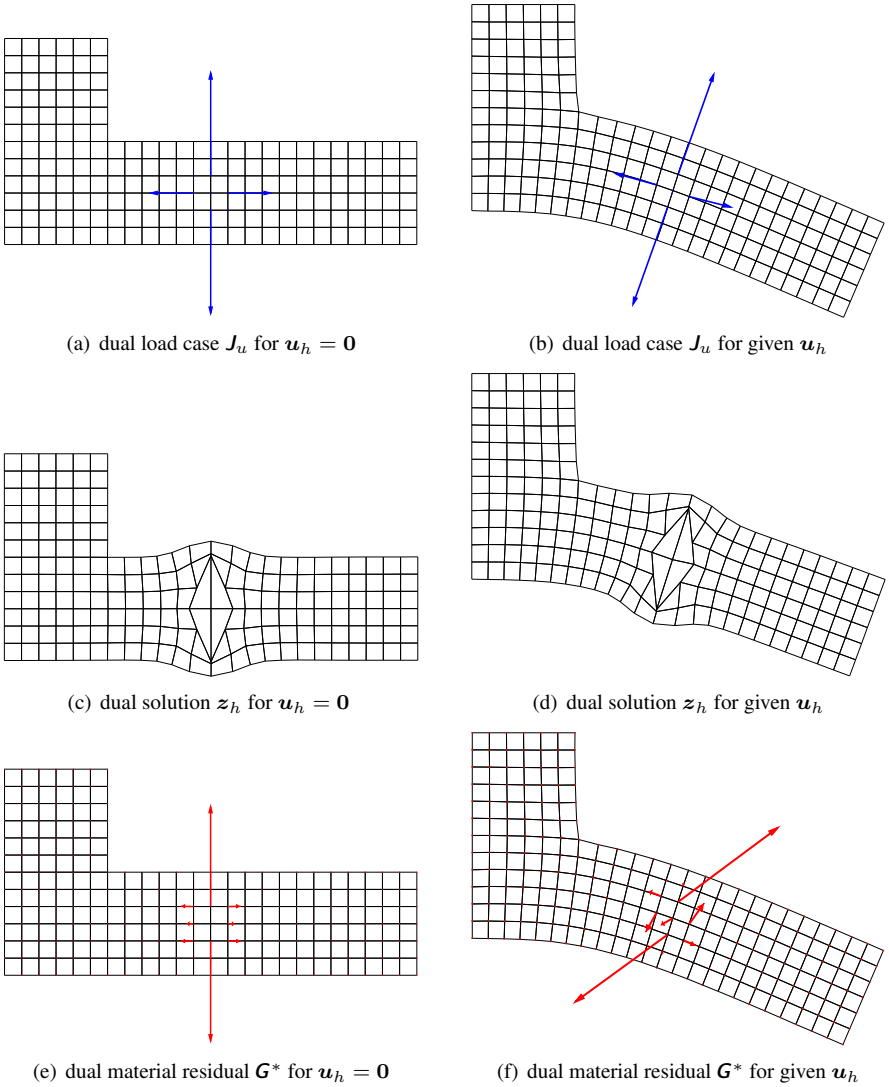

(a) dual load case $\boldsymbol{J}_u$ for $\boldsymbol{u}_h = \boldsymbol{0}$

(b) dual load case $\boldsymbol{J}_u$ for given $\boldsymbol{u}_h$

(c) dual solution $\boldsymbol{z}_h$ for $\boldsymbol{u}_h = \boldsymbol{0}$

(d) dual solution $\boldsymbol{z}_h$ for given $\boldsymbol{u}_h$

(e) dual material residual $\boldsymbol{G}^*$ for $\boldsymbol{u}_h = \boldsymbol{0}$

(f) dual material residual $\boldsymbol{G}^*$ for given $\boldsymbol{u}_h$

Figure 6.3: L-shaped plate: dual problems (equivalent nodal forces $\boldsymbol{J}_u$), dual solutions and dual material residuals for the undeformed and a given deformed state for $J(\boldsymbol{u}, \boldsymbol{s}) = S_{22}(\boldsymbol{X}_p)$; (the dual solutions are scaled and the nodal forces are normalized to unity)

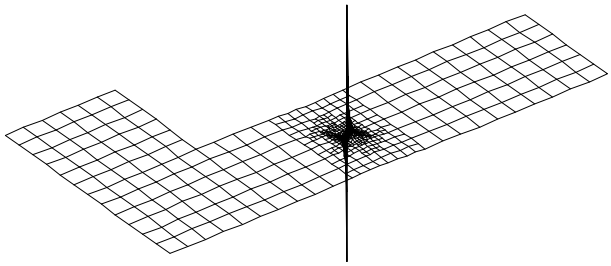

Figure 6.4: L-shaped plate: 3D plot of the approximate dual solution z_y

The primal and dual material residuals. The primal solution $\boldsymbol{u}_h$ as well as the corresponding primal material residual $\boldsymbol{G}(\boldsymbol{u}_h, \boldsymbol{s}_h)$ for the chosen mesh are given in Fig. 6.2b. The nodal values of $\boldsymbol{G}$ are scaled to unity in order to guarantee the visibility. The material residual does in general not vanish in the discrete case. The primal material residual $\boldsymbol{G}$ in Fig. 6.2b can be interpreted as the sensitivity of the primal energy functional $E(\boldsymbol{u}_h, \boldsymbol{s}_h)$ with respect to changes in the material configuration. In the same manner, the dual material residuals $\boldsymbol{G}^*$ shown in Fig. 6.3e and Fig. 6.3f, respectively, can be interpreted as the sensitivity of the dual energy functional $E^*(\boldsymbol{u}_h)(\boldsymbol{z}_h, \boldsymbol{s}_h)$. Hence, the changes in the primal energy $\delta_s E$ and the dual energy $\delta_s E^*$ due to given changes in the discrete design variables $\delta\boldsymbol{s}$ are given by the discrete sensitivity relations

$$\delta_s E = \boldsymbol{G}^T \delta\boldsymbol{s} \qquad \text{and} \qquad \delta_s E^* = \boldsymbol{G}^{*T} \delta\boldsymbol{s}. \tag{6.106}$$

A large material residual on a nodal coordinate s_i indicates that a change in this design variable causes a large change in the primal and dual energy, respectively, i.e. the residual reflects the influence of the design variable s_i on energy changes.

6.9 Summary and concluding remarks

In the present chapter a novel formulation for the dual problem with respect to configurational variations has been presented. The dual problem can be formulated at a given deformed state. In the same manner as for the primal problem the complete variational and discrete formulations of the dual problem were proposed. Variations of a dual energy functional yield a dual physical and material residual, respectively. The corresponding tangent forms have been derived, which are the basis for sensitivity analysis of the dual solution itself. The most important sensitivity relations are summarized in Table 6.1.

The change in the dual solution $\delta\boldsymbol{z}$ due to changes in the design of the material body on a given deformed state can be computed by solving the sensitivity relation (6.98) given as

$$\boldsymbol{K}\delta\boldsymbol{z} = -\boldsymbol{Q}^*_{\text{full}},$$

Table 6.1: Summary of important variational and discrete sensitivity relations

Variational formulation	Discrete formulation
dual physical residual (fixed $\boldsymbol{v}$)	
$\delta R^* = k(\boldsymbol{v}, \boldsymbol{s}; \delta \boldsymbol{z}, \cdot) + p^*(\boldsymbol{v}, \boldsymbol{s}; \boldsymbol{z}, \cdot, \delta \boldsymbol{s})$	$\delta \boldsymbol{R}^* = \boldsymbol{K} \delta \boldsymbol{z} + \boldsymbol{P}^* \delta \boldsymbol{s}$
dual material residual (fixed $\boldsymbol{v}$)	
$\delta G^* = p^*(\boldsymbol{v}, \boldsymbol{s}; \boldsymbol{z}, \delta \boldsymbol{z}, \cdot) + d^*(\boldsymbol{v}, \boldsymbol{s}; \boldsymbol{z}; \cdot, \delta \boldsymbol{s})$	$\delta \boldsymbol{G}^* = \boldsymbol{P}^{*T} \delta \boldsymbol{z} + \boldsymbol{D}^* \delta \boldsymbol{s}$
dual pseudo load (fixed $\boldsymbol{v}$)	
$Q_p^*(\boldsymbol{v}, \boldsymbol{s}; \boldsymbol{z}, \cdot) = p^*(\boldsymbol{v}, \boldsymbol{s}; \boldsymbol{z}, \cdot, \delta \hat{\boldsymbol{s}})$	$\boldsymbol{Q}_p^* = \boldsymbol{P}^* \delta \hat{\boldsymbol{s}}$
sensitivity of $\boldsymbol{z}$ (fixed $\boldsymbol{v}$)	
$k(\boldsymbol{v}, \boldsymbol{s}; \delta \boldsymbol{z}, \cdot) = -Q_p^*(\boldsymbol{v}, \boldsymbol{s}; \boldsymbol{z}, \cdot)$	$\boldsymbol{K} \delta \boldsymbol{z} = -\boldsymbol{Q}_p^*$
sensitivity of E^* (fixed $\boldsymbol{v}$)	
$\delta_s E^* = G^*(\boldsymbol{v}, \boldsymbol{s}; \boldsymbol{z}; \delta \boldsymbol{s})$	$\delta_s E^* = \boldsymbol{G}^{*T} \delta \boldsymbol{s}$
full dual pseudo load	
$Q_{\text{full}}^*(\boldsymbol{v}, \boldsymbol{s}; \boldsymbol{z}, \cdot)$	$\boldsymbol{Q}_{\text{full}}^* = [\, \boldsymbol{P}^* - \boldsymbol{B}^* \boldsymbol{K}^{-1} \boldsymbol{P} \,] \, \delta \hat{\boldsymbol{s}}$
sensitivity of $\boldsymbol{z}$	
$k(\boldsymbol{v}, \boldsymbol{s}; \delta \boldsymbol{z}, \cdot) = -Q_{\text{full}}^*(\boldsymbol{v}, \boldsymbol{s}; \boldsymbol{z}, \cdot)$	$\boldsymbol{K} \delta \boldsymbol{z} = -\boldsymbol{Q}_{\text{full}}^*$
sensitivity of E^*	
$\delta E^* = G^*(\boldsymbol{v}, \boldsymbol{s}; \boldsymbol{z}; \delta \boldsymbol{s}) + L^*(\boldsymbol{v}, \boldsymbol{s}; \boldsymbol{z}; \delta \boldsymbol{v})$	$\delta E^* = [\, \boldsymbol{G}^{*T} - \boldsymbol{L}^{*T} \boldsymbol{K}^{-1} \boldsymbol{P} \,] \, \delta \boldsymbol{s}$
sensitivity of $J(\boldsymbol{v}, \boldsymbol{s})$	
$J'_v(\boldsymbol{v}, \boldsymbol{s}; \delta \boldsymbol{v}) = -Q_p(\boldsymbol{v}, \boldsymbol{s}; \boldsymbol{z})$	$J'_v(\boldsymbol{v}_h, \boldsymbol{s}_h; \delta \boldsymbol{v}_h) = -\boldsymbol{z}^T \boldsymbol{Q}_p$

where $\boldsymbol{Q}_{\text{full}}^*$ is the total dual pseudo load for a given design variation $\delta \hat{\boldsymbol{s}}$. This can be used within the error analysis of sensitivity relations or model adaptivity for local quantities of interest, because the change in a chosen quantity of interest due to design or model changes depends on the change in the dual solution $\delta \boldsymbol{z}$, which is caused by the same design or model changes. The change of the physical model can be interpreted as a change in the design. This is discussed in Section 10.4 and Section 10.5. Therefore, the first-order approximation for the change in the dual solution obtained from (6.98) can be used to estimate the change in the quantity of interest, see Section 10.4.3.

Chapter 7

Global r-adaptive mesh optimization

A direct application of the proposed energy minimization problem is r-adaptive mesh optimization. In this case the nodal coordinates in the domain and the nodal coordinates in tangential direction on the boundaries are chosen as design variables. The lowest potential energy of the primal problem yields the smallest discretization error on the current mesh. The derived residuals and tangent forms of the primal problem are the basis for global r-adaptive mesh optimization.

7.1 Introduction

The optimization of finite element meshes with a fixed number of nodes by relocating a subset of nodes is well-known as r-adaptivity. This problem has a long tradition. First steps for the optimization of finite element meshes based on a discrete formulation of energy minimization date back to the nineteen seventies and were outlined for instance in [23, 24, 41, 75, 99]. The energy is minimized with respect to the state and the position of the nodes. The best mesh is defined as the one associated with the lowest potential energy.

Another approach is based on the well-known fact, that the mesh is optimal if the discretization error is uniformly distributed on the mesh [33]. For computed error estimators on all elements, the nodes are positioned such that the error is uniformly distributed, i.e. the error in every element is the same.

Furthermore, r-adaptive techniques are also known as the so-called moving mesh algorithms, see e.g. [22] for an overview. Local minimization problems with few degrees of freedom are often solved instead of the global problem [103].

In recent years r-adaptivity became very popular in the context of configurational mechanics or mechanics in the material space, see e.g. [2, 20, 77, 80, 101].

Furthermore, in the context of structural optimization and sensitivity analysis this has been investigated in [66, 69, 70]. The overall energy depends on the state function and on a design function, which specifies in an abstract sense the material configuration. The partial variation

with respect to the state variable leads to the classical physical residual and the partial variation with respect to the design function leads to the material residual. In the context of the finite element method, we obtain a material residual due to the non-optimal numerical solution, which is a result of the non-optimal discretization in the sense of the minimization of the overall energy. Hence, a non-vanishing material residual within the domain is an indicator for a non-optimal finite element mesh.

Within r-adaptivity we can improve the finite element solution on the same mesh. Furthermore, the method is easy to implement in comparison to other adaptivity algorithms, e.g. h-, p- or hp-adaptivity, because no new degrees of freedom have to be introduced and the nodal connectivities are fixed. But there are also some disadvantages of the method. The r-adaptivity based on direct energy minimization requires the solution of a highly nonlinear optimization problem, because all the nodal coordinates or a large subset of nodal coordinates are the design variables. In addition, some numerical difficulties arise during the solution process, e.g. the system matrices are often ill-conditioned and we have to control the mesh distortion. Due to the non-convexity of the energy functional the solution may not be unique, but yields an improvement of the initial mesh.

Nevertheless, r-adaptive mesh optimization algorithms are useful in many cases, for instance:

- At the beginning of an adaptive process, i.e. for an initial coarse mesh before the application of the h- or p-adaptive methods.

- For problems with changes in the reference configuration, e.g. shape optimization or fracture mechanics, where the mesh may become distorted due to the change of the shape.

- For problems, where moving and large local phenomena occur, e.g. shock waves or moving interfaces.

In h- or p-adaptive algorithms the approximation spaces are enhanced in every iteration step, i.e. new degrees of freedom are introduced by selectively subdividing elements or by selective enrichment of elements. This leads to a minimization of the overall discretization error for $h \to 0$ or $p \to \infty$, respectively. In contrast, the r-adaptivity yields an improvement of the solution on the same mesh, i.e. the approximation spaces are fixed and hence we may in general not expect the minimization of the overall discretization error. But the discretization error on the current mesh can be minimized. Therefore, the r-adaptive optimization can not be seen as a real competitor to h- or p-adaptivity but rather a supplement. The combination of r- and h- or p-adaptivity seems to be promising. A combined rh-adaption is more efficient than a pure h-adaptive algorithm [89]. Therefore, a rhp-adaptive method seems to be the most efficient strategy.

7.2 The energy minimization problem

The discrete energy minimization problem which has been introduced in Section 4.4.1 is considered. Within this chapter the displacement field $\boldsymbol{u}$ is chosen as primary unknown. The discrete energy functional depends on the discrete state $\boldsymbol{u}_h \in \mathcal{V}_h \subset \mathcal{V}$ and discrete design $\boldsymbol{s}_h \in \mathcal{S}_h \subset \mathcal{S}$.

In the context of the finite element method and r-adaptivity, the discrete design variables are a subset of nodal coordinates which are allowed to vary and the current mesh is the reference configuration. All inner nodes or a subset of nodes build up the design space $\mathcal{S}_h$. Additional we can include nodal coordinates in tangential direction on the boundary. The nodal coordinates in normal direction on the boundaries are fixed in order to keep the shape of the body.

The minimization of the energy with respect to the state and the nodal coordinates yields a r-adaptive mesh optimization algorithm. Hence, $\boldsymbol{u}_h$ and $\boldsymbol{s}_h$ are determined by problem (4.4), i.e. the following optimization problem has to be solved: Find $\{\boldsymbol{u}_h, \boldsymbol{s}_h\} \in \mathcal{V}_h \times \mathcal{S}_h$ such that

$$E(\boldsymbol{u}_h, \boldsymbol{s}_h) = \min_{\{\boldsymbol{p}_h, \boldsymbol{r}_h\} \in \mathcal{V}_h \times \mathcal{S}_h} E(\boldsymbol{p}_h, \boldsymbol{r}_h). \tag{7.1}$$

For the optimal solutions $\boldsymbol{u}_h^* \in \mathcal{V}_h$ and $\boldsymbol{s}_h^* \in \mathcal{S}_h$ in the chosen approximation spaces $\mathcal{V}_h$ and $\mathcal{S}_h$ it is required that

$$E(\boldsymbol{u}_h^*, \boldsymbol{s}_h^*) \leq E(\boldsymbol{u}_h, \boldsymbol{s}_h) \quad \forall\, \boldsymbol{u}_h, \boldsymbol{s}_h \in \mathcal{V}_h \times \mathcal{S}_h. \tag{7.2}$$

The error of the state $\boldsymbol{e}_{u,h}$ and the design $\boldsymbol{e}_{s,h}$ in the chosen approximation spaces are introduced by

$$\boldsymbol{e}_{u,h} := \boldsymbol{u}_h^* - \boldsymbol{u}_h \quad \text{and} \quad \boldsymbol{e}_{s,h} := \boldsymbol{s}_h^* - \boldsymbol{s}_h. \tag{7.3}$$

The optimal solution $\boldsymbol{u}_h^*$ depends on the optimal design, i.e. $\boldsymbol{u}_h^* = \boldsymbol{u}_h(\boldsymbol{s}_h^*)$ and we can rewrite the energy in the form $\hat{E}(\boldsymbol{u}_h^*) = E(\boldsymbol{u}_h(\boldsymbol{s}_h^*), \boldsymbol{s}_h^*)$. In the linear theory, we have a simple energy representation of the form

$$E(\boldsymbol{u}) = \frac{1}{2}\, a(\boldsymbol{u}, \boldsymbol{u}) - F(\boldsymbol{u}). \tag{7.4}$$

It can easily be proved that

$$\hat{E}(\boldsymbol{u}_h^*) \leq \hat{E}(\boldsymbol{u}_h) \tag{7.5}$$

because, using linearity and symmetry of bilinear form $a(\cdot,\cdot)$, we have

$$\begin{aligned}\hat{E}(\boldsymbol{u}_h) &= \hat{E}(\boldsymbol{u}_h^* - \boldsymbol{e}_{u,h}) \\ &= \frac{1}{2}\, a(\boldsymbol{u}_h^* - \boldsymbol{e}_{u,h}, \boldsymbol{u}_h^* - \boldsymbol{e}_{u,h}) - F(\boldsymbol{u}_h^* - \boldsymbol{e}_{u,h}) \\ &= \frac{1}{2}\, a(\boldsymbol{u}_h^*, \boldsymbol{u}_h^*) - a(\boldsymbol{u}_h^*, \boldsymbol{e}_{u,h}) + \frac{1}{2}\, a(\boldsymbol{e}_{u,h}, \boldsymbol{e}_{u,h}) \\ &\quad - F(\boldsymbol{u}_h^*) + F(\boldsymbol{e}_{u,h}) \\ &= \hat{E}(\boldsymbol{u}_h^*) + \frac{1}{2}\, a(\boldsymbol{e}_{u,h}, \boldsymbol{e}_{u,h}).\end{aligned} \tag{7.6}$$

Here, we have used $a(\boldsymbol{u}_h^*, \boldsymbol{e}_{u,h}) - F(\boldsymbol{e}_{u,h}) = 0$. Due to the fact that $a(\boldsymbol{e}_{u,h}, \boldsymbol{e}_{u,h}) \geq 0$ follows the relation (7.5).

This is the motivation for r-adaptive mesh optimization. We reduce the energy with respect to $\boldsymbol{u}$ and $\boldsymbol{s}$ in order to find the state with the lowest energy and hence the optimal solution $\boldsymbol{u}_h^*$ and $\boldsymbol{s}_h^*$ in the chosen approximation spaces $\mathcal{V}_h$ and $\mathcal{S}_h$.

7.3 Error measures in the context of r-adaptivity

Different error measures can be introduced in the context of r-adaptivity.

Definition 7.1 (Error measures within r-adaptivity) *Let $\boldsymbol{u} \in \mathcal{V}$ be the exact solution of the considered variational problem. Then, the error*

$$\boldsymbol{e}_u := \boldsymbol{u} - \boldsymbol{u}_h \tag{7.7}$$

measures the overall discretization error *with respect to a solution $\boldsymbol{u}_h(\boldsymbol{s}_h) \in \mathcal{V}_h$. In contrast, the error*

$$\boldsymbol{e}_{u,h} := \boldsymbol{u}_h^* - \boldsymbol{u}_h \tag{7.8}$$

measures the discretization error on the current mesh*, i.e. the distance between the optimal solution $\boldsymbol{u}_h^* = \boldsymbol{u}_h(\boldsymbol{s}_h^*) \in \mathcal{V}_h$ and a solution $\boldsymbol{u}_h(\boldsymbol{s}_h) \in \mathcal{V}_h$. Furthermore, the* least obtainable discretization error *on the current mesh is introduced as*

$$\boldsymbol{e}_u^* := \boldsymbol{u} - \boldsymbol{u}_h^*, \tag{7.9}$$

i.e. the distance between the true solution $\boldsymbol{u}$ and the optimal solution $\boldsymbol{u}_h^*$ on the current approximation spaces $\mathcal{V}_h$ and $\mathcal{S}_h$.

For the error $\boldsymbol{e}_u^*$ holds

$$\boldsymbol{e}_u^* = \boldsymbol{u} - \boldsymbol{u}_h^* = (\boldsymbol{u} - \boldsymbol{u}_h) - (\boldsymbol{u}_h^* - \boldsymbol{u}_h) = \boldsymbol{e}_u - \boldsymbol{e}_{u,h}. \tag{7.10}$$

Hence, the error $\boldsymbol{e}_u$ can be split into the error $\boldsymbol{e}_u^*$ and the error on the current mesh $\boldsymbol{e}_{u,h}$, i.e.

$$\boldsymbol{e}_u = \boldsymbol{e}_u^* + \boldsymbol{e}_{u,h}. \tag{7.11}$$

For instance, for the linear problem (7.4), the error $\boldsymbol{e}_u$ in terms of the energy norm $||\cdot||_E$ is given as

$$\begin{aligned} ||\boldsymbol{e}_u||_E^2 &= a(\boldsymbol{e}_u, \boldsymbol{e}_u) = a(\boldsymbol{e}_u^* + \boldsymbol{e}_{u,h}, \boldsymbol{e}_u^* + \boldsymbol{e}_{u,h}) \\ &= a(\boldsymbol{e}_u^*, \boldsymbol{e}_u^*) + 2a(\boldsymbol{e}_u^*, \boldsymbol{e}_{u,h}) + a(\boldsymbol{e}_{u,h}, \boldsymbol{e}_{u,h}) \\ &= a(\boldsymbol{e}_u^*, \boldsymbol{e}_u^*) + a(\boldsymbol{e}_{u,h}, \boldsymbol{e}_{u,h}) \\ &= ||\boldsymbol{e}_u^*||_E^2 + ||\boldsymbol{e}_{u,h}||_E^2, \end{aligned} \tag{7.12}$$

where the orthogonality condition $a(\boldsymbol{e}_u^*, \boldsymbol{\eta}) = 0 \,\forall\, \boldsymbol{\eta} \in \mathcal{V}_h$ has been used. Due to the fact that $||\boldsymbol{e}_{u,h}||_E^2 \geq 0$ follows the relation

$$||\boldsymbol{e}_u^*||_E^2 \leq ||\boldsymbol{e}_u||_E^2. \tag{7.13}$$

For the optimal discretization, i.e. $\boldsymbol{u}_h = \boldsymbol{u}_h^* = \boldsymbol{u}_h(\boldsymbol{s}_h^*)$ follows $\boldsymbol{e}_{u,h} = \boldsymbol{0}$ and hence $\boldsymbol{e}_u = \boldsymbol{e}_u^*$. This means, even in the case that the best distribution of the nodal coordinates $\boldsymbol{s}_h^*$ is obtained, there is still an error contribution. On coarse meshes the contribution of the part $\boldsymbol{e}_{u,h}$ on the overall error $\boldsymbol{e}_u$ is large. This is illustrated in Figure 8.4.

Furthermore, let $||\boldsymbol{e}_u^*||$ be an error norm of the optimal discretization error on the current mesh $\boldsymbol{e}_u^* = \boldsymbol{u} - \boldsymbol{u}_h^*$. If the true error $||\boldsymbol{e}_u|| \to 0$, the error measure $||\boldsymbol{e}_{u,h}||$ is asymptotically exact if

$$\frac{||\boldsymbol{e}_u^*||}{||\boldsymbol{e}_u||} \to 0. \tag{7.14}$$

The proof is straightforward. Using the triangular inequality we have from $\boldsymbol{e}_{u,h} = \boldsymbol{e}_u - \boldsymbol{e}_u^*$

$$||\boldsymbol{e}_u|| - ||\boldsymbol{e}_u^*|| \leq ||\boldsymbol{e}_{u,h}|| \leq ||\boldsymbol{e}_u|| + ||\boldsymbol{e}_u^*|| \tag{7.15}$$

or

$$\left(1 - \frac{||\boldsymbol{e}_u^*||}{||\boldsymbol{e}_u||}\right) \leq \frac{||\boldsymbol{e}_{u,h}||}{||\boldsymbol{e}_u||} \leq \left(1 + \frac{||\boldsymbol{e}_u^*||}{||\boldsymbol{e}_u||}\right). \tag{7.16}$$

The effectivity index

$$I_{\text{eff}} := \frac{||\boldsymbol{e}_{u,h}||}{||\boldsymbol{e}_u||} \tag{7.17}$$

tends to unity as $\dfrac{||\boldsymbol{e}_u^*||}{||\boldsymbol{e}_u||} \to 0$.

Finally, in contrast to other adaptivity techniques, e.g. h or p-adaptivity, the r-adaptivity leads only to a minimization of the discretization error $\boldsymbol{e}_{u,h}$ on the current mesh, i.e. we keep the same approximation spaces $\mathcal{V}_h$ and $\mathcal{S}_h$. This means that for the optimal solution $\boldsymbol{u}_h^*$ the error $\boldsymbol{e}_u^*$ remains. In h or p-adaptivity we extend in every step the approximation spaces $\mathcal{V}_h$ and $\mathcal{S}_h$. This leads to a minimization of the true error $\boldsymbol{e}_u$ for $h \to 0$ or $p \to \infty$, respectively. Nevertheless, the r-adaptivity provides an improved solution on the same mesh with low computational cost. If we require a lower discretization error, we have to extend the approximation spaces, i.e. we have to perform a h- or p-adaptive step. The best performance could be achieved if we combine r-adaptivity with h- and/or p-adaptivity.

7.4 The error in the material residual

The physical residual is fulfilled for every admissible design, i.e.

$$R(\boldsymbol{u}_h, \boldsymbol{s}_h; \boldsymbol{\eta}_h) = 0 \quad \forall\, \boldsymbol{s}_h \in \mathcal{S}_h. \tag{7.18}$$

The optimality condition (4.42) for the material problem holds only for stationary points $\boldsymbol{u}_h^*$ and $\boldsymbol{s}_h^*$, i.e. $E_s' = G(\boldsymbol{u}_h^*, \boldsymbol{s}_h^*; \boldsymbol{\psi}_h) = 0$. This means, that the material residual is not fulfilled for every $\boldsymbol{u}_h \neq \boldsymbol{u}_h^* = \boldsymbol{u}_h(\boldsymbol{s}_h^*)$, i.e.

$$G(\boldsymbol{u}_h, \boldsymbol{s}_h; \boldsymbol{\psi}_h) \neq 0 \quad \forall\, \boldsymbol{u}_h \neq \boldsymbol{u}_h^* = \boldsymbol{u}_h(\boldsymbol{s}_h^*) \in \mathcal{V}_h. \tag{7.19}$$

Hence, we obtain a material residual as a result of the non-optimal solution $\boldsymbol{u}_h$, which is a result of the non-optimal design $\boldsymbol{s}_h$ in the sense of the minimization of problem (4.41). With the definition of the errors (7.3) we have $\boldsymbol{s}_h^* = \boldsymbol{s}_h + \boldsymbol{e}_{s,h}$ and

$$G(\boldsymbol{u}_h^*, \boldsymbol{s}_h^*; \boldsymbol{\psi}_h) = G(\boldsymbol{u}_h(\boldsymbol{s}_h + \boldsymbol{e}_{s,h}), \boldsymbol{s}_h + \boldsymbol{e}_{s,h}; \boldsymbol{\psi}_h) = 0. \tag{7.20}$$

From this, a suitable approximation for the error could be obtained from the linearization

$$G(\boldsymbol{u}_h, \boldsymbol{s}_h; \boldsymbol{\psi}_h) + D_s G(\boldsymbol{u}_h, \boldsymbol{s}_h; \boldsymbol{\psi}_h) \cdot \boldsymbol{e}_{s,h} + \mathcal{O} = 0. \tag{7.21}$$

The material tangent operator

$$D_s G(\boldsymbol{u}_h, \boldsymbol{s}_h; \boldsymbol{\psi}_h) \cdot \boldsymbol{e}_{s,h} = m(\boldsymbol{u}_h, \boldsymbol{s}_h; \boldsymbol{\psi}_h, \boldsymbol{e}_{s,h}) \tag{7.22}$$

is given in (4.80), where we have replaced the design increment by the error in the design $\boldsymbol{e}_{s,h}$. The remainder of higher-order $\mathcal{O}$ and can be neglected. The material tangent operator has to be evaluated in each step at the current state $\{\boldsymbol{u}_h, \boldsymbol{s}_h\}$. Finally, we obtain an equation for the error in the design or rather for the error in the material residual in the form

$$m(\boldsymbol{u}_h, \boldsymbol{s}_h; \boldsymbol{\psi}_h, \boldsymbol{e}_{s,h}) = -G(\boldsymbol{u}_h, \boldsymbol{s}_h; \boldsymbol{\psi}_h) \quad \forall\, \boldsymbol{\psi}_h \in \mathcal{S}_h. \tag{7.23}$$

This is comparable to the discrete version of Eq. 4.81, in which we have replaced the design increment $\Delta \boldsymbol{s}_h$ by $\boldsymbol{e}_{s,h}$.

Finally, the discrete material residual vector $\boldsymbol{G}$ corresponding to the functional $G(\boldsymbol{u}_h, \boldsymbol{s}_h; \cdot)$ is an error indicator for a non-optimal finite element discretization. The minimization of the residual on the mesh nodes by relocating the nodes yields a lower energy and therefore a smaller discretization error on the current mesh.

Remark 7.1 *The material residual as an error indicator for mesh optimization can also be used within h-adaptive algorithms [79]. Furthermore, it seems promising to combine r- and h-adaptivity as well as remeshing strategies based on the above mentioned error indicators [78, 89].*

7.5 Numerical solution, regularization and algorithmic details

7.5.1 Solution algorithms

For the mesh optimization problem a subset the nodal coordinates $\boldsymbol{X}_s$ are chosen as design variables, i.e. $\boldsymbol{s} = \boldsymbol{X}_s$. The optimal nodal positions (the design) of a given mesh (the reference configuration) can be computed by solving Eq. 4.71, i.e.

$$\begin{bmatrix} \boldsymbol{K} & \boldsymbol{P} \\ \boldsymbol{P}^T & \boldsymbol{D} \end{bmatrix} \begin{bmatrix} \Delta \boldsymbol{u} \\ \Delta \boldsymbol{X}_s \end{bmatrix} = - \begin{bmatrix} \boldsymbol{R} \\ \boldsymbol{G} \end{bmatrix}. \tag{7.24}$$

Alternatively, other solution algorithms could be used for the mesh optimization problem. The staggered solution algorithm (4.83) yields the form

$$\boldsymbol{M} \Delta \boldsymbol{X}_s = -\boldsymbol{G} \qquad \text{with} \qquad \boldsymbol{M} = \boldsymbol{D} - \boldsymbol{P}^T \boldsymbol{K}^{-1} \boldsymbol{P}. \tag{7.25}$$

Furthermore, the simple steepest descent method (4.84) becomes

$$\boldsymbol{X}_s^{i+1} = \boldsymbol{X}_s^i - \varepsilon \, \boldsymbol{G}(\boldsymbol{u}(\boldsymbol{X}_s^i), \boldsymbol{X}_s^i). \tag{7.26}$$

7.5.2 Regularization

The mesh optimization problem can be interpreted as an inverse problem. It requires the solution of the material residual problem within a staggered algorithm (7.25) or the coupled system (7.24). Several numerical difficulties arise due to the solution of this problem. In many cases, the Hessian matrix of the system is ill-conditioned and becomes singular or close to singular during the iterations and therefore the Newton algorithm is not stable and fails. The optimization problem is non-convex in general and hence, the solution needs not to be unique. Therefore, the problem could be termed ill-posed in the sense of HADAMARD

and reasonable regularization methods should be used in order to regularize the problem. A classical regularization is given by adding a penalty functional $\mathcal{P}$ to the original objective E, i.e.

$$\tilde{E}(\boldsymbol{u}, \boldsymbol{s}) = E(\boldsymbol{u}, \boldsymbol{s}) + \mathcal{P}(\gamma, \boldsymbol{s}), \tag{7.27}$$

where γ is a penalty parameter. The choice of the penalty functional and the penalty parameter depends on the problem. For a classical TIKHONOV-type regularization we often have a functional in the form

$$\mathcal{P}(\gamma, \boldsymbol{s}) = \frac{\gamma}{2} \left|\left| \boldsymbol{s} - \boldsymbol{s}_0 \right|\right|^2, \tag{7.28}$$

see for instance [36] and the references therein for details. The numerical difficulties for the mesh optimization problem are also mentioned by [2, 77]. The authors have proposed different strategies in order to overcome these problems.

An ill-conditioned problem is indicated by a large condition number c of the system matrix $\boldsymbol{A}$ from the system $\boldsymbol{A}\boldsymbol{x} = \boldsymbol{b}$, which can be defined by

$$c(\boldsymbol{A}) = \frac{\sigma_{max}(\boldsymbol{A})}{\sigma_{min}(\boldsymbol{A})}. \tag{7.29}$$

Here, $\sigma_{max}(\boldsymbol{A})$ and $\sigma_{min}(\boldsymbol{A})$ are the maximal and minimal *singular values* of $\boldsymbol{A}$, respectively. A large condition number is caused by nearly zero singular values of $\boldsymbol{A}$. In the context of sensitivity analysis, the condition number quantifies the sensitivity of the system $\boldsymbol{A}\boldsymbol{x} = \boldsymbol{b}$ with respect to small perturbations $(\boldsymbol{A} + \varepsilon\tilde{\boldsymbol{A}})\boldsymbol{x}(\varepsilon) = \boldsymbol{b} + \varepsilon\tilde{\boldsymbol{b}}$. Small changes in $\boldsymbol{A}$ or $\boldsymbol{b}$ can induce large changes in $\boldsymbol{x}$ if the condition number in large. The singular values can be obtained by a *singular value decomposition* (SVD) of the system matrix. The SVD is used in many fields of engineering and physics, which deal with inverse problems.

For a rectangular matrix $\boldsymbol{A} \in \mathbb{R}^{n\times m}$, the SVD is a decomposition of the form

$$\boldsymbol{A} = \boldsymbol{V}\boldsymbol{\Sigma}\boldsymbol{Y}^T = \sum_{i=1}^{m} \sigma_i \boldsymbol{v}_i \boldsymbol{y}_i^T \tag{7.30}$$

where $\boldsymbol{V} \in \mathbb{R}^{n\times n}$ and $\boldsymbol{Y} \in \mathbb{R}^{m\times m}$ are matrices with orthonormal columns, i.e. we have $\boldsymbol{V}\boldsymbol{V}^T = \boldsymbol{I} \in \mathbb{R}^{n\times n}$ and $\boldsymbol{Y}\boldsymbol{Y}^T = \boldsymbol{I} \in \mathbb{R}^{m\times m}$. The matrix $\boldsymbol{\Sigma} = \mathrm{diag}(\sigma_1, \ldots, \sigma_m) \in \mathbb{R}^{n\times m}$ is a diagonal matrix with non-negative diagonal elements σ_i. The quantities σ_i are called singular values of $\boldsymbol{A}$ and they appearing in decreasing order such that $\sigma_1 \geq \sigma_2 \geq \ldots \geq \sigma_m \geq 0$. The column vectors of $\boldsymbol{V} = [\boldsymbol{v}_1, \ldots, \boldsymbol{v}_n]$ and $\boldsymbol{Y} = [\boldsymbol{y}_1, \ldots, \boldsymbol{y}_m]$ are called *left and right singular vectors* of $\boldsymbol{A}$, respectively, see e.g. [43] for details.

We use the singular value decomposition in order to calculate the condition number and therefore information about the solution behavior as well as for a regularization of the Hessian matrix.

The SVD is a reliable method in order to identify the numerical rank. The singular vectors, which are corresponding to the non-zero singular values σ_i of $\boldsymbol{A}$ span the range of $\boldsymbol{A}$. With these, we can define the numerical rank r of $\boldsymbol{A}$ as the number of the non-zero singular values of $\boldsymbol{A}$, which are larger than a defined tolerance. The solution of the system $\boldsymbol{A}\boldsymbol{x} = \boldsymbol{b}$ could be expressed in terms of the left and right singular vectors

$$\boldsymbol{x} = \boldsymbol{A}^{-1}\boldsymbol{b} = \boldsymbol{Y}\boldsymbol{\Sigma}^{-1}\boldsymbol{V}^T\boldsymbol{b} = \sum_{i=1}^{m} \frac{1}{\sigma_i}\, \boldsymbol{y}_i\, \boldsymbol{v}_i^T \boldsymbol{b}\,. \tag{7.31}$$

The solution $\boldsymbol{x}$ is given by linear combination of $\boldsymbol{y}_i \boldsymbol{v}_i^T \boldsymbol{b}$ weighted with the inverse singular values σ_i^{-1}. At this point, we see the influence of nearly zero singular values σ_i, i.e. we have

$$\lim_{\sigma_i \to 0} \frac{1}{\sigma_i}\, \boldsymbol{y}_i\, \boldsymbol{v}_i^T \boldsymbol{b} = \infty\,. \tag{7.32}$$

If we truncate the sum in Eq. 7.31 after r terms, the result is a rank-r approximation to the original Hessian. The error in the approximation depends upon the magnitude of the neglected singular values. This could be interpreted as filtering out the noisy data.

7.5.3 Mesh distortion control

The quality of the mesh (the distortion of the mesh) has an important influence on the shape derivatives and hence on the results and the success of the optimization process.

In order to control the mesh distortion a simple geometrical distortion parameter ξ is used, which is also utilized in shape optimization [106]. The distortion parameter for a quadrilateral element with four nodes is given by

$$\xi = \frac{4}{A}\, \min(\det \mathbf{J}_i) \qquad i = 1, ..., 4\,. \tag{7.33}$$

Here, $\min(\det \mathbf{J}_i)$ denotes the minimum value of the Jacobian determinant and A the element area. The distortion parameter has the following properties:

$$\xi \begin{cases} = 1 & \text{element is a parallelogram} \\ > 0 & \text{element is convex} \\ = 0 & \text{element is degenerate (triangle)} \\ < 0 & \text{element is concave} \end{cases}$$

The parameter ξ must be greater than zero to avoid degeneracy of the element. In practical computations, the condition $\xi \geq tol_\xi$ is used with a tolerance $tol_\xi \in [0.2, 0.5]$.

1. Solve the physical problem within a Newton Method.
2. Solve the material problem:
   Compute the material tangent operator $\boldsymbol{M} = \boldsymbol{D} - \boldsymbol{P}^T \boldsymbol{K}^{-1} \boldsymbol{P}$.
   Check the condition number and the numerical rank of $\boldsymbol{M}$ with SVD. If necessary, compute a rank-r approximation in order to overcome the ill-conditioning.
   Compute $\Delta \boldsymbol{X}_s$.
3. Line search:
   Compute α such that $\xi(\alpha) \geq tol_\xi$.
   Compute β such that $\mathcal{E}(\boldsymbol{X}_h + \beta \Delta \boldsymbol{X}_h) < \mathcal{E}(\boldsymbol{X}_h)$.
4. Update $\boldsymbol{X}_s$ with $\Delta \bar{\boldsymbol{X}}_s = \varepsilon \, \Delta \boldsymbol{X}_s$, where $\varepsilon = \min[\alpha, \beta]$.
5. Update $\boldsymbol{u}$ with sensitivity relation $\Delta \boldsymbol{u} \approx \boldsymbol{S}_p \Delta \bar{\boldsymbol{X}}_s$.
   After that, the system is usually still unbalanced, see Remark 7.2.
   Goto 1 and find the new state of equilibrium.

Box 7.1: Staggered solution algorithm for global r-adaptive mesh optimization

7.5.4 Overall solution algorithm

We consider a staggered solution algorithm for Eq. 7.25, i.e. the algorithm introduced in Section 4.5.2 is used. The energy functional (4.74) has to be minimized, which has the particular form $\mathcal{E}(\boldsymbol{X}_h) := E(\boldsymbol{u}_h(\boldsymbol{X}_h), \boldsymbol{X}_h)$. The overall solution scheme for mesh optimization is given in Box 7.1.

The line search consists of two parts. In the first part, we compute a step size parameter α in order to avoid mesh distortion. For a given tolerance tol_ξ, the step size parameter is given explicitly for every element from (7.33)

$$\xi(\alpha) = \frac{4}{A(\boldsymbol{X}_e + \alpha \Delta \boldsymbol{X}_e)} \det \mathbf{J}(\boldsymbol{X}_e + \alpha \Delta \boldsymbol{X}_e) \geq tol_\xi. \tag{7.34}$$

where $\boldsymbol{X}_e$ denotes the element coordinate vector. The maximum step length α along a given search direction can be computed in closed form from this expression [106]. The second part is the computation of the usual step size β used in nonlinear programming in order to guarantee the decrease in the energy. For this, we use the Armijo-Goldstein condition.

An algorithm for the simultaneous solution of the physical and material problem (7.24) can be obtained in the same manner by using the regularization and line search as in the staggered solution algorithm.

Remark 7.2 (Update of the state) *The computation of the accurate material residual $\boldsymbol{G}$ for the next iteration step requires the solution of the state variable $\boldsymbol{u}_h$ for the updated current*

design, i.e. the equation $R(\boldsymbol{u}_h, \boldsymbol{s}_h; \boldsymbol{\eta}_h) = 0$ has to be solved. For a simple linear physical problem, only the solution of one linear equation is required. In the general nonlinear case, some Newton iterations for the physical problem have to be performed in order to find the new state of equilibrium for the current design. The best performance of the algorithm could be achieved, if beforehand the data of the state $\boldsymbol{u}_h$ are transferred to the new design. To do this, the sensitivity relation for the physical problem (4.54) can be used. With a sufficient small $\Delta \boldsymbol{X}_s$ an approximation for the change in the state is obtained from

$$\Delta \boldsymbol{u} \approx -\boldsymbol{K}^{-1} \boldsymbol{P}\, \Delta \boldsymbol{X}_s = \boldsymbol{S}_p\, \Delta \boldsymbol{X}_s \,. \tag{7.35}$$

After this, the system is usually still unbalanced, but only few Newton iterations are required in order to find the new state of equilibrium.

7.6 Numerical examples

In this section two numerical examples for global r-adaptive mesh optimization are presented. In the first example, the model problem of linearized elasticity is considered and in the second example a problem from nonlinear elasticity is studied. Further examples with some details on the proposed error measures in the context of r-adaptivity are given in the next chapter in Section 8.5.

7.6.1 Unit square

System and model problem. A two-dimensional unit square $\Omega = (0, 1)^2$ with homogeneous Dirichlet boundary conditions $\boldsymbol{u} = \boldsymbol{0}$ on Γ is considered. The body is loaded with a horizontal body load $b_x = 50$. We consider in this first example the model problem of linearized elasticity given in Appendix B.2. The displacement field is governed by Eq. B.77. The problem is modeled with the plane strain condition with $E = 1000$ and $\nu = 0.3$.

We discretize the model with 153 Q4 elements and we choose an arbitrary irregular initial discretization, see Fig. 7.1a.

The design variables. For the mesh optimization problem a subset the nodal coordinates $\boldsymbol{X}_s$ are chosen as design variables. The optimal nodal positions (the design) of a given mesh (the reference configuration) can be computed by using the solution algorithms given in Section 7.5.1.

For simplicity, in this first example only horizontal movements of all inner nodes are allowed. This restriction stabilize the algorithm especially by using the simultaneous solution of the physical and material problems.

The mesh consists of overall 360 degrees of freedom (DOF) but only 128 nodal coordinates are chosen as design variables.

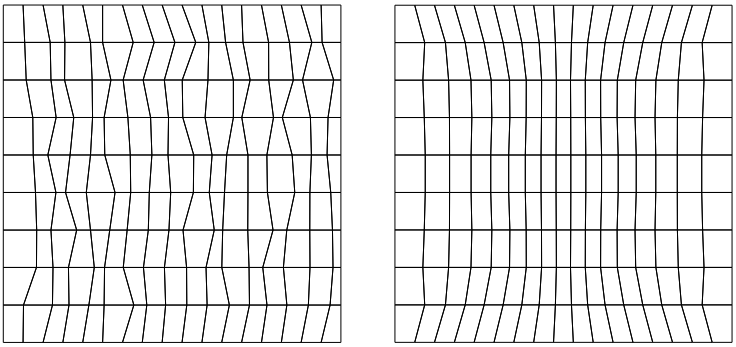

(a) Initial mesh (b) Optimized mesh

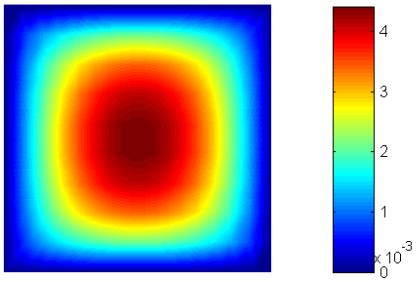

(c) Solution u_x on the optimized mesh

Figure 7.1: Unit square with horizontal body load

Solution algorithm and mesh distortion. We consider the simultaneous solution of the physical and material problem. In order to find the minimum of the objective $E(\boldsymbol{u}, \boldsymbol{X})$ we have to solve Eq. 7.24 in each Newton step. The Newton algorithm stops when the norm of the physical and material residuals are lower than given tolerances TOL_R and TOL_G, respectively. In the computation the tolerances are chosen as $TOL_R = TOL_G = 10^{-12}$.

The distortion of the mesh during the optimization process has been controlled by a distortion parameter as described in Section 7.5.3. The mesh distortion control parameter (7.33) with $tol_\xi = 0.2$ was used. The elements are well-shaped during the optimization process in this example such that the distortion constraint is not active.

Results of the simultaneous solution algorithm. The results of the full Newton algorithm are given in Table 7.1. The solution $E(\boldsymbol{u}_h^*, \boldsymbol{X}_h^*)$ was obtained after 7 iterations. The corresponding optimal mesh is given in Fig. 7.1b.

Table 7.1: Results of the full Newton algorithm

i	$\|\|\boldsymbol{R}\|\|$	$\|\|\boldsymbol{G}\|\|$	$\|\|\varepsilon\,\Delta\boldsymbol{u}\|\|$	$\|\|\varepsilon\,\Delta\boldsymbol{X}\|\|$	$E(\boldsymbol{u}_h, \boldsymbol{X}_h)$	$\varepsilon = \min[\alpha, \beta]$
0	5.292E-14	1.646E-03	3.111E-02	0.000E+00	-5.232E-02	1.00E+00
1	5.364E-02	1.274E-03	1.326E-03	1.269E-01	-5.238E-02	2.50E-01
2	1.729E-01	4.882E-04	1.949E-03	2.208E-01	-5.245E-02	7.66E-01
3	3.575E-02	9.226E-05	5.271E-04	8.298E-02	-5.247E-02	1.00E+00
4	1.763E-02	1.022E-05	4.869E-04	7.695E-02	-5.247E-02	1.00E+00
5	2.468E-04	5.255E-07	2.529E-05	4.125E-03	-5.247E-02	1.00E+00
6	1.791E-07	4.820E-10	2.444E-06	3.757E-04	-5.247E-02	1.00E+00
7	2.134E-14	8.843E-15	2.245E-09	3.359E-07	-5.247E-02	1.00E+00

During the iteration the free nodes move in the opposite direction of the material residual forces and the energy decrease from $E(\boldsymbol{u}_h^0, \boldsymbol{X}_h^0) = -5.2323 \times 10^{-2}$ (initial mesh) to the value $E(\boldsymbol{u}_h^*, \boldsymbol{X}_h^*) = -5.2466 \times 10^{-2}$ (optimized mesh), see Table 7.1.

Here, $\boldsymbol{u}_h^* \in \mathcal{V}_h$ and $\boldsymbol{X}_h^* \in \mathcal{S}_h$ are the optimal solution in the chosen approximation spaces $\mathcal{V}_h$ and $\mathcal{S}_h$ in the sense of the minimization problem (7.1).

The optimal mesh. The optimal solution $\boldsymbol{X}_h^*$ (the optimal design) for $E(\boldsymbol{u}_h, \boldsymbol{X}_h)$ for this simple model problem under the given load case is a symmetric discretization as shown in Fig. 7.1b. This discretization leads to the best approximation for the given problem in the chosen approximation spaces $\mathcal{V}_h$ and $\mathcal{S}_h$.

The mesh is finer in the middle of the domain and tends to a coarser discretization on the boundary. This behavior reflects the solution for the given load case. The solution $\boldsymbol{u}_h$ has the maximum in the middle and goes to zero on the boundary, see Fig. 7.1c.

The errors in the state, design and energy. With the optimal solutions $\{\boldsymbol{u}_h^*, \boldsymbol{X}_h^*\}$ at hand, we introduce the error in the energy $e_{E,h} := E(\boldsymbol{u}_h^*, \boldsymbol{X}_h^*) - E(\boldsymbol{u}_h, \boldsymbol{X}_h)$, the error in the state $\boldsymbol{e}_{u,h} := \boldsymbol{u}_h^* - \boldsymbol{u}_h$ and the design $\boldsymbol{e}_{X,h} := \boldsymbol{X}_h^* - \boldsymbol{X}_h$, respectively, see Eq. 7.3. The relative errors are given by

$$\eta_E^{rel} := \left| \frac{e_{h,E}}{E(\boldsymbol{u}_h^*, \boldsymbol{X}_h^*)} \right|, \qquad \eta_u^{rel} := \frac{||\boldsymbol{e}_{h,u}||_{L_2}}{||\boldsymbol{u}_h^*||_{L_2}}, \qquad \eta_X^{rel} := \frac{||\boldsymbol{e}_{h,X}||_{L_2}}{||\boldsymbol{X}_h^*||_{L_2}}, \tag{7.36}$$

where $||\cdot||_{L_2}$ denotes the usual L_2 norm. The behavior of the errors during the iterations are shown in Table 7.2. The reduction of the error in the energy is merely marginal, but the reduction of the error in the displacement is about $12.5\,\%$.

Table 7.2: Relative errors during the mesh optimization process.

Iteration	η_u^{rel} [%]	η_X^{rel} [%]	η_E^{rel} [%]
0	1.2475e+001	4.3465e+000	2.7233e-001
1	8.5868e+000	3.2306e+000	1.6568e-001
2	2.7892e+000	1.2628e+000	2.6839e-002
3	1.4723e+000	7.0776e-001	2.5854e-003
4	7.6473e-002	3.8580e-002	2.6867e-005
5	7.3401e-003	3.3895e-003	1.1397e-007
6	6.7417e-006	3.0294e-006	1.0000e-013
7	0	0	0

Concluding remarks. This example can be used as a benchmark for the performance and reliability of the considered solution algorithm, because the optimal solution is known for this simple problem.

Furthermore, the material residual on the mesh nodes vanish completely. This is in general not the case, because the mesh distortion control usually avoid this. This is further discussed in the next example.

As mentioned in Remark 4.12, the full Newton algorithm (7.24) is very sensitive and in many cases not stable for a large number of design variables. Therefore, in general, suitable regularization methods have to be considered, see Section 7.5.2. A staggered solution algorithm is more stable for complex problems. Such an algorithm is used in the next example. Furthermore, quasi-Newton methods based on gradient information can be alternatively used, see Remark 4.13.

7.6.2 Cracked beam

System and model problem. In this second example a cracked cantilever beam under self-weight loading $b_y = -10$ is considered, see Fig. 7.2. The dimensions of the rectangular domain are $L = 4$ and $H = 1$ as well as the crack length is $a = 0.4$. We consider as an example of isothermal hyperelasticity a classical compressible Neo-Hookean material. The strain energy function under consideration in terms of the invariant $I_C = \text{tr}(\mathbf{F}^T\mathbf{F})$ and $J = \det \mathbf{F}$ is given by

$$W_R(I_C, J) = \frac{1}{2}\,\mu\,(I_C - 3 - 2\ln J) + \frac{1}{2}\,\lambda\,(J-1)^2, \tag{7.37}$$

see Box B.2 for details and the corresponding stress and elasticity tensors. The Lamé parameters are chosen as $\lambda = 5.769 \times 10^3$ and $\mu = 3.846 \times 10^3$, which correspond to $E = 10^4$ and $\nu = 0.3$.

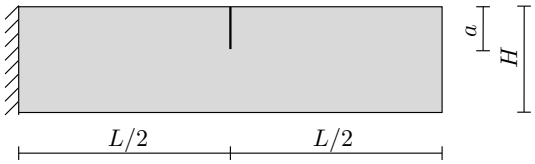

Figure 7.2: Cracked beam: system

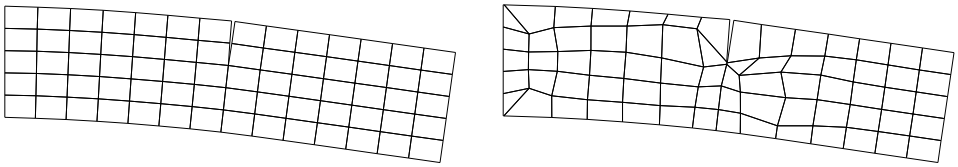

(a) initial mesh (b) optimized mesh

Figure 7.3: Cracked beam: deformed initial and optimized mesh

All inner nodes as well as all nodal coordinates in tangential direction on the free boundaries are chosen as design variables. Only the nodal coordinates on the Dirichlet boundary are fixed.

The mesh consists of 70 Q4 element with 184 degrees of freedom. Overall 131 nodal coordinates are chosen as design variables.

Results of the staggered solution algorithm. The staggered solution algorithm Eq. 7.25 is used in order to solve the problem. The solution was attained within 16 iterations. The deformed initial and optimized meshes are shown in Fig. 7.3a and Fig. 7.3b, respectively.

The system matrix was ill-conditioned for some Newton iterations and a regularization method has been used as proposed in Section 7.5.2. The algorithm works but the usual quadratic convergence can not be achieved, because the original tangent operator $\boldsymbol{M}$ is replaced by a rank-r approximation as described in Box. 7.1.

The overall energy decreases from -3.23597 (initial mesh) to -3.33385 (optimized mesh). The norm of the material residual $||\boldsymbol{G}||_{L_2}$ decreases from 2.8793×10^{-1} to 8.7777×10^{-2}, i.e. a reduction of $69.51\,\%$ with respect to the initial mesh. The material residual does not vanish completely as a result of the mesh distortion control.

Therefore, a usual stoping criterion as used in the Newton method for the physical problem can not be used. But the algorithm stops if the change in the norm of the material residual is smaller than a given tolerance or if a maximal admissible number of iterations is achieved. In practical computations the tolerance can be chosen as $[\,10^{-4}, 10^{-8}\,]$.

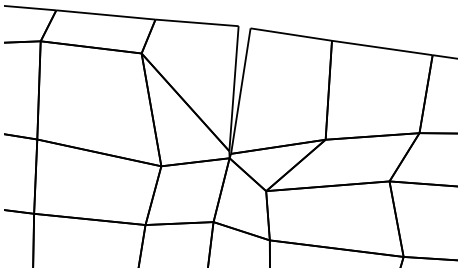

Figure 7.4: Cracked beam: elements on the crack tip

The largest improvements of the mesh occur within the first few iterations. The gain of accuracy by performing many iterations in order to minimize the material residual further can be low in comparison to the numerical work involved. Hence, in practical computations it is sufficient to do just few iterations in order to obtain the largest improvements of the solution.

Mesh distortion control. In order to control the distortion of the mesh during the optimization process, a simple geometrical distortion parameter has been used as described in Section 7.5.3. The mesh distortion control parameter (7.33) with $tol_\xi = 0.1$ was used.

As mentioned above, the material residual does not vanish completely as a result of the mesh distortion control. This means that there is still an ambition to move the nodes in order to minimize the energy but the elements may become distorted. A remeshing strategy with a change of the nodal connectivities as well as h-adaptivity techniques for patches with distorted elements could be considered to improve the algorithm further. Furthermore, other mesh distortion control criteria could be used, see e.g. [92].

Due to the singularity at the crack the nodes are concentrated at the crack tip and the elements around the tip seem distorted. But this is not the case, see Fig. 7.4. The mesh distortion control avoid the distortion. By choosing a larger value of the distortion control parameter (7.33) this effect will be reduced and the elements become more well-shaped.

Control of a displacement. In order to quantify the capability of the optimized mesh, we control as a quantity of interest the vertical displacement at the lower right corner. We use a reference solution $u_y^* = -0.440225$ obtained from a fine mesh with 4258 nodes.

The vertical displacement of the initial mesh is $u_y^0 = -0.406161$. The relative error with respect to u_y^* is given by $7.74\,\%$. The optimized mesh yields the displacement $u_y = -0.420303$ and hence a relative error of $4.53\,\%$. Finally, we obtain a reduction of $41.52\,\%$ in the relative error for the displacement at the lower right corner with respect to the reference solution.

This demonstrates the potential of r-adaptive mesh optimization techniques. The discretization error is significantly reduced with a fixed number of nodes.

Chapter 8

Goal-oriented r-adaptive mesh optimization

A novel approach for goal-oriented r-adaptive mesh optimization based on minimization principles of the primal and dual energy functionals is proposed within this chapter. The mesh is optimized with respect to a chosen quantity of interest. The variational framework is first presented for a linear elliptic problem and later on extended to nonlinear problems. Furthermore, error measures for a chosen quantity of interest are investigated.

8.1 Introduction

The proposed approach for global r-adaptive mesh optimization in Chapter 7 is based on global energy minimization. The resulting mesh is optimal with respect to the overall energy of the primal problem. The discretization error measured in terms of the global energy norm can be computed using standard residual based error estimators or averaging techniques, see e.g. [3, 59] and [109], respectively. But nothing can be said about the quality of a certain quantities of interest, such as pointwise stresses and displacements or average stresses. The error in a local quantity of interest depends on the error in the corresponding dual solution or generalized Green's function. This fact is used in dual-weighted based goal-oriented error estimation techniques and adaptivity algorithms. The error is measured with respect to a specific structural response quantity and the mesh is optimized with respect to the chosen quantity of interest.

A posteriori error analysis for quantities of interest using duality techniques was first presented in [37]. A generalization with exact weighted a posteriori error estimates was proposed in [11]. Furthermore, the terms *goal-oriented error estimation* was introduced in [88], who presented upper and lower error bounds based on the parallelogram law. An engineering motivation by means of Betti's principle was given in [31]. In the context of fracture mechanics and mechanics in the material space duality techniques and a posteriori error estimates were investigated for instance in [52, 90, 91]. A goal-oriented a posteriori error estimation technique for the pointwise error of finite element approximations using fundamental solutions

has been presented in [47]. The approach is based on an integral representation of the pointwise quantity of interest using the corresponding Green's function, which is decomposed into an unknown regular part and a fundamental solution. See also for instance [4, 46] for an overview of different problems and applications.

Furthermore, in recent years the goal-oriented techniques are used for combined model and discretization error analysis and adaptive algorithms, see e.g. [18, 84, 95] for an overview. The modeling error is a part of the error due to the natural imperfections in abstract models of actual physical phenomena.

In this chapter, a novel approach for goal-oriented r-adaptivity based on energy minimization principles for the primal and the dual problems is proposed. The primal and dual energy functionals are the basis for a goal-oriented mesh optimization algorithm. The corresponding primal and dual material residuals yield an error indicator for mesh optimization. Therefore, the approach is referred to as *Primal Dual Material Residual* (PDMR) method. The resulting mesh yields an optimal solution with respect to a chosen quantity of interest.

As mentioned above, r-adaptive methods based on energy minimization of the primal problem are well-known since several decades. But the extension to goal-oriented r-adaptive mesh optimization based on energy minimization principles has not been investigated so far. Some parts of this chapter are published in [68, 72].

8.2 Linear problems

For motivation and notational simplicity the model problem of linearized elasticity is considered. The problem formulation is given in Appendix B.2. The linear primal problem is defined by the variational equation (B.80) as

$$a(\boldsymbol{u}, \boldsymbol{\eta}) = F(\boldsymbol{\eta}) \quad \forall\, \boldsymbol{\eta} \in \mathcal{V}. \tag{8.1}$$

Furthermore, the dual problem is given in (B.109) in form of

$$a(\boldsymbol{z}, \boldsymbol{\eta}) = J(\boldsymbol{\eta}) \quad \forall\, \boldsymbol{\eta} \in \mathcal{V}. \tag{8.2}$$

These problems are solved for a fixed design $\boldsymbol{s}$. The corresponding primal and dual residuals are introduced as

$$R(\boldsymbol{u}, \boldsymbol{\eta}) := a(\boldsymbol{u}, \boldsymbol{\eta}) - F(\boldsymbol{\eta}), \tag{8.3}$$

$$R^*(\boldsymbol{z}, \boldsymbol{\eta}) := a(\boldsymbol{z}, \boldsymbol{\eta}) - J(\boldsymbol{\eta}). \tag{8.4}$$

8.2.1 The error in a quantity of interest

The Galerkin approximations of the primal (8.1) and the dual problem (8.2) are given by using finite dimensional subspaces $\mathcal{V}_h \subset \mathcal{V}$. The approximate primal problem reads: Find $\boldsymbol{u}_h \in \mathcal{V}_h \subset \mathcal{V}$ such that

$$a(\boldsymbol{u}_h, \boldsymbol{\eta}_h) = F(\boldsymbol{\eta}_h) \quad \forall\, \boldsymbol{\eta}_h \in \mathcal{V}_h. \tag{8.5}$$

Furthermore, the approximate dual problem is given by

$$a(\boldsymbol{z}_h, \boldsymbol{\eta}_h) = J(\boldsymbol{\eta}_h) \quad \forall\, \boldsymbol{\eta}_h \in \mathcal{V}_h. \tag{8.6}$$

Using once again the symmetry of the bilinear form we have for the approximation of the quantity of interest $J(\boldsymbol{u}_h)$

$$J(\boldsymbol{u}_h) = a(\boldsymbol{z}_h, \boldsymbol{u}_h) = a(\boldsymbol{u}_h, \boldsymbol{z}_h) = F(\boldsymbol{z}_h). \tag{8.7}$$

Finally, if the approximate dual solution $\boldsymbol{z}_h$ is known, the quantity of interest $J(\boldsymbol{u}_h)$ can be computed for arbitrary functionals $F(\cdot)$, i.e. $J(\boldsymbol{u}_h) = F(\boldsymbol{z}_h)$.

The error in the primal solution $\boldsymbol{e}_u$ and the error in the dual solution $\boldsymbol{e}_z$ are introduced as

$$\boldsymbol{e}_u := \boldsymbol{u} - \boldsymbol{u}_h \qquad \text{and} \qquad \boldsymbol{e}_z := \boldsymbol{z} - \boldsymbol{z}_h. \tag{8.8}$$

These errors are used within error representations for $J(\boldsymbol{u})$. The error in the quantity of interest is given by

$$J(\boldsymbol{e}_u) := J(\boldsymbol{u}) - J(\boldsymbol{u}_h) = F(\boldsymbol{z} - \boldsymbol{z}_h) = F(\boldsymbol{e}_z). \tag{8.9}$$

The error can be expressed in terms of the primal physical residual $R(\cdot)$ as

$$\begin{aligned} J(\boldsymbol{e}_u) &= a(\boldsymbol{z}, \boldsymbol{e}_u) = a(\boldsymbol{e}_u, \boldsymbol{z}) = a(\boldsymbol{u}, \boldsymbol{z}) - a(\boldsymbol{u}_h, \boldsymbol{z}) \\ &= F(\boldsymbol{z}) - a(\boldsymbol{u}_h, \boldsymbol{z}) = -R(\boldsymbol{u}_h, \boldsymbol{z}). \end{aligned} \tag{8.10}$$

By using the Galerkin orthogonality

$$a(\boldsymbol{u} - \boldsymbol{u}_h, \boldsymbol{\eta}_h) = 0 \quad \forall\, \boldsymbol{\eta}_h \in \mathcal{V}_h, \tag{8.11}$$

the error in the quantity of interest can be written as

$$\begin{aligned} J(\boldsymbol{e}_u) &= a(\boldsymbol{e}_u, \boldsymbol{z}) = a(\boldsymbol{e}_u, \boldsymbol{z} - \boldsymbol{z}_h) = F(\boldsymbol{z} - \boldsymbol{z}_h) - a(\boldsymbol{u}_h, \boldsymbol{z} - \boldsymbol{z}_h) \\ &= -R(\boldsymbol{u}_h, \boldsymbol{z} - \boldsymbol{z}_h). \end{aligned} \tag{8.12}$$

The error can be also expressed in terms of the dual physical residual $R^*(\cdot)$ in the form

$$\begin{aligned} J(\boldsymbol{e}_u) &= a(\boldsymbol{z}, \boldsymbol{e}_u) = a(\boldsymbol{e}_z, \boldsymbol{e}_u) = a(\boldsymbol{e}_z, \boldsymbol{u}) = a(\boldsymbol{z}, \boldsymbol{u}) - a(\boldsymbol{z}_h, \boldsymbol{u}) \\ &= J(\boldsymbol{u}) - a(\boldsymbol{z}_h, \boldsymbol{u}) = -R^*(\boldsymbol{z}_h, \boldsymbol{u}). \end{aligned} \tag{8.13}$$

Furthermore, using the Galerkin orthogonality the error becomes

$$\begin{aligned} J(\boldsymbol{e}_u) &= a(\boldsymbol{e}_z, \boldsymbol{u}) = a(\boldsymbol{e}_z, \boldsymbol{u} - \boldsymbol{u}_h) = J(\boldsymbol{u} - \boldsymbol{u}_h) - a(\boldsymbol{z}_h, \boldsymbol{u} - \boldsymbol{u}_h) \\ &= -R^*(\boldsymbol{z}_h, \boldsymbol{u} - \boldsymbol{u}_h). \end{aligned} \tag{8.14}$$

Due to the linear model problem, the error can be alternatively written as

$$J(\boldsymbol{e}_u) = -\left[\frac{1}{2} R(\boldsymbol{u}_h, \boldsymbol{z} - \boldsymbol{z}_h) + \frac{1}{2} R^*(\boldsymbol{z}_h, \boldsymbol{u} - \boldsymbol{u}_h) \right]. \tag{8.15}$$

The equations (8.12) and (8.14) are the basis for different error estimators for the error $J(\boldsymbol{e}_u)$, see e.g. [4, 11]. A simple error estimator in the energy norm $||\cdot||_E$ follows directly from the error representation (8.12). Using the Cauchy-Schwarz inequality, we obtain the upper error bound

$$|J(\boldsymbol{e}_u)| = |a(\boldsymbol{u} - \boldsymbol{u}_h, \boldsymbol{z} - \boldsymbol{z}_h)| \leq ||\boldsymbol{u} - \boldsymbol{u}_h||_E ||\boldsymbol{z} - \boldsymbol{z}_h||_E. \tag{8.16}$$

In practical computations, the relation is applied element-wise as

$$|J(\boldsymbol{e}_u)| \leq \sum_{K \in \mathcal{T}_h} ||\boldsymbol{u} - \boldsymbol{u}_h||_{E,K} ||\boldsymbol{z} - \boldsymbol{z}_h||_{E,K}. \tag{8.17}$$

The error in the quantity of interest is bounded by the energy norm error of the primal problem weighted with the energy norm error of the dual solution.

The element contributions $||\boldsymbol{u} - \boldsymbol{u}_h||_{E,K}$ and $||\boldsymbol{z} - \boldsymbol{z}_h||_{E,K}$ are computed using standard residual based error estimators, see e.g. [3, 59]. Furthermore, local or global averaging techniques for a posteriori error control can be used, e.g. the ZZ-error estimator [109].

Finally, the most important fact is, that the error in $J(\boldsymbol{u})$ depends on the error in the corresponding dual solution. Therefore, in the context of goal-oriented r-adaptivity, we have to optimize the mesh with respect to the dual solution.

8.2.2 Error measures in the context of r-adaptivity

Different global error measures in the context of r-adaptivity have been introduced in Section 7.3. In the same manner, for the discrete solutions of the quantity of interest the overall error

$$J(\boldsymbol{e}_u) := J(\boldsymbol{u}) - J(\boldsymbol{u}_h) \tag{8.18}$$

the error on the current mesh

$$J(\boldsymbol{e}_{u,h}) := J(\boldsymbol{u}_h^*) - J(\boldsymbol{u}_h) \tag{8.19}$$

as well as the least obtainable error on the current mesh

$$J(\boldsymbol{e}_u^*) := J(\boldsymbol{u}) - J(\boldsymbol{u}_h^*) \tag{8.20}$$

are introduced. Furthermore, the overall error can be split into

$$J(\boldsymbol{e}_u) = J(\boldsymbol{e}_u^*) + J(\boldsymbol{e}_{u,h}). \tag{8.21}$$

8.2.3 Energy principles for the primal and dual problem

In order to use the same arguments from energy minimization as for the global mesh optimization, we consider in the following energy principles for the primal and dual problems.

The weak form of the primal problem is given in (8.1) as $a(\boldsymbol{u}, \boldsymbol{\eta}) = F(\boldsymbol{\eta})$. We assume that an energy functional

$$E(\boldsymbol{u}) := \frac{1}{2}\, a(\boldsymbol{u}, \boldsymbol{u}) - F(\boldsymbol{u}) \tag{8.22}$$

exists such that

$$R(\boldsymbol{u}, \boldsymbol{\eta}) = E'_u(\boldsymbol{u}, \boldsymbol{\eta}) = 0 \quad \forall\, \boldsymbol{\eta} \in \mathcal{V}. \tag{8.23}$$

The solution $\boldsymbol{u}$ is a minimizer of the corresponding energy functional $E(\boldsymbol{u})$. The first-order optimality condition leads to the primal physical residual (8.3).

In the same manner, the variational equation for the dual problem is given in (8.2) and reads $a(\boldsymbol{z}, \boldsymbol{\eta}) = J(\boldsymbol{\eta})$. We assume, that $J(\boldsymbol{u})$ is a regularized functional and well defined on $\mathcal{V}$. Then, the dual solution $\boldsymbol{z}$ is a minimizer of the corresponding energy functional of the dual problem

$$E^*(\boldsymbol{z}) := \frac{1}{2}\, a(\boldsymbol{z}, \boldsymbol{z}) - J(\boldsymbol{z}). \tag{8.24}$$

The first-order optimality condition leads to the dual physical residual (8.4), i.e.

$$R^*(\boldsymbol{z}, \boldsymbol{\eta}) = E^{*\prime}_z(\boldsymbol{z}, \boldsymbol{\eta}) = 0 \quad \forall\, \boldsymbol{\eta} \in \mathcal{V}. \tag{8.25}$$

The minimization of the energy of the primal problem $E(\boldsymbol{u})$ and the dual problem $E^*(\boldsymbol{z})$ lead to the primal and dual physical residuals, respectively. The consecutive solution of both problems provide the solutions $\boldsymbol{u}$ and $\boldsymbol{z}$. In order to solve these problems simultaneously, the functional

$$I(\boldsymbol{u}, \boldsymbol{z}) := \gamma_u\, E(\boldsymbol{u}) + \gamma_z\, E^*(\boldsymbol{z}) \tag{8.26}$$

is introduced which contains both energy quantities. Here, for later use, the scaling factors or weights γ_u and γ_z have been introduced in order to favor either one or the other. This ends in the following problem.

Problem 8.1 (Energy minimization w.r.t. $\{\boldsymbol{u}, \boldsymbol{z}\}$) *Find $\{\boldsymbol{u}, \boldsymbol{z}\} \in \mathcal{V} \times \mathcal{V}$ such that the energy functional (8.26) is minimized, i.e.*

$$I(\boldsymbol{u}, \boldsymbol{z}) = \min_{\{\boldsymbol{p}, \boldsymbol{q}\} \in \mathcal{V} \times \mathcal{V}} I(\boldsymbol{p}, \boldsymbol{q}). \tag{8.27}$$

The first-order optimality condition for this problem reads

$$\left\{ \begin{array}{l} I'_u(\boldsymbol{u},\boldsymbol{\eta}) \\ \\ I'_z(\boldsymbol{z},\boldsymbol{\nu}) \end{array} \right\} = \left\{ \begin{array}{l} \gamma_u \, R(\boldsymbol{u},\boldsymbol{\eta}) \\ \\ \gamma_z \, R^*(\boldsymbol{z},\boldsymbol{\nu}) \end{array} \right\} = \boldsymbol{0} \tag{8.28}$$

for all $\{\boldsymbol{\eta},\boldsymbol{\nu}\} \in \mathcal{V} \times \mathcal{V}$. The variation with respect to $\boldsymbol{u}$ leads to the primal physical residual $R(\boldsymbol{u},\boldsymbol{\eta}) = E'_u(\boldsymbol{u},\boldsymbol{\eta})$ defined in (8.3) and the variation with respect to $\boldsymbol{z}$ yields the dual physical residual $R^*(\boldsymbol{z},\boldsymbol{\nu}) = E^{*\prime}_z(\boldsymbol{z},\boldsymbol{\nu})$ which is given in (8.4).

The optimality condition (8.28) yields two independent equations, i.e. there is no coupling between $\boldsymbol{u}$ and $\boldsymbol{z}$ at this point and the scaling factors or weights can be set to $\gamma_u = \gamma_z = 1$. Finally, the minimizers $\{\boldsymbol{u},\boldsymbol{z}\} \in \mathcal{V} \times \mathcal{V}$ of the functional (8.26) are given by the solution of the set of equations

$$\begin{aligned} a(\boldsymbol{u},\boldsymbol{\eta}) &= F(\boldsymbol{\eta}) \quad \forall\, \boldsymbol{\eta} \in \mathcal{V} \\ a(\boldsymbol{z},\boldsymbol{\nu}) &= J(\boldsymbol{\nu}) \quad \forall\, \boldsymbol{\nu} \in \mathcal{V}. \end{aligned} \tag{8.29}$$

Remark 8.1 (Optimal control approach) *The optimal control approach from Section 5.2 is applied to the linear problem (8.1), which results in the following constraint optimization problem:*

$$\min_{\boldsymbol{u}\in\mathcal{V}} J(\boldsymbol{u}) \qquad \textit{s.t.} \qquad a(\boldsymbol{u},\boldsymbol{\eta}) = F(\boldsymbol{\eta}) \quad \forall\, \boldsymbol{\eta} \in \mathcal{V}. \tag{8.30}$$

The Lagrangian functional is given by $L(\boldsymbol{u},\boldsymbol{z}) = J(\boldsymbol{u}) + F(\boldsymbol{z}) - a(\boldsymbol{u},\boldsymbol{z})$ and the optimality condition becomes

$$\left\{ \begin{array}{l} L'_z(\boldsymbol{u},\boldsymbol{\eta}) \\ \\ L'_u(\boldsymbol{z},\boldsymbol{\nu}) \end{array} \right\} = \left\{ \begin{array}{l} F(\boldsymbol{\eta}) - a(\boldsymbol{u},\boldsymbol{\eta}) \\ \\ J(\boldsymbol{\nu}) - a(\boldsymbol{\nu},\boldsymbol{z}) \end{array} \right\} = \boldsymbol{0} \quad \forall\, \{\boldsymbol{\eta},\boldsymbol{\nu}\} \in \mathcal{V} \times \mathcal{V}. \tag{8.31}$$

These equations obtained from the optimal control approach are equivalent to (8.29). Hence, the two approaches are equivalent.

8.2.4 Energy minimization with respect to the design

The global mesh optimization is based on the minimization of the energy with respect to the state and the design. For the goal-oriented mesh optimization, the functional (8.26) is extended by the design function $\boldsymbol{s}$, i.e.

$$I(\boldsymbol{u},\boldsymbol{z},\boldsymbol{s}) = \gamma_u \, E(\boldsymbol{u},\boldsymbol{s}) + \gamma_z \, E^*(\boldsymbol{z},\boldsymbol{s}), \tag{8.32}$$

where $E(\boldsymbol{u},\boldsymbol{s}) = \frac{1}{2}\, a(\boldsymbol{s};\boldsymbol{u},\boldsymbol{u}) - F(\boldsymbol{s};\boldsymbol{u})$ and $E^*(\boldsymbol{z},\boldsymbol{s}) = \frac{1}{2}\, a(\boldsymbol{s};\boldsymbol{z},\boldsymbol{z}) - J(\boldsymbol{s};\boldsymbol{z})$. The energy of the primal problem depends on $\boldsymbol{s}$ and the energy of the dual problem depends on the same design function, because both problems have the same reference configuration. Hence, the optimization problem is now coupled by the design function $\boldsymbol{s}$.

Remark 8.2 *In the context of the finite element method and mesh optimization, the discrete design variables are a subset of nodal coordinates. Then, the primal and dual problems are approximated on the same mesh. In general, it can also be imagined that the primal and dual problems are solved on different meshes. In this work, only the first case is considered, i.e. the same design function $\boldsymbol{s}$ is used for the primal and the dual problem.*

In this case, the following problem is introduced.

Problem 8.2 (Energy minimization w.r.t. $\{\boldsymbol{u}, \boldsymbol{z}, \boldsymbol{s}\}$) *Find $\{\boldsymbol{u}, \boldsymbol{z}, \boldsymbol{s}\} \in \mathcal{V} \times \mathcal{V} \times \mathcal{S}$ such that the energy functional (8.32) is minimized, i.e.*

$$I(\boldsymbol{u}, \boldsymbol{z}, \boldsymbol{s}) = \min_{\{\boldsymbol{p},\boldsymbol{q},\boldsymbol{r}\}\in\mathcal{V}\times\mathcal{V}\times\mathcal{S}} I(\boldsymbol{p}, \boldsymbol{q}, \boldsymbol{r}). \tag{8.33}$$

The optimality condition is given as

$$\left\{ \begin{array}{l} I'_u(\boldsymbol{u}, \boldsymbol{z}, \boldsymbol{s})(\boldsymbol{\eta}) \\ I'_z(\boldsymbol{u}, \boldsymbol{z}, \boldsymbol{s})(\boldsymbol{\nu}) \\ I'_s(\boldsymbol{u}, \boldsymbol{z}, \boldsymbol{s})(\boldsymbol{\psi}) \end{array} \right\} = \left\{ \begin{array}{l} \gamma_u \, R(\boldsymbol{s}; \boldsymbol{u}, \boldsymbol{\eta}) \\ \gamma_z \, R^*(\boldsymbol{s}; \boldsymbol{z}, \boldsymbol{\nu}) \\ \gamma_u \, G(\boldsymbol{s}; \boldsymbol{u}; \boldsymbol{\psi}) + \gamma_z \, G^*(\boldsymbol{s}; \boldsymbol{z}; \boldsymbol{\psi}) \end{array} \right\} = \boldsymbol{0} \tag{8.34}$$

for all $\{\boldsymbol{\eta}, \boldsymbol{\nu}, \boldsymbol{\psi}\} \in \mathcal{V} \times \mathcal{V} \times \mathcal{S}$, where

$$\begin{aligned} R(\boldsymbol{s}; \boldsymbol{u}, \boldsymbol{\eta}) &= E'_u(\boldsymbol{u}, \boldsymbol{s}; \boldsymbol{\eta}) && \text{primal physical residual} \\ R^*(\boldsymbol{s}; \boldsymbol{z}, \boldsymbol{\nu}) &= E^{*\prime}_z(\boldsymbol{z}, \boldsymbol{s}; \boldsymbol{\nu}) && \text{dual physical residual} \\ G(\boldsymbol{s}; \boldsymbol{u}; \boldsymbol{\psi}) &= E'_s(\boldsymbol{u}, \boldsymbol{s}; \boldsymbol{\psi}) && \text{primal material residual} \\ G^*(\boldsymbol{s}; \boldsymbol{z}; \boldsymbol{\psi}) &= E^{*\prime}_s(\boldsymbol{z}, \boldsymbol{s}; \boldsymbol{\psi}) && \text{dual material residual.} \end{aligned}$$

The first and the second equations are the primal and dual physical residuals (8.3) and (8.4), respectively. The last two equations are the primal and dual material residuals

$$G(\boldsymbol{s}; \boldsymbol{u}; \boldsymbol{\psi}) = \frac{1}{2} \, a'_s(\boldsymbol{s}; \boldsymbol{u}; \boldsymbol{\psi}) - F'_s(\boldsymbol{s}; \boldsymbol{u}, \boldsymbol{\psi}), \tag{8.35}$$

$$G^*(\boldsymbol{s}; \boldsymbol{z}; \boldsymbol{\psi}) = \frac{1}{2} \, a'_s(\boldsymbol{s}; \boldsymbol{z}; \boldsymbol{\psi}) - J'_s(\boldsymbol{s}; \boldsymbol{z}, \boldsymbol{\psi}). \tag{8.36}$$

Remark 8.3 (Linear vs. nonlinear arguments) *The bilinear forms $a(\boldsymbol{s}; \boldsymbol{u}, \cdot)$ and $a(\boldsymbol{s}; \boldsymbol{z}, \cdot)$ in the physical residuals $R(\boldsymbol{s}; \boldsymbol{u}, \cdot)$ and $R^*(\boldsymbol{s}; \boldsymbol{z}, \cdot)$ are linear with respect to all arguments right from the semicolon, i.e. the primal and the dual solutions $\boldsymbol{u}$ and $\boldsymbol{z}$ are linear. In contrast, in the material residuals $G(\boldsymbol{s}; \boldsymbol{u}; \cdot)$ and $G^*(\boldsymbol{s}; \boldsymbol{z}; \cdot)$ the primal and the dual solutions $\boldsymbol{u}$ and $\boldsymbol{z}$ appear still as quadratic terms, because the variations of the internal energies $\frac{1}{2} \, a'_s(\boldsymbol{s}; \boldsymbol{u}; \cdot) := \frac{1}{2} \, a'_s(\boldsymbol{s}; \boldsymbol{u}, \boldsymbol{u}, \cdot)$ and $\frac{1}{2} \, a'_s(\boldsymbol{s}; \boldsymbol{z}; \cdot) := \frac{1}{2} \, a'_s(\boldsymbol{s}; \boldsymbol{z}, \boldsymbol{z}, \cdot)$ are quadratic in $\boldsymbol{u}$ and $\boldsymbol{z}$, respectively. This is indicated by the second semicolon, i.e. only the arguments right from the second semicolon are linear.*

For a homogeneous elastic body with the chosen model problem of linearized elasticity (B.77) the energy functionals (8.22) and (8.24) are given by

$$E(\boldsymbol{u}, \boldsymbol{s}) = \int_{\Omega_R} W_R(\boldsymbol{u})\, d\Omega - F(\boldsymbol{s}; \boldsymbol{u}), \tag{8.37}$$

$$E^*(\boldsymbol{z}, \boldsymbol{s}) = \int_{\Omega_R} W_R(\boldsymbol{z})\, d\Omega - J(\boldsymbol{s}; \boldsymbol{z}), \tag{8.38}$$

where the quadratic strain energy function $W_R(\cdot)$ reads

$$W_R(\cdot) = \frac{1}{2}\, \boldsymbol{\sigma}(\cdot) : \boldsymbol{\varepsilon}(\cdot). \tag{8.39}$$

The explicit forms of the residuals are obtained as

$$R(\boldsymbol{s}; \boldsymbol{u}, \boldsymbol{\eta}) = \int_{\Omega_R} \boldsymbol{\sigma}(\boldsymbol{u}) : \operatorname{Grad} \boldsymbol{\eta}\, d\Omega - F(\boldsymbol{s}; \boldsymbol{\eta}), \tag{8.40}$$

$$G(\boldsymbol{s}; \boldsymbol{u}; \boldsymbol{\psi}) = \int_{\Omega_R} \boldsymbol{\Sigma}(\boldsymbol{u}) : \operatorname{Grad} \boldsymbol{\psi}\, d\Omega - F'_s(\boldsymbol{s}; \boldsymbol{u}, \boldsymbol{\psi}), \tag{8.41}$$

$$R^*(\boldsymbol{s}; \boldsymbol{z}, \boldsymbol{\eta}) = \int_{\Omega_R} \boldsymbol{\sigma}(\boldsymbol{z}) : \operatorname{Grad} \boldsymbol{\eta}\, d\Omega - J(\boldsymbol{s}; \boldsymbol{\eta}), \tag{8.42}$$

$$G^*(\boldsymbol{s}; \boldsymbol{z}; \boldsymbol{\psi}) = \int_{\Omega_R} \boldsymbol{\Sigma}(\boldsymbol{z}) : \operatorname{Grad} \boldsymbol{\psi}\, d\Omega - J'_s(\boldsymbol{s}; \boldsymbol{z}, \boldsymbol{\psi}), \tag{8.43}$$

where the Eshelby tensor in terms of linear elasticity is given as

$$\boldsymbol{\Sigma}(\cdot) := W_R(\cdot)\mathbf{I} - \operatorname{Grad}(\cdot)^T \boldsymbol{\sigma}(\cdot). \tag{8.44}$$

8.3 Nonlinear problems

The extension to nonlinear problems is proposed within this section. The variational equation of the primal problem is given by

$$a(\boldsymbol{u}, \boldsymbol{s}; \boldsymbol{\eta}) = F(\boldsymbol{s}; \boldsymbol{\eta}) \qquad \forall\, \boldsymbol{\eta} \in \mathcal{V}, \tag{8.45}$$

For a given nonlinear primal problem, the corresponding dual problem is formulated at the current linearization point and determined by the linear equation

$$k(\boldsymbol{u}, \boldsymbol{s}; \boldsymbol{z}, \boldsymbol{\eta}) = J'_u(\boldsymbol{u}, \boldsymbol{s}; \boldsymbol{\eta}) \qquad \forall\, \boldsymbol{\eta} \in \mathcal{V}, \tag{8.46}$$

where the tangent operator $k(\boldsymbol{u}, \boldsymbol{s}; \boldsymbol{z}, \boldsymbol{\eta}) = a'_u(\boldsymbol{u}, \boldsymbol{s}; \boldsymbol{z}, \boldsymbol{\eta})$ is the tangent physical stiffness operator (4.87) of the primal problem. The corresponding primal and dual residuals have been introduced in (4.7) and (6.7) as

$$R(\boldsymbol{u}, \boldsymbol{s}; \boldsymbol{\eta}) = a(\boldsymbol{u}, \boldsymbol{s}; \boldsymbol{\eta}) - F(\boldsymbol{s}; \boldsymbol{\eta}), \tag{8.47}$$

$$R^*(\boldsymbol{u}, \boldsymbol{s}; \boldsymbol{z}, \boldsymbol{\eta}) = k(\boldsymbol{u}, \boldsymbol{s}; \boldsymbol{z}, \boldsymbol{\eta}) - J'_u(\boldsymbol{u}, \boldsymbol{s}; \boldsymbol{\eta}). \tag{8.48}$$

8.3.1 The error in a quantity of interest

We consider the physical problem for a given fixed design and therefore the variable $\boldsymbol{s}$ is omitted for notational simplicity within this section. A representation of the error in a quantity of interest $J(\boldsymbol{u}) - J(\boldsymbol{u}_h)$ for general nonlinear problems can be obtain by using an optimal control approach [12].

In Section 5.3.2 we have introduced the Lagrangian functional $L(\boldsymbol{u}, \boldsymbol{z}) = J(\boldsymbol{u}) - R(\boldsymbol{u}; \boldsymbol{z})$ with the corresponding optimality condition

$$L'(\boldsymbol{u}, \boldsymbol{z})(\boldsymbol{\eta}, \boldsymbol{\nu}) = \left\{ \begin{array}{l} J'_u(\boldsymbol{u}; \boldsymbol{\eta}) - R'_u(\boldsymbol{u}; \boldsymbol{z}, \boldsymbol{\eta}) \\ \\ - R(\boldsymbol{u}; \boldsymbol{\nu}) \end{array} \right\} = \boldsymbol{0} \tag{8.49}$$

for all $\{\boldsymbol{\eta}, \boldsymbol{\nu}\} \in \mathcal{V} \times \mathcal{V}$.

The Galerkin approximation of (8.49) for solutions $\{\boldsymbol{u}_h, \boldsymbol{z}_h\} \in \mathcal{V}_h \times \mathcal{V}_h$ is given by

$$L'(\boldsymbol{u}_h, \boldsymbol{z}_h)(\boldsymbol{\eta}_h, \boldsymbol{\nu}_h) = \left\{ \begin{array}{l} J'_u(\boldsymbol{u}_h; \boldsymbol{\eta}_h) - R'_u(\boldsymbol{u}_h; \boldsymbol{z}_h, \boldsymbol{\eta}_h) \\ \\ - R(\boldsymbol{u}_h; \boldsymbol{\nu}_h) \end{array} \right\} = \boldsymbol{0} \tag{8.50}$$

for all $\{\boldsymbol{\eta}_h, \boldsymbol{\nu}_h\} \in \mathcal{V}_h \times \mathcal{V}_h$.

For an error representation the relation

$$\begin{aligned} J(\boldsymbol{u}) - J(\boldsymbol{u}_h) &= L(\boldsymbol{u}, \boldsymbol{z}) - L(\boldsymbol{u}_h, \boldsymbol{z}_h) \\ &= \frac{1}{2} L'(\boldsymbol{u}_h, \boldsymbol{z}_h)(\boldsymbol{e}_u, \boldsymbol{e}_z) + r_{uz}(\boldsymbol{u}_h, \boldsymbol{z}_h, \boldsymbol{e}_u, \boldsymbol{e}_z) \end{aligned} \tag{8.51}$$

can be used. The first term is given as

$$\begin{aligned} L'(\boldsymbol{u}_h, \boldsymbol{z}_h)(\boldsymbol{e}_u, \boldsymbol{e}_z) &= L'_u(\boldsymbol{u}_h, \boldsymbol{z}_h)(\boldsymbol{u} - \boldsymbol{u}_h) + L'_z(\boldsymbol{u}_h, \boldsymbol{z}_h)(\boldsymbol{z} - \boldsymbol{z}_h) \\ &= J'_u(\boldsymbol{u}_h; \boldsymbol{u} - \boldsymbol{u}_h) - R'_u(\boldsymbol{u}_h; \boldsymbol{z}_h, \boldsymbol{u} - \boldsymbol{u}_h) - R(\boldsymbol{u}_h; \boldsymbol{z} - \boldsymbol{z}_h) \\ &= -[\, R^*(\boldsymbol{u}_h; \boldsymbol{z}_h, \boldsymbol{u} - \boldsymbol{u}_h) + R(\boldsymbol{u}_h; \boldsymbol{z} - \boldsymbol{z}_h)\,] \end{aligned} \tag{8.52}$$

and the remainder reads

$$\begin{aligned} r_{uz}(\boldsymbol{u}_h, \boldsymbol{z}_h, \boldsymbol{e}_u, \boldsymbol{e}_z) := \frac{1}{2} \int_0^1 \{ & J'''_{uuu}(\boldsymbol{u}_h + \lambda \boldsymbol{e}_u)(\boldsymbol{e}_u, \boldsymbol{e}_u, \boldsymbol{e}_u) \\ & - R'''_{uuu}(\boldsymbol{u}_h + \lambda \boldsymbol{e}_u)(\boldsymbol{e}_u, \boldsymbol{e}_u, \boldsymbol{e}_u, \boldsymbol{z}_h + \lambda \boldsymbol{e}_z) \\ & - 3R''_{uu}(\boldsymbol{u}_h + \lambda \boldsymbol{e}_u)(\boldsymbol{e}_u, \boldsymbol{e}_u, \boldsymbol{e}_z)\} \, \lambda(\lambda - 1)\, d\lambda, \end{aligned} \tag{8.53}$$

which is cubic in $\boldsymbol{e}_u := \boldsymbol{u} - \boldsymbol{u}_h$ and $\boldsymbol{e}_z := \boldsymbol{z} - \boldsymbol{z}_h$.

Finally, for the error in the quantity of interest holds

$$J(\boldsymbol{u}) - J(\boldsymbol{u}_h) = -\left[\frac{1}{2}\,R(\boldsymbol{u}_h; \boldsymbol{z} - \boldsymbol{z}_h) + \frac{1}{2}\,R^*(\boldsymbol{u}_h; \boldsymbol{z}_h, \boldsymbol{u} - \boldsymbol{u}_h)\right] + r_{uz}. \tag{8.54}$$

The proof is straightforward and can be found in [4, 12]. The error in the quantity of interest $J(\boldsymbol{u}) - J(\boldsymbol{u}_h)$ depends directly on the error in the corresponding dual solution.

Remark 8.4 (Linear vs. nonlinear problem) *In the linear case the primal and dual residuals coincide, i.e. $R(\boldsymbol{u}_h; \boldsymbol{z} - \boldsymbol{z}_h) = R^*(\boldsymbol{z}_h; \boldsymbol{u} - \boldsymbol{u}_h)$. Therefore, (8.12) and (8.14) yield the same error in the quantity of interest. But this does not apply to the nonlinear case.*

Remark 8.5 (Error measures in the context of r-adaptivity) *Error measures in the context of r-adaptivity have been introduced in Section 7.3. The corresponding errors for linear quantities of interest are given in Section 8.2.2. For nonlinear quantities of interest these errors are introduced in the same manner as*

$$J_{e_u}(\boldsymbol{u}, \boldsymbol{u}_h) := J(\boldsymbol{u}) - J(\boldsymbol{u}_h), \tag{8.55}$$

$$J_{e_{u,h}}(\boldsymbol{u}_h^*, \boldsymbol{u}_h) := J(\boldsymbol{u}_h^*) - J(\boldsymbol{u}_h), \tag{8.56}$$

$$J_{e_u^*}(\boldsymbol{u}, \boldsymbol{u}_h^*) := J(\boldsymbol{u}) - J(\boldsymbol{u}_h^*). \tag{8.57}$$

8.3.2 Energy minimization with respect to the design

In the same manner as for the linear problem in Section 8.2.4, the combined energy functional for the primal problem (4.1) as well as for the dual problem (6.2) is given as

$$I(\boldsymbol{u}, \boldsymbol{z}, \boldsymbol{s}) = \gamma_u\, E(\boldsymbol{u}, \boldsymbol{s}) + \gamma_z\, E^*(\boldsymbol{u})(\boldsymbol{z}, \boldsymbol{s}). \tag{8.58}$$

The minimization of the overall energy is given by a sequence of minimization problems at every linearization point $\{\boldsymbol{u}, \boldsymbol{s}, \boldsymbol{z}\}$, i.e. we have to solve the following problem in each linearization point.

Problem 8.3 (Energy minimization w.r.t. $\{\boldsymbol{u}, \boldsymbol{z}, \boldsymbol{s}\}$) *Find $\{\boldsymbol{u}, \boldsymbol{z}, \boldsymbol{s}\} \in \mathcal{V} \times \mathcal{V} \times \mathcal{S}$ such that the energy functional (8.58) is minimized, i.e.*

$$I(\boldsymbol{u}, \boldsymbol{z}, \boldsymbol{s}) = \min_{\{\boldsymbol{p}, \boldsymbol{q}, \boldsymbol{r}\} \in \mathcal{V} \times \mathcal{V} \times \mathcal{S}} I(\boldsymbol{p}, \boldsymbol{q}, \boldsymbol{r}). \tag{8.59}$$

The first-order optimality condition is given as

$$\left\{\begin{array}{l} I_u'(\boldsymbol{u}, \boldsymbol{z}, \boldsymbol{s})(\boldsymbol{\eta}) \\ I_z'(\boldsymbol{u}, \boldsymbol{z}, \boldsymbol{s})(\boldsymbol{\nu}) \\ I_s'(\boldsymbol{u}, \boldsymbol{z}, \boldsymbol{s})(\boldsymbol{\psi}) \end{array}\right\} = \left\{\begin{array}{l} \gamma_u\, R(\boldsymbol{u}, \boldsymbol{s}; \boldsymbol{\eta}) \\ \gamma_z\, R^*(\boldsymbol{u}, \boldsymbol{s}; \boldsymbol{z}, \boldsymbol{\nu}) \\ \gamma_u\, G(\boldsymbol{u}, \boldsymbol{s}; \boldsymbol{\psi}) + \gamma_z\, G^*(\boldsymbol{u}, \boldsymbol{s}; \boldsymbol{z}; \boldsymbol{\psi}) \end{array}\right\} = \boldsymbol{0} \tag{8.60}$$

for all $\{\boldsymbol{\eta}, \boldsymbol{\nu}, \boldsymbol{\psi}\} \in \mathcal{V} \times \mathcal{V} \times \mathcal{S}$. The structure of this system coincides with the system of the linear problem (8.34), but in contrast the first equation is still a nonlinear variational equation for the state $\boldsymbol{u}$ and the second equation is a linear equation for $\boldsymbol{z}$ formulated at the current linearization point, i.e. at a given deformed state.

The primal physical and material residuals R and G are given in (4.7) and (4.8). Furthermore, the dual physical and material residuals R^* and G^* are given in (6.7) and (6.8), respectively.

For the computational treatment it is useful to reformulate the optimization problem (8.59) only in terms of $\boldsymbol{s}$, i.e. we introduce the functional

$$\mathcal{I}(\boldsymbol{s}) := \gamma_u \, E(\boldsymbol{u}(\boldsymbol{s}), \boldsymbol{s}) + \gamma_z \, E^*(\boldsymbol{u}(\boldsymbol{s}))(\boldsymbol{z}(\boldsymbol{s}), \boldsymbol{s}) \tag{8.61}$$

and we seek for $\boldsymbol{s} \in \mathcal{S}$ such that

$$\mathcal{I}(\boldsymbol{s}) = \min_{\boldsymbol{r} \in \mathcal{S}} \mathcal{I}(\boldsymbol{r}). \tag{8.62}$$

For given solutions $\{\boldsymbol{u}, \boldsymbol{z}\}$ this optimization problem can be solved by using standard gradient based algorithms or a staggered Newton method like for the global mesh optimization problem from Section 4.5.2.

Remark 8.6 (Energy as quantity of interest) *If the overall energy $E(\boldsymbol{u}, \boldsymbol{s})$ of the primal problem is chosen as quantity of interest, i.e.*

$$J(\boldsymbol{u}, \boldsymbol{s}) = E(\boldsymbol{u}, \boldsymbol{s}), \tag{8.63}$$

the corresponding dual problem reads

$$k(\boldsymbol{u}, \boldsymbol{s}; \boldsymbol{z}, \boldsymbol{\eta}) = J'_u(\boldsymbol{u}, \boldsymbol{s}; \boldsymbol{\eta}) = R(\boldsymbol{u}, \boldsymbol{s}; \boldsymbol{\eta}) = 0. \tag{8.64}$$

Hence, the dual solution $\boldsymbol{z}$ becomes zero and $E^*(\boldsymbol{u})(\boldsymbol{z}, \boldsymbol{s})$ vanishes. In this trivial case we obtain just the global mesh optimization problem (4.4) with the optimality condition (4.6).

8.4 Solution algorithm and practical aspects

In practice, we propose a staggered solution algorithm, i.e. we solve first the primal and the dual problem and thereafter the optimization problem for the optimal design. For a given initial mesh $\mathcal{T}_h(\boldsymbol{s}_h)$ and a certain load step the solution scheme is given in Box 8.1.

Different numerical difficulties arise due to the solution of this problem. Reasonable regularization methods should be used in order to regularize the energy functional. Furthermore, the quality of the mesh (the distortion of the mesh) has an important influence on the shape derivatives and hence on the results and the success of the optimization process. Hence, we have to control the mesh distortion during the optimization progress, see Section 7.5.3.

1. Solve the primal problem for a given load scale λ and for a given design $\hat{\boldsymbol{s}}_h$. Find $\boldsymbol{u}_h \in \mathcal{V}_h$ such that

$$a(\boldsymbol{u}_h, \hat{\boldsymbol{s}}_h; \boldsymbol{\eta}_h) = \lambda \cdot F(\hat{\boldsymbol{s}}_h; \boldsymbol{\eta}_h) \quad \forall\, \boldsymbol{\eta}_h \in \mathcal{V}_h.$$

2. Solve the corresponding dual problem for given $\{\hat{\boldsymbol{u}}_h, \hat{\boldsymbol{s}}_h\}$. Find $\boldsymbol{z}_h \in \mathcal{V}_h$ such that

$$k(\hat{\boldsymbol{u}}_h, \hat{\boldsymbol{s}}_h; \boldsymbol{z}_h, \boldsymbol{\eta}_h) = J'_u(\hat{\boldsymbol{u}}_h, \hat{\boldsymbol{s}}_h; \boldsymbol{\eta}_h) \quad \forall\, \boldsymbol{\eta}_h \in \mathcal{V}_h.$$

3. Solve the minimization problem for given $\{\hat{\boldsymbol{u}}_h, \hat{\boldsymbol{s}}_h, \hat{\boldsymbol{z}}_h\}$. Find $\boldsymbol{s}_h \in \mathcal{S}_h$ such that (8.61) is minimized, i.e.

$$\mathcal{I}(\boldsymbol{s}_h) = \min_{\boldsymbol{r}_h \in \mathcal{S}_h} \mathcal{I}(\boldsymbol{r}_h).$$

   Compute the primal and the dual material residuals G and G^* for $\{\boldsymbol{u}_h, \boldsymbol{s}_h, \boldsymbol{z}_h\}$ and the search direction $\boldsymbol{d}$ by using gradient based or Newton-type methods.
   Compute a step size parameter ε and update the design, i.e. $\boldsymbol{s}_{i+1} = \boldsymbol{s}_i + \Delta\boldsymbol{s}$ with $\Delta\boldsymbol{s} = \varepsilon \boldsymbol{d}$.
   Update $\boldsymbol{u}$ with the sensitivity relation $\Delta\boldsymbol{u} \approx \boldsymbol{S}\, \Delta\boldsymbol{s}$, see Remark 7.2. Goto (1) and find the new state of equilibrium.

Box 8.1: Staggered solution algorithm for goal-oriented r-adaptive mesh optimization

Furthermore, the dimension of the numerical values of the primal and the dual material residuals can be very different, because they depend directly on the dimension of the primal and dual energy. In order to find a new search direction we have to choose the weights γ_u and γ_z in an adequate manner. Within the following examples normalized material residuals are used, i.e the weights γ_u and γ_z are chosen in such a way that both residuals are normalized to unity with the corresponding sign. Afterwards, the new search direction $\boldsymbol{d}$ has to be scaled back to a suitable value in dependency on the dimension of the primal solution, the decrease in the energy functional and the distortion of the mesh.

Of course, due to the complexity of the multi-objective problem different solutions may be possible in dependency on the parameters γ_u and γ_z. Furthermore, from a theoretical point of view an *objective conflict* may appear, i.e. none of the feasible solutions allows the simultaneous minimization of both objectives, see e.g. [38, 98]. In such a case, the weights have to be set to $\gamma_u = 1$ and $\gamma_z = 0$ or $\gamma_u = 0$ and $\gamma_z = 1$, i.e. the single primal or the single dual problem is solved. In the author's experience, for a proper choice of the weights the algorithm works.

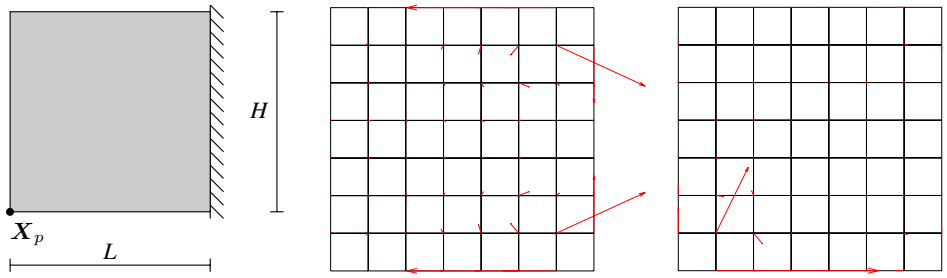

(a) system (b) primal material residual G (c) dual material residual G^*

Figure 8.1: Short cantilever: system and material residuals on the design variables for the initial mesh

8.5 Numerical examples

In this section, numerical examples concerning global and goal-oriented mesh optimization are presented. In the first example, the theory of linearized elasticity is considered and in the second example a problem from nonlinear elasticity is investigated.

8.5.1 Short cantilever

System and model problem. We examine a short cantilever under self-weight loading $b_y = -100$, see Fig. 8.1a. In this first example, the model problem of linearized elasticity is considered, see Appendix B.2. The problem is modeled with the plane strain condition with $E = 1000$ and $\nu = 0.3$ and we discretize the model with standard Q4 elements.

The simple mesh consists of 49 Q4 elements and overall 128 degrees of freedom. The design variables are the nodal coordinates of all inner nodes and the nodal coordinates in tangential direction on the boundaries, i.e. 96 nodal coordinates are chosen as design variables.

We consider as a quantity of interest the vertical displacement u_y at the point $\boldsymbol{X}_p$ as indicated in Fig. 8.1a , i.e.

$$J(\boldsymbol{u}, \boldsymbol{s}) = u_y(\boldsymbol{X}_p). \tag{8.65}$$

The dual load for this quantity of interest is just a unit load in y-direction at point $\boldsymbol{X}_p$ and the resulting displacement field due to this load case is the dual solution $\boldsymbol{z}_h$ for $u_y(\boldsymbol{X}_p)$.

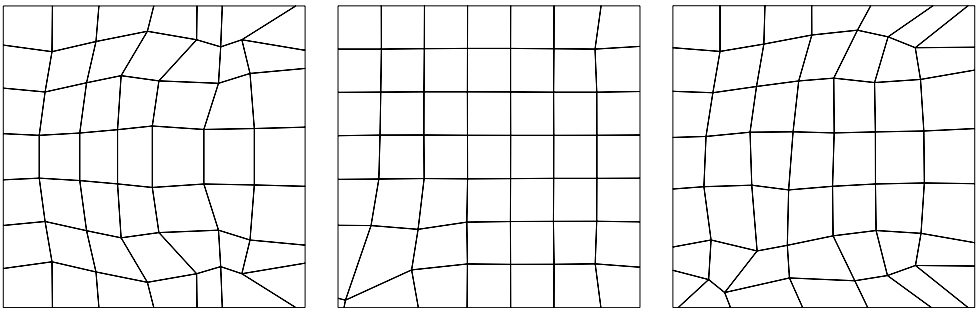

(a) global mesh optimization for the primal problem

(b) global mesh optimization for the dual problem

(c) goal-oriented mesh optimization

Figure 8.2: Short cantilever: optimized meshes

The primal and dual material residuals. The discrete primal material residual $\boldsymbol{G}(\boldsymbol{u}_h, \boldsymbol{s}_h)$ due to the primal load case b_y is given in Fig. 8.1b and the discrete dual material residual $\boldsymbol{G}^*(\boldsymbol{z}_h, \boldsymbol{s}_h)$ due to the dual load is shown in Fig. 8.1c. Both residuals are given for the same initial discretization (design) and only for the design variables, i.e. for the nodal coordinates, which are allowed to vary. These are error indicators for the non-optimal discretizations of the primal and the dual problem, respectively.

Results of the mesh optimization algorithm. A simple steepest descent method was used in order to solve the minimization problem (8.62). Therefore, only the gradients of the primal and dual energy, i.e. the primal and dual material residuals, are required. The solution was attained within 10 iterations by using the solution algorithm in Box. 8.1.

The global mesh optimization for the primal problem as well as the global mesh optimization for the dual problem itself have been investigated. The resulting meshes are given in Fig. 8.2a and Fig. 8.2b, respectively. The meshes are optimized with respect to the overall energy of the primal problem $E(\boldsymbol{u})$ and the overall energy of the dual problem $E^*(\boldsymbol{z})$.

Furthermore, the goal-oriented optimized mesh with respect to the chosen quantity of interest is shown in Fig. 8.2c. The resulting mesh yields an optimal solution with respect to $J(\boldsymbol{u}, \boldsymbol{s})$.

The error in the quantity of interest. In order to quantify the capability of the optimized meshes, we compare the finite element solution $J(\boldsymbol{u}_h, \boldsymbol{s}_h)$ in every iteration with a reference solution $J(\boldsymbol{u}, \boldsymbol{s}) = -0.28525$ obtained on a fine mesh with 10201 nodes. The results of the relative errors for the global mesh optimization and the goal-oriented approach are shown in Fig. 8.3. For the initial mesh we have $J(\boldsymbol{u}_h^0, \boldsymbol{s}_h^0) = -0.27756$ and a relative error of $2.70\,\%$ with respect to the reference solution.

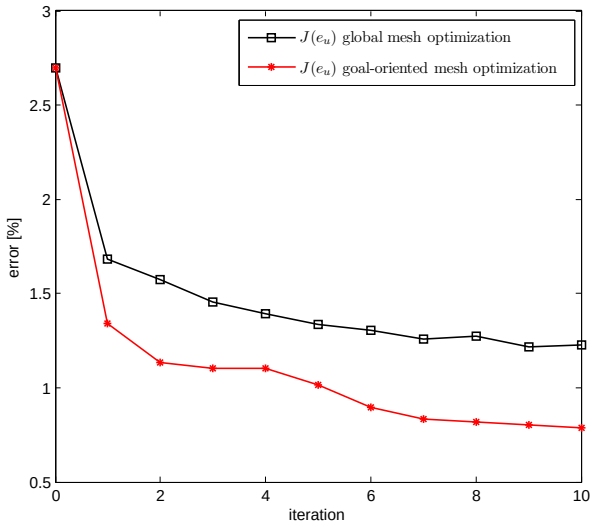

Figure 8.3: Short cantilever: relative error $J(\boldsymbol{e}_u)$ during the mesh optimization

The global mesh optimization procedure yields after 10 iterations to $J(\boldsymbol{u}_h^*, \boldsymbol{s}_h^*) = -0.28176$ and the relative error of about $1.23\,\%$, i.e. the error is reduced of about $54\,\%$. In contrast, the goal-oriented mesh optimization leads to $J(\boldsymbol{u}_h^*, \boldsymbol{s}_h^*) = -0.28301$ and hence to the relative error of $0.79\,\%$, i.e. a reduction of $71\,\%$ with respect to the error of the initial mesh. Hence, the goal-oriented approach yields a much better accuracy in the quantity of interest than the global mesh optimization procedure.

Error measures within r-adaptivity. In Section 7.3 and in Remark 8.2.2 we have introduced error measures within r-adaptivity for the global and the goal-oriented mesh optimization problems. Due to the fact that we keep the current approximation spaces $\mathcal{V}_h$ and $\mathcal{S}_h$ fixed, we minimize only the error on the current mesh $J(\boldsymbol{e}_{u,h}) = J(\boldsymbol{u}_h^*) - J(\boldsymbol{u}_h)$ and obtain the least obtainable error $J(\boldsymbol{e}_u^*) = J(\boldsymbol{u}) - J(\boldsymbol{u}_h^*)$. Hence, the errors shown in Fig. 8.3 tend to the errors $J(\boldsymbol{e}_u^*)$ and not to zero. In case a smaller error is desired, we have to extend the approximation spaces, i.e. we have to perform a h or p-adaptive step.

The overall error is given by $J(\boldsymbol{e}_u) = J(\boldsymbol{e}_u^*) + J(\boldsymbol{e}_{u,h})$. The contribution of the error $J(\boldsymbol{e}_{u,h})$ on the overall error is very large for the initial mesh and the first and second iterations. The contributions of all errors for the goal-oriented mesh optimization during the iterations are shown in Fig. 8.4.

Uniform mesh refinement vs. r-adaptivity. The r-adaptivity provides an improved solution on the same mesh with low computational cost. On a coarse mesh with 64 nodes, we

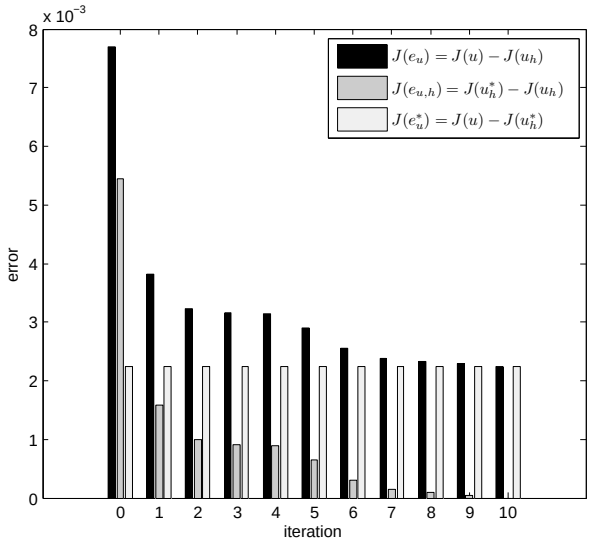

Figure 8.4: Short cantilever: distribution of the absolute errors $J(\boldsymbol{e}_u)$, $J(\boldsymbol{e}_{u,h})$ and $J(\boldsymbol{e}_u^*)$ for goal-oriented mesh optimization

have reduced the relative error of about $71\,\%$. If we use a uniform mesh refinement we need about 280 nodes in order to obtain the same accuracy, i.e. more than the fourfold number of nodes. This is shown in Fig. 8.5. The relative error due to a uniform mesh refinement is compared with the errors $J(\boldsymbol{e}_u^*)$ obtained from the global and goal-oriented mesh optimization procedures.

This demonstrates the potential of r-adaptive mesh optimization techniques. Especially on coarse meshes, the error can be significantly reduced.

Mesh distortion control. In order to control the distortion of the mesh during the optimization process, the same algorithm as for the global mesh optimization has been used, which is described in Section 7.5.3. A remeshing strategy with a change of the nodal connectivities as well as h-adaptivity techniques for patches with distorted elements could be considered to improve the algorithm further.

As we can see in Fig. 8.3 and Fig. 8.4 the largest error contribution $J(\boldsymbol{e}_{u,h})$ occurs on the initial mesh and the first and second iterations. The gain of accuracy by using complex methods for mesh distortion control can be low as compared to the numerical work involved. Hence, in practical computations it is sufficient to do just few iterations in order to obtain the largest improvements of the solution.

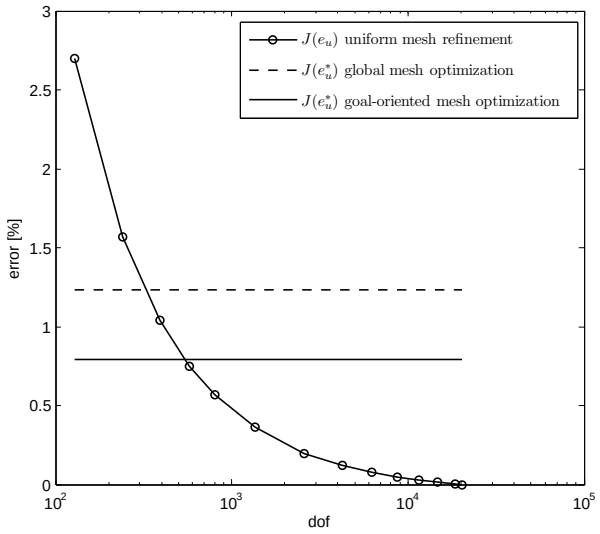

Figure 8.5: Short cantilever: comparison of the relative error $J(\boldsymbol{e}_u)$ due to uniform mesh refinement with the optimal error $J(\boldsymbol{e}_u^*)$ obtained from global and goal-oriented mesh optimization

8.5.2 Plate with a slit

System and model problem. We consider a classical compressible Neo-Hookean material. The strain energy function under consideration is given in (B.20) as

$$W_R(I_C, J) = \frac{1}{2}\,\mu\,(I_C - 3 - 2\ln J) + \frac{1}{2}\,\lambda\,(J-1)^2.$$

The corresponding stress and elasticity tensors are given in Box B.2.

We investigate a plate with a slit as indicated in Figure 8.6. The plate is loaded by a body force $\boldsymbol{b}_R = [0\,,\,100]^T$. The Lamé parameters are chosen as $\lambda = 5.769 \times 10^2$ and $\mu = 3.846 \times 10^2$, which correspond to $E = 10^3$ and $\nu = 0.3$.

The design variables are the nodal coordinates of all inner nodes and the nodal coordinates in tangential direction on the free boundary. The nodal coordinates on the Dirichlet boundary Γ_{D} are fixed.

The finite element model consists of 288 Q4 elements with 331 nodes and 662 degrees of freedom. Overall 505 nodal coordinates are chosen as design variables.

The quantity of interest is the vertical displacement u_y at the point $\boldsymbol{X}_p$, i.e. $J(\boldsymbol{u}, \boldsymbol{s}) = u_y(\boldsymbol{X}_p)$.

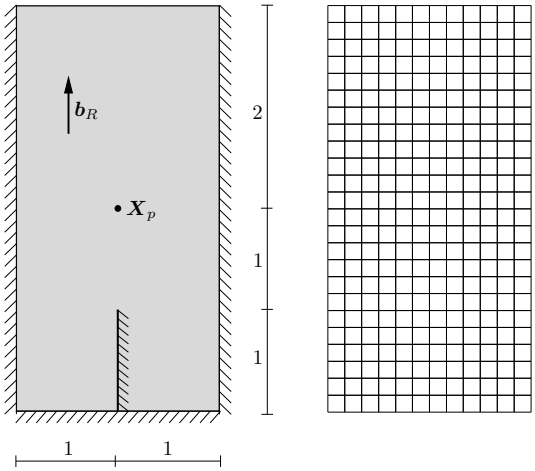

Figure 8.6: Plate with a slit: system and initial mesh

Results of the global and the goal-oriented mesh optimization approach. As in the former example, a steepest descent method has been used in order to solve the problem and up to 100 iterations have been investigated using the global and the goal-oriented mesh optimization approach.

A reference solution $J(\boldsymbol{u}, \boldsymbol{s}) = 9.667878 \times 10^{-2}$ obtained on a fine mesh with 29221 nodes is used in order to quantify the error. The energy of the primal problem for this reference solution is $E(\boldsymbol{u}, \boldsymbol{s}) = -22.642969$. For the initial mesh we have $J(\boldsymbol{u}_h^0, \boldsymbol{s}_h^0) = 9.4824 \times 10^{-2}$, which corresponds to a relative error of $1.92\,\%$ with respect to the reference solution. Furthermore, the primal energy for the initial mesh is $E(\boldsymbol{u}_h^0, \boldsymbol{s}_h^0) = -2.2018 \times 10^1$, which corresponds to a relative error of $2.76\,\%$.

The values of the quantity of interest $J(\boldsymbol{u}_h, \boldsymbol{s}_h)$ and the primal energy $E(\boldsymbol{u}_h, \boldsymbol{s}_h)$ after every tenth iteration are given in Table 8.1 and Table 8.2, respectively. In addition, the relative errors in the quantity of interest η_J^{rel} and the primal energy η_E^{rel} with respect to the reference solutions are listed in the tables. The corresponding meshes for some selected iterations are shown in Fig. 8.8 and Fig. 8.9, respectively. The meshes obtained from the global mesh optimization reflect the primal solution for the given primal load case, see Fig. 8.8f. The goal-oriented optimized meshes reflect the influence of the dual solution. The dual solution is shown in Fig. 8.9f.

The largest improvements occur within the first thirty iterations. The global mesh optimization leads after 30 iterations to $J(\boldsymbol{u}_h, \boldsymbol{s}_h) = 9.5647 \times 10^{-2}$ and a relative error of $1.07\,\%$, i.e. a reduction of the error of the initial mesh of about $44\,\%$. The goal-oriented approach yields $J(\boldsymbol{u}_h, \boldsymbol{s}_h) = 9.5950 \times 10^{-2}$, which corresponds to a relative error of $0.75\,\%$, i.e. a reduction of $61\,\%$ with respect to the error of the initial mesh.

Table 8.1: Global and goal-oriented mesh optimization: relative errors in $J(\boldsymbol{u}_h, \boldsymbol{s}_h)$

Iteration	global		goal-oriented	
	$J(\boldsymbol{u}_h, \boldsymbol{s}_h)$	η_J^{rel} [%]	$J(\boldsymbol{u}_h, \boldsymbol{s}_h)$	η_J^{rel} [%]
0	9.4824e-002	1.9186	9.4824e-002	1.9186
10	9.5600e-002	1.1160	9.5664e-002	1.0495
20	9.5628e-002	1.0867	9.5849e-002	0.8585
30	9.5647e-002	1.0667	9.5950e-002	0.7538
40	9.5659e-002	1.0546	9.5971e-002	0.7325
50	9.5667e-002	1.0470	9.5978e-002	0.7246
60	9.5675e-002	1.0383	9.5985e-002	0.7175
70	9.5681e-002	1.0320	9.5993e-002	0.7089
80	9.5695e-002	1.0180	9.5998e-002	0.7041
90	9.5707e-002	1.0055	9.6002e-002	0.6999
100	9.5717e-002	0.9949	9.6006e-002	0.6961

Table 8.2: Global and goal-oriented mesh optimization: relative errors in $E(\boldsymbol{u}_h, \boldsymbol{s}_h)$

Iteration	global		goal-oriented	
	$E(\boldsymbol{u}_h, \boldsymbol{s}_h)$	η_E^{rel} [%]	$E(\boldsymbol{u}_h, \boldsymbol{s}_h)$	η_E^{rel} [%]
0	-2.2018e+001	2.7584	-2.2018e+001	2.7584
10	-2.2200e+001	1.9582	-2.2112e+001	2.3461
20	-2.2207e+001	1.9249	-2.2190e+001	2.0022
30	-2.2212e+001	1.9022	-2.2213e+001	1.9005
40	-2.2215e+001	1.8905	-2.2217e+001	1.8830
50	-2.2215e+001	1.8884	-2.2218e+001	1.8772
60	-2.2217e+001	1.8813	-2.2219e+001	1.8719
70	-2.2217e+001	1.8815	-2.2221e+001	1.8653
80	-2.2220e+001	1.8680	-2.2221e+001	1.8616
90	-2.2221e+001	1.8614	-2.2222e+001	1.8585
100	-2.2223e+001	1.8563	-2.2223e+001	1.8556

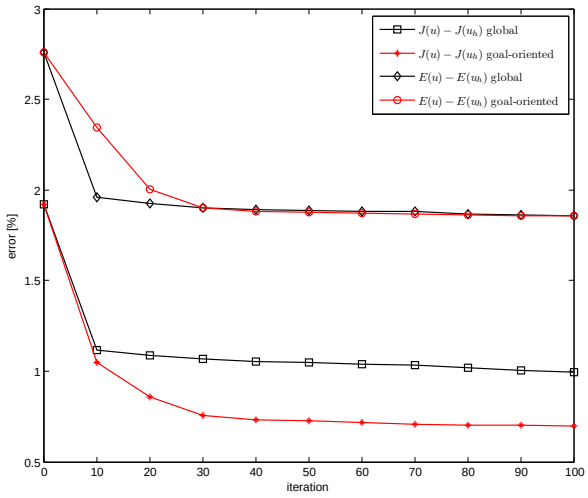

Figure 8.7: Plate with a slit: relative errors in $J(\boldsymbol{u}_h, \boldsymbol{s}_h)$ and the primal energy $E(\boldsymbol{u}_h, \boldsymbol{s}_h)$ with respect to the reference solution

The goal-oriented approach yields much better results for the quantity of interest within all iterations. In contrast, the global mesh optimization approach leads to better results for the primal energy within the first thirty iterations. After that, both the global and the goal-oriented optimized meshes give roughly the same primal energy $E(\boldsymbol{u}_h, \boldsymbol{s}_h)$. This is shown in Fig. 8.7 and all values are given in Table 8.2.

Notes on the non-convex optimization problem. It is noteworthy that different meshes yield the same amount of primal energy, because the optimization problem is non-convex in general and several local minima may occur. For instance, the global and the goal-oriented optimized meshes after 30 iterations are shown in Fig. 8.8c and Fig. 8.9c, respectively. The relative error in the primal energy of both meshes is about $1.90\,\%$ with respect to the reference solution, i.e. two local minima have been found, see Fig. 8.7.

Therefore, due to the complexity of the optimization problem, a global minima can in general not be achieved. However, the error in the energy with respect to the error of the initial mesh is reduced of about $32\,\%$.

Hence, the errors in the quantity of interest and in the primal energy are significantly reduced with respect to the initial discretization, in which the number of nodes as well as the mesh topology are fixed.

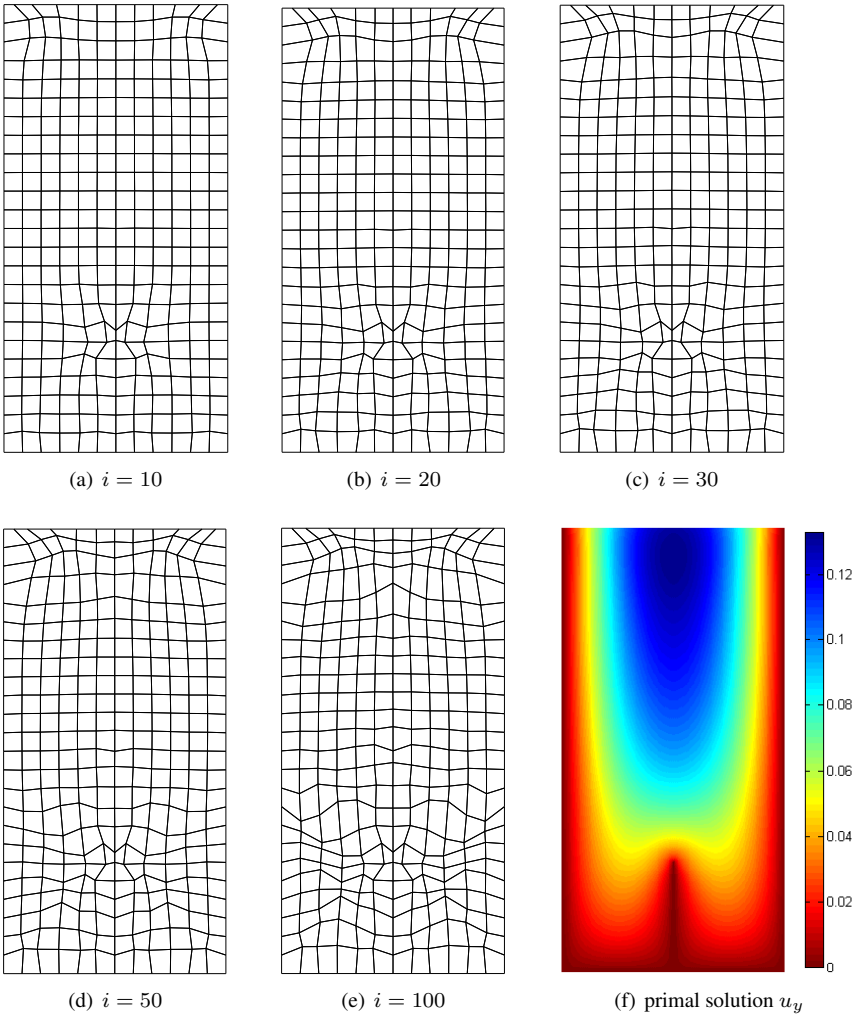

(a) $i = 10$ (b) $i = 20$ (c) $i = 30$

(d) $i = 50$ (e) $i = 100$ (f) primal solution u_y

Figure 8.8: Global mesh optimization: optimized meshes and the vertical component of the primal solution on the reference mesh

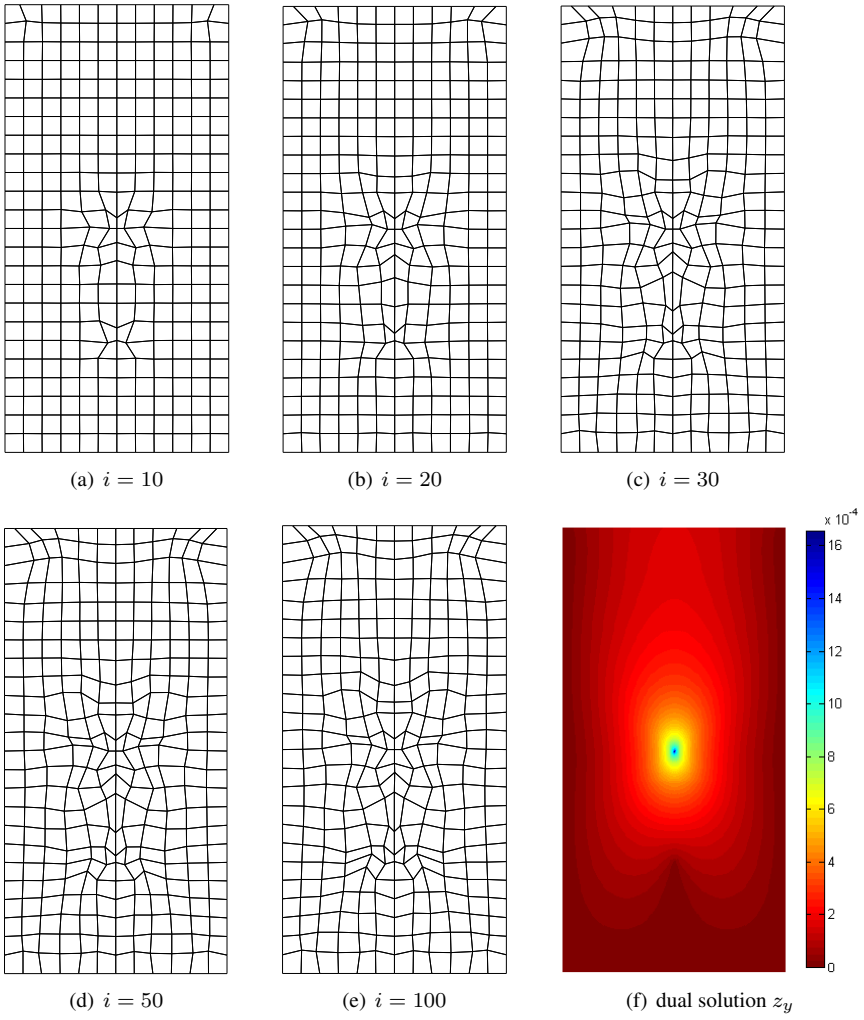

(a) $i = 10$ (b) $i = 20$ (c) $i = 30$

(d) $i = 50$ (e) $i = 100$ (f) dual solution z_y

Figure 8.9: Goal-oriented mesh optimization: optimized meshes and the vertical component of the dual solution on the reference mesh

Approximations of the dual solution. As shown in Section 8.3.1, the error in the quantity depends on the error in the corresponding dual solution. Hence, the mesh has to be optimized with respect to the dual solution in order to minimize the error. The mesh which yields a good approximation of the dual solution can be associated with a good approximation of the quantity of interest.

A good approximation of the dual solution on a h-adaptive refined mesh is given in Fig. 8.10c. The figure shows a 3D plot of the vertical component z_y in order to illustrate the solution behavior. On the initial mesh only a rough approximation of the exact dual solution can be computed. This is shown in Fig. 8.10a. The goal-oriented optimized mesh yields a better approximation of the dual solution as the initial mesh, see Fig. 8.10b.

Concluding remarks. The proposed r-adaptive mesh optimization algorithm yields an improved solution on the same mesh with a fixed number of nodes and mesh topology, i.e. the current approximation spaces $\mathcal{V}_h$ and $\mathcal{S}_h$ are fixed. If a lower discretization error is required, we have to extend the approximation spaces, i.e. we have to perform a h- or p-adaptive step.

Classical h- and p-methods are superior as compared to r-adaptive methods and it is not intended to substitute any h- or p-method by a r-adaptivity. However, r-adaptive mesh optimization algorithms are powerful at the beginning of an adaptive process, i.e. for an initial coarse mesh before the application of h- or p-adaptive methods.

It is well-known that the combination of h- and p-methods is more efficient than each individual method. Therefore, a combined rhp-method seems to be the most efficient way in order to optimize the mesh and to improve the finite element solution. The development of such a rhp-method for global and goal-oriented mesh optimization should be addressed to future work.

Moreover, there are other challenging problems from shape optimization where r-adaptivity can be used. For instance, a r-adaptive method could be used to reallocate the nodal position of all interior nodes if the shape optimization algorithm has modified the boundary. Especially the goal-oriented r-adaptivity can be used if a local quantity of interest is considered as a constraint of the optimization problem.

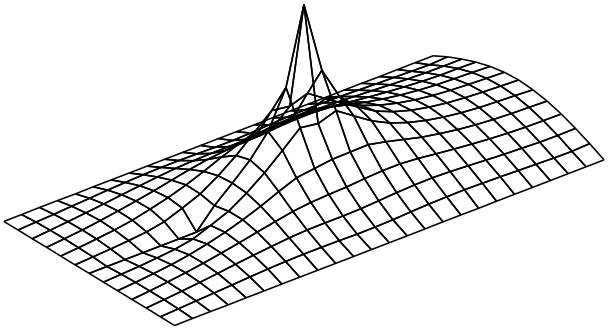

(a) initial mesh

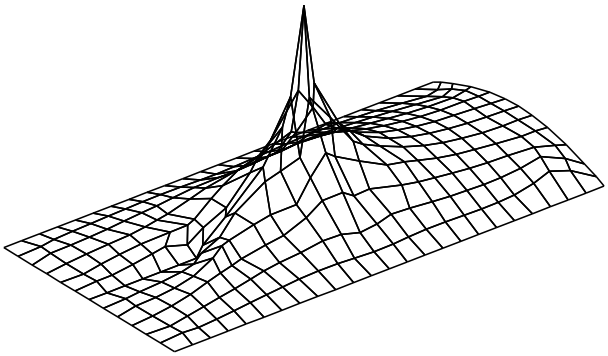

(b) goal-oriented r-adaptive optimized mesh ($i = 100$)

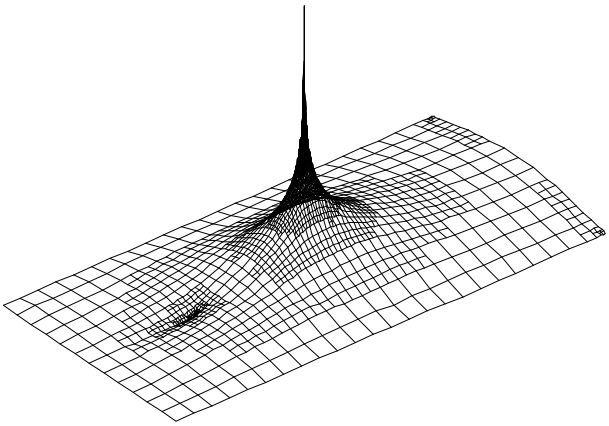

(c) h-adaptive optimized mesh with respect to $\boldsymbol{z}$

Figure 8.10: Approximative dual solutions z_y on the initial and the goal-oriented r-adaptive optimized meshes as well as a good approximation of the dual solution on a h-adaptive optimized mesh

Chapter 9

Shape optimization and configurational mechanics

The shape optimization problem in the context of configurational mechanics is considered in this chapter. At first, an abstract framework for structural optimization problems is introduced. The shape optimization problem is investigated later on and the internal energy is chosen as objective functional. It is shown that the material residual on the design boundary is an indicator in which direction the boundary has to move in order to minimize the internal energy.

9.1 Introduction

Many fields deal with configurational changes. A classical field is structural optimization, e.g. shape or topology optimization, in which the changes of the objective functional and the state variable due to changes in the material configuration are of interest, see e.g. [13, 14, 29, 58]. An interesting objective functional in shape and topology optimization is the energy, because the minimization of the energy is directly related to the minimization of the compliance of the system or equivalently to the maximization of the stiffness.

In this chapter the shape optimization problem is considered and the goal is to minimize the internal energy of the primal problem. The shape of the body is described by a geometry model, which is controlled by a set of discrete control points of geometrical objects. In the examples, the geometry is modeled using Bézier curves.

Furthermore, different applications in the context of structural optimization and configurational mechanics or mechanics in the material space can be found in the literature. The shape optimization of elastic inclusions was studied in [101, 102] and an application to the optimization of truss structures were presented in [1, 21].

In addition to these applications, the shape optimization problem for elastic solids is investigated within this work and the relations to configurational mechanics are highlighted. Both disciplines deal with changes in the material configuration but they use merely different designations for the same quantities. For instance, the so-called *configurational* or *material forces*

or *material residual* are called *sensitivities of the energy* in the context of structural optimization, see (4.13) in Section 4.3.1. It turns out that the discrete material residuals on the design boundaries are the negative gradients within the shape optimization process. Therefore, material residuals are indicators in which direction the boundary has to move in order to minimize the compliance (internal energy) or equivalently to maximize of the structural stiffness. Some results of this chapter are published in [66, 69].

9.2 On structural optimization and variational balance laws

9.2.1 An abstract framework for structural optimization

A classical structural optimization problem in an abstract setting is considered. In general, the following optimization problem has to be solved.

Problem 9.1 (General structural optimization problem) *Find* $\{\boldsymbol{v}, \boldsymbol{s}\} \in \mathcal{V} \times \mathcal{S}$ *such that a chosen objective functional* $I : \mathcal{V} \times \mathcal{S} \to \mathbb{R}$ *is minimized, i.e*

$$I(\boldsymbol{v}, \boldsymbol{s}) = \min_{\{\boldsymbol{p},\boldsymbol{r}\} \in \mathcal{V} \times \mathcal{S}} I(\boldsymbol{p}, \boldsymbol{r}) \tag{9.1}$$

subject to the constraint

$$R(\boldsymbol{v}, \boldsymbol{s}; \boldsymbol{\eta}) = a(\boldsymbol{v}, \boldsymbol{s}; \boldsymbol{\eta}) - F(\boldsymbol{s}; \boldsymbol{\eta}) = 0 \qquad \forall\, \boldsymbol{\eta} \in \mathcal{V}. \tag{9.2}$$

Additionally other conditions and side constraints for the design $\boldsymbol{s}$ may be introduced. The corresponding Lagrangian functional reads

$$L(\boldsymbol{v}, \boldsymbol{s}, \boldsymbol{z}) := I(\boldsymbol{v}, \boldsymbol{s}) + R(\boldsymbol{v}, \boldsymbol{s}; \boldsymbol{z})\,, \tag{9.3}$$

where $\boldsymbol{z} \in \mathcal{V}$ denotes the *dual* or *adjoint variable*. We seek for stationary points of L which are given by the solution of

$$L'(\boldsymbol{v}, \boldsymbol{s}, \boldsymbol{z})(\boldsymbol{\eta}, \boldsymbol{\psi}, \boldsymbol{\nu}) = 0. \tag{9.4}$$

The triple $\{\boldsymbol{v}, \boldsymbol{s}, \boldsymbol{z}\} \in \mathcal{V} \times \mathcal{S} \times \mathcal{V}$ is determined by the saddle-point problem

$$\left\{ \begin{array}{l} L'_v(\boldsymbol{v}, \boldsymbol{s}, \boldsymbol{z})(\boldsymbol{\eta}) \\ L'_s(\boldsymbol{v}, \boldsymbol{s}, \boldsymbol{z})(\boldsymbol{\psi}) \\ L'_z(\boldsymbol{v}, \boldsymbol{s}, \boldsymbol{z})(\boldsymbol{\nu}) \end{array} \right\} = \left\{ \begin{array}{l} I'_v(\boldsymbol{v}, \boldsymbol{s}; \boldsymbol{\eta}) + R'_v(\boldsymbol{v}, \boldsymbol{s}; \boldsymbol{z}, \boldsymbol{\eta}) \\ I'_s(\boldsymbol{v}, \boldsymbol{s}; \boldsymbol{\psi}) + R'_s(\boldsymbol{v}, \boldsymbol{s}; \boldsymbol{z}, \boldsymbol{\psi}) \\ R(\boldsymbol{v}, \boldsymbol{s}; \boldsymbol{\nu}) \end{array} \right\} = \boldsymbol{0} \tag{9.5}$$

for all $\{\boldsymbol{\eta}, \boldsymbol{\psi}, \boldsymbol{\nu}\} \in \mathcal{V} \times \mathcal{S} \times \mathcal{V}$. Here, I'_v, I'_s, R'_v, R'_s are the partial variations of the objective functional I and the primal physical residual R with respect to $\boldsymbol{v}$ and $\boldsymbol{s}$. The last equation of

(9.5) is simply the variational problem (9.2) for the state $\boldsymbol{v}$. Using the notation from Chapter 4 with $R'_v(\cdot,\cdot) = k(\cdot,\cdot)$ and $R'_s(\cdot,\cdot) = p(\cdot,\cdot)$ the problem becomes

$$\left\{ \begin{array}{l} I'_v(\boldsymbol{v},\boldsymbol{s};\boldsymbol{\eta}) + k(\boldsymbol{v},\boldsymbol{s};\boldsymbol{z},\boldsymbol{\eta}) \\ I'_s(\boldsymbol{v},\boldsymbol{s};\boldsymbol{\psi}) + p(\boldsymbol{v},\boldsymbol{s};\boldsymbol{z},\boldsymbol{\psi}) \\ R(\boldsymbol{v},\boldsymbol{s};\boldsymbol{\nu}) \end{array} \right\} = \boldsymbol{0} \quad \forall \{\boldsymbol{\eta},\boldsymbol{\psi},\boldsymbol{\nu}\} \in \mathcal{V}\times\mathcal{S}\times\mathcal{V}. \tag{9.6}$$

Remark 9.1 (Dual or adjoint problem) *Eq. 9.5$_1$ is the* dual *or* adjoint problem *corresponding to the solution $\boldsymbol{v} \in \mathcal{V}$ at the current linearization point, i.e. $\boldsymbol{z} \in \mathcal{V}$ is the solution of*

$$k(\boldsymbol{v},\boldsymbol{s};\boldsymbol{z},\boldsymbol{\eta}) = -I'_v(\boldsymbol{v},\boldsymbol{s};\boldsymbol{\eta}) \qquad \forall\, \boldsymbol{\eta} \in \mathcal{V}. \tag{9.7}$$

The bilinear form $k(\boldsymbol{v},\boldsymbol{s};\boldsymbol{z},\boldsymbol{\eta}) = R'_v(\boldsymbol{v},\boldsymbol{s};\boldsymbol{z},\boldsymbol{\eta})$ is the tangent physical stiffness operator at the current linearization point $\boldsymbol{v}$ defined in (4.87).

9.2.2 The energy functional as objective function

The objective function I of the optimization problem (9.1) is arbitrary and depends on the particular application. In many engineering applications, the energy functional of the problem is used as the objective functional, because there is a relation between the overall minimization of the energy and the maximization of the stiffness.

For the particular choice of $I(\boldsymbol{v},\boldsymbol{s}) = E(\boldsymbol{v},\boldsymbol{s})$ we have for a given solution $\boldsymbol{v} \in \mathcal{V}$

$$I'_v(\boldsymbol{v},\boldsymbol{s};\boldsymbol{\eta}) = E'_v(\boldsymbol{v},\boldsymbol{s};\boldsymbol{\eta}) = R(\boldsymbol{v},\boldsymbol{s};\boldsymbol{\eta}) = 0 \quad \forall\, \boldsymbol{\eta} \in \mathcal{V}. \tag{9.8}$$

Therefore, the dual solution $\boldsymbol{z}$ becomes zero in (9.7) as well as the Lagrangian (9.3) remains $L(\boldsymbol{v},\boldsymbol{s}) = I(\boldsymbol{v},\boldsymbol{s}) = E(\boldsymbol{v},\boldsymbol{s})$. Hence, the optimality condition (9.5) is reduced to the optimality condition of the primal physical problem (4.6), i.e.

$$\left\{ \begin{array}{l} E'_v(\boldsymbol{v},\boldsymbol{s})(\boldsymbol{\eta}) \\ E'_s(\boldsymbol{v},\boldsymbol{s})(\boldsymbol{\psi}) \end{array} \right\} = \left\{ \begin{array}{l} R(\boldsymbol{v},\boldsymbol{s};\boldsymbol{\eta}) \\ G(\boldsymbol{v},\boldsymbol{s};\boldsymbol{\psi}) \end{array} \right\} = \boldsymbol{0} \qquad \forall\, \{\boldsymbol{\eta},\boldsymbol{\psi}\} \in \mathcal{V}\times\mathcal{S}. \tag{9.9}$$

The partial variations of $I = E$ with respect to $\boldsymbol{v}$ and $\boldsymbol{s}$ yield the primal physical and material residuals defined in (4.7) and (4.8), respectively.

9.3 The minimum compliance problem

The model problem of linearized elasticity is considered and its formulation is given in Section B.2. Let

$$C(\boldsymbol{u}) = \int_{\Omega_R} W_R \,\mathrm{d}\Omega = \frac{1}{2}\, a(\boldsymbol{u},\boldsymbol{u}) \tag{9.10}$$

be the internal energy of the structure and $F(\boldsymbol{u})$ a linear functional associated with the external energy. The overall energy of this problem can be written in the form

$$\begin{aligned} E(\boldsymbol{u}) &= \int_{\Omega_R} W_R \, \mathrm{d}\Omega - F(\boldsymbol{u}) = \frac{1}{2}\, a(\boldsymbol{u},\boldsymbol{u}) - F(\boldsymbol{u}) = -\frac{1}{2}\, F(\boldsymbol{u}) \\ &= -\int_{\Omega_R} W_R \, \mathrm{d}\Omega = -\frac{1}{2}\, a(\boldsymbol{u},\boldsymbol{u}) = -C(\boldsymbol{u}), \end{aligned} \tag{9.11}$$

where the equilibrium equation $a(\boldsymbol{u},\boldsymbol{\eta}) = F(\boldsymbol{\eta}) \;\; \forall\, \boldsymbol{\eta} \in \mathcal{V}$ has been used.

Assume the overall potential energy as a measure for the mean structural stiffness S, i.e. $S = E$. Note, that $S = -C$, i.e. the internal energy can be assumed as a measure for the mean structural compliance. The maximization of the stiffness S is equivalent to the minimization of the compliance C.

The goal is now to find the optimal design for which the structure attains a minimum of mean elastic compliance among the structures of constant volume V_0 or material cost. We use a staggered solution algorithm and we formulate the optimization problem only in terms of the design. This ends in the following problem.

Problem 9.2 (Minimum of mean elastic compliance) *Find $\boldsymbol{s} \in \mathcal{S}$ such that the internal energy $C(\boldsymbol{u}(\boldsymbol{s}),\boldsymbol{s})$ is minimized, i.e.*

$$I(\boldsymbol{s}) = \min_{\boldsymbol{r}\in\mathcal{S}} C(\boldsymbol{u}(\boldsymbol{r}),\boldsymbol{r}) \tag{9.12}$$

subject to the constraints

$$R(\boldsymbol{u},\boldsymbol{s};\boldsymbol{\eta}) = 0 \quad \forall\, \boldsymbol{\eta} \in \mathcal{V} \tag{9.13}$$

$$V - V_0 = 0\,. \tag{9.14}$$

From the above stated definitions, it turns out that the variation of the objective functional, i.e. the variation of the internal energy with respect to $\boldsymbol{s}$ is the negative material residual G, which is defined as the variation of the overall energy E with respect to $\boldsymbol{s}$, i.e.

$$E'_s = G(\boldsymbol{u},\boldsymbol{s};\boldsymbol{\psi}) \tag{9.15}$$

$$C'_s = -E'_s = -G(\boldsymbol{u},\boldsymbol{s};\boldsymbol{\psi})\,. \tag{9.16}$$

Hence, the gradients which are used in the shape optimization process contain the negative configurational or material forces or material residual G. The negative gradients are the search directions within a simple gradient based method in order to find a decrease in the objective functional. This means in the context of shape optimization that the negative gradients on the design boundaries represents the search directions. Finally, the negative material residual can be interpreted as an indicator in which direction the boundary has to move in order to minimize the internal energy or to maximize the structural stiffness.

Remark 9.2 (Alternative formulation) *In topology optimization the compliance minimization problem is often written in an equivalent form in terms of the potential $F(\boldsymbol{u})$, i.e. $F(\boldsymbol{u})$ is minimized in (9.12), see e.g. [14]. The internal energy $C(\boldsymbol{u})$ and $F(\boldsymbol{u})$ are related by a constant factor, i.e.*

$$F(\boldsymbol{u}) = 2\, C(\boldsymbol{u}). \tag{9.17}$$

9.4 Design velocity fields

The *design velocity field* in the language of structural optimization corresponds to the 'displacement' in the material space. An initial domain $\Omega_R(s)$ is perturbed to a domain Ω_s by using a (time-like) design parametrization s, which parameterizes in an abstract sense the material body in the reference configuration, see Section 3.1.2. This change in the shape can be expressed by the mapping $\boldsymbol{T} : \boldsymbol{X} \to \boldsymbol{X}_s(\boldsymbol{X}),\ \boldsymbol{X} \in \Omega_R$, where $\boldsymbol{X}_s$ is the material point in the perturbed domain. By thinking of s as a time-like design parametrization, a design velocity field $\boldsymbol{V}$ can be defined as

$$\boldsymbol{V}(\boldsymbol{X}_s, s) = \frac{d\boldsymbol{X}_s}{ds} = \frac{d\boldsymbol{T}(\boldsymbol{X}, s)}{ds} = \frac{\partial \boldsymbol{T}(\boldsymbol{X}, s)}{\partial s}\,. \tag{9.18}$$

If we assume regularity in the neighborhood of the initial design $s = 0$, we have around the initial mapping point $\boldsymbol{T}(\boldsymbol{X}, 0)$ the Taylor expansion

$$\boldsymbol{T}(\boldsymbol{X}, s) = \boldsymbol{T}(\boldsymbol{X}, 0) + s\, \frac{\partial \boldsymbol{T}(\boldsymbol{X}, 0)}{\partial s} + \mathcal{O}. \tag{9.19}$$

Finally, with $\boldsymbol{T}(\boldsymbol{X}, 0) = \boldsymbol{X}$ and by ignoring high-order terms $\mathcal{O}$, we obtain the relation

$$\boldsymbol{X}_s = \boldsymbol{X} + s\, \boldsymbol{V}(\boldsymbol{X}). \tag{9.20}$$

The design velocity field characterizes the direction of domain variation. For a given $\boldsymbol{V}$, the change of the domain is uniquely controlled by the scalar parameter s. For more details see e.g. [27, 28] and the references therein.

For a geometry model representation of the domain, this field is generated by a variation of the underlying geometry mappings, i.e. the Bézier representation of patches describing the geometry of the structure, respectively. In the continuum domain, the velocity fields associate the geometry parametrization to the movement of material points. In the discrete case, this is the association between the geometry parametrization and the movement of mesh nodes.

We consider a vector of design variables $\boldsymbol{p} \in \mathbb{R}^m$, which parameterize the shape of the current domain Ω_R. Within this chapter the design variables p_i are control points of Bézier curves. The design velocity field corresponding to the design variable p_i is given by

$$\boldsymbol{V}_i(\boldsymbol{X}) = \frac{\partial \boldsymbol{X}}{\partial p_i}\,. \tag{9.21}$$

In the context of the finite element method, the design velocity field $\boldsymbol{V}_i(\boldsymbol{X})$ characterizes the changes of the finite element nodal point coordinates $\boldsymbol{X}$ with respect to the changes of arbitrary design parameter p_i. Examples for such design velocity fields are given in Example 9.5.2 in Figure 9.7a and 9.7b, respectively.

Furthermore, the velocity fields are also important and fundamental in the context of mesh updating and smoothing. Let $\boldsymbol{X}$ be the vector of nodal coordinates, then the new shape $\boldsymbol{X}_s$ is obtained from

$$\boldsymbol{X}_s = \boldsymbol{X}(\boldsymbol{p}) + \varepsilon \Delta \boldsymbol{X}(\boldsymbol{p}, \Delta \boldsymbol{p}) \tag{9.22}$$

with

$$\Delta \boldsymbol{X}(\boldsymbol{p}, \Delta \boldsymbol{p}) = \frac{\partial \boldsymbol{X}}{\partial \boldsymbol{p}} \Delta \boldsymbol{p} = \sum_{i=1}^{m} \frac{\partial \boldsymbol{X}}{\partial p_i} \Delta p_i = \sum_{i=1}^{m} \boldsymbol{V}_i \, \Delta p_i \, . \tag{9.23}$$

Here, $\boldsymbol{V}_i$ is the discrete design velocity field corresponding to the design parameter p_i. Furthermore, ε is a step size parameter, which controls the decrease in the objective and the mesh distortion as well as $\Delta \boldsymbol{p}$ is the increment of the design variables obtained from the solution at the current iteration.

The design velocity field can be multiplied with the vector field of energy variation, i.e. the material residual or configurational forces $\boldsymbol{G}$, to build up the sensitivity of the objective (the energy) with respect to a variation of the design variable p_i, i.e.

$$E'_{p_i} = \boldsymbol{G}^T \delta \boldsymbol{X}_i = \boldsymbol{G}^T \frac{\partial \boldsymbol{X}}{\partial p_i} \, \delta p_i = \boldsymbol{G}^T \boldsymbol{V}_i \, \delta p_i \, . \tag{9.24}$$

Hence, the design velocity fields connect the variation in the geometrical design variable p_i with the variation in the objective functional.

9.5 Numerical examples

9.5.1 Cantilever beam

System and model problem. As a first simple example from shape optimization the well-known cantilever beam problem is considered. The cantilever is clamped on the left side and loaded by a point load $f_0 = 5$ at $(L, 0)$, see Fig. 9.1. The initial design consists of the rectangular domain with dimensions of $L = 4$ and $H = 2$, respectively.

The model problem of linearized elasticity is considered, see Appendix B.2. The cantilever is modeled with the plane strain condition with $E = 1000$ and $\nu = 0.3$. A regular finite element mesh with overall 16 by 8 elements is chosen to guarantee visibility of the meshes in all pictures.

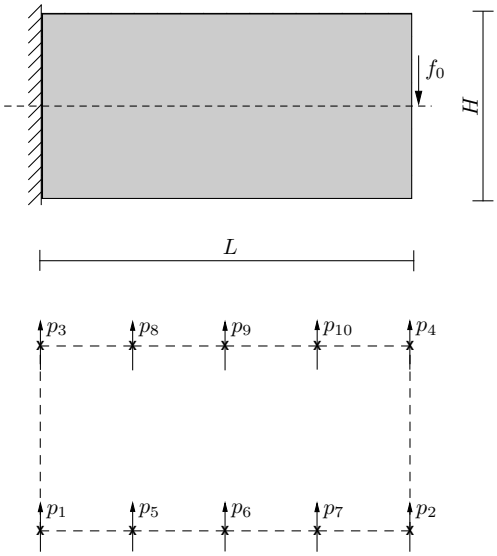

Figure 9.1: System of the cantilever and geometry model with 10 design variables p_i in vertical direction. The lower and upper boundaries are modeled with Bézier curves with three internal control points (p_5–p_{10}).

The optimization problem and the design variables. The optimization task is to generate the most efficient material distribution with respect to the overall stiffness of the structure. The nonlinear programming problem consists of the objective function (internal elastic energy), the constraint function (constant volume) and the geometrical design variables, i.e. Problem 9.2 has to be solved.

Here, the lower and upper boundaries of the structure are modeled using Bézier curves with three internal control points which are equally distributed over the length of the structure. Including the corner points, overall 10 vertical coordinates are design variables p_i, see Fig. 9.1. The design variables p_i are bounded by upper p_o and lower p_u side constraints

$$-10 = p_u \leq p_i \leq p_o = -0.25 \quad \forall\, i = \{1, 2, 5, 6, 7\}$$

$$0.25 = p_u \leq p_i \leq p_o = 10 \qquad \forall\, i = \{3, 4, 8, 9, 10\}\,.$$

Results of the shape optimization. The optimum was attained within 19 iterations. The initial and final solutions as well as some selected iterations are shown in Fig. 9.2.

The optimal shape leads to a uniform distribution of the material residual on the design boundary. The norm of the material residual $\boldsymbol{G}$ on the design variables $\boldsymbol{p}$ decreases from

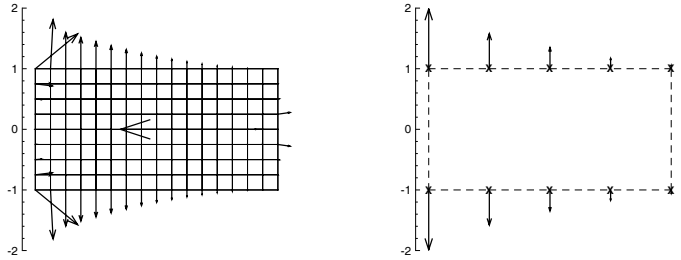

(a) $i = 0$ $C(\boldsymbol{u}_h) = 0.437534$ $||\boldsymbol{G}(\boldsymbol{p})|| = 0.450822$

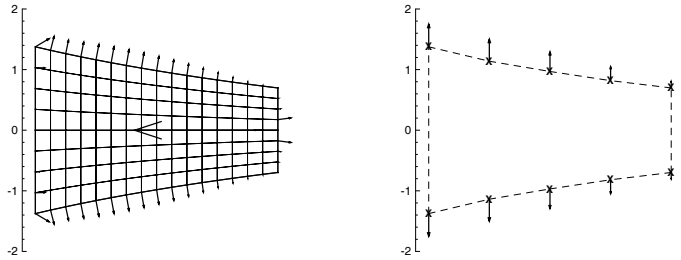

(b) $i = 2$ $C(\boldsymbol{u}_h) = 0.319063$ $||\boldsymbol{G}(\boldsymbol{p})|| = 0.248540$

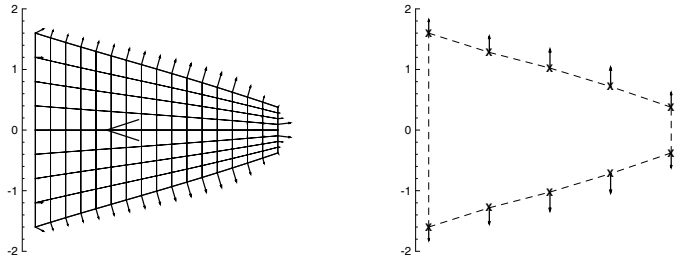

(c) $i = 5$ $C(\boldsymbol{u}_h) = 0.293381$ $||\boldsymbol{G}(\boldsymbol{p})|| = 0.231787$

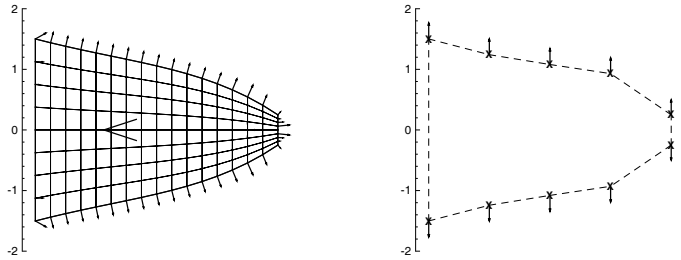

(d) $i = 19$ $C(\boldsymbol{u}_h) = 0.286983$ $||\boldsymbol{G}(\boldsymbol{p})|| = 0.217522$

Figure 9.2: Distribution of the material residuals on the mesh nodes $\boldsymbol{G}(\boldsymbol{X})$ (left side) and design variables $\boldsymbol{G}(\boldsymbol{p})$ (control points of the Bézier curves) (right side) during the optimization progress, (a) initial shape (d) final shape

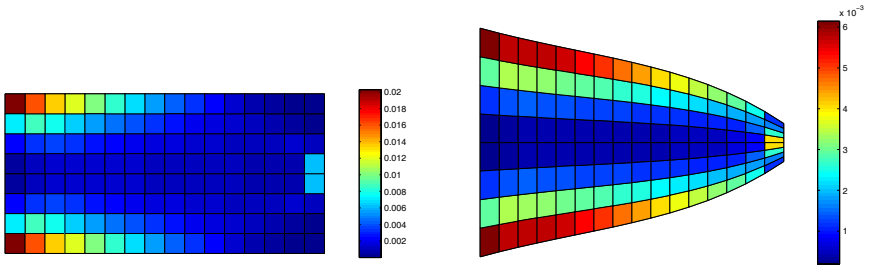

(a) initial design (b) optimal design

Figure 9.3: Distribution of the internal energy

0.4508 to 0.2175, i.e. a reduction of $51.8\,\%$. The internal energy $C(\boldsymbol{u}_h)$ decreases from 0.4375 to 0.2869, i.e. a reduction of $34.4\,\%$.

The distribution of the internal energy for the initial and optimized design is shown in Fig. 9.3. The energy distribution of the optimized shape is more smooth in comparison to the initial shape.

9.5.2 L-shape

System and model problem. We consider as a more complex example from shape optimization a L-shaped cantilever problem, see Fig. 9.4. The nonlinear programming problem under consideration consists of the objective function (internal elastic energy), the constraint function (constant volume) and the geometrical design variables, i.e. we solve Problem 9.2.

The L-shape consists of three geometry patches as indicated in Fig. 9.4. The boundaries of the patches are modeled using Bézier curves each with three internal control points. We consider only the lower and right boundary of the L-shape as design boundary and keep the loaded boundary fixed. Including the corner points, overall 14 coordinates of the control points are design variables p_i. The L-shape is modeled with the plane strain condition with $E = 10^5$ and $\nu = 0.3$ and loaded by line loads $t_x = t_y = 5$.

Results of the shape optimization. The initial and final solutions as well as a selected iteration are shown in Fig. 9.6. The optimal shape is obtained, if the material residual $\boldsymbol{G}(\boldsymbol{X})$ is uniformly distributed over the design boundary, see Fig. 9.6 (c). The optimal solution was attained within 37 iterations. The norm of the material residual $\boldsymbol{G}(\boldsymbol{p})$ on the design variables decreases from 0.4009 to 0.1911, i.e. a reduction of $52\,\%$.

The design variables p_2 and p_3 connect two geometry patches, respectively. Therefore, they have a large influence domain, i.e. small variations result in large changes in the geometry

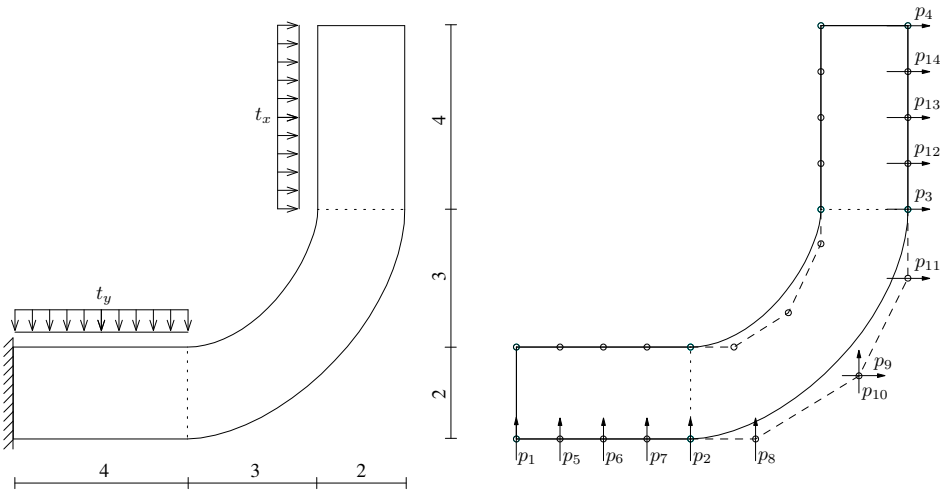

Figure 9.4: L-shape: system (left) and geometry model with 14 design variables p_i (right)

and hence in the internal energy. This is indicated by large material residuals $\boldsymbol{G}(p_i)$ on these design variables, see Fig. 9.6.

The internal energy $C(\boldsymbol{u}_h)$ decreases from 0.9015 to 0.5409, i.e. a reduction of $40\,\%$. The distribution of the energy of the optimized shape is once again more smooth in comparison to the initial shape, see Fig. 9.5.

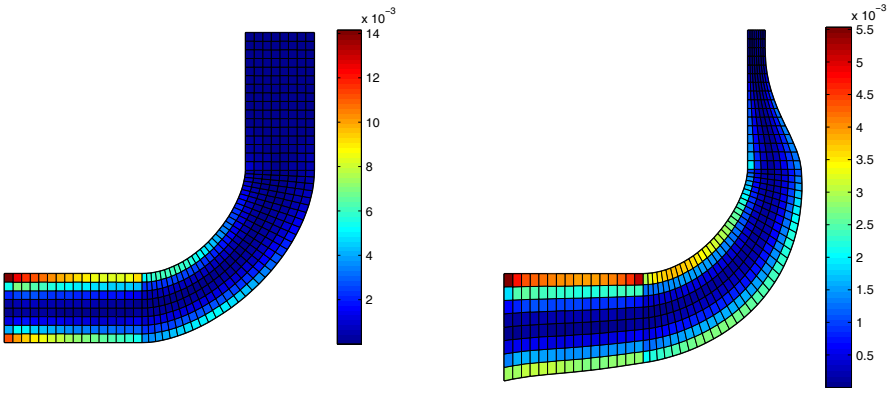

(a) initial design (b) optimized design

Figure 9.5: Distribution of the internal energy

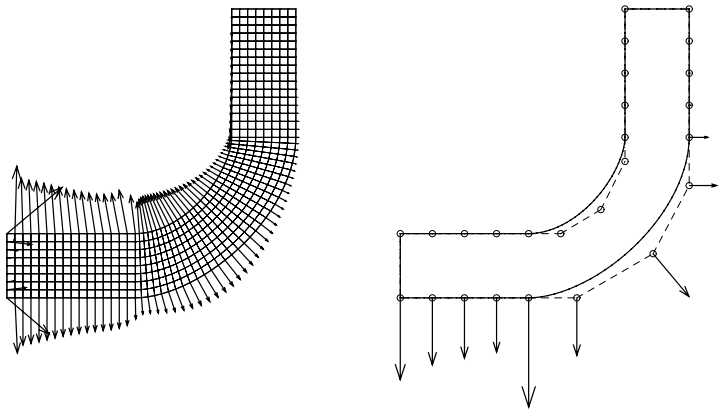

(a) $i = 0$ $C(\boldsymbol{u}_h) = 0.9015$ $||\boldsymbol{G}(\boldsymbol{p})|| = 0.4009$

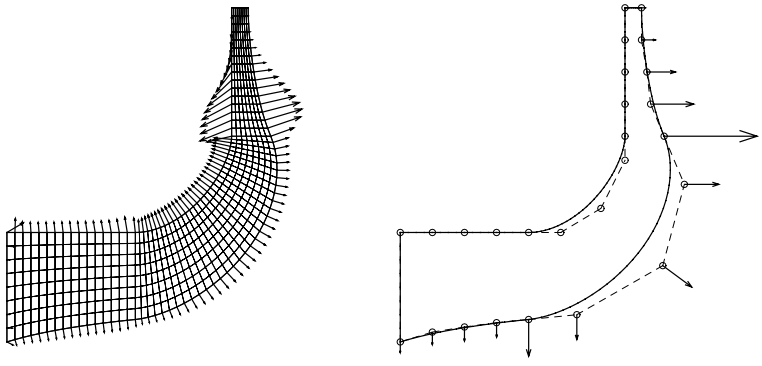

(b) $i = 6$ $C(\boldsymbol{u}_h) = 0.5698$ $||\boldsymbol{G}(\boldsymbol{p})|| = 0.2684$

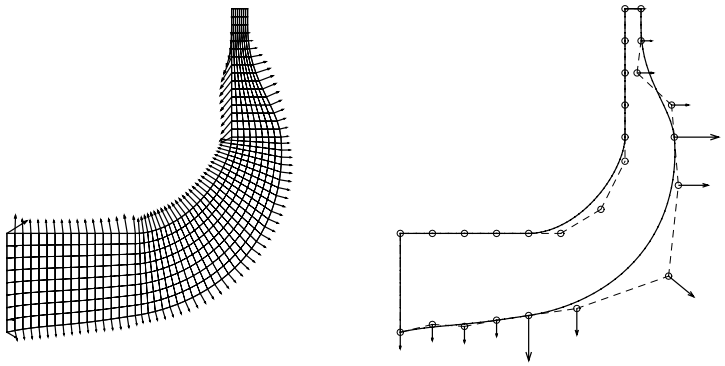

(c) $i = 37$ $C(\boldsymbol{u}_h) = 0.5409$ $||\boldsymbol{G}(\boldsymbol{p})|| = 0.1911$

Figure 9.6: Distribution of the material residuals on the mesh nodes $\boldsymbol{G}(\boldsymbol{X})$ (left side) and design variables $\boldsymbol{G}(\boldsymbol{p})$ (control points of the Bézier curves) (right side) during the optimization progress, (a) initial shape, (b) iteration 6, (c) final shape

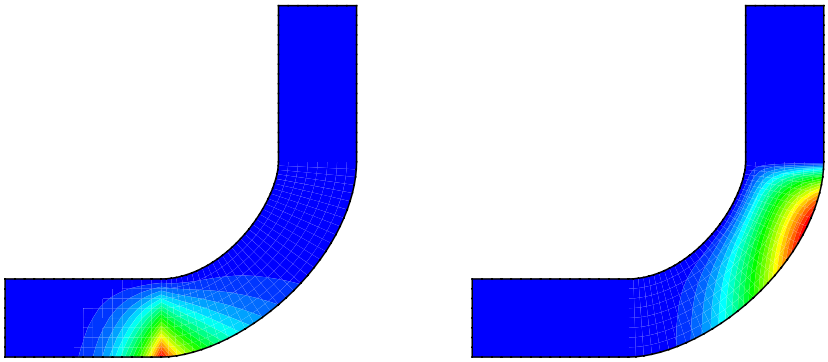

(a) Field $\boldsymbol{V}_2$ corresponding to p_2 (b) Field $\boldsymbol{V}_{11}$ corresponding to p_{11}

Figure 9.7: Design velocity fields $\boldsymbol{V}_i$ for p_2 (a) and p_{11} (b)

Design velocity fields. As mentioned in Section 9.4, the design velocity field $\boldsymbol{V}_i(\boldsymbol{X})$ characterizes the changes of the finite element nodal point coordinates $\boldsymbol{X}$ with respect to the changes of arbitrary design parameter p_i. For example, a variation of the vertical position of the design variables p_2 and p_{11} of the design boundary of the L-shape generate the fields shown in Figure 9.7a and 9.7b, respectively. Hence, these fields reflect the influence domains of the design variations.

Distribution of the material residual. It is interesting to note, that for the compliance or internal energy optimization problem, the material residual G on the design boundary is the indicator in which direction the boundary has to move in order to minimize the internal energy. The optimal shape is obtained, if the material residual is uniformly distributed over the design boundary, see Fig. 9.2d and Fig. 9.6c, respectively.

The material residual on the boundary does not vanish, because there is still an ambition to find a state with lower internal energy, i.e. a more stiffer structure. The side constraints for the design variables and the volume constraint avoid this movement.

Chapter 10

Error analysis and improvement of sensitivity relations

This chapter is concerned with error analysis and improvement of first-order sensitivity relations for the state and quantities of interest. At first, novel exact sensitivity and error relations are presented. Based on the exact sensitivity relations an improvement algorithm is proposed. The improved design sensitivities are used to estimate the error between the exact change in the state due to design perturbations and the changes in the state obtained from a classical first-order sensitivity relation.

10.1 Introduction

The reliability and accuracy of design sensitivities is an important question within sensitivity analysis. For numerically obtained design sensitivities, such as *finite difference methods*, this has been widely studied in the literature, see e.g. [104] for a compressive overview with many references.

Within this work a variational approach is used in order to obtain the design sensitivities. Variational methods are known since several decades, see e.g. [27, 28] and the references therein. But as far as the author knows, the following approach for error analysis and improvement of variational sensitivity relations has not been studied before. Here, only the error in the design sensitivity is studied. Other errors such as the discretization error as well as the combined sensitivity and discretization error are addressed to future work.

Variational sensitivity relations for the state $\boldsymbol{v}$ and a chosen quantity of interest $J(\boldsymbol{v}, \boldsymbol{s})$ have been introduced in Section 4.3.2 and Section 6.3.4, respectively. These relations are based on an invariant requirement of the physical residual $R(\boldsymbol{v}, \boldsymbol{s}; \boldsymbol{\eta})$. This means that for a fixed initial design $\boldsymbol{s}_0$ and a given initial solution $\boldsymbol{v}_0 \in \mathcal{V}$ the residual vanishes, i.e.

$$R(\boldsymbol{v}_0, \boldsymbol{s}_0; \boldsymbol{\eta}) = 0 \qquad \forall\, \boldsymbol{\eta} \in \mathcal{V}.$$

Furthermore, also the total variation has to be zero, i.e.

$$\delta R = \delta_v R(\boldsymbol{v}_0, \boldsymbol{s}_0; \boldsymbol{\eta}, \delta\boldsymbol{v}) + \delta_s R(\boldsymbol{v}_0, \boldsymbol{s}_0; \boldsymbol{\eta}, \delta\boldsymbol{s}) = 0.$$

From this, the sensitivity relation for the state has been derived in (4.21) in form of

$$\delta_v R(\boldsymbol{v}_0, \boldsymbol{s}_0; \boldsymbol{\eta}, \delta\boldsymbol{v}) = -\delta_s R(\boldsymbol{v}_0, \boldsymbol{s}_0; \boldsymbol{\eta}, \delta\hat{\boldsymbol{s}}) \tag{10.1}$$

or

$$k(\boldsymbol{v}_0, \boldsymbol{s}_0; \boldsymbol{\eta}, \delta\boldsymbol{v}) = -Q(\boldsymbol{v}_0, \boldsymbol{s}_0; \boldsymbol{\eta}), \tag{10.2}$$

where $k(\boldsymbol{v}_0, \boldsymbol{s}_0; \boldsymbol{\eta}, \delta\boldsymbol{v}) = \delta_v R(\boldsymbol{v}_0, \boldsymbol{s}_0; \boldsymbol{\eta}, \delta\boldsymbol{v})$ is the tangent stiffness operator (4.87) and

$$Q(\boldsymbol{v}_0, \boldsymbol{s}_0; \boldsymbol{\eta}) = p(\boldsymbol{v}_0, \boldsymbol{s}_0; \boldsymbol{\eta}, \delta\hat{\boldsymbol{s}}) = \delta_s R(\boldsymbol{v}_0, \boldsymbol{s}_0; \boldsymbol{\eta}, \delta\hat{\boldsymbol{s}}) \tag{10.3}$$

is the pseudo load for a given fixed design variation $\delta\hat{\boldsymbol{s}}$. Furthermore, a sensitivity relation for a chosen quantity of interest can be obtained from the above relation. This has been given in (6.27) and reads

$$J'_v(\boldsymbol{v}_0, \boldsymbol{s}_0; \delta\boldsymbol{v}) = -Q(\boldsymbol{v}_0, \boldsymbol{s}_0; \boldsymbol{z}_0), \tag{10.4}$$

where $\boldsymbol{z}_0$ denotes the dual solution corresponding to the quantity of interest obtained on the initial design $\boldsymbol{s}_0$.

It is important to note that these relations are valid only for infinitesimal variations $\delta\boldsymbol{v}$ and $\delta\boldsymbol{s}$. In practical computations the changes in the design have a finite value, i.e. design increments $\Delta\boldsymbol{s}$ and state increments $\Delta\boldsymbol{v}$ are considered. Let $\Delta\boldsymbol{v} \in \mathcal{V}$ be the exact change in the state due to the design change $\Delta\boldsymbol{s}$. The pseudo load $Q(\boldsymbol{v}_0, \boldsymbol{s}_0; \cdot)$ is therefore computed for a given design increment $\Delta\hat{\boldsymbol{s}}$, i.e.

$$Q(\boldsymbol{v}_0, \boldsymbol{s}_0; \boldsymbol{\eta}) = p(\boldsymbol{v}_0, \boldsymbol{s}_0; \boldsymbol{\eta}, \Delta\hat{\boldsymbol{s}}) = \delta_s R(\boldsymbol{v}_0, \boldsymbol{s}_0; \boldsymbol{\eta}, \Delta\hat{\boldsymbol{s}}). \tag{10.5}$$

Then, in the general case, the relations (10.2) and (10.4) are not fulfilled, i.e.

$$k(\boldsymbol{v}_0, \boldsymbol{s}_0; \boldsymbol{\eta}, \Delta\boldsymbol{v}) \approx -Q(\boldsymbol{v}_0, \boldsymbol{s}_0; \boldsymbol{\eta}) \quad \text{and} \quad J'_v(\boldsymbol{v}_0, \boldsymbol{s}_0; \Delta\boldsymbol{v}) \approx -Q(\boldsymbol{v}_0, \boldsymbol{s}_0; \boldsymbol{z}_0). \tag{10.6}$$

Hence, only an approximation for the change in the state $\Delta\tilde{\boldsymbol{v}}$ and a quantity of interest $J'_v(\boldsymbol{v}_0, \boldsymbol{s}_0; \Delta\tilde{\boldsymbol{v}})$ due to changes $\Delta\boldsymbol{s}$ are obtained by solving (10.2) and (10.4), i.e.

$$k(\boldsymbol{v}_0, \boldsymbol{s}_0; \boldsymbol{\eta}, \Delta\tilde{\boldsymbol{v}}) = -Q(\boldsymbol{v}_0, \boldsymbol{s}_0; \boldsymbol{\eta}) \tag{10.7}$$

and

$$J'_v(\boldsymbol{v}_0, \boldsymbol{s}_0; \Delta\tilde{\boldsymbol{v}}) = -Q(\boldsymbol{v}_0, \boldsymbol{s}_0; \boldsymbol{z}_0). \tag{10.8}$$

Therefore, the goal is now to study the error

$$\boldsymbol{e}_{\Delta v} := \Delta\boldsymbol{v} - \Delta\tilde{\boldsymbol{v}}, \tag{10.9}$$

i.e. the distance between the exact change in the state $\Delta\boldsymbol{v}$ and the approximative change $\Delta\tilde{\boldsymbol{v}}$ obtained from the sensitivity relation (10.7). This is illustrated in Fig. 10.1, which shows the increments and the error for a one-dimensional problem.

To do this, first an exact representation of the sensitivity relation is derived.

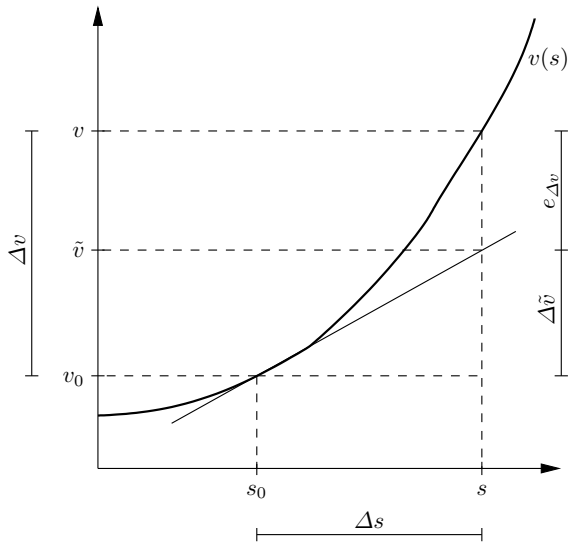

error in the change of the state:

$$e_{\Delta v} = v - \tilde{v} = \Delta v - \Delta\tilde{v}$$

first-order sensitivity relation:

$$\Delta\tilde{v} = -K^{-1}\,[\partial R/\partial s]\,\Delta s = -K^{-1}\,P\,\Delta s = -K^{-1}\,Q$$

Figure 10.1: One-dimensional illustration of the first-order increment $\Delta\tilde{\boldsymbol{v}}$ and the error in the increment $\boldsymbol{e}_{\Delta v} = \Delta\boldsymbol{v} - \Delta\tilde{\boldsymbol{v}}$.

10.2 An exact sensitivity relation and error analysis for the state

10.2.1 Taylor expansion with an exact integral remainder

In this section an exact sensitivity relation for the state is proposed. This is based on well-known Taylor expansions with exact integral remainders, see e.g. [30]. Such Taylor expansions are also used within error estimation techniques for discretization and model errors, see for instance [12, 18, 84].

The Taylor expansions are exemplary shown for a one-dimensional function. Let $f(x)$ be an arbitrary nonlinear function with an independent variable x. Furthermore, let x_0 be some initial value and Δx be a given increment. Then, the changed function value of $f(x_0)$ due to Δx is given as

$$f(x_0 + \Delta x) = f(x_0) + \Delta f(x_0; \Delta x)$$

The exact increment

$$\Delta f(x_0; \Delta x) := f(x_0 + \Delta x) - f(x_0) \tag{10.10}$$

is a nonlinear function and can be expressed using different Taylor expansions with integral remainders. In particular, we have

$$\Delta f(x_0;\Delta x) = r_x^1(x_0;\Delta x) \tag{10.11}$$

$$= f_x'(x_0;\Delta x) + r_x^2(x_0;\Delta x) \tag{10.12}$$

$$= \frac{1}{2}\, f_x'(x_0;\Delta x) + \frac{1}{2}\, f_x'(x_0+\Delta x;\Delta x) + \frac{1}{2}\, r_x^3(x_0;\Delta x) \tag{10.13}$$

with the exact remainders

$$r_x^1(x_0;\Delta x) := \int_0^1 f_x'(x_0+\lambda\Delta x;\Delta x)\, d\lambda \tag{10.14}$$

$$r_x^2(x_0;\Delta x) := \int_0^1 f_{xx}''(x_0+\lambda\Delta x;\Delta x,\Delta x)\,(1-\lambda)\, d\lambda \tag{10.15}$$

$$r_x^3(x_0;\Delta x) := \int_0^1 f_{xxx}'''(x_0+\lambda\Delta x;\Delta x,\Delta x,\Delta x)\,\lambda(\lambda-1)\, d\lambda. \tag{10.16}$$

These relations are exact if the remainders are computable and can easily be verified for arbitrary continuously differentiable functions. A one-dimensional illustration of the first-order approximation $f_x'(x_0;\Delta x)$ and the corresponding remainder $r_x^2(x_0;\Delta x)$ is given in Fig. 10.2. The extension to general functionals and semilinear forms is straightforward and used within the following sections.

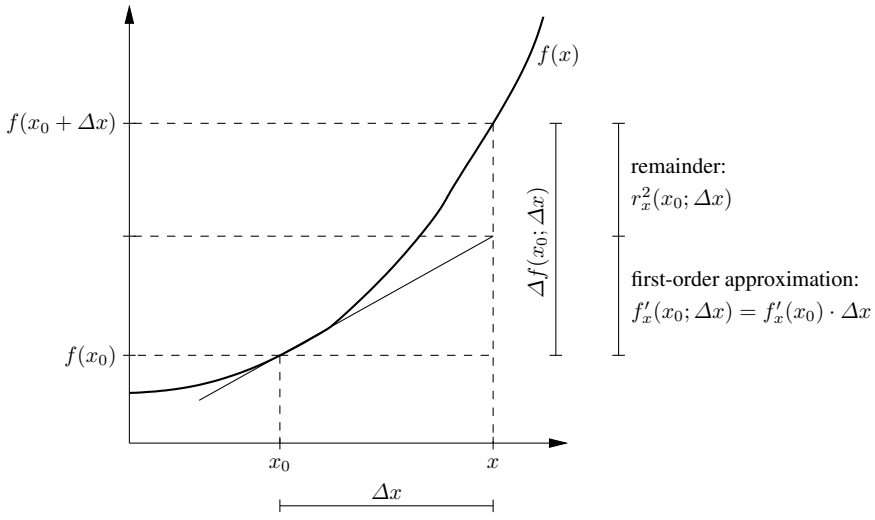

Figure 10.2: One-dimensional illustration of the first-order approximation and the remainder.

10.2.2 An exact sensitivity relation

Let $\boldsymbol{v}_0 \in \mathcal{V}$ be the solution of the initial problem with a given initial design $\boldsymbol{s}_0 \in \mathcal{S}$. Furthermore, let $\boldsymbol{v} \in \mathcal{V}$ be the solution for the changed design $\boldsymbol{s} = \boldsymbol{s}_0 + \Delta\boldsymbol{s} \in \mathcal{S}$. Then, both problems are given as

$$R(\boldsymbol{v}_0, \boldsymbol{s}_0; \boldsymbol{\eta}) = 0 \quad \forall\, \boldsymbol{\eta} \in \mathcal{V} \qquad \text{initial design } \boldsymbol{s}_0 \tag{10.17}$$

$$R(\boldsymbol{v}, \boldsymbol{s}; \boldsymbol{\eta}) \quad = 0 \quad \forall\, \boldsymbol{\eta} \in \mathcal{V} \qquad \text{changed design } \boldsymbol{s} = \boldsymbol{s}_0 + \Delta\boldsymbol{s}. \tag{10.18}$$

In the general case, the residuals depend nonlinear on $\boldsymbol{v}$ and $\boldsymbol{s}$ and we have

$$R(\boldsymbol{v}, \boldsymbol{s}; \boldsymbol{\eta}) = R(\boldsymbol{v}_0 + \Delta\boldsymbol{v}, \boldsymbol{s}; \boldsymbol{\eta}) \neq R(\boldsymbol{v}_0, \boldsymbol{s}; \boldsymbol{\eta}) + R(\Delta\boldsymbol{v}, \boldsymbol{s}; \boldsymbol{\eta}), \tag{10.19}$$

$$R(\boldsymbol{v}, \boldsymbol{s}; \boldsymbol{\eta}) = R(\boldsymbol{v}, \boldsymbol{s}_0 + \Delta\boldsymbol{s}; \boldsymbol{\eta}) \neq R(\boldsymbol{v}, \boldsymbol{s}_0; \boldsymbol{\eta}) + R(\boldsymbol{v}, \Delta\boldsymbol{s}; \boldsymbol{\eta}). \tag{10.20}$$

Using a Taylor expansion with an exact integral remainder the variational form for the changed design (10.18) can be written as

$$\begin{aligned} R(\boldsymbol{v}, \boldsymbol{s}; \boldsymbol{\eta}) &= R(\boldsymbol{v}_0 + \Delta\boldsymbol{v}, \boldsymbol{s}; \boldsymbol{\eta}) \\ &= R(\boldsymbol{v}_0, \boldsymbol{s}; \boldsymbol{\eta}) + R'_v(\boldsymbol{v}_0, \boldsymbol{s}; \boldsymbol{\eta}, \Delta\boldsymbol{v}) + r_v(\boldsymbol{v}_0, \boldsymbol{s}; \boldsymbol{\eta}, \Delta\boldsymbol{v}) \\ &= R(\boldsymbol{v}_0, \boldsymbol{s}; \boldsymbol{\eta}) + \Delta_v R(\boldsymbol{v}_0, \boldsymbol{s}; \boldsymbol{\eta}) = 0. \end{aligned} \tag{10.21}$$

The change in the residual due to changes $\Delta\boldsymbol{v}$ is given by the nonlinear increment

$$\Delta_v R(\boldsymbol{v}_0, \boldsymbol{s}; \boldsymbol{\eta}) := R'_v(\boldsymbol{v}_0, \boldsymbol{s}; \boldsymbol{\eta}, \Delta\boldsymbol{v}) + r_v(\boldsymbol{v}_0, \boldsymbol{s}; \boldsymbol{\eta}, \Delta\boldsymbol{v}) \tag{10.22}$$

with the remainder

$$r_v(\boldsymbol{v}_0, \boldsymbol{s}; \boldsymbol{\eta}, \Delta\boldsymbol{v}) := \int_0^1 R''_{vv}(\boldsymbol{v}_0 + \lambda\Delta\boldsymbol{v}, \boldsymbol{s}; \boldsymbol{\eta}, \Delta\boldsymbol{v}, \Delta\boldsymbol{v})\,(1-\lambda)\,d\lambda. \tag{10.23}$$

Furthermore, (10.18) can be also written as

$$\begin{aligned} R(\boldsymbol{v}, \boldsymbol{s}; \boldsymbol{\eta}) &= R(\boldsymbol{v}, \boldsymbol{s}_0 + \Delta\boldsymbol{s}; \boldsymbol{\eta}) \\ &= R(\boldsymbol{v}, \boldsymbol{s}_0; \boldsymbol{\eta}) + R'_s(\boldsymbol{v}, \boldsymbol{s}_0; \boldsymbol{\eta}, \Delta\boldsymbol{s}) + r_s(\boldsymbol{v}, \boldsymbol{s}_0; \boldsymbol{\eta}, \Delta\boldsymbol{s}) \\ &= R(\boldsymbol{v}, \boldsymbol{s}_0; \boldsymbol{\eta}) + \Delta_s R(\boldsymbol{v}, \boldsymbol{s}_0; \boldsymbol{\eta}) = 0. \end{aligned} \tag{10.24}$$

The change in the residual due to changes $\Delta\boldsymbol{s}$ is given by the nonlinear increment

$$\Delta_s R(\boldsymbol{v}, \boldsymbol{s}_0; \boldsymbol{\eta}) := R'_s(\boldsymbol{v}, \boldsymbol{s}_0; \boldsymbol{\eta}, \Delta\boldsymbol{s}) + r_s(\boldsymbol{v}, \boldsymbol{s}_0; \boldsymbol{\eta}, \Delta\boldsymbol{s}) \tag{10.25}$$

with the remainder

$$r_s(\boldsymbol{v}, \boldsymbol{s}_0; \boldsymbol{\eta}, \Delta\boldsymbol{s}) := \int_0^1 R''_{ss}(\boldsymbol{v}, \boldsymbol{s}_0 + \lambda\Delta\boldsymbol{s}; \boldsymbol{\eta}, \Delta\boldsymbol{s}, \Delta\boldsymbol{s})\,(1-\lambda)\,d\lambda. \tag{10.26}$$

If the remainders are computable, these relations are exact. With this at hand, the residual $R(\boldsymbol{v}, \boldsymbol{s}; \boldsymbol{\eta})$ can be expressed only in terms of the initial state $\boldsymbol{v}_0$ or the initial design $\boldsymbol{s}_0$.

The goal is now to obtain an exact sensitivity relation for the state $\boldsymbol{v}$ due to changes in the design $\Delta\boldsymbol{s}$, i.e. the exact distance between the solutions $\boldsymbol{v}_0$ and $\boldsymbol{v}$ from (10.17) and (10.18), respectively. This is accomplished in the following result.

Theorem 10.1 (Exact sensitivity relation for the state) *Let the residual $R(\boldsymbol{v}, \boldsymbol{s}; \cdot)$ be sufficiently differentiable with respect to $\boldsymbol{v}$ and $\boldsymbol{s}$. Then it holds for the change in the state $\Delta\boldsymbol{v} = \boldsymbol{v} - \boldsymbol{v}_0$ due to changes in the design $\Delta\boldsymbol{s}$ that*

$$k(\boldsymbol{v}_0, \boldsymbol{s}_0; \boldsymbol{\eta}, \Delta\boldsymbol{v}) = -Q_{\mathrm{ex}}(\boldsymbol{v})(\boldsymbol{v}_0, \boldsymbol{s}_0; \boldsymbol{\eta}) \qquad \forall\, \boldsymbol{\eta} \in \mathcal{V} \tag{10.27}$$

with the exact pseudo load *functional*

$$\begin{aligned} Q_{\mathrm{ex}}(\boldsymbol{v})(\boldsymbol{v}_0, \boldsymbol{s}_0; \boldsymbol{\eta}) := R'_s(\boldsymbol{v}_0, \boldsymbol{s}_0; \boldsymbol{\eta}, \Delta\boldsymbol{s}) + R''_{sv}(\boldsymbol{v}_0, \boldsymbol{s}_0; \boldsymbol{\eta}, \Delta\boldsymbol{s}, \Delta\boldsymbol{v}) \\ + r(\boldsymbol{v}, \boldsymbol{v}_0, \boldsymbol{s}_0; \boldsymbol{\eta}, \Delta\boldsymbol{v}, \Delta\boldsymbol{s}) \end{aligned} \tag{10.28}$$

for a given $\Delta\boldsymbol{s}$. The remainder is quadratic in $\Delta\boldsymbol{v}$ and $\Delta\boldsymbol{s}$ and reads

$$\begin{aligned} r(\boldsymbol{v}, \boldsymbol{v}_0, \boldsymbol{s}_0; \boldsymbol{\eta}, \Delta\boldsymbol{v}, \Delta\boldsymbol{s}) := \int_0^1 \{\, & R''_{vv}(\boldsymbol{v}_0 + \lambda\Delta\boldsymbol{v}, \boldsymbol{s}_0; \boldsymbol{\eta}, \Delta\boldsymbol{v}, \Delta\boldsymbol{v}) \\ & + R''_{ss}(\boldsymbol{v}, \boldsymbol{s}_0 + \lambda\Delta\boldsymbol{s}; \boldsymbol{\eta}, \Delta\boldsymbol{s}, \Delta\boldsymbol{s}) \\ & + R'''_{svv}(\boldsymbol{v}_0 + \lambda\Delta\boldsymbol{v}, \boldsymbol{s}_0; \boldsymbol{\eta}, \Delta\boldsymbol{s}, \Delta\boldsymbol{v}, \Delta\boldsymbol{v})\}\, (1 - \lambda)\, d\lambda. \end{aligned} \tag{10.29}$$

Proof. Obviously we have, subtract Eq. 10.17 from Eq. 10.18 and by using (10.24),

$$\begin{aligned} R(\boldsymbol{v}, \boldsymbol{s}; \boldsymbol{\eta}) - R(\boldsymbol{v}_0, \boldsymbol{s}_0; \boldsymbol{\eta}) = R(\boldsymbol{v}, \boldsymbol{s}_0; \boldsymbol{\eta}) - R(\boldsymbol{v}_0, \boldsymbol{s}_0; \boldsymbol{\eta}) \\ + R'_s(\boldsymbol{v}, \boldsymbol{s}_0; \boldsymbol{\eta}, \Delta\boldsymbol{s}) + r_s(\boldsymbol{v}, \boldsymbol{s}_0; \boldsymbol{\eta}, \Delta\boldsymbol{s}) = 0. \end{aligned} \tag{10.30}$$

Furthermore, we can write

$$\begin{aligned} R(\boldsymbol{v}, \boldsymbol{s}_0; \boldsymbol{\eta}) - R(\boldsymbol{v}_0, \boldsymbol{s}_0; \boldsymbol{\eta}) &= R(\boldsymbol{v}_0 + \Delta\boldsymbol{v}, \boldsymbol{s}_0; \boldsymbol{\eta}) - R(\boldsymbol{v}_0, \boldsymbol{s}_0; \boldsymbol{\eta}) \\ &= R'_v(\boldsymbol{v}_0, \boldsymbol{s}_0; \boldsymbol{\eta}, \Delta\boldsymbol{v}) + r_v(\boldsymbol{v}_0, \boldsymbol{s}_0; \boldsymbol{\eta}, \Delta\boldsymbol{v}) \\ &= \Delta_v R(\boldsymbol{v}_0, \boldsymbol{s}_0; \boldsymbol{\eta}), \end{aligned} \tag{10.31}$$

where $r_v(\boldsymbol{v}_0, \boldsymbol{s}_0; \boldsymbol{\eta}, \Delta\boldsymbol{v})$ is defined in (10.23), in which $\boldsymbol{s}$ is replaced by $\boldsymbol{s}_0$. This yields

$$\begin{aligned} R(\boldsymbol{v}, \boldsymbol{s}; \boldsymbol{\eta}) - R(\boldsymbol{v}_0, \boldsymbol{s}_0; \boldsymbol{\eta}) = R'_v(\boldsymbol{v}_0, \boldsymbol{s}_0; \boldsymbol{\eta}, \Delta\boldsymbol{v}) + R'_s(\boldsymbol{v}, \boldsymbol{s}_0; \boldsymbol{\eta}, \Delta\boldsymbol{s}) \\ + r_v(\boldsymbol{v}_0, \boldsymbol{s}_0; \boldsymbol{\eta}, \Delta\boldsymbol{v}) + r_s(\boldsymbol{v}, \boldsymbol{s}_0; \boldsymbol{\eta}, \Delta\boldsymbol{s}) = 0 \end{aligned} \tag{10.32}$$

or

$$\begin{aligned} R_v'(\boldsymbol{v}_0, \boldsymbol{s}_0; \boldsymbol{\eta}, \Delta\boldsymbol{v}) = &- R_s'(\boldsymbol{v}, \boldsymbol{s}_0; \boldsymbol{\eta}, \Delta\boldsymbol{s}) \\ &- r_v(\boldsymbol{v}_0, \boldsymbol{s}_0; \boldsymbol{\eta}, \Delta\boldsymbol{v}) - r_s(\boldsymbol{v}, \boldsymbol{s}_0; \boldsymbol{\eta}, \Delta\boldsymbol{s}). \end{aligned} \tag{10.33}$$

The term $R_s'(\boldsymbol{v}, \boldsymbol{s}_0; \boldsymbol{\eta}, \Delta\boldsymbol{s})$ depends still on $\boldsymbol{v}$. A Taylor expansion yields

$$\begin{aligned} R_s'(\boldsymbol{v}, \boldsymbol{s}_0; \boldsymbol{\eta}, \Delta\boldsymbol{s}) &= R_s'(\boldsymbol{v}_0 + \Delta\boldsymbol{v}, \boldsymbol{s}_0; \boldsymbol{\eta}, \Delta\boldsymbol{s}) \\ &= R_s'(\boldsymbol{v}_0, \boldsymbol{s}_0; \boldsymbol{\eta}, \Delta\boldsymbol{s}) + R_{sv}''(\boldsymbol{v}_0, \boldsymbol{s}_0; \boldsymbol{\eta}, \Delta\boldsymbol{s}, \Delta\boldsymbol{v}) \\ &\quad + r_{sv}(\boldsymbol{v}_0, \boldsymbol{s}_0; \boldsymbol{\eta}, \Delta\boldsymbol{s}, \Delta\boldsymbol{v}) \end{aligned} \tag{10.34}$$

with the remainder

$$r_{sv}(\boldsymbol{v}_0, \boldsymbol{s}_0; \boldsymbol{\eta}, \Delta\boldsymbol{s}, \Delta\boldsymbol{v}) := \int_0^1 R_{svv}'''(\boldsymbol{v}_0 + \lambda\Delta\boldsymbol{v}, \boldsymbol{s}_0; \boldsymbol{\eta}, \Delta\boldsymbol{s}, \Delta\boldsymbol{v}, \Delta\boldsymbol{v})\,(1-\lambda)\,d\lambda. \tag{10.35}$$

Finally, this leads to

$$\begin{aligned} R_v'(\boldsymbol{v}_0, \boldsymbol{s}_0; \boldsymbol{\eta}, \Delta\boldsymbol{v}) = &- R_s'(\boldsymbol{v}_0, \boldsymbol{s}_0; \boldsymbol{\eta}, \Delta\boldsymbol{s}) - R_{sv}''(\boldsymbol{v}_0, \boldsymbol{s}_0; \boldsymbol{\eta}, \Delta\boldsymbol{s}, \Delta\boldsymbol{v}) \\ &- r_v(\boldsymbol{v}_0, \boldsymbol{s}_0; \boldsymbol{\eta}, \Delta\boldsymbol{v}) - r_s(\boldsymbol{v}, \boldsymbol{s}_0; \boldsymbol{\eta}, \Delta\boldsymbol{s}) \\ &- r_{sv}(\boldsymbol{v}_0, \boldsymbol{s}_0; \boldsymbol{\eta}, \Delta\boldsymbol{s}, \Delta\boldsymbol{v}). \end{aligned} \tag{10.36}$$

A rearrangement of all terms and the reminders as well as by using

$$k(\boldsymbol{v}_0, \boldsymbol{s}_0; \boldsymbol{\eta}, \Delta\boldsymbol{v}) := R_v'(\boldsymbol{v}_0, \boldsymbol{s}_0; \boldsymbol{\eta}, \Delta\boldsymbol{v}) \tag{10.37}$$

gives the stated result. □

In Theorem 10.1 an *exact pseudo load* for the state $Q_{\mathrm{ex}}(\boldsymbol{v}, \boldsymbol{v}_0, \boldsymbol{s}_0; \cdot)$ has been introduced. For chosen fixed $\Delta\boldsymbol{v}$ and $\Delta\boldsymbol{s}$ this is a linear functional $Q_{\mathrm{ex}} : \mathcal{V} \to \mathbb{R}$. The structure of the exact sensitivity relation (10.27) is equivalent to the standard approximative sensitivity relation (10.7). But obviously, the exact pseudo load contains the exact solution $\boldsymbol{v}$ or the exact increment $\Delta\boldsymbol{v}$. For practical computations the exact solution can be replaced by a good approximation. This will be discussed in detail in Section 10.3.

Remark 10.1 (Exact pseudo load vs. approximation) *The derived exact pseudo load functional $Q_{\mathrm{ex}}(\boldsymbol{v})(\boldsymbol{v}_0, \boldsymbol{s}_0; \cdot)$ in (10.27) and the approximate pseudo load $Q(\boldsymbol{v}_0, \boldsymbol{s}_0; \cdot)$ in (10.7) are related by*

$$\begin{aligned} Q_{\mathrm{ex}}(\boldsymbol{v})(\boldsymbol{v}_0, \boldsymbol{s}_0; \boldsymbol{\eta}) = Q(\boldsymbol{v}_0, \boldsymbol{s}_0; \boldsymbol{\eta}) &+ Q_v'(\boldsymbol{v}_0, \boldsymbol{s}_0; \boldsymbol{\eta}, \Delta\boldsymbol{v}) \\ &+ r(\boldsymbol{v}, \boldsymbol{v}_0, \boldsymbol{s}_0; \boldsymbol{\eta}, \Delta\boldsymbol{v}, \Delta\boldsymbol{s}), \end{aligned} \tag{10.38}$$

where the relations

$$Q(\boldsymbol{v}_0, \boldsymbol{s}_0; \cdot) = R'_s(\boldsymbol{v}_0, \boldsymbol{s}_0; \cdot, \Delta\boldsymbol{s}), \tag{10.39}$$

$$Q'_v(\boldsymbol{v}_0, \boldsymbol{s}_0; \cdot, \Delta\boldsymbol{v}) = R''_{sv}(\boldsymbol{v}_0, \boldsymbol{s}_0; \cdot, \Delta\boldsymbol{s}, \Delta\boldsymbol{v}) \tag{10.40}$$

have been used. Furthermore, the remainder (10.29) in terms of $Q(\cdot, \cdot; \cdot)$ is given as

$$\begin{aligned} r(\boldsymbol{v}, \boldsymbol{v}_0, \boldsymbol{s}_0; \boldsymbol{\eta}, \Delta\boldsymbol{v}, \Delta\boldsymbol{s}) = \int_0^1 \{ & R''_{vv}(\boldsymbol{v}_0 + \lambda\Delta\boldsymbol{v}, \boldsymbol{s}_0; \boldsymbol{\eta}, \Delta\boldsymbol{v}, \Delta\boldsymbol{v}) \\ & + Q'_s(\boldsymbol{v}, \boldsymbol{s}_0 + \lambda\Delta\boldsymbol{s}; \boldsymbol{\eta}, \Delta\boldsymbol{s}) \\ & + Q''_{vv}(\boldsymbol{v}_0 + \lambda\Delta\boldsymbol{v}, \boldsymbol{s}_0; \boldsymbol{\eta}, \Delta\boldsymbol{v}, \Delta\boldsymbol{v})\} (1 - \lambda)\, d\lambda. \end{aligned} \tag{10.41}$$

Remark 10.2 (The error in the pseudo load) *The error in the pseudo load is easily obtained from (10.38) as*

$$\begin{aligned} Q_{\mathrm{ex}}(\boldsymbol{v})(\boldsymbol{v}_0, \boldsymbol{s}_0; \boldsymbol{\eta}) - Q(\boldsymbol{v}_0, \boldsymbol{s}_0; \boldsymbol{\eta}) = & Q'_v(\boldsymbol{v}_0, \boldsymbol{s}_0; \boldsymbol{\eta}, \Delta\boldsymbol{v}) \\ & + r(\boldsymbol{v}, \boldsymbol{v}_0, \boldsymbol{s}_0; \boldsymbol{\eta}, \Delta\boldsymbol{v}, \Delta\boldsymbol{s}). \end{aligned} \tag{10.42}$$

Remark 10.3 (First-order sensitivity relation) *The approximative pseudo load $Q(\boldsymbol{v}_0, \boldsymbol{s}_0; \cdot)$ in (10.7) is just the first partial variation of the residual of the initial design $R(\boldsymbol{v}_0, \boldsymbol{s}_0; \cdot)$ with respect to $\boldsymbol{s}$. Therefore, the approximate sensitivity relation (10.7) given as*

$$k(\boldsymbol{v}_0, \boldsymbol{s}_0; \boldsymbol{\eta}, \Delta\tilde{\boldsymbol{v}}) = -Q(\boldsymbol{v}_0, \boldsymbol{s}_0; \boldsymbol{\eta})$$

is in the following referred to as the first-order sensitivity relation *for the state. The* first order approximation *for the state $\tilde{\boldsymbol{v}}$ is introduced as*

$$\tilde{\boldsymbol{v}} := \boldsymbol{v}_0 + \Delta\tilde{\boldsymbol{v}}. \tag{10.43}$$

10.2.3 Different formulations depending on the order of linearization

Depending in which order the exact linearization is performed, different formulations of the residuals and therefore different formulations of the exact sensitivity relations are obtained. If the first linearization is done with respect to $\boldsymbol{v}$ and the second with respect to $\boldsymbol{s}$ we have

$$\begin{aligned} R(\boldsymbol{v}, \boldsymbol{s}; \boldsymbol{\eta}) &= R(\boldsymbol{v}_0, \boldsymbol{s}; \boldsymbol{\eta}) + R'_v(\boldsymbol{v}_0, \boldsymbol{s}; \boldsymbol{\eta}, \Delta\boldsymbol{v}) + r_v(\boldsymbol{v}_0, \boldsymbol{s}; \boldsymbol{\eta}, \Delta\boldsymbol{v}) \\ &= R(\boldsymbol{v}_0, \boldsymbol{s}_0; \boldsymbol{\eta}) + R'_v(\boldsymbol{v}_0, \boldsymbol{s}; \boldsymbol{\eta}, \Delta\boldsymbol{v}) + R'_s(\boldsymbol{v}_0, \boldsymbol{s}_0; \boldsymbol{\eta}, \Delta\boldsymbol{s}) \\ &\quad + r_v(\boldsymbol{v}_0, \boldsymbol{s}; \boldsymbol{\eta}, \Delta\boldsymbol{v}) + r_s(\boldsymbol{v}_0, \boldsymbol{s}_0; \boldsymbol{\eta}, \Delta\boldsymbol{s}) \\ &= R(\boldsymbol{v}_0, \boldsymbol{s}_0; \boldsymbol{\eta}) + \Delta_s R(\boldsymbol{v}_0, \boldsymbol{s}_0; \boldsymbol{\eta}) + \Delta_v R(\boldsymbol{v}_0, \boldsymbol{s}; \boldsymbol{\eta}) = 0. \end{aligned} \tag{10.44}$$

Furthermore, this can be written as

$$\begin{aligned} R(\boldsymbol{v},\boldsymbol{s};\boldsymbol{\eta}) &= R(\boldsymbol{v}_0,\boldsymbol{s}_0;\boldsymbol{\eta}) \\ &\quad + R'_v(\boldsymbol{v}_0,\boldsymbol{s}_0;\boldsymbol{\eta},\Delta\boldsymbol{v}) + R'_s(\boldsymbol{v}_0,\boldsymbol{s}_0;\boldsymbol{\eta},\Delta\boldsymbol{s}) + R''_{vs}(\boldsymbol{v}_0,\boldsymbol{s}_0;\boldsymbol{\eta},\Delta\boldsymbol{v},\Delta\boldsymbol{s}) \\ &\quad + r_v(\boldsymbol{v}_0,\boldsymbol{s};\boldsymbol{\eta},\Delta\boldsymbol{v}) + r_s(\boldsymbol{v}_0,\boldsymbol{s}_0;\boldsymbol{\eta},\Delta\boldsymbol{s}) + r_{vs}(\boldsymbol{v}_0,\boldsymbol{s}_0;\boldsymbol{\eta},\Delta\boldsymbol{v},\Delta\boldsymbol{s}) = 0. \end{aligned} \tag{10.45}$$

The remainders r_v, r_s and r_{vs} are defined in (10.23), (10.26) and (10.35), respectively.

On the other hand, if the first linearization is done with respect to $\boldsymbol{s}$ and the second with respect to $\boldsymbol{v}$ we have

$$\begin{aligned} R(\boldsymbol{v},\boldsymbol{s};\boldsymbol{\eta}) &= R(\boldsymbol{v},\boldsymbol{s}_0;\boldsymbol{\eta}) + R'_s(\boldsymbol{v},\boldsymbol{s}_0;\boldsymbol{\eta},\Delta\boldsymbol{s}) + r_s(\boldsymbol{v},\boldsymbol{s}_0;\boldsymbol{\eta},\Delta\boldsymbol{s}) \\ &= R(\boldsymbol{v}_0,\boldsymbol{s}_0;\boldsymbol{\eta}) + R'_v(\boldsymbol{v}_0,\boldsymbol{s}_0;\boldsymbol{\eta},\Delta\boldsymbol{v}) + R'_s(\boldsymbol{v},\boldsymbol{s}_0;\boldsymbol{\eta},\Delta\boldsymbol{s}) \\ &\quad + r_v(\boldsymbol{v}_0,\boldsymbol{s}_0;\boldsymbol{\eta},\Delta\boldsymbol{v}) + r_s(\boldsymbol{v},\boldsymbol{s}_0;\boldsymbol{\eta},\Delta\boldsymbol{s}) \\ &= R(\boldsymbol{v}_0,\boldsymbol{s}_0;\boldsymbol{\eta}) + \Delta_v R(\boldsymbol{v}_0,\boldsymbol{s}_0;\boldsymbol{\eta}) + \Delta_s R(\boldsymbol{v},\boldsymbol{s}_0;\boldsymbol{\eta}) = 0 \end{aligned} \tag{10.46}$$

and

$$\begin{aligned} R(\boldsymbol{v},\boldsymbol{s};\boldsymbol{\eta}) &= R(\boldsymbol{v}_0,\boldsymbol{s}_0;\boldsymbol{\eta}) \\ &\quad + R'_v(\boldsymbol{v}_0,\boldsymbol{s}_0;\boldsymbol{\eta},\Delta\boldsymbol{v}) + R'_s(\boldsymbol{v}_0,\boldsymbol{s}_0;\boldsymbol{\eta},\Delta\boldsymbol{s}) + R''_{sv}(\boldsymbol{v}_0,\boldsymbol{s}_0;\boldsymbol{\eta},\Delta\boldsymbol{s},\Delta\boldsymbol{v}) \\ &\quad + r_v(\boldsymbol{v}_0,\boldsymbol{s}_0;\boldsymbol{\eta},\Delta\boldsymbol{v}) + r_s(\boldsymbol{v},\boldsymbol{s}_0;\boldsymbol{\eta},\Delta\boldsymbol{s}) + r_{sv}(\boldsymbol{v}_0,\boldsymbol{s}_0;\boldsymbol{\eta},\Delta\boldsymbol{s},\Delta\boldsymbol{v}) = 0. \end{aligned} \tag{10.47}$$

Obviously, from (10.44) and (10.46) we have

$$\left\{\begin{array}{l} R'_v(\boldsymbol{v}_0,\boldsymbol{s};\boldsymbol{\eta},\Delta\boldsymbol{v}) \\ \quad + R'_s(\boldsymbol{v}_0,\boldsymbol{s}_0;\boldsymbol{\eta},\Delta\boldsymbol{s}) \\ \quad + r_v(\boldsymbol{v}_0,\boldsymbol{s};\boldsymbol{\eta},\Delta\boldsymbol{v}) \\ \quad + r_s(\boldsymbol{v}_0,\boldsymbol{s}_0;\boldsymbol{\eta},\Delta\boldsymbol{s}) \end{array}\right\} = \left\{\begin{array}{l} R'_v(\boldsymbol{v}_0,\boldsymbol{s}_0;\boldsymbol{\eta},\Delta\boldsymbol{v}) \\ \quad + R'_s(\boldsymbol{v},\boldsymbol{s}_0;\boldsymbol{\eta},\Delta\boldsymbol{s}) \\ \quad + r_v(\boldsymbol{v}_0,\boldsymbol{s}_0;\boldsymbol{\eta},\Delta\boldsymbol{v}) \\ \quad + r_s(\boldsymbol{v},\boldsymbol{s}_0;\boldsymbol{\eta},\Delta\boldsymbol{s}) \end{array}\right\} \tag{10.48}$$

or

$$\left\{\begin{array}{l} R''_{vs}(\boldsymbol{v}_0,\boldsymbol{s}_0;\boldsymbol{\eta},\Delta\boldsymbol{v},\Delta\boldsymbol{s}) \\ \quad + r_v(\boldsymbol{v}_0,\boldsymbol{s};\boldsymbol{\eta},\Delta\boldsymbol{v}) \\ \quad + r_s(\boldsymbol{v}_0,\boldsymbol{s}_0;\boldsymbol{\eta},\Delta\boldsymbol{s}) \\ \quad + r_{vs}(\boldsymbol{v}_0,\boldsymbol{s}_0;\boldsymbol{\eta},\Delta\boldsymbol{v},\Delta\boldsymbol{s}) \end{array}\right\} = \left\{\begin{array}{l} R''_{sv}(\boldsymbol{v}_0,\boldsymbol{s}_0;\boldsymbol{\eta},\Delta\boldsymbol{s},\Delta\boldsymbol{v}) \\ \quad + r_v(\boldsymbol{v}_0,\boldsymbol{s}_0;\boldsymbol{\eta},\Delta\boldsymbol{v}) \\ \quad + r_s(\boldsymbol{v},\boldsymbol{s}_0;\boldsymbol{\eta},\Delta\boldsymbol{s}) \\ \quad + r_{sv}(\boldsymbol{v}_0,\boldsymbol{s}_0;\boldsymbol{\eta},\Delta\boldsymbol{s},\Delta\boldsymbol{v}) \end{array}\right\}. \tag{10.49}$$

From this follows that the change in the state $\Delta\boldsymbol{v}$ can be computed using different formulations. For given $\Delta\boldsymbol{s}$ the bilinear form $R'_v(\boldsymbol{v}_0,\boldsymbol{s};\boldsymbol{\eta},\Delta\boldsymbol{v}) = R'_v(\boldsymbol{v}_0,\boldsymbol{s}_0+\Delta\boldsymbol{s};\boldsymbol{\eta},\Delta\boldsymbol{v})$ is

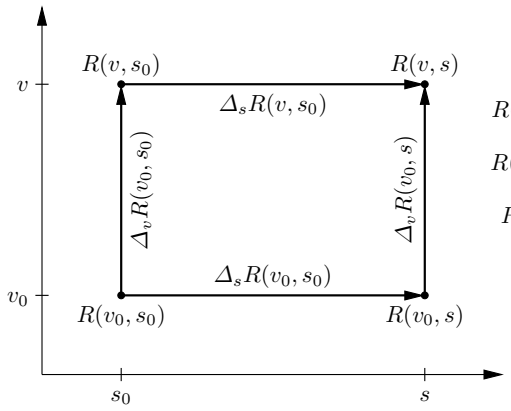

$$R(v_0, s) = R(v_0, s_0) + \Delta_s R(v_0, s_0)$$

$$R(v, s_0) = R(v_0, s_0) + \Delta_v R(v_0, s_0)$$

$$\begin{aligned} R(v, s) &= R(v_0, s_0) + \Delta_s R(v_0, s_0) + \Delta_v R(v_0, s) \\ &= R(v_0, s_0) + \Delta_v R(v_0, s_0) + \Delta_s R(v, s_0) \end{aligned}$$

Figure 10.3: Illustration of the different order of linearization of a given functional $R(v, s)$.

explicitly known and $\Delta \boldsymbol{v} \in \mathcal{V}$ is the solution of

$$\begin{aligned} R'_v(\boldsymbol{v}_0, \boldsymbol{s}; \boldsymbol{\eta}, \Delta \boldsymbol{v}) = R'_s(\boldsymbol{v}_0, \boldsymbol{s}_0; \boldsymbol{\eta}, \Delta \boldsymbol{s}) \\ + r_v(\boldsymbol{v}_0, \boldsymbol{s}; \boldsymbol{\eta}, \Delta \boldsymbol{v}) + r_s(\boldsymbol{v}_0, \boldsymbol{s}_0; \boldsymbol{\eta}, \Delta \boldsymbol{s}) \end{aligned} \qquad \forall\, \boldsymbol{\eta} \in \mathcal{V}. \tag{10.50}$$

On the other hand, $\Delta \boldsymbol{v} \in \mathcal{V}$ is also the solution of

$$\begin{aligned} R'_v(\boldsymbol{v}_0, \boldsymbol{s}_0; \boldsymbol{\eta}, \Delta \boldsymbol{v}) = R'_s(\boldsymbol{v}, \boldsymbol{s}_0; \boldsymbol{\eta}, \Delta \boldsymbol{s}) \\ + r_v(\boldsymbol{v}_0, \boldsymbol{s}_0; \boldsymbol{\eta}, \Delta \boldsymbol{v}) + r_s(\boldsymbol{v}, \boldsymbol{s}_0; \boldsymbol{\eta}, \Delta \boldsymbol{s}) \end{aligned} \qquad \forall\, \boldsymbol{\eta} \in \mathcal{V}. \tag{10.51}$$

Hence, both formulations are equivalent.

A graphical illustration of (10.44) and (10.46) is given in Fig. 10.3. The linearization of $R(\boldsymbol{v}, \boldsymbol{s}; \boldsymbol{\eta})$ can be performed first with respect $\boldsymbol{v}$ or equivalently with respect to $\boldsymbol{s}$, i.e.

$$\begin{aligned} R(\boldsymbol{v}, \boldsymbol{s}; \boldsymbol{\eta}) &= R(\boldsymbol{v}_0, \boldsymbol{s}_0; \boldsymbol{\eta}) + \Delta_s R(\boldsymbol{v}_0, \boldsymbol{s}_0; \boldsymbol{\eta}) + \Delta_v R(\boldsymbol{v}_0, \boldsymbol{s}; \boldsymbol{\eta}) \\ &= R(\boldsymbol{v}_0, \boldsymbol{s}_0; \boldsymbol{\eta}) + \Delta_v R(\boldsymbol{v}_0, \boldsymbol{s}_0; \boldsymbol{\eta}) + \Delta_s R(\boldsymbol{v}, \boldsymbol{s}_0; \boldsymbol{\eta}). \end{aligned} \tag{10.52}$$

Finally, we have

$$\Delta_s R(\boldsymbol{v}_0, \boldsymbol{s}_0; \boldsymbol{\eta}) + \Delta_v R(\boldsymbol{v}_0, \boldsymbol{s}; \boldsymbol{\eta}) = \Delta_v R(\boldsymbol{v}_0, \boldsymbol{s}_0; \boldsymbol{\eta}) + \Delta_s R(\boldsymbol{v}, \boldsymbol{s}_0; \boldsymbol{\eta}). \tag{10.53}$$

10.2.4 The error in the change of the state

The first-order approximation for the change in the state $\Delta \tilde{\boldsymbol{v}}$ due to changes in the design $\Delta \boldsymbol{s}$ is given in (10.7) as

$$k(\boldsymbol{v}_0, \boldsymbol{s}_0; \boldsymbol{\eta}, \Delta \tilde{\boldsymbol{v}}) = -Q(\boldsymbol{v}_0, \boldsymbol{s}_0; \boldsymbol{\eta}) \qquad \forall\, \boldsymbol{\eta} \in \mathcal{V}.$$

Furthermore, an exact relation has been introduced in (10.27) and the exact change $\Delta \boldsymbol{v}$ is the solution of

$$k(\boldsymbol{v}_0, \boldsymbol{s}_0; \boldsymbol{\eta}, \Delta \boldsymbol{v}) = -Q_{\mathrm{ex}}(\boldsymbol{v})(\boldsymbol{v}_0, \boldsymbol{s}_0; \boldsymbol{\eta}) \qquad \forall\, \boldsymbol{\eta} \in \mathcal{V}.$$

The goal is to now to obtain an exact error representation of the error in the increment

$$\boldsymbol{e}_{\Delta v} := \boldsymbol{v} - \tilde{\boldsymbol{v}} = \Delta \boldsymbol{v} - \Delta \tilde{\boldsymbol{v}}. \tag{10.54}$$

This relation is illustrated for a one-dimensional problem in Fig. 10.1.

The error $\boldsymbol{e}_{\Delta v}$ depends directly on the error in the pseudo load introduced in (10.42). An equation for the error $\boldsymbol{e}_{\Delta v}$ can now be obtained with the results from Theorem 10.1. This is accomplished in the following result.

Theorem 10.2 *Let $\Delta \tilde{\boldsymbol{v}}$ be the solution of the approximative first-order sensitivity relation (10.7) and let $\Delta \boldsymbol{v}$ be the solution of the exact sensitivity relation (10.27). Then, it holds for the error $\boldsymbol{e}_{\Delta v} = \Delta \boldsymbol{v} - \Delta \tilde{\boldsymbol{v}}$ that*

$$\begin{aligned} k(\boldsymbol{v}_0, \boldsymbol{s}_0; \boldsymbol{\eta}, \boldsymbol{e}_{\Delta v}) &= -[\, Q_{\mathrm{ex}}(\boldsymbol{v})(\boldsymbol{v}_0, \boldsymbol{s}_0; \boldsymbol{\eta}) - Q(\boldsymbol{v}_0, \boldsymbol{s}_0; \boldsymbol{\eta})\,] \\ &= -[\, R''_{sv}(\boldsymbol{v}_0, \boldsymbol{s}_0; \boldsymbol{\eta}, \Delta \boldsymbol{s}, \Delta \boldsymbol{v}) + r(\boldsymbol{v}, \boldsymbol{v}_0, \boldsymbol{s}_0; \boldsymbol{\eta}, \Delta \boldsymbol{v}, \Delta \boldsymbol{s})\,] \\ &= -[\, Q'_v(\boldsymbol{v}_0, \boldsymbol{s}_0; \boldsymbol{\eta}, \Delta \boldsymbol{v}) + r(\boldsymbol{v}, \boldsymbol{v}_0, \boldsymbol{s}_0; \boldsymbol{\eta}, \Delta \boldsymbol{v}, \Delta \boldsymbol{s})\,] \end{aligned} \tag{10.55}$$

for all $\boldsymbol{\eta} \in \mathcal{V}$. The remainder $r(\boldsymbol{v}, \boldsymbol{v}_0, \boldsymbol{s}_0; \boldsymbol{\eta}, \Delta \boldsymbol{v}, \Delta \boldsymbol{s})$ is given in (10.29).

Proof. The proof is easily obtained if we subtract (10.7) from (10.27), i.e.

$$k(\boldsymbol{v}_0, \boldsymbol{s}_0; \boldsymbol{\eta}, \Delta \boldsymbol{v}) - k(\boldsymbol{v}_0, \boldsymbol{s}_0; \boldsymbol{\eta}, \Delta \tilde{\boldsymbol{v}}) = -[\, Q_{\mathrm{ex}}(\boldsymbol{v})(\boldsymbol{v}_0, \boldsymbol{s}_0; \boldsymbol{\eta}) - Q(\boldsymbol{v}_0, \boldsymbol{s}_0; \boldsymbol{\eta})\,].$$

Due to the linearity of the bilinear form $k(\boldsymbol{v}_0, \boldsymbol{s}_0; \cdot, \cdot)$ it holds that

$$k(\boldsymbol{v}_0, \boldsymbol{s}_0; \boldsymbol{\eta}, \boldsymbol{e}_{\Delta v}) = -[\, Q_{\mathrm{ex}}(\boldsymbol{v})(\boldsymbol{v}_0, \boldsymbol{s}_0; \boldsymbol{\eta}) - Q(\boldsymbol{v}_0, \boldsymbol{s}_0; \boldsymbol{\eta})\,].$$

The right hand side is given by the error in the pseudo load (10.42). This gives the stated result. □

Hence, the error in the change of the state $\boldsymbol{e}_{\Delta v}$ depends directly on the error in the pseudo load. The relation (10.55) is exact if the exact pseudo load $Q_{\mathrm{ex}}(\boldsymbol{v})(\boldsymbol{v}_0, \boldsymbol{s}_0; \boldsymbol{\eta})$ is computable.

10.2.5 An error estimator for the design sensitivity of the state

The exact error representation (10.55) contains in the right hand side the exact increment $\Delta \boldsymbol{v}$. Hence, the practical computation requires a good approximation of the increment.

Let $\Delta \tilde{\boldsymbol{v}}^*$ be a computed higher-order approximation of the increment such that $\Delta \tilde{\boldsymbol{v}}^* \approx \Delta \boldsymbol{v}$. Then, an approximation of the error relation (10.55) reads

$$\begin{aligned} k(\boldsymbol{v}_0, \boldsymbol{s}_0; \boldsymbol{\eta}, \boldsymbol{e}_{\Delta v}) &\approx -[\, Q_{\mathrm{ex}}(\boldsymbol{v}_0 + \Delta \tilde{\boldsymbol{v}}^*)(\boldsymbol{v}_0, \boldsymbol{s}_0; \boldsymbol{\eta}) - Q(\boldsymbol{v}_0, \boldsymbol{s}_0; \boldsymbol{\eta}) \,] \\ &= -[\, R''_{sv}(\boldsymbol{v}_0, \boldsymbol{s}_0; \boldsymbol{\eta}, \Delta \boldsymbol{s}, \Delta \tilde{\boldsymbol{v}}^*) \\ &\qquad + r(\boldsymbol{v}_0 + \Delta \tilde{\boldsymbol{v}}^*, \boldsymbol{v}_0, \boldsymbol{s}_0; \boldsymbol{\eta}, \Delta \tilde{\boldsymbol{v}}^*, \Delta \boldsymbol{s}) \,]. \end{aligned} \tag{10.56}$$

In the simplest case, the solution $\Delta \tilde{\boldsymbol{v}}$ of the first-order sensitivity relation (10.7) can be used, i.e. we set $\Delta \tilde{\boldsymbol{v}}^* = \Delta \tilde{\boldsymbol{v}}$.

Furthermore, higher-order approximations can be computed using the exact sensitivity relation (10.27) within an iterative algorithm. Such an improvement algorithm is proposed in Section 10.3 in Box. 10.1.

The exact new state due to design changes $\Delta \boldsymbol{s}$ is obtained with the exact increment $\Delta \boldsymbol{v}$ as

$$\boldsymbol{v} := \boldsymbol{v}_0 + \Delta \boldsymbol{v}. \tag{10.57}$$

A first-order approximation for the state $\tilde{\boldsymbol{v}}$ for the changed design using the first-order solution $\Delta \tilde{\boldsymbol{v}}$ is given from

$$\tilde{\boldsymbol{v}} := \boldsymbol{v}_0 + \Delta \tilde{\boldsymbol{v}}. \tag{10.58}$$

Furthermore, with an improved solution $\Delta \tilde{\boldsymbol{v}}^*$ the new *improved state* is introduced as

$$\tilde{\boldsymbol{v}}^* := \boldsymbol{v}_0 + \Delta \tilde{\boldsymbol{v}}^*. \tag{10.59}$$

A simple error estimator can be obtained using such an improved solution $\Delta \tilde{\boldsymbol{v}}^*$. Let $\tilde{\boldsymbol{e}}_{\Delta v}$ be an *error estimator for the error of the design sensitivity of the state* introduced as

$$\tilde{\boldsymbol{e}}_{\Delta v} := \tilde{\boldsymbol{v}}^* - \tilde{\boldsymbol{v}} = \Delta \tilde{\boldsymbol{v}}^* - \Delta \tilde{\boldsymbol{v}}. \tag{10.60}$$

For a good approximation $\tilde{\boldsymbol{v}}^* \approx \boldsymbol{v}$ the exact error representation (10.55) is the basis for the computation of the error estimator $\tilde{\boldsymbol{e}}_{\Delta v}$.

Finally, $\tilde{\boldsymbol{e}}_{\Delta v}$ is computable and just the solution of the following problem: Find $\tilde{\boldsymbol{e}}_{\Delta v} \in \mathcal{V}$ such that

$$\begin{aligned} k(\boldsymbol{v}_0, \boldsymbol{s}_0; \boldsymbol{\eta}, \tilde{\boldsymbol{e}}_{\Delta v}) &= -[\, Q_{\mathrm{ex}}(\tilde{\boldsymbol{v}}^*)(\boldsymbol{v}_0, \boldsymbol{s}_0; \boldsymbol{\eta}) - Q(\boldsymbol{v}_0, \boldsymbol{s}_0; \boldsymbol{\eta}) \,] \\ &= -[\, R''_{sv}(\boldsymbol{v}_0, \boldsymbol{s}_0; \boldsymbol{\eta}, \Delta \boldsymbol{s}, \Delta \tilde{\boldsymbol{v}}^*) + r(\tilde{\boldsymbol{v}}^*, \boldsymbol{v}_0, \boldsymbol{s}_0; \boldsymbol{\eta}, \Delta \tilde{\boldsymbol{v}}^*, \Delta \boldsymbol{s}) \,] \end{aligned} \tag{10.61}$$

for all $\boldsymbol{\eta} \in \mathcal{V}$. The estimate $\tilde{\boldsymbol{e}}_{\Delta v}$ tends to the exact solution $\boldsymbol{e}_{\Delta v}$ if $\Delta \tilde{\boldsymbol{v}}^* \to \Delta \boldsymbol{v}$.

Remark 10.4 (Least obtainable error) *In practical computations the improved solution $\tilde{\boldsymbol{v}}^*$ can be very close to the exact solution $\boldsymbol{v}$ for sufficiently small design changes, i.e. $\boldsymbol{v} \approx \tilde{\boldsymbol{v}}^*$. But especially for large design changes there is still a difference even if the best improved solution $\tilde{\boldsymbol{v}}^*$ is obtained. Therefore, the* least obtainable error *can be introduced as*

$$\tilde{\boldsymbol{e}}^*_{\Delta v} := \boldsymbol{e}_{\Delta v} - \tilde{\boldsymbol{e}}_{\Delta v} = \Delta\boldsymbol{v} - \Delta\tilde{\boldsymbol{v}}^*, \tag{10.62}$$

which measures the distance between the exact solution $\Delta\boldsymbol{v}$ and the improved solution $\Delta\tilde{\boldsymbol{v}}^*$.

Remark 10.5 (Error estimator in the L_2 norm) *The error $\tilde{\boldsymbol{e}}_{\Delta v}$ measures the distance between the solution $\Delta\tilde{\boldsymbol{v}}$ and an improved solution $\Delta\tilde{\boldsymbol{v}}^*$ obtained from an higher-order approximation. The error estimator in terms of the L_2 norm as well as the corresponding relative error are introduced as*

$$\tilde{\eta}_{\Delta v} := ||\tilde{\boldsymbol{e}}_{\Delta v}||_{L_2} = ||\tilde{\boldsymbol{v}}^* - \tilde{\boldsymbol{v}}||_{L_2} = ||\Delta\tilde{\boldsymbol{v}}^* - \Delta\tilde{\boldsymbol{v}}||_{L_2}, \tag{10.63}$$

$$\tilde{\eta}^{\mathrm{rel}}_{\Delta v} := \frac{||\tilde{\boldsymbol{v}}^* - \tilde{\boldsymbol{v}}||_{L_2}}{||\tilde{\boldsymbol{v}}^*||_{L_2}} = \frac{||\Delta\tilde{\boldsymbol{v}}^* - \Delta\tilde{\boldsymbol{v}}||_{L_2}}{||\tilde{\boldsymbol{v}}^*||_{L_2}}. \tag{10.64}$$

Furthermore, the exact error measured in the L_2 norm as well as the corresponding relative error are given as

$$\eta_{\Delta v} := ||\boldsymbol{e}_{\Delta v}||_{L_2} = ||\boldsymbol{v} - \tilde{\boldsymbol{v}}||_{L_2} = ||\Delta\boldsymbol{v} - \Delta\tilde{\boldsymbol{v}}||_{L_2}, \tag{10.65}$$

$$\eta^{\mathrm{rel}}_{\Delta v} := \frac{||\boldsymbol{v} - \tilde{\boldsymbol{v}}||_{L_2}}{||\boldsymbol{v}||_{L_2}} = \frac{||\Delta\boldsymbol{v} - \Delta\tilde{\boldsymbol{v}}||_{L_2}}{||\boldsymbol{v}||_{L_2}}. \tag{10.66}$$

Remark 10.6 (Effectivity index) *In order to quantify the error estimator the* effectivity index

$$I_{\mathrm{eff}} := \frac{||\tilde{\boldsymbol{e}}_{\Delta v}||_{L_2}}{||\boldsymbol{e}_{\Delta v}||_{L_2}} = \frac{\tilde{\eta}_{\Delta v}}{\eta_{\Delta v}} \tag{10.67}$$

is used. The error estimator is asymptotically exact if I_{eff} tends to unity. The effectivity index is a measure for the accuracy of the resulting error estimator $\tilde{\eta}_{\Delta v}$.

10.3 Improvement of sensitivity relations

The exact sensitivity representation (10.27) contains in the right hand side the exact solution $\boldsymbol{v}$ or the exact increment $\Delta\boldsymbol{v}$ for the changed design. From this relation an improvement algorithm can be derived.

10.3.1 An improvement approach

Let $\Delta\tilde{\boldsymbol{v}}_0$ be a good approximation of the exact change $\Delta\boldsymbol{v}$ such that $\Delta\tilde{\boldsymbol{v}}_0 \approx \Delta\boldsymbol{v}$. An approximation of the state $\boldsymbol{v}$ for the changed design is given from

$$\tilde{\boldsymbol{v}}_0 = \boldsymbol{v}_0 + \Delta\tilde{\boldsymbol{v}}_0. \tag{10.68}$$

The exact pseudo load $Q_{\mathrm{ex}}(\boldsymbol{v})(\boldsymbol{v}_0, \boldsymbol{s}_0; \boldsymbol{\eta})$ in (10.28) contains higher-order variations of the considered residual $R(\cdot,\cdot;\cdot)$ obtained from the exact Taylor expansion with integral reminder. Using the initial solution $\Delta\tilde{\boldsymbol{v}}_0$ within the exact sensitivity relation (10.27) we obtain an *improved design sensitivity solution* $\Delta\tilde{\boldsymbol{v}}_1^* \in \mathcal{V}$ by solving

$$k(\boldsymbol{v}_0, \boldsymbol{s}_0; \boldsymbol{\eta}, \Delta\tilde{\boldsymbol{v}}_1^*) = -Q_{\mathrm{ex}}(\tilde{\boldsymbol{v}}_0)(\boldsymbol{v}_0, \boldsymbol{s}_0; \boldsymbol{\eta}) \qquad \forall\, \boldsymbol{\eta} \in \mathcal{V} \tag{10.69}$$

with

$$\begin{aligned} Q_{\mathrm{ex}}(\tilde{\boldsymbol{v}}_0)(\boldsymbol{v}_0, \boldsymbol{s}_0; \boldsymbol{\eta}) := {} & R'_s(\boldsymbol{v}_0, \boldsymbol{s}_0; \boldsymbol{\eta}, \Delta\boldsymbol{s}) + R''_{sv}(\boldsymbol{v}_0, \boldsymbol{s}_0; \boldsymbol{\eta}, \Delta\boldsymbol{s}, \Delta\tilde{\boldsymbol{v}}_0) \\ & + r(\tilde{\boldsymbol{v}}_0, \boldsymbol{v}_0, \boldsymbol{s}_0; \boldsymbol{\eta}, \Delta\tilde{\boldsymbol{v}}_0, \Delta\boldsymbol{s}). \end{aligned} \tag{10.70}$$

This can be repeated within an iteration loop until no further improvements occur, i.e. no changes in the state. The algorithm stops if the change is smaller than a given tolerance TOL, i.e.

$$||\Delta\tilde{\boldsymbol{v}}_{i+1}^* - \Delta\tilde{\boldsymbol{v}}_i^*||_{L_2} \leq \mathrm{TOL}, \tag{10.71}$$

or if a maximal admissible number of iterations is achieved. In practical computations the tolerance is chosen as $[\,10^{-10}, 10^{-14}\,]$.

The overall solution algorithm is given in Box. 10.1. The algorithm corresponds formally with a classical Newton algorithm used within the solution of a nonlinear problem.

10.3.2 Computational aspects and efficiency

The proposed improvement approach for the design sensitivity of the state based on the formulation of the exact sensitivity relation is very efficient for several reasons.

- The tangent stiffness matrix $\boldsymbol{K}_0$ and its inverse $\boldsymbol{K}_0^{-1}$ in Box. 10.1 are the same as used for the solution of the primal structural problem $\boldsymbol{K}_0\Delta\boldsymbol{v} = -\boldsymbol{R}$ in the last iteration step of the Newton algorithm. Therefore, these matrices have not to be computed once again for the sensitivity relation improvement.
- Hence, $\boldsymbol{K}_0^{-1}$ is already known and the computation of $\Delta\tilde{\boldsymbol{v}}_{i+1}^*$ in (10.72) requires only the matrix-vector multiplication $\Delta\tilde{\boldsymbol{v}}_{i+1}^* = -\boldsymbol{K}_0^{-1}\boldsymbol{Q}_{\mathrm{ex}}(\tilde{\boldsymbol{v}}_i^*)$. In all iteration steps the same tangent stiffness matrix $\boldsymbol{K}_0^{-1}$ is used.

Compute an initial value $\Delta\tilde{\boldsymbol{v}}_0$: Solve the first-order sensitivity relation (10.7) for given $\boldsymbol{v}_0$ and $\boldsymbol{s}_0$. Find $\Delta\tilde{\boldsymbol{v}}_0 \in \mathcal{V}$ such that

$$k(\boldsymbol{v}_0, \boldsymbol{s}_0; \boldsymbol{\eta}, \Delta\tilde{\boldsymbol{v}}_0) = -Q(\boldsymbol{v}_0, \boldsymbol{s}_0; \boldsymbol{\eta}) \quad \forall\, \boldsymbol{\eta} \in \mathcal{V},$$

i.e. solve the discrete linear equation

$$\boldsymbol{K}_0 \Delta\tilde{\boldsymbol{v}}_0 = -\boldsymbol{Q}(\boldsymbol{v}_0).$$

Iteration loop: Set $i = 0$, $\Delta\tilde{\boldsymbol{v}}_i^* = \Delta\tilde{\boldsymbol{v}}_0$ and $\tilde{\boldsymbol{v}}_i^* = \boldsymbol{v}_0 + \Delta\tilde{\boldsymbol{v}}_0$

1. Solve the exact sensitivity relation (10.27) with $\tilde{\boldsymbol{v}}_i^*$. Find $\Delta\tilde{\boldsymbol{v}}_{i+1}^* \in \mathcal{V}$ such that

   $$k(\boldsymbol{v}_0, \boldsymbol{s}_0; \boldsymbol{\eta}, \Delta\tilde{\boldsymbol{v}}_{i+1}^*) = -Q_{\mathrm{ex}}(\tilde{\boldsymbol{v}}_i^*)(\boldsymbol{v}_0, \boldsymbol{s}_0; \boldsymbol{\eta}) \quad \forall\, \boldsymbol{\eta} \in \mathcal{V},$$

   i.e. solve the discrete linear equation

   $$\boldsymbol{K}_0 \Delta\tilde{\boldsymbol{v}}_{i+1}^* = -\boldsymbol{Q}_{\mathrm{ex}}(\tilde{\boldsymbol{v}}_i^*). \tag{10.72}$$

2. Update improved state: $\tilde{\boldsymbol{v}}_{i+1}^* = \tilde{\boldsymbol{v}}_i^* + \Delta\tilde{\boldsymbol{v}}_{i+1}^*$

3. Check convergence:
   if $\quad ||\Delta\tilde{\boldsymbol{v}}_{i+1}^* - \Delta\tilde{\boldsymbol{v}}_i^*||_{L_2} \leq \mathrm{TOL} \quad$ or $\quad i \geq$ max. # of iterations $\quad \rightarrow \quad$ END

   else $\quad \rightarrow \quad$ set $i = i + 1$ and GOTO (1)

Box 10.1: Solution algorithm for the improvement of $\Delta\boldsymbol{v}$ due to changes in the design $\Delta\boldsymbol{s}$

- The most contributions of the exact pseudo load $Q_{\mathrm{ex}}(\boldsymbol{v})(\boldsymbol{v}_0, \boldsymbol{s}_0; \boldsymbol{\eta})$ in (10.28) are only affected by elements which share nodes with design variations $\Delta\boldsymbol{s}$. Therefore, only those elements have to be considered within the assembling routine and all other element contributions are zero. The assembling routine can be modified in such a way that the loop runs not over all elements, but only over the elements which are affected by design changes. In the most cases this is a small number of elements and the computational effort is small.

  The only contribution of $Q_{\mathrm{ex}}(\boldsymbol{v})(\boldsymbol{v}_0, \boldsymbol{s}_0; \boldsymbol{\eta})$ which is affected by all elements is the term $R''_{vv}(\boldsymbol{v}, \boldsymbol{s}; \boldsymbol{\eta}, \Delta\boldsymbol{v}, \Delta\boldsymbol{v})$ in the remainder (10.29). This term is quadratic in $\Delta\boldsymbol{v}$ and tends for small changes in the state very quickly to zero. Therefore, in practical computations this terms has to be computed for all elements only for large values of $\Delta\boldsymbol{v}$. The computational experience shows that R''_{vv} has not to be considered for

  $$||\Delta\boldsymbol{v}||_{L_2} \leq \mathrm{TOL}, \tag{10.73}$$

  with a chosen tolerance of $[\,10^{-5}, 10^{-7}\,]$. For instance, let $\boldsymbol{R}_{vv}(\Delta\boldsymbol{v})$ be the discrete vector corresponding to the functional R''_{vv} for a given $\Delta\boldsymbol{v}$. Then, the chosen tolerance

TOL $= 10^{-6}$ leads to a norm of the residual of about $||\boldsymbol{R}_{vv}(\Delta\boldsymbol{v})||_{L_2} \approx 10^{-12}$, because the functional is quadratic in $\Delta\boldsymbol{v}$. Hence, for small design changes $\Delta\boldsymbol{s}$ which cause small changes in the state $\Delta\boldsymbol{v}$ the term R''_{vv} vanishes and only the elements which are affected by design changes have to be considered as mentioned above.

The computation of the exact pseudo load $Q_{\mathrm{ex}}(\boldsymbol{v})(\boldsymbol{v}_0, \boldsymbol{s}_0; \boldsymbol{\eta})$ requires higher-order variations of the residual $R(\cdot,\cdot;\cdot)$ with respect to $\boldsymbol{v}$ and $\boldsymbol{s}$. These terms can be derived using the same variational approach as in the former chapters. Furthermore, the corresponding discrete formulations are also obtained in the same manner. Explicit variational formulations for shape design sensitivity of all required higher-order variations are given in Section 10.6. Furthermore, compact formulations used within the numerical implementation are stated in Appendix B.1.2. These terms can be computed and assembled in the same routine as the classical stiffness matrix and the residual vector without considerable computational cost.

Remark 10.7 (Linear problems) *The second variations with respect to $\boldsymbol{v}$ vanish in the exact pseudo load $Q_{\mathrm{ex}}(\boldsymbol{v})(\boldsymbol{v}_0, \boldsymbol{s}_0; \boldsymbol{\eta})$ in (10.28) if a linear model problem is considered, i.e.*

$$R''_{vv}(\boldsymbol{v}, \boldsymbol{s}; \boldsymbol{\eta}, \Delta\boldsymbol{v}, \Delta\boldsymbol{v}) = 0 \qquad \textit{and} \qquad R'''_{svv}(\boldsymbol{v}, \boldsymbol{s}; \boldsymbol{\eta}, \Delta\boldsymbol{s}, \Delta\boldsymbol{v}, \Delta\boldsymbol{v}) = 0.$$

Therefore, if the problem is linear in $\boldsymbol{v}$ only the elements which are affected by design changes $\Delta\boldsymbol{s}$ have to be considered within the assembling process. This makes the proposed approach very efficient. For the model problem of linearized elasticity all required variations are given in Section B.2.7.

10.3.3 Computation of the remainder

The exact pseudo load $Q_{\mathrm{ex}}(\boldsymbol{v})(\boldsymbol{v}_0, \boldsymbol{s}_0; \boldsymbol{\eta})$ contains an exact integral remainder defined in (10.29) as

$$\begin{aligned} r(\boldsymbol{v}, \boldsymbol{v}_0, \boldsymbol{s}_0; \boldsymbol{\eta}, \Delta\boldsymbol{v}, \Delta\boldsymbol{s}) = \int_0^1 \{ & R''_{vv}(\boldsymbol{v}_0 + \lambda\Delta\boldsymbol{v}, \boldsymbol{s}_0; \boldsymbol{\eta}, \Delta\boldsymbol{v}, \Delta\boldsymbol{v}) \\ & + R''_{ss}(\boldsymbol{v}, \boldsymbol{s}_0 + \lambda\Delta\boldsymbol{s}; \boldsymbol{\eta}, \Delta\boldsymbol{s}, \Delta\boldsymbol{s}) \\ & + R'''_{svv}(\boldsymbol{v}_0 + \lambda\Delta\boldsymbol{v}, \boldsymbol{s}_0; \boldsymbol{\eta}, \Delta\boldsymbol{s}, \Delta\boldsymbol{v}, \Delta\boldsymbol{v})\} \, (1-\lambda) \, d\lambda. \end{aligned}$$

Such integral remainders are usually neglected. In the present work the exact sensitivity and error relations are based on the fully computation of the remainder. In the general case, the integral $\int_0^1 (\cdot)\, d\lambda$ cannot be computed analytically. In this work a numerical integration scheme (Gauss integration) is used in order to solve the integral.

For instance, for notational simplicity only the first term in the remainder

$$r_v(\boldsymbol{v}_0, \boldsymbol{s}_0; \boldsymbol{\eta}, \Delta\boldsymbol{v}) = \int_0^1 R''_{vv}(\boldsymbol{v}_0 + \lambda\Delta\boldsymbol{v}, \boldsymbol{s}_0; \boldsymbol{\eta}, \Delta\boldsymbol{v}, \Delta\boldsymbol{v}) \, (1-\lambda) \, d\lambda$$

is considered. Let $\boldsymbol{R}_{vv}(\boldsymbol{v}_0) \in \mathbb{R}^n$ be the discrete vector corresponding to the functional $R''_{vv}(\boldsymbol{v}_0, \boldsymbol{s}_0; \cdot, \Delta\boldsymbol{v}, \Delta\boldsymbol{v})$ for any given $\Delta\boldsymbol{v}$. Furthermore, let $\boldsymbol{r}_v \in \mathbb{R}^n$ be the discrete vector corresponding to the remainder functional $r_v(\boldsymbol{v}_0, \boldsymbol{s}_0; \cdot, \Delta\boldsymbol{v})$. Then, the discrete vector $\boldsymbol{r}_v$ is given from

$$\boldsymbol{r}_v = \int_0^1 \boldsymbol{R}_{vv}(\boldsymbol{v}_0 + \lambda\Delta\boldsymbol{v})\,(1-\lambda)\,d\lambda \cong \sum_{i=1}^{\mathrm{NGP}} \boldsymbol{R}_{vv}(\boldsymbol{v}_0 + \xi_i\,\Delta\boldsymbol{v})\,(1-\xi_i)\,\omega_i, \qquad (10.74)$$

where ξ_i and ω_i are the Gauss-points and weights of the one-dimensional integration scheme. The accuracy of $\boldsymbol{r}_v$ depends on the number of Gauss-points NGP. For an adequate number of Gauss-points the integration scheme yields good results, i.e. the remainder can be computed with high accuracy. In practical computations 2 to 4 Gauss-points should be used in order to obtain sufficient results. All other remainder contributions can be computed within the same integration loop.

10.4 An exact sensitivity relation and error analysis for quantities of interest

The extension of the above presented framework to chosen quantities of interest is presented within this section. The goal is to establish an exact relation for the change in the quantity of interest due to design changes. The problem is more complex as the sensitivity relation of the state because the dual problem is in general formulated at a given deformed state. The corresponding dual solution is the deformation due to the dual load case applied on the deformed structure.

The following approach has been inspired by an article on modeling error estimation [18]. This subject is in an abstract sense closely related to design sensitivity analysis if the change in a model is interpreted as a design change, see Section 10.5.

10.4.1 An exact sensitivity relation

Let again $\boldsymbol{v}_0 \in \mathcal{V}$ be the solution of the initial problem (10.17) with a given initial design $\boldsymbol{s}_0 \in \mathcal{S}$ and let $\boldsymbol{v} \in \mathcal{V}$ be the solution for the changed design $\boldsymbol{s} = \boldsymbol{s}_0 + \Delta\boldsymbol{s} \in \mathcal{S}$, i.e. the solution of (10.18). The quantity of interest for the initial and changed design are given as

$$J(\boldsymbol{v}_0, \boldsymbol{s}_0) \qquad \text{initial design } \boldsymbol{s}_0 \qquad (10.75)$$

$$J(\boldsymbol{v}, \boldsymbol{s}) \qquad \text{changed design } \boldsymbol{s} = \boldsymbol{s}_0 + \Delta\boldsymbol{s}. \qquad (10.76)$$

The goal is now to predict the change in the quantity of interest due to design changes, which is given by the increment

$$\Delta J = J(\boldsymbol{v}, \boldsymbol{s}) - J(\boldsymbol{v}_0, \boldsymbol{s}_0). \qquad (10.77)$$

The quantity of interest can be computed using an optimal control approach as shown in Section 5.2. The corresponding Lagrangian functionals for the initial and changed design are introduced as

$$L(\boldsymbol{s}_0)(\boldsymbol{v}_0, \boldsymbol{z}_0) = J(\boldsymbol{v}_0, \boldsymbol{s}_0) - R(\boldsymbol{v}_0, \boldsymbol{s}_0; \boldsymbol{z}_0), \tag{10.78}$$

$$L(\boldsymbol{s})(\boldsymbol{v}, \boldsymbol{z}) = J(\boldsymbol{v}, \boldsymbol{s}) - R(\boldsymbol{v}, \boldsymbol{s}; \boldsymbol{z}), \tag{10.79}$$

where $\boldsymbol{z}_0$ and $\boldsymbol{z}$ are the dual solutions for the initial and changed design, respectively.

Furthermore, the Lagrangian $L(\boldsymbol{s})(\boldsymbol{v}, \boldsymbol{z})$ can be expressed in terms of the initial design as

$$\begin{aligned} L(\boldsymbol{s})(\boldsymbol{v}, \boldsymbol{z}) &= L(\boldsymbol{s}_0 + \Delta\boldsymbol{s})(\boldsymbol{v}, \boldsymbol{z}) \\ &= L(\boldsymbol{s}_0)(\boldsymbol{v}, \boldsymbol{z}) + \Delta_s L(\boldsymbol{s}_0)(\boldsymbol{v}, \boldsymbol{z}) \end{aligned} \tag{10.80}$$

with the increment of the Lagrangian

$$\Delta_s L(\boldsymbol{s}_0)(\boldsymbol{v}, \boldsymbol{z}) := \Delta_s J(\boldsymbol{v}, \boldsymbol{s}_0) - \Delta_s R(\boldsymbol{v}, \boldsymbol{s}_0; \boldsymbol{z}). \tag{10.81}$$

The increments $\Delta_s J$ and $\Delta_s R$ are given as

$$\Delta_s J(\boldsymbol{v}, \boldsymbol{s}_0) := J'_s(\boldsymbol{v}, \boldsymbol{s}_0; \Delta\boldsymbol{s} + r_s^J(\boldsymbol{v}, \boldsymbol{s}_0; \Delta\boldsymbol{s}) \tag{10.82}$$

$$\Delta_s R(\boldsymbol{v}, \boldsymbol{s}_0; \boldsymbol{z}) := R'_s(\boldsymbol{v}, \boldsymbol{s}_0; \boldsymbol{z}, \Delta\boldsymbol{s}) + r_s^R(\boldsymbol{v}, \boldsymbol{s}_0; \boldsymbol{z}, \Delta\boldsymbol{s}) \tag{10.83}$$

with the remainders

$$r_s^J(\boldsymbol{v}, \boldsymbol{s}_0; \Delta\boldsymbol{s}) := \int_0^1 J''_{ss}(\boldsymbol{v}, \boldsymbol{s}_0 + \lambda\Delta\boldsymbol{s}; \Delta\boldsymbol{s}, \Delta\boldsymbol{s})\,(1-\lambda)\,d\lambda, \tag{10.84}$$

$$r_s^R(\boldsymbol{v}, \boldsymbol{s}_0; \boldsymbol{z}, \Delta\boldsymbol{s}) := \int_0^1 R''_{ss}(\boldsymbol{v}, \boldsymbol{s}_0 + \lambda\Delta\boldsymbol{s}; \boldsymbol{z}, \Delta\boldsymbol{s}, \Delta\boldsymbol{s})\,(1-\lambda)\,d\lambda. \tag{10.85}$$

The first-order optimality conditions for the initial problem (10.78) and the changed design (10.79) read

$$L'(\boldsymbol{s}_0)(\boldsymbol{v}_0, \boldsymbol{z}_0)(\Delta\boldsymbol{v}, \Delta\boldsymbol{z}) = 0 \qquad \forall\,\{\Delta\boldsymbol{v}, \Delta\boldsymbol{z}\} \in \mathcal{V} \times \mathcal{V}, \tag{10.86}$$

$$L'(\boldsymbol{s})(\boldsymbol{v}, \boldsymbol{z})(\Delta\boldsymbol{v}, \Delta\boldsymbol{z}) = 0 \qquad \forall\,\{\Delta\boldsymbol{v}, \Delta\boldsymbol{z}\} \in \mathcal{V} \times \mathcal{V}. \tag{10.87}$$

By using (10.80), the total variation $L'(\boldsymbol{s})(\boldsymbol{v}, \boldsymbol{z})(\Delta\boldsymbol{v}, \Delta\boldsymbol{z})$ in (10.87) can also be written as

$$\begin{aligned} L'(\boldsymbol{s})(\boldsymbol{v}, \boldsymbol{z})(\Delta\boldsymbol{v}, \Delta\boldsymbol{z}) &= L'(\boldsymbol{s}_0)(\boldsymbol{v}, \boldsymbol{z})(\Delta\boldsymbol{v}, \Delta\boldsymbol{z}) \\ &\quad + (\Delta_s L)'(\boldsymbol{s}_0)(\boldsymbol{v}, \boldsymbol{z})(\Delta\boldsymbol{v}, \Delta\boldsymbol{z}). \end{aligned} \tag{10.88}$$

The total variation of $L(\boldsymbol{s}_0)(\boldsymbol{v}_0, \boldsymbol{z}_0)$ is given by

$$L'(\boldsymbol{s}_0)(\boldsymbol{v}_0, \boldsymbol{z}_0)(\Delta\boldsymbol{v}, \Delta\boldsymbol{z}) = L'_v(\boldsymbol{s}_0)(\boldsymbol{v}_0, \boldsymbol{z}_0)(\Delta\boldsymbol{v}) + L'_z(\boldsymbol{s}_0)(\boldsymbol{v}_0, \boldsymbol{z}_0)(\Delta\boldsymbol{z}) \tag{10.89}$$

with

$$L'_v(\boldsymbol{s}_0)(\boldsymbol{v}_0,\boldsymbol{z}_0)(\Delta\boldsymbol{v}) = J'_v(\boldsymbol{v}_0,\boldsymbol{s}_0;\Delta\boldsymbol{v}) - R'_v(\boldsymbol{v}_0,\boldsymbol{s}_0;\boldsymbol{z}_0,\Delta\boldsymbol{v}), \tag{10.90}$$

$$L'_z(\boldsymbol{s}_0)(\boldsymbol{v}_0,\boldsymbol{z}_0)(\Delta\boldsymbol{z}) = -R(\boldsymbol{v}_0,\boldsymbol{s}_0;\Delta\boldsymbol{z}). \tag{10.91}$$

In the same manner, the total variation of $\Delta_s L(\boldsymbol{s}_0)(\boldsymbol{v}_0,\boldsymbol{z}_0)$ reads

$$\begin{aligned}(\Delta_s L)'(\boldsymbol{s}_0)(\boldsymbol{v}_0,\boldsymbol{z}_0)(\Delta\boldsymbol{v},\Delta\boldsymbol{z}) = (\Delta_s L)'_v(\boldsymbol{s}_0)(\boldsymbol{v}_0,\boldsymbol{z}_0)(\Delta\boldsymbol{v})\\ + (\Delta_s L)'_z(\boldsymbol{s}_0)(\boldsymbol{v}_0,\boldsymbol{z}_0)(\Delta\boldsymbol{z})\end{aligned} \tag{10.92}$$

with

$$(\Delta_s L)'_v(\boldsymbol{s}_0)(\boldsymbol{v}_0,\boldsymbol{z}_0)(\Delta\boldsymbol{v}) = (\Delta_s J)'_v(\boldsymbol{v}_0,\boldsymbol{s}_0;\Delta\boldsymbol{v}) - (\Delta_s R)'_v(\boldsymbol{v}_0,\boldsymbol{s}_0;\boldsymbol{z}_0,\Delta\boldsymbol{v}), \tag{10.93}$$

$$(\Delta_s L)'_z(\boldsymbol{s}_0)(\boldsymbol{v}_0,\boldsymbol{z}_0)(\Delta\boldsymbol{z}) = -\Delta_s R(\boldsymbol{v}_0,\boldsymbol{s}_0;\Delta\boldsymbol{z}). \tag{10.94}$$

The variations of the increments $\Delta_s J$ and $\Delta_s R$ are given as

$$(\Delta_s J)'_v(\boldsymbol{v}_0,\boldsymbol{s}_0;\Delta\boldsymbol{v}) = J''_{sv}(\boldsymbol{v}_0,\boldsymbol{s}_0;\Delta\boldsymbol{s},\Delta\boldsymbol{v}) + (r^J_s)'_v(\boldsymbol{v}_0,\boldsymbol{s}_0;\Delta\boldsymbol{s},\Delta\boldsymbol{v}) \tag{10.95}$$

$$(\Delta_s R)'_v(\boldsymbol{v}_0,\boldsymbol{s}_0;\boldsymbol{z}_0,\Delta\boldsymbol{v}) = R''_{sv}(\boldsymbol{v}_0,\boldsymbol{s}_0;\boldsymbol{z}_0,\Delta\boldsymbol{s},\Delta\boldsymbol{v}) + (r^R_s)'_v(\boldsymbol{v}_0,\boldsymbol{s}_0;\boldsymbol{z}_0,\Delta\boldsymbol{s},\Delta\boldsymbol{v}) \tag{10.96}$$

with the variations of the remainders

$$(r^J_s)'_v(\boldsymbol{v}_0,\boldsymbol{s}_0;\Delta\boldsymbol{s},\Delta\boldsymbol{v}) = \int_0^1 J'''_{ssv}(\boldsymbol{v}_0,\boldsymbol{s}_0+\lambda\Delta\boldsymbol{s};\Delta\boldsymbol{s},\Delta\boldsymbol{s},\Delta\boldsymbol{v})\,(1-\lambda)\,d\lambda, \tag{10.97}$$

$$\begin{aligned}&(r^R_s)'_v(\boldsymbol{v}_0,\boldsymbol{s}_0;\boldsymbol{z}_0,\Delta\boldsymbol{s},\Delta\boldsymbol{v})\\ &\qquad = \int_0^1 R'''_{ssv}(\boldsymbol{v}_0,\boldsymbol{s}_0+\lambda\Delta\boldsymbol{s};\boldsymbol{z}_0,\Delta\boldsymbol{s},\Delta\boldsymbol{s},\Delta\boldsymbol{v})\,(1-\lambda)\,d\lambda.\end{aligned} \tag{10.98}$$

Furthermore, let $\{\boldsymbol{v}_0,\boldsymbol{z}_0\} \in \mathcal{V}\times\mathcal{V}$ and $\{\boldsymbol{v},\boldsymbol{z}\} \in \mathcal{V}\times\mathcal{V}$ be solutions of (10.86) and (10.87), respectively. Then, the quantity of interest is given by evaluating $L(\boldsymbol{s}_0)(\boldsymbol{v}_0,\boldsymbol{z}_0)$ and $L(\boldsymbol{s})(\boldsymbol{v},\boldsymbol{z})$, i.e.

$$J(\boldsymbol{v}_0,\boldsymbol{s}_0) = L(\boldsymbol{s}_0)(\boldsymbol{v}_0,\boldsymbol{z}_0), \tag{10.99}$$

$$J(\boldsymbol{v},\boldsymbol{s}) \quad = L(\boldsymbol{s})(\boldsymbol{v},\boldsymbol{z}) = L(\boldsymbol{s}_0)(\boldsymbol{v},\boldsymbol{z}) + \Delta_s L(\boldsymbol{s}_0)(\boldsymbol{v},\boldsymbol{z}), \tag{10.100}$$

because $R(\boldsymbol{v}_0,\boldsymbol{s}_0;\boldsymbol{z}_0) = 0$ and $R(\boldsymbol{v},\boldsymbol{s};\boldsymbol{z}) = 0$.

Finally, the change in the quantity of interest $\Delta J = J(\boldsymbol{v},\boldsymbol{s}) - J(\boldsymbol{v}_0,\boldsymbol{s}_0)$ can be equivalently expressed in terms of the change in the Lagrangian functionals $L(\boldsymbol{s})(\boldsymbol{v},\boldsymbol{z}) - L(\boldsymbol{s}_0)(\boldsymbol{v}_0,\boldsymbol{z}_0)$. This is accomplished in the following result.

Theorem 10.3 (Exact change in the quantity of interest) *Let the residual $R(\boldsymbol{v}, \boldsymbol{s}; \cdot)$ and the functional $J(\boldsymbol{v}, \boldsymbol{s})$ be sufficiently differentiable with respect to $\boldsymbol{v}$ and $\boldsymbol{s}$. Then it holds for the change in the quantity of interest $\Delta J = J(\boldsymbol{v}, \boldsymbol{s}) - J(\boldsymbol{v}_0, \boldsymbol{s}_0)$ due to changes in the design $\Delta \boldsymbol{s}$ that*

$$\begin{aligned} J(\boldsymbol{v}, \boldsymbol{s}) - J(\boldsymbol{v}_0, \boldsymbol{s}_0) &= \Delta J(\boldsymbol{v}_0, \boldsymbol{s}_0, \boldsymbol{z}_0)(\Delta \boldsymbol{v}, \Delta \boldsymbol{s}, \Delta \boldsymbol{z}) \\ &= \Delta_s J(\boldsymbol{v}_0, \boldsymbol{s}_0) - \Delta_s R(\boldsymbol{v}_0, \boldsymbol{s}_0; \boldsymbol{z}_0) - \frac{1}{2}\, \Delta_s R(\boldsymbol{v}_0, \boldsymbol{s}_0; \Delta \boldsymbol{z}) \\ &\quad + \frac{1}{2}\, [\, (\Delta_s J)'_v(\boldsymbol{v}_0, \boldsymbol{s}_0; \Delta \boldsymbol{v}) - (\Delta_s R)'_v(\boldsymbol{v}_0, \boldsymbol{s}_0; \boldsymbol{z}_0, \Delta \boldsymbol{v})\,] \\ &\quad + \frac{1}{2}\, r^L(\boldsymbol{s})(\boldsymbol{v}_0, \boldsymbol{z}_0; \Delta \boldsymbol{v}, \Delta \boldsymbol{z}). \end{aligned} \tag{10.101}$$

The increments $\Delta_s J$ and $\Delta_s R$ are defined in (10.82) and (10.83) and the variations of the increments $(\Delta_s J)'_v$ and $(\Delta_s R)'_v$ are given in (10.95) and (10.96), respectively. Furthermore, the remainder $r^L(\boldsymbol{s})(\boldsymbol{v}_0, \boldsymbol{z}_0; \Delta \boldsymbol{v}, \Delta \boldsymbol{z})$ is cubic in $\Delta \boldsymbol{v}$ and reads

$$\begin{aligned} & r^L(\boldsymbol{s})(\boldsymbol{v}_0, \boldsymbol{z}_0; \Delta \boldsymbol{v}, \Delta \boldsymbol{z}) \\ &= \int_0^1 \{\, J'''_{vvv}(\boldsymbol{v}_0 + \lambda \Delta \boldsymbol{v}, \boldsymbol{s}_0; \Delta \boldsymbol{v}, \Delta \boldsymbol{v}, \Delta \boldsymbol{v}) \\ &\qquad - R'''_{vvv}(\boldsymbol{v}_0 + \lambda \Delta \boldsymbol{v}, \boldsymbol{s}_0; \boldsymbol{z}_0 + \lambda \Delta \boldsymbol{z}, \Delta \boldsymbol{v}, \Delta \boldsymbol{v}, \Delta \boldsymbol{v}) \\ &\qquad - 3\, R''_{vv}(\boldsymbol{v}_0 + \lambda \Delta \boldsymbol{v}, \boldsymbol{s}_0; \Delta \boldsymbol{z}, \Delta \boldsymbol{v}, \Delta \boldsymbol{v}) \\ &\qquad + (\Delta_s J)'''_{vvv}(\boldsymbol{v}_0 + \lambda \Delta \boldsymbol{v}, \boldsymbol{s}_0; \Delta \boldsymbol{v}, \Delta \boldsymbol{v}, \Delta \boldsymbol{v}) \\ &\qquad - (\Delta_s R)'''_{vvv}(\boldsymbol{v}_0 + \lambda \Delta \boldsymbol{v}, \boldsymbol{s}_0; \boldsymbol{z}_0 + \lambda \Delta \boldsymbol{z}, \Delta \boldsymbol{v}, \Delta \boldsymbol{v}, \Delta \boldsymbol{v}) \\ &\qquad - 3\, (\Delta_s R)''_{vv}(\boldsymbol{v}_0 + \lambda \Delta \boldsymbol{v}, \boldsymbol{s}_0; \Delta \boldsymbol{z}, \Delta \boldsymbol{v}, \Delta \boldsymbol{v})\} \, \lambda(\lambda - 1)\, d\lambda. \end{aligned} \tag{10.102}$$

Proof. Let $\mathcal{X} := \mathcal{V} \times \mathcal{V}$ be a product space and set $\boldsymbol{x}_0 := \{\boldsymbol{v}_0, \boldsymbol{z}_0\} \in \mathcal{X}$, $\boldsymbol{x} := \{\boldsymbol{v}, \boldsymbol{z}\} \in \mathcal{X}$ as well as $\Delta \boldsymbol{x} := \{\Delta \boldsymbol{v}, \Delta \boldsymbol{z}\} \in \mathcal{X}$. Then, the Lagrangian functionals (10.78) and (10.80) are given by

$$\begin{aligned} \mathcal{L}(\boldsymbol{s}_0)(\boldsymbol{x}_0) &= L(\boldsymbol{s}_0)(\boldsymbol{v}_0, \boldsymbol{z}_0), \\ \mathcal{L}(\boldsymbol{s})(\boldsymbol{x}) &= L(\boldsymbol{s})(\boldsymbol{v}, \boldsymbol{z}) \\ &= \mathcal{L}(\boldsymbol{s}_0)(\boldsymbol{x}) + \Delta_s \mathcal{L}(\boldsymbol{s}_0)(\boldsymbol{x}) = L(\boldsymbol{s}_0)(\boldsymbol{v}, \boldsymbol{z}) + \Delta_s L(\boldsymbol{s}_0)(\boldsymbol{v}, \boldsymbol{z}). \end{aligned}$$

Furthermore, we have

$$\mathcal{L}(\boldsymbol{s}_0)(\boldsymbol{x}_0) = \mathcal{L}(\boldsymbol{s})(\boldsymbol{x}_0) - \Delta_s \mathcal{L}(\boldsymbol{s}_0)(\boldsymbol{x}_0).$$

The change in the quantity of interest can be expressed in terms of the change in the Lagrangian functionals, i.e.

$$\begin{aligned} J(\boldsymbol{v},\boldsymbol{s}) - J(\boldsymbol{v}_0,\boldsymbol{s}_0) &= \mathcal{L}(\boldsymbol{s})(\boldsymbol{x}) - \mathcal{L}(\boldsymbol{s}_0)(\boldsymbol{x}_0) \\ &= \mathcal{L}(\boldsymbol{s})(\boldsymbol{x}) - \mathcal{L}(\boldsymbol{s})(\boldsymbol{x}_0) + \Delta_s\mathcal{L}(\boldsymbol{s}_0)(\boldsymbol{x}_0) \\ &= \mathcal{L}(\boldsymbol{s})(\boldsymbol{x}) - \mathcal{L}(\boldsymbol{s})(\boldsymbol{x}_0) + \Delta_s J(\boldsymbol{v}_0,\boldsymbol{s}_0) - \Delta_s R(\boldsymbol{v}_0,\boldsymbol{s}_0;\boldsymbol{z}_0). \end{aligned}$$

Using (10.13) we obtain the representation

$$\begin{aligned} \mathcal{L}(\boldsymbol{s})(\boldsymbol{x}) - \mathcal{L}(\boldsymbol{s})(\boldsymbol{x}_0) = \frac{1}{2}\,[\,\mathcal{L}'(\boldsymbol{s})(\boldsymbol{x}_0)(\Delta\boldsymbol{x}) + \mathcal{L}'(\boldsymbol{s})(\boldsymbol{x}_0+\Delta\boldsymbol{x})(\Delta\boldsymbol{x})\,] \\ + \frac{1}{2}\,r^L(\boldsymbol{s})(\boldsymbol{x}_0;\Delta\boldsymbol{x}). \end{aligned}$$

Because of (10.87), the second term vanishes, i.e.

$$\mathcal{L}'(\boldsymbol{s})(\boldsymbol{x}_0+\Delta\boldsymbol{x})(\Delta\boldsymbol{x}) = \mathcal{L}'(\boldsymbol{s})(\boldsymbol{x})(\Delta\boldsymbol{x}) = 0.$$

Furthermore, using (10.88) and (10.86), we have for the first term

$$\begin{aligned} \mathcal{L}'(\boldsymbol{s})(\boldsymbol{x}_0)(\Delta\boldsymbol{x}) &= \mathcal{L}'(\boldsymbol{s}_0)(\boldsymbol{x}_0)(\Delta\boldsymbol{x}) + (\Delta_s\mathcal{L})'(\boldsymbol{s}_0)(\boldsymbol{x}_0)(\Delta\boldsymbol{x}) \\ &= (\Delta_s\mathcal{L})'(\boldsymbol{s}_0)(\boldsymbol{x}_0)(\Delta\boldsymbol{x}). \end{aligned}$$

The variation $(\Delta_s\mathcal{L})'(\boldsymbol{s}_0)(\boldsymbol{x}_0;\Delta\boldsymbol{x})$ is given with (10.93) and (10.94) in form of

$$\begin{aligned} (\Delta_s\mathcal{L})'(\boldsymbol{s}_0)(\boldsymbol{x}_0)(\Delta\boldsymbol{x}) &= (\Delta_s L)'_v(\boldsymbol{s}_0)(\boldsymbol{v}_0,\boldsymbol{z}_0)(\Delta\boldsymbol{v}) + (\Delta_s L)'_z(\boldsymbol{s}_0)(\boldsymbol{v}_0,\boldsymbol{z}_0)(\Delta\boldsymbol{z}) \\ &= (\Delta_s J)'_v(\boldsymbol{v}_0,\boldsymbol{s}_0;\Delta\boldsymbol{v}) - (\Delta_s R)'_v(\boldsymbol{v}_0,\boldsymbol{s}_0;\boldsymbol{z}_0,\Delta\boldsymbol{v}) \\ &\quad - \Delta_s R(\boldsymbol{v}_0,\boldsymbol{s}_0;\Delta\boldsymbol{z}). \end{aligned}$$

Finally, the reminder term $r^L(\boldsymbol{s})(\boldsymbol{x}_0;\Delta\boldsymbol{x})$ according to (10.16) is cubic in $\Delta\boldsymbol{x}$ and reads

$$\begin{aligned} r^L(\boldsymbol{s})(\boldsymbol{x}_0;\Delta\boldsymbol{x}) &= \int_0^1 \mathcal{L}'''(\boldsymbol{s})(\boldsymbol{x}_0+\lambda\Delta\boldsymbol{x})(\Delta\boldsymbol{x},\Delta\boldsymbol{x},\Delta\boldsymbol{x})\,\lambda(\lambda-1)\,d\lambda \\ &= \int_0^1 \{\,\mathcal{L}'''(\boldsymbol{s}_0)(\boldsymbol{x}_0+\lambda\Delta\boldsymbol{x})(\Delta\boldsymbol{x},\Delta\boldsymbol{x},\Delta\boldsymbol{x}) \\ &\quad + (\Delta_s\mathcal{L})'''(\boldsymbol{s}_0)(\boldsymbol{x}_0+\lambda\Delta\boldsymbol{x})(\Delta\boldsymbol{x},\Delta\boldsymbol{x},\Delta\boldsymbol{x})\}\,\lambda(\lambda-1)\,d\lambda, \end{aligned}$$

where

$$\begin{aligned} &\mathcal{L}'''(\boldsymbol{s}_0)(\boldsymbol{x}_0+\lambda\Delta\boldsymbol{x})(\Delta\boldsymbol{x},\Delta\boldsymbol{x},\Delta\boldsymbol{x}) \\ &\quad = J'''_{vvv}(\boldsymbol{v}_0+\lambda\Delta\boldsymbol{v},\boldsymbol{s}_0;\Delta\boldsymbol{v},\Delta\boldsymbol{v},\Delta\boldsymbol{v}) \\ &\quad - R'''_{vvv}(\boldsymbol{v}_0+\lambda\Delta\boldsymbol{v},\boldsymbol{s}_0;\boldsymbol{z}_0+\lambda\Delta\boldsymbol{z},\Delta\boldsymbol{v},\Delta\boldsymbol{v},\Delta\boldsymbol{v}) \\ &\quad - 3\,R''_{vv}(\boldsymbol{v}_0+\lambda\Delta\boldsymbol{v},\boldsymbol{s}_0;\Delta\boldsymbol{z},\Delta\boldsymbol{v},\Delta\boldsymbol{v}), \end{aligned}$$

$$
\begin{aligned}
(\Delta_s \mathcal{L})'''(\boldsymbol{s}_0)(\boldsymbol{x}_0 + \lambda \Delta \boldsymbol{x})(\Delta \boldsymbol{x}, \Delta \boldsymbol{x}, \Delta \boldsymbol{x}) \\
&= (\Delta_s J)'''_{vvv}(\boldsymbol{v}_0 + \lambda \Delta \boldsymbol{v}, \boldsymbol{s}_0; \Delta \boldsymbol{v}, \Delta \boldsymbol{v}, \Delta \boldsymbol{v}) \\
&- (\Delta_s R)'''_{vvv}(\boldsymbol{v}_0 + \lambda \Delta \boldsymbol{v}, \boldsymbol{s}_0; \boldsymbol{z}_0 + \lambda \Delta \boldsymbol{z}, \Delta \boldsymbol{v}, \Delta \boldsymbol{v}, \Delta \boldsymbol{v}) \\
&- 3\,(\Delta_s R)''_{vv}(\boldsymbol{v}_0 + \lambda \Delta \boldsymbol{v}, \boldsymbol{s}_0; \Delta \boldsymbol{z}, \Delta \boldsymbol{v}, \Delta \boldsymbol{v}).
\end{aligned}
$$

This yields the stated result in (10.101). □

10.4.2 The error in the change of the quantity of interest

A first-order sensitivity relation for the change in the quantity of interest due to variations $\delta \boldsymbol{s}$ has been introduced in Section 6.3.4 in Eq. 6.27 in form of

$$
\begin{aligned}
\delta J = J'_v(\boldsymbol{v}_0, \boldsymbol{s}_0; \delta \boldsymbol{v}) &= -Q(\boldsymbol{v}_0, \boldsymbol{s}_0; \boldsymbol{z}_0) \\
&= -p(\boldsymbol{v}_0, \boldsymbol{s}_0; \boldsymbol{z}_0, \delta \boldsymbol{s}) = -R'_s(\boldsymbol{v}_0, \boldsymbol{s}_0; \boldsymbol{z}_0, \delta \boldsymbol{s}),
\end{aligned}
$$

where $\boldsymbol{z}_0$ denotes the dual solution corresponding to the quantity of interest obtained on the initial design $\boldsymbol{s}_0$. For a finite value of design changes $\Delta \boldsymbol{s}$ this relations yields just an approximation $\Delta \tilde{J}$ for the change in the quantity of interest, i.e.

$$
J(\boldsymbol{v}, \boldsymbol{s}) - J(\boldsymbol{v}_0, \boldsymbol{s}_0) \approx \Delta \tilde{J} = J'_v(\boldsymbol{v}_0, \boldsymbol{s}_0; \Delta \tilde{\boldsymbol{v}}) = -R'_s(\boldsymbol{v}_0, \boldsymbol{s}_0; \boldsymbol{z}_0, \Delta \boldsymbol{s}). \tag{10.103}
$$

Furthermore, a representation for the exact increment ΔJ has been derived in (10.101). The distance between the first-order approximation $\Delta \tilde{J}$ and ΔJ can now easily be obtained.

Theorem 10.4 *Let $\Delta \tilde{J}$ be the solution of the first-order sensitivity relation (10.103) and let ΔJ be the solution of the exact sensitivity relation (10.101). Then, it holds for the error $\Delta J - \Delta \tilde{J}$ that*

$$
\begin{aligned}
\Delta J - \Delta \tilde{J} = \Delta_s J(\boldsymbol{v}_0, \boldsymbol{s}_0) &- \frac{1}{2}\,\Delta_s R(\boldsymbol{v}_0, \boldsymbol{s}_0; \Delta \boldsymbol{z}) - r^R_s(\boldsymbol{v}_0, \boldsymbol{s}_0; \boldsymbol{z}_0, \Delta \boldsymbol{s}) \\
&+ \frac{1}{2}\,[\,(\Delta_s J)'_v(\boldsymbol{v}_0, \boldsymbol{s}_0; \Delta \boldsymbol{v}) - (\Delta_s R)'_v(\boldsymbol{v}_0, \boldsymbol{s}_0; \boldsymbol{z}_0, \Delta \boldsymbol{v})\,] \\
&+ \frac{1}{2}\,r^L(\boldsymbol{s})(\boldsymbol{v}_0, \boldsymbol{z}_0; \Delta \boldsymbol{v}, \Delta \boldsymbol{z}),
\end{aligned} \tag{10.104}
$$

where the reminders $r^R_s(\boldsymbol{v}_0, \boldsymbol{s}_0; \boldsymbol{z}_0, \Delta \boldsymbol{s})$ and $r^L(\boldsymbol{s})(\boldsymbol{v}_0, \boldsymbol{z}_0; \Delta \boldsymbol{v}, \Delta \boldsymbol{z})$ are defined in (10.85) and (10.102), respectively.

***Proof*.** The proof is straightforward. We subtract (10.103) from (10.101) and use the definition of the increment $\Delta_s R(\boldsymbol{v}_0, \boldsymbol{s}_0; \boldsymbol{z}_0)$ in (10.83). □

10.4.3 An error estimator for the change in the quantity of interest

The exact sensitivity relation (10.101) contains the exact increments $\Delta \boldsymbol{v}$ and $\Delta \boldsymbol{z}$ which are in general unknown. But the first-order approximations for the change in the state $\Delta \tilde{\boldsymbol{v}}$ and the change in the dual solution $\Delta \tilde{\boldsymbol{z}}$ can be used in order to obtain a better approximation as the first-order sensitivity relation (10.103).

These relations have been introduced in (4.21) and (6.94) in form of

$$k(\boldsymbol{v}_0, \boldsymbol{s}_0; \boldsymbol{\eta}, \Delta \tilde{\boldsymbol{v}}) = -Q(\boldsymbol{v}_0, \boldsymbol{s}_0; \boldsymbol{\eta}) \quad \forall\, \boldsymbol{\eta} \in \mathcal{V},$$

$$k(\boldsymbol{v}_0, \boldsymbol{s}_0; \Delta \tilde{\boldsymbol{z}}, \boldsymbol{\eta}) = -Q^*_{\text{full}}(\boldsymbol{v}_0, \boldsymbol{s}_0; \boldsymbol{z}_0, \boldsymbol{\eta}) \quad \forall\, \boldsymbol{\eta} \in \mathcal{V}.$$

The discrete formulations of these relations are given in (4.52) and (6.98) as

$$\boldsymbol{K} \Delta \tilde{\boldsymbol{v}} = -\boldsymbol{Q} \qquad \text{and} \qquad \boldsymbol{K} \Delta \tilde{\boldsymbol{z}} = -\boldsymbol{Q}^*_{\text{full}},$$

where $\boldsymbol{Q} = \boldsymbol{P} \Delta \boldsymbol{s}$ and $\boldsymbol{Q}^*_{\text{full}} = [\, \boldsymbol{P}^* - \boldsymbol{B}^* \boldsymbol{K}^{-1} \boldsymbol{P} \,] \, \Delta \boldsymbol{s}$, respectively.

With $\Delta \tilde{\boldsymbol{v}}$ and $\Delta \tilde{\boldsymbol{z}}$ at hand, an improved solution for the change in the quantity of interest $\Delta \tilde{J}^*$ can be obtained from (10.101) as

$$\begin{aligned} J(\boldsymbol{v}, \boldsymbol{s}) - J(\boldsymbol{v}_0, \boldsymbol{s}_0) &\cong \Delta \tilde{J}^*(\boldsymbol{v}_0, \boldsymbol{s}_0, \boldsymbol{z}_0)(\Delta \tilde{\boldsymbol{v}}, \Delta \boldsymbol{s}, \Delta \tilde{\boldsymbol{z}}) \\ &= \Delta_s J(\boldsymbol{v}_0, \boldsymbol{s}_0) - \Delta_s R(\boldsymbol{v}_0, \boldsymbol{s}_0; \boldsymbol{z}_0) - \frac{1}{2} \Delta_s R(\boldsymbol{v}_0, \boldsymbol{s}_0; \Delta \tilde{\boldsymbol{z}}) \\ &\quad + \frac{1}{2} \left[\, (\Delta_s J)'_v(\boldsymbol{v}_0, \boldsymbol{s}_0; \Delta \tilde{\boldsymbol{v}}) - (\Delta_s R)'_v(\boldsymbol{v}_0, \boldsymbol{s}_0; \boldsymbol{z}_0, \Delta \tilde{\boldsymbol{v}}) \, \right], \end{aligned} \tag{10.105}$$

in which the cubic reminder $r^L(\boldsymbol{s})(\boldsymbol{v}_0, \boldsymbol{z}_0; \Delta \tilde{\boldsymbol{v}}, \Delta \tilde{\boldsymbol{z}})$ has been omitted. For suitable chosen design changes $\Delta \boldsymbol{s}$ and good approximations $\Delta \tilde{\boldsymbol{v}}$ and $\Delta \tilde{\boldsymbol{z}}$ this relation yields an adequate estimator for the true change in the quantity of interest.

Furthermore, the relation (10.105) could be advanced further if some improved solutions of the state $\Delta \tilde{\boldsymbol{v}}^*$ and the dual solution $\Delta \tilde{\boldsymbol{z}}^*$ are used, which could be obtained by an improvement algorithm as proposed in Section 10.3.

10.5 On model error and design sensitivity analysis

The *model error* is a part of the error due to the natural imperfections in abstract models of actual physical phenomena. This has been studied in recent years in a series of papers, see e.g. [18, 84, 86, 94, 95] and the references therein for an overview. Furthermore, combined model and discretization error control and adaptive algorithms have been investigated.

The estimation of the modeling error is in an abstract sense closely related to design sensitivity analysis, if the change in a model is interpreted as a design change. It is assumed that the considered model is parameterized by a design function $\boldsymbol{s}$.

For instance, an important applications of the modeling error estimation is the analysis of heterogeneous elastic materials [84, 86]. In this application the elasticity tensor depends in an abstract sense on a design variable, i.e. $\mathbb{C} = \mathbb{C}(\boldsymbol{s})$. The tensor $\mathbb{C}_0 = \mathbb{C}(\boldsymbol{s}_0)$ is an approximation obtained through some homogenization process and the homogenization is controlled by $\boldsymbol{s}$. Let $\boldsymbol{v}_0 \in \mathcal{V}$ be the solution of this initial problem or *coarse model* with $\mathbb{C}_0$. Furthermore, let $\boldsymbol{v} \in \mathcal{V}$ be the solution for the changed problem or *fine model* with some $\mathbb{C}(\boldsymbol{s})$. Then, both problems are given as

$$R(\boldsymbol{v}_0, \boldsymbol{s}_0; \boldsymbol{\eta}) = 0 \quad \forall\, \boldsymbol{\eta} \in \mathcal{V} \quad \text{initial or coarse model (design)} \tag{10.106}$$

$$R(\boldsymbol{v}, \boldsymbol{s}; \boldsymbol{\eta}) \quad = 0 \quad \forall\, \boldsymbol{\eta} \in \mathcal{V} \quad \text{changed or fine model (design).} \tag{10.107}$$

These equations correspond to those introduced for the initial and changed design in (10.17) and (10.18), respectively.

The error or the difference between the solutions $\boldsymbol{e}_m = \boldsymbol{v} - \boldsymbol{v}_0 = \Delta\boldsymbol{v}$ is the modeling error $\boldsymbol{e}_m$ or the change in the state $\Delta\boldsymbol{v}$ due to different homogenized elasticity tensors. With this in mind, the above proposed sensitivity and error relations can be used to estimate the modeling error for the state or a chosen quantity of interest if the design function controls in an abstract sense the considered model.

10.6 Explicit variational formulations for shape sensitivity

The computation of the the exact pseudo load $Q_{\mathrm{ex}}(\boldsymbol{v})(\boldsymbol{v}_0, \boldsymbol{s}_0; \boldsymbol{\eta})$ requires higher-order variations of the residual $R(\cdot, \cdot; \cdot)$ with respect to $\boldsymbol{v}$ and $\boldsymbol{s}$. Explicit formulations of these higher-order variations for shape sensitivity for the model problem of nonlinear elasticity are derived within this section. A compact specification of all higher-order variations of $R(\boldsymbol{v}, \boldsymbol{s}, \cdot)$ are given in Appendix B.1.2. Those formulations can directly be implemented in standard finite element programs as the usual residuals. Furthermore, the explicit formulations in terms of linearized elasticity are stated in Appendix B.2.7.

Computation of R''_{vv}. The second variation of the primal physical residual $R(\boldsymbol{v}, \boldsymbol{s}; \cdot)$ given in (4.85) with respect to the state $\boldsymbol{v}$ is obtained in form of

$$\begin{aligned} R''_{vv}(\boldsymbol{v}, \boldsymbol{s}; \boldsymbol{\eta}, \Delta\boldsymbol{v}, \Delta\boldsymbol{v}) &= k'_v(\boldsymbol{v}, \boldsymbol{s}; \boldsymbol{\eta}, \Delta\boldsymbol{v}, \Delta\boldsymbol{v}) \\ &= \int_{\Omega_R} \{\, 2\, \mathbf{E}''_{vv}(\boldsymbol{\eta}, \Delta\boldsymbol{v}) : \mathbb{C} : \mathbf{E}'_v(\boldsymbol{v}, \Delta\boldsymbol{v}) \\ &\qquad + \mathbf{E}'_v(\boldsymbol{v}, \boldsymbol{\eta}) : \mathbb{C} : \mathbf{E}''_{vv}(\Delta\boldsymbol{v}, \Delta\boldsymbol{v}) \\ &\qquad + \mathbf{E}'_v(\boldsymbol{v}, \boldsymbol{\eta}) : \boldsymbol{\mathcal{D}} : \mathbf{E}'_v(\boldsymbol{v}, \Delta\boldsymbol{v}) : \mathbf{E}'_v(\boldsymbol{v}, \Delta\boldsymbol{v}) \,\}\, \mathrm{d}\Omega. \end{aligned} \tag{10.108}$$

The form is quadratic in $\Delta\boldsymbol{v}$. For chosen fixed $\Delta\boldsymbol{v}$ the form R''_{vv} is a linear form. An explicit and compact specification of R''_{vv} is given in Box B.6.

Computation of R''_{ss}. The second variation with respect to $\boldsymbol{s}$ reads

$$\begin{aligned}
R''_{ss}(\boldsymbol{v},\boldsymbol{s};\boldsymbol{\eta},\Delta\boldsymbol{s},\Delta\boldsymbol{s}) &= p'_s(\boldsymbol{v},\boldsymbol{s};\boldsymbol{\eta},\Delta\boldsymbol{s},\Delta\boldsymbol{s}) \\
&= \int_{\Omega_R} \{\, 2\,\mathbf{E}''_{vs}(\boldsymbol{v},\boldsymbol{\eta},\Delta\boldsymbol{s}) : \mathbb{C} : \mathbf{E}'_s(\boldsymbol{v},\Delta\boldsymbol{s}) \\
&\qquad + \mathbf{S} : \mathbf{E}'''_{vss}(\boldsymbol{v},\boldsymbol{\eta},\Delta\boldsymbol{s},\Delta\boldsymbol{s}) \\
&\qquad + \mathbf{E}'_v(\boldsymbol{v},\boldsymbol{\eta}) : \mathbb{C} : \mathbf{E}''_{ss}(\boldsymbol{v},\Delta\boldsymbol{s},\Delta\boldsymbol{s}) \\
&\qquad + \mathbf{E}'_v(\boldsymbol{v},\boldsymbol{\eta}) : \boldsymbol{\mathcal{D}} : \mathbf{E}'_s(\boldsymbol{v},\Delta\boldsymbol{s}) : \mathbf{E}'_s(\boldsymbol{v},\Delta\boldsymbol{s}) \\
&\qquad + 2\,[\,\mathbf{S} : \mathbf{E}''_{vs}(\boldsymbol{v},\boldsymbol{\eta},\Delta\boldsymbol{s}) + \mathbf{E}'_v(\boldsymbol{v},\boldsymbol{\eta}) : \mathbb{C} : \mathbf{E}'_s(\boldsymbol{v},\Delta\boldsymbol{s})\,]\,\mathrm{Div}\,\Delta\boldsymbol{s} \\
&\qquad - [\,\mathbf{S} : \mathbf{E}'_v(\boldsymbol{v},\boldsymbol{\eta}) - \boldsymbol{b}_R\cdot\boldsymbol{\eta}\,]\,\mathbf{I} : \mathrm{Grad}\,\Delta\boldsymbol{s}\,\mathrm{Grad}\,\Delta\boldsymbol{s} \\
&\qquad + [\,\mathbf{S} : \mathbf{E}'_v(\boldsymbol{v},\boldsymbol{\eta}) - \boldsymbol{b}_R\cdot\boldsymbol{\eta}\,]\,\mathrm{Div}\,\Delta\boldsymbol{s}\,\mathrm{Div}\,\Delta\boldsymbol{s}\,\}\,\mathrm{d}\Omega,
\end{aligned} \tag{10.109}$$

where

$$\begin{aligned}
\mathbf{E}'''_{vss}(\boldsymbol{v},\boldsymbol{\eta},\Delta\boldsymbol{s},\Delta\boldsymbol{s}) = 2\,\mathrm{sym}\{\,&\mathrm{Grad}\,\Delta\boldsymbol{s}^T\,\mathrm{Grad}\,\Delta\boldsymbol{s}^T\,\mathrm{Grad}\,\boldsymbol{v}^T\,\mathrm{Grad}\,\boldsymbol{\eta} \\
&+ \mathrm{Grad}\,\Delta\boldsymbol{s}^T\,\mathrm{Grad}\,\boldsymbol{v}^T\,\mathrm{Grad}\,\boldsymbol{\eta}\,\mathrm{Grad}\,\Delta\boldsymbol{s} \\
&+ \mathbf{F}^T\,\mathrm{Grad}\,\boldsymbol{\eta}\,\mathrm{Grad}\,\Delta\boldsymbol{s}\,\mathrm{Grad}\,\Delta\boldsymbol{s}\,\}.
\end{aligned} \tag{10.110}$$

For chosen fixed $\Delta\boldsymbol{s}$ the form becomes is a linear functional, see Box B.7.

Computation of R''_{sv}. The mixed variation of $R(\boldsymbol{v},\boldsymbol{s};\cdot)$ is obtained as

$$\begin{aligned}
R''_{sv}(\boldsymbol{v},\boldsymbol{s};\boldsymbol{\eta},\Delta\boldsymbol{s},\Delta\boldsymbol{v}) &= p'_v(\boldsymbol{v},\boldsymbol{s};\boldsymbol{\eta},\Delta\boldsymbol{s},\Delta\boldsymbol{v}) \\
&= \int_{\Omega_R} \{\, \mathbf{E}''_{vs}(\boldsymbol{v},\boldsymbol{\eta},\Delta\boldsymbol{s}) : \mathbb{C} : \mathbf{E}'_v(\boldsymbol{v},\Delta\boldsymbol{v}) \\
&\qquad + \mathbf{S} : \mathbf{E}'''_{vsv}(\boldsymbol{\eta},\Delta\boldsymbol{s},\Delta\boldsymbol{v}) \\
&\qquad + \mathbf{E}''_{vv}(\boldsymbol{\eta},\Delta\boldsymbol{v}) : \mathbb{C} : \mathbf{E}'_s(\boldsymbol{v},\Delta\boldsymbol{s}) \\
&\qquad + \mathbf{E}'_v(\boldsymbol{v},\boldsymbol{\eta}) : \mathbb{C} : \mathbf{E}''_{sv}(\boldsymbol{v},\Delta\boldsymbol{s},\Delta\boldsymbol{v}) \\
&\qquad + \mathbf{E}'_v(\boldsymbol{v},\boldsymbol{\eta}) : \boldsymbol{\mathcal{D}} : \mathbf{E}'_v(\boldsymbol{v},\Delta\boldsymbol{v}) : \mathbf{E}'_s(\boldsymbol{v},\Delta\boldsymbol{s}) \\
&\qquad + [\,\mathbf{S} : \mathbf{E}''_{vv}(\boldsymbol{\eta},\Delta\boldsymbol{v}) + \mathbf{E}'_v(\boldsymbol{v},\boldsymbol{\eta}) : \mathbb{C} : \mathbf{E}'_v(\boldsymbol{v},\Delta\boldsymbol{v})\,]\,\mathrm{Div}\,\Delta\boldsymbol{s}\,\}\,\mathrm{d}\Omega,
\end{aligned} \tag{10.111}$$

where

$$\begin{aligned}\mathbf{E}'''_{vsv}(\boldsymbol{\eta}, \Delta\boldsymbol{s}, \Delta\boldsymbol{v}) = -\operatorname{sym}\{ &\operatorname{Grad}\Delta\boldsymbol{s}^T \operatorname{Grad}\Delta\boldsymbol{v}^T \operatorname{Grad}\boldsymbol{\eta} \\ &+ \operatorname{Grad}\Delta\boldsymbol{v}^T \operatorname{Grad}\boldsymbol{\eta} \operatorname{Grad}\Delta\boldsymbol{s}\}.\end{aligned} \tag{10.112}$$

A compact representation is given in Box B.8.

Computation of R'''_{svv}. The third variation of the primal physical residual $R(\boldsymbol{v}, \boldsymbol{s}; \cdot)$ with respect to $\boldsymbol{v}$ reads

$$\begin{aligned}R'''_{svv}(\boldsymbol{v}, \boldsymbol{s}; \boldsymbol{\eta}, \Delta\boldsymbol{s}, \Delta\boldsymbol{v}, \Delta\boldsymbol{v}) &= p'''_{vv}(\boldsymbol{v}, \boldsymbol{s}; \boldsymbol{\eta}, \Delta\boldsymbol{s}, \Delta\boldsymbol{v}, \Delta\boldsymbol{v}) \\ = \int_{\Omega_R} \{ &\mathbf{E}''_{vs}(\boldsymbol{v}, \boldsymbol{\eta}, \Delta\boldsymbol{s}) : \mathbb{C} : \mathbf{E}''_{vv}(\Delta\boldsymbol{v}, \Delta\boldsymbol{v}) \\ &+ 2\,\mathbf{E}'''_{vsv}(\boldsymbol{\eta}, \Delta\boldsymbol{s}, \Delta\boldsymbol{v}) : \mathbb{C} : \mathbf{E}'_{v}(\boldsymbol{v}, \Delta\boldsymbol{v}) \\ &+ 2\,\mathbf{E}''_{vv}(\boldsymbol{\eta}, \Delta\boldsymbol{v}) : \mathbb{C} : \mathbf{E}''_{sv}(\boldsymbol{v}, \Delta\boldsymbol{s}, \Delta\boldsymbol{v}) \\ &+ \mathbf{E}'_{v}(\boldsymbol{v}, \boldsymbol{\eta}) : \mathbb{C} : \mathbf{E}'''_{svv}(\Delta\boldsymbol{s}, \Delta\boldsymbol{v}, \Delta\boldsymbol{v}) \\ &+ 2\,\mathbf{E}''_{vv}(\boldsymbol{\eta}, \Delta\boldsymbol{v}) : \boldsymbol{\mathcal{D}} : \mathbf{E}'_{v}(\boldsymbol{v}, \Delta\boldsymbol{v}) : \mathbf{E}'_{s}(\boldsymbol{v}, \Delta\boldsymbol{s}) \\ &+ 2\,\mathbf{E}'_{v}(\boldsymbol{v}, \boldsymbol{\eta}) : \boldsymbol{\mathcal{D}} : \mathbf{E}'_{v}(\boldsymbol{v}, \Delta\boldsymbol{v}) : \mathbf{E}''_{sv}(\boldsymbol{v}, \Delta\boldsymbol{s}, \Delta\boldsymbol{v}) \\ &+ \mathbf{E}''_{vs}(\boldsymbol{v}, \boldsymbol{\eta}, \Delta\boldsymbol{s}) : \boldsymbol{\mathcal{D}} : \mathbf{E}'_{v}(\boldsymbol{v}, \Delta\boldsymbol{v}) : \mathbf{E}'_{v}(\boldsymbol{v}, \Delta\boldsymbol{v}) \\ &+ \mathbf{E}'_{v}(\boldsymbol{v}, \boldsymbol{\eta}) : \boldsymbol{\mathcal{D}} : \mathbf{E}''_{vv}(\Delta\boldsymbol{v}, \Delta\boldsymbol{v}) : \mathbf{E}'_{s}(\boldsymbol{v}, \Delta\boldsymbol{s}) \\ &+ \mathbf{E}'_{v}(\boldsymbol{v}, \boldsymbol{\eta}) : \boldsymbol{\mathfrak{E}} : \mathbf{E}'_{v}(\boldsymbol{v}, \Delta\boldsymbol{v}) : \mathbf{E}'_{v}(\boldsymbol{v}, \Delta\boldsymbol{v}) : \mathbf{E}'_{s}(\boldsymbol{v}, \Delta\boldsymbol{s}) \\ &+ 2\,\mathbf{E}''_{vv}(\boldsymbol{\eta}, \Delta\boldsymbol{v}) : \mathbb{C} : \mathbf{E}'_{v}(\boldsymbol{v}, \Delta\boldsymbol{v}) \operatorname{Div}\Delta\boldsymbol{s} \\ &+ \mathbf{E}'_{v}(\boldsymbol{v}, \boldsymbol{\eta}) : \mathbb{C} : \mathbf{E}''_{vv}(\Delta\boldsymbol{v}, \Delta\boldsymbol{v}) \operatorname{Div}\Delta\boldsymbol{s} \\ &+ \mathbf{E}'_{v}(\boldsymbol{v}, \boldsymbol{\eta}) : \boldsymbol{\mathcal{D}} : \mathbf{E}'_{v}(\boldsymbol{v}, \Delta\boldsymbol{v}) : \mathbf{E}'_{v}(\boldsymbol{v}, \Delta\boldsymbol{v}) \operatorname{Div}\Delta\boldsymbol{s} \}\, \mathrm{d}\Omega,\end{aligned} \tag{10.113}$$

The form $R'''_{svv}(\boldsymbol{v}, \boldsymbol{s}; \boldsymbol{\eta}, \Delta\boldsymbol{s}, \Delta\boldsymbol{v}, \Delta\boldsymbol{v})$ is quadratic in $\Delta\boldsymbol{v}$ and linear in $\Delta\boldsymbol{s}$. A straightforward but lengthy calculation yields a compact representation of R'''_{svv} which is given in Box B.9.

Furthermore, the specifications of the fourth-order tangent operator $\mathbb{C}$, the sixth-order tensor $\boldsymbol{\mathcal{D}}$ and the eighth-order tensor $\boldsymbol{\mathfrak{E}}$ are given in Appendix B.1.

Computation of R'''_{ssv}. For the sensitivity analysis of quantities of interest the variation

$$R'''_{ssv}(\boldsymbol{v}, \boldsymbol{s}; \boldsymbol{\eta}, \Delta\boldsymbol{s}, \Delta\boldsymbol{s}, \Delta\boldsymbol{v}) = p'''_{sv}(\boldsymbol{v}, \boldsymbol{s}; \boldsymbol{\eta}, \Delta\boldsymbol{s}, \Delta\boldsymbol{s}, \Delta\boldsymbol{v}) \tag{10.114}$$

is required in order to compute the remainder (10.98). This remainder occurs in the exact sensitivity relation (10.101). The explicit formulation is quite lengthy and therefore omitted at this point. But a compact representation is given in Box B.10.

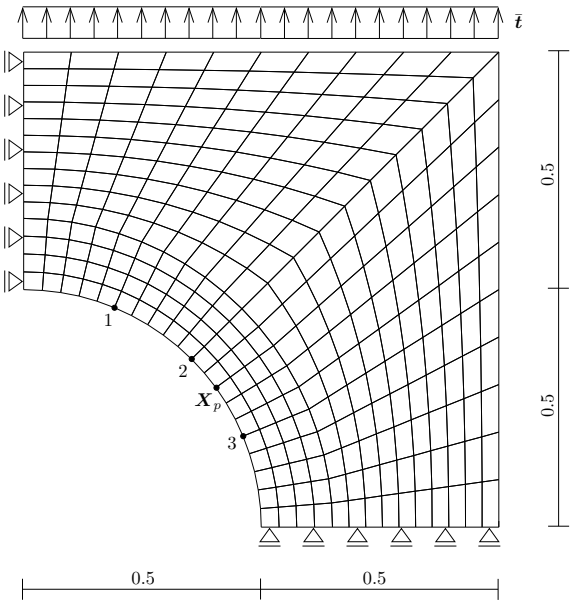

Figure 10.4: Plate with a hole: initial configuration, nodal coordinates of nodes 1-3 are chosen as design variables.

10.7 Numerical example

A numerical example concerning error analysis and improvement of design sensitivity relations is presented in this section. The above derived framework for the sensitivity of the state and for a chosen quantity of interest is investigated for a problem from nonlinear elasticity.

System and model problem. Within this example a plate with a hole under tension is considered. Only a quarter model is used for the sensitivity analysis as well as the improvement algorithm. Due to geometric and load symmetry conditions, simply supported boundary conditions are imposed on each edge and symmetric conditions are imposed on the cutting edges, see Fig. 10.4. In the upper line, the distributed tension $\bar{\boldsymbol{t}} = [0\,,\ 20]^T$ is applied. A mesh with overall 280 Q4 elements and 315 nodes is chosen in order to guarantee the visibility of the design changes. The corresponding deformed configuration is given in Fig. 10.6b.

A compressible Neo-Hookean material with the strain energy function given in (B.20) is considered. The corresponding stress and elasticity tensors are given in Box B.2. The Lamé parameters are chosen as $\lambda = 5.769 \times 10^2$ and $\mu = 3.846 \times 10^2$, which correspond to $E = 10^3$ and $\nu = 0.3$.

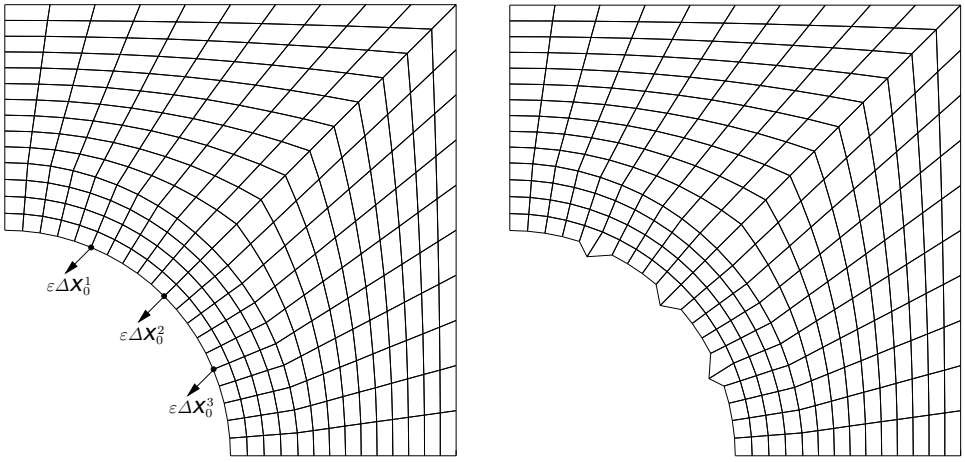

(a) design increments (b) perturbed mesh for $\varepsilon = 1$

Figure 10.5: Plate with a hole: changes in the design variables and perturbed mesh for $\varepsilon = 1$.

The design variables. The shape design sensitivity problem from Section 10.6 is considered. The discrete design variables are a subset of nodal coordinates of the mesh $\boldsymbol{X}_s$. For simplicity, only the nodal coordinates of 3 nodes on the curved boundary are chosen as design variables as indicated Fig. 10.4. The change in the design is defined by the increment in the nodal coordinates

$$\Delta \boldsymbol{X}_s = \varepsilon \, \Delta \boldsymbol{X}_0 \qquad \text{with} \qquad \Delta \boldsymbol{X}_0 = \begin{bmatrix} \Delta \boldsymbol{X}_0^1 \\ \Delta \boldsymbol{X}_0^2 \\ \Delta \boldsymbol{X}_0^3 \end{bmatrix} . \tag{10.115}$$

The changes in the design variables $\Delta \boldsymbol{X}_s$ are controlled by a *design scaling parameter* ε. Hence, the sensitivity of the state due to changes in the design is studied with respect to different values of ε. The nodal vectors $\Delta \boldsymbol{X}_0^i$ on the nodes 1, 2 and 3 are chosen as

$$\Delta \boldsymbol{X}_0^1 = \Delta \boldsymbol{X}_0^2 = \Delta \boldsymbol{X}_0^3 = \begin{bmatrix} -0.02 \\ -0.02 \end{bmatrix} . \tag{10.116}$$

The possible directions of design changes in dependency of the scaling parameter ε are shown in Fig. 10.5a. Furthermore, the perturbed mesh for $\varepsilon = 1$ is given in Fig. 10.5b. The mesh consists of overall 280 elements but only 6 elements are affected by design changes, see Fig. 10.6a.

Improvement of the state sensitivity. The classical first-order sensitivity relation (10.7) yields for large design changes just a rough approximation for the change in the state $\Delta \tilde{\boldsymbol{v}}$.

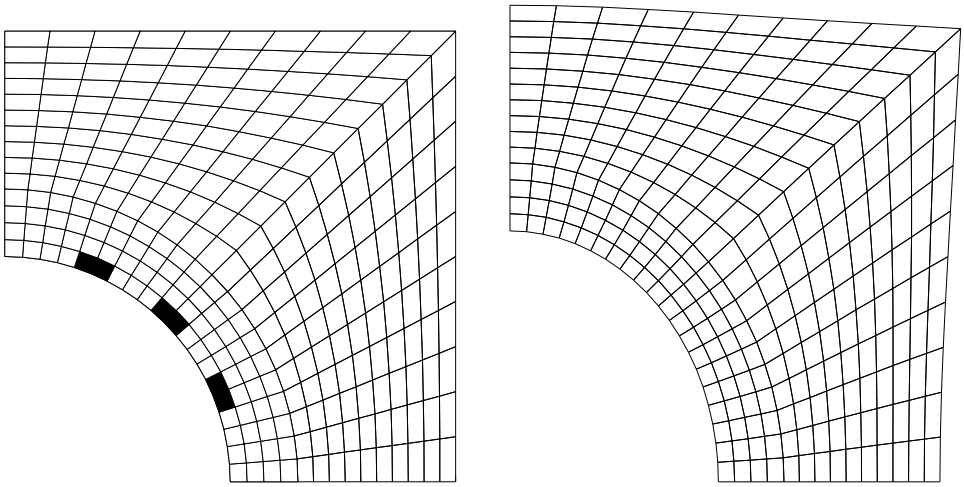

(a) elements which are affected by design changes (b) deformed mesh for the initial design

Figure 10.6: Plate with a hole: elements which are affected by design changes and deformed mesh.

An improvement algorithm has been proposed in Section 10.3 which is based on an exact sensitivity relation given in (10.69). This algorithm yields an improved solution $\Delta\tilde{\boldsymbol{v}}^*$.

For the considered example the improvement algorithm in Box. 10.1 has been applied for different values of design scaling parameter ε. The tolerance within the convergence test is chosen as TOL $= 10^{-14}$ such that the algorithm stops if

$$||\Delta\tilde{\boldsymbol{v}}^*_{i+1} - \Delta\tilde{\boldsymbol{v}}^*_i||_{L_2} \leq \text{TOL} = 10^{-14}.$$

Furthermore, maximum 9 improvement iterations are allowed.

The results are shown in Fig. 10.7. The exact absolute and relative errors $\eta_{\Delta v}$ and $\eta^{\text{rel}}_{\Delta v}$, defined in (10.65) as well as (10.66), are shown in dependency of ε in Fig. 10.7a and Fig. 10.7b, respectively.

The errors are given for different number of improvement iterations. The error $\Delta\boldsymbol{u} - \Delta\tilde{\boldsymbol{u}}^*_0$ denotes the error by using just the initial first-order sensitivity relation (10.7). Furthermore, the error $\Delta\boldsymbol{u} - \Delta\tilde{\boldsymbol{u}}^*_1$ gives the result if one improvement iteration is performed and $\Delta\boldsymbol{u} - \Delta\tilde{\boldsymbol{u}}^*_2$ shows the error if two improvement iterations are used and so on.

The relative error of the first-order solution $\Delta\tilde{\boldsymbol{u}}^*_0$ for $\varepsilon = 10^0$ is about $\eta^{\text{rel}}_{\Delta v} = 4.8546 \times 10^{-1}\,\%$ and is reduced to $\eta^{\text{rel}}_{\Delta v} = 2.9801 \times 10^{-2}\,\%$ by using 9 improvement iterations. Furthermore, the relative error of $\Delta\tilde{\boldsymbol{u}}^*_0$ for $\varepsilon = 10^{-1}$ is about $\eta^{\text{rel}}_{\Delta v} = 6.5779 \times 10^{-3}\,\%$ and is reduced to $\eta^{\text{rel}}_{\Delta v} = 7.2934 \times 10^{-7}\,\%$ with 3 improvement iterations and to $\eta^{\text{rel}}_{\Delta v} = 1.9687 \times 10^{-10}\,\%$ by

using 6 iterations. For smaller design scaling parameter ε the solution is improved in just one or two iterations so that the error becomes numerically zero.

Hence, the error is significantly reduced. For suitable chosen ε the error is numerically zero, i.e. the 'exact' change in the state due to changes in the design can be computed. This demonstrates the capability of the proposed improvement algorithm.

Number of required improvement iterations. The number of required improvement iterations in order to achieve the chosen tolerance TOL depends on the value of the design change and the quality of the initial solution $\Delta\tilde{\boldsymbol{u}}_0^*$. In the considered example the design change is controlled by a design scaling parameter ε. Furthermore, as mentioned above in this example maximum 9 iterations are allowed within the improvement algorithm in Box. 10.1.

The required improvement iterations for different values of ε are given in Fig. 10.8. For the first value $\varepsilon = 10^0$ more than 9 iterations are required in order to fulfil the chosen tolerance. A numerical test has shown that overall 16 iterations have to be performed in order to achieve the convergence criteria. But this is not efficient in comparison with the gain of accuracy. This can be seen in Fig. 10.9, which shows the behavior of the relative error within the improvement iterations. For $\varepsilon = 10^0$ the relative error decreases slowly in comparison with smaller values of ε.

For smaller ε only few iterations are required in order to fulfill the chosen tolerance. For instance, for $\varepsilon = 10^{-4}$ only 2 iterations are performed and the error becomes numerically zero.

Investigations of the error estimator. In Section 10.2.5 a novel error estimator for the error in the change of the state has been proposed. The error estimator is defined in (10.60) as

$$\tilde{\boldsymbol{e}}_{\Delta v} := \tilde{\boldsymbol{v}}^* - \tilde{\boldsymbol{v}} = \Delta\tilde{\boldsymbol{v}}^* - \Delta\tilde{\boldsymbol{v}}.$$

The improved solution $\Delta\tilde{\boldsymbol{v}}^*$ can be computed using the above improvement algorithm. Furthermore, the corresponding error estimator in the L_2 norm $\tilde{\eta}_{\Delta v}$ as well as the relative error $\tilde{\eta}_{\Delta v}^{\mathrm{rel}}$ are given in (10.63) and (10.64), respectively.

The results of the error estimator $\tilde{\eta}_{\Delta v}^{\mathrm{rel}}$ are stated in Table 10.1 for some selected values of design scaling parameter ε. In the table head the parameter ε and the exact error $\eta_{\Delta v}^{\mathrm{rel}}$ are given. The error estimator $\tilde{\eta}_{\Delta v}^{\mathrm{rel}}$ has been computed for all improvement iterations. Up to 9 iterations were performed. Even for large design perturbations with $\varepsilon = 10^0$ the error estimator $\tilde{\eta}_{\Delta v}^{\mathrm{rel}}$ tends to the exact value $\eta_{\Delta v}^{\mathrm{rel}}$. For smaller values of ε only a few improvement iterations are required in order to obtain a good approximation of the exact error.

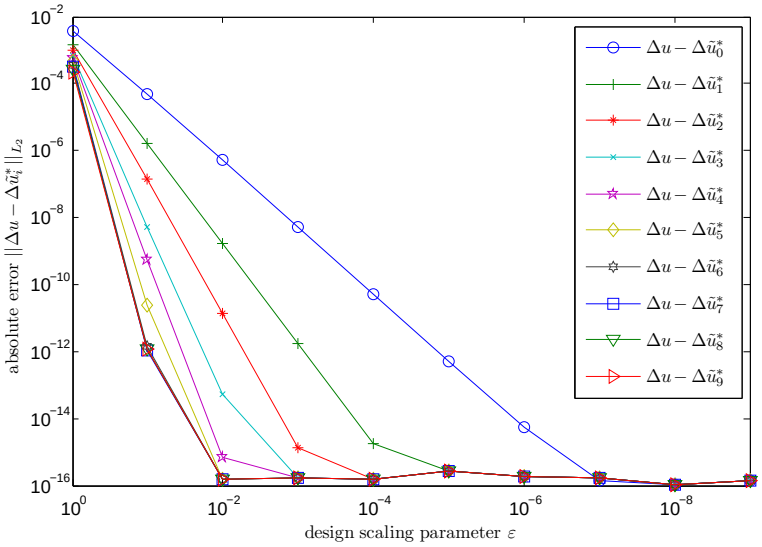

(a) absolute error of different improved solutions vs. design scaling parameter ε

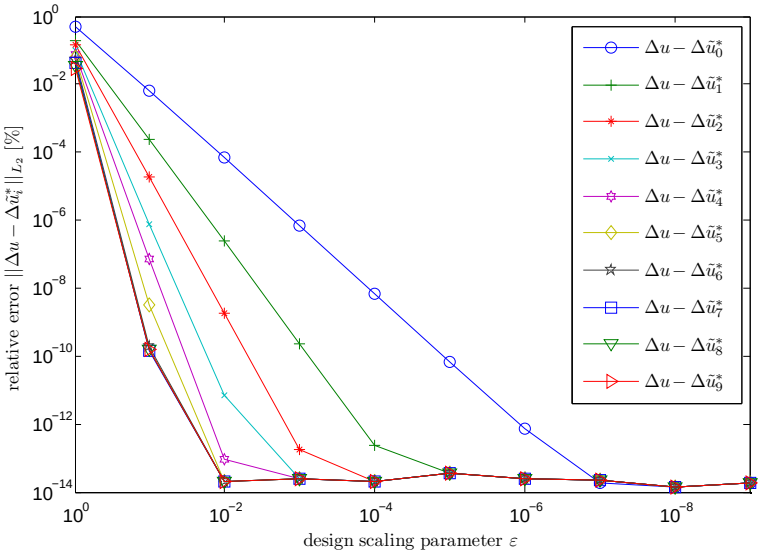

(b) relative error of different improved solutions vs. design scaling parameter ε

Figure 10.7: Plate with a hole: absolute and relative errors of different improved solutions $\Delta\tilde{\boldsymbol{v}}_i^* = \Delta\tilde{\boldsymbol{u}}_i^*$.

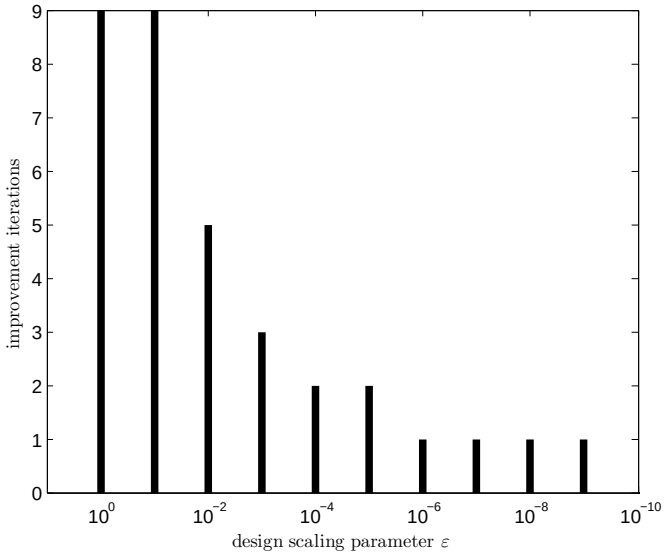

Figure 10.8: Plate with a hole: number of required improvement iterations in order to achieve the chosen tolerance TOL $= 10^{-14}$.

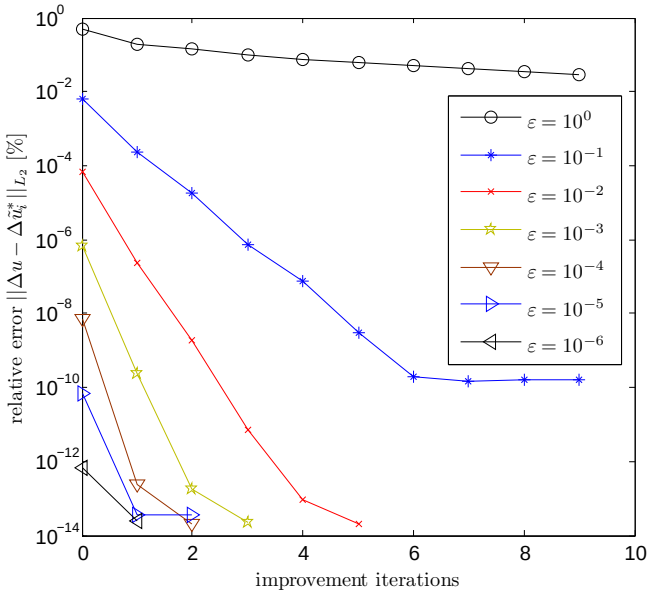

Figure 10.9: Plate with a hole: relative error for different design scaling parameters ε vs. number of improvement iterations.

Table 10.1: Plate with a hole: error estimator $\tilde{\eta}^{\mathrm{rel}}_{\Delta v}$ and effectivity index $I_{\mathrm{eff}} = \tilde{\eta}_{\Delta v}/\eta_{\Delta v}$ within the improvement iterations for different design scaling parameters ε

Iter	$\varepsilon = 10^{0},\ \eta^{\mathrm{rel}}_{\Delta v} = 4.85458571 \times 10^{-1}\ \%$		$\varepsilon = 10^{-1},\ \eta^{\mathrm{rel}}_{\Delta v} = 6.57790116 \times 10^{-3}\ \%$	
	$\tilde{\eta}^{\mathrm{rel}}_{\Delta v}$ [%]	I_{eff}	$\tilde{\eta}^{\mathrm{rel}}_{\Delta v}$ [%]	I_{eff}
1	6.43739722e-001	1.32763426	6.77127823e-003	1.02939965
2	3.71243538e-001	0.76396310	6.55979904e-003	0.99724787
3	5.46847139e-001	1.12688412	6.57825683e-003	1.00005407
4	4.43658387e-001	0.91360716	6.57783019e-003	0.99998921
5	5.15985381e-001	1.06304978	6.57790144e-003	1.00000004
6	4.66555175e-001	0.96095444	6.57790097e-003	0.99999997
7	5.02646821e-001	1.03548158	6.57790129e-003	1.00000002
8	4.75508284e-001	0.97946475	6.57790130e-003	1.00000002
9	4.95914720e-001	1.02157541	6.57790130e-003	1.00000002

Iter	$\varepsilon = 10^{-2},\ \eta^{\mathrm{rel}}_{\Delta v} = 6.79501825 \times 10^{-5}\ \%$		$\varepsilon = 10^{-3},\ \eta^{\mathrm{rel}}_{\Delta v} = 6.81720441 \times 10^{-7}\ \%$	
	$\tilde{\eta}^{\mathrm{rel}}_{\Delta v}$ [%]	I_{eff}	$\tilde{\eta}^{\mathrm{rel}}_{\Delta v}$ [%]	I_{eff}
1	6.81470953e-005	1.00289790	6.81917715e-007	1.00028937
2	6.79482952e-005	0.99997222	6.81720266e-007	0.99999974
3	6.79501854e-005	1.00000004	6.81720457e-007	1.00000002
4	6.79501824e-005	0.99999999	6.81720457e-007	1.00000002
5	6.79501825e-005	0.99999999	6.81720457e-007	1.00000002
6	6.79501825e-005	0.99999999	6.81720457e-007	1.00000002
7	6.79501825e-005	0.99999999	6.81720457e-007	1.00000002
8	6.79501825e-005	0.99999999	6.81720457e-007	1.00000002
9	6.79501825e-005	0.99999999	6.81720457e-007	1.00000002

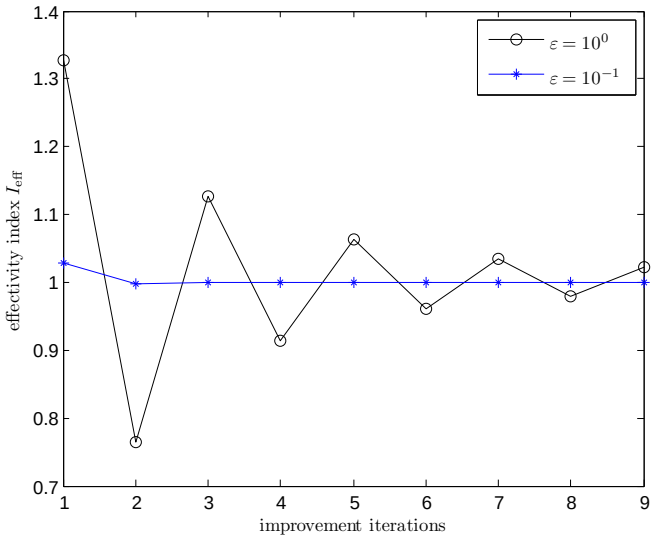

Figure 10.10: Plate with a hole: effectivity index $I_{\text{eff}} = \tilde{\eta}_{\Delta v}/\eta_{\Delta v}$ within the improvement iterations for design scaling parameter $\varepsilon = 10^0$ and $\varepsilon = 10^{-1}$.

Reliability and accuracy of the error estimator. The reliability and accuracy of the error estimator is measured with the effectivity index $I_{\text{eff}} = \tilde{\eta}_{\Delta v}/\eta_{\Delta v}$ introduced in (10.67). The error estimator yields good results if I_{eff} tends to unity. The effectivity index for all improvement iterations for some selected values of the design scaling parameter ε is given Table 10.1.

The values of I_{eff} oscillate for large design perturbations with $\varepsilon = 10^0$ and $\varepsilon = 10^{-1}$ but converge to unity. This is illustrated in Fig. 10.10.

Furthermore, even in the case that just 1 improvement iteration is performed, the error estimator yields good results. This is shown in Fig. 10.11. For a large design perturbation with $\varepsilon = 10^0$ the error is a little overestimated, i.e. $\tilde{\eta}^{\text{rel}}_{\Delta v} = 6.43739722 \times 10^{-1}$ instead of the exact error $\eta^{\text{rel}}_{\Delta v} = 4.85458571 \times 10^{-1}$. For smaller values of ε the estimator tends quickly to the exact error until $\varepsilon = 10^{-6}$. For ε smaller than $\varepsilon = 10^{-6}$ the error is underestimated and tends to zero from $\varepsilon = 10^{-8}$. However, in the wide range of $\varepsilon = 10^{-1}$ to $\varepsilon = 10^{-7}$ the estimator yields good results with just 1 improvement iteration. This can be further improved if more than 1 improvement iterations are performed.

Finally, these results demonstrate the reliability and accuracy of the proposed error estimator. For suitable chosen design changes the error estimator yields very good approximations of the exact error in the state.

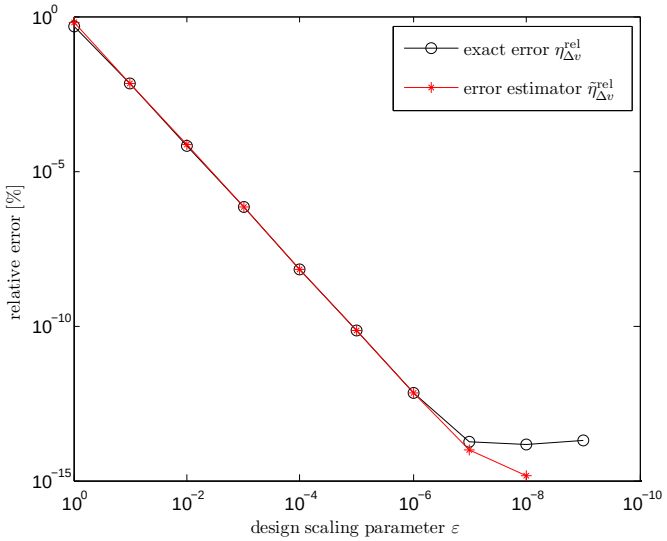

Figure 10.11: Plate with a hole: exact relative error $\eta^{\mathrm{rel}}_{\Delta v}$ and error estimator $\tilde{\eta}^{\mathrm{rel}}_{\Delta v}$ obtained with one improvement iteration.

The change in the quantity of interest. The considered quantity of interest is the vertical component of the nodal displacement at a given point $\boldsymbol{X}_P$, i.e. $J(\boldsymbol{v}, \boldsymbol{s}) = u_y(\boldsymbol{X}_P)$. The material point $\boldsymbol{X}_P$ is shown in Fig. 10.4. This specific quantity of interest is close to the design perturbation region and therefore strongly affected by design changes. The value for the undisturbed design of the vertical displacement is $J(\boldsymbol{v}_0, \boldsymbol{s}_0) = 3.15304776 \times 10^{-2}$.

The change in the quantity of interest is predicted by evaluating the first-order sensitivity relation (10.103) as well as the improved sensitivity relation (10.105), which has been proposed in Section 10.4.3. These relations yield the first-order solution $\Delta\tilde{J}$ and the improved solution $\Delta\tilde{J}^*$, respectively.

The relative errors of the first-order solution $\Delta\tilde{J}$ as well as the improved solution $\Delta\tilde{J}^*$ for different values of design scaling parameters ε are given in Fig. 10.12. The relative error of $\Delta\tilde{J}$ for $\varepsilon = 10^0$ is of about $5.85 \times 10^{-1}\,\%$ and the error of $\Delta\tilde{J}^*$ is of about $2.52 \times 10^{-1}\,\%$. Furthermore, the error of the first-order solution $\Delta\tilde{J}$ for $\varepsilon = 10^{-2}$ is $8.21 \times 10^{-5}\,\%$ and reduced to $3.30 \times 10^{-7}\,\%$ using the improved solution $\Delta\tilde{J}^*$.

Finally, the improved sensitivity relation (10.105) based on higher-order variations of the considered residual and the quantity of interest yields better results for the change in the quantity of interest due to design perturbations than the first-order sensitivity relation (10.103).

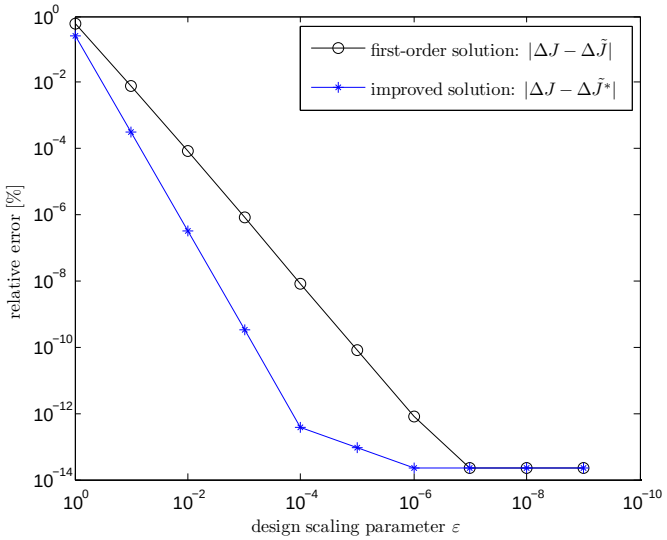

Figure 10.12: Plate with a hole: relative errors of the first-order solution $\Delta\tilde{J}$ and the improved solution $\Delta\tilde{J}^*$, which is obtained by using the first-order approximations of the state $\Delta\tilde{\boldsymbol{v}}$ and the dual solution $\Delta\tilde{\boldsymbol{z}}$.

10.8 Summary and concluding remarks

A novel exact sensitivity relation as well as an error estimator for the error of the sensitivity of the state and quantities of interest have been presented within this chapter. This was based on a fully variational framework for the exact initial and the changed design. Several important results have been derived which are summarized below.

The starting point was the classical first-order sensitivity relation introduced in (10.7) as

$$k(\boldsymbol{v}_0, \boldsymbol{s}_0; \boldsymbol{\eta}, \Delta\tilde{\boldsymbol{v}}) = -Q(\boldsymbol{v}_0, \boldsymbol{s}_0; \boldsymbol{\eta}) \qquad \forall\, \boldsymbol{\eta} \in \mathcal{V}.$$

This relation yields just a rough approximation for the change in the state $\Delta\tilde{\boldsymbol{v}}$ due to large design perturbations $\Delta\boldsymbol{s}$. Here, $Q(\boldsymbol{v}_0, \boldsymbol{s}_0; \boldsymbol{\eta})$ is the classical first-order pseudo load.

In Theorem 10.1 an exact sensitivity relation (10.27) has been derived in form of

$$k(\boldsymbol{v}_0, \boldsymbol{s}_0; \boldsymbol{\eta}, \Delta\boldsymbol{v}) = -Q_{\mathrm{ex}}(\boldsymbol{v})(\boldsymbol{v}_0, \boldsymbol{s}_0; \boldsymbol{\eta}) \qquad \forall\, \boldsymbol{\eta} \in \mathcal{V},$$

in which $Q_{\mathrm{ex}}(\boldsymbol{v})(\boldsymbol{v}_0, \boldsymbol{s}_0; \boldsymbol{\eta})$ is the exact pseudo load given in (10.28). This relation is based on an exact integral remainder representation within the Taylor expansion. Hence, as stated

in Theorem 10.2 in Eq. 10.55 the error $\boldsymbol{e}_{\Delta v} = \Delta\boldsymbol{v} - \Delta\tilde{\boldsymbol{v}}$ depends on the error in the pseudo loads, i.e.

$$k(\boldsymbol{v}_0, \boldsymbol{s}_0; \boldsymbol{\eta}, \boldsymbol{e}_{\Delta v}) = -[\, Q_{\mathrm{ex}}(\boldsymbol{v})(\boldsymbol{v}_0, \boldsymbol{s}_0; \boldsymbol{\eta}) - Q(\boldsymbol{v}_0, \boldsymbol{s}_0; \boldsymbol{\eta})\,] \qquad \forall\, \boldsymbol{\eta} \in \mathcal{V}.$$

This relation is exact if $Q_{\mathrm{ex}}(\boldsymbol{v})(\boldsymbol{v}_0, \boldsymbol{s}_0; \boldsymbol{\eta})$ is explicitly computable.

The exact pseudo load contains the true solution $\boldsymbol{v}$, which is in general unknown. An improved solution $\tilde{\boldsymbol{v}}^* = \boldsymbol{v}_0 + \Delta\tilde{\boldsymbol{v}}^*$ can be used in order to make this relation computable. Such an improved solution can be obtained by using an iterative improvement algorithm based on the exact sensitivity relation (10.27) as proposed in Section 10.3.

For a good approximation $\tilde{\boldsymbol{v}}^* \approx \boldsymbol{v}$ the exact error representation is the basis for an error estimator $\tilde{\boldsymbol{e}}_{\Delta v}$. This estimator is the solution of the error relation (10.61) given as

$$k(\boldsymbol{v}_0, \boldsymbol{s}_0; \boldsymbol{\eta}, \tilde{\boldsymbol{e}}_{\Delta v}) = -[\, Q_{\mathrm{ex}}(\tilde{\boldsymbol{v}}^*)(\boldsymbol{v}_0, \boldsymbol{s}_0; \boldsymbol{\eta}) - Q(\boldsymbol{v}_0, \boldsymbol{s}_0; \boldsymbol{\eta})\,] \qquad \forall\, \boldsymbol{\eta} \in \mathcal{V}.$$

For suitable chosen design changes this relation yields a good approximation of the exact error $\boldsymbol{e}_{\Delta v}$.

This has been demonstrated within the numerical example. Much better solutions for the change in the state due to design changes are obtained by using the improvement algorithm in comparison to the classical first-order solution. The obtained improved solution is used within the error representation as mentioned above. The estimated error tends quickly to the exact error for suitable chosen design changes.

Furthermore, an exact sensitivity relation for quantities of interest has been derived. This problem is more complex because the dual problem is formulated on a given deformed state. Therefore, additional higher-order variations of the considered residual as well as of the quantity of interest occur. The exact sensitivity relation is the basis for an improvement algorithm for changes in the quantity of interest, in which the exact changes in the state and the dual solution are replaced by first-order approximations. The proposed improved relation yields better results than the first-order sensitivity relation.

In the present work only the first-order approximations of the state $\Delta\tilde{\boldsymbol{v}}$ and the dual solution $\Delta\tilde{\boldsymbol{z}}$ are used in order to evaluate the improved sensitivity relation (10.105). This relation could be further enhanced if some improved solutions of the state $\Delta\tilde{\boldsymbol{v}}^*$ and the dual solution $\Delta\tilde{\boldsymbol{z}}^*$ are used.

Chapter 11

Conclusion

In this concluding chapter, the work is briefly summarized and the main goals and results are once more highlighted. Furthermore, an outlook on further research topics and possible other investigations concludes the work.

11.1 Summary

In the present work a general framework for structural analysis and variational sensitivity analysis of the primal and the dual problems has been presented. The main intention was to provide a complete description of the primal and dual problems with respect to variations in the physical and material spaces. A complete description means that changes in the physical and material spaces are allowed. Therefore, not only the structural analysis of the problem is considered but also the sensitivity of functionals and field quantities with respect to configurational changes.

In summary, overall eight problems have been considered for a complete description of the primal and dual problems, i.e. we have

$$\begin{array}{c}\text{structural \& sensitivity}\\ \text{analysis}\end{array} \times \begin{array}{c}\text{primal \& dual}\\ \text{problems}\end{array} \times \begin{array}{c}\text{physical \& material}\\ \text{spaces}\end{array} .$$

These problems are symbolically summarized in the following table.

	primal problem		**dual problem**	
	physical	**material**	**physical**	**material**
structural analysis	$R = 0$	$G = 0$	$R^* = 0$	$G^* = 0$
sensitivity analysis	$\delta R = 0$	$\delta G = 0$	$\delta R^* = 0$	$\delta G^* = 0$

There are several problems which can be now solved based on the corresponding residuals and tangent forms which have been derived in this thesis. In particular, the following results have been presented in the present work.

A complete framework for the primal problem. The starting point was the energy functional of the primal problem. Every functional quantity of the primal problem depends on the state and on a design or control function, which controls in an abstract sense the material configuration. Variations of the energy with respect to the state yield the physical residual and variations with respect to configurational changes lead to the material residual. Additionally, the sensitivities of these residuals were presented. The complete variations of the primal energy with respect to state and design provide all residuals and tangent forms, which are required for analysis and sensitivity of the primal problem. The derived variational formulations were the basis for a consistent finite element formulation. It is important to notice that all discrete residuals and tangent matrices can be computed and assembled in the same way as the usual physical residual and stiffness matrix.

Duality techniques in the physical and material spaces. A variational framework for dual solutions in the physical and material spaces has been proposed in Chapter 5. This is based on an optimal control approach, which provides the general framework for duality relations of variational equations. The form of the dual problem and the corresponding dual solution depend on the kind of the considered variational problem.

A complete framework for the dual problem. The dual problem has been embedded in the same framework as the primal problem in Chapter 6. A novel formulation for the dual problem with respect to configurational variations has been presented. An energy functional of the dual problem has been introduced and the complete variations with respect to the dual solution and the design yield the corresponding dual physical and material residuals as well as the dual tangent forms. These quantities are essential for structural analysis and sensitivity investigations of the dual problem. A sensitivity relation for the change in the dual solution itself due to configurational changes has been derived.

Different applications and several numerical examples based on the derived residuals and tangent forms of the primal and dual problems were proposed in Chapter 7, Chapter 8 and Chapter 9. In particular, the following applications were presented.

- **Global r-adaptive mesh optimization** based on energy minimization of the primal problem. This is a direct application of the energy minimization problem by taking the nodal coordinates as design variables. The discrete primal material residual on the mesh nodes is an error indicator for a non-optimal finite element discretization. These indicators represent the sensitivity of the primal energy with respect to changes of the position of the mesh nodes. The mesh can be optimized with respect to the energy of the primal problem.

- **Goal-oriented r-adaptive mesh optimization** based on the simultaneous minimization of the primal and the dual energy functionals. This novel approach is referred to

as *Primal Dual Material Residual* (PDMR) method, because both the primal and dual material residuals provide an error indicator for mesh optimization. The mesh can be optimized with respect to a chosen quantity of interest.

- **Shape optimization** based on the minimization of the primal internal energy (compliance). The relations to configurational mechanics have been highlighted. Both disciplines deal with changes in the material configuration but they use merely different designations for the same quantities. The primal material residual on the design boundary is an indicator in which direction the boundary has to move in order to minimize the internal energy, i.e. it represents the sensitivity of the internal energy with respect to changes of the design boundary.

Error analysis of sensitivity relations. A novel theorem for error analysis of sensitivity relations as well as an improvement strategy have been stated in Chapter 10. This is based on an exact sensitivity relation with an exact integral remainder within the Taylor expansion. The remainder can be computed explicitly based on higher-order variations of the considered residual. This has been shown for the shape sensitivity problem and the required variations have been derived for nonlinear and linearized elasticity in Section 10.6 and Section B.2.7, respectively. Much better solutions for the change in the state due to design changes are obtained by using the improvement algorithm in comparison to the classical first-order solution. Furthermore, an exact sensitivity relation for quantities of interest has been presented in Section 10.4. This relation is the basis for an estimator for the change in the quantity of interest due to changes in the design and yields better results as the first-order sensitivity relation.

11.2 Future work

There are several challenging problems which can be treated in the future using the techniques derived in this thesis.

Complete element formulation and extension to inelastic material. Within this work a complete variational and finite element formulation has been proposed. The formulation is complete in the sense that changes in the physical and material spaces are allowed. Future finite element formulations should consider all residuals and tangent matrices in order to obtain a complete description of the primal and dual problems as mentioned in Section 4.7 and Section 6.6, respectively. In the present work, a Neo-Hookean material has been investigated and non-standard sixth-order and eighth-order tensors have been derived in Section B.1. The next step should be to extend the proposed approach also to inelastic materials.

Combination of r-, h- and p-adaptivity. In the context of mesh optimization and r-adaptivity a global and a goal-oriented approach were presented. The next step should be to combine r-adaptivity with h- and/or p-adaptive methods. It is well-known that the combination of h- and p-methods is more efficient than each individual method. Therefore, a combined rhp-method seems to be the most efficient way in order to optimize the mesh and to improve the

finite element solution. By means of the primal and dual material residuals r-adaptivity is easy to implement in an existing finite element code. These residuals can be computed without considerable computational cost. Thus, the development of such a rhp-method for global and goal-oriented mesh optimization should be addressed in future work.

Shape optimization and r-adaptivity. There are other challenging problems from shape optimization where r-adaptivity can be used. For instance, a r-adaptive method could be used to reallocate the nodal position of all interior nodes if the shape optimization algorithm has modified the boundary. Often this is based only on a smooth mapping from the original nodal position to the new one under certain geometrical requirements. But nothing can be said about the quality of the mesh with respect to the discretization error. It is known in shape optimization that h- and p-adaptive methods yield a non-differentiability of objectives and constraints due to the modified mesh topology which has a severe impact on the overall gradient driven nonlinear programming algorithm. Furthermore, it is not suitable to spend to much effort in h- or p-adaptivity for any non-optimal design. Especially the goal-oriented r-adaptivity can be used if a local quantity of interest is considered as a constraint of the optimization problem. For instance, a displacement or a stress at some certain point of the body has to be controlled, i.e. the quantity has to be smaller or greater than a given value. The accuracy of the quantity of interest depends directly on the error in corresponding dual solution and the mesh should be optimized with respect to the dual solution if the shape has been modified. Hence, the combination of r-adaptive methods with shape optimization could be a valuable tool.

Error analysis for state and design within shape optimization. Another interesting issue in the above context is the error analysis for the state and the design functions within shape optimization. Assume that a chosen objective functional or quantity of interest depends on both the design and the state function. Then, the goal is to estimate the error in the state and the design function, i.e. distance between the optimal solutions and some given solutions within the optimization process. In addition, the errors which result from the discretization of the state and the design using finite dimensional spaces have to be considered.

Improved sensitivity relations and structural optimization. A novel improvement algorithm for sensitivity relations has been proposed in this work and a benchmark example of shape sensitivity has been investigated. The algorithm can be used within different structural optimization problems. Therefore, future work should address the application of the proposed framework to a large class of optimization problems. Furthermore, it can be used within parameter identification problems, if some material parameters are chosen as design variables.

In addition, the combination of design sensitivity error with discretization error analysis should be addressed in future work. In this context it would be interesting to study the influence of the discretization error on a chosen mesh to the design sensitivity error.

Appendix A

Summary of important variations

Important variations in the physical and material spaces are summarized within this chapter. Furthermore, some lengthy derivations are given explicitly. Firstly, details on the variation of kinematical quantities in local coordinates are stated.

A.1 Variations of kinematical quantities in local coordinates

The following variations are based on an *intrinsic formulation in local coordinates* presented in [5, 7, 9]. The variations are exemplarily performed for selected quantities. In particular, only the first variations of $\mathbf{F}$ and $\mathbf{E}$ with respect to $\boldsymbol{v}$ and $\boldsymbol{s}$ are stated. The extension to higher-order variations is straightforward.

The variations are based on a multiplicative decomposition of the deformation gradients $\mathbf{F}$ and $\mathbf{f} = \mathbf{F}^{-1}$ using the local mappings $\mathbf{K}$ and $\mathbf{M}$, which are introduced in Section 3.1.2 and shown in Figure 3.2. Both gradients can be written as

$$\mathbf{F} = \mathbf{M}\mathbf{K}^{-1}, \tag{A.1}$$

$$\mathbf{f} = \mathbf{K}\mathbf{M}^{-1}. \tag{A.2}$$

The total variations are given as

$$\delta\mathbf{F} = \delta\mathbf{M}\mathbf{K}^{-1} + \mathbf{M}\delta[\mathbf{K}^{-1}], \tag{A.3}$$

$$\delta\mathbf{f} = \delta\mathbf{K}\mathbf{M}^{-1} + \mathbf{K}\delta[\mathbf{M}^{-1}]. \tag{A.4}$$

The variation of an inverse tensor $\mathbf{A}^{-1}$ can be computed using the identity $\mathbf{A}\mathbf{A}^{-1} = \mathbf{I}$. Hence, the variation is given from

$$\delta(\mathbf{A}\mathbf{A}^{-1}) = \delta\mathbf{A}\mathbf{A}^{-1} + \mathbf{A}\delta[\mathbf{A}^{-1}] = \delta\mathbf{I} = \mathbf{0} \quad \text{or} \quad \delta[\mathbf{A}^{-1}] = -\mathbf{A}^{-1}\delta\mathbf{A}\mathbf{A}^{-1}. \tag{A.5}$$

The corresponding variations of $\mathbf{K}$ and $\mathbf{M}$ are obtained as

$$\delta[\mathbf{K}^{-1}] = -\mathbf{K}^{-1}\delta\mathbf{K}\mathbf{K}^{-1}, \tag{A.6}$$

Table A.1: Summary of transformation relations for local gradients

$\operatorname{Grad}\boldsymbol{\varphi} = \mathbf{M}\mathbf{K}^{-1} = \mathbf{F}$	$\operatorname{Grad}\boldsymbol{\varphi}^T = \mathbf{K}^{-T}\mathbf{M}^T = \mathbf{F}^T$
$\operatorname{Grad}\delta\boldsymbol{\varphi} = \delta\mathbf{M}\mathbf{K}^{-1}$	$\operatorname{Grad}\delta\boldsymbol{\varphi}^T = \mathbf{K}^{-T}\delta\mathbf{M}^T$
$\operatorname{Grad}\delta\boldsymbol{\Phi} = \delta\mathbf{K}\mathbf{K}^{-1}$	$\operatorname{Grad}\delta\boldsymbol{\Phi}^T = \mathbf{K}^{-T}\delta\mathbf{K}^T$
$\operatorname{grad}\boldsymbol{\Phi} = \mathbf{K}\mathbf{M}^{-1} = \mathbf{f}$	$\operatorname{grad}\boldsymbol{\Phi}^T = \mathbf{M}^{-T}\mathbf{K}^T = \mathbf{f}^T = \mathbf{F}^{-T}$
$\operatorname{grad}\delta\boldsymbol{\Phi} = \delta\mathbf{K}\mathbf{M}^{-1}$	$\operatorname{grad}\delta\boldsymbol{\Phi}^T = \mathbf{M}^{-T}\delta\mathbf{K}^T$
$\operatorname{grad}\delta\boldsymbol{\varphi} = \delta\mathbf{M}\mathbf{M}^{-1}$	$\operatorname{grad}\delta\boldsymbol{\varphi}^T = \mathbf{M}^{-T}\delta\mathbf{M}^T$

$$\delta[\mathbf{M}^{-1}] = -\mathbf{M}^{-1}\delta\mathbf{M}\mathbf{M}^{-1}. \tag{A.7}$$

In order to identify the compositions with known quantities, the relations from Tab. A.1 are used. Finally, the total variations of the deformation gradients are given as

$$\delta\mathbf{F} = \delta\mathbf{M}\mathbf{K}^{-1} - \mathbf{M}\mathbf{K}^{-1}\delta\mathbf{K}\mathbf{K}^{-1} = \operatorname{Grad}\delta\boldsymbol{\varphi} - \mathbf{F}\operatorname{Grad}\delta\boldsymbol{\Phi}, \tag{A.8}$$

$$\delta\mathbf{f} = \delta\mathbf{K}\mathbf{M}^{-1} - \mathbf{K}\mathbf{M}^{-1}\delta\mathbf{M}\mathbf{M}^{-1} = \operatorname{grad}\delta\boldsymbol{\Phi} - \mathbf{f}\operatorname{grad}\delta\boldsymbol{\varphi}. \tag{A.9}$$

The partial variations are identified as

$$\delta_{\varphi}\mathbf{F}(\boldsymbol{\varphi}, \delta\boldsymbol{\varphi}) = \operatorname{Grad}\delta\boldsymbol{\varphi}, \tag{A.10}$$

$$\delta_{\Phi}\mathbf{F}(\boldsymbol{\varphi}, \delta\boldsymbol{\Phi}) = -\mathbf{F}\operatorname{Grad}\delta\boldsymbol{\Phi}, \tag{A.11}$$

$$\delta_{\varphi}\mathbf{f}(\boldsymbol{\Phi}, \delta\boldsymbol{\varphi}) = -\mathbf{f}\operatorname{grad}\delta\boldsymbol{\varphi}, \tag{A.12}$$

$$\delta_{\Phi}\mathbf{f}(\boldsymbol{\Phi}, \delta\boldsymbol{\Phi}) = \operatorname{grad}\delta\boldsymbol{\Phi}. \tag{A.13}$$

Alternatively, the deformation can be expressed in terms of the displacement field $\boldsymbol{u}$, i.e. $\mathbf{F}(\boldsymbol{u}) = \mathbf{I} + \operatorname{Grad}\boldsymbol{u}$. For this, the partial variations are given as

$$\delta_{u}\mathbf{F}(\boldsymbol{u}, \delta\boldsymbol{u}) = \operatorname{Grad}\delta\boldsymbol{u}, \tag{A.14}$$

$$\delta_{\Phi}\mathbf{F}(\boldsymbol{u}, \delta\boldsymbol{\Phi}) = -\mathbf{H}\operatorname{Grad}\delta\boldsymbol{\Phi}. \tag{A.15}$$

The partial variations with respect to $\boldsymbol{\Phi}$ are different, i.e. $\delta_{\Phi}\mathbf{F}(\boldsymbol{u},\delta\boldsymbol{\Phi}) \neq \delta_{\Phi}\mathbf{F}(\boldsymbol{\varphi},\delta\boldsymbol{\Phi})$, but the total variations of $\mathbf{F}$ yield the same results, i.e.

$$\begin{aligned}\delta\mathbf{F}(\boldsymbol{u}) &= \delta_u\mathbf{F}(\boldsymbol{u},\delta\boldsymbol{u}) + \delta_{\Phi}\mathbf{F}(\boldsymbol{u},\delta\boldsymbol{\Phi}) \\ &= \delta_{\varphi}\mathbf{F}(\boldsymbol{\varphi},\delta\boldsymbol{\varphi}) + \delta_{\Phi}\mathbf{F}(\boldsymbol{\varphi},\delta\boldsymbol{\Phi}) = \delta\mathbf{F}(\boldsymbol{\varphi})\end{aligned} \tag{A.16}$$

because we have with $\delta\boldsymbol{\varphi} = \delta\boldsymbol{\Phi} + \delta\boldsymbol{u}$

$$\begin{aligned}\delta\mathbf{F}(\boldsymbol{\varphi}) &= \operatorname{Grad}\delta\boldsymbol{\varphi} - \operatorname{Grad}\boldsymbol{\varphi}\operatorname{Grad}\delta\boldsymbol{\Phi} \\ &= \operatorname{Grad}\delta\boldsymbol{\Phi} + \operatorname{Grad}\delta\boldsymbol{u} - \operatorname{Grad}\boldsymbol{\varphi}\operatorname{Grad}\delta\boldsymbol{\Phi} \\ &= \operatorname{Grad}\delta\boldsymbol{u} + (\mathbf{I} - \operatorname{Grad}\boldsymbol{\varphi})\operatorname{Grad}\delta\boldsymbol{\Phi} \\ &= \operatorname{Grad}\delta\boldsymbol{u} - \operatorname{Grad}\boldsymbol{u}\operatorname{Grad}\delta\boldsymbol{\Phi} \\ &= \delta\mathbf{F}(\boldsymbol{u}).\end{aligned} \tag{A.17}$$

Furthermore, the Green-Lagrange strain tensor

$$\mathbf{E} = \frac{1}{2}\left(\mathbf{F}^T\mathbf{F} - \mathbf{I}\right) = \frac{1}{2}\left(\mathbf{K}^{-T}\mathbf{M}^T\mathbf{M}\mathbf{K}^{-1} - \mathbf{I}\right) \tag{A.18}$$

is considered as strain measure within this work.

The first total variation of $\mathbf{E}$ written in terms of $\mathbf{K}$ and $\mathbf{M}$ reads

$$\begin{aligned}\delta\mathbf{E} &= \frac{1}{2}\,\delta(\,\mathbf{K}^{-T}\mathbf{M}^T\mathbf{M}\mathbf{K}^{-1} - \mathbf{I}\,) \\ &= \frac{1}{2}\,(\,\delta[\mathbf{K}^{-T}]\mathbf{M}^T\mathbf{M}\mathbf{K}^{-1} + \mathbf{K}^{-T}\delta\mathbf{M}^T\mathbf{M}\mathbf{K}^{-1} \\ &\qquad + \mathbf{K}^{-T}\mathbf{M}^T\delta\mathbf{M}\mathbf{K}^{-1} + \mathbf{K}^{-T}\mathbf{M}^T\mathbf{M}\delta[\mathbf{K}^{-1}]\,)\end{aligned} \tag{A.19}$$

Using (A.6), (A.7) and Tab. A.1 the variation becomes

$$\begin{aligned}\delta\mathbf{E} &= \frac{1}{2}\,(\,-\operatorname{Grad}\delta\boldsymbol{\Phi}^T\mathbf{F}^T\mathbf{F} + \operatorname{Grad}\delta\boldsymbol{\varphi}^T\mathbf{F} \\ &\qquad + \mathbf{F}^T\operatorname{Grad}\delta\boldsymbol{\varphi} - \mathbf{F}^T\mathbf{F}\operatorname{Grad}\delta\boldsymbol{\Phi}\,) \\ &= \operatorname{sym}\{\,\mathbf{F}^T\operatorname{Grad}\delta\boldsymbol{\varphi} - \mathbf{F}^T\mathbf{F}\operatorname{Grad}\delta\boldsymbol{\Phi}\,\}.\end{aligned} \tag{A.20}$$

The partial variations are identified as

$$\delta_{\varphi}\mathbf{E}(\boldsymbol{\varphi},\delta\boldsymbol{\varphi}) = \operatorname{sym}\{\,\mathbf{F}^T\operatorname{Grad}\delta\boldsymbol{\varphi}\,\}, \tag{A.21}$$

$$\delta_{\Phi}\mathbf{E}(\boldsymbol{\varphi},\delta\boldsymbol{\Phi}) = -\operatorname{sym}\{\,\mathbf{F}^T\mathbf{F}\operatorname{Grad}\delta\boldsymbol{\Phi}\,\}. \tag{A.22}$$

Higher-order variations of $\mathbf{E}$ can be obtained in the same manner. A complete list of the required variations in terms of the generalized state $\boldsymbol{v}$ and design $\boldsymbol{s}$ is given in the following section.

A.2 Variations of gradients and strains

The calculations of the sensitivities require the variations of $\mathbf{E}$ with respect to $\boldsymbol{v} \in \mathcal{V}$ and $\boldsymbol{s} \in \mathcal{S}$. Let $\boldsymbol{\eta}$, $\boldsymbol{\lambda} \in \mathcal{V}$ be admissible variations for the state and $\boldsymbol{\psi}$, $\boldsymbol{\chi} \in \mathcal{S}$ be admissible design variations. Some important relations are listed below.

A.2.1 Variations of gradients

For the displacement gradient $\mathbf{H} := \operatorname{Grad} \boldsymbol{u}$ we have

$$\mathbf{H}'_u(\boldsymbol{\eta}) = \operatorname{Grad} \boldsymbol{\eta} \tag{A.23}$$

$$\mathbf{H}'_s(\boldsymbol{u}, \boldsymbol{\psi}) = -\operatorname{Grad} \boldsymbol{u} \operatorname{Grad} \boldsymbol{\psi} = -\mathbf{H} \operatorname{Grad} \boldsymbol{\psi}. \tag{A.24}$$

The variation of the deformation gradient $\mathbf{F} = \operatorname{Grad} \boldsymbol{\varphi} = \mathbf{1} + \mathbf{H}$ reads

$$\mathbf{F}'_v(\boldsymbol{\eta}) = \operatorname{Grad} \boldsymbol{\eta} \tag{A.25}$$

$$\mathbf{F}'_s(\boldsymbol{v}, \boldsymbol{\psi}) = -\operatorname{Grad} \boldsymbol{v} \operatorname{Grad} \boldsymbol{\psi}. \tag{A.26}$$

A.2.2 Variations of strains

Hence, the variations of the Green-Lagrange strain tensor $\mathbf{E} = \frac{1}{2}(\mathbf{F}^T\mathbf{F} - \mathbf{1})$ follow from the above definitions in the form

$$\mathbf{E}'_v(\boldsymbol{v}, \boldsymbol{\eta}) = \frac{1}{2}\left(\operatorname{Grad} \boldsymbol{\eta}^T \mathbf{F} + \mathbf{F}^T \operatorname{Grad} \boldsymbol{\eta}\right) = \operatorname{sym}\{\mathbf{F}^T \operatorname{Grad} \boldsymbol{\eta}\} \tag{A.27}$$

$$\begin{aligned} \mathbf{E}'_s(\boldsymbol{u}, \boldsymbol{\psi}) &= -\frac{1}{2}\left(\operatorname{Grad} \boldsymbol{\psi}^T \operatorname{Grad} \boldsymbol{v}^T \mathbf{F} + \mathbf{F}^T \operatorname{Grad} \boldsymbol{v} \operatorname{Grad} \boldsymbol{\psi}\right) \\ &= -\operatorname{sym}\{\mathbf{F}^T \operatorname{Grad} \boldsymbol{v} \operatorname{Grad} \boldsymbol{\psi}\}. \end{aligned} \tag{A.28}$$

The second and mixed variations are obtained in a straightforward manner as

$$\begin{aligned} \mathbf{E}''_{vv}(\boldsymbol{\eta}, \boldsymbol{\lambda}) &= \frac{1}{2}\left(\operatorname{Grad} \boldsymbol{\eta}^T \operatorname{Grad} \boldsymbol{\lambda} + \operatorname{Grad} \boldsymbol{\lambda}^T \operatorname{Grad} \boldsymbol{\eta}\right) \\ &= \operatorname{sym}\{\operatorname{Grad} \boldsymbol{\lambda}^T \operatorname{Grad} \boldsymbol{\eta}\} \end{aligned} \tag{A.29}$$

$$\begin{aligned} \mathbf{E}''_{vs}(\boldsymbol{v}, \boldsymbol{\eta}, \boldsymbol{\psi}) &= -\frac{1}{2}\left(\operatorname{Grad} \boldsymbol{\psi}^T \operatorname{Grad} \boldsymbol{\eta}^T \mathbf{F} + \operatorname{Grad} \boldsymbol{\eta}^T \operatorname{Grad} \boldsymbol{v} \operatorname{Grad} \boldsymbol{\psi}\right. \\ &\qquad \left. + \operatorname{Grad} \boldsymbol{\psi}^T \operatorname{Grad} \boldsymbol{v}^T \operatorname{Grad} \boldsymbol{\psi}^T \operatorname{Grad} \boldsymbol{\eta} + \mathbf{F}^T \operatorname{Grad} \boldsymbol{\eta} \operatorname{Grad} \boldsymbol{\psi}\right) \\ &= -\operatorname{sym}\{\operatorname{Grad} \boldsymbol{\psi}^T \operatorname{Grad} \boldsymbol{v}^T \operatorname{Grad} \boldsymbol{\eta} + \mathbf{F}^T \operatorname{Grad} \boldsymbol{\eta} \operatorname{Grad} \boldsymbol{\psi}\}. \end{aligned} \tag{A.30}$$

$$\begin{aligned}\mathbf{E}''_{ss}(\boldsymbol{v},\boldsymbol{\psi},\boldsymbol{\chi}) = \frac{1}{2}\,(\,&\mathrm{Grad}\,\boldsymbol{\chi}^T\,\mathrm{Grad}\,\boldsymbol{\psi}^T\,\mathrm{Grad}\,\boldsymbol{v}^T\mathbf{F}\\ &+\mathrm{Grad}\,\boldsymbol{\psi}^T\,\mathrm{Grad}\,\boldsymbol{\chi}^T\,\mathrm{Grad}\,\boldsymbol{v}^T\mathbf{F}\\ &+\mathrm{Grad}\,\boldsymbol{\psi}^T\,\mathrm{Grad}\,\boldsymbol{v}^T\,\mathrm{Grad}\,\boldsymbol{v}\,\mathrm{Grad}\,\boldsymbol{\chi}\\ &+\mathrm{Grad}\,\boldsymbol{\chi}^T\,\mathrm{Grad}\,\boldsymbol{v}^T\,\mathrm{Grad}\,\boldsymbol{v}\,\mathrm{Grad}\,\boldsymbol{\psi}\\ &+\mathbf{F}^T\,\mathrm{Grad}\,\boldsymbol{v}\,\mathrm{Grad}\,\boldsymbol{\chi}\,\mathrm{Grad}\,\boldsymbol{\psi}\\ &+\mathbf{F}^T\,\mathrm{Grad}\,\boldsymbol{v}\,\mathrm{Grad}\,\boldsymbol{\psi}\,\mathrm{Grad}\,\boldsymbol{\chi}\,)\\ =\,&\mathrm{sym}\{\mathrm{Grad}\,\boldsymbol{\chi}^T\,\mathrm{Grad}\,\boldsymbol{v}^T\,\mathrm{Grad}\,\boldsymbol{v}\,\mathrm{Grad}\,\boldsymbol{\psi}\\ &+\mathbf{F}^T\,\mathrm{Grad}\,\boldsymbol{v}\,\mathrm{Grad}\,\boldsymbol{\chi}\,\mathrm{Grad}\,\boldsymbol{\psi}\\ &+\mathbf{F}^T\,\mathrm{Grad}\,\boldsymbol{v}\,\mathrm{Grad}\,\boldsymbol{\psi}\,\mathrm{Grad}\,\boldsymbol{\chi}\}\end{aligned} \tag{A.31}$$

$$\begin{aligned}\mathbf{E}''_{sv}(\boldsymbol{v},\boldsymbol{\psi},\boldsymbol{\eta}) = -\frac{1}{2}\,(\,&\mathrm{Grad}\,\boldsymbol{\psi}^T\,\mathrm{Grad}\,\boldsymbol{\eta}^T\mathbf{F}+\mathrm{Grad}\,\boldsymbol{\psi}^T\,\mathrm{Grad}\,\boldsymbol{v}^T\,\mathrm{Grad}\,\boldsymbol{\eta}\\ &+\mathrm{Grad}\,\boldsymbol{\eta}^T\,\mathrm{Grad}\,\boldsymbol{v}\,\mathrm{Grad}\,\boldsymbol{\psi}+\mathbf{F}^T\,\mathrm{Grad}\,\boldsymbol{\eta}\;\mathrm{Grad}\,\boldsymbol{\psi}\,)\\ =\,&-\mathrm{sym}\{\mathrm{Grad}\,\boldsymbol{\psi}^T\,\mathrm{Grad}\,\boldsymbol{v}^T\,\mathrm{Grad}\,\boldsymbol{\eta}+\mathbf{F}^T\,\mathrm{Grad}\,\boldsymbol{\eta}\;\mathrm{Grad}\,\boldsymbol{\psi}\}\\ =\,&-\mathrm{sym}\{\mathrm{Grad}\,\boldsymbol{\eta}^T\,\mathrm{Grad}\,\boldsymbol{v}\,\mathrm{Grad}\,\boldsymbol{\psi}+\mathbf{F}^T\,\mathrm{Grad}\,\boldsymbol{\eta}\;\mathrm{Grad}\,\boldsymbol{\psi}\}.\end{aligned} \tag{A.32}$$

Hence, as a result of symmetry, we have

$$\mathbf{E}''_{sv}(\boldsymbol{v},\boldsymbol{\psi},\boldsymbol{\eta}) = \mathbf{E}''_{vs}(\boldsymbol{v},\boldsymbol{\eta},\boldsymbol{\psi}). \tag{A.33}$$

In addition, the following higher-order variations are required and obtained in short form as

$$\begin{aligned}\mathbf{E}'''_{vvs}(\boldsymbol{\eta},\boldsymbol{\lambda},\boldsymbol{\psi}) = -\,\mathrm{sym}\{\;&\mathrm{Grad}\,\boldsymbol{\psi}^T\,\mathrm{Grad}\,\boldsymbol{\lambda}^T\,\mathrm{Grad}\,\boldsymbol{\eta}\\ &+\mathrm{Grad}\,\boldsymbol{\lambda}^T\,\mathrm{Grad}\,\boldsymbol{\eta}\;\mathrm{Grad}\,\boldsymbol{\psi}\},\end{aligned} \tag{A.34}$$

$$\begin{aligned}\mathbf{E}'''_{vsv}(\boldsymbol{\eta},\boldsymbol{\psi},\boldsymbol{\lambda}) = -\,\mathrm{sym}\{\;&\mathrm{Grad}\,\boldsymbol{\psi}^T\,\mathrm{Grad}\,\boldsymbol{\lambda}^T\,\mathrm{Grad}\,\boldsymbol{\eta}\\ &+\mathrm{Grad}\,\boldsymbol{\lambda}^T\,\mathrm{Grad}\,\boldsymbol{\eta}\,\mathrm{Grad}\,\boldsymbol{\psi}\},\end{aligned} \tag{A.35}$$

$$\begin{aligned}\mathbf{E}'''_{svv}(\boldsymbol{\psi},\boldsymbol{\eta},\boldsymbol{\lambda}) = -\,\mathrm{sym}\{\;&\mathrm{Grad}\,\boldsymbol{\psi}^T\,\mathrm{Grad}\,\boldsymbol{\lambda}^T\,\mathrm{Grad}\,\boldsymbol{\eta}\\ &+\mathrm{Grad}\,\boldsymbol{\lambda}^T\,\mathrm{Grad}\,\boldsymbol{\eta}\,\mathrm{Grad}\,\boldsymbol{\psi}\;\},\end{aligned} \tag{A.36}$$

$$\begin{aligned}\mathbf{E}'''_{vss}(\boldsymbol{v},\boldsymbol{\eta},\boldsymbol{\psi},\boldsymbol{\chi}) = \operatorname{sym}\{\ &\operatorname{Grad}\boldsymbol{\chi}^T \operatorname{Grad}\boldsymbol{\psi}^T \operatorname{Grad}\boldsymbol{v}^T \operatorname{Grad}\boldsymbol{\eta}\\ &+ \operatorname{Grad}\boldsymbol{\psi}^T \operatorname{Grad}\boldsymbol{\chi}^T \operatorname{Grad}\boldsymbol{v}^T \operatorname{Grad}\boldsymbol{\eta}\\ &+ \operatorname{Grad}\boldsymbol{\psi}^T \operatorname{Grad}\boldsymbol{v}^T \operatorname{Grad}\boldsymbol{\eta} \operatorname{Grad}\boldsymbol{\chi}\\ &+ \operatorname{Grad}\boldsymbol{\chi}^T \operatorname{Grad}\boldsymbol{v}^T \operatorname{Grad}\boldsymbol{\eta} \operatorname{Grad}\boldsymbol{\psi}\\ &+ \mathbf{F}^T \operatorname{Grad}\boldsymbol{\eta} \operatorname{Grad}\boldsymbol{\chi} \operatorname{Grad}\boldsymbol{\psi}\\ &+ \mathbf{F}^T \operatorname{Grad}\boldsymbol{\eta} \operatorname{Grad}\boldsymbol{\psi} \operatorname{Grad}\boldsymbol{\chi}\ \}.\end{aligned} \tag{A.37}$$

$$\begin{aligned}\mathbf{E}''''_{vvss}(\boldsymbol{\eta},\boldsymbol{\lambda},\boldsymbol{\psi},\boldsymbol{\chi}) = \operatorname{sym}\{\ &\operatorname{Grad}\boldsymbol{\chi}^T \operatorname{Grad}\boldsymbol{\psi}^T \operatorname{Grad}\boldsymbol{\lambda}^T \operatorname{Grad}\boldsymbol{\eta}\\ &+ \operatorname{Grad}\boldsymbol{\psi}^T \operatorname{Grad}\boldsymbol{\chi}^T \operatorname{Grad}\boldsymbol{\lambda}^T \operatorname{Grad}\boldsymbol{\eta}\\ &+ \operatorname{Grad}\boldsymbol{\psi}^T \operatorname{Grad}\boldsymbol{\lambda}^T \operatorname{Grad}\boldsymbol{\eta} \operatorname{Grad}\boldsymbol{\chi}\\ &+ \operatorname{Grad}\boldsymbol{\chi}^T \operatorname{Grad}\boldsymbol{\lambda}^T \operatorname{Grad}\boldsymbol{\eta} \operatorname{Grad}\boldsymbol{\psi}\\ &+ \operatorname{Grad}\boldsymbol{\lambda}^T \operatorname{Grad}\boldsymbol{\eta} \operatorname{Grad}\boldsymbol{\chi} \operatorname{Grad}\boldsymbol{\psi}\\ &+ \operatorname{Grad}\boldsymbol{\lambda}^T \operatorname{Grad}\boldsymbol{\eta} \operatorname{Grad}\boldsymbol{\psi} \operatorname{Grad}\boldsymbol{\chi}\ \}.\end{aligned} \tag{A.38}$$

Again, due to symmetry, we have

$$\mathbf{E}'''_{vsv}(\boldsymbol{\eta},\boldsymbol{\psi},\boldsymbol{\lambda}) = \mathbf{E}'''_{svv}(\boldsymbol{\psi},\boldsymbol{\eta},\boldsymbol{\lambda}). \tag{A.39}$$

A.3 Variations of stresses

A.3.1 Standard variations

We consider a hyperelastic material, i.e. there exists a strain energy function $W_R(\mathbf{F})$ such that

$$\mathbf{P} = \frac{\partial W_R}{\partial \mathbf{F}} \quad \text{and} \quad \mathbf{S} = \frac{\partial W_R}{\partial \mathbf{E}}, \tag{A.40}$$

where $\mathbf{P}$ and $\mathbf{S}$ are the first and second Piola-Kirchhoff stress tensors, respectively. The variations read

$$\mathbf{P}'_v(\boldsymbol{v},\boldsymbol{\eta}) = \frac{\partial \mathbf{P}}{\partial \mathbf{F}} : \mathbf{F}'_v = \mathbb{A} : \mathbf{F}'_v = \mathbb{A} : \operatorname{Grad}\boldsymbol{\eta}, \tag{A.41}$$

$$\mathbf{P}'_s(\boldsymbol{v},\boldsymbol{\psi}) = \frac{\partial \mathbf{P}}{\partial \mathbf{F}} : \mathbf{F}'_s = \mathbb{A} : \mathbf{F}'_s = -\mathbb{A} : \operatorname{Grad}\boldsymbol{v} \operatorname{Grad}\boldsymbol{\psi}, \tag{A.42}$$

$$\mathbf{S}'_v(\boldsymbol{v},\boldsymbol{\eta}) = \frac{\partial \mathbf{S}}{\partial \mathbf{E}} : \mathbf{E}'_v(\boldsymbol{v},\boldsymbol{\eta}) = \mathbb{C} : \mathbf{E}'_v(\boldsymbol{v},\boldsymbol{\eta}) = \mathbb{C} : \mathbf{F}^T \operatorname{Grad}\boldsymbol{\eta}, \tag{A.43}$$

$$\mathbf{S}'_s(\boldsymbol{v},\boldsymbol{\psi}) = \frac{\partial \mathbf{S}}{\partial \mathbf{E}} : \mathbf{E}'_s(\boldsymbol{v},\boldsymbol{\psi}) = \mathbb{C} : \mathbf{E}'_s(\boldsymbol{v},\boldsymbol{\psi}) = -\mathbb{C} : \mathbf{F}^T \operatorname{Grad}\boldsymbol{v} \operatorname{Grad}\boldsymbol{\psi}, \tag{A.44}$$

where

$$\mathbb{A} := \frac{\partial \mathbf{P}}{\partial \mathbf{F}} = \frac{\partial^2 W_R}{\partial \mathbf{F}\,\partial \mathbf{F}} \quad \text{and} \quad \mathbb{C} := \frac{\partial \mathbf{S}}{\partial \mathbf{E}} = \frac{\partial^2 W_R}{\partial \mathbf{E}\,\partial \mathbf{E}}. \tag{A.45}$$

A.3.2 Higher-order variations

Within this work non-standard higher-order variations are required, which are obtained as

$$\mathbb{C}'_v(\boldsymbol{v},\boldsymbol{\eta}) = \frac{\partial \mathbb{C}}{\partial \mathbf{E}} : \mathbf{E}'_v(\boldsymbol{v},\boldsymbol{\eta}) = \boldsymbol{\mathcal{D}} : \mathbf{E}'_v(\boldsymbol{v},\boldsymbol{\eta}), \tag{A.46}$$

$$\mathbb{C}'_s(\boldsymbol{v},\boldsymbol{\psi}) = \frac{\partial \mathbb{C}}{\partial \mathbf{E}} : \mathbf{E}'_s(\boldsymbol{v},\boldsymbol{\psi}) = \boldsymbol{\mathcal{D}} : \mathbf{E}'_s(\boldsymbol{v},\boldsymbol{\psi}), \tag{A.47}$$

$$\boldsymbol{\mathcal{D}}'_v(\boldsymbol{v},\boldsymbol{\eta}) = \frac{\partial \boldsymbol{\mathcal{D}}}{\partial \mathbf{E}} : \mathbf{E}'_v(\boldsymbol{v},\boldsymbol{\eta}) = \boldsymbol{\mathfrak{E}} : \mathbf{E}'_v(\boldsymbol{v},\boldsymbol{\eta}), \tag{A.48}$$

$$\boldsymbol{\mathcal{D}}'_s(\boldsymbol{v},\boldsymbol{\psi}) = \frac{\partial \boldsymbol{\mathcal{D}}}{\partial \mathbf{E}} : \mathbf{E}'_s(\boldsymbol{v},\boldsymbol{\psi}) = \boldsymbol{\mathfrak{E}} : \mathbf{E}'_s(\boldsymbol{v},\boldsymbol{\psi}), \tag{A.49}$$

where the sixth-order tensor $\boldsymbol{\mathcal{D}}$ and the eighth-order tensor $\boldsymbol{\mathfrak{E}}$ are given as

$$\boldsymbol{\mathcal{D}} := \frac{\partial \mathbb{C}}{\partial \mathbf{E}} \quad \text{and} \quad \boldsymbol{\mathfrak{E}} := \frac{\partial \boldsymbol{\mathcal{D}}}{\partial \mathbf{E}}. \tag{A.50}$$

A.4 Variations of the strain energy function

The variations of the strain energy function $W_R(\mathbf{F})$ are obtained in form of

$$\begin{aligned}
(W_R)'_v(\boldsymbol{v},\boldsymbol{\eta}) &= \frac{\partial W_R}{\partial \mathbf{F}} : \mathbf{F}'_v(\boldsymbol{v},\boldsymbol{\eta}) = \mathbf{P} : \mathbf{F}'_v(\boldsymbol{v},\boldsymbol{\eta}) = \mathbf{P} : \operatorname{Grad}\boldsymbol{\eta} \\
&= \mathbf{F}\mathbf{S} : \operatorname{Grad}\boldsymbol{\eta} = \mathbf{S} : \mathbf{F}^T \operatorname{Grad}\boldsymbol{\eta} \\
&= \mathbf{S} : \mathbf{E}'_v(\boldsymbol{v},\boldsymbol{\eta}),
\end{aligned} \tag{A.51}$$

$$\begin{aligned}
(W_R)'_s(\boldsymbol{v},\boldsymbol{\psi}) &= \frac{\partial W_R}{\partial \mathbf{F}} : \mathbf{F}'_s(\boldsymbol{v},\boldsymbol{\psi}) = \mathbf{P} : \mathbf{F}'_s(\boldsymbol{v},\boldsymbol{\psi}) = -\mathbf{P} : \operatorname{Grad}\boldsymbol{v} \operatorname{Grad}\boldsymbol{\psi} \\
&= -\mathbf{F}\mathbf{S} : \operatorname{Grad}\boldsymbol{v} \operatorname{Grad}\boldsymbol{\psi} = -\mathbf{S} : \mathbf{F}^T \operatorname{Grad}\boldsymbol{v} \operatorname{Grad}\boldsymbol{\psi} \\
&= \mathbf{S} : \mathbf{E}'_s(\boldsymbol{v},\boldsymbol{\psi}).
\end{aligned} \tag{A.52}$$

In a concrete situation $\boldsymbol{\varphi}$ or $\boldsymbol{u}$ is chosen as the state variable. For $\boldsymbol{v} = \boldsymbol{\varphi}$ we obtain

$$\begin{aligned}(W_R)'_{\varphi}(\boldsymbol{\varphi},\boldsymbol{\eta}) &= \frac{\partial W_R}{\partial \mathbf{F}} : \mathbf{F}'_{\varphi}(\boldsymbol{\varphi},\boldsymbol{\eta}) = \mathbf{P} : \mathbf{F}'_{\varphi}(\boldsymbol{\varphi},\boldsymbol{\eta}) = \mathbf{P} : \operatorname{Grad}\boldsymbol{\eta} \\ &= \mathbf{S} : \mathbf{E}'_{\varphi}(\boldsymbol{\varphi},\boldsymbol{\eta}),\end{aligned} \tag{A.53}$$

$$\begin{aligned}(W_R)'_{s}(\boldsymbol{\varphi},\boldsymbol{\psi}) &= \frac{\partial W_R}{\partial \mathbf{F}} : \mathbf{F}'_{s}(\boldsymbol{\varphi},\boldsymbol{\psi}) = \mathbf{P} : \mathbf{F}'_{s}(\boldsymbol{\varphi},\boldsymbol{\psi}) = -\mathbf{P} : \mathbf{F}\operatorname{Grad}\boldsymbol{\psi} = \\ &= -\mathbf{F}\mathbf{S} : \mathbf{F}\operatorname{Grad}\boldsymbol{\psi} = -\mathbf{S} : \mathbf{F}^T\mathbf{F}\operatorname{Grad}\boldsymbol{\psi} \\ &= \mathbf{S} : \mathbf{E}'_{s}(\boldsymbol{\varphi},\boldsymbol{\psi}).\end{aligned} \tag{A.54}$$

For $\boldsymbol{v} = \boldsymbol{u}$ we have

$$\begin{aligned}(W_R)'_{u}(\boldsymbol{u},\boldsymbol{\eta}) &= \frac{\partial W_R}{\partial \mathbf{F}} : \mathbf{F}'_{u}(\boldsymbol{u},\boldsymbol{\eta}) = \mathbf{P} : \mathbf{F}'_{u}(\boldsymbol{u},\boldsymbol{\eta}) = \mathbf{P} : \operatorname{Grad}\boldsymbol{\eta} \\ &= \mathbf{S} : \mathbf{E}'_{u}(\boldsymbol{u},\boldsymbol{\eta}),\end{aligned} \tag{A.55}$$

$$\begin{aligned}(W_R)'_{s}(\boldsymbol{u},\boldsymbol{\psi}) &= \frac{\partial W_R}{\partial \mathbf{F}} : \mathbf{F}'_{s}(\boldsymbol{u},\boldsymbol{\psi}) = \mathbf{P} : \mathbf{F}'_{s}(\boldsymbol{u},\boldsymbol{\psi}) = -\mathbf{P} : \mathbf{H}\operatorname{Grad}\boldsymbol{\psi} \\ &= -\mathbf{F}\mathbf{S} : \mathbf{H}\operatorname{Grad}\boldsymbol{\psi} = -\mathbf{S} : \mathbf{F}^T\mathbf{H}\operatorname{Grad}\boldsymbol{\psi} \\ &= \mathbf{S} : \mathbf{E}'_{s}(\boldsymbol{u},\boldsymbol{\psi}).\end{aligned} \tag{A.56}$$

A.5 Variations of line, surface and volume elements

The variations of line, surface and volume elements with respect to $\boldsymbol{s}$ are given by

$$(d\boldsymbol{X})'_s = \operatorname{Grad}\boldsymbol{\psi}\, d\boldsymbol{X}, \tag{A.57}$$

$$(d\boldsymbol{A})'_s = [\operatorname{Div}\boldsymbol{\psi}\,\mathbf{1} - \operatorname{Grad}\boldsymbol{\psi}^T]\, d\boldsymbol{A}, \tag{A.58}$$

$$(dV)'_s = \operatorname{Div}\boldsymbol{\psi}\, dV. \tag{A.59}$$

Following the chain rule, the variation of a quantity $\mathcal{F} = \int_{\Omega_R}(\cdot)\,\mathrm{d}\Omega$ is given by

$$\mathcal{F}'_v(\boldsymbol{v},\boldsymbol{\eta}) = \int_{\Omega_R}(\cdot)'_v(\boldsymbol{v},\boldsymbol{\eta})\,\mathrm{d}\Omega, \tag{A.60}$$

$$\begin{aligned}\mathcal{F}'_s(\boldsymbol{v},\boldsymbol{\psi}) &= \int_{\Omega_R}(\cdot)'_s(\boldsymbol{v},\boldsymbol{\psi}) + (\cdot)\operatorname{Div}\boldsymbol{\psi}\,\mathrm{d}\Omega \\ &= \int_{\Omega_R}(\cdot)'_s(\boldsymbol{v},\boldsymbol{\psi}) + (\cdot)\mathbf{I} : \operatorname{Grad}\boldsymbol{\psi}\,\mathrm{d}\Omega.\end{aligned} \tag{A.61}$$

Appendix B

Model problems and explicit formulations

Within this work the model problem of nonlinear elasticity has been considered. All residuals and tangent forms have been derived with respect to the general nonlinear case. In this chapter explicit formulations of constitutive relations as well as the explicit formulations of higher-order variations of the primal physical residual are stated. Furthermore, for completeness, the most important variational and discrete relations are given for the theory of linearized elasticity.

B.1 Nonlinear elasticity

B.1.1 Constitutive relations

As an example of isothermal hyperelasticity a classical compressible Neo-Hookean material is considered. The strain energy function $W_R(I_C, J)$ under consideration is written in terms of the first invariant of $\mathbf{C} = \mathbf{F}^T\mathbf{F}$ given by

$$I_C := \mathrm{tr}(\mathbf{C}) = \mathrm{tr}(\mathbf{F}^T\mathbf{F}) = \mathbf{F} : \mathbf{F} \tag{B.1}$$

and $J := \det \mathbf{F}$.

The complete derivatives of the strain energy function with respect to the Green-Lagrange strain tensor $\mathbf{E}$ or equivalent with respect to the $\mathbf{C}$ are given as

$$\mathbf{S} := \frac{\partial W_R}{\partial \mathbf{E}} = 2\,\frac{\partial W_R}{\partial \mathbf{C}}, \tag{B.2}$$

$$\mathbb{C} := \frac{\partial \mathbf{S}}{\partial \mathbf{E}} = 2\,\frac{\partial \mathbf{S}}{\partial \mathbf{C}}, \tag{B.3}$$

$$\boldsymbol{\mathcal{D}} := \frac{\partial \mathbb{C}}{\partial \mathbf{E}} = 2\,\frac{\partial \mathbb{C}}{\partial \mathbf{C}}, \tag{B.4}$$

$$\mathfrak{E} := \frac{\partial \boldsymbol{\mathcal{D}}}{\partial \mathbf{E}} = 2\,\frac{\partial \boldsymbol{\mathcal{D}}}{\partial \mathbf{C}}. \tag{B.5}$$

Additional to the standard second Piola-Kirchhoff stress tensor $\mathbf{S}$ and the fourth-order tangent operator $\mathbb{C}$, nonstandard higher-order derivatives of the strain energy function W_R are required. A lengthy calculation yields a sixth-order tensor $\boldsymbol{\mathcal{D}}$ and a eighth-order tensor $\mathfrak{E}$. Within these tensors appear the derivatives of $\mathbf{C}^{-1}$ with respect to $\mathbf{C}$, i.e.

$$\mathbb{V} := \frac{\partial \mathbf{C}^{-1}}{\partial \mathbf{C}}, \tag{B.6}$$

$$\boldsymbol{\mathcal{W}} := \frac{\partial \mathbb{V}}{\partial \mathbf{C}}, \tag{B.7}$$

$$\boldsymbol{\mathfrak{X}} := \frac{\partial \boldsymbol{\mathcal{W}}}{\partial \mathbf{C}}. \tag{B.8}$$

The explicit formulations of all stress tensors and corresponding tangent operators for two Neo-Hookean materials are given in Box B.1 and Box B.2 as well as in Box B.3 and Box B.4. Furthermore, the specifications of $\mathbb{V}$, $\boldsymbol{\mathcal{W}}$ and $\boldsymbol{\mathfrak{X}}$ are given in Box B.5.

Within this work a formulation in terms of $\mathbf{E}$ and $\mathbf{S}$ is used. All terms can be also written in terms of $\mathbf{F}$ and the first Piola-Kirchhoff stress tensor $\mathbf{P} := \partial W_R / \partial \mathbf{F}$. For completeness, $\mathbf{P}$, the Cauchy stress tensor $\boldsymbol{\sigma} = J^{-1}\,\mathbf{P}\mathbf{F}^T = J^{-1}\,\mathbf{F}\mathbf{S}\mathbf{F}^T$ and the fourth-order tangent operator $\mathbb{A} := \partial \mathbf{P} / \partial \mathbf{F}$ are also given for the considered strain energy functions.

Strain energy function:

$$W_R(I_C, J) = \frac{1}{2}\,\mu\,(I_C - n^{dim} - 2\ln J) + \frac{1}{2}\,\lambda\,(J-1)^2. \tag{B.9}$$

Second-order stress tensors:

$$\mathbf{P} = \mu\,\mathbf{F} - [\,\mu - \lambda\,(J^2 - J)\,]\mathbf{F}^{-T} \tag{B.10}$$

$$\mathbf{S} = \mu\,\mathbf{I} - [\,\mu - \lambda\,(J^2 - J)\,]\mathbf{C}^{-T} \tag{B.11}$$

$$\boldsymbol{\sigma} = \frac{1}{J}\,\mu\,\mathbf{b} - \frac{1}{J}\,[\,\mu - \lambda\,(J^2 - J)\,]\mathbf{I} \tag{B.12}$$

Fourth-order tangent operators:

$$\mathbb{A} = \mu\,\mathbf{I}\bar{\otimes}\mathbf{I} + \lambda\,(2\,J^2 - J)\,\mathbf{F}^{-T}\otimes\mathbf{F}^{-T} + [\,\mu - \lambda\,(J^2 - J)\,]\,\mathbf{F}^{-T}\hat{\otimes}\mathbf{F}^{-1} \tag{B.13}$$

$$\mathbb{C} = \lambda\,(2\,J^2 - J)\,\mathbf{C}^{-T}\otimes\mathbf{C}^{-T} - 2\,[\,\mu - \lambda\,(J^2 - J)\,]\,\mathbb{V} \tag{B.14}$$

Component representation:

$$P_{ij} = \mu\,F_{ij} - [\,\mu - \lambda\,(J^2 - J)\,]F^{-1}_{ji} \tag{B.15}$$

$$S_{ij} = \mu\,\delta_{ij} - [\,\mu - \lambda\,(J^2 - J)\,]C^{-1}_{ji} \tag{B.16}$$

$$\sigma_{ij} = \frac{1}{J}\,(\,\mu\,b_{ij} - [\,\mu - \lambda\,(J^2 - J)\,])\,\delta_{ij} \tag{B.17}$$

$$\mathsf{A}_{ijkl} = \mu\,\delta_{ik}\,\delta_{jl} + \lambda\,(2\,J^2 - J)\,F^{-1}_{ji}F^{-1}_{lk} + [\,\mu - \lambda\,(J^2 - J)\,]\,F^{-1}_{li}F^{-1}_{jk} \tag{B.18}$$

$$\begin{aligned}\mathsf{C}_{ijkl} &= \lambda\,(2\,J^2 - J)\,C^{-1}_{ji}C^{-1}_{lk} + [\,\mu - \lambda\,(J^2 - J)\,]\,[C^{-1}_{ik}C^{-1}_{jl} + C^{-1}_{il}C^{-1}_{jk}] \\ &= \lambda\,(2\,J^2 - J)\,C^{-1}_{ji}C^{-1}_{lk} - 2\,[\,\mu - \lambda\,(J^2 - J)\,]\,\mathsf{V}_{ijkl}\end{aligned} \tag{B.19}$$

The tensor $\mathbb{V}$ is given in (B.41) and $\mathbf{b} = \mathbf{F}\mathbf{F}^T$.

Box B.1: Stress tensors and standard tangent operators for a Neo-Hookean material

Strain energy function:

$$W_R(I_C, J) = \frac{1}{2}\,\mu\,(I_C - n^{dim} - 2\ln J) + \frac{1}{2}\,\lambda\,(J-1)^2. \tag{B.20}$$

Second-order stress tensor:

$$S_{ij} = \mu\,\delta_{ij} - [\,\mu - \lambda\,(J^2 - J)\,]C^{-1}_{ij} \tag{B.21}$$

Fourth-order tangent operator:

$$\mathsf{C}_{ijkl} = \lambda\,(2\,J^2 - J)\,C^{-1}_{ij}C^{-1}_{kl} - 2\,[\,\mu - \lambda\,(J^2 - J)\,]\,\mathsf{V}_{ijkl} \tag{B.22}$$

Sixth-order tangent operator:

$$\begin{aligned}\mathcal{D}_{ijklmn} = {}& \lambda\,(4\,J^2 - J)C^{-1}_{ij}C^{-1}_{kl}C^{-1}_{mn} \\ & + 2\,\lambda\,(2\,J^2 - J)\,[\,C^{-1}_{ij}\mathsf{V}_{klmn} + C^{-1}_{kl}\mathsf{V}_{ijmn} + C^{-1}_{mn}\mathsf{V}_{ijkl}\,] \\ & - 4\,[\,\mu - \lambda\,(J^2 - J)\,]\,\mathcal{W}_{ijklmn}\end{aligned} \tag{B.23}$$

Eighth-order tangent operator:

$$\begin{aligned}\mathfrak{E}_{ijklmnop} = {}& \lambda\,(8\,J^2 - J)C^{-1}_{ij}C^{-1}_{kl}C^{-1}_{mn}C^{-1}_{op} \\ & + 2\,\lambda\,(4\,J^2 - J)\,[\,C^{-1}_{ij}C^{-1}_{kl}\mathsf{V}_{mnop} + C^{-1}_{ij}C^{-1}_{mn}\mathsf{V}_{klop} \\ & \qquad + C^{-1}_{ij}C^{-1}_{op}\mathsf{V}_{klmn} + C^{-1}_{kl}C^{-1}_{mn}\mathsf{V}_{ijop} \\ & \qquad + C^{-1}_{kl}C^{-1}_{op}\mathsf{V}_{ijmn} + C^{-1}_{mn}C^{-1}_{op}\mathsf{V}_{ijkl}\,] \\ & + 4\,\lambda\,(2\,J^2 - J)\,[\,\mathsf{V}_{ijop}\mathsf{V}_{klmn} + \mathsf{V}_{klop}\mathsf{V}_{ijmn} + \mathsf{V}_{mnop}\mathsf{V}_{ijkl} \\ & \qquad + C^{-1}_{ij}\mathcal{W}_{klmnop} + C^{-1}_{kl}\mathcal{W}_{ijmnop} \\ & \qquad + C^{-1}_{mn}\mathcal{W}_{ijklop} + C^{-1}_{op}\mathcal{W}_{ijklmn}\,] \\ & - 8\,[\,\mu - \lambda\,(J^2 - J)\,]\,\mathfrak{X}_{ijklmnop}\end{aligned} \tag{B.24}$$

The components of the tensors $\mathbb{V}$, $\boldsymbol{\mathcal{W}}$ and $\boldsymbol{\mathfrak{X}}$ are given in Box B.5.

Box B.2: Complete derivatives of W_R with respect to $\mathbf{E}$ for a Neo-Hookean material

Strain energy function:

$$W_R(I_C, J) = \frac{1}{2}\,\mu\,(I_C - n^{dim} - 2\ln J) + \frac{1}{2}\,\lambda\,\ln^2(J). \tag{B.25}$$

Second-order stress tensors:

$$\mathbf{P} = \mu(\mathbf{F} - \mathbf{F}^{-T}) + \lambda\ln(J)\mathbf{F}^{-T} = \mu\,\mathbf{F} - [\,\mu - \lambda\ln(J)\,]\mathbf{F}^{-T} \tag{B.26}$$

$$\mathbf{S} = \mu(\mathbf{I} - \mathbf{C}^{-T}) + \lambda\ln(J)\mathbf{C}^{-T} = \mu\,\mathbf{I} - [\,\mu - \lambda\ln(J)\,]\mathbf{C}^{-T} \tag{B.27}$$

$$\boldsymbol{\sigma} = \frac{1}{J}\,(\,\mu\,\mathbf{b} - [\,\mu - \lambda\ln(J)\,])\mathbf{I} \tag{B.28}$$

Fourth-order tangent operators:

$$\mathbb{A} = \lambda\,\mathbf{F}^{-T}\otimes\mathbf{F}^{-T} + \mu\,\mathbf{I}\bar{\otimes}\mathbf{I} + [\,\mu - \lambda\ln(J)\,]\,\mathbf{F}^{-T}\hat{\otimes}\mathbf{F}^{-1} \tag{B.29}$$

$$\mathbb{C} = \lambda\,\mathbf{C}^{-T}\otimes\mathbf{C}^{-T} - 2\,[\,\mu - \lambda\ln(J)\,]\,\mathbb{V} \tag{B.30}$$

Component representation:

$$P_{ij} = \mu\,F_{ij} - [\,\mu - \lambda\ln(J)\,]\,F^{-1}_{ji} \tag{B.31}$$

$$S_{ij} = \mu\,\delta_{ij} - [\,\mu - \lambda\ln(J)\,]\,C^{-1}_{ji} \tag{B.32}$$

$$\sigma_{ij} = \frac{1}{J}\,(\,\mu\,b_{ij} - [\,\mu - \lambda\ln(J)\,])\,\delta_{ij} \tag{B.33}$$

$$\mathsf{A}_{ijkl} = \lambda\,F^{-1}_{ji}F^{-1}_{lk} + \mu\,\delta_{ik}\delta_{jl} + [\,\mu - \lambda\ln(J)\,]\,F^{-1}_{li}F^{-1}_{jk} \tag{B.34}$$

$$\begin{aligned}\mathsf{C}_{ijkl} &= \lambda\,C^{-1}_{ji}C^{-1}_{lk} + [\,\mu - \lambda\ln(J)\,]\,[\,C^{-1}_{ik}C^{-1}_{jl} + C^{-1}_{il}C^{-1}_{jk}\,] \\ &= \lambda\,C^{-1}_{ji}C^{-1}_{lk} - 2\,[\,\mu - \lambda\ln(J)\,]\,\mathsf{V}_{ijkl}\end{aligned} \tag{B.35}$$

The tensor V_{ijkl} is given in (B.41) and $\mathbf{b} = \mathbf{F}\mathbf{F}^T$.

Box B.3: Stress tensors and standard tangent operators for a Neo-Hookean material

Strain energy function:

$$W_R(I_C, J) = \frac{1}{2}\,\mu\,(I_C - n^{dim} - 2\ln J) + \frac{1}{2}\,\lambda\,\ln^2(J). \tag{B.36}$$

Second-order stress tensor:

$$S_{ij} = \mu\,\delta_{ij} - [\,\mu - \lambda \ln(J)\,]\,C^{-1}_{ij} \tag{B.37}$$

Fourth-order tangent operator:

$$\mathsf{C}_{ijkl} = \lambda\,C^{-1}_{ij}C^{-1}_{kl} - 2\,[\,\mu - \lambda\ln(J)\,]\,\mathsf{V}_{ijkl} \tag{B.38}$$

Sixth-order tangent operators:

$$\begin{aligned}\mathcal{D}_{ijklmn} = {} & 2\,\lambda\,[\,C^{-1}_{ij}\mathsf{V}_{klmn} + C^{-1}_{kl}\mathsf{V}_{ijmn} + C^{-1}_{mn}\mathsf{V}_{ijkl}\,] \\ & - 4\,[\,\mu - \lambda\ln(J)\,]\,\mathcal{W}_{ijklmn}\end{aligned} \tag{B.39}$$

Eighth-order tangent operator:

$$\begin{aligned}\mathfrak{E}_{ijklmnop} = {} & 4\,\lambda\,[\,\mathsf{V}_{ijop}\mathsf{V}_{klmn} + \mathsf{V}_{klop}\mathsf{V}_{ijmn} + \mathsf{V}_{mnop}\mathsf{V}_{ijkl} \\ & + C^{-1}_{ij}\mathcal{W}_{klmnop} + C^{-1}_{kl}\mathcal{W}_{ijmnop} \\ & + C^{-1}_{mn}\mathcal{W}_{ijklop} + C^{-1}_{op}\mathcal{W}_{ijklmn}\,] \\ & - 8\,[\,\mu - \lambda\ln(J)\,]\,\mathfrak{X}_{ijklmnop}\end{aligned} \tag{B.40}$$

The components of the tensors $\mathbb{V}$, $\boldsymbol{\mathcal{W}}$ and $\boldsymbol{\mathfrak{X}}$ are given in Box B.5.

Box B.4: Complete derivatives of W_R with respect to $\mathbf{E}$ for a Neo-Hookean material

$$\mathsf{V}_{ijkl} := \frac{\partial C^{-1}_{ij}}{\partial C_{kl}} = -\frac{1}{2}\left(C^{-1}_{ik}C^{-1}_{jl} + C^{-1}_{il}C^{-1}_{jk}\right) \tag{B.41}$$

$$\begin{aligned}
\mathcal{W}_{ijklmn} :=& \frac{\partial \mathsf{V}_{ijkl}}{\partial C_{mn}} \qquad (B.42)\\
=& \frac{1}{4}\,(\, C^{-1}_{ik}C^{-1}_{jm}C^{-1}_{ln} + C^{-1}_{ik}C^{-1}_{jn}C^{-1}_{lm} + C^{-1}_{il}C^{-1}_{jm}C^{-1}_{kn} + C^{-1}_{il}C^{-1}_{jn}C^{-1}_{km}\\
&+ C^{-1}_{im}C^{-1}_{jk}C^{-1}_{ln} + C^{-1}_{im}C^{-1}_{jl}C^{-1}_{kn} + C^{-1}_{in}C^{-1}_{jk}C^{-1}_{lm} + C^{-1}_{in}C^{-1}_{jl}C^{-1}_{km}\,)
\end{aligned}$$

$$\begin{aligned}
\mathfrak{x}_{ijklmnop} :=& \frac{\partial \mathcal{W}_{ijklmn}}{\partial C_{op}}\\
=& -\frac{1}{8}\,(\, C^{-1}_{io}C^{-1}_{kp}C^{-1}_{jm}C^{-1}_{ln} + C^{-1}_{ip}C^{-1}_{ko}C^{-1}_{jm}C^{-1}_{ln} + C^{-1}_{ik}C^{-1}_{jo}C^{-1}_{mp}C^{-1}_{ln}\\
&+ C^{-1}_{ik}C^{-1}_{jp}C^{-1}_{mo}C^{-1}_{ln} + C^{-1}_{ik}C^{-1}_{jm}C^{-1}_{lo}C^{-1}_{np} + C^{-1}_{ik}C^{-1}_{jm}C^{-1}_{lp}C^{-1}_{no}\\
&+ C^{-1}_{io}C^{-1}_{kp}C^{-1}_{jn}C^{-1}_{lm} + C^{-1}_{ip}C^{-1}_{ko}C^{-1}_{jn}C^{-1}_{lm} + C^{-1}_{ik}C^{-1}_{jo}C^{-1}_{np}C^{-1}_{lm}\\
&+ C^{-1}_{ik}C^{-1}_{jp}C^{-1}_{no}C^{-1}_{lm} + C^{-1}_{ik}C^{-1}_{jn}C^{-1}_{lo}C^{-1}_{mp} + C^{-1}_{ik}C^{-1}_{jn}C^{-1}_{lp}C^{-1}_{mo}\\
&+ C^{-1}_{io}C^{-1}_{lp}C^{-1}_{jm}C^{-1}_{kn} + C^{-1}_{ip}C^{-1}_{lo}C^{-1}_{jm}C^{-1}_{kn} + C^{-1}_{il}C^{-1}_{jo}C^{-1}_{mp}C^{-1}_{kn}\\
&+ C^{-1}_{il}C^{-1}_{jp}C^{-1}_{mo}C^{-1}_{kn} + C^{-1}_{il}C^{-1}_{jm}C^{-1}_{ko}C^{-1}_{np} + C^{-1}_{il}C^{-1}_{jm}C^{-1}_{kp}C^{-1}_{no}\\
&+ C^{-1}_{io}C^{-1}_{lp}C^{-1}_{jn}C^{-1}_{km} + C^{-1}_{ip}C^{-1}_{lo}C^{-1}_{jn}C^{-1}_{km} + C^{-1}_{il}C^{-1}_{jo}C^{-1}_{np}C^{-1}_{km}\\
&+ C^{-1}_{il}C^{-1}_{jp}C^{-1}_{no}C^{-1}_{km} + C^{-1}_{il}C^{-1}_{jn}C^{-1}_{ko}C^{-1}_{mp} + C^{-1}_{il}C^{-1}_{jn}C^{-1}_{kp}C^{-1}_{mo}\\
&+ C^{-1}_{io}C^{-1}_{mp}C^{-1}_{jk}C^{-1}_{ln} + C^{-1}_{ip}C^{-1}_{mo}C^{-1}_{jk}C^{-1}_{ln} + C^{-1}_{im}C^{-1}_{jo}C^{-1}_{kp}C^{-1}_{ln}\\
&+ C^{-1}_{im}C^{-1}_{jp}C^{-1}_{ko}C^{-1}_{ln} + C^{-1}_{im}C^{-1}_{jk}C^{-1}_{lo}C^{-1}_{np} + C^{-1}_{im}C^{-1}_{jk}C^{-1}_{lp}C^{-1}_{no}\\
&+ C^{-1}_{io}C^{-1}_{mp}C^{-1}_{jl}C^{-1}_{kn} + C^{-1}_{ip}C^{-1}_{mo}C^{-1}_{jl}C^{-1}_{kn} + C^{-1}_{im}C^{-1}_{jo}C^{-1}_{lp}C^{-1}_{kn}\\
&+ C^{-1}_{im}C^{-1}_{jp}C^{-1}_{lo}C^{-1}_{kn} + C^{-1}_{im}C^{-1}_{jl}C^{-1}_{ko}C^{-1}_{np} + C^{-1}_{im}C^{-1}_{jl}C^{-1}_{kp}C^{-1}_{no}\\
&+ C^{-1}_{io}C^{-1}_{np}C^{-1}_{jk}C^{-1}_{lm} + C^{-1}_{ip}C^{-1}_{no}C^{-1}_{jk}C^{-1}_{lm} + C^{-1}_{in}C^{-1}_{jo}C^{-1}_{kp}C^{-1}_{lm}\\
&+ C^{-1}_{in}C^{-1}_{jp}C^{-1}_{ko}C^{-1}_{lm} + C^{-1}_{in}C^{-1}_{jk}C^{-1}_{lo}C^{-1}_{mp} + C^{-1}_{in}C^{-1}_{jk}C^{-1}_{lp}C^{-1}_{mo}\\
&+ C^{-1}_{io}C^{-1}_{np}C^{-1}_{jl}C^{-1}_{km} + C^{-1}_{ip}C^{-1}_{no}C^{-1}_{jl}C^{-1}_{km} + C^{-1}_{in}C^{-1}_{jo}C^{-1}_{lp}C^{-1}_{km}\\
&+ C^{-1}_{in}C^{-1}_{jp}C^{-1}_{lo}C^{-1}_{km} + C^{-1}_{in}C^{-1}_{jl}C^{-1}_{ko}C^{-1}_{mp} + C^{-1}_{in}C^{-1}_{jl}C^{-1}_{kp}C^{-1}_{mo}\,)
\end{aligned} \tag{B.43}$$

Box B.5: Summary of derivatives of $\mathbf{C}^{-1}$ with respect to $\mathbf{C} = \mathbf{F}^T\mathbf{F}$

B.1.2 Explicit formulations for higher-order variations of the residual

An exact error representation as well as an improvement algorithm of sensitivity relations have been proposed in Chapter 10. The explicit computation of the exact pseudo load $Q_{\mathrm{ex}}(\cdot)(\cdot)$ in (10.28) requires higher-order variations of the residual $R(\cdot)$ with respect to $\boldsymbol{v}$ and $\boldsymbol{s}$. Explicit formulations of these higher-order variations for shape sensitivity are stated in Section 10.6.

Compact specifications of R''_{vv}, R''_{ss}, R''_{sv}, R'''_{svv} and R'''_{ssv} for shape sensitivity are given below. For given $\{\boldsymbol{v}, \boldsymbol{s}\}$ and $\{\Delta\boldsymbol{v}, \Delta\boldsymbol{s}\}$ these forms become linear functionals and have the same structure as the usual residual $R(\boldsymbol{v}, \boldsymbol{s}; \cdot)$. Hence, they can be directly implemented in standard finite element programs as the residual R.

$$R''_{vv}(\boldsymbol{v}, \boldsymbol{s}; \boldsymbol{\eta}, \Delta\boldsymbol{v}, \Delta\boldsymbol{v}) = k'_v(\boldsymbol{v}, \boldsymbol{s}; \boldsymbol{\eta}, \Delta\boldsymbol{v}, \Delta\boldsymbol{v}) = \int_{\Omega_R} \mathbf{A}_1 : \mathrm{Grad}\,\boldsymbol{\eta}\,\mathrm{d}\Omega \tag{B.44}$$

with the second-order tensor

$$\mathbf{A}_1 := 2\ \mathrm{Grad}\,\boldsymbol{v}\,\Delta_v\mathbf{S}^{(1)} + \mathbf{F}\,(\,\Delta_v\mathbf{S}^{(2)} + \Delta_v\mathbf{S}^{(3)}\,). \tag{B.45}$$

The stress increments due to changes in the state $\Delta\boldsymbol{v}$ are introduced as

$$\Delta_v\mathbf{S}^{(1)} := \mathbb{C} : \mathbf{E}'_v(\boldsymbol{v}, \Delta\boldsymbol{v}) \tag{B.46}$$

$$\Delta_v\mathbf{S}^{(2)} := \mathbb{C} : \mathbf{E}''_{vv}(\Delta\boldsymbol{v}, \Delta\boldsymbol{v}) \tag{B.47}$$

$$\Delta_v\mathbf{S}^{(3)} := \boldsymbol{\mathcal{D}} : \mathbf{E}'_v(\boldsymbol{v}, \Delta\boldsymbol{v}) : \mathbf{E}'_v(\boldsymbol{v}, \Delta\boldsymbol{v}) \tag{B.48}$$

with

$$\mathbf{E}'_v(\boldsymbol{v}, \Delta\boldsymbol{v}) = \mathbf{F}^T\,\mathrm{Grad}\,\Delta\boldsymbol{v} \tag{B.49}$$

$$\mathbf{E}''_{vv}(\Delta\boldsymbol{v}, \Delta\boldsymbol{v}) = \mathrm{Grad}\,\Delta\boldsymbol{v}^T\,\mathrm{Grad}\,\Delta\boldsymbol{v}. \tag{B.50}$$

Box B.6: Explicit formulation of R''_{vv} for nonlinear elasticity

$$R''_{ss}(\boldsymbol{v},\boldsymbol{s};\boldsymbol{\eta},\Delta\boldsymbol{s},\Delta\boldsymbol{s}) = p'_s(\boldsymbol{v},\boldsymbol{s};\boldsymbol{\eta},\Delta\boldsymbol{s},\Delta\boldsymbol{s}) = \int_{\Omega_R} \{\, \mathbf{A}_1 : \operatorname{Grad}\boldsymbol{\eta} + \boldsymbol{A}_2 \cdot \boldsymbol{\eta} \,\} \,\mathrm{d}\Omega \tag{B.51}$$

with the second-order tensor $\mathbf{A}_1$ and the vector $\boldsymbol{A}_2$ which are given as

$$\begin{aligned}\mathbf{A}_1 := 2\,[\,&\operatorname{Grad}\boldsymbol{v}\operatorname{Grad}\Delta\boldsymbol{s}\,(\operatorname{Grad}\Delta\boldsymbol{s}\,\mathbf{S} + \mathbf{S}\operatorname{Grad}\Delta\boldsymbol{s}^T - \Delta_s\mathbf{S}^{(1)}\,)\\ &+ \mathbf{FS}\,\operatorname{Grad}\Delta\boldsymbol{s}^T\operatorname{Grad}\Delta\boldsymbol{s}^T - \mathbf{F}\Delta_s\mathbf{S}^{(1)}\operatorname{Grad}\Delta\boldsymbol{s}^T\\ &- (\,\operatorname{Grad}\boldsymbol{v}\operatorname{Grad}\Delta\boldsymbol{s}\,\mathbf{S} + \mathbf{FS}\,\operatorname{Grad}\Delta\boldsymbol{s}^T - \mathbf{F}\Delta_s\mathbf{S}^{(1)}\,)\operatorname{Div}\Delta\boldsymbol{s}\,]\\ &+ \mathbf{F}\,(\,\Delta_s\mathbf{S}^{(2)} + \Delta_s\mathbf{S}^{(3)}\,)\\ &- \mathbf{FS}\,(\,\mathbf{I} : \operatorname{Grad}\Delta\boldsymbol{s}\operatorname{Grad}\Delta\boldsymbol{s} - \operatorname{Div}\Delta\boldsymbol{s}\operatorname{Div}\Delta\boldsymbol{s}\,),\end{aligned} \tag{B.52}$$

$$\boldsymbol{A}_2 := \boldsymbol{b}_R\,(\,\mathbf{I} : \operatorname{Grad}\Delta\boldsymbol{s}\operatorname{Grad}\Delta\boldsymbol{s} - \operatorname{Div}\Delta\boldsymbol{s}\operatorname{Div}\Delta\boldsymbol{s}\,). \tag{B.53}$$

The stress increments due to design changes $\Delta\boldsymbol{s}$ are introduced as

$$\Delta_s\mathbf{S}^{(1)} := \mathbb{C} : \mathbf{E}'_s(\boldsymbol{v},\Delta\boldsymbol{s}) \tag{B.54}$$

$$\Delta_s\mathbf{S}^{(2)} := \mathbb{C} : \mathbf{E}''_{ss}(\boldsymbol{v},\Delta\boldsymbol{s},\Delta\boldsymbol{s}) \tag{B.55}$$

$$\Delta_s\mathbf{S}^{(3)} := \boldsymbol{\mathcal{D}} : \mathbf{E}'_s(\boldsymbol{v},\Delta\boldsymbol{s}) : \mathbf{E}'_s(\boldsymbol{v},\Delta\boldsymbol{s}) \tag{B.56}$$

with

$$\mathbf{E}'_s(\boldsymbol{v},\Delta\boldsymbol{s}) = -\mathbf{F}^T\operatorname{Grad}\boldsymbol{v}\operatorname{Grad}\Delta\boldsymbol{s}, \tag{B.57}$$

$$\begin{aligned}\mathbf{E}''_{ss}(\boldsymbol{v},\Delta\boldsymbol{s},\Delta\boldsymbol{s}) = \operatorname{sym}\{\,&\operatorname{Grad}\Delta\boldsymbol{s}^T\operatorname{Grad}\boldsymbol{v}^T\operatorname{Grad}\boldsymbol{v}\operatorname{Grad}\Delta\boldsymbol{s}\\ &+ 2\,\mathbf{F}^T\operatorname{Grad}\boldsymbol{v}\operatorname{Grad}\Delta\boldsymbol{s}\operatorname{Grad}\Delta\boldsymbol{s}\,\}.\end{aligned} \tag{B.58}$$

Box B.7: Explicit formulation of R''_{ss} for nonlinear elasticity

$$R''_{sv}(\boldsymbol{v},\boldsymbol{s};\boldsymbol{\eta},\Delta\boldsymbol{s},\Delta\boldsymbol{v}) = p'_v(\boldsymbol{v},\boldsymbol{s};\boldsymbol{\eta},\Delta\boldsymbol{s},\Delta\boldsymbol{v}) = \int_{\Omega_R} \mathbf{A}_1 : \operatorname{Grad}\boldsymbol{\eta}\,\mathrm{d}\Omega, \tag{B.59}$$

where the second-order tensor $\mathbf{A}_1$ is given by

$$\begin{aligned}\mathbf{A}_1 := {} & \operatorname{Grad}\Delta\boldsymbol{v}\,(\,\Delta_s\mathbf{S}^{(1)} - \mathbf{S}\operatorname{Grad}\Delta\boldsymbol{s}^T - \operatorname{Grad}\Delta\boldsymbol{s}\,\mathbf{S}\,)\\ & - \operatorname{Grad}\boldsymbol{v}\operatorname{Grad}\Delta\boldsymbol{s}\,\Delta_v\mathbf{S}^{(1)} - \mathbf{F}\Delta_v\mathbf{S}^{(1)}\operatorname{Grad}\Delta\boldsymbol{s}^T\\ & + \mathbf{F}\,(\,\Delta_{sv}\mathbf{S}^{(1)} + \Delta_{sv}\mathbf{S}^{(2)}\,)\\ & + [\,\mathbf{F}\Delta_v\mathbf{S}^{(1)} + \operatorname{Grad}\Delta\boldsymbol{v}\,\mathbf{S}\,]\operatorname{Div}\Delta\boldsymbol{s}.\end{aligned} \tag{B.60}$$

The stress increments due to changes $\Delta\boldsymbol{v}$ and $\Delta\boldsymbol{s}$ are introduced as

$$\Delta_{sv}\mathbf{S}^{(1)} := \mathbb{C} : \mathbf{E}''_{sv}(\boldsymbol{v},\Delta\boldsymbol{s},\Delta\boldsymbol{v}) = \mathbb{C} : \mathbf{E}''_{vs}(\boldsymbol{v},\Delta\boldsymbol{v},\Delta\boldsymbol{s}) \tag{B.61}$$

$$\Delta_{sv}\mathbf{S}^{(2)} := \boldsymbol{\mathcal{D}} : \mathbf{E}'_v(\boldsymbol{v},\Delta\boldsymbol{v}) : \mathbf{E}'_s(\boldsymbol{v},\Delta\boldsymbol{s}) \tag{B.62}$$

$$\begin{aligned}\mathbf{E}''_{sv}(\boldsymbol{v},\Delta\boldsymbol{v},\Delta\boldsymbol{s}) = {} & -\operatorname{sym}\{\operatorname{Grad}\Delta\boldsymbol{s}^T\operatorname{Grad}\boldsymbol{v}^T\operatorname{Grad}\Delta\boldsymbol{v}\\ & + \mathbf{F}^T\operatorname{Grad}\Delta\boldsymbol{v}\operatorname{Grad}\Delta\boldsymbol{s}\,\}.\end{aligned} \tag{B.63}$$

The stress increments $\Delta_v\mathbf{S}^{(1)}$ and $\Delta_s\mathbf{S}^{(1)}$ are defined in (B.46) and (B.54), respectively.

Box B.8: Explicit formulation of R''_{sv} for nonlinear elasticity

$$R'''_{svv}(\boldsymbol{v},\boldsymbol{s};\boldsymbol{\eta},\Delta\boldsymbol{s},\Delta\boldsymbol{v},\Delta\boldsymbol{v}) = p''_{vv}(\boldsymbol{v},\boldsymbol{s};\boldsymbol{\eta},\Delta\boldsymbol{s},\Delta\boldsymbol{v},\Delta\boldsymbol{v}) = \int_{\Omega_R} \mathbf{A}_1 : \operatorname{Grad}\boldsymbol{\eta}\,\mathrm{d}\Omega, \tag{B.64}$$

where the second-order tensor $\mathbf{A}_1$ is given by

$$\begin{aligned}\mathbf{A}_1 :=& -2\,\operatorname{Grad}\Delta\boldsymbol{v}\,(\operatorname{Grad}\Delta\boldsymbol{s}\,\Delta_v\mathbf{S}^{(1)} + \Delta_v\mathbf{S}^{(1)}\operatorname{Grad}\Delta\boldsymbol{s}^T)\\ &- \operatorname{Grad}\boldsymbol{v}\operatorname{Grad}\Delta\boldsymbol{s}\,\Delta_v\mathbf{S}^{(2)} - \mathbf{F}\Delta_v\mathbf{S}^{(2)}\operatorname{Grad}\Delta\boldsymbol{s}^T\\ &- \operatorname{Grad}\boldsymbol{v}\operatorname{Grad}\Delta\boldsymbol{s}\,\Delta_v\mathbf{S}^{(3)} - \mathbf{F}\Delta_v\mathbf{S}^{(3)}\operatorname{Grad}\Delta\boldsymbol{s}^T\\ &+ 2\,\operatorname{Grad}\Delta\boldsymbol{v}\,(\Delta_{sv}\mathbf{S}^{(1)} + \Delta_{sv}\mathbf{S}^{(2)})\\ &+ \mathbf{F}\,(\Delta_{svv}\mathbf{S}^{(1)} + 2\,\Delta_{svv}\mathbf{S}^{(2)} + \Delta_{svv}\mathbf{S}^{(3)} + \Delta_{svv}\mathbf{S}^{(4)})\\ &+ [\,2\,\operatorname{Grad}\Delta\boldsymbol{v}\,\Delta_v\mathbf{S}^{(1)} + \mathbf{F}\Delta_v\mathbf{S}^{(2)} + \mathbf{F}\Delta_v\mathbf{S}^{(3)}\,]\operatorname{Div}\Delta\boldsymbol{s}.\end{aligned} \tag{B.65}$$

The stress increments due to changes $\Delta\boldsymbol{v}$ and $\Delta\boldsymbol{s}$ are introduced as

$$\Delta_{svv}\mathbf{S}^{(1)} := \mathbb{C} : \mathbf{E}'''_{svv}(\Delta\boldsymbol{s},\Delta\boldsymbol{v},\Delta\boldsymbol{v}) \tag{B.66}$$

$$\Delta_{svv}\mathbf{S}^{(2)} := \boldsymbol{\mathcal{D}} : \mathbf{E}'_v(\boldsymbol{v},\Delta\boldsymbol{v}) : \mathbf{E}''_{sv}(\boldsymbol{v},\Delta\boldsymbol{s},\Delta\boldsymbol{v}) \tag{B.67}$$

$$\Delta_{svv}\mathbf{S}^{(3)} := \boldsymbol{\mathcal{D}} : \mathbf{E}''_{vv}(\Delta\boldsymbol{v},\Delta\boldsymbol{v}) : \mathbf{E}'_s(\boldsymbol{v},\Delta\boldsymbol{s}) \tag{B.68}$$

$$\Delta_{svv}\mathbf{S}^{(4)} := \boldsymbol{\mathfrak{E}} : \mathbf{E}'_v(\boldsymbol{v},\Delta\boldsymbol{v}) : \mathbf{E}'_v(\boldsymbol{v},\Delta\boldsymbol{v}) : \mathbf{E}'_s(\boldsymbol{v},\Delta\boldsymbol{s}) \tag{B.69}$$

with

$$\mathbf{E}'''_{svv}(\Delta\boldsymbol{s},\Delta\boldsymbol{v},\Delta\boldsymbol{v}) = -\operatorname{sym}\{\operatorname{Grad}\Delta\boldsymbol{s}^T\operatorname{Grad}\Delta\boldsymbol{v}^T\operatorname{Grad}\Delta\boldsymbol{v} + \operatorname{Grad}\Delta\boldsymbol{v}^T\operatorname{Grad}\Delta\boldsymbol{v}\operatorname{Grad}\Delta\boldsymbol{s}\}. \tag{B.70}$$

Explicit formulation of $\mathbb{C}$, $\boldsymbol{\mathcal{D}}$ and $\boldsymbol{\mathfrak{E}}$ are given in Box B.2 and Box B.4. The stress increments $\Delta_v\mathbf{S}^{(1)}$, $\Delta_v\mathbf{S}^{(2)}$ and $\Delta_v\mathbf{S}^{(3)}$ are defined in (B.46), (B.47) and (B.48), respectively. Furthermore, $\Delta_{sv}\mathbf{S}^{(1)}$ and $\Delta_{sv}\mathbf{S}^{(2)}$ are given in (B.61) and (B.62).

Box B.9: Explicit formulation of R'''_{svv} for nonlinear elasticity

$$R'''_{ssv}(\boldsymbol{v},\boldsymbol{s};\boldsymbol{\eta},\Delta\boldsymbol{s},\Delta\boldsymbol{s},\Delta\boldsymbol{v}) = p''_{sv}(\boldsymbol{v},\boldsymbol{s};\boldsymbol{\eta},\Delta\boldsymbol{s},\Delta\boldsymbol{s},\Delta\boldsymbol{v}) = \int_{\Omega_R} \mathbf{A}_1 : \operatorname{Grad}\boldsymbol{\eta}\,\mathrm{d}\Omega, \tag{B.71}$$

$$\begin{aligned}\mathbf{A}_1 := 2\,[\,&\operatorname{Grad}\Delta\boldsymbol{v}\operatorname{Grad}\Delta\boldsymbol{s}\,(\operatorname{Grad}\Delta\boldsymbol{s}\,\mathbf{S} + \mathbf{S}\operatorname{Grad}\Delta\boldsymbol{s}^T - \Delta_s\mathbf{S}^{(1)}) \\ &+ \operatorname{Grad}\boldsymbol{v}\operatorname{Grad}\Delta\boldsymbol{s}\,(\operatorname{Grad}\Delta\boldsymbol{s}\,\Delta_v\mathbf{S}^{(1)} + \Delta_v\mathbf{S}^{(1)}\operatorname{Grad}\Delta\boldsymbol{s}^T) \\ &- \operatorname{Grad}\boldsymbol{v}\operatorname{Grad}\Delta\boldsymbol{s}(\Delta_s\mathbf{S}^{(1)})'_v(\Delta\boldsymbol{v}) \\ &+ \operatorname{Grad}\Delta\boldsymbol{v}\,(\mathbf{S}\operatorname{Grad}\Delta\boldsymbol{s}^T\operatorname{Grad}\Delta\boldsymbol{s}^T - \Delta_s\mathbf{S}^{(1)}\operatorname{Grad}\Delta\boldsymbol{s}^T) \\ &+ \mathbf{F}\,(\Delta_v\mathbf{S}^{(1)}\operatorname{Grad}\Delta\boldsymbol{s}^T\operatorname{Grad}\Delta\boldsymbol{s}^T - (\Delta_s\mathbf{S}^{(1)})'_v(\Delta\boldsymbol{v})\operatorname{Grad}\Delta\boldsymbol{s}^T) \\ &- \operatorname{Grad}\Delta\boldsymbol{v}\,(\operatorname{Grad}\Delta\boldsymbol{s}\,\mathbf{S} + \mathbf{S}\operatorname{Grad}\Delta\boldsymbol{s}^T - \Delta_s\mathbf{S}^{(1)})\operatorname{Div}\Delta\boldsymbol{s} \\ &- (\operatorname{Grad}\boldsymbol{v}\operatorname{Grad}\Delta\boldsymbol{s}\,\Delta_v\mathbf{S}^{(1)} + \mathbf{F}\Delta_v\mathbf{S}^{(1)}\operatorname{Grad}\Delta\boldsymbol{s}^T)\operatorname{Div}\Delta\boldsymbol{s} \\ &+ \mathbf{F}(\Delta_s\mathbf{S}^{(1)})'_v(\Delta\boldsymbol{v})\operatorname{Div}\Delta\boldsymbol{s}\,] \\ &+ \operatorname{Grad}\Delta\boldsymbol{v}\,(\Delta_s\mathbf{S}^{(2)} + \Delta_s\mathbf{S}^{(3)}) + \mathbf{F}\,((\Delta_s\mathbf{S}^{(2)})'_v(\Delta\boldsymbol{v}) + (\Delta_s\mathbf{S}^{(3)})'_v(\Delta\boldsymbol{v})) \\ &- (\operatorname{Grad}\Delta\boldsymbol{v}\mathbf{S} + \mathbf{F}\Delta_v\mathbf{S}^{(1)})\,(\mathbf{I} : \operatorname{Grad}\Delta\boldsymbol{s}\operatorname{Grad}\Delta\boldsymbol{s} - \operatorname{Div}\Delta\boldsymbol{s}\operatorname{Div}\Delta\boldsymbol{s}),\end{aligned} \tag{B.72}$$

$$(\Delta_s\mathbf{S}^{(1)})'_v(\Delta\boldsymbol{v}) := \mathbb{C} : \mathbf{E}''_{sv}(\boldsymbol{v},\Delta\boldsymbol{s},\Delta\boldsymbol{v}) + \boldsymbol{\mathcal{D}} : \mathbf{E}'_v(\boldsymbol{v},\Delta\boldsymbol{v}) : \mathbf{E}'_s(\boldsymbol{v},\Delta\boldsymbol{s}), \tag{B.73}$$

$$\begin{aligned}(\Delta_s\mathbf{S}^{(2)})'_v(\Delta\boldsymbol{v}) := {}& \mathbb{C} : \mathbf{E}'''_{ssv}(\boldsymbol{v},\Delta\boldsymbol{s},\Delta\boldsymbol{s},\Delta\boldsymbol{v}) \\ &+ \boldsymbol{\mathcal{D}} : \mathbf{E}'_v(\boldsymbol{v},\Delta\boldsymbol{v}) : \mathbf{E}''_{ss}(\boldsymbol{v},\Delta\boldsymbol{s},\Delta\boldsymbol{s}),\end{aligned} \tag{B.74}$$

$$\begin{aligned}(\Delta_s\mathbf{S}^{(3)})'_v(\Delta\boldsymbol{v}) := {}& 2\,\boldsymbol{\mathcal{D}} : \mathbf{E}''_{sv}(\boldsymbol{v},\Delta\boldsymbol{s},\Delta\boldsymbol{v}) : \mathbf{E}'_s(\boldsymbol{v},\Delta\boldsymbol{s}) \\ &+ \boldsymbol{\mathfrak{E}} : \mathbf{E}'_v(\boldsymbol{v},\Delta\boldsymbol{v}) : \mathbf{E}'_s(\boldsymbol{v},\Delta\boldsymbol{s}) : \mathbf{E}'_s(\boldsymbol{v},\Delta\boldsymbol{s}),\end{aligned} \tag{B.75}$$

$$\begin{aligned}\mathbf{E}'''_{ssv}(\boldsymbol{v},\Delta\boldsymbol{s},\Delta\boldsymbol{s},\Delta\boldsymbol{v}) = \operatorname{sym}\{&\operatorname{Grad}\Delta\boldsymbol{s}^T\operatorname{Grad}\Delta\boldsymbol{v}^T\operatorname{Grad}\boldsymbol{v}\operatorname{Grad}\Delta\boldsymbol{s} \\ &+ \operatorname{Grad}\Delta\boldsymbol{s}^T\operatorname{Grad}\boldsymbol{v}^T\operatorname{Grad}\Delta\boldsymbol{v}\operatorname{Grad}\Delta\boldsymbol{s} \\ &+ 2\operatorname{Grad}\Delta\boldsymbol{v}^T\operatorname{Grad}\boldsymbol{v}\operatorname{Grad}\Delta\boldsymbol{s}\operatorname{Grad}\Delta\boldsymbol{s} \\ &+ 2\,\mathbf{F}^T\operatorname{Grad}\Delta\boldsymbol{v}\operatorname{Grad}\Delta\boldsymbol{s}\operatorname{Grad}\Delta\boldsymbol{s}\}.\end{aligned} \tag{B.76}$$

Box B.10: Explicit formulation of R'''_{ssv} for nonlinear elasticity

B.2 Linear elasticity

For the sake of completeness, the model problem of linearized elasticity is considered. The most relevant variational and discrete relations are briefly stated.

B.2.1 The primal problem

The state $\boldsymbol{u} \in C^2$ is determined by

$$\boldsymbol{A}\boldsymbol{u} = -[\,\mu\,\Delta\boldsymbol{u} + (\lambda+\mu)\,\nabla\ \mathrm{Div}\ \boldsymbol{u}\,] = \boldsymbol{b}_R \quad \text{in } \Omega_R, \tag{B.77}$$

where $\boldsymbol{A}$ denotes an elliptic differential operator and $\boldsymbol{b}_R$ are body forces per unit volume in Ω_R. Additionally, we have to fulfill the boundary condition

$$\boldsymbol{u} = \bar{\boldsymbol{u}} \quad \text{on } \Gamma_{\mathrm{D}} \qquad \text{and} \qquad \boldsymbol{t} = \bar{\boldsymbol{t}} \quad \text{on } \Gamma_{\mathrm{N}}. \tag{B.78}$$

For notational simplicity, we assume that no prescribed displacements and no prescribed tractions are applied, i.e. $\bar{\boldsymbol{u}} = \boldsymbol{0}$ and $\bar{\boldsymbol{t}} = \boldsymbol{0}$, respectively.

Let $\mathcal{V}$ be a Sobolev space of states $\boldsymbol{u}$, which is defined as

$$\mathcal{V} = \{\boldsymbol{\eta} \in [H^1(\Omega)]^3 :\ \boldsymbol{\eta} = \boldsymbol{0} \text{ on } \Gamma_{\mathrm{D}}\}. \tag{B.79}$$

Furthermore, let $a(\cdot,\cdot)$ be a bilinear form on $\mathcal{V}\times\mathcal{V}$ as well as $F(\cdot)$ a linear functional defined on $\mathcal{V}$. The weak form of the above problem for a given fixed $\boldsymbol{s}$ reads: Find $\boldsymbol{u} \in \mathcal{V}$ such that

$$a(\boldsymbol{s};\boldsymbol{u},\boldsymbol{\eta}) = F(\boldsymbol{s};\boldsymbol{\eta}) \quad \forall\,\boldsymbol{\eta} \in \mathcal{V}. \tag{B.80}$$

For the given model problem of linearized elasticity and under the above assumptions these quantities are given as

$$a(\boldsymbol{s};\boldsymbol{u},\boldsymbol{\eta}) = \int_{\Omega_R} \boldsymbol{\sigma}(\boldsymbol{u}) : \boldsymbol{\varepsilon}(\boldsymbol{\eta})\, d\Omega, \tag{B.81}$$

$$F(\boldsymbol{s};\boldsymbol{\eta}) = \int_{\Omega_R} \boldsymbol{b}_R \cdot \boldsymbol{\eta}\, d\Omega, \tag{B.82}$$

where $\boldsymbol{\sigma}(\boldsymbol{u}) = \mathbb{C} : \boldsymbol{\varepsilon}(\boldsymbol{u})$ denotes the Cauchy stress tensor, $\boldsymbol{\varepsilon}(\boldsymbol{u}) = \mathrm{sym}\{\mathrm{Grad}\,\boldsymbol{u}\}$ is the linear strain tensor and $\mathbb{C}$ is the fourth-order isotropic material tensor corresponding to (B.77).

Remark B.1 *The problem (B.80) is linear in $\boldsymbol{u}$ but possible nonlinear in $\boldsymbol{s}$. This is indicated by the semicolon in $a(\boldsymbol{s};\cdot,\cdot)$ and $F(\boldsymbol{s};\cdot)$, i.e. all arguments on the right of the semicolon are linear.*

B.2.2 Variations of strains

We consider the linear strain tensor

$$\boldsymbol{\varepsilon}(\boldsymbol{u}) := \frac{1}{2}\left(\nabla\boldsymbol{u} + \nabla\boldsymbol{u}^T\right) = \operatorname{sym}\{\nabla\boldsymbol{u}\}. \tag{B.83}$$

The variations of $\boldsymbol{\varepsilon}$ with respect to $\boldsymbol{u}$ and $\boldsymbol{s}$ as well as the mixed variations are given by

$$\boldsymbol{\varepsilon}'_u(\boldsymbol{\eta}) = \frac{1}{2}\left(\nabla\boldsymbol{\eta} + \nabla\boldsymbol{\eta}^T\right) = \operatorname{sym}\{\nabla\boldsymbol{\eta}\} = \boldsymbol{\varepsilon}(\boldsymbol{\eta}) \tag{B.84}$$

$$\boldsymbol{\varepsilon}'_s(\boldsymbol{u},\boldsymbol{\psi}) = -\frac{1}{2}\left(\nabla\boldsymbol{u}\,\nabla\boldsymbol{\psi} + \nabla\boldsymbol{\psi}^T\nabla\boldsymbol{u}^T\right) = -\operatorname{sym}\{\nabla\boldsymbol{u}\,\nabla\boldsymbol{\psi}\} \tag{B.85}$$

$$\boldsymbol{\varepsilon}''_{us}(\boldsymbol{\eta},\boldsymbol{\psi}) = -\frac{1}{2}\left(\nabla\boldsymbol{\eta}\,\nabla\boldsymbol{\psi} + \nabla\boldsymbol{\psi}^T\nabla\boldsymbol{\eta}^T\right) = -\operatorname{sym}\{\nabla\boldsymbol{\eta}\,\nabla\boldsymbol{\psi}\} \tag{B.86}$$

$$\boldsymbol{\varepsilon}''_{su}(\boldsymbol{\psi},\boldsymbol{\eta}) = \boldsymbol{\varepsilon}''_{us}(\boldsymbol{\eta},\boldsymbol{\psi}) = -\operatorname{sym}\{\nabla\boldsymbol{\eta}\,\nabla\boldsymbol{\psi}\} \tag{B.87}$$

$$\begin{aligned}\boldsymbol{\varepsilon}''_{ss}(\boldsymbol{u},\boldsymbol{\psi},\boldsymbol{\chi}) = \frac{1}{2}\big(&\nabla\boldsymbol{u}\,\nabla\boldsymbol{\chi}\,\nabla\boldsymbol{\psi} + \nabla\boldsymbol{u}\,\nabla\boldsymbol{\psi}\,\nabla\boldsymbol{\chi}\\ &+ \nabla\boldsymbol{\psi}^T\nabla\boldsymbol{\chi}^T\nabla\boldsymbol{u}^T + \nabla\boldsymbol{\chi}^T\nabla\boldsymbol{\psi}^T\nabla\boldsymbol{u}^T\big)\\ = \operatorname{sym}\{&\nabla\boldsymbol{u}\,\nabla\boldsymbol{\chi}\,\nabla\boldsymbol{\psi} + \nabla\boldsymbol{u}\,\nabla\boldsymbol{\psi}\,\nabla\boldsymbol{\chi}\}\,.\end{aligned} \tag{B.88}$$

B.2.3 Variations of the primal energy

The energy functional reads

$$E(\boldsymbol{u},\boldsymbol{s}) = C(\boldsymbol{u},\boldsymbol{s}) - F(\boldsymbol{s};\boldsymbol{u}) \tag{B.89}$$

where

$$C(\boldsymbol{u},\boldsymbol{s}) = \frac{1}{2}\,a(\boldsymbol{s};\boldsymbol{u},\boldsymbol{u}) = \int_{\Omega_R} W_R(\boldsymbol{u})\,\mathrm{d}\Omega, \tag{B.90}$$

$$W_R(\boldsymbol{u}) := \frac{1}{2}\,\boldsymbol{\sigma}(\boldsymbol{u}) : \boldsymbol{\varepsilon}(\boldsymbol{u}). \tag{B.91}$$

The primal physical and material residuals are given by

$$R(\boldsymbol{u},\boldsymbol{s};\boldsymbol{\eta}) = E'_u(\boldsymbol{u},\boldsymbol{s})(\boldsymbol{\eta}) = a(\boldsymbol{s};\boldsymbol{u},\boldsymbol{\eta}) - F(\boldsymbol{s};\boldsymbol{\eta}), \tag{B.92}$$

$$G(\boldsymbol{u},\boldsymbol{s};\boldsymbol{\psi}) = E'_s(\boldsymbol{u},\boldsymbol{s})(\boldsymbol{\psi}) = b(\boldsymbol{s},\boldsymbol{u};\boldsymbol{\psi}) - F'_s(\boldsymbol{s};\boldsymbol{u},\boldsymbol{\psi}), \tag{B.93}$$

where $a(\boldsymbol{s};\boldsymbol{u},\boldsymbol{\eta}) = C'_u(\boldsymbol{u},\boldsymbol{s})(\boldsymbol{\eta})$ is given in (B.81) and

$$b(\boldsymbol{s},\boldsymbol{u};\boldsymbol{\psi}) := C'_s(\boldsymbol{u},\boldsymbol{s})(\boldsymbol{\psi}) = \int_{\Omega_R} \boldsymbol{\Sigma}(\boldsymbol{u}) : \nabla\boldsymbol{\psi}\,\mathrm{d}\Omega. \tag{B.94}$$

The energy-momentum or Eshelby tensor in terms of linear elasticity is obtained as

$$\boldsymbol{\Sigma}(\boldsymbol{u}) := W_R(\boldsymbol{u})\mathbf{I} - \nabla\boldsymbol{u}^T\boldsymbol{\sigma}. \tag{B.95}$$

B.2.4 Variational formulations of the primal residuals and tangent forms

The residuals written in terms of $\boldsymbol{\sigma}$ and $\boldsymbol{\varepsilon}$ are given by

$$R(\boldsymbol{u}, \boldsymbol{s}; \boldsymbol{\eta}) = \int_{\Omega_R} \boldsymbol{\sigma} : \boldsymbol{\varepsilon}(\boldsymbol{\eta}) \, \mathrm{d}\Omega - F(\boldsymbol{s}; \boldsymbol{\eta}) \tag{B.96}$$

$$G(\boldsymbol{u}, \boldsymbol{s}; \boldsymbol{\psi}) = \int_{\Omega_R} [\, \boldsymbol{\sigma} : \boldsymbol{\varepsilon}'_s(\boldsymbol{u}, \boldsymbol{\psi}) + W_R \mathbf{I} : \nabla \boldsymbol{\psi} \,] \, \mathrm{d}\Omega - F'_s(\boldsymbol{s}; \boldsymbol{v}, \boldsymbol{\psi}) \tag{B.97}$$

The tangent forms for linear elasticity are obtained as

$$k(\boldsymbol{u}, \boldsymbol{s}; \boldsymbol{\eta}, \delta\boldsymbol{u}) = \int_{\Omega_R} \boldsymbol{\varepsilon}'_u(\boldsymbol{\eta}) : \mathbb{C} : \boldsymbol{\varepsilon}'_u(\delta\boldsymbol{u}) \, \mathrm{d}\Omega = \int_{\Omega_R} \boldsymbol{\varepsilon}(\boldsymbol{\eta}) : \mathbb{C} : \boldsymbol{\varepsilon}(\delta\boldsymbol{u}) \, \mathrm{d}\Omega, \tag{B.98}$$

$$\begin{aligned} p(\boldsymbol{u}, \boldsymbol{s}; \boldsymbol{\eta}, \delta\boldsymbol{s}) = \int_{\Omega_R} \{\, & \boldsymbol{\varepsilon}'_u(\boldsymbol{\eta}) : \mathbb{C} : \boldsymbol{\varepsilon}'_s(\boldsymbol{u}, \delta\boldsymbol{s}) + \boldsymbol{\sigma} : \boldsymbol{\varepsilon}''_{us}(\boldsymbol{\eta}, \delta\boldsymbol{s}) \\ & + \boldsymbol{\sigma} : \boldsymbol{\varepsilon}(\boldsymbol{\eta}) \operatorname{Div} \delta\boldsymbol{s} \,\} \, \mathrm{d}\Omega \\ & - F'_s(\boldsymbol{s}; \boldsymbol{\eta}, \delta\boldsymbol{s}), \end{aligned} \tag{B.99}$$

$$\begin{aligned} t(\boldsymbol{u}, \boldsymbol{s}; \boldsymbol{\psi}, \delta\boldsymbol{u}) = \int_{\Omega_R} \{\, & \boldsymbol{\varepsilon}'_s(\boldsymbol{u}, \boldsymbol{\psi}) : \mathbb{C} : \boldsymbol{\varepsilon}'_u(\delta\boldsymbol{u}) + \boldsymbol{\sigma} : \boldsymbol{\varepsilon}''_{su}(\boldsymbol{\psi}, \delta\boldsymbol{u}) \\ & + \boldsymbol{\sigma} : \boldsymbol{\varepsilon}(\delta\boldsymbol{u}) \operatorname{Div} \boldsymbol{\psi} \,\} \, \mathrm{d}\Omega \\ & - F'_s(\boldsymbol{s}; \delta\boldsymbol{v}, \boldsymbol{\psi}), \end{aligned} \tag{B.100}$$

$$\begin{aligned} d(\boldsymbol{u}, \boldsymbol{s}; \boldsymbol{\psi}, \delta\boldsymbol{s}) = \int_{\Omega_R} \{\, & \boldsymbol{\varepsilon}'_s(\boldsymbol{u}, \boldsymbol{\psi}) : \mathbb{C} : \boldsymbol{\varepsilon}'_s(\boldsymbol{u}, \delta\boldsymbol{s}) + \boldsymbol{\sigma} : \boldsymbol{\varepsilon}''_{ss}(\boldsymbol{u}, \boldsymbol{\psi}, \delta\boldsymbol{s}) \\ & + \boldsymbol{\sigma} : [\, \boldsymbol{\varepsilon}'_s(\boldsymbol{u}, \boldsymbol{\psi}) \operatorname{Div} \delta\boldsymbol{s} + \boldsymbol{\varepsilon}'_s(\boldsymbol{u}, \delta\boldsymbol{s}) \operatorname{Div} \boldsymbol{\psi} \,] \\ & + W_R \, [\operatorname{Div} \boldsymbol{\psi} \operatorname{Div} \delta\boldsymbol{s} - \mathbf{I} : \nabla\boldsymbol{\psi} \nabla\delta\boldsymbol{s} \,] \,\} \, \mathrm{d}\Omega \\ & - F''_{ss}(\boldsymbol{s}; \boldsymbol{v}, \boldsymbol{\psi}, \delta\boldsymbol{s}). \end{aligned} \tag{B.101}$$

The explicit formulations of $F(\boldsymbol{s}; \boldsymbol{\eta})$, $F'_s(\boldsymbol{s}; \boldsymbol{v}, \boldsymbol{\psi})$, $F'_s(\boldsymbol{s}; \boldsymbol{\eta}, \delta\boldsymbol{s})$ and $F''_{ss}(\boldsymbol{s}; \boldsymbol{v}, \boldsymbol{\psi}, \delta\boldsymbol{s})$ depend on the form of the functional $F(\cdot)$. They are equal to the quantities from the nonlinear problem given in (4.92), (4.93), (4.94) and (4.95), respectively.

B.2.5 Discrete formulations of the primal residuals and tangent matrices

The nodal contributions of the discrete residual vectors are given by

$$\boldsymbol{R}_i^e = \int_{\Omega_R^e} \boldsymbol{B}_i^T \underline{\boldsymbol{\sigma}} \, \mathrm{d}\Omega - \boldsymbol{F}^e(\boldsymbol{s})_i, \tag{B.102}$$

$$\boldsymbol{G}_i^e = \int_{\Omega_R^e} \{ \, \boldsymbol{B}_{si}^T \underline{\boldsymbol{\sigma}} + W_R \boldsymbol{I} \boldsymbol{L}_i \} \, \mathrm{d}\Omega - \boldsymbol{F}_s^e(\boldsymbol{s}; \boldsymbol{v})_i, \tag{B.103}$$

and the tangent matrices are obtained as

$$\boldsymbol{K}_{ij}^e = \int_{\Omega_R^e} \boldsymbol{B}_i^T \boldsymbol{C} \boldsymbol{B}_j \, \mathrm{d}\Omega, \tag{B.104}$$

$$\begin{aligned} \boldsymbol{P}_{ij}^e = & \int_{\Omega_R^e} \{ \, \boldsymbol{B}_i^T \boldsymbol{C} \boldsymbol{B}_{sj} - \boldsymbol{\sigma} \boldsymbol{L}_j \boldsymbol{L}_i^T + \boldsymbol{\sigma} \boldsymbol{L}_i \boldsymbol{L}_j^T \, \} \, \mathrm{d}\Omega \\ & - \boldsymbol{F}_s^e(\boldsymbol{s})_{ij}, \end{aligned} \tag{B.105}$$

$$\begin{aligned} \boldsymbol{D}_{ij}^e = & \int_{\Omega_R^e} \{ \, \boldsymbol{B}_{si}^T \boldsymbol{C} \boldsymbol{B}_{sj} + \nabla \boldsymbol{u}^T \boldsymbol{\sigma} \boldsymbol{L}_j \boldsymbol{L}_i^T + \boldsymbol{L}_j \boldsymbol{L}_i^T \boldsymbol{\sigma}^T \nabla \boldsymbol{u} \\ & \quad - \nabla \boldsymbol{u}^T \boldsymbol{\sigma} \boldsymbol{L}_i \boldsymbol{L}_j^T - \boldsymbol{L}_i \boldsymbol{L}_j^T \boldsymbol{\sigma}^T \nabla \boldsymbol{u} \\ & \quad + W_R \, [\, \boldsymbol{L}_i \boldsymbol{L}_j^T - \boldsymbol{L}_j \boldsymbol{L}_i^T \,] \, \} \, \mathrm{d}\Omega \\ & - \boldsymbol{F}_{ss}^e(\boldsymbol{s}; \boldsymbol{v})_{ij}, \end{aligned} \tag{B.106}$$

where

$$\boldsymbol{B}_i = \begin{bmatrix} \phi_{i,1} & 0 \\ 0 & \phi_{i,2} \\ \phi_{i,2} & \phi_{i,1} \end{bmatrix}, \qquad \boldsymbol{B}_{si} = -\boldsymbol{B}_i \nabla \boldsymbol{u}, \qquad \boldsymbol{L}_i := \nabla \phi_i = \begin{bmatrix} \phi_{i,1} \\ \phi_{i,2} \end{bmatrix}, \tag{B.107}$$

$$\boldsymbol{\sigma} = \begin{bmatrix} \sigma_{11} & \sigma_{12} \\ \sigma_{21} & \sigma_{22} \end{bmatrix}, \qquad \underline{\boldsymbol{\sigma}} = \begin{bmatrix} \sigma_{11} & \sigma_{22} & \sigma_{12} \end{bmatrix}^T. \tag{B.108}$$

Details about the numerical implementation are given in Appendix C.

The quantities $\boldsymbol{F}^e(\boldsymbol{s})_i$ and $\boldsymbol{F}_s^e(\boldsymbol{s}; \boldsymbol{v})_i$ are the element nodal vectors on a node i corresponding to the functionals $F(\boldsymbol{s}; \cdot)$ and $F_s'(\boldsymbol{s}; \boldsymbol{v}, \cdot)$. In the same manner, $\boldsymbol{F}_s^e(\boldsymbol{s})_{ij}$ and $\boldsymbol{F}_{ss}^e(\boldsymbol{s}; \boldsymbol{v})_{ij}$ are the element nodal matrices corresponding to the bilinear forms $F_s'(\boldsymbol{s}; \cdot, \cdot)$ and $F_{ss}''(\boldsymbol{s}; \boldsymbol{v}, \cdot, \cdot)$, respectively. These contributions are equal to the quantities from the nonlinear problem and they are given in (4.103), (4.104), (4.105) and (4.106).

B.2.6 The dual problem

The weak form of the dual problem for a given fixed $\boldsymbol{s}$ reads: Find $\boldsymbol{z} \in \mathcal{V}$ such that

$$a(\boldsymbol{s}; \boldsymbol{z}, \boldsymbol{\eta}) = J(\boldsymbol{s}; \boldsymbol{\eta}) \quad \forall\, \boldsymbol{\eta} \in \mathcal{V}. \tag{B.109}$$

The corresponding energy functional is given as

$$E^*(\boldsymbol{z}, \boldsymbol{s}) = C^*(\boldsymbol{z}, \boldsymbol{s}) - J(\boldsymbol{s}; \boldsymbol{u}) \tag{B.110}$$

where

$$C^*(\boldsymbol{z}, \boldsymbol{s}) = C(\boldsymbol{z}, \boldsymbol{s}) = \frac{1}{2}\, a(\boldsymbol{s}; \boldsymbol{z}, \boldsymbol{z}) = \int_{\Omega_R} W_R(\boldsymbol{z})\, \mathrm{d}\Omega. \tag{B.111}$$

This coincides with (B.90). Hence, in the linear case the strain energy functions of the primal and the dual problems coincide. Therefore, all variations of the internal energy $C^*(\boldsymbol{z}, \boldsymbol{s}) = C(\boldsymbol{z}, \boldsymbol{s})$ yield the same results as for the primal problem.

Finally, the variational formulations of all dual residuals $R^*(\cdot)$ and $G^*(\cdot)$ as well as the dual tangent forms $p^*(\cdot, \cdot)$, $t^*(\cdot, \cdot)$ and $d^*(\cdot, \cdot)$ are given in Section B.2.4, in which $\boldsymbol{u}$ has to be replaced by $\boldsymbol{z}$. In the same manner, the corresponding discrete formulations are given in Section B.2.5.

Only the variations of the functional $F(\boldsymbol{s}; \boldsymbol{\eta})$ in the primal problem have to be replaced by the corresponding variations of the functional $J(\boldsymbol{s}; \boldsymbol{\eta})$.

B.2.7 Explicit formulations for higher-order variations of the residual

This section deals with higher-order variations of the residual $R(\boldsymbol{u}, \boldsymbol{s}; \cdot)$ with respect to $\boldsymbol{u}$ and $\boldsymbol{s}$ for shape sensitivity. For the general nonlinear problem these terms have been derived in Section 10.6. The variations are required for error analysis and improvement of sensitivity relations as proposed in Chapter 10. Furthermore, compact specifications of R''_{uu}, R''_{ss}, R''_{su} and R''_{suu} are stated. These relations can be directly computed as the usual residual $R(\boldsymbol{u}, \boldsymbol{s}; \cdot)$.

For the model problem of linearized elasticity the second variation of $R(\boldsymbol{u}, \boldsymbol{s}; \boldsymbol{\eta}$ with respect to $\boldsymbol{u}$ vanishes, i.e.

$$R''_{uu}(\boldsymbol{u}, \boldsymbol{s}; \boldsymbol{\eta}, \Delta\boldsymbol{u}) = k'_u(\boldsymbol{u}, \boldsymbol{s}; \boldsymbol{\eta}, \Delta\boldsymbol{u}) = 0. \tag{B.112}$$

Therefore, the remainder $r^u(\boldsymbol{u}_0, \boldsymbol{s}_0, \Delta\boldsymbol{u})$ defined in (10.23) does not contribute to (10.29).

The second variation of the primal physical residual $R(\boldsymbol{u}, \boldsymbol{s}; \cdot)$ with respect to $\boldsymbol{s}$ reads

$$
\begin{aligned}
R''_{ss}(\boldsymbol{u}, \boldsymbol{s}; \boldsymbol{\eta}, \Delta\boldsymbol{s}, \Delta\boldsymbol{s}) &= p'_s(\boldsymbol{u}, \boldsymbol{s}; \boldsymbol{\eta}, \Delta\boldsymbol{s}, \Delta\boldsymbol{s}) \qquad \text{(B.113)}\\
&= \int_{\Omega_R} \{\, 2\, \boldsymbol{\varepsilon}''_{us}(\boldsymbol{\eta}, \Delta\boldsymbol{s}) : \mathbb{C} : \boldsymbol{\varepsilon}'_s(\boldsymbol{u}, \Delta\boldsymbol{s}) \\
&\qquad + \boldsymbol{\sigma} : \boldsymbol{\varepsilon}'''_{uss}(\boldsymbol{\eta}, \Delta\boldsymbol{s}, \Delta\boldsymbol{s}) + \boldsymbol{\varepsilon}'_u(\boldsymbol{\eta}) : \mathbb{C} : \boldsymbol{\varepsilon}''_{ss}(\boldsymbol{u}, \Delta\boldsymbol{s}, \Delta\boldsymbol{s}) \\
&\qquad + [\, \boldsymbol{\varepsilon}'_s(\boldsymbol{u}, \Delta\boldsymbol{s}) : \mathbb{C} : \boldsymbol{\varepsilon}(\boldsymbol{\eta}) + \boldsymbol{\sigma} : \boldsymbol{\varepsilon}''_{us}(\boldsymbol{\eta}, \Delta\boldsymbol{s}) \,]\mathbf{I} : \operatorname{Grad} \Delta\boldsymbol{s} \\
&\qquad - [\, \boldsymbol{\sigma} : \boldsymbol{\varepsilon}(\boldsymbol{\eta}) - \boldsymbol{b}_R \cdot \boldsymbol{\eta} \,]\mathbf{I} : \operatorname{Grad} \Delta\boldsymbol{s} \operatorname{Grad} \Delta\boldsymbol{s} \\
&\qquad + [\, \boldsymbol{\sigma} : \boldsymbol{\varepsilon}''_{us}(\boldsymbol{\eta}, \Delta\boldsymbol{s}) + \boldsymbol{\varepsilon}'_u(\boldsymbol{\eta}) : \mathbb{C} : \boldsymbol{\varepsilon}'_s(\boldsymbol{u}, \Delta\boldsymbol{s}) \,]\mathbf{I} : \operatorname{Grad} \Delta\boldsymbol{s} \\
&\qquad + [\, (\, \boldsymbol{\sigma} : \boldsymbol{\varepsilon}(\boldsymbol{\eta}) - \boldsymbol{b}_R \cdot \boldsymbol{\eta} \,)\mathbf{I} : \operatorname{Grad} \Delta\boldsymbol{s} \,]\mathbf{I} : \operatorname{Grad} \Delta\boldsymbol{s} \,\}\, \mathrm{d}\Omega.
\end{aligned}
$$

In the same manner, the mixed variation of the primal physical residual $R(\boldsymbol{u}, \boldsymbol{s}; \cdot)$ with respect to $\boldsymbol{u}$ is obtained as

$$
\begin{aligned}
R''_{su}(\boldsymbol{u}, \boldsymbol{s}; \boldsymbol{\eta}, \Delta\boldsymbol{s}, \Delta\boldsymbol{u}) &= p'_u(\boldsymbol{u}, \boldsymbol{s}; \boldsymbol{\eta}, \Delta\boldsymbol{s}, \Delta\boldsymbol{u}) \qquad \text{(B.114)}\\
&= \int_{\Omega_R} \{\, \boldsymbol{\varepsilon}''_{us}(\boldsymbol{\eta}, \Delta\boldsymbol{s}) : \mathbb{C} : \boldsymbol{\varepsilon}'_u(\Delta\boldsymbol{u}) + \boldsymbol{\varepsilon}'_u(\boldsymbol{\eta}) : \mathbb{C} : \boldsymbol{\varepsilon}'_s(\Delta\boldsymbol{u}, \Delta\boldsymbol{s}) \\
&\qquad + \boldsymbol{\varepsilon}'_u(\boldsymbol{\eta}) : \mathbb{C} : \boldsymbol{\varepsilon}(\Delta\boldsymbol{u})\mathbf{I} : \operatorname{Grad} \Delta\boldsymbol{s} \,\}\, \mathrm{d}\Omega
\end{aligned}
$$

Finally, the third variation R'''_{suu} vanishes in the case of linear elasticity, i.e.

$$
R'''_{suu}(\boldsymbol{u}, \boldsymbol{s}; \boldsymbol{\eta}, \Delta\boldsymbol{s}, \Delta\boldsymbol{u}, \Delta\boldsymbol{u}) = p''_{uu}(\boldsymbol{u}, \boldsymbol{s}; \boldsymbol{\eta}, \Delta\boldsymbol{s}, \Delta\boldsymbol{u}, \Delta\boldsymbol{u}) = 0. \qquad \text{(B.115)}
$$

For given $\{\boldsymbol{u}, \boldsymbol{s}\}$ and $\{\Delta\boldsymbol{u}, \Delta\boldsymbol{s}\}$ all of the above forms become linear functionals. The compact formulations for the problem of linear elasticity are collected in Box B.11 in the same manner as in Section B.1.2 for the nonlinear problem.

$$R''_{uu}(\boldsymbol{u}, \boldsymbol{s}; \boldsymbol{\eta}, \Delta\boldsymbol{u}) = k'_u(\boldsymbol{u}, \boldsymbol{s}; \boldsymbol{\eta}, \Delta\boldsymbol{u}) = 0 \tag{B.116}$$

$$\begin{aligned} R''_{ss}(\boldsymbol{u}, \boldsymbol{s}; \boldsymbol{\eta}, \Delta\boldsymbol{s}, \Delta\boldsymbol{s}) &= p'_s(\boldsymbol{u}, \boldsymbol{s}; \boldsymbol{\eta}, \Delta\boldsymbol{s}, \Delta\boldsymbol{s}) \\ &= \int_{\Omega_R} \{\, \mathbf{A}_1 : \operatorname{Grad} \boldsymbol{\eta} + \boldsymbol{A}_2 \cdot \boldsymbol{\eta} \,\} \,\mathrm{d}\Omega \end{aligned} \tag{B.117}$$

with

$$\begin{aligned} \mathbf{A}_1 := 2\,[\, &\Delta_s\boldsymbol{\sigma}^{(1)} \operatorname{Grad} \Delta\boldsymbol{s}^T + \boldsymbol{\sigma} \operatorname{Grad} \Delta\boldsymbol{s}^T \operatorname{Grad} \Delta\boldsymbol{s}^T + \Delta_s\boldsymbol{\sigma}^{(2)} \\ &- (\, \Delta_s\boldsymbol{\sigma}^{(1)} + \boldsymbol{\sigma} \operatorname{Grad} \Delta\boldsymbol{s}^T \,) \operatorname{Div} \Delta\boldsymbol{s} \,] \\ &- \boldsymbol{\sigma}\,(\, \mathbf{I} : \operatorname{Grad} \Delta\boldsymbol{s} \operatorname{Grad} \Delta\boldsymbol{s} - \operatorname{Div} \Delta\boldsymbol{s} \operatorname{Div} \Delta\boldsymbol{s} \,), \end{aligned} \tag{B.118}$$

$$\boldsymbol{A}_2 := \boldsymbol{b}_R\,(\, \mathbf{I} : \operatorname{Grad} \Delta\boldsymbol{s} \operatorname{Grad} \Delta\boldsymbol{s} - \operatorname{Div} \Delta\boldsymbol{s} \operatorname{Div} \Delta\boldsymbol{s} \,), \tag{B.119}$$

$$\Delta_s\boldsymbol{\sigma}^{(1)} := \mathbb{C} : \operatorname{Grad} \boldsymbol{u} \operatorname{Grad} \Delta\boldsymbol{s}, \tag{B.120}$$

$$\Delta_s\boldsymbol{\sigma}^{(2)} := \mathbb{C} : \operatorname{Grad} \boldsymbol{u} \operatorname{Grad} \Delta\boldsymbol{s} \operatorname{Grad} \Delta\boldsymbol{s}. \tag{B.121}$$

$$R''_{su}(\boldsymbol{u}, \boldsymbol{s}; \boldsymbol{\eta}, \Delta\boldsymbol{s}, \Delta\boldsymbol{u}) = p'_u(\boldsymbol{u}, \boldsymbol{s}; \boldsymbol{\eta}, \Delta\boldsymbol{s}, \Delta\boldsymbol{u}) = \int_{\Omega_R} \mathbf{A}_3 : \operatorname{Grad} \boldsymbol{\eta} \,\mathrm{d}\Omega \tag{B.122}$$

with

$$\mathbf{A}_3 := -\Delta_{us}\boldsymbol{\sigma} - \Delta_u\boldsymbol{\sigma} \operatorname{Grad} \Delta\boldsymbol{s}^T + \Delta_u\boldsymbol{\sigma} \operatorname{Div} \Delta\boldsymbol{s} \tag{B.123}$$

$$\Delta_u\boldsymbol{\sigma} := \mathbb{C} : \operatorname{Grad} \Delta\boldsymbol{u}, \tag{B.124}$$

$$\Delta_{us}\boldsymbol{\sigma} := \mathbb{C} : \operatorname{Grad} \Delta\boldsymbol{u} \operatorname{Grad} \Delta\boldsymbol{s}. \tag{B.125}$$

$$R'''_{suu}(\boldsymbol{u}, \boldsymbol{s}; \boldsymbol{\eta}, \Delta\boldsymbol{s}, \Delta\boldsymbol{u}, \Delta\boldsymbol{u}) = p''_{uu}(\boldsymbol{u}, \boldsymbol{s}; \boldsymbol{\eta}, \Delta\boldsymbol{s}, \Delta\boldsymbol{u}, \Delta\boldsymbol{u}) = 0 \tag{B.126}$$

Box B.11: Explicit formulations of R''_{uu}, R''_{ss}, R''_{su} and R'''_{suu} for linear elasticity

Appendix C

Details on the numerical implementation

This chapter is concerned with some details about the numerical implementation. The approximations of the considered residuals and tangent forms are briefly stated. For notational simplicity only the two-dimensional case is considered. The extension to general three-dimensional problems is straightforward.

C.1 Preliminaries

The finite element approximation is given as usual by using shape functions $\phi_i(\boldsymbol{\xi})$. Following the isoparametric concept, the state $\boldsymbol{v}_h$ and the geometry $\boldsymbol{X}_h$ are approximated by the same shape functions defined on a fixed parameter space with coordinates $\boldsymbol{\xi}$. According to the classical Bubnov-Galerkin technique also the test functions are interpolated using the shape functions $\phi_i(\boldsymbol{\xi})$. For details about the finite element technique we refer to standard text books, e.g. [10, 17, 105, 107, 108].

The state function $\boldsymbol{v}_h$ and the geometry $\boldsymbol{X}_h$ as well as their derivatives are approximated in every element in the form

$$\boldsymbol{v}_h^e = \sum_{i=1}^{n} \boldsymbol{v}_i \, \phi_i \qquad \boldsymbol{v}_{h,\beta} = \sum_{i=1}^{n} \boldsymbol{v}_i \, \phi_{i,\beta} \quad \text{with} \quad \boldsymbol{v}_i = \begin{bmatrix} v_1^{(i)} \\ v_2^{(i)} \end{bmatrix},$$

$$\boldsymbol{X}_h^e = \sum_{i=1}^{n} \boldsymbol{X}_i \, \phi_i \qquad \boldsymbol{X}_{h,\beta} = \sum_{i=1}^{n} \boldsymbol{X}_i \, \phi_{i,\beta} \quad \text{with} \quad \boldsymbol{X}_i = \begin{bmatrix} X_1^{(i)} \\ X_2^{(i)} \end{bmatrix},$$

where $\boldsymbol{v}_i$ and $\boldsymbol{X}_i$ are the nodal components at node i and n denotes the number of nodes per element. Furthermore, the gradient and the divergence are approximated by

$$\operatorname{Grad} \boldsymbol{v}_h^e = \sum_{i=1}^{n} \boldsymbol{v}_i \otimes \nabla_X \phi_i = \sum_{i=1}^{n} \boldsymbol{v}_i \nabla_X \phi_i^T = \sum_{i=1}^{n} \begin{bmatrix} v_1^{(i)} \, \phi_{i,1} & v_1^{(i)} \, \phi_{i,2} \\ v_2^{(i)} \, \phi_{i,1} & v_2^{(i)} \, \phi_{i,2} \end{bmatrix},$$

$$\operatorname{Grad} \boldsymbol{X}_h^e = \sum_{i=1}^{n} \boldsymbol{X}_i \otimes \nabla_X \phi_i = \sum_{i=1}^{n} \boldsymbol{X}_i \nabla_X \phi_i^T = \sum_{i=1}^{n} \begin{bmatrix} X_1^{(i)}\,\phi_{i,1} & X_1^{(i)}\,\phi_{i,2} \\ X_2^{(i)}\,\phi_{i,1} & X_2^{(i)}\,\phi_{i,2} \end{bmatrix},$$

$$\operatorname{Div} \boldsymbol{v}_h^e = \sum_{i=1}^{n} \nabla_X \phi_i \cdot \boldsymbol{v}_i = \sum_{i=1}^{n} \nabla_X \phi_i^T \boldsymbol{v}_i,$$

$$\operatorname{Div} \boldsymbol{X}_h^e = \sum_{i=1}^{n} \nabla_X \phi_i \cdot \boldsymbol{X}_i = \sum_{i=1}^{n} \nabla_X \phi_i^T \boldsymbol{X}_i.$$

We introduce for the gradient of the shape functions the vectors

$$\boldsymbol{L}_i := \nabla_X \phi_i = \begin{bmatrix} \phi_{i,1} \\ \phi_{i,2} \end{bmatrix}, \qquad \boldsymbol{L}_j := \nabla_X \phi_j = \begin{bmatrix} \phi_{j,1} \\ \phi_{j,2} \end{bmatrix}. \tag{C.1}$$

C.2 Approximations of the Green-Lagrange strain tensor

We consider the Green-Lagrange strain tensor and its variations with respect to $\boldsymbol{v}$ and $\boldsymbol{s}$ given in Section A.2. In addition to the classical well-known approximation of the variation $\mathbf{E}'_v$, we introduce in the same manner similar approximations of different variations of $\mathbf{E}$.

C.2.1 General approximation of symmetric strain measures

Let $\mathbf{T}'_v(\boldsymbol{v}, \delta\boldsymbol{v})$ be the variation of a two point tensor $\mathbf{T}(\boldsymbol{v})$ with respect to $\boldsymbol{v}$. We assume that the variation $\mathbf{T}'_v$ has the particular form

$$\mathbf{T}'_v(\boldsymbol{v}, \delta\boldsymbol{v}) = \frac{1}{2} \left[\operatorname{Grad} \delta\boldsymbol{v}^T \mathbf{A} + \mathbf{A}^T \operatorname{Grad} \delta\boldsymbol{v}\right] = \operatorname{sym}\{\mathbf{A}^T \operatorname{Grad} \delta\boldsymbol{v}\} \tag{C.2}$$

with some tensor $\mathbf{A}(\boldsymbol{v})$. For a matrix formulation we use the symmetry of $\mathbf{T}'_v$ and we can introduce a vector $\boldsymbol{T}'_v$ with three independent components such that its finite element approximation can be written as

$$\boldsymbol{T}'_v(\boldsymbol{v}_h, \delta\boldsymbol{v}_h) = \begin{bmatrix} (T'_v)_{11} \\ (T'_v)_{22} \\ 2\,(T'_v)_{12} \end{bmatrix} = \sum_{i=1}^{n} \boldsymbol{B}_{vi} \delta\boldsymbol{v}_i \tag{C.3}$$

with

$$\boldsymbol{B}_{vi} = \begin{bmatrix} A_{11}\,\phi_{i,1} & A_{21}\,\phi_{i,1} \\ A_{12}\,\phi_{i,2} & A_{22}\,\phi_{i,2} \\ A_{11}\,\phi_{i,2} + A_{12}\,\phi_{i,1} & A_{21}\,\phi_{i,2} + A_{22}\,\phi_{i,1} \end{bmatrix}, \qquad \delta\boldsymbol{v}_i = \begin{bmatrix} \delta v_1^{(i)} \\ \delta v_2^{(i)} \end{bmatrix}. \tag{C.4}$$

C.2.2 Approximation of variations of the Green-Lagrange strain tensor

Approximation of $\mathbf{E}'_v(\boldsymbol{v},\boldsymbol{\eta})$. The variation with respect to the state is given as

$$\mathbf{E}'_v(\boldsymbol{v},\boldsymbol{\eta}) = \operatorname{sym}\{\mathbf{F}^T \operatorname{Grad}\boldsymbol{\eta}\} = \operatorname{sym}\{\mathbf{A}_v^T \operatorname{Grad}\boldsymbol{\eta}\}, \tag{C.5}$$

$$\mathbf{A}_v := \mathbf{F}. \tag{C.6}$$

The finite element approximation can be written as

$$\boldsymbol{E}'_v(\boldsymbol{v}_h,\boldsymbol{\eta}_h) = \begin{bmatrix} (E'_v)_{11} \\ (E'_v)_{22} \\ 2\,(E'_v)_{12} \end{bmatrix} = \sum_{i=1}^{n} \boldsymbol{B}_{vi}\boldsymbol{\eta}_i \tag{C.7}$$

with

$$\boldsymbol{B}_{vi} = \begin{bmatrix} A_v^{11}\,\phi_{i,1} & A_v^{21}\,\phi_{i,1} \\ A_v^{12}\,\phi_{i,2} & A_v^{22}\,\phi_{i,2} \\ A_v^{11}\,\phi_{i,2} + A_v^{12}\,\phi_{i,1} & A_v^{21}\,\phi_{i,2} + A_v^{22}\,\phi_{i,1} \end{bmatrix}, \qquad \boldsymbol{\eta}_i = \begin{bmatrix} \eta_1^{(i)} \\ \eta_2^{(i)} \end{bmatrix}. \tag{C.8}$$

Approximation of $\mathbf{E}'_s(\boldsymbol{v},\boldsymbol{\psi})$. The variation of $\mathbf{E}$ with respect to the geometry can be written in terms of the deformation $\boldsymbol{\varphi}$ or the displacement $\boldsymbol{u}$ or in terms of the generalized state $\boldsymbol{v}$ as

$$\mathbf{E}'_s(\boldsymbol{v},\boldsymbol{\psi}) = -\operatorname{sym}\{\mathbf{F}^T \operatorname{Grad}\boldsymbol{v} \operatorname{Grad}\boldsymbol{\eta}\} = \operatorname{sym}\{\mathbf{A}_s^T \operatorname{Grad}\boldsymbol{\eta}\}, \tag{C.9}$$

$$\mathbf{A}_s := -\operatorname{Grad}\boldsymbol{v}^T\mathbf{F}. \tag{C.10}$$

The finite element approximation follows as

$$\boldsymbol{E}'_s(\boldsymbol{v}_h,\boldsymbol{\psi}_h) = \begin{bmatrix} (E'_s)_{11} \\ (E'_s)_{22} \\ 2\,(E'_s)_{12} \end{bmatrix} = \sum_{i=1}^{n} \boldsymbol{B}_{si}\boldsymbol{\psi}_i \tag{C.11}$$

with

$$\boldsymbol{B}_{si} = \begin{bmatrix} A_s^{11}\,\phi_{i,1} & A_s^{21}\,\phi_{i,1} \\ A_s^{12}\,\phi_{i,2} & A_s^{22}\,\phi_{i,2} \\ A_s^{11}\,\phi_{i,2} + A_s^{12}\,\phi_{i,1} & A_s^{21}\,\phi_{i,2} + A_s^{22}\,\phi_{i,1} \end{bmatrix}, \qquad \boldsymbol{\psi}_i = \begin{bmatrix} \psi_1^{(i)} \\ \psi_2^{(i)} \end{bmatrix}. \tag{C.12}$$

Approximation of $\mathbf{E}''_{vv}(\boldsymbol{\eta},\boldsymbol{z})$. The variation $\mathbf{E}''_{vv}(\boldsymbol{\eta},\boldsymbol{z}) = \mathbf{E}''_{vv}(\boldsymbol{z},\boldsymbol{\eta})$ reads

$$\mathbf{E}'_{vv}(\boldsymbol{\eta},\boldsymbol{z}) = \operatorname{sym}\{\operatorname{Grad}\boldsymbol{z}^T \operatorname{Grad}\boldsymbol{\eta}\} = \operatorname{sym}\{\mathbf{A}_z^T \operatorname{Grad}\boldsymbol{\eta}\}, \tag{C.13}$$

$$\mathbf{A}_z := \operatorname{Grad}\boldsymbol{z}. \tag{C.14}$$

The finite element approximation follows as $\boldsymbol{E}''_{vv}(\boldsymbol{\eta}_h,\boldsymbol{z}_h) = \sum_{i=1}^{n} \boldsymbol{B}_{zi}\boldsymbol{\eta}_i$ with

$$\boldsymbol{B}_{zi} = \begin{bmatrix} A_z^{11}\,\phi_{i,1} & A_z^{21}\,\phi_{i,1} \\ A_z^{12}\,\phi_{i,2} & A_z^{22}\,\phi_{i,2} \\ A_z^{11}\,\phi_{i,2} + A_{12}\,\phi_{i,1} & A_z^{21}\,\phi_{i,2} + A_z^{22}\,\phi_{i,1} \end{bmatrix}. \tag{C.15}$$

Approximation of $\mathbf{E}''_{vs}(\boldsymbol{v},\boldsymbol{z},\boldsymbol{\psi})$. The partial variation can be expressed as

$$\begin{aligned}\mathbf{E}''_{vs}(\boldsymbol{v},\boldsymbol{z},\boldsymbol{\psi}) &= -\operatorname{sym}\{\operatorname{Grad}\boldsymbol{z}^T \operatorname{Grad}\boldsymbol{v} \operatorname{Grad}\boldsymbol{\psi} + \mathbf{F}^T \operatorname{Grad}\boldsymbol{z} \operatorname{Grad}\boldsymbol{\psi}\} \\ &= \operatorname{sym}\{\mathbf{A}^T_{vs} \operatorname{Grad}\boldsymbol{\psi}\},\end{aligned} \tag{C.16}$$

$$\mathbf{A}_{vs} := -(\operatorname{Grad}\boldsymbol{v}^T \operatorname{Grad}\boldsymbol{z} + \operatorname{Grad}\boldsymbol{z}^T\mathbf{F}). \tag{C.17}$$

The approximation follows as $\boldsymbol{E}''_{vs}(\boldsymbol{v}_h,\boldsymbol{z}_h,\boldsymbol{\psi}_h) = \sum_{i=1}^n \boldsymbol{B}_{vsi}\boldsymbol{\psi}_i$ with

$$\boldsymbol{B}_{vsi} = \begin{bmatrix} A^{11}_{vs}\,\varphi_{i,1} & A^{21}_{vs}\,\varphi_{i,1} \\ A^{12}_{vs}\,\varphi_{i,2} & A^{22}_{vs}\,\varphi_{i,2} \\ A^{11}_{vs}\,\varphi_{i,2} + A^{12}_{vs}\,\varphi_{i,1} & A^{21}_{vs}\,\varphi_{i,2} + A^{22}_{vs}\,\varphi_{i,1} \end{bmatrix}. \tag{C.18}$$

Approximation of $\mathbf{E}'''_{vvs}(\boldsymbol{z},\boldsymbol{z},\boldsymbol{\psi})$. From (A.34) we have

$$\begin{aligned}\mathbf{E}'''_{vvs}(\boldsymbol{z},\boldsymbol{z},\boldsymbol{\psi}) &= -\operatorname{sym}\{\operatorname{Grad}\boldsymbol{z}^T \operatorname{Grad}\boldsymbol{z} \operatorname{Grad}\boldsymbol{\psi} + \operatorname{Grad}\boldsymbol{z}^T \operatorname{Grad}\boldsymbol{z} \operatorname{Grad}\boldsymbol{\psi}\} \\ &= \operatorname{sym}\{\mathbf{A}^T_{vvs} \operatorname{Grad}\boldsymbol{\psi}\},\end{aligned}$$

$$\mathbf{A}_{vvs} := -2 \operatorname{Grad}\boldsymbol{z}^T \operatorname{Grad}\boldsymbol{z}. \tag{C.19}$$

The finite element approximation reads $\boldsymbol{E}'''_{vvs}(\boldsymbol{v}_h,\boldsymbol{z}_h,\boldsymbol{\psi}_h) = \sum_{i=1}^n \boldsymbol{B}_{vvsi}\boldsymbol{\psi}_i$ with

$$\boldsymbol{B}_{vvsi} = \begin{bmatrix} A^{11}_{vvs}\,\varphi_{i,1} & A^{21}_{vvs}\,\varphi_{i,1} \\ A^{12}_{vvs}\,\varphi_{i,2} & A^{22}_{vvs}\,\varphi_{i,2} \\ A^{11}_{vvs}\,\varphi_{i,2} + A^{12}_{vvs}\,\varphi_{i,1} & A^{21}_{vvs}\,\varphi_{i,2} + A^{22}_{vvs}\,\varphi_{i,1} \end{bmatrix}. \tag{C.20}$$

C.3 Approximation of residuals

The approximation of the considered residuals and the introduction of the corresponding matrix formulations are given below. This is exemplarily shown for the physical and material residuals of the primal problem. The approach can be applied in the same manner to the residuals of the dual problem R^* and G^*, respectively.

The discretization of the primal physical residual (4.85) for given $\{\hat{\boldsymbol{v}}_h, \hat{\boldsymbol{s}}_h\}$ is obtained as usual in the form

$$\begin{aligned}R(\hat{\boldsymbol{v}}_h,\hat{\boldsymbol{s}}_h;\boldsymbol{\eta}_h) &= \bigcup_{e=1}^{NEL} \int_{\Omega^e_R} \mathbf{S} : \mathbf{E}'_v(\hat{\boldsymbol{v}}^e_h,\boldsymbol{\eta}^e_h)\,\mathrm{d}\Omega - F(\boldsymbol{s}^e_h;\boldsymbol{\eta}^e_h) \\ &= \bigcup_{e=1}^{NEL} \int_{\Omega^e_R} \boldsymbol{S} \cdot \boldsymbol{E}'_v(\hat{\boldsymbol{v}}^e_h,\boldsymbol{\eta}^e_h)\,\mathrm{d}\Omega - F(\boldsymbol{s}^e_h;\boldsymbol{\eta}^e_h) \\ &= \bigcup_{e=1}^{NEL} \sum_{i=1}^{n} \boldsymbol{\eta}^T_i \boldsymbol{R}^e_i = \boldsymbol{\eta}^T \boldsymbol{R},\end{aligned} \tag{C.21}$$

where the nodal contribution $\boldsymbol{R}_i^e$ is given in (4.96). In order to indicate the assembly over all finite elements we use the operator $\bigcup$. Furthermore, due to the symmetry of the two point tensors $\mathbf{S}$ and $\mathbf{E}'_v$ the residual can be written in terms of the vectors $\boldsymbol{S}$ and $\boldsymbol{E}'_v$. In the two-dimensional case these vectors have three independent components and are given as

$$\boldsymbol{S} = \begin{bmatrix} S_{11} & S_{22} & S_{12} \end{bmatrix}^T, \qquad \boldsymbol{E}'_v = \begin{bmatrix} (E'_v)_{11} & (E'_v)_{22} & 2\,(E'_v)_{12} \end{bmatrix}^T.$$

In the same manner, the primal material residual (4.86) is given as

$$\begin{aligned} G(\hat{\boldsymbol{v}}_h, \hat{\boldsymbol{s}}_h; \boldsymbol{\psi}_h) &= \bigcup_{e=1}^{NEL} \int_{\Omega_R^e} \mathbf{S} : \mathbf{E}'_s(\hat{\boldsymbol{v}}_h^e, \boldsymbol{\psi}_h^e) + W_R \mathbf{I} : \operatorname{Grad} \boldsymbol{\psi}_h^e \, \mathrm{d}\Omega - F'_s(\hat{\boldsymbol{s}}_h^e; \hat{\boldsymbol{v}}_h^e, \boldsymbol{\psi}_h^e) \\ &= \bigcup_{e=1}^{NEL} \int_{\Omega_R^e} \boldsymbol{S} \cdot \boldsymbol{E}'_s(\hat{\boldsymbol{v}}_h^e, \boldsymbol{\psi}_h^e) + W_R \mathbf{I} : \operatorname{Grad} \boldsymbol{\psi}_h^e \, \mathrm{d}\Omega - F'_s(\hat{\boldsymbol{s}}_h^e; \hat{\boldsymbol{v}}_h^e, \boldsymbol{\psi}_h^e) \\ &= \bigcup_{e=1}^{NEL} \sum_{i=1}^{n} \boldsymbol{\psi}_i^T \boldsymbol{G}_i^e = \boldsymbol{\psi}^T \boldsymbol{G}, \end{aligned} \tag{C.22}$$

where $\boldsymbol{G}_i^e$ is given in (4.97).

Finally, for a four node element with 8 degrees of freedom the element vectors $\boldsymbol{R}^e \in \mathbb{R}^8$ and $\boldsymbol{G}^e \in \mathbb{R}^8$ are given by the vectors $\boldsymbol{R}_i^e \in \mathbb{R}^2$ and $\boldsymbol{G}_i^e \in \mathbb{R}^2$ as

$$\boldsymbol{R}^e = \begin{bmatrix} \boldsymbol{R}_1^e \\ \boldsymbol{R}_2^e \\ \boldsymbol{R}_3^e \\ \boldsymbol{R}_4^e \end{bmatrix}, \qquad \boldsymbol{G}^e = \begin{bmatrix} \boldsymbol{G}_1^e \\ \boldsymbol{G}_2^e \\ \boldsymbol{G}_3^e \\ \boldsymbol{G}_4^e \end{bmatrix}. \tag{C.23}$$

The residuals of the dual problem $\boldsymbol{R}^*$ and $\boldsymbol{G}^*$ can be computed in the same manner in the same routine as $\boldsymbol{R}$ and $\boldsymbol{G}$. The nodal contributions of these residuals are given in Section 6.5.3.

C.4 Approximation of tangent forms

The discretization of the considered primal and dual tangent forms from Section 4.6.2 and Section 6.5.2 can be obtained in a straightforward manner. This is exemplarily shown for the primal physical stiffness tangent form $k(\boldsymbol{v}, \boldsymbol{s}; \boldsymbol{\eta}, \delta\boldsymbol{v})$ and the primal physical pseudo load tangent form $p(\boldsymbol{v}, \boldsymbol{s}; \boldsymbol{\eta}, \delta\boldsymbol{s})$, which have been introduced in (4.87) and (4.88), respectively.

For instance, for given $\{\hat{\boldsymbol{v}}_h, \hat{\boldsymbol{s}}_h\}$ the primal physical stiffness tangent form read

$$\begin{aligned} k(\hat{\boldsymbol{v}}_h, \hat{\boldsymbol{s}}_h; \boldsymbol{\eta}_h, \delta\boldsymbol{v}_h) &= \bigcup_{e=1}^{NEL} \int_{\Omega_R^e} \mathbf{S} : \mathbf{E}''_{vv}(\boldsymbol{\eta}_h^e, \delta\boldsymbol{v}_h^e) + \mathbf{E}'_v(\hat{\boldsymbol{v}}_h^e, \boldsymbol{\eta}_h^e) : \mathbb{C} : \mathbf{E}'_v(\hat{\boldsymbol{v}}_h^e, \delta\boldsymbol{v}_h^e) \\ &= \bigcup_{e=1}^{NEL} \sum_{i=1}^{n} \sum_{j=1}^{n} \boldsymbol{\eta}_i^T \boldsymbol{K}_{ij}^e \, \delta\boldsymbol{v}_j = \boldsymbol{\eta}^T \boldsymbol{K} \delta\boldsymbol{v}, \end{aligned} \tag{C.24}$$

In the same manner, the primal physical pseudo load tangent form becomes the matrix representation

$$\begin{aligned} p(\hat{\boldsymbol{v}}_h, \hat{\boldsymbol{s}}_h; \boldsymbol{\eta}_h, \delta\boldsymbol{s}_h) = \bigcup_{e=1}^{NEL} \int_{\Omega_R^e} \{ & \mathbf{S} : \mathbf{E}''_{vs}(\hat{\boldsymbol{v}}_h^e, \boldsymbol{\eta}_h^e, \delta\boldsymbol{s}_h^e) \\ & + \mathbf{E}'_v(\hat{\boldsymbol{v}}_h^e, \boldsymbol{\eta}_h^e) : \mathbb{C} : \mathbf{E}'_s(\hat{\boldsymbol{v}}_h^e, \delta\boldsymbol{s}_h^e) \\ & + \mathbf{S} : \mathbf{E}'_v(\hat{\boldsymbol{v}}_h^e, \boldsymbol{\eta}_h^e) \operatorname{Div} \delta\boldsymbol{s}_h^e \} \, \mathrm{d}\Omega - F'_s(\hat{\boldsymbol{s}}_h^e; \boldsymbol{\eta}_h^e, \delta\boldsymbol{s}_h^e) \\ = \bigcup_{e=1}^{NEL} \sum_{i=1}^{n} \sum_{j=1}^{n} & \boldsymbol{\eta}_i^T \boldsymbol{P}_{ij}^e \, \delta\boldsymbol{s}_j = \boldsymbol{\eta}^T \boldsymbol{P} \delta\boldsymbol{s}, \end{aligned} \tag{C.25}$$

where the nodal contribution $\boldsymbol{K}_{ij}^e$ and $\boldsymbol{P}_{ij}^e$ are given in (4.98). and (4.99), respectively.

Finally, for a four node element the element matrices $\boldsymbol{K}^e \in \mathbb{R}^{8\times8}$ and $\boldsymbol{P}^e \in \mathbb{R}^{8\times8}$ are given by the submatrices $\boldsymbol{K}_{ij}^e \in \mathbb{R}^{2\times2}$ and $\boldsymbol{P}_{ij}^e \in \mathbb{R}^{2\times2}$ as

$$\boldsymbol{K}^e = \begin{bmatrix} \boldsymbol{K}_{11}^e & \boldsymbol{K}_{12}^e & \boldsymbol{K}_{13}^e & \boldsymbol{K}_{14}^e \\ \boldsymbol{K}_{21}^e & \boldsymbol{K}_{22}^e & \boldsymbol{K}_{23}^e & \boldsymbol{K}_{24}^e \\ \boldsymbol{K}_{31}^e & \boldsymbol{K}_{32}^e & \boldsymbol{K}_{33}^e & \boldsymbol{K}_{34}^e \\ \boldsymbol{K}_{41}^e & \boldsymbol{K}_{42}^e & \boldsymbol{K}_{43}^e & \boldsymbol{K}_{44}^e \end{bmatrix}, \qquad \boldsymbol{P}^e = \begin{bmatrix} \boldsymbol{P}_{11}^e & \boldsymbol{P}_{12}^e & \boldsymbol{P}_{13}^e & \boldsymbol{P}_{14}^e \\ \boldsymbol{P}_{21}^e & \boldsymbol{P}_{22}^e & \boldsymbol{P}_{23}^e & \boldsymbol{P}_{24}^e \\ \boldsymbol{P}_{31}^e & \boldsymbol{P}_{32}^e & \boldsymbol{P}_{33}^e & \boldsymbol{P}_{34}^e \\ \boldsymbol{P}_{41}^e & \boldsymbol{P}_{42}^e & \boldsymbol{P}_{43}^e & \boldsymbol{P}_{44}^e \end{bmatrix}. \tag{C.26}$$

The approach can be applied in the same manner to the other tangent forms of the primal and the dual problems in order to obtain the primal tangent material stiffness matrix $\boldsymbol{D}$ as well as the dual pseudo load matrix $\boldsymbol{P}^*$ and the dual tangent material stiffness matrix $\boldsymbol{D}^*$. The nodal contributions of these matrices are given in Section 4.6.2 and Section 6.5.3, respectively. All matrices can be computed in the same routine as the classical stiffness matrix $\boldsymbol{K}$ without considerable computational cost.

Note, that the tangent physical and material stiffness matrices $\boldsymbol{K}$, $\boldsymbol{D}$ and $\boldsymbol{D}^*$ are symmetric. But this does not apply, in general, to the tangent pseudo load matrices $\boldsymbol{P}$ and $\boldsymbol{P}^*$.

Bibliography

[1] ASKES, H., BARGMANN, S., KUHL, E., AND STEINMANN, P. Structural optimisation by simultaneous equilibration of spatial and material forces. *Commun. Numer. Meth. Engng. 21* (2005), 433–442.

[2] ASKES, H., KUHL, E., AND STEINMANN, P. An ALE formulation based on spatial and material settings of continuum mechanics. Part 2: Classification and applications. *Comput. Methods Appl. Mech. Engrg.*, 193 (2004), 4223–4245.

[3] BABUŠKA, I., AND RHEINBOLDT, W. C. Error estimates for adaptive finite element computations. *SIAM J. Numer. Anal. 15* (1978), 736–754.

[4] BANGERTH, W., AND RANNACHER, R. *Adaptive Finite Element Methods for Differential Equations*. Lectures in Mathematics, ETH Zürich. Birkhäuser, Basel, 2003.

[5] BARTHOLD, F.-J. Zur Kontinuumsmechanik inverser Geometrieprobleme. Habilitationsschrift, Braunschweiger Schriften zur Mechanik 44-2002, TU Braunschweig, 2002.

[6] BARTHOLD, F.-J. A structural optimization viewpoint on configurational mechanics. *Proc. Appl. Math. Mech. 3* (2003), 246–247.

[7] BARTHOLD, F.-J. Remarks on variational shape sensitivity analysis based on local coordinates. *Engineering Analysis with Boundary Elements 32*, 11 (2008), 971–985.

[8] BARTHOLD, F.-J., AND MESECKE, S. Remarks on computing the energy release rate and its sensitivities. In *Mechanics of Composite Materials and Structures*, C. Mota Soares, C. Mota Soares, and M. Freitas, Eds., vol. 361 of *NATO Science Series, Serie E: Applied Science*. Kluwer Academic Publishers, 1999, pp. 341–350.

[9] BARTHOLD, F.-J., AND STEIN, E. A continuum mechanical based formulation of the variational sensitivity analysis in structural optimization. Part I: Analysis. *Structural Optimization 11*, 1/2 (1996), 29–42.

[10] BATHE, K.-J. *Finite Element Procedures*. Prentice-Hall, 1996.

[11] BECKER, R., AND RANNACHER, R. A feed-back approach to error control in finite element methods: basic analysis and examples. *East-West J. Numer. Math. 4* (1996), 237–264.

[12] BECKER, R., AND RANNACHER, R. An optimal control approach to a posteriori error estimation in finite element methods. *Acta Numerica 10* (2001), 1–102.

[13] BENDSØE, M. P. *Optimization of Structural Topology, Shape, and Material*. Springer-Verlag, 1995.

[14] BENDSØE, M. P., AND SIGMUND, O. *Topology Optimization - Theory, Methods and Applications*. Springer-Verlag, 2003.

[15] BENZI, M., AND GOLUB, G. H. A preconditioner for generalized saddle point problems. *Siam J. Matrix Anal. Appl. 26*, 1 (2004), 20–41.

[16] BLANCHARD, P., AND BRÜNING, E. *Direkte Methoden der Variationsrechnung. Ein Lehrbuch*. Springer-Verlag, Wien, 1982.

[17] BONET, J., AND WOOD, R. D. *Nonlinear Continuum Mechanics for Finite Element Analysis*. Cambridge University Press, 1997.

[18] BRAACK, M., AND ERN, A. A posteriori control of modeling errors and discretization errors. *Multiscale Model. Simul. 1*, 2 (2003), 221–238.

[19] BRAESS, D. *Finite Elemente*. Springer-Verlag, 1997.

[20] BRAUN, M. Configurational forces induced by finite-element discretisation. *Proc. Estonian Acad. Sci. Phys. Math. 46* (1997), 24–31.

[21] BRAUN, M. Structural optimization by material forces. In *Mechanics of Material Forces* (2005), P. Steinmann and G. A. Maugin, Eds., vol. 11, Springer-Verlag, pp. 211–218.

[22] CAO, W., HUANG, W., AND RUSSELL, R. D. Approaches for generating moving adaptive meshes: location versus velocity. *Applied Numerical Mathematics 47* (2003), 121–138.

[23] CARPENTER, W. C., AND ZENDEGUI, S. Optimum nodal locations for a finite element idealization. *Engineering Optimization 5* (1982), 215–221.

[24] CARROLL, W. E., AND BARKER, R. M. A theorem for optimum finite-element idealizations. *Int. J. Solids. Struct. 9* (1973), 883–895.

[25] CÉA, J. Problems of shape optimal design. In *Optimization of Distributed Parameter Structures* (1981), E. J. Haug and J. Céa, Eds., Sijthoff & Noordhoff, pp. 1005–1048.

[26] CHADWICK, P. Applications of an energy-momentum tensor in non-linear elastostatics. *Journal of Elasticity 5*, 3-4 (1975), 249–258.

[27] CHOI, K. K., AND KIM, N.-H. *Structural Sensitivity Analysis and Optimization 1 - Linear Systems*. Mechanical Engineering Series. Springer-Verlag, Berlin, 2005.

[28] CHOI, K. K., AND KIM, N.-H. *Structural Sensitivity Analysis and Optimization 2 - Nonlinear Systems and Applications*. Mechanical Engineering Series. Springer-Verlag, Berlin, 2005.

[29] CHRISTENSEN, P. W., AND KLARBRING, A. *An Introduction to Structural Optimization*. Springer-Verlag, 2009.

[30] CIARLET, P. G. *Mathematical Elasticity, Volume I: Three-Dimensional Elasticity*. Studies in Mathematics and its Applications. Elsevier, Amsterdam, 1994.

[31] CIRAK, F., AND RAMM, E. A posteriori error estimation and adaptivity for linear elasticity using the reciprocal theorem. *Comput. Methods Appl. Mech. Engrg. 156*, 1-4 (1998), 351–362.

[32] DEMS, K., AND MRÓZ, Z. Multiparameter structural shape optimization by the finite element method. *Int. J. Numer. Meth. Engng. 13*, 2 (1978), 247–263.

[33] DIAZ, A. R., KIKUCHI, N., AND TAYLOR, J. E. A method of grid optimization for finite element methods. *Comput. Methods Appl. Mech. Engrg. 41*, 1 (1983), 29–45.

[34] DUFFY, D. G. *Green's Functions with Applications*. Chapman & Hall, 2001.

[35] EDELEN, D. G. B. Aspects of variational arguments in the theory of elasticity: Fact and folklore. *Int. J. Solids. Struct. 17*, 8 (1981), 729–740.

[36] ENGL, H. W., HANKE, M., AND NEUBAUER, A. *Regularization of Inverse Problems*. Kluver Academic Publishers, 2000.

[37] ERIKSSON, K., AND JOHNSON, C. An adaptive finite element method for linear elliptic problems. *Math. Comput. 50* (1988), 361–383.

[38] ESCHENAUER, H., KOSKI, J., AND OSYCZKA, A., Eds. *Multicriteria Design Optimization: Procedures and Applications*. Springer-Verlag, 1990.

[39] ESHELBY, J. D. The force on an elastic singularity. *Philosophical Transactions of the Royal Society of London 244* (1951), 87–112.

[40] ESHELBY, J. D. The elastic energy-momentum tensor. *Journal of Elasticity 5* (1975), 321–335.

[41] FELIPPA, C. A. Optimization of finite element grids by direct energy search. *Appl. Math. Modelling 1* (1976), 93–96.

[42] GELFAND, I. M., AND FOMIN, S. V. *Calculus of Variations*. Dover Publications, New York, 2000.

[43] GOLUB, G. H., AND LOAN, C. F. V. *Matrix Computations*, 3rd ed. The Johns Hopkins University Press, Baltimore, 1996.

[44] GOVINDJEE, S., AND MIHALIC, P. A. Computational methods for inverse finite elastostatics. *Comput. Methods Appl. Mech. Engrg. 136*, 1-2 (1996), 47–57.

[45] GOVINDJEE, S., AND MIHALIC, P. A. Computational methods for inverse deformations in quasi-incompressible finite elasticity. *Int. J. Numer. Meth. Engng. 43*, 5 (1998), 821–838.

[46] GRÄTSCH, T., AND BATHE, K.-J. A posteriori error estimation techniques in practical finite element analysis. *Computers & Structures 83*, 4-5 (2005), 235–265.

[47] GRÄTSCH, T., AND HARTMANN, F. Pointwise error estimation and adaptivity for the finite element method using fundamental solutions. *Computational Mechanics 37*, 5 (2006), 394–407.

[48] GURTIN, M. E. *Configurational Forces as Basic Concepts of Continuum Physics*. Springer-Verlag, New York, 2000.

[49] HARTMANN, F. *The Mathematical Foundation of Structural Mechanics*. Springer-Verlag, Berlin Heidelberg, 1985.

[50] HARTMANN, F. *Introduction to Boundary Elements, Theory and Applications*. Springer-Verlag, 1989.

[51] HARTMANN, F., AND KATZ, C. *Structural Analysis with Finite Elements*. Springer-Verlag, 2007.

[52] HEINTZ, P., LARSSON, F., HANSBO, P., AND RUNESSON, K. Adaptive strategies and error control for computing material forces in fracture mechanics. *Int. J. Numer. Meth. Engng. 60* (2004), 1287–1299.

[53] HERRMANN, G., AND KIENZLER, R. Reciprocity relations in Eshelbian mechanics. *Mech. Res. Commun. 34* (2007), 338–343.

[54] HERRMANN, G., AND KIENZLER, R. A reciprocity relation couples newtonian and eshelbian mechanics. *ASME J. Appl. Mech. 75*, 1 (2008), 011017.

[55] HOLZAPFEL, G. A. *Nonlinear Solid Mechanics: A Continuum Approach for Engineering*. Wiley & Sons, 2000.

[56] HUGHES, T. *The Finite Element Method*. Prentice-Hall, 1987.

[57] KALPAKIDES, V. K., AND BALASSAS, K. G. The inverse deformation mapping in the finite element method. *Philosophical Magazine 85*, 33-35 (2005), 4257–4275.

[58] KAMAT, M. P. *Structural Optimization: Status and Promise*. Washington: American Institute of Aeronautics and Astronautics, 1993.

[59] KELLY, D. W., GAGO, J. P. D. S. R., ZIENKIEWICZ, O. C., AND BABUŠKA, I. A posteriori error analysis and adaptive processes in the finite element method: Part I - error analysis. *Int. J. Numer. Meth. Engng. 19* (1983), 1593–1619.

[60] KIENZLER, R., AND HERRMANN, G. *Mechanics in Material Space*. Springer-Verlag, Berlin Heidelberg New York, 2000.

[61] KUHL, E., ASKES, H., AND STEINMANN, P. An ALE formulation based on spatial and material settings of continuum mechanics. Part 1: Generic hyperelastic formulation. *Comput. Methods Appl. Mech. Engrg.*, 193 (2004), 4207–4222.

[62] LIONS, J. L. *Optimal Control of Systems Governed by Partial Differential Equations*. Springer-Verlag, 1971.

[63] LOVELOCK, D., AND RUND, H. *Tensors, Differential Forms, and Variational Principles*. Dover Publications, New York, 1989.

[64] MARSDEN, J. E., AND HUGHES, T. J. R. *Mathematical Foundations of Elasticity*. Dover, New York, 1994.

[65] MATERNA, D., AND BARTHOLD, F.-J. Relations between structural optimization and configurational mechanics with applications to mesh optimization. In *Proc. of the 6th ASMO-UK/ISSMO Conf. on Engineering Design Optimization, St Edmund Hall, Oxford, UK* (2006), J. Sienz, O. M. Querin, V. V. Toropov, and P. D. Gosling, Eds., University of Leeds, UK, pp. 173–181.

[66] MATERNA, D., AND BARTHOLD, F.-J. Variational design sensitivity analysis in the context of structural optimization and configurational mechanics. *Int. J. Fract. 147*, 1-4 (2007), 133–155.

[67] MATERNA, D., AND BARTHOLD, F.-J. Variational sensitivity analysis and changes in the material configuration. *Proc. Appl. Math. Mech. 7*, 1 (2007), 1090105–1090106.

[68] MATERNA, D., AND BARTHOLD, F.-J. Goal-oriented r-adaptivity based on the evaluation of the physical and material residual. *Proc. Appl. Math. Mech. 8*, 1 (2008), 10307–10308.

[69] MATERNA, D., AND BARTHOLD, F.-J. On variational sensitivity analysis and configurational mechanics. *Computational Mechanics 41*, 5 (2008), 661–681.

[70] MATERNA, D., AND BARTHOLD, F.-J. *Computational Optimization: New Research Developments*. Nova Science Publishers, 2009, ch. Theoretical aspects and applications of variational sensitivity analysis in the physical and material space. accepted for publication.

[71] MATERNA, D., AND BARTHOLD, F.-J. Configurational variations for the primal and dual problem in elasticity. *Z. Angew. Math. Mech. 89*, 8 (2009), 666–676.

[72] MATERNA, D., AND BARTHOLD, F.-J. Goal-oriented r-adaptivity based on variational arguments in the physical and material spaces. *Comput. Methods Appl. Mech. Engrg. 198*, 41-44 (2009), 3335–3351.

[73] MATERNA, D., AND BARTHOLD, F.-J. A variational framework for dual solutions in the physical and material space. In *IUTAM Symposium on Progress in the Theory and Numerics of Configurational Mechanics* (2009), P. Steinmann, Ed., vol. 17 of *IUTAM Bookseries*, Springer-Verlag, pp. 95–105.

[74] MAUGIN, G. A. *Material inhomogeneities in elasticity*. Chapman & Hall, London, 1993.

[75] MCNEICE, G. M., AND MARCAL, P. E. Optimization of finite element grids based on minimum potential energy. *ASME Journal of Engineering for Industry 95*, 1 (1973), 186–190.

[76] MELNIKOV, Y. A. *Green's functions in applied mechanics*. Computational Mechanics Publications, Southampton, UK, 1995.

[77] MOSLER, J., AND ORTIZ, M. On the numerical modeling of variational arbitrary lagrangian-eulerian (vale) formulations. *Int. J. Numer. Meth. Engng. 67* (2006), 1272–1289.

[78] MOSLER, J., AND ORTIZ, M. Variational h-adaption in finite deformation elasticity and plasticity. *Int. J. Numer. Meth. Engng. 72* (2007), 505–523.

[79] MUELLER, R., GROSS, D., AND MAUGIN, G. A. Use of material forces in adaptive finite element methods. *Computational Mechanics*, 33 (2004), 421–434.

[80] MUELLER, R., AND MAUGIN, G. A. On material forces and finite element discretizations. *Computational Mechanics 29* (2002), 52–60.

[81] NOCEDAL, J., AND WRIGHT, S. J. *Numerical Optimization*. Springer-Verlag, 1999.

[82] NOLL, W. A new mathematical theory of simple materials. *Arch. Rational Mech. Anal. 48*, 1 (1972), 1–50.

[83] NOVOTNY, A. A., FEIJÓO, R. A., TAROCO, E., AND PADRA, C. Topological sensitivity analysis. *Comput. Methods Appl. Mech. Engrg. 192* (2003), 803–829.

[84] ODEN, J. T., AND PRUDHOMME, S. Estimation of modeling error in computational mechanics. *Journal of Computational Physics 182* (2002), 496–515.

[85] ODEN, J. T., AND REDDY, J. N. *An introduction to the mathematical theory of finite elements*. John Wiley & Sons, 1976.

[86] ODEN, J. T., AND VEMAGANTI, K. Estimation of local modeling error and goal-oriented modeling of heterogeneous materials; Part i: Error estimates and adaptive algorithms. *J. Comput. Phys. 164* (2000), 22–47.

[87] OGDEN, R. W. *Non-Linear Elastic Deformations*. Dover Publications, 1997.

[88] PRUDHOMME, S., AND ODEN, J. T. On goal-oriented error estimation for elliptic problems: application to the control of pointwise errors. *Comput. Methods Appl. Mech. Engrg. 176*, 1-4 (1999), 313–331.

[89] RAJAGOPAL, A., AND SIVAKUMAR, S. M. A combined r-h adaptive strategy based on material forces and error assessment for plane problems and bimaterial interfaces. *Comput. Mech. 41*, 1 (2007), 49–72.

[90] RÜTER, M., AND STEIN, E. Adaptive finite element analysis of crack propagation in elastic fracture mechanics based on averaging techniques. *Computational Materials Science 31* (2004), 247–257.

[91] RÜTER, M., AND STEIN, E. On the duality of finite element discretization error control in computational newtonian and eshelbian mechanics. *Comput. Mech. 39*, 5 (2007), 609–630.

[92] SCHERER, M., DENZER, R., AND STEINMANN, P. Energy-based r-adaptivity: a solution strategy and applications to fracture mechanics. *Int. J. Fract. 147*, 1-4 (2007), 117–132.

[93] SHIELD, R. T. Inverse Deformation Results in Finite Elasticity. *Z. Angew. Math. Phys. 18* (1967), 490–500.

[94] STEIN, E., AND OHNIMUS, S. Anisotropic discretization- and model-error estimation in solid mechanics by local neumann problems. *Comput. Methods Appl. Mech. Engrg. 176* (1999), 363–385.

[95] STEIN, E., RÜTER, M., AND OHNIMUS, S. Error-controlled adaptive goal-oriented modeling and finite element approximations in elasticity. *Comput. Methods Appl. Mech. Engrg. 196* (2007), 3598–3613.

[96] STEINMANN, P. Application of material forces to hyperelastic fracture mechanics. I. Continuum mechanical settings. *Int. J. Solids. Struct. 37* (2000), 7371–7391.

[97] STEINMANN, P., AND MAUGIN, G. A., Eds. *Mechanics of Material Forces*. Springer-Verlag, 2005.

[98] STEUER, R. E. *Multiple Criteria Optimization: Theory, Computations and Application*. Wiley & Sons, 1986.

[99] SUSSMAN, T., AND BATHE, K.-J. The gradient of the finite element variational indicator with respect to nodal point coordinates: An explicit calculation and applications in fracture mechanics and mesh optimization. *Int. J. Numer. Meth. Engng. 21*, 4 (1985), 763–774.

[100] TAROCO, E. Shape sensitivity analysis in linear elastic fracture mechanics. *Comput. Methods Appl. Mech. Engrg. 188* (2000), 697–712.

[101] THOUTIREDDY, P. *Variational Arbitrary Lagrangian-Eulerian Method*. Phd thesis, California Institute of Technology, Passadena, California, 2003.

[102] THOUTIREDDY, P., AND ORTIZ, M. A variational r-adaption and shape-optimization method for finite-deformation elasticity. *Int. J. Numer. Meth. Engng. 61*, 1 (2004), 1–21.

[103] TOURIGNY, Y., AND HÜLSEMANN, F. A new moving mesh algorithm for the finite element solution of variational problems. *SIAM J. Numer. Anal. 35*, 4 (1998), 1416–1438.

[104] VAN KEULEN, F., HAFTKA, R., AND KIM, N. Review of options for structural design sensitivity analysis. Part 1: Linear systems. *Comput. Methods Appl. Mech. Engrg. 194* (2005), 3213–3243.

[105] WRIGGERS, P. *Nichtlineare Finite-Element-Methoden*. Springer-Verlag, 2001.

[106] ZHANG, S., AND BELEGUNDU, A. Mesh distortion control in shape optimization. *AIAA Journal 31*, 7 (1993), 1360–1362.

[107] ZIENKIEWICZ, O., AND TAYLOR, R. *The Finite Element Method. Volume 1: The Basis*, fifth ed. Butterworth-Heinemann, 2000.

[108] ZIENKIEWICZ, O., AND TAYLOR, R. *The Finite Element Method. Volume 2: Solid Mechanics*, fifth ed. Butterworth-Heinemann, 2000.

[109] ZIENKIEWICZ, O. C., AND ZHU, J. Z. A simple error estimator and adaptive procedure for practical engineering analysis. *Int. J. Numer. Meth. Engng. 24* (1987), 337–357.